antibiotics

Antimicrobial Activity of Different Plant Extracts, Plant-Derived Compounds and Synthetic Derivatives of Natural Compounds on Pathogenic Microorganisms

Edited by
Joanna Kozłowska and Anna Duda-Madej

MDPI

Antimicrobial Activity of Different Plant Extracts, Plant-Derived Compounds and Synthetic Derivatives of Natural Compounds on Pathogenic Microorganisms

Antimicrobial Activity of Different Plant Extracts, Plant-Derived Compounds and Synthetic Derivatives of Natural Compounds on Pathogenic Microorganisms

Editors

Joanna Kozłowska
Anna Duda-Madej

Editors

Joanna Kozłowska
Department of Food
Chemistry and Biocatalysis
Wroclaw University of
Environmental and Life Sciences
Wrocław
Poland

Anna Duda-Madej
Department of Microbiology
Wroclaw Medical University
Wrocław
Poland

For citation purposes, cite each article independently as indicated on the article page online and as indicated below:

Lastname, A.A.; Lastname, B.B. Article Title. *Journal Name* **Year**, *Volume Number*, Page Range.

Contents

Article

Ether Derivatives of Naringenin and Their Oximes as Factors Modulating Bacterial Adhesion

Anna Duda-Madej [1,*], Joanna Kozłowska [2], Dagmara Baczyńska [3] and Paweł Krzyżek [1,*]

1   Department of Microbiology, Faculty of Medicine, Wroclaw Medical University, Chałubińskiego 4,
    50-368 Wrocław, Poland
2   Department of Food Chemistry and Biocatalysis, Faculty of Biotechnology and Food Science,
    Wrocław University of Environmental and Life Sciences, C.K. Norwida 25, 50-375 Wrocław, Poland;
    joanna.kozlowska@upwr.edu.pl
3   Department of Molecular and Cellular Biology, Faculty of Pharmacy, Wroclaw Medical University,
    Borowska 211A, 50-556 Wrocław, Poland; dagmara.baczynska@umw.edu.pl
*   Correspondence: anna.duda-madej@umw.edu.pl (A.D.-M.); pawel.krzyzek@umw.edu.pl (P.K.)

Abstract: Because of the close connection between adhesion and many vital cellular functions, the search for new compounds modulating the adhesion of bacteria belonging to the intestinal microbiota is a great challenge and a clinical need. Based on our previous studies, we discovered that *O*-lkyl naringenin derivatives and their oximes exhibit antimicrobial activity against antibiotic-resistant pathogens. The current study was aimed at determining the modulatory effect of these compounds on the adhesion of selected representatives of the intestinal microbiota: *Escherichia coli*, a commensal representative of the intestinal microbiota, and *Enterococcus faecalis*, a bacterium that naturally colonizes the intestines but has disease-promoting potential. To better reflect the variety of real-life scenarios, we performed these studies using two different intestinal cell lines: the physiologically functioning ("healthy") 3T3-L1 cell line and the disease-mimicking, cancerous HT-29 line. The study was performed in vitro under static and microfluidic conditions generated by the Bioflux system. We detected the modulatory effect of the tested *O*-alkyl naringenin derivatives on bacterial adhesion, which was dependent on the cell line studied and was more significant for *E. coli* than for *E. faecalis*. In addition, it was noticed that this activity was affected by the concentration of the tested compound and its structure (length of the carbon chain). In summary, *O*-alkyl naringenin derivatives and their oximes possess a promising modulatory effect on the adhesion of selected representatives of the intestinal microbiota.

Keywords: adhesion; biofilm; Bioflux; microfluidic conditions; naringenin derivatives; intestinal microflora

1. Introduction

Cell adhesion is a phenomenon of paramount importance in various physiological processes. It affects a plethora of physiological functions of cells, e.g., growth, differentiation, and migration. Interactions during adhesion can occur either on the cell-to-cell or cell-to-extracellular matrix (ECM; extracellular matrix) pathway, which for eukaryotic cells is essential for the development of tissues, organs, and even whole organisms [1]. Non-specific factors responsible for cell adhesion include van der Waals forces, hydrogen and ionic bonds, and the presence of hydrophobic groups [2]. Cell–cell inter-adhesion is additionally stabilized by specific mechanisms, including the production of cell membrane glycoproteins, known as cell adhesion molecules (CAMs). The role of CAMs has been confirmed in many processes, both physiological and pathological. Under natural conditions, they are involved in, e.g., embryogenesis, wound healing, and the maintenance of normal tissue organization [3,4]. The negative effects of CAMs include their involvement in tumorigenesis by allowing: (1) progression (growth of the primary tumor by affecting

cell differentiation); (2) tissue invasion (morphological abnormalities and disorganization of the cytoskeleton); and (3) metastasis (involvement in detachment of tumor cells from the neoplastic mass and migration to other organs) [5–7].

Adhesion is, however, not limited to eukaryotic cells. This phenomenon is also of high importance for prokaryotic cells, which, using a number of factors, e.g., motile cilia, fimbriae, lipopolysaccharide, and outer membrane proteins [8], easily reach the epithelial surface. A model example of the relevance of the ligation process of microbes with cell receptors is the gastrointestinal tract, the largest organ of our body. There are many factors preventing the adhesion of microbes to the gastrointestinal tract, including mucus production, intestinal peristalsis, antibodies, and other components of the non-specific immune response. This greatly underscores the importance of this environment in the context of modulating microbial adhesion. However, despite these processes, microorganisms constituting the gastrointestinal microbiome can easily cope with this microenvironment and overcome the above-mentioned disadvantages, reaching a final biomass of 10^{13}–10^{14} cells [9]. Over the years, it has become clear that the gastrointestinal microbiota coordinates the proper functioning of metabolism, immunity, and the development of the human body. Intestinal bacteria exhibit a number of positive effects on the health of the host, such as the synthesis of vitamins (vitamin K or B group vitamins), degradation and detoxification of toxic and mutagenic compounds, maintenance of intestinal epithelial integrity (production of short-chain fatty acids), adsorption of electrolytes and mineral salts (sodium, calcium, magnesium, potassium), as well as production of compounds with bactericidal activity (e.g., bacteriocins) [10,11]. However, in this unique environment, the adhesion process of potentially pathogenic microorganisms can also negatively influence the human body. It initiates the production of pro-inflammatory cytokines, which stimulate the development of an inflammatory, destructive cascade in the intestinal mucosa. Simultaneously, effective adherence of microbes increases the risk of their transition into the deeper layers of the mucosa and the production of systemic infections. In that respect, of particular interest are reports highlighting the involvement of intestinal bacteria in the development of some severe neurodegenerative conditions, such as Parkinson's and Alzheimer's disease [12,13]. Because of the double-edged nature of the adhesion process (involvement in cancer progression and infectious diseases or maintaining the physiology of the host), proper control of this process seems to be of high scientific relevance. So far, several adhesion-modulatory strategies have been described, including: (1) modification of the microbial surface [14], (2) blockage of adhesin biosynthesis [15], (3) interference with adhesin modification processes [16], or (4) the use of methods blocking interactions between adhesins and cell receptors, e.g., anti-adhesion antibodies [17]. It is worth highlighting that adhesive molecules also have a positive effect on the immune response. This has allowed the development of anti-adhesion strategies aimed at modulating disorders of the immune system, including asthma, psoriasis, Crohn's disease, multiple sclerosis, inflammatory bowel disease (IBD), and cancer [18–23].

In the last decade, it has become very popular in the scientific community to screen various substances for their ability to modulate the virulence of different pathogens, including interference with the production of adhesins. There are already the first indications that compounds from natural sources (e.g., lycopene) affect the adhesion process both in vitro and in vivo [24]. Therefore, it is advisable to find new substances that have a modulating effect on the adhesion process. A very promising group of compounds commonly found in nature are flavonoids. They exhibit a wide range of positive effects on human health. They modulate the activity of the immune system and present anti-cancer, anti-inflammatory, anti-atherosclerotic, and neuroprotective effects [25]. Previous studies performed by our team underscore the attractiveness of bioflavonoid derivatives. Indeed, we demonstrated the antimicrobial activity of *O*-alkyl derivatives of naringenin and their oximes against multidrug-resistant strains, e.g., *Staphylococcus aureus* MRSA (methicillin-resistant *S. aureus*), *Enterococcus faecalis* VRE (vancomycin-resistant *Enterococcus*), and clarithromycin-resistant
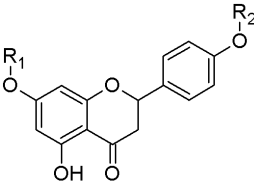
Helicobacter pylori [26]. In addition to this, our latest report showed the anticancer activity of these compounds against the human colorectal adenocarcinoma cell line (HT-29) [27].

Accordingly, the aim of the present study was to test the ability of *O*-alkyl derivatives of naringenin and their oximes to modulate the adhesion of selected microorganisms colonizing the gastrointestinal tract to cell lines derived from this organ.

2. Results

In our investigations, we determined the impact of *O*-alkyl derivatives of naringenin (**1a–10a**) and their oximes (**1b–10b**) on the adhesion of two representative strains of gut microbiota to HT-29 and 3T3-L1 cell lines. All compounds that were used in our research are presented in Table 1. The chemical data and methods of obtaining these derivatives were described by us in previous works [26,27].

Table 1. Structures of selected *O*-alkyl derivatives of naringenin (**1a–10a**) and their oximes (**1b–10b**).

Compound	R₁	R₂
1a-7-*O*-hexylnaringenin	hexyl	H
1b-7-*O*-hexylnaringenin oxime		
2a-7,4′-di-*O*-hexylnaringenin	hexyl	hexyl
2b-7,4′-di-*O*-hexylnaringenin oxime		
3a-7-*O*-heptylnaringenin	heptyl	H
3b-7-*O*-heptylnaringenin oxime		
4a-7,4′-di-*O*-heptylnaringenin	heptyl	heptyl
4b-7,4′-di-*O*-heptylnaringenin oxime		
5a-7-*O*-octylnaringenin	octyl	H
5b-7-*O*-octylnaringenin oxime		
6a-7,4′-di-*O*-octylnaringenin	octyl	octyl
6b-7,4′-di-*O*-octylnaringenin oxime		
7a-7-*O*-nonylnaringenin	nonyl	H
7b-7-*O*-nonylnaringenin oxime		
8a-7,4′-di-*O*-nonylnaringenin	nonyl	nonyl
8b-7,4′-di-*O*-nonylnaringenin oxime		
9a-7-*O*-undecylnaringenin	undecyl	H
9b-7-*O*-undecylnaringenin oxime		
10a-7,4′-di-*O*-undecylnaringenin	undecyl	undecyl
10b-7,4′-di-*O*-undecylnaringenin oxime		

Legend: H—hydrogen atom.

In the first stage of determining the activity of our newly synthesized compounds, we decided to check the effect of their different concentrations on the adhesive properties of two selected bacterial species: *E. coli*, a commensal representative of the intestinal microbiota, and *E. faecalis*, a bacterium that naturally colonizes the intestines but has disease-promoting potential. To better reflect the variety of real-life scenarios, we performed these studies using two different intestinal cell lines, i.e., the physiologically functioning ("healthy") 3T3-L1 cell line and the disease-mimicking, cancerous HT-29 line.

When *E. coli* was co-incubated with the 3T3-L1 line, we noticed a very interesting correlation between the structure/chain length of tested compounds and their ability to modulate a physical bacteria-cell line interaction (Figure 1). We—observed that short—chain **a** compounds very strongly promoted the adhesion of *E. coli* to the 3T3-L1 line (e.g., **1a** at 1–50 μg/mL increased attachment by 3 to 16 times). The longer the chain of these com-

pounds, the weaker the effect was, until the moment when bacterial adhesion was disturbed by substances **9a** ($\approx$1.1- to 2-fold for 10–100 µg/mL) and **10a** ($\approx$2-fold, regardless of the concentration used). Interestingly, we observed a completely opposite effect for **b** compounds. In this case, long-chain compounds promoted adhesion (**10b** was the strongest and induced this process 1.5- to 5.5-fold), while short-chain ones significantly reduced this phenomenon (e.g., **1b** at 1 µg/mL decreased attachment to 63%, while at a concentration of 25 µg/mL adherence was practically not observed). For all the tested compounds promoting adhesion, both from the **a** and **b** groups, we noticed attachment-inducing activity only when using low-level concentrations.

For *E. coli* co-incubated with the HT-29 line, the obtained results were much more homogeneous—all the tested substances reduced the bacterial adhesion to eukaryotic cells (Figure 1). In this case, the exceptions were substances **1a**, **3b**, **4b**, **5b**, **6b**, and **10b** at 50 µg/mL as well as **4b** and **5b** at 25 µg/mL. The most interesting results in this regard were obtained for compound **4b**, because at concentrations within the range of 1–10µg/mL or 75–100 µg/mL the level of adherence was very low (often only a few percent), while at concentrations equal to 25 µg/mL and 50 µg/mL adhesion was 17- and 5-fold higher than in the control.

The results described in the above paragraphs suggest that the effect of tested compounds on *E. coli* is: (a) dependent on the tested cell line and often has a positive effect on adhesion to the physiological 3T3-L1 line; (b) in general terms, in both tested cell lines, the positive effect of low concentrations and the negative effect of high concentrations on the adherence of *E. coli* were noticed, while co-incubation studies of this bacterium with the HT-29 line indicate also that precisely selected, high concentrations of some compounds can strongly induce bacterial adhesion to the cell line.

In an alternative research scenario, taking into account the co-incubation of *E. faecalis* with eukaryotic cells and the presence of various concentrations of tested compounds, the effect of the cell line was not as significant as in the case of *E. coli*. When we used the 3T3-L1 line, we again noticed the relationship between the length of the side chain of compounds and their impact on bacterial adhesion (Figure 1). This effect was, however, visible exclusively when increasing the side chain only from the C-7 position of naringenin (**1a**/**1b** vs. **3a**/**3b** vs. **5a**/**5b** vs. **7a**/**7b** vs. **9a**/**9b**), but not from both C-7 and C-4′ sites of naringenin simultaneously (**2a**/**2b** vs. **4a**/**4b** vs. **6a**/**6b** vs. **8a**/**8b** vs. **10a**/**10b**). For both tested groups of compounds (annotated as **a** and **b**), we observed that the extension of the side chain has a negative effect on the pro-adhesive activity of these substances. For example, the compounds **1a** and **3a** as well as **1b** and **3b** had a much more beneficial effect on the adhesion of *E. faecalis* (at 1–10 µg/mL they increased this process 1.5- to 3-fold) than **7a** and **9a** as well as **7b** and **9b**, which often actually limited the attachment.

When using the HT-29 line, co-incubation with *E. faecalis* showed a similar relationship between the structure of the tested compounds and their effect on adhesion as presented previously (Figure 1). We noticed that substances with the attachment of the eight- or nine-carbon chain(s) in the C-7 and C-4′ positions of naringenin (**6a**–**8a** and **6b**–**8b**) promoted the adhesion of bacteria to eukaryotic cells (depending on the concentration used, up to two times), while both compounds with shorter or longer side chains reduced this process.

In general, the results described above indicate that the effect of tested substances on *E. faecalis* is: (a) dependent on the tested cell line, although this effect is much less significant than in the case of *E. coli*; (b) influenced by the compounds' structure; (c) in simple terms, a positive effect of low concentrations and a negative effect of high concentrations were observed; similarly to *E. coli*, when co-incubating *E. faecalis* with the HT-29 line, some precisely selected, high concentrations of the tested compounds can strongly increase the adhesion of this bacterium to the cell line.
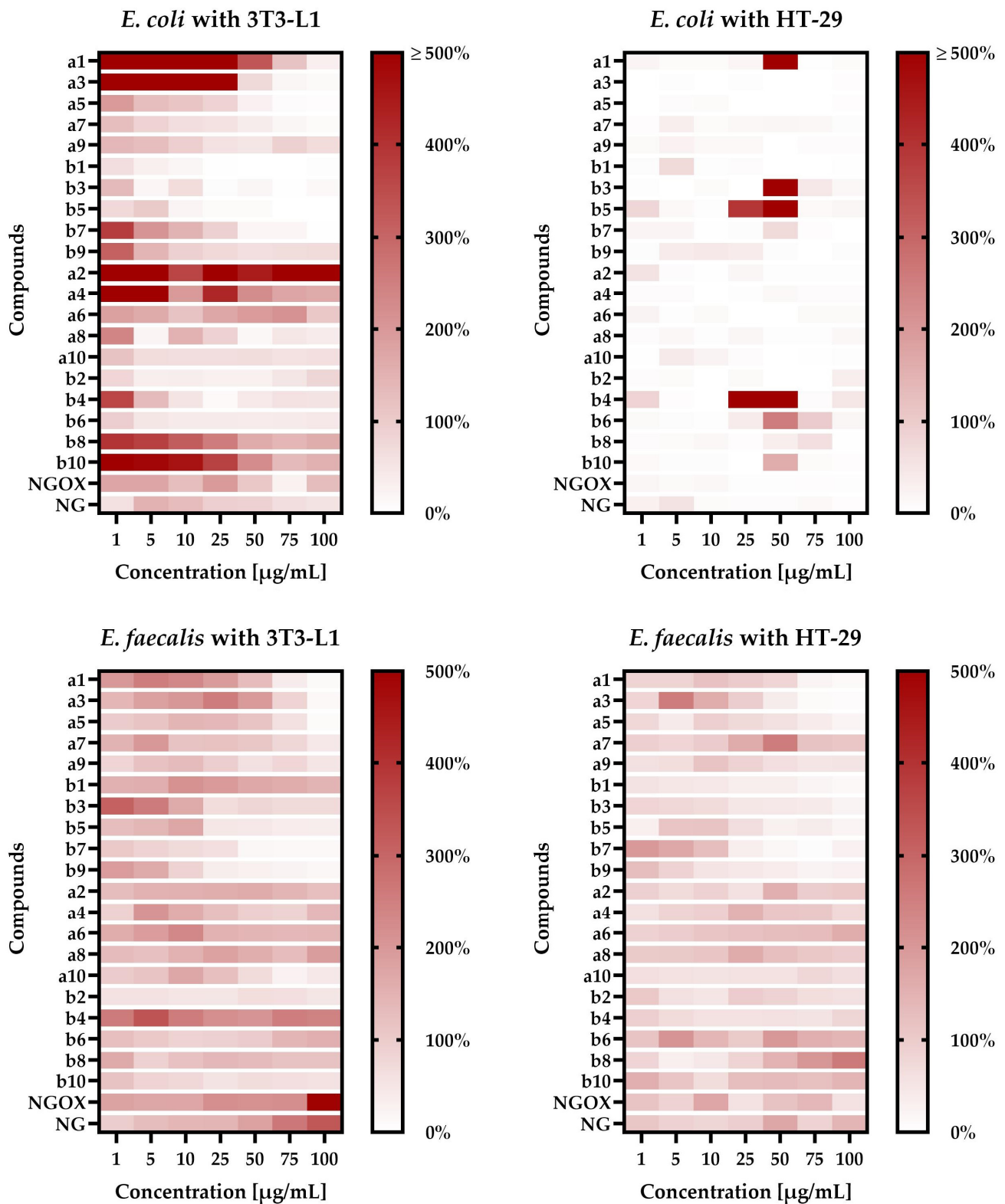
Figure 1. The results presenting the influence of the tested *O*-alkyl derivatives of naringenin (**1a–10a**) and their oximes (**1b–10b**) on the adhesion of *E. coli* and *E. faecalis* to the surface of the 3T3-L1 and HT-29 cell lines in static conditions. The data are presented in the form of heat maps. The study was performed with triplicate biological replications with three technical repetitions (*n* = 9); **NG**—naringenin; **NGOX**—naringenin oxime.

In the next step, we decided to determine whether the tested naringenin derivatives negatively affect the viability of the examined intestinal cell lines. The cytotoxic effect of *O*-alkyl naringenin derivatives (**1a–10a**) and their oximes (**1b–10b**) against the human colon cancer line (HT-29) and "healthy" murine fibroblasts (3T3-L1) is reported as survival index (SI) IC_{50} [μg/mL], being a concentration able to induce 50% inhibition of cell proliferation. The obtained data are presented in Table 2 and were compared with the values determined for the reference substances—naringenin (**NG**) and naringenin oxime (**NGOX**).

Table 2. Antiproliferative activity of *O*-alkyl derivatives of naringenin (**1a–10a**) and their oximes (**1b–10b**) against the HT-29 and 3T3-L1 cell lines, after 2 h incubation, tested with the SRB assay.

Compound	HT-29	3T3-L1	Compound	HT-29	3T3-L1
	IC_{50} [μg/mL]	IC_{50} [μg/mL]		IC_{50} [μg/mL]	IC_{50} [μg/mL]
1a	25.39	25.81	**1b**	38.44	34.99
2a	>100	>100	**2b**	>100	>100
3a	28.70	25.55	**3b**	29.15	32.12
4a	>100	>100	**4b**	43.35	>100
5a	38.35	20.09	**5b**	49.78	49.93
6a	>100	>100	**6b**	>100	>100
7a	46.72	22.23	**7b**	57.81	41.56
8a	>100	>100	**8b**	>100	>100
9a	>100	80.56	**9b**	>100	>100
10a	>100	>100	**10b**	48.23	>100
NG	>100	>100	**NGOX**	>100	>100

Naringenin and its oxime showed no proliferative effects against both cell lines, 3T3-L1 and HT-29, over the concentration range tested. The IC_{50} value for these two model compounds was >100 μg/mL.

Among the tested naringenin derivatives lacking an oxime group, cytotoxic activity against the 3T3-L1 line was demonstrated for monosubstituted *O*-alkyl derivatives of naringenin, e.g., **1a**, **3a**, **5a**, **7a**, and **9a**. The same compounds, with the exception of **9a**, also showed antiproliferative activity against the HT-29 line. It is interesting to note that the cytotoxic effect was observed only for compounds having one carbon chain attached at the C-7 position of the naringenin ring. Furthermore, a correlation between the number of carbon atoms and the level of cytotoxic activity was observed. Indeed, the shorter the attached carbon chain, the greater the effect of the compound on the proliferation of the adenocarcinoma cells examined. In fact, the IC_{50} value for compound **1a**, which contains a hexyl group attached to the C-7 position of naringenin, was 25.39 μg/mL, which was 1.8 times lower than compound **7a** (IC_{50} = 46.72 μg/mL), which possesses a nonyl moiety.

In contrast, against the 3T3-L1 line, compounds having chains with 6 to 9 carbon atoms showed an effect on proliferation at a level 3–4 times higher than compounds with longer chains (e.g., **9a** having 10 carbon atoms). Naringenin derivatives with two alkyl chains attached (the second at the C-4' position) with different numbers of carbon atoms (compounds **2a**, **4a**, **6a**, **8a**, and **10a**) showed no effect on the proliferation of the tested cell lines in the tested concentration range.

In the case of naringenin derivatives bearing an additional oxime group (compounds **1b–10b**), an effect on 3T3-L1 cell proliferation was also noted only for monosubstituted compounds, e.g., **1b**, **3b**, **5b**, and **7b**. For them, IC_{50} values were in the range of 32.12 µg/mL to 49.93 µg/mL. A similar relationship was observed for the human adenocarcinoma cell line because the same compounds (**1b**, **3b**, **5b**, and **7b**) showed cytotoxic effects against this cell line. The IC_{50} value depended on the length of the attached chain and was higher for the oxime derivatives with a longer alkyl chain attached to the naringenin ring. On the other hand, both **4b** and **10b**, oximes of *O*-alkyl naringenin derivatives with attached alkyl chains at the C-7 and C-4' positions, affected cell differentiation of the HT-29 line with comparable IC_{50} values of 43.35 and 48.23 µg/mL, respectively. In contrast, the other di-substituted compounds, e.g., **2b**, **6b**, and **8b**, showed no harmful effects against human colon cancer cells in the concentration range tested ($IC_{50} > 100$ µg/mL).

Based on the results of the experiments presented above (adhesion in static conditions and cytotoxicity against cell lines) as well as our detailed review of the literature indicating the highest biological activity of flavonoids with a C8–C10 side chain [28–33], at the final proof-of-concept stage of this research, compound **8b** at 50 µg/mL was administered. In this context, our priority was the ability of **8b** to strongly enhance the adhesion of *E. coli* to the physiological 3T3-L1 cell line without causing any cytotoxic effects. The choice of concentration was, in turn, related to our willingness to obtain a noticeable biological effect of this substance in an experimental model with high dynamics of physicochemical conditions—microfluidic studies.

Applying microfluidic conditions, we observed that the use of **8b** at 50 µg/mL had a very strong, pro-adhesive effect on *E. coli* with respect to both cell lines tested. Here, for the physiological 3T3-L1 cell line, the ratio of the area of bacterial biomass (BB) adhered to the surface of the eukaryotic cells (EC) [the BB/EC ratio] was 0.6 ± 0.12 vs. 0.37 ± 0.13 for compound-exposed and control samples, respectively (Figure 2). For the tumor-altered HT-29 cell line, the BB/EC ratio was 1.03 ± 0.06 vs. 0.65 ± 0.07 for substance-exposed and control samples, respectively (Figure 2). Interestingly, under identical environmental conditions, we did not detect such an effect for *E. faecalis*. In that case, for both cell lines, the effect was neutral (the BB/EC ratio for treated and control samples was: 0.28 ± 0.15 vs. 0.29 ± 0.11 for 3T3-L1 and 1.36 ± 0.08 vs. 1.55 ± 0.15 for the HT-29 cell line) (Figure 2). Representative photographs showing the adhesion of both tested bacteria to the surface of the physiological cell line, 3T3-L1, with and without exposure to **8b**, are shown in Figure 3. The results obtained by us in the current set of microfluidic experiments indicate a high selectivity in the pro-adhesive effect of the chosen substance. As demonstrated in the example above, this activity can promote the adherence of commensal microorganisms with a beneficial effect on the host's gut (e.g., physiological strains of *E. coli*) without a negative, dysbiotic effect on other representatives of the microbiota (including opportunistic bacteria, e.g., *E. faecalis*).

E. coli with 3T3-L1

E. coli with HT-29

E. faecalis with 3T3-L1

E. faecalis with HT-29
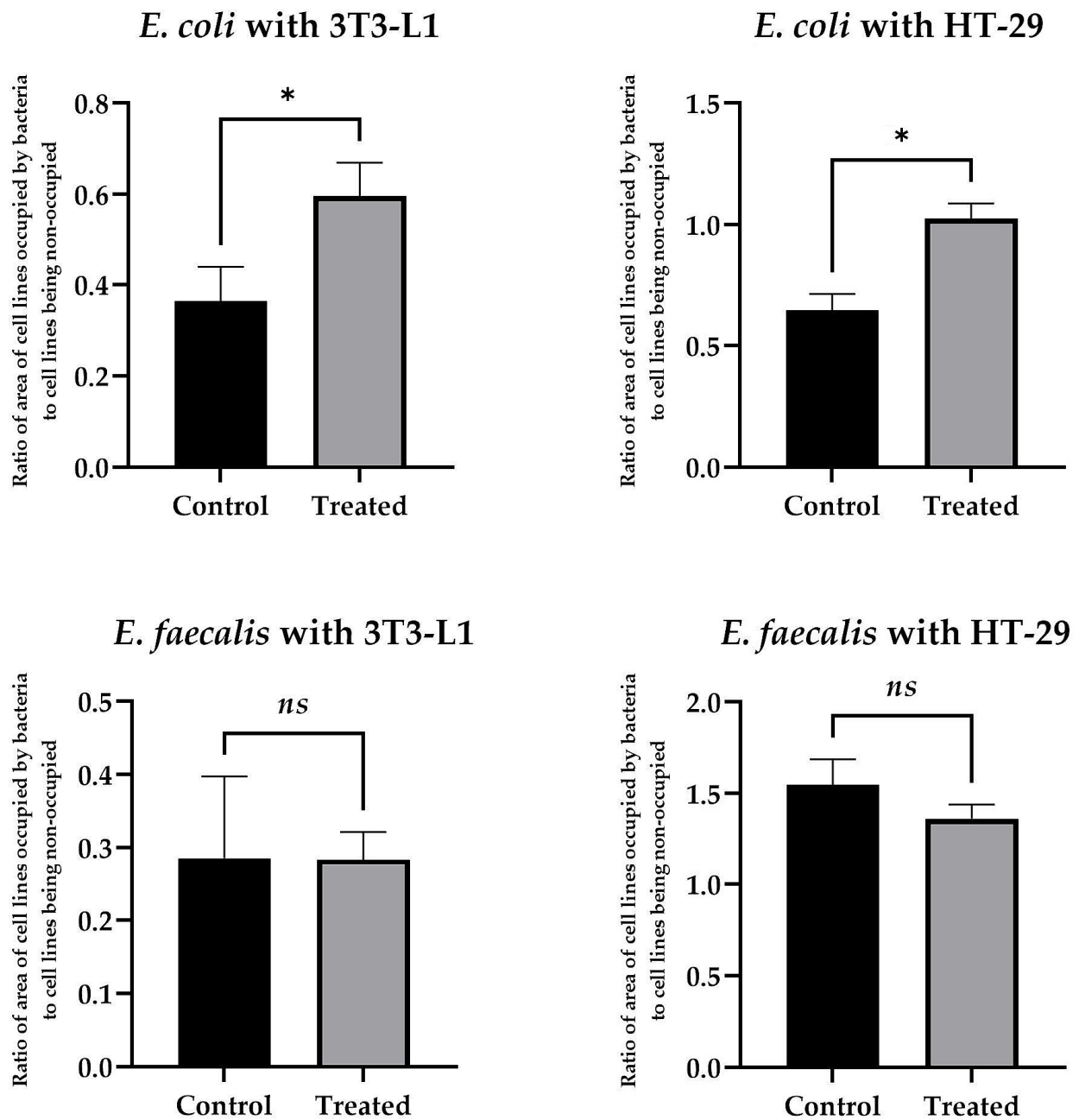
Figure 2. The results presenting the influence of **8b** at 50 μg/mL on the adhesion of *E. coli* and *E. faecalis* to the surface of the 3T3-L1 and HT-29 cell lines in the microfluidic conditions generated by the Bioflux system. The study was performed with triplicate biological replications with three technical repetitions (*n* = 9). The *p*-value represented by *ns* was statistically insignificant, while a *p*-value of <0.05 was considered statistically significant and presented as "*".
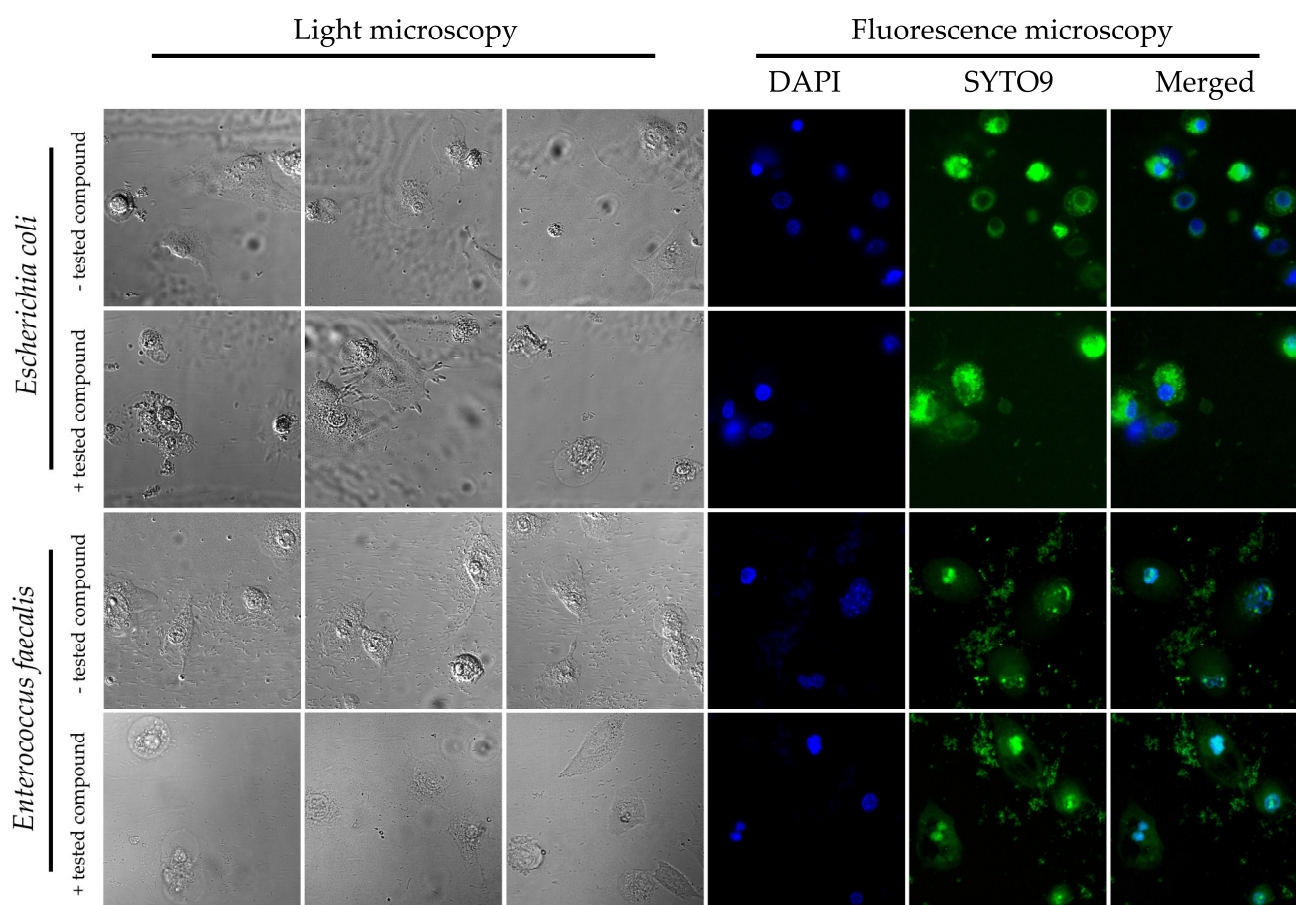
Figure 3. Representative photographs of light and fluorescence microscopy showing the adhesion of *E. coli* and *E. faecalis* to the surface of the physiological cell line, 3T3-L1, with and without exposure to **8b** (50 μg/mL), in the microfluidic conditions generated by the Bioflux system. DAPI stains the nucleus of the 3T3-L1 cell line, while SYTO9 stains bacterial cells (*E. coli* and *E. faecalis*).

3. Discussion

Naringenin is an organic flavonoid compound that is widely distributed in nature. The largest source of naringenin is citrus fruits (grapefruit, orange, and tangerine), although it is also present in smaller amounts in grapes, cherries, fenugreek, and Greek oregano, as well as in coffee, tea, and red wine. The literature review confirms the broad-spectrum, health-promoting effect of this flavonoid on the human body. It has been shown that such activity is closely related to the affinity of naringenin for scavenging reactive oxygen species and increasing the antioxidant defense of the host. This strictly translates into its anti-inflammatory effect and determines its anti-atherosclerotic and neuroprotective features. Additionally, it has been documented that naringenin also has anti-microbial and anti-cancer activity [25,28].

The cell membrane is one of the main target sites of flavonoids against microorganisms [34]. As observed in mechanistic studies on flavonoids, these compounds localize themselves within the hydrophobic fractions of the lipid membrane bilayer and lead to change in its fluidity and stiffness [35,36]. For this reason, the chemical structure of flavonoids and their ability to modulate membrane fluidity are important parameters affecting their biological activity [36]. For naringin and naringenin, two flavonoids relevant to the current study, the capacity to preferentially localize in the polar lipid membrane bilayer and exert an ordering effect on the hydrophobic region of this compartment has been demonstrated [37,38]. Such activity of flavonoids, including naringenin, contributes to the loss of the fluidity of cell membranes [35]. It is worth mentioning, however, that this membrane-solidifying effect of naringenin is revealed only at higher concentrations

of ≥2.5 µg/mL [39]. Quite obviously, such changes in cell membrane fluidity affect the physiological properties of microorganisms [40]. In the study of Cazzola et al. [41], a close correlation was observed between the increase in *E. coli* adhesion to eukaryotic cells and the decrease in cell membrane fluidity of these bacteria. In another study carried out on four selected bacterial species, it was shown that, together with the entry into the biofilm (sedentary) phase, microorganisms accumulate saturated fatty acids in their cell membranes, leading to a decrease in their membranes' fluidity [42]. Identical observations were made in another article [43], where, using *Pseudomonas aeruginosa* as a model organism, the participation of extracellular vesicles in membrane stiffening and promotion of biofilm formation was additionally noticed. The above-described observations seem to perfectly complement our team's observations made in this paper, as we noticed that exposure of bacteria to naringenin and the panel of its derivatives is accompanied by modifications in the ability of the tested bacteria to adhere to host cells. Undoubtedly, this effect was dependent on many factors, including both the chemical structure of the compound and its concentration, as well as the type of bacteria or intestinal cell line used. Nevertheless, under conditions of dynamic medium flow, we noticed the ability of the selected naringenin derivative **8b** to promote the adhesion of *E. coli* to both cell lines while having no impact on *E. faecalis*. Based on our knowledge of the cell structure of both species of bacteria (Gram-negative *E. coli* and Gram-positive *E. faecalis*), we suspect that the physical proximity between the cell membrane of *E. coli* and the culture medium with the tested compound had a direct impact on the results obtained. Gram-positive bacteria have no outer membrane, and the only one that exists is physically separated from the external environment by a densely cross-linked layer of peptidoglycan [44,45]. The physiology of Gram-negative bacteria is more closely related to the presence of cell membranes as they produce two of them (inner and outer membranes) [46,47], and therefore we postulate that the action of naringenin derivatives may have a greater impact on changes in *E. coli* membrane fluidity and its adhesive properties.

When assessing the influence of naringenin derivatives on the adhesive properties of bacteria, one cannot ignore the role of their chemical structure in modulating the physiology of microorganisms. In this context, consideration of our results obtained for the panel of chemical modifiers of naringenin (alkoxy derivatives and their oximes) seems very helpful. In general terms, we noticed that the appearance of the oxime residue affects the activity of the tested compounds, but this effect was variable and largely dependent on chemical modifications within the structure of naringenin, especially on the length of the alkyl chain attached. In our opinion, much more interesting observations were obtained with respect to the correlation between the presence of aliphatic chains in the C-7 and C-4′ positions and the pro-adhesive properties of these substances. Here, we noticed that the highest biological activity was most often found for naringenin derivatives with 8- to 10-carbon side chains. Both shorter- and longer-chain compounds had reduced activity. When considering the causes of this phenomenon, it is worth focusing on the physicochemical implications of the above chemical modifications. Lipophilicity is one of the key parameters determining the activity of flavonoids [34,48]. Therefore, hydrophobic substituents (including alkyl chains) usually increase the biological activity of substances [48]. The elongation of the side chain increases the hydrophobicity of the compound and, consequently, leads to a stronger affinity for biological membranes [34,48]. However, it is suggested that excessive elongation of compounds' side chains is related to the decline of their optimal solubility, eventually leading to a drastic decrease in their biological activity (the so-called "cut-off effect") [29,34]. These observations are in great agreement with the results obtained by other research teams, suggesting that the presence of medium-chain substituents has the most beneficial effect on the increase in the flavonoids' activity [29–33]. To sum up, in the current article, we proved that the chemical modification of naringenin and attachment of medium-length side chains have a positive effect on their pro-adhesive properties towards bacteria.

The gastrointestinal tract is the most heterogeneous and microbiologically dense organ of the human body. A long residence time in the intestines is a characteristic pharmacoki-

netic feature of flavonoids. For this obvious reason, it has been proven that during this prolonged period, they interact with a variety of representatives of the microbiota [49]. This type of interaction translates into two important aspects. Firstly, microorganisms are involved in the transformation of naringin (inactive form) into a host-beneficial naringenin (active form) [50]. Thus, the gastrointestinal microbiota plays a critical role in the bioavailability of this bioflavonoid in the human body. On the other hand, the presence of flavonoids, including naringenin, is not indifferent to the microbiota residing in the intestines. Many flavonoids (e.g., naringin, naringenin, hesperetin-7-*O*-glucoside, prunin, isoquercitrin, hesperidin, rutin, and quercetin) have been shown to interact with the vast majority of microorganisms belonging to the intestinal microbiota. In this way, flavonoids present a modulatory effect on both the structure and qualitative composition of the gastrointestinal microbiota [51]. The interaction of naringenin with representatives of the natural intestinal flora and their metabolites has been shown to improve animal health, e.g., in polycystic ovary syndrome (PCOS) [52] and non-alcoholic fatty liver disease (NAFLD) [53]. Next-generation sequencing showed that administration of naringenin increases the abundance of a plethora of health-promoting bacterial species that are part of the gastrointestinal microbiome, including *Lactobacillus* spp., *Faecalibacterium* spp., *Butyricicoccus* spp., *Coprococcus* spp., and *Roseburia* spp. [54]. It is also worth emphasizing that the "metagenome", a whole pool of genes of the microbiome, encodes information about the metabolism of different classes of carbohydrates, amino acids, or xenobiotics, sometimes being the only source for their degradation and absorption in a human organism [55,56]. Therefore, it is significant that naringenin, by enriching the microbiome of the gastrointestinal tract with species of "beneficial" bacteria, promotes homeostasis of the host not only by regulating inflammatory reactions but also by increasing its digestive abilities. In addition, through this unique function, it prevents intestinal dysbiosis and thus protects against the development of inflammatory bowel disease (IBD) (Crohn's disease, ulcerative colitis, and indeterminate colitis), irritable bowel syndrome (IBS), and celiac disease.

4. Materials and Methods
4.1. Naringenin Derivatives

Naringenin used for the synthesis of ether derivatives (**1a–10a**) and their oximes (**1b–10b**) was purchased from Sigma-Aldrich Co. (St. Louis, MO, USA). The *O*-alkyl derivatives of naringenin and oximes were synthesized according to methods described by us in previous works [26,27]. Briefly, to obtain ether derivatives **1a–10a**, to naringenin dissolved in organic solvent (anhydrous acetone or DMF; Chempur, Piekary Śląskie; Poland), potassium carbonate and appropriate alkyl iodide in a molar ratio of 1:1.5:5 were added, respectively. The reaction mixture was kept on a magnetic stirrer at room temperature (when the reaction was performed in DMF) or at 45 °C (when the reaction was performed in anhydrous acetone). The progress of the reaction was monitored by thin-layer chromatography (TLC), and after observing two products (mono- and di-*O*-alkyl derivatives), the crude mixture was extracted with an organic solvent (ethyl acetate or diethyl ether). The organic fractions were collected and concentrated on a vacuum evaporator, and the products were separated by liquid column chromatography.

In the next step, compounds **1a–10a** were modified into their oximes **1b–10b**. Briefly, the *O*-alkyl derivative was dissolved in anhydrous ethanol, and then hydroxylamine hydrochloride and anhydrous sodium acetate in a molar ratio of 1:3:3 were added, respectively. After complete conversion of substrate, the reaction mixture was poured into ice water, and precipitated white products were collected and purified by liquid column chromatography. Using the same method, naringenin oxime (**NGOX**) was obtained.

4.2. Prokaryotic Cells

The study used two reference strains, *Escherichia coli* K12 (ATCC 10798) and *Enterococcus faecalis* (ATCC 29212), obtained from the American Type Culture Collection. Both strains were stored in trypticase soy broth (TSB; OXOID, Basingstoke, UK) with the addition of

30% glycerol at −70 °C in the museum resources of the Department of Microbiology at the Wroclaw Medical University.

Strains were reactivated from deep freeze by inoculation into TSB and an overnight incubation under shaking conditions (MaxQTM6000 incubator shaker, Thermo Scientific, Waltham, MA, USA) at 125 rpm and 37 °C. The purity of the strains was assessed using enriched media: MacConkey (MC, OXOID, Basingstoke, UK) for *E. coli* and Columbia Agar (CA, Becton, Dickinson and Company, San Diego, CA, USA) for *E. faecalis*. A fresh 18–20 h culture was prepared for each experiment on tryptic soy agar (TSA, OXOID, Basingstoke, UK).

For studies determining the interaction of bacteria with eukaryotic cells, suspensions of the tested strains were prepared in Luria broth (LB, Becton, Dickinson and Company, USA) medium with a bacterial density of 6×10^8 CFU/mL.

4.3. Cell Culture Procedure

The human adenocarcinoma cell line, HT-29 (ATCC HTB-38), was cultured in αMEM medium (IITD PAN) supplemented with 10% fetal bovine serum, FBS (Sigma-Aldrich, Taufkirchen, Germany), 100 U/mL penicillin, 100 μg/mL streptomycin antibiotic solution (Sigma-Aldrich, Taufkirchen, Germany), and 2 mM glutamine solution (Sigma-Aldrich, Taufkirchen, Germany). Cells from less than 20 passages were used for the study. In turn, preadipocytes from mouse embryos with the morphology of fibroblast cells, line 3T3-L1 (ATCC CL-173), were cultured in DMEM high-glucose medium (Life Technologies Corporation, Carlsbad, CA, USA) with the same supplements as above. Cells from less than 14 passages were used for the study. Both tested cell lines were grown at 37 °C in 5% CO_2.

4.4. SRB Assay

The effect of *O*-alkyl derivatives of naringenin and their oximes on eukaryotic cells was checked using a slightly modified SRB test described earlier [57]. Firstly, HT-29 (1×10^5 cells/mL) and 3T3-L1 (5×10^4 cells/mL) cell lines were incubated in adherent microtiter plates under the conditions described above. The cells were then treated for 2 h with the tested compounds **1a–10a** and **1b–10b** at concentrations of 1, 5, 10, 25, 50, 75, and 100 μg/mL each. After this time, the medium was removed and replaced with one containing 50% (wt/vol) trichloroacetic acid (TCA; Sigma-Aldrich, Taufkirchen, Germany). Following 1 h of incubation at 4 °C, the plate was rinsed with water, and then an acidic solution of 0.4% sulforhodamine B (SRB) (Sigma-Aldrich, Taufkirchen, Germany), was added to the dried wells and incubated in the dark for half an hour. At the end of this time, the SRB solution was replaced by 1% (vol/vol) acetic acid, and the stained protein precipitate was dissolved in 10 mM Tris base solution (pH 10.5). Absorbance was measured at 560 nm in a plate reader (GloMax Discover Microplate Reader, Promega).

The cytotoxic effect of *O*-alkyl derivatives of naringenin and their oximes on eukaryotic cells was expressed as the concentration of the tested compounds at which 50% growth inhibition of the tested cell lines was observed. Values were presented in the form of the survival index (SI)–IC$_{50}$. All determinations were repeated in three independent experiments, each performed in three technical replicates. Moreover, the effect of DMSO (Sigma-Aldrich, Taufkirchen, Germany), the solvent present in all the initial solutions of the tested compounds, on the growth of the cell lines used in the study was also verified.

4.5. Adhesion Assay

The adhesion ability of the tested bacterial strains to HT-29 and 3T3-L1 cell lines was determined by an in vitro adhesion assay as described previously [58]. Eukaryotic cells were infected with prokaryotic cells in the presence of the examined compounds in pre-selected concentrations at an MOI (multiplicity of infection) ratio of 50. Cells were exposed to the tested strains and compounds for 2 h. After this time, unbound bacteria were removed by washing with PBS (Life Technologies Corporation, Carlsbad, CA, USA). The

lysates acquired by cell lysis (0.5% Triton X-100 in LB): 90 min, 37 °C, 5% CO_2 atmosphere, were then seeded onto TSA and MC media for *E. faecalis* and *E. coli*, respectively. The assays were performed in at least three independent experiments (cells from subsequent passages), each in triplicate. A control without tested compounds was set for each strain.

4.6. Bioflux

Determination of the impact of a dynamic medium flow on the adhesive capacity of bacteria was performed using the Bioflux 1000Z (Fluxion, San Francisco, CA, USA) with a coupled microscope environmental chamber (Pecton Incubator XL S1, Carl Zeiss, Jena, Germany), enabling the maintenance of 37 °C and microaerophilic conditions. At the very beginning, all channels of dedicated microfluidic plates (Fluxion, San Francisco, CA, USA) were flushed with 100 μL of αMEM or DMEM high-glucose medium with supplements (further named "cell line medium"; for details of the supplementation see "Cell culture procedure") applying an intensive flow of 10 dyne/cm^2 for 10 s. After unblocking the lumen of the channels, the inlet and outlet wells were emptied, and 20 μL of 100 μg/mL fibronectin solution (Sigma-Aldrich, Taufkirchen, Germany) was added to each inlet channel. The medium was turned in the outlet direction at a flow rate of 1 dyne/cm^2 for 1 min. After this step, the plate was left for a 1 h incubation period to allow fibronectin to be absorbed on the surface of the microcapillaries. After the incubation period, the microcapillaries were rinsed again with 100 μL of the cell line medium at 10 dyne/cm^2 for 10 s to remove excess non-attached fibronectin. The outlet wells were emptied and then refilled with 100 μL of the cell line medium containing 3T3-L1 or HT-29 cells (10^8 cells/mL). An outlet-to-inlet medium flow of 5 dyne/cm^2 was turned on for 5 s, then the flow was stopped, and the cells were incubated for 0.5 h to allow them to effectively adhere to the surface of the microcapillaries. After this time, 1 mL of the cell line medium was added to the inlet wells, and the inlet-to-outlet flow was adjusted to 0.5 dyne/cm^2 for 24 h, thus allowing the growth of the cell line monolayer. After one day of incubation, the inlet and outlet wells were emptied, and then 1 mL of the cell line medium [without antibiotics] containing one of the tested bacterial strains (*E. coli* or *E. faecalis*; 10^8 CFU/mL) and a selected flavonoid, **8b** (50 μg/mL), was added to the inlet wells. In the control sample, the above compound was not added (the cell line medium [without antibiotics] together with bacteria). In regard to this, in both tested and control samples, the cell line-to-bacteria ratio was maintained at MOI = 50. After this, the medium was set to flow from inlets to outlets at 0.5 dyne/cm^2 for 4 h. In the next step, the inlet wells were emptied, and 100 μL of saline solution containing a mix of two fluorescent dyes, SYTO9 (L10316, ThermoFisher, Waltham, MA, USA) to visualize bacterial biomass and DAPI (62248, ThermoFisher, Waltham, MA, USA), to detect eukaryotic cells, was added to each well. The inlet-to-outlet flow was turned on at 0.5 dyne/cm^2 for 10 min, followed by a 0.5 h incubation to induce the absorption of the dyes by cells. After completing this stage, photographs of the microcapillaries containing the tested biological materials were taken using an inverted fluorescence microscope (GabH, Jena, Germany) and the Bioflux Montage software (Fluxion, San Francisco, CA, USA). When determining the area occupied by bacterial cells adhered to the surface of eukaryotic cells, the entire bacterial biomass attached was taken into account (vertically and horizontally). These calculations did not include bacterial cells adhering only to the surface of the microcapillaries. The tests were performed in three biological repetitions with three technical replications (constituting images from different fragments of the examined microcapillaries).

4.7. Statistical Analysis

Statistical analysis was performed using GraphPad Prism version 9 (GraphPad Co., San Diego, CA, USA). The normality of the distribution was checked by the Shapiro–Wilk test. As all values were normally distributed, Student's *t*-test was further used. The results of statistical analyses were considered significant for values with $p < 0.05$.

5. Conclusions

The present study showed that the synthesized naringenin derivatives modulate the adhesion of selected intestinal microbiota to the tested cell lines. It was noticed that this activity was affected by the concentration of the tested naringenin derivatives and their structure (length of the carbon chain). To better reflect the variety of real-life scenarios, the current research on *O*-alkyl derivatives of naringenin was focused not only on different intestinal cell lines (physiological and cancerous) but also on both static and microfluidic conditions. Therefore, the promising results obtained here provide a basis for in vivo animal studies to clarify the effect of these bioflavonoids on the gut environment. This may provide valuable information on the bioavailability and effect of these compounds on the whole intestinal microbiome.

References

1. McEver, R.P.; Luscinskas, F.W. *Cell Adhesion*, 7th ed.; Elsevier Inc.: Amsterdam, The Netherlands, 2017; ISBN 9780323357623.
2. Quintero-Villegas, M.I.; Aam, B.B.; Rupnow, J.; Sørlie, M.; Eijsink, V.G.H.; Hutkins, R.W. Adherence Inhibition of Enteropathogenic *Escherichia coli* by Chitooligosaccharides with Specific Degrees of Acetylation and Polymerization. *J. Agric. Food Chem.* **2013**, *61*, 2748–2754. [CrossRef] [PubMed]
3. Houreld, N.N.; Ayuk, S.M.; Abrahamse, H. Cell Adhesion Molecules Are Mediated by Photobiomodulation at 660 Nm in Diabetic Wounded Fibroblast Cells. *Cells* **2018**, *7*, 30. [CrossRef] [PubMed]
4. Koivisto, L.; Heino, J.; Häkkinen, L.; Larjava, H. Integrins in Wound Healing. *Adv. Wound Care* **2014**, *3*, 762–783. [CrossRef]
5. Ch, G.; Charalabopoulos, A.; Peschos, D.; Maritsi, D.; Charalabopoulos, K.; Batistatou, A. Adhesion Molecules in Invasion and Metastasis. *Clin. Exp. Metastasis* **2005**, *10*, 35–44. [CrossRef]
6. Okegawa, T.; Pong, R.-C.; Li, Y.; Hsieh, J.-T. The Role of Cell Adhesion Molecule in Cancer Progression and Its Application in Cancer Therapy. *Acta Biochim. Pol.* **2004**, *51*, 445–457. [CrossRef]
7. Lauko, A.; Mu, Z.; Gutmann, D.H.; Naik, U.P.; Lathia, J.D. Junctional Adhesion Molecules in Cancer: A Paradigm for the Diverse Functions of Cell-Cell Interactions in Tumor Progression. *Cancer Res.* **2020**, *80*, 4878–4885. [CrossRef] [PubMed]
8. Koebnik, R.; Locher, K.P.; Van Gelder, P. Structure and Function of Bacterial Outer Membrane Proteins: Barrels in a Nutshell. *Mol. Microbiol.* **2000**, *37*, 239–253. [CrossRef] [PubMed]
9. Kho, Z.Y.; Lal, S.K. The Human Gut Microbiome—A Potential Controller of Wellness and Disease. *Front. Microbiol.* **2018**, *9*, 1835. [CrossRef]
10. Valdes, A.M.; Walter, J.; Segal, E.; Spector, T.D. Role of the Gut Microbiota in Nutrition and Health. *BMJ* **2018**, *361*, 36–44. [CrossRef]
11. Jandhyala, S.M.; Talukdar, R.; Subramanyam, C.; Vuyyuru, H.; Sasikala, M.; Reddy, D.N. Role of the Normal Gut Microbiota. *World J. Gastroenterol.* **2015**, *21*, 8836–8847. [CrossRef]

12. Varesi, A.; Pierella, E.; Romeo, M.; Piccini, G.B.; Alfano, C.; Bjørklund, G.; Oppong, A.; Ricevuti, G.; Esposito, C.; Chirumbolo, S.; et al. The Potential Role of Gut Microbiota in Alzheimer's Disease: From Diagnosis to Treatment. *Nutrients* **2022**, *14*, 668. [CrossRef] [PubMed]

13. Romano, S.; Savva, G.M.; Bedarf, J.R.; Charles, I.G.; Hildebrand, F.; Narbad, A. Meta-Analysis of the Parkinson's Disease Gut Microbiome Suggests Alterations Linked to Intestinal Inflammation. *NPJ Park. Dis.* **2021**, *7*, 27. [CrossRef] [PubMed]

14. Chen, L.; Wen, Y.M. The Role of Bacterial Biofilm in Persistent Infections and Control Strategies. *Int. J. Oral Sci.* **2011**, *3*, 66–73. [CrossRef] [PubMed]

15. Ofek, I.; Hasty, D.L.; Sharon, N. Anti-Adhesion Therapy of Bacterial Diseases: Prospects and Problems. *FEMS Immunol. Med. Microbiol.* **2003**, *38*, 181–191. [CrossRef] [PubMed]

16. Svensson, M.; Platt, F.M.; Svanborg, C. Glycolipid Receptor Depletion as an Approach to Specific Antimicrobial Therapy. *FEMS Microbiol. Lett.* **2006**, *258*, 1–8. [CrossRef]

17. Okuda, K.; Hanada, N.; Usui, Y.; Takeuchi, H.; Koba, H.; Nakao, R.; Watanabe, H.; Senpuku, H. Inhibition of *Streptococcus mutans* Adherence and Biofilm Formation Using Analogues of the SspB Peptide. *Arch. Oral Biol.* **2010**, *55*, 754–762. [CrossRef]

18. Woodside, D.G.; Vanderslice, P. Cell Adhesion Antagonists: Therapeutic Potential in Asthma and Chronic Obstructive Pulmonary Disease. *BioDrugs* **2008**, *22*, 85–100. [CrossRef]

19. Bauer, R.J.; Dedrick, R.L.; White, M.L.; Murray, M.J.; Garovoy, M.R. Population Pharmacokinetics and Pharmacodynamics of the Anti-Cd11a Antibody Hu1124 in Human Subjects with Psoriasis. *J. Pharmacokinet. Pharmacodyn.* **1999**, *27*, 397–420. [CrossRef]

20. Leung, Y.; Panaccione, R. Anti-Adhesion Molecule Strategies for Crohn Disease. *BioDrugs* **2008**, *22*, 259–264. [CrossRef]

21. Miller, D.H.; Khan, O.A.; Sheremata, W.A.; Blumhardt, L.D.; Rice, G.P.A.; Libonati, M.A.; Willmer-Hulme, A.J.; Dalton, C.M.; Miszkiel, K.A.; O'Connor, P.W. A Controlled Trial of Natalizumab for Relapsing Multiple Sclerosis. *N. Engl. J. Med.* **2003**, *348*, 15–23. [CrossRef]

22. Steinman, L. Blocking Adhesion Molecules as Therapy for Multiple Sclerosis: Natalizumab. *Nat. Rev. Drug Discov.* **2005**, *4*, 510–518. [CrossRef] [PubMed]

23. Stefanelli, T.; Malesci, A.; De La Rue, S.A.; Danese, S. Anti-Adhesion Molecule Therapies in Inflammatory Bowel Disease: Touch and Go. *Autoimmun. Rev.* **2008**, *7*, 364–369. [CrossRef]

24. Shih, C.M.; Hsieh, C.K.; Huang, C.Y.; Huang, C.Y.; Wang, K.H.; Fong, T.H.; Trang, N.T.T.; Liu, K.T.; Lee, A.W. Lycopene Inhibit IMQ-Induced Psoriasis-like Inflammation by Inhibiting ICAM-1 Production in Mice. *Polymers* **2020**, *12*, 1521. [CrossRef] [PubMed]

25. Duda-Madej, A.; Stecko, J.; Sobieraj, J.; Szymańska, N.; Kozłowska, J. Naringenin and Its Derivatives—Health-Promoting Phytobiotic against Resistant Bacteria and Fungi in Humans. *Antibiotics* **2022**, *11*, 1628. [CrossRef] [PubMed]

26. Duda-Madej, A.; Kozłowska, J.; Krzyzek, P.; Anioł, M.; Seniuk, A.; Jermakow, K.; Dworniczek, E. Antimicrobial O-Alkyl Derivatives of Naringenin and Their Oximes against Multidrug-Resistant Bacteria. *Molecules* **2020**, *25*, 3642. [CrossRef] [PubMed]

27. Kozłowska, J.; Duda-Madej, A.; Baczynska, D. Antiproliferative Activity and Impact on Human Gut Microbiota of New O-Alkyl Derivatives of Naringenin and Their Oximes. *Int. J. Mol. Sci.* **2023**, *24*, 9856. [CrossRef]

28. Kozłowska, J.; Grela, E.; Baczynska, D.; Grabowiecka, A.; Anioł, M. Novel O-Alkyl Derivatives of Naringenin and Their Oximes with Antimicrobial and Anticancer Activity. *Molecules* **2019**, *24*, 679. [CrossRef]

29. Andrade, M.; Benfeito, S.; Soares, P.; Magalhães e Silva, D.; Loureiro, J.; Borges, A.; Borges, F.; Simões, M. Fine-Tuning of the Hydrophobicity of Caffeic Acid: Studies on the Antimicrobial Activity against *Staphylococcus aureus* and *Escherichia coli*. *RSC Adv.* **2015**, *5*, 53915–53925. [CrossRef]

30. Kubo, I.; Fujita, K.I.; Nihei, K.I.; Nihei, A. Antibacterial Activity of Akyl Gallates against *Bacillus subtilis*. *J. Agric. Food Chem.* **2004**, *52*, 1072–1076. [CrossRef]

31. Park, K.D.; Cho, S.J. Synthesis and Antimicrobial Activities of 3-*O*-Alkyl Analogues of (+)-Catechin: Improvement of Stability and Proposed Action Mechanism. *Eur. J. Med. Chem.* **2010**, *45*, 1028–1033. [CrossRef]

32. Sung, H.K.; Sang, J.L.; Joo, H.L.; Won, S.S.; Jung, H.K. Antimicrobial Activity of 9-O-Acyl- and 9-O-Alkylberberrubine Derivatives. *Planta Med.* **2002**, *68*, 277–281.

33. Oliveira, H.; Correia, P.; Bessa, L.J.; Guimarães, M.; Gameiro, P.; de Freitas, V.; Mateus, N.; Cruz, L.; Fernandes, I. Cyanidin-3-Glucoside Lipophilic Conjugates for Topical Application: Tuning the Antimicrobial Activities with Fatty Acid Chain Length. *Processes* **2021**, *9*, 340. [CrossRef]

34. Yuan, G.; Guan, Y.; Yi, H.; Lai, S.; Sun, Y.; Cao, S. Antibacterial Activity and Mechanism of Plant Flavonoids to Gram-Positive Bacteria Predicted from Their Lipophilicities. *Sci. Rep.* **2021**, *11*, 10471. [CrossRef] [PubMed]

35. Arora, A.; Byrem, T.M.; Nair, M.G.; Strasburg, G.M. Modulation of Liposomal Membrane Fluidity by Flavonoids and Isoflavonoids. *Arch. Biochem. Biophys.* **2000**, *373*, 102–109. [CrossRef] [PubMed]

36. Selvaraj, S.; Krishnaswamy, S.; Devashya, V.; Sethuraman, S.; Krishnan, U.M. Influence of Membrane Lipid Composition on Flavonoid–Membrane Interactions: Implications on Their Biological Activity. *Prog. Lipid Res.* **2015**, *58*, 1–13. [CrossRef]

37. Altunayar-Unsalan, C.; Unsalan, O.; Mavromoustakos, T. Insights into Molecular Mechanism of Action of Citrus Flavonoids Hesperidin and Naringin on Lipid Bilayers Using Spectroscopic, Calorimetric, Microscopic and Theoretical Studies. *J. Mol. Liq.* **2022**, *347*, 118411. [CrossRef]

38. Tedeschi, A.; D'Errico, G.; Lauro, M.R.; Sansone, F.; Di Marino, S.; D'Ursi, A.M.; Aquino, R.P. Effect of Flavonoids on the Aβ(25-35)-Phospholipid Bilayers Interaction. *Eur. J. Med. Chem.* **2010**, *45*, 3998–4003. [CrossRef]

39. Tsuchiya, H.; Iinuma, M. Reduction of Membrane Fluidity by Antibacterial Sophoraflavanone G Isolated from Sophora Exigua. *Phytomedicine* **2000**, *7*, 161–165. [CrossRef]

40. Marrelli, M.; Karonen, M. Insights into Polyphenol–Lipid Interactions: Chemical Methods, Molecular Aspects and Their Effects on Membrane Structures. *Plants* **2022**, *11*, 1809. [CrossRef]

41. Cazzola, H.; Lemaire, L.; Acket, S.; Prost, E.; Duma, L.; Erhardt, M.; Čechová, P.; Trouillas, P.; Mohareb, F.; Rossi, C.; et al. The Impact of Plasma Membrane Lipid Composition on Flagellum-Mediated Adhesion of Enterohemorrhagic *Escherichia coli. mSphere* **2020**, *5*, e00702-20. [CrossRef]

42. Cao, P.; Wall, D. The Fluidity of the Bacterial Outer Membrane Is Species Specific. *BioEssays* **2020**, *42*, 1900246. [CrossRef]

43. Mozaheb, N.; Van Der Smissen, P.; Opsomer, T.; Mignolet, E.; Terrasi, R.; Paquot, A.; Larondelle, Y.; Dehaen, W.; Muccioli, G.G.; Mingeot-Leclercq, M.-P. Contribution of Membrane Vesicle to Reprogramming of Bacterial Membrane Fluidity in *Pseudomonas aeruginosa. mSphere* **2022**, *7*, e00187-22. [CrossRef]

44. Rajagopal, M.; Walker, S. Envelope Structures of Gram-Positive Bacteria. *Curr. Top. Microbiol. Immunol.* **2017**, *404*, 44. [CrossRef]

45. Silhavy, T.J.; Kahne, D.; Walker, S. The Bacterial Cell Envelope. *Cold Spring Harb. Perspect. Biol.* **2010**, *2*, a000414. [CrossRef] [PubMed]

46. Huang, K.C.; Mukhopadhyay, R.; Wen, B.; Gitai, Z.; Wingreen, N.S. Cell Shape and Cell-Wall Organization in Gram-Negative Bacteria. *Proc. Natl. Acad. Sci. USA* **2008**, *105*, 19282–19287. [CrossRef]

47. Henderson, J.C.; Zimmerman, S.M.; Crofts, A.A.; Boll, J.M.; Kuhns, L.G.; Herrera, C.M.; Trent, M.S. The Power of Asymmetry: Architecture and Assembly of the Gram-Negative Outer Membrane Lipid Bilayer. *Annu. Rev. Microbiol.* **2016**, *70*, 255–278. [CrossRef] [PubMed]

48. Xie, Y.; Yang, W.; Tang, F.; Chen, X.; Ren, L. Antibacterial Activities of Flavonoids: Structure-Activity Relationship and Mechanism. *Curr. Med. Chem.* **2014**, *22*, 132–149. [CrossRef] [PubMed]

49. Braune, A.; Blaut, M. Bacterial Species Involved in the Conversion of Dietary Flavonoids in the Human Gut. *Gut Microbes* **2016**, *7*, 216–234. [CrossRef]

50. Stevens, Y.; Van Rymenant, E.; Grootaert, C.; Van Camp, J.; Possemiers, S.; Masclee, A.; Jonkers, D. The Intestinal Fate of Citrus Flavanones and Their Effects on Gastrointestinal Health. *Nutrients* **2019**, *11*, 1464. [CrossRef] [PubMed]

51. Pan, L.; Ye, H.; Pi, X.; Liu, W.; Wang, Z.; Zhang, Y.; Zheng, J. Effects of Several Flavonoids on Human Gut Microbiota and Its Metabolism by In Vitro Simulated Fermentation. *Front. Microbiol.* **2023**, *14*, 1092729. [CrossRef]

52. Wu, Y.-X.; Yang, X.-Y.; Han, B.-S.; Hu, Y.-Y.; An, T.; Lv, B.-H.; Lian, J.; Wang, T.-Y.; Bao, X.-L.; Gao, L.; et al. Naringenin Regulates Gut Microbiota and SIRT1/PGC-1αSignaling Pathway in Rats with Letrozole-Induced Polycystic Ovary Syndrome. *Biomed. Pharmacother.* **2022**, *153*, 113286. [CrossRef] [PubMed]

53. Mu, H.; Zhou, Q.; Yang, R.; Zeng, J.; Li, X.; Zhang, R.; Tang, W.; Li, H.; Wang, S.; Shen, T.; et al. Naringin Attenuates High Fat Diet Induced Non-Alcoholic Fatty Liver Disease and Gut Bacterial Dysbiosis in Mice. *Front. Microbiol.* **2020**, *11*, 585066. [CrossRef] [PubMed]

54. Wu, Y.-X.; Yang, X.-Y.; Hu, Y.-Y.; An, T.; Lv, B.-H.; Lian, J.; Wang, T.-Y.; Bao, X.-L.; Zhu, J.-J.; Gao, L.; et al. Naringenin, a Flavonoid, Modulates Gut Microbiome and Ameliorates Hormone Levels to Improve Polycystic Ovary Syndrome in Letrozole-Induced Rats. *Res. Sq.* **2020**, preprint. [CrossRef]

55. Gill, S.; Pop, M.; Deboy, R.; Eckburg, P.; Turnbaugh, P.; Samuel, B.; Gordon, J.; Relman, D.; Fraser-Liggett, C.; Nelson, K. Metagenomic Analysis of the Human Distal Gut Microbiome. *Science* **2006**, *312*, 1355–1359. [CrossRef]

56. Prakash, S.; Rodes, L.; Coussa-Charley, M.; Tomaro-Duchesneau, C. Gut Microbiota: Next Frontier in Understanding Human Health and Development of Bio-Therapeutics. *Biologics* **2011**, *5*, 71–86. [CrossRef]

57. Vajrabhaya, L.-O.; Korsuwannawong, S. Cytotoxicity Evaluation of a Thai Herb Using Tetrazolium (MTT) and Sulforhodamine B (SRB) Assays. *J. Anal. Sci. Technol.* **2018**, *9*, 15. [CrossRef]

58. Drolia, R.; Tenguria, S.; Durkes, A.C.; Turner, J.R.; Bhunia, A.K. Listeria Adhesion Protein Induces Intestinal Epithelial Barrier Dysfunction for Bacterial Translocation. *Cell Host Microbe* **2018**, *23*, 470–484. [CrossRef]

Review

Carvacrol—A Natural Phenolic Compound with Antimicrobial Properties

Wanda Mączka *[ID], Martyna Twardawska, Małgorzata Grabarczyk *[ID] and Katarzyna Wińska *[ID]

Department of Food Chemistry and Biocatalysis, Wrocław University of Environmental and Life Sciences, Norwida 25, 50-375 Wrocław, Poland; 121626@student.upwr.edu.pl
* Correspondence: wanda.maczka@upwr.edu.pl (W.M.); malgorzata.grabarczyk@upwr.edu.pl (M.G.); katarzyna.winska@upwr.edu.pl (K.W.)

Abstract: The main purpose of this article is to present the latest research related to selected biological properties of carvacrol, such as antimicrobial, anti-inflammatory, and antioxidant activity. As a monoterpenoid phenol, carvacrol is a component of many essential oils and is usually found in plants together with its isomer, thymol. Carvacrol, either alone or in combination with other compounds, has a strong antimicrobial effect on many different strains of bacteria and fungi that are dangerous to humans or can cause significant losses in the economy. Carvacrol also exerts strong anti-inflammatory properties by preventing the peroxidation of polyunsaturated fatty acids by inducing SOD, GPx, GR, and CAT, as well as reducing the level of pro-inflammatory cytokines in the body. It also affects the body's immune response generated by LPS. Carvacrol is considered a safe compound despite the limited amount of data on its metabolism in humans. This review also discusses the biotransformations of carvacrol, because the knowledge of the possible degradation pathways of this compound may help to minimize the risk of environmental contamination with phenolic compounds.

Keywords: carvacrol; antimicrobial; biotransformation

1. Introduction

Carvacrol (5-isopropyl-2-methylphenol) is a monoterpenoid alcohol, a liquid with a boiling point of 236–237 °C and a density of 0.976 g/mL at 20 °C. It is insoluble in water but very soluble in ethanol, acetone, and diethyl ether [1]. It is a component of essential oils obtained from many plants, e.g., *Corido thymus*, *Lippia pepperwort* [2], black cumin (*Nigella sativa*), oregano (*Origanum compactum*), *O. dictamnus*, *O. microphyllum*, *O. onites*, *O. scabrum*, *O. vulgare*, pepperwort (*Lepidium flavum*), wild bergamot (*Citrus aurantium* var. bergamia Loisel), *Monarda didyma*, thyme (*Thymus glandulosus*), and savory (*Satureja hortensis*) [3]. It is worth noting that the content of carvacrol may vary depending on the tissue. In *Origanum vulgare* "Hot and Spicy", carvacrol is the main component found in petals (94.40 ± 1.23%), tepals (96.92 ± 0.85%), bracts (96.07 ± 0.67%), and leaves (84.71 ± 1.59%), while *p*-cymene was dominant in the stems (65.44 ± 5.77%) and carvacrol was present in a minor amount (13.06 ± 6.74%) [4].

In plants, carvacrol is biosynthesized from γ-terpinene, which is formed by the mevalonate pathway [5] or by the plastid-based methylerythritol pathway (MEP) [6]. Recently, Krause et al. [7] proposed a carvacrol biosynthesis pathway in Lamiaceae plants in which γ-terpinene is oxidized by cytochrome P450 (CYP) monooxygenases of the CYP71D subfamily to produce an unstable cyclohexadienol intermediate. The resulting compound was then dehydrogenated by a short-chain dehydrogenase/reductase (SDR) to the corresponding ketone, which was converted to carvacrol. The combination of these enzymes produced carvacrol with γ-terpinene in both in vitro and in vivo tests in *Nicotiana benthamiana*. On the other hand, in the absence of SDR, no carvacrol formation was observed and only *p*-cymene was formed. Carvacrol's biosynthetic pathway genes are highly co-expressed

with transcription factor genes such as ZIP and basic helix–loop–helix (bHLH), indicating their involvement in the regulation of carvacrol biosynthesis [4]. CYP71D subfamily enzymes have also been detected in *Origanum vulgare* L. (CYP71D178, CYP71D180, and CYP71D181) [8]. In addition, Sun et al. [9] found genes in the *Thymus quinquecostatus* genome encoding terpene synthase (TPS), CYP, SDR, R2R3-MYB, and homeodomain–leucine zipper (HD-ZIP) IV. Researchers have shown that *Tq02G002290.1* (*TqTPS1*) encodes the terpene synthase responsible for the biosynthesis of γ-terpinene from geranyl diphosphate (GPP) [9]. TPS-encoding genes are found in *Origanum vulgare* (*OvTPS2*) [8], *Thymus vulgaris* (*TvTPS2*) [10], and *Thymus caespititius* (*TcTPS2*) [11]. The formation of γ-terpinene is also crucial in the synthesis of thymol—an isomer of carvacrol [9].

In turn, by organic synthesis, carvacrol is obtained as a result of Friedel–Crafts alkylation of *o*-cresol with propylene or isopropyl alcohol on solid acid catalysts (e.g., UDCaT-5, aluminum, or iron (III) chloride) [1,12]. Carvacrol can also be obtained by sulfonation of *p*-cymene followed by alkaline fusion [13], chlorination of α-pinene with *tert*-butyl hypochlorite [14], or as a result of the aromatization of carvone [12].

Carvacrol has been approved by the FDA for use in food and listed by the Council of Europe as a Category B chemical flavoring agent that may be added to foodstuffs at a level of 2 ppm in beverages, 5 ppm in flakes, and 25 ppm in candies [15]. Acute toxicity studies have been performed on a variety of animals, which is described in the next part of this publication.

Due to its flavoring (oregano-like smell and pizza-like flavor) [16] and antimicrobial properties, it is most often used in the food industry as a natural food preservative [17]. In dental practice, carvacrol has been used as a substitute for cretol and carbolic acid in the treatment of toothache, sensitive dentine, and alveolar abscess, and as an antiseptic in the pulp canals of the teeth [18]. It can also be used in the fight against mosquitoes, because it has much greater activity as a mosquito repellent than the commercial preparation, *N*,*N*-diethyl-*m*-methylbenzamide [19]. In addition, it reduces egg hatchability and induces infertility in mosquitoes.

In addition to antimicrobial properties, this compound also exhibits a wide range of other biological activities, including cardio-, reno-, and neuroprotective [20]; immune response-modulating [21]; antioxidant; anti-inflammatory [22]; anticancer [23–25]; analgesic [26]; anticonvulsant [27]; antidiabetic; hepatoprotective [28]; and anti-obesity properties [29,30] (Figure 1).

In the first part of our publication, the metabolism of carvacrol was discussed in detail, with particular emphasis on its effect on CYP. When discussing the antimicrobial properties, we paid attention to new forms of application of this compound. The challenges surrounding the wider use of carvacrol in food or feed are its unpleasant and pungent taste at higher doses; low bioavailability; high volatility; sensitivity to the surrounding environment, such as in processing conditions (e.g., heat or other ingredients); and the acidic environment in the digestive tract. The solution to the above problems seems to be the use of colloidal systems, including microencapsulation and nanotechnology, which were extensively discussed in the review by Wang and Wu [31]. Herein, we focused on the impact of these forms of application on the antimicrobial activity of carvacrol. Since infections are often accompanied by massive inflammation, an important advantage of an antimicrobial agent is its anti-inflammatory and antioxidant effects, which are discussed in the next part of our publication. We also called attention to the biotransformations that carvacrol can undergo in the environment, because the awareness of human impact on the environment is of great importance and it is essential not to contribute to the increase in pollution when introducing new products into the market.
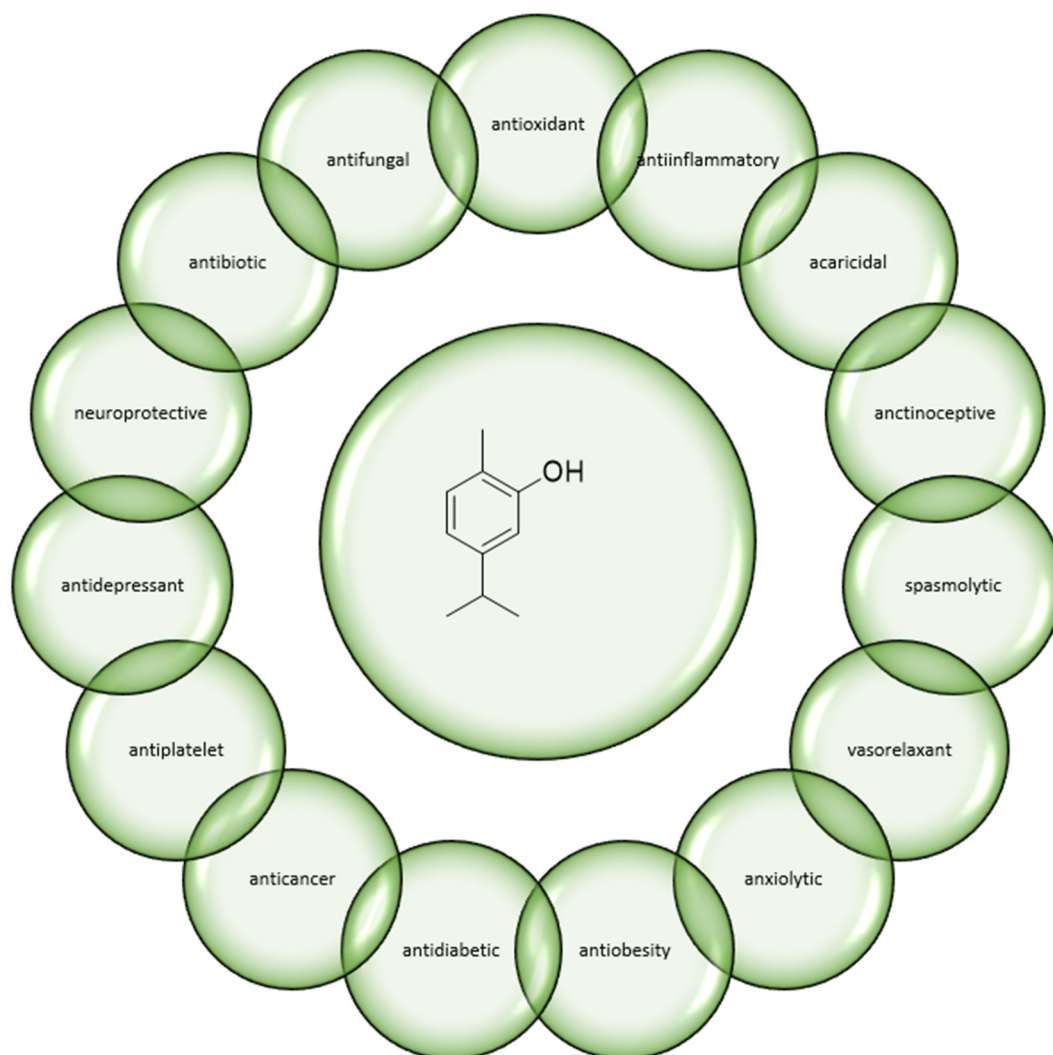
Figure 1. The broad spectrum of carvacrol activity.

2. Antimicrobial Activity of Carvacrol

Carvacrol has a strong antimicrobial effect against many strains of bacteria and fungi that are dangerous to humans or cause significant losses in the economy (Table 1). A strain of *Candida albicans*, next to *C. glabrata*, *C. krusei*, *C. tropicalis*, and *C. parapsilosis*, is one of the few species of fungi that causes diseases in humans [32]. In people with a healthy immune system, *C. albicans* is often harmless, remaining in balance with other members of the local microflora and asymptomatically colonizing the digestive tract, reproductive system, mouth, and skin. However, changes in the host microbiota (e.g., due to antibiotic intake), changes in the host's immune response (e.g., during stress, infection with another microorganism, or immunosuppressive therapy), or changes in the local environment (e.g., changes in pH or nutrients) may allow for excessive growth of *C. albicans* and cause infection. These infections range from superficial mucosal and skin infections, such as thrush, vaginal yeast infections, and diaper rashes, to blood-borne disseminated infections, which have a high mortality rate. Infections with this pathogen account for 15% of all cases of hospital-acquired sepsis and are particularly serious in immunocompromised individuals (e.g., those with AIDS or those undergoing cancer or immunosuppressive therapies) and those with implanted medical devices [33]. This strain of *C. albicans* produces highly structured biofilms composed of multiple cell types encased in an extracellular matrix. It is worth noting that fungal biofilms are largely resistant to current antifungal drugs, so high doses are generally required to treat infections [34]. In the research by Jafri et al. [35] and Niu et al. [36], *C. albicans* cells treated with carvacrol showed irregular surfaces, multiple

hyphal lesions, reductions in cell number, inhibition of biofilm formation by up to 80%, and inhibition of ergosterol synthesis. In turn, Miranda et al. [37] tested the activity of carvacrol against *C. albicans*, *C. glabrata*, *C. krusei*, and *C. dubliniensis*, confirming the antifungal activity of this compound from MIC 161.3 mg/L.

Ismail et al. [38] undertook research on the activity of carvacrol against the pathogenic *Candida auris* strain. They showed that the growth of all *C. auris* isolates was inhibited by carvacrol in the MIC range of 125–500 μg/mL, and the MFC values for the same isolates were in the range of 250–1000 μg/mL. *C. auris* antioxidant enzymes such as catalase (CAT), superoxide dismutase (SOD), glutathione peroxidase (GPx), glutathione reductase (GR), and glutathione transferase (GST) were analyzed and evaluated after exposure to carvacrol. It was observed that exposing the cell to increasing concentrations of carvacrol resulted in an increase in the activity of CAT, SOD, and GPx. In contrast to GR and GST, there was an obvious decrease in activity after exposure to carvacrol. The authors of the study proved that carvacrol is able to reduce the expression of genes encoding antioxidant enzymes. They also confirmed the effect of carvacrol on hemolysis in the range of 0.9–26.8%.

The antifungal activity of carvacrol in combination with antibiotics such as fluconazole, ketoconazole, or amphotericin B was tested against eight strains of *Candida*, including *C. tropicalis*, *C. parapsilosis*, *C. guilliermondii*, and *C. krusei*. The MIC for carvacrol alone ranged from 128 to 512 μg/mL. Different forms of interactions between carvacrol and antifungal agents have been observed: synergism in 25% of the combinations, additivity in 25%, and, finally, inertness in 50% of the combinations. No antagonist effect was observed. A synergistic effect was observed with the combination of carvacrol/ketoconazole and Amphotericin B against *C. guilliermondii* LM-103 and carvacrol/fluconazole against *C. parapsilosis* ATCC 22019 [39].

Regarding the wider use of carvacrol as an antimicrobial agent, its bioavailability is a major limitation. To this end, Mauriello et al. [40] encapsulated carvacrol using various stabilizers, such as whey protein isolate and surfactant Tween 80, and measured its antimicrobial activity against *Saccharomyces cerevisiae*. The obtained results indicated antifungal activity at a carvacrol concentration of <500 mg/L. Pure carvacrol had a stronger fungicidal effect than the Tween 80 emulsion containing 25% and 50% carvacrol. When whey protein isolate was used, the antimicrobial activity was proportional to the dissolution of carvacrol, suggesting that the emulsion droplets act as micrometric reservoirs for the compound, which is gradually released in the aqueous phase. Researchers postulate that the use of encapsulation may also contribute to extending its durability.

A certain strain of *Aspergillus flavus* is a common contaminant in grain, oil, and their products. Its metabolite, aflatoxin B1 (AFB1), has been proven to be highly carcinogenic. Therefore, it is very important to find antifungal substances that could inhibit the growth and production of toxins by *A. flavus* [41]. The optimal pH for the growth of the eight toxigenic Aspergillus strains was reported to be pH 6 in unmodified potato dextrose broth. Carvacrol, at 1.0 mM, completely inhibited fungal growth, but only at pH 4 and 8. At lower concentrations (0.1 and 0.5 mM), partial inhibition of mycelial growth was observed at all pH levels, with significantly less mycelial growth at pH 4 and 8 [42]. Qu et al. [43] found that carvacrol was effective in inhibiting *A. flavus* growth and AFB1 production. Carvacrol, when used at concentrations of 0, 50, 100, and 200 μg/mL, inhibited spore germination, mycelial growth, and AFB1 production in proportion to the concentration. In studies on the mechanism of action of carvacrol against *A. flavus*, it was found that the production of ergosterol (5,7-diene oxysterol) in the mycelium decreased with the increasing concentration of carvacrol [43]. Ergosterol is synthesized in the endoplasmic reticulum through the sequential activity of 25 different enzymes [44]. It is important for the structure of the cell membrane because its absence causes defects in the integrity of the cell membrane of the microorganism and an imbalance in cell permeability [45,46], which, in turn, can lead to eventual cell death. Thus, carvacrol was able to damage the cell membrane. The effect of carvacrol on *A. flavus* lipids was also investigated using a lipidomic metabolism analysis. When carvacrol was used at 200 μg/mL, a decrease in the

level of most glycerolipids and phospholipids in the mycelium of *A. flavus* was observed. Neutral lipids decreased, as did phosphatidylcholines, phosphatidylethanolamines, and phosphatidylserines, while phosphatidylinositol and phosphatidylglycerols increased [43]. Glycerophospholipids are key components of the cellular lipid bilayer, and the composition of fatty acids has a significant impact on properties of the cell membrane such as its fluidity or its transport of triacylglycerols and cholesterol. Proper glycerophospholipid metabolism is essential for optimal cell membrane dynamics [47]. Therefore, external factors that induce changes in the amount of certain types of glycerophospholipids can affect the overall cellular metabolism [43].

Carvacrol placed on nanofibers is used to produce packaging. Fonseca et al. [48] conducted an experiment using nanofibers containing starch and carvacrol. Carvacrol alone contributed to a greater inhibition of growth on day 7 by 13% of *Penicillium* sp. and by 30% of *A. flavus* ATCC 204304. The MIC values for both carvacrol and nanofibers depended on the concentration. It is worth emphasizing that both Penicillium and Aspergillus fungi are responsible for food spoilage, and, thus, an active antifungal agent is being sought for use in packaging that will effectively limit the growth of these microorganisms and, at the same time, will not pass into food. The use of nanofibers with the addition of carvacrol seems to be a promising alternative to the currently used solutions.

Carvacrol was also active against plant soilborne pathogens (*Alternaria tomatophila*, *Podosphaera xanthii*, and *Xanthomonas perforans*) which are common in South Florida of the United States [49].

The antifungal activity of carvacrol was also tested on strains of Hyphomycetes (*Alternaria solani*, *Botrytis cinerea*, *Fusarium oxysporum*, *Pyricularia grisea*, and *Rhizoctonia solani*) and Oomycetes (*Phytophthora capsici* and *Phytophthora nicotianae*). Carvacrol, at a dose of 50 µg/mL, was active against the above strains, with a degree of inhibition greater than 90% against *B. cinerea*, which was equal to the commercial fungicide chlorothalonil [50]. The search for an effective antimicrobial agent is particularly important for *B. cinerea*, as it affects more than 1400 plant species, including many economically important ornamentals, fruits, and vegetables. It causes stem and fruit rot both before and after harvest. The economic losses caused by this phytopathogen are estimated to be between USD 10 and 100 billion worldwide [51]. The MIC for carvacrol was 120 mg/L, and the MBC was 140 mg/L. It changed the morphology of *B. cinerea* hyphae by disrupting and distorting the mycelium. It also negatively affected cell membrane permeability and caused a marked decrease in the total lipid content in *B. cinerea* cells, suggesting that cell membrane structures were destroyed [52].

On the other hand, harvesting fresh citrus fruits in warm and humid regions such as Florida destroys *Lasiodiplodia theobromae*, which causes Diplodia stem-end rot (SER). The EC_{50} value was 0.045 mg/mL. Carvacrol and thymol were then incorporated into a commercial shellac coating and applied to "Ruby Red" grapefruit inoculated with *L. theobromae* to determine their activity against Diplodia SER in vivo. Fruits were artificially inoculated with *L. theobromae* 12 h before or immediately after coating, then incubated at 29 °C and 90% relative humidity for 48 h. Lesion development was inhibited more effectively when a coating containing 10 mg/mL carvacrol was applied prior to pathogen inoculation. In addition, the inclusion of carvacrol in the shell did not adversely affect fruit weight loss, skin color, or titrated acidity [53].

Bacteria such as *Enterobacter cloacae*, *Escherichia coli*, *Listeria monocytogenes*, *Pseudomonas fluorescens*, *Pseudomonas putida*, and *Staphylococcus aureus* often develop during meat storage. Eating meat contaminated with bacteria can be dangerous to human health. Therefore, work is underway to develop packaging that would effectively inhibit the growth of microorganisms. Xiao et al. [54] obtained a film containing chitosan, pullulan, and carvacrol, which had acceptable technical parameters such as water vapor permeability, tensile strength, and percentage elongation at break. At the same time, its use allowed the shelf life of goat meat to be extended to more than 15 days. Another solution was to incorporate carvacrol and carboxybetaine into the polyurethane, slowing down the release of carvacrol from

the material. A synergistic antibacterial effect of bio-derived "kill and gun" polyurethane against *E. coli* and *S. aureus* was observed [55].

On the surface of materials commonly used in medicine and food production, a microbial biofilm often develops which is difficult to remove and promotes the development of pathogenic bacteria. Carvacrol inhibited biofilm formation by up to 74–88% for *Pseudomonas aeruginosa* ATCC15442, and up to 86–100% for *S. aureus* ATCC6538 [56].

An interesting solution seems to be the combination of carvacrol with proteolytic enzymes. Mechmechani et al. [57] found a synergistic effect of a combination of carvacrol with pepsin and trypsin on the degradation of *P. aeruginosa* and *E. faecalis* biofilms growing on polystyrene or stainless steel surfaces. The effect was best after sequential treatment with two enzymes prior to administration of carvacrol. The enzymes were effective in destroying biofilms without causing cell death. By interacting with proteins, they caused structural defects in biofilms, thus worsening the barrier properties.

A strain of *Streptococcus pyogenes* (group A streptococcus (GAS)) is a Gram-positive bacterium commonly associated with pharyngitis. However, it can also cause scarlet fever, impetigo, cellulitis, type II necrotizing fasciitis, streptococcal toxic shock syndrome, acute rheumatic fever, and post-streptococcal glomerulonephritis. Approximately 18.1 million people currently suffer from the serious disease GAS, with 1.78 million new cases and 500,000 deaths each year [58]. A strain of *S. pyogenes* has the ability to form a biofilm to evade host defense systems. The biofilm is formed by microbial cells that are irreversibly bound to a substrate or interface, or to each other. They are encapsulated in the EPS matrix which they produce, and exhibit an altered phenotype in terms of growth rate and gene transcription. In the studies of Wijesundar et al. [59], it was found that carvacrol induced deformations and damage to the bacterial cells, as well as deactivation of extracellular polymers (EPS), which, in the bacterial cell, are responsible for protecting the cell against toxic substances and ensuring its strength. In addition, carvacrol reduced the hydrophobic properties of multicellular bacterial structures by up to 84.2%, and was able to reduce the expression of the *LuxS* gene associated with the formation of biofilms by *S. pyogenes* [59]. Carvacrol also resulted to be a promising antifungal agent against *S. aureus* and *S. epidermidis*, which mainly cause diseases of the skin and the respiratory, urinary, and digestive systems, as well as osteomyelitis of the bone and meningitis. In a study by Mauriello et al. [40], the authors attempted to correlate carvacrol with whey emulsion and compared the effect of pure carvacrol with that of an emulsion. The obtained results indicated a strong bactericidal effect against *S. epidermidis* ATCC 12228 and *P. fluorescens* ATCC 13525 at a carvacrol dose of <500 mg/L. In turn, Luna et al. [60] used nanotechnology, which increased the chemical and physical stability of carvacrol, extended its duration, and increased its effectiveness. For the synthesis of carvacrol-delivering nanoparticles by ionotropic gelation, they used chitosan due to its biocompatibility, biodegradability, intrinsic antibacterial activity, and hemostatic and mucoadhesive properties. Its activity against *E. coli* ATCC 25922 and *S. aureus* ATCC 25923 was tested, and it showed higher antibacterial activity compared to nanoparticles. However, it is worth noting that the total amount of carvacrol released from the nanoparticles after 24 h was significantly lower than that of the free chemical. In turn, Cui et al. [61] obtained a nanomaterial based on cationic starch nanofibers containing carvacrol and casein nanoparticles, and studied the effect of this material on the presence of *Bacillus cereus* in soy products. It was found that the obtained nanofibers were able to effectively inhibit the growth of *B. cereus* during cold storage and to maintain the sensory qualities of soybean products.

In turn, Mechmechani et al. [62] investigated the effect of microcapsules of carvacrol on the biofilm-forming capacity of *P. aeruginosa* and *Enterococcus faecalis*. Carvacrol was able to reduce the *P. aeruginosa* biofilm to below the limit of detection after only 15 min. A 4-fold lower MIC (1.25 mg/mL) than free carvacrol was observed for *P. aeruginosa* (MIC = 5 mg/mL) when microcapsules were used. However, in relation to *E. faecalis*, comparable results were obtained for both free carvacrol and microcapsules

(MIC = 0.625 mg/mL). Carvacrol destabilized the bacterial cell membrane, leading to cell death.

The effect of carvacrol in the form of nanocapsules on the formation of a biofilm by *Salmonella* Enteritidis adhering to stainless steel was investigated by Yammine et al. [63]. Spherical nanocapsules with sizes of 159.25–234.76 nm were obtained using spray drying. Although, in the case of free carvacrol, the MIC was present at the level of 1.25 mg/L, after the application of this compound in the form of nanocapsules, the MIC decreased to 0.31 mg/L. It is worth noting that the MIC of thymol in the form of nanocapsules was 0.62 mg/L. The anti-biofilm activity of free and nanoencapsulated carvacrol was dose-dependent. Elimination of *S.* Enteritidis biofilms developed on stainless steel was achieved after 15 min of treatment with carvacrol nanocapsules at twice the MIC dose. Carvacrol, in the form of nanocapsules, showed no toxicity to *Daphnia magna* crustaceans after 48 h of exposure.

In addition, Fang et al. [64] determined that the MIC values for carvacrol against *Vibrio parahemolyticus* ATCC 17802, *Shewanella putrefaciens* ATCC 49138, *S. aureus* ATCC 6538, and *P. fluorescens* ATCC 13525 were 0.5, 0.5, 0.125, and 0.5 mg/mL, respectively. Carvacrol was found to alter cell membrane permeability, causing nucleic acids and proteins to leak and resulting in cell death. This mechanism was confirmed by the observation of alkaline phosphatase (AKP) leakage. This is an intracellular enzyme located between the cell wall and the cell membrane, and in the event of damage to the cell wall, there is a strong leakage of AKP outside the bacteria into the extracellular environment. The same researchers also obtained a carvacrol/β-cyclodextrin emulsion, which they applied to edible films of flaxseed gum (FSG)-sodium alginate (SA) to test the application of such a system for storing Chinese sea bass (*Lateolabrax maculatus*) fillets. The addition of carvacrol at a concentration of 1.0 mg/L ensured excellent organoleptic properties during cold storage of the meat. However, carvacrol at 2.0 mg/L imparted a strong characteristic taste, which is not desirable [64].

Carvacrol was also effective against multidrug-resistant *Klebsiella pneumoniae*, which is responsible for the development of pneumonia, as it eliminated all bacterial cells within 4 h. It showed low MIC and MBC values (ranging from 130 to 260 mg/L) for *K. pneumoniae* strains resistant to carbapenems and polymyxins. The obtained results encouraged the researchers to test its effectiveness in a mouse model of pneumonia. Administration of carvacrol to mice (10, 25, 50 mg/kg) was associated with increased survival and significantly reduced bacterial load in peritoneal washings. In addition, the carvacrol-treated groups had a significant reduction in the total white blood cell count and a significantly increased platelet count compared to the group of mice not given carvacrol [65].

In addition, Khan et al. [66] studied the activity of carvacrol against *E. coli* producing extended-spectrum β-lactamases (ESBLs) that were isolated from the blood of patients with urinary tract infections. Carvacrol, which has a minimum inhibitory concentration of 150 μg/mL and a minimum bactericidal concentration of 300 μg/mL, reduced the number of *E. coli* cells in a time-dependent manner. In addition, carvacrol was found to cause greater membrane depolarization and increased oxidative stress in *E. coli* cells; it also induced the release of cellular DNA, proteins, and potassium ions from bacterial cells and reduced both the quantity of bacteria in macrophage invasion assays and the levels of the inflammatory proteins TNF-α and COX-2. It has also been verified that carvacrol inhibits the activity of β-lactamase.

Carvacrol also inhibited the growth of *Dickeya zeae* (formerly *Erwinia chrysanthemi* pv. *zeae*), which causes huge economic losses because it attacks banana, rice, maize, and potato crops. Its presence has been noted in the USA, Asia, Australia, Africa, and Europe. The MIC (0.1 mg/mL) and MBC (0.2 mg/mL) values were determined against the *D. zeae* strain MS1, which was isolated from banana stems with soft rot symptoms. In addition, carvacrol damaged the cell membrane, as a reduction in membrane potential, a decrease in ATP concentration, and nucleic acid leakage were found. In addition, at sub-inhibitory concentrations, a significant inhibition of the swimming motility and biofilm formation of *D. zeae* MS1 was observed. A tissue infection test was also performed, showing that carvacrol

significantly reduced the pathogenicity of *D. zeae* MS1. Inoculated banana seedlings showed significantly fewer disease symptoms after treatment with carvacrol, and the effectiveness against banana soft rot was 32.0% 14 days after inoculation [67].

Kasthuri et al. [68] tested the activity of carvacrol against *S. aureus* ATCC 6538, *P. aeruginosa* ATCC 15442, *E. coli* ATCC 10536, and *Enterococcus hirae* ATCC 10541 according to the protocol of the British Standard European Norm 1276: phase2/step1 (EN1276). In addition, a synergistic effect of the combination of carvacrol and nerol in the proportions of 0.625% carvacrol + 1.25% nerol and 0.781% carvacrol + 1.56% nerol was found. In addition, this combination destroyed the pre-formed biofilm. The effect of these terpenes on benign keratinocyte (HaCaT) cells was also tested, and no toxic effects were found. On this basis, the researchers postulate that the above combinations of carvacrol and nerol may be active ingredients in preparations for washing and disinfecting the hands of people in both hospital and home environments.

The synergistic effect of carvacrol with other terpenoids was also found by Sousa et al. [69] against *Gardnerella* sp. In bacterial vaginosis (BV), an increase in anaerobic bacteria is observed, leading to the formation of a multimicrobial biofilm consisting mainly of *Gardnerella* sp. BV is usually treated with broad-spectrum antibiotics such as metronidazole and clindamycin, resulting in a high number of relapses due to the simultaneous eradication of the beneficial *Lactobacillus* strains as well. For this reason, new alternative treatments are sought. Carvacrol in combination with *p*-cymene showed strong synergistic antimicrobial activity against *Gardnerella* sp. planktonic cultures. For biofilm elimination, the combination of carvacrol and linalool at concentrations below the MIC was found to be effective without exhibiting the cytotoxicity observed in reconstituted human vaginal epithelium [69].

A synergistic effect of carvacrol and nisin was found against *Listeria monocytogenes* and *S. aureus* BNCC 186335 strains. For *S. aureus* BNCC 186335, the combination of carvacrol and nisin resulted in a FICI of 0.281 and an FBCI of 0.09375. In addition, a decrease in biofilm formation was observed. Nisin facilitates the entry of carvacrol into the cell. The combination of carvacrol and nisin reduced the number of microorganisms growing in pasteurized milk and maintained the milk quality at 25 °C and 4 °C [70]. Carvacrol alone gave a MIC of 250 μg/mL and an MBC of 250 to 500 μg/mL when tested on 9 strains of *L. monocytogenes*. Bacterial cells exposed to carvacrol showed depolarization of the cell membrane and its increased permeability and changes in respiratory activity. The effectiveness of the combination of carvacrol and nisin was tested by storing sliced Bolognese sausages at 4 °C. A significant reduction in the growth rate of *L. monocytogenes* was then observed compared to the controls [71]. This bacterium is able to survive and multiply at refrigerator temperatures and is ubiquitous in the environment, easily contaminating vegetables, fruits, dairy products, meat, seafood, and ready-to-eat foods. It causes listeriosis in susceptible individuals, including the elderly, the immunocompromised, and pregnant women, with an overall mortality rate of 20–30%, depending on the country [72].

A synergistic effect against *E. coli* CICC 10664 and *S. aureus* CICC 21600 was also found for the combination of ε-poly-L-lysine (ε-PL) with carvacrol [73]. ε-PL is a polymer consisting of a series of 25–35 L-lysine monomers that is derived from metabolites produced by fermentation by *Streptomyces albus* 346 [74]. ε-PL has been approved as a safe food preservative in China and the United States, and is widely used to preserve various foods, such as cooked meat products, fruit and vegetable juices, and egg products. Apart from its antibacterial properties, it also shows resistance to high temperatures, good solubility in water, and low toxicity [75]. The combination of ε-PL and carvacrol was synergistic against *E. coli* CICC 10664 and *S. aureus* CICC 21600, with fractional inhibitory concentration indices (FICI) of 0.375 and 0.5, respectively. Damage to cell membranes and a change in its permeability, as well as a decrease in the activity of the respiratory chain dehydrogenase, were observed [73].

The latest publication of Addo et al. describes the synergistic effect of a combination of carvacrol and cineole against *E. coli* ATCC 35150 growing on cucumbers. Strains of *E. coli* O157:H7 usually cause diarrhea, and they have a high capacity to form biofilms. The

combination of carvacrol and cineole effectively inhibited the growth of *E. coli*, destroying the structure of the cell membrane and causing leakage of the bacterial cell contents. The ability to form a biofilm was also limited. In addition, the carvacrol–cineole mixture reduced the transcription of *E. coli* virulence genes, shiga toxin (*stx1*), intimin (*eae*), flagellar regulation (*flhD*), and quorum sensing gene AI-2 (*luxS*) [76].

In turn, Fan et al. [77] showed the synergistic effect of carvacrol and thermosonication in combating microorganisms infecting carrot juices. In the developed method, despite heating to 52 °C, the juices retained their original color and β-carotene content. In addition, the use of high-frequency thermosonication together with carvacrol allowed the shelf life of carrot juice to be extended by 25 days at 6 °C, while maintaining high sedimentation stability.

Table 1. Antimicrobial activity of carvacrol against strains of microorganisms.

Microorganism	Determination Method	MIC and/or MFC Value	References
Aspergillus flavus ATCC 204304	Serial dilution method in liquid medium	MIC: 0.098 mg/mL MFC: 0.098 mg/mL	[48]
Candida albicans	Serial dilution method in liquid medium	MFC: 256 mg/L	[37]
Candida albicans SC5314	Microdilution	MIC: 250 mg/L	[38]
Candida albicans SC5314	Microdilution	MIC: 247 μg/mL	[36]
Candida auris	Microdilution	MIC: 125 μg/mL	[38]
Candida dubliniensis	Serial dilution method in liquid medium	MFC: 161.3 mg/L	[37]
Candida glabrata	Serial dilution method in liquid medium	MFC: 238.9 mg/L	[37]
Candida krusei	Serial dilution method in liquid medium	MFC: 256 mg/L	[37]
Penicillium sp. isolated from soybeans	Serial dilution method in liquid medium	MIC: 0.098 mg/mL MFC: 0.98 mg/mL	[48]
Saccharomyces cerevisiae	Serial dilution method in liquid medium	MIC: <500 mg/L	[40]
Bacterial strains			
Bacillus cereus ATCC 14579	Double dilution method in liquid medium	MIC: 0.2 mg/mL	[61]
Dickeya zeae MS1	Serial dilution method in liquid medium	MIC: 0.1 mg/mL	[67]
Enterococcus faecalis isolated from French cheese	Serial dilution method in liquid medium	MIC: 0.625 mg/mL	[62]
Enterococcus hirae ATCC 10541	Serial dilution method in liquid medium	MIC: 312.5 μg/mL	[68]
Escherichia coli ATCC 25922	Microdilution	MIC: 0.225 mg/mL	[60]
Escherichia coli KBN10P03335	Serial dilution method in liquid medium	MIC: 150 μg/mL MBC: 300 μg/mL	[66]
Gardnerella sp. UM241	Microdilution	MIC: 0.08 μL/mL	[69]
Klebsiella pneumoniae CTX-M-8, OXA-48, KPC	Serial dilution method in liquid medium	MIC: 130 mg/L	[65]
Pseudomonas aeruginosa CIP 103467	Serial dilution method in liquid medium	MIC: 1.25 mg/mL	[62]
Pseudomonas aeruginosa ATCC 15442	Serial dilution method in liquid medium	MIC: 625 μg/mL	[68]
Pseudomonas fluorescens ATCC 13525	Double dilution method in liquid medium	MIC: 0.5 mg/mL	[64]
Shewanella putrefaciens ATCC 49138	Double dilution method in liquid medium	MIC: 0.5 mg/mL	[64]
Staphylococcus epidermidis ATCC 12228	Serial dilution method in liquid medium	MIC: <500 mg/L	[40]

Microorganism	Determination Method	MIC and/or MFC Value	References
Staphylococcus aureus ATCC 25923	Microdilution	MIC: 0.45 mg/mL	[60]
Staphylococcus aureus ATCC 6538	Double dilution method in liquid medium	MIC: 0.125 mg/mL	[64]
Staphylococcus aureus ATCC 6538	Serial dilution method in liquid medium	MIC: 78 µg/mL	[68]
Streptococcus pyogenes ATCC 19615, ATCC 49399	Serial dilution method in liquid medium	MBIC: 125 µg/mL MBEC: 250 µg/mL	[59]
Vibrio parahaemolyticus ATCC 17802	Double dilution method in liquid medium	MIC: 0.5 mg/mL	[64]

3. Antioxidant and Anti-Inflammatory Activity of Carvacrol

During normal cellular metabolism, free radicals or reactive oxygen intermediates are produced by cells. However, excessive accumulation of free radicals such as superoxide radicals, hydrogen peroxide, and hydroxyl radicals lead to tissue damage [3]. Infectious diseases often develop inflammation because the controlled accumulation of inflammatory factors such as leukotrienes, prostaglandins, TNF-α, or interleukins (e.g., IL-1, IL-6, IL-8, IL-10) has a beneficial effect in the fight against microbes. For example, cytokines are the link between cell damage and inflammation symptoms (cell migration, swelling, fever, or hyperalgesia). They are produced and released by many cell types in response to inflammatory stimuli [78]. It is worth emphasizing that the generally beneficial pro-inflammatory response, as a result of overstimulation, can contribute to the development of dangerous disease syndromes such as sepsis and septic shock [79,80]. For this reason, it is essential that the antimicrobial drug utilized also has antioxidant and anti-inflammatory activity. The antioxidant and anti-inflammatory activity of carvacrol is described in Table 2.

Carvacrol showed significant antioxidant activity in in vitro FRAP, DPPH, and TEAC assays, and Al-Mansori et al. [81] observed an increase in its activity with increasing compound concentration in the range of 50 to 1000 ppm. It is worth noting that carvacrol showed a stronger antioxidant effect than its isomer, thymol, and there was no synergistic effect found when using their mixture at the tested concentrations.

In studies conducted in guinea pigs, carvacrol concentrations of 120 and 240 µg/mL have been shown to reduce malondialdehyde levels compared to the control group [82]. Malondialdehyde is the main marker of polyunsaturated fatty acid peroxidation, as the breakdown of cell membrane integrity deactivates membrane proteins, receptors, and their associated enzymes, intensifying oxidative damage to cells [83]. It is worth emphasizing that in the concentrations utilized, the effect of carvacrol was comparable to that of dexamethasone—a glucocorticosteroid with strong and long-lasting anti-inflammatory, anti-allergic, and immunosuppressive effects [82]. A decrease in the level of malondialdehyde was also observed in the study by Carvalho et al. [84], where, in order to increase the bioavailability of carvacrol, it was encapsulated in solid lipid nanoparticles (SLN), and the effect of SLN on lung damage caused by inhalation of smoke through the respiratory tract was investigated. The study was conducted on 30 rats, which were sacrificed 24 h after inhalation trauma. SLN significantly reduced malondialdehyde levels compared to the control group [84]. Carvacrol significantly improves the level of available glutathione (GSH), which is mainly due to the removal of ROS. Carvacrol prevents lipid peroxidation by inducing SOD, GPx, GR, and CAT [85,86].

In an in vivo animal study, the administration of carvacrol at doses of 50–100 mg/kg was shown to have an anti-inflammatory effect, to relieve inflammatory edema in the paws of mice, and to reduce IL-1β and PGE2 levels. At the same time, they showed that the administration of a dose of 100 mg/kg reduces the expression of COX-2 and IL-1β mRNA. In turn, the level of IL-10 was increased by carvacrol [5,85,87]. Another study evaluated the anti-inflammatory effects of carvacrol in experimental models of edema induced by various phlogistic agents. In models of dextran or histamine-induced paw edema, carvacrol, at

50 mg/kg, reduced swelling by 46% and 35%, respectively. On the other hand, in the case of substance P-induced edema, carvacrol (100 mg/kg) reduced the edema by 46%. In addition, carvacrol reduced 12-*O*-tetradecanoyl phorbol acetate-induced ear swelling by 43% [88].

The anti-inflammatory properties of carvacrol were also tested in C57BL/6 mice administered 5% acetic acid rectally, thereby inducing epithelial changes in the intestinal mucosa and mimicking the phenotype of ulcerative colitis (UC), as ulcerative lesions of the distal colon or abnormalities of the intestinal crypts were formed that extended to the lamina propria. Prior to the induction of UC, rats were administered carvacrol at doses of 25, 50, or 100 mg/kg every 12 h for 3 days. Carvacrol significantly increased CAT, SOD, and GPx activity. In addition, reductions in abdominal hyperalgesia, colonic myeloperoxidase (MPO) activity, lipid peroxidation, and TNF-1 and IL-1 levels were observed [89,90].

The anti-inflammatory activity of carvacrol was tested in an in vitro model of streptococcal pharyngitis using human tonsil epithelial cells (HTonEpiCs) induced with *S. pyogenes* cell wall antigens. Pro-inflammatory cytokines such as IL-6, IL-8, ENA-78, and GCP-2 were found to decrease in a dose-dependent manner with carvacrol. In addition, HBD-2 production was significantly suppressed during the 24 h carvacrol treatment. Carvacrol also had an effect on PGE2 and COX-2 levels in cell suspensions [91].

Prostaglandins also play an important role in the inflammatory process. Cyclooxygenase (COX) is involved in the synthesis of these chemicals and has three isoforms, namely, COX-1, COX-2, and COX-3. COX-2 is rapidly expressed by extracellular stimuli as part of the inflammatory response, and is actually associated with inflammatory symptoms such as pain and fever [92]. The effect of carvacrol on the expression of the COX-2 gene in the LPS-stimulated macrophage cell line J774A.1 was studied. A decrease in COX-2 gene expression was found at carvacrol concentrations of 0.008% and 0.016% [93].

The effect of carvacrol on COX-2 has been studied in in vitro tests. Carvacrol ($IC_{50} = 0.8$ μM) inhibited the production of COX-2-catalysed prostaglandin E2, and was comparable to standard inhibitors such as indomethacin ($IC_{50} = 0.7$ μM) and NS-398 (N-[2-(cyclohexyloxy)-4-nitrophenyl]-methanesulfonamide; $IC_{50} = 0.8$ μM) [94].

The control of COX-2 expression is mediated by peroxisome proliferator-activated receptors (PPARs), which are ligand-dependent transcription factors belonging to the superfamily of nuclear receptors. PPAR-dependent suppression of COX-2 promoter activity by carvacrol was observed. This monoterpene is suggested to regulate COX-2 expression through its agonistic effect on PPARγ [95].

When male rats were given carvacrol at a dose of 20 mg/kg, it was found to positively modulate the Nrf2 transcription factor gene, which is an integral part of the host cell defense mechanism against oxidative stress. Nrf2 binds to antioxidant response elements (AREs) at the promoter sites of genes that encode several essential enzymes of the body's anti-inflammatory response [96].

The compound that facilitates the colonization of host cells by bacteria through adhesion is lipopolysaccharide (LPS). It is the major component of the outer membrane of Gram-negative bacteria and is a foreign substance to higher organisms. However, LPS induces a rapid response in the immune system of the infected person. LPS is highly toxic when present in human blood, which is why it is often called an endotoxin. It causes fever and physical discomfort [97], and interacts with host cells, e.g., with monocytes, macrophages, polymorphonuclear leukocytes, and B and T lymphocytes, as well as various endothelial and epithelial cells. One of the pathways that triggers inflammation and is activated by LPS is the pathway with adapter proteins TRAM and TRIF, which are involved in the transduction of the LPS-derived signal. This pathway leads to the NF-κB-activated transcription of genes responsible for the production of proteins related to the body's immune response [98]. LPS may also stimulate the inflammasome of NALP3, a high-molecular-weight multiprotein caspase-1-activating platform that coordinates the maturation of highly potent pro-inflammatory cytokines such as IL-1β and IL-18 [99]. The NALP3 inflammasome plays a key role in tissue damage caused by inflammation. In turn, TLR4 stimulation initiates the signaling pathway of bone marrow differentiation

factor 88 (MyD88), which promotes rapid activation of NF-κB, consequently leading to an increase in IL-18, IL-6, IL-1β, tumor necrosis factor-α (TNF-α), and monocyte chemotactic protein-1 (MCP-1) [100]. It is worth noting that an overreaction of the infected body to LPS can result in immune suppression and organ dysfunction, which can even lead to death [101].

Lipopolysaccharide from *Porphyromonas gingivalis* (LPS-G), alone and in combination with carvacrol, was used in studies on the potential protective role of carvacrol in the inflammatory process. In an in vitro experiment, HL-1 cardiomyocytes were exposed to LPS-G and incubated with carvacrol. Carvacrol has been shown to have an anti-inflammatory effect by reducing the expression of TLR4, NF-κB, NALP3, and IL-1β. Therefore, the researchers suggest that carvacrol may provide a significant protective effect against the inflammatory stimulus generated by LPS-G, including suppression of the TLR4/NF-κB/NALP3/IL-1β signaling pathway [102].

In addition, studies conducted on mouse spleen cells have shown that carvacrol enhances anti-inflammatory cytokines, increasing the expression of interferon gamma (IFN-γ) and forkhead box P3 (FOXP3) genes while reducing pro-inflammatory activity and modifying the expression of IL-4 and IL-17 genes, as well as transforming growth factor beta (TGF-β) [103].

Carvacrol inhibited the activation of ERK1/2 by LPS. Carvacrol does not act at the extracellular level; at least, it does not affect the binding of LPS to TLR4/CD14. It is possible that carvacrol has a specific effect on the Ras/Raf pathway or that it acts on various membrane receptors that are also modulated by LPS. The pro-inflammatory effects of LPS are also mediated by NF-κB-dependent activation of transcription, and carvacrol blocks the effect of LPS on the translocation of NF-κB (p65) from the cytoplasm to the nucleus and its luciferase-coupled transcription. It has been shown to inhibit NF-κB transactivation even in the absence of LPS, demonstrating its role as an inhibitor of basal NF-κB activation in RAW 264.7 macrophages [104]. Activation of NF-κB by TLR4-mediated LPS is postulated to be dependent on TAK1, an upstream activator of both JNK and IKK [105], but studies by Somensi et al. have shown that carvacrol simultaneously inhibits ERK1/2 and NF-κB, suggesting an alternative pathway for its anti-inflammatory effect [104].

Another important signaling molecule besides LPS that plays an important role in the development of inflammatory immune responses is nitric oxide (NO) [25]. Carvacrol removed NO which had formed as a result of spontaneous degradation of sodium nitroprusside [106].

Carvacrol also affects heat shock proteins (Hsp), the overexpression of which is observed in inflammation caused by infection, high temperature, hypoxia, malnutrition, and exposure to chemicals or UV radiation, among other factors. HSPs are important factors regulating cell survival, differentiation, and death [107]. They prevent cellular damage and increase immunoregulation by activating anti-inflammatory T cells [108]. Carvacrol was able to co-induce the cellular expression of Hsp70 in Hsp70-specific T cell hybridomas in vitro. On the other hand, in in vivo studies on Peyer's patches in mice, amplification of the T-cell responses to Hsp70 was observed after intragastric administration of carvacrol. Carvacrol administration also increased the number of CD4+CD25+FoxP3+ T cells, both systemically in the spleen and locally in the joint, and almost completely suppressed experimental proteoglycan-induced arthritis [109]. It is worth noting that Hsp70 interacts with the viral components of human cytomegalovirus, rabies virus, respiratory syncytial virus, human papilloma virus, and herpes simplex virus [107].

Table 2. Anti-inflammatory and antioxidant effects of carvacrol. (↑ increased or upregulate, ↓ decreased or downregulate).

Animal/Model	Doses of Carvacrol	Main Results	Reference
In vitro tests (ABTS, DPPH, FRAP, TEAC)	From 50 to 1000 ppm	Antioxidant activity	[81]
Guinea pigs exposed to cigarette smoke	120 and 240 µg/mL	Malondialdehyde↓	[82]
Inhalation of smoke in rats	Nanoparticles of carvacrol in form of SLN	Malondialdehyde↓	[84]
Induction of diabetes in rats	75 mg/kg for 8 weeks	SOD↓, GPx↓, Bax↓, Bcl-2↑, malondialdehyde↓	[86]
Mice	50–100 mg/kg	COX-2↓, IL-1β↓, PGE2↓, IL-10↑	[11]
C57BL/6 mice	25, 50, or 100 mg/kg	IL-1β↓, TNF-α↓, CAT↑, SOD↑, GPx↑	[89]
Model of streptococcal pharyngitis (HTonEpiCs)	4–125 µg/mL	IL-6↓, IL-8↓, ENA-78↓, GCP-2↓, HBD-2↓, PGE2↓, COX-2↓	[91]
LPS-stimulated cell line J774A.1	0.008% and 0.016%	COX-2↓	[93]
Ovine COX-2 activity assay	$IC_{50} = 0.8$ µM	Prostaglandin E2↓	[94]
Male Sprague–Dawley rats	20 mg/kg	Nrf2↑	[96]
HL-1 cardiomyocytes exposed to LPS-G	6.25–50 µM	IL-1β↓, TLR4↓, NFκ-B↓, NALP3↓	[102]
Mouse splenocytes	75–300 µg/mL	Gene expression of IL-4↓, IL-17↓, IFN-γ↓, FOXP3↓	[103]
RAW264.7 cells	0.2 mM	Hsp70↑	[109]

4. The Metabolism of Carvacrol

Carvacrol is generally considered to be a safe compound. Therefore, the lack of detailed data on its metabolism in humans is surprising. In a Phase I clinical trial, carvacrol was administered to healthy subjects at 1 and 2 mg/kg/day for 1 month, and no critical adverse reactions or clinically significant changes in biochemical, hematological, endocrine, renal, or hepatic function tests were observed [110]. More than 80% of carvacrol is absorbed or metabolized in the duodenum and stomach. Encapsulation of carvacrol in microcapsules of calcium alginate can effectively reduce its early absorption in the upper gastrointestinal tract after oral administration [111]. The involvement of CYP in the metabolism of carvacrol in humans has been confirmed in studies by Dong et al. [112] in 2012, when the compound was incubated with human liver microsomes (HLM) in the presence of NADPH. The CYP2A6 isoform was shown to be the major enzyme involved in the metabolism of carvacrol in humans. CYP1A2 and CYP2B6 isoforms also contributed to a lesser extent. In addition, 1-aminobenzotriazole (ABT), a non-specific CYP inhibitor, was found to almost completely inhibit the formation of carvacrol metabolites. Conversely, among the selective inhibitors of the CYP isoforms, 8-methoxypsoralen, a specific CYP2A6 inhibitor, significantly inhibited the formation of carvacrol metabolites, confirming that this isoform is primarily responsible for the metabolism of carvacrol in humans. The obtained results indicate that when carvacrol is co-administered with other drugs that are mainly metabolized by CYP2A6, further pharmacokinetic and clinical studies of these combinations of compounds should be performed [112]. Carvacrol may affect the toxicity of other compounds. CYP2E1 is involved in the metabolism of galactosamine. Significant increases in hepatic CYP2E1 mRNA and protein expression were found in rats intoxicated with d-galactosamine. In contrast, carvacrol supplementation suppressed mRNA expression of this protein, suggesting that carvacrol may have a remarkable hepatoprotective effect in the case of d-galactosamine poisoning [113].

There are more data on the metabolism of carvacrol in animals [109].In rats given oral carvacrol by gavage, the LD$_{50}$ was 810 mg/kg body weight [114], while in mice, the LD$_{50}$ was 80 mg/kg body weight after intravenous administration, 73.30 mg/kg body weight when administered intraperitoneally (i.p.), and 680 mg/kg body weight after subcutaneous administration. At very high doses (110–233.3 mg/kg bw), ataxia, decreased spontaneous motor activity, and somnolence were observed in mice before death [29,115]. In dogs, however, the lethal dose of intravenous carvacrol was 0.31 g/kg [116]. As early as 1932, it was found that carvacrol is rapidly excreted in the urine of rats and rabbits [117,118]. Carvacrol appears to be slowly adsorbed in the rabbit intestine, as 22 h after administration of 1.5 g, only about 25% of the dose was excreted in the urine [15]. More detailed studies on the metabolism of carvacrol were carried out by Austgulen et al. on Wistar rats in 1987. The compound (1 mmol/kg), dissolved in propylene glycol, was administered to the rats through a gastric tube. It was found to be excreted either unchanged or as glucuronides and sulfates. In much smaller amounts, hydroxylation of the methyl and isopropyl groups and further oxidation to the acid take place. Only traces of hydroxylation in the aromatic ring were observed, leading to the formation of 2,3-dihydroxy-*p*-cymene (Figure 2) [118,119].
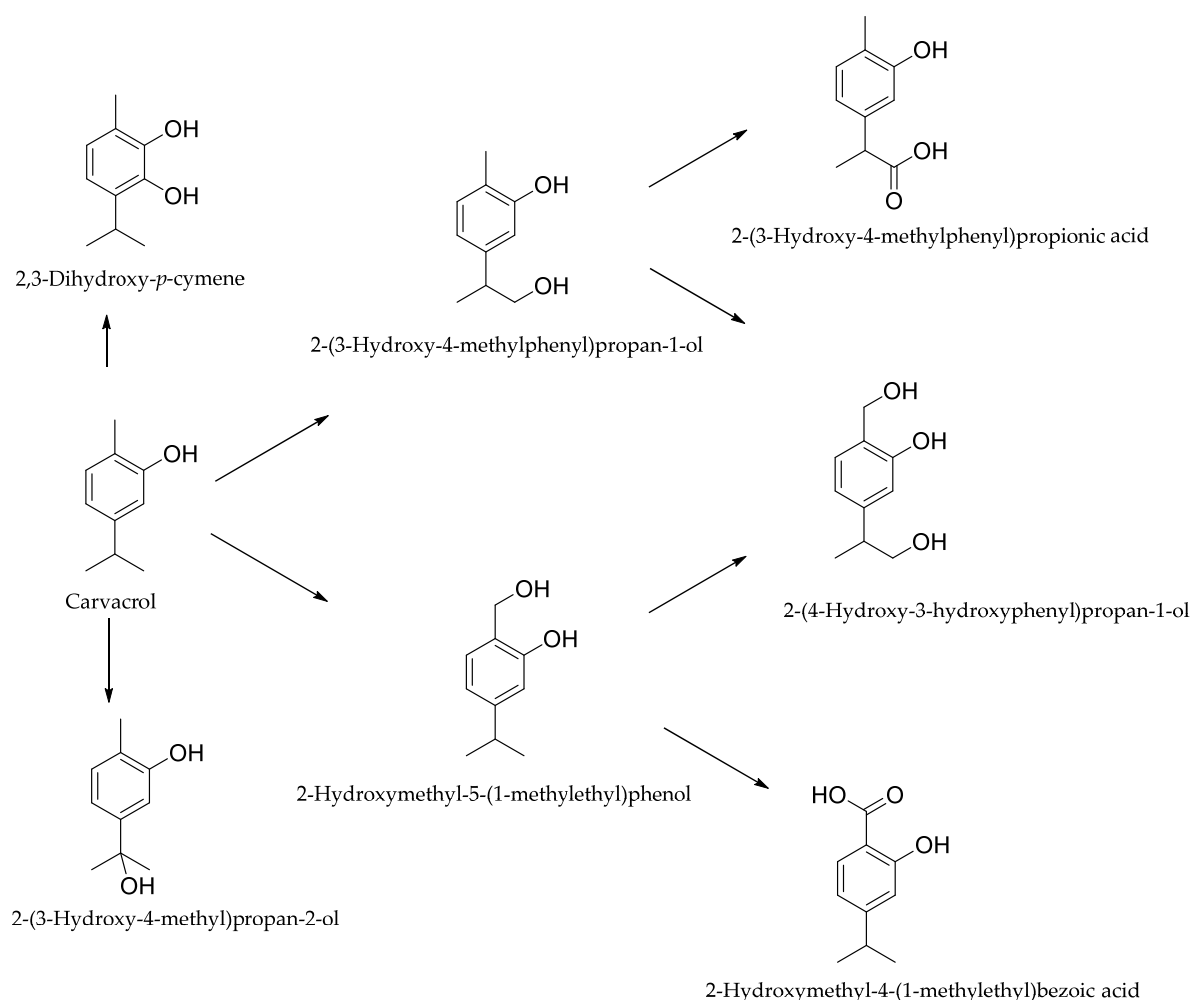
Figure 2. Metabolism and urinary excretion in rats.

5. Biotransformation of Carvacrol

Care for the environment forces the consideration of the impact of each antimicrobial agent on the surface water and soil ecosystem. For this reason, it is extremely important to determine the possible degradation pathways of each new antimicrobial drug, including

carvacrol. Biotransformation processes are often the first stage of degradation, and are discussed in detail in this chapter.

The first reports on the biotransformation of carvacrol date back to 1972, when Herber et al. [120] transformed carvacrol into a hydroquinone derivative using a *Mucor hiemalis* culture. In addition, in their research, Numpaqe et al. [121] used the fungi *Colletotrichum acutatum* and *Botryodiplodia theobromae*, isolated from infected fruits of *Solanum betacea* (tamarillo) and *Persea americana* (avocado). In the culture of *C. acutatum*, the following were obtained: 2-methyl-5-isopropylhydroquinone (thymohydroquinone), 5-(1-hydroxy-1-methylethyl)-2-methylphenol, 2-isopropenyl-5-methylbenzene-1,4-diol, thymoquinone, and carvacrol ether derivative. In the culture of *B. theobromae*, 5-(2-hydroxy-1-methylethyl)-2-methylphenol, 2-hydroxymethyl-5-isopropylphenol, and 5-isopropenyl-2-methylphenol were observed. The transformation efficiency of *B. theobromae* for 5-(2-hydroxy-1-methylethyl)-2-methylphenol and 5-(1-hydroxy-1-methylethyl)-2-methylphenol was about 20%, and for the other compounds, it was much lower. It resulted that *C. acutatum* metabolized carvacrol much more quickly than *B. theobromae*, while the efficiency was only about 12% for the carvacrol ether derivative, and the values were lower for the other compounds [121] (Figure 3). In *Cladosporium* sp. culture, carvacrol was converted to 9-hydroxycarvacrol, which was then oxidized to carvacrol-9-oic acid [122].
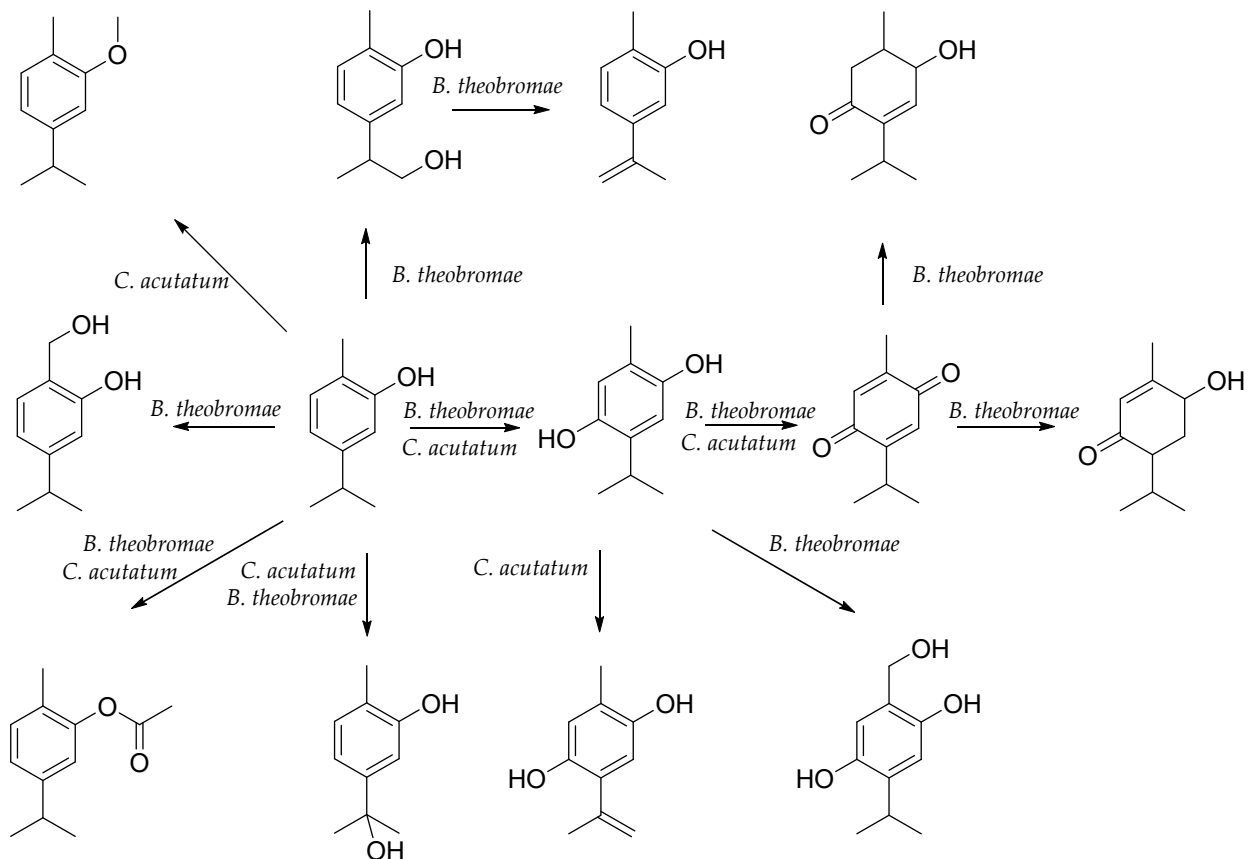
Figure 3. Biotransformation of carvacrol in plant culture.

6. Future Fields of Carvacrol Research

Due to its flavoring and antimicrobial properties, carvacrol is most often used in the food industry as a natural food preservative. An area of research that has recently been intensively developed is the possibility of using carvacrol as a component of active packaging, especially for food storage. Carvacrol placed on specific carriers or included in modified release preparations can limit the growth of pathogenic bacteria in food and slow down the process of its spoilage. Currently, research is also being carried out on

the use of carvacrol as a feed additive in order to maintain the sensory and nutritional quality of poultry meat by inhibiting tissue lipid oxidation. It is debatable whether it is considered a safe antimicrobial compound despite the lack of modern research in this area. In particular, there are no unequivocal results indicating whether or to what extent carvacrol acts as an inducer or inhibitor of the CYP isoforms found in humans. Therefore, further research is needed in this area using modern methods, such as transcriptomic and proteomic techniques, metabolomics, X-ray crystallography, spectroscopy, and computer modeling. There are also no studies to date on the interaction of carvacrol with other food ingredients and drugs.

Although most scientific studies have shown significant potential for carvacrol as an antimicrobial agent, it is important to conduct appropriate clinical trials to determine the safety of the optimal doses and to further study their effectiveness against the strains of microorganisms that have been isolated from patients. Research is needed on the interaction of carvacrol with antibiotics, and in the search for such combinations of carvacrol with other drugs, researchers seek to prove that achieving a synergistic effect of both substances is possible.

In recent years, an intensively developed area of research in microbiology has been the structure and importance of microbial biofilms. In medicine, biofilm formation involving pathogenic strains is often a major therapeutic challenge, as such infections are extremely difficult to treat due to their natural tolerance to commonly used antibiotics and host immune responses. On the other hand, it is known that biofilms of non-pathogenic bacteria can effectively protect the body against infection with pathogenic strains. It is already known that carvacrol disrupts formed biofilms and prevents their formation. However, further research is needed on its mechanism of action on biofilms.

A serious challenge that stands in the way of the widespread use of carvacrol as an antimicrobial drug is its limited bioavailability, which results from unfavorable physico-chemical properties such as high volatility, instability, and low solubility in water. Some studies have attempted to address this problem through the use of specific carriers or modified-release carvacrol formulations, which may result in improvements to the uptake of the active compound and its residence time in various organs or matrices. However, the systems developed so far, especially with the use of nanotechnology, require detailed toxicological studies in order to objectively assess the safety of their use.

Since carvacrol has a strong antimicrobial effect, it is very difficult to find strains of microorganisms capable of biotransforming this compound. Finding strains of microorganisms capable of transforming compounds with antimicrobial activity is particularly tedious and laborious, which may explain the very limited number of publications on this subject. However, research of this type is currently of particular importance in the context of a holistic view of the functioning of all chemical compounds in the environment.

7. Conclusions

Carvacrol is a naturally occurring compound that has achieved great importance, mainly due to its well-documented antimicrobial activity against many strains of bacteria, yeasts, and fungi (Table 1). The combination of the hydroxyl group and the delocalized electrons of the aromatic ring is essential for its activity. Importantly, the position of the hydroxy group is of less importance, as carvacrol often has comparable activity to its isomer, thymol. Carvacrol easily penetrates the cell membrane and can bind ATP or monovalent cations (e.g., K^+), changing the cell membrane potential and influencing homeostasis. Changes in the respiratory chain and, consequently, decreases in ATP synthesis are also observed. Retained lipophilicity contributes to damage to the cell membrane of fungal and spore hyphae, changing the size and shape of cells, allowing for the leakage of cytoplasmic contents, and causing cell death. Carvacrol also disrupts formed biofilms and prevents their formation, especially in the case of *Candida*.

Serious infections are often accompanied by massive inflammation, which, in extreme cases, can lead to sepsis. Carvacrol prevents polyunsaturated fatty acid peroxidation by

inducing SOD, GPx, GR, and CAT. It also contributes to the reduction in pro-inflammatory cytokines such as IL-6, IL-8, ENA-78, and GCP-2 in a dose-dependent manner. It also inhibits the synthesis of prostaglandins, affecting the cellular level of COX-2. It also reduces the level of the body's immune response generated by LPS. Carvacrol also affects heat shock proteins (Hsp), which are overexpressed in infection-induced inflammation.

In the case of the antimicrobials utilized herein, it is important to understand the degradation pathways of the compounds in the environment. So far, it is known that strains of *B. theobromae*, *C. acutatum*, *M. hiemalis*, and *Cladosporium* sp. are capable of carvacrol biotransformation.

References

1. Yadav, G.; Kamble, S.B. Synthesis of carvacrol by Friedel–Crafts alkylation of *o*-cresol with isopropanol using superacidic catalyst UDCaT-5. *J. Chem. Technol. Biotechnol.* **2009**, *84*, 1499–1508. [CrossRef]
2. Marinelli, L.; di Stefano, A.; Cacciatore, I. Carvacrol and its derivatives as antibacterial agents. *Phytochem. Rev.* **2018**, *17*, 903–921. [CrossRef]
3. Gholami-Ahangaran, M.; Ahmadi-Dastgerdi, A.; Azizi, S.; Basiratpour, A.; Zokaei, M.; Derakhshan, M. Thymol and carvacrol supplementation in poultry health and performance. *Vet. Med. Sci.* **2022**, *8*, 267–288. [CrossRef]
4. Hao, Y.; Guo, X.; Yang, R.; Yan, Y.; Sun, M.; Li, H.; Bai, H.; Cui, H.; Li, J.; Shi, L. Unraveling the Biosynthesis of Carvacrol in Different Tissues of *Origanum vulgare*. *Int. J. Mol. Sci.* **2022**, *23*, 13231. [CrossRef] [PubMed]
5. Friedman, M. Chemistry and multibeneficial bioactivities of carvacrol (4-isopropyl-2-methylphenol), a component of essential oils produced by aromatic plants and spices. *J. Agric. Food Chem.* **2014**, *62*, 7652–7670. [CrossRef]
6. Ramak, P.; Kazempour Osaloo, S.; Ebrahimzadeh, H.; Sharifi, M.; Behmanesh, M. Inhibition of the mevalonate pathway enhances carvacrol biosynthesis and DXR gene expression in shoot cultures of *Satureja khuzistanica* Jamzad. *J. Plant Physiol.* **2013**, *170*, 1187–1193. [CrossRef]
7. Krause, S.; Liao, P.; Crocoll, C.; Boachon, B.; Forster, C.; Leidecker, F.; Wiese, N.; Zhaoe, D.; Joshua, C.; Wood, J.C.; et al. The biosynthesis of thymol, carvacrol, and thymohydroquinone in Lamiaceae proceeds via cytochrome P450s and a short-chain dehydrogenase. *Proc. Natl. Acad. Sci. USA* **2021**, *118*, e2110092118. [CrossRef]
8. Crocoll, C.; Asbach, J.; Novak, J.; Gershenzon, J.; Degenhardt, J. Terpene synthases of oregano (*Origanum vulgare* L.) and their roles in the pathway and regulation of terpene biosynthesis. *Plant Mol. Biol.* **2010**, *73*, 587–603. [CrossRef]
9. Sun, M.; Zhang, Y.; Zhu, L.; Liu, N.; Bai, H.; Sun, G.; Zhang, J.; Shi, L. Chromosome-level assembly and analysis of the *Thymus* genome provide insights into glandular secretory trichome formation and monoterpenoid biosynthesis in thyme. *Plant Community* **2022**, *3*, 100413. [CrossRef]
10. Tohidi, B.; Rahimmalek, M.; Arzani, A.; Trindade, H. Sequencing and variation of terpene synthase gene (TPS2) as the major gene in biosynthesis for thymol in different *Thymus* Species. *Phytochemistry* **2020**, *169*, 112126. [CrossRef]
11. Lima, A.S.; Schimmel, J.; Lukas, B.; Novak, J.; Barroso, J.G.; Figueiredo, A.C.; Pedro, L.G.; Degenhardt, J.; Trindade, H. Genomic characterization, molecular cloning and expression analysis of two terpene synthases from *Thymus caespititius* (Lamiaceae). *Planta* **2013**, *238*, 191–204. [CrossRef] [PubMed]
12. Vrbková, E.; Šímová, A.; Vyskocilová, E.; Lhotka, M.; Cervený, L. Acid Treated Montmorillonite—Eco-Friendly Clay as Catalyst in Carvone Isomerization to Carvacrol. *Reactions* **2021**, *2*, 486–498. [CrossRef]
13. Phillips, M. The sulfonation of *para*-cymene. *J. Am. Chem. Soc.* **1924**, *46*, 686–694. [CrossRef]
14. Ritter, J.J.; Ginsburg, D. Preparation of chlorination of alpha-pinene with *tert*-butyl hypochlorite. *J. Am. Chem. Soc.* **1950**, *72*, 2381–2384. [CrossRef]
15. De Vincenzi, M.; Stammati, A.; de Vincenzi, A.; Silano, M. Constituents of aromatic plants: Carvacrol. *Fitoterapia* **2004**, *75*, 801–804. [CrossRef]
16. Melo, C.I.; Bogel-Łukasik, R.; Bogel-Łukasik, E. Combination of supercritical carbon dioxide and ionic liquid in a novel assembly of carvacrol. *J. Supercrit. Fluids* **2012**, *61*, 191–198. [CrossRef]

17. Salehi, B.; Mishra, A.P.; Shukla, I.; Sharifi-Rad, M.; Contreras, M.D.M.; Segura-Carretero, A.; Fathi, H.; Nasri Nasrabadi, N.; Kobarfard, F.; Sharifi-Rad, J. Thymol, thyme, and other plant sources: Health and potential uses. *Phytother. Res.* **2018**, *32*, 1688–1706. [CrossRef]

18. Xu, H.; Delling, M.; Jun, J.C.; Clapham, D.E. Oregano, thyme and clove-derived flavors and skin sensitizers activate specific TRP channels. *Nat. Neurosci.* **2006**, *9*, 628–635. [CrossRef]

19. Park, B.S.; Choi, W.S.; Kim, J.H.; Kim, K.H.; Lee, S.E. Monoterpenes from thyme (*Thymus vulgaris*) as potential mosquito repellents. *J. Am. Mosq. Control Assoc.* **2005**, *21*, 80–83. [CrossRef]

20. Azizi, Z.; Majlessi, N.; Choopani, S.; Naghdi, N. Neuroprotective effects of carvacrol against Alzheimer's disease and other neurodegenerative diseases: A review. *Avicenna J. Phytomed.* **2022**, *12*, 371.

21. Pelvan, E.; Karaoğlu, Ö.; Fırat, E.Ö.; Kalyon, K.B.; Ros, E.; Alasalvar, C. Immunomodulatory effects of selected medicinal herbs and their essential oils: A comprehensive review. *J. Funct. Foods* **2022**, *94*, 105108. [CrossRef]

22. Chen, Y.; Ba, L.; Huang, W.; Liu, Y.; Pan, H.; Mingyao, E.; Shi, P.; Wang, Y.; Li, S.; Qi, H. Role of carvacrol in cardioprotection against myocardial ischemia/reperfusion injury in rats through activation of MAPK/ERK and Akt/eNOS signaling pathways. *Eur. J. Pharmacol.* **2017**, *796*, 90–100. [CrossRef] [PubMed]

23. Sampaio, L.A.; Pina, L.T.S.; Serafini, M.R.; Tavares, D.D.S.; Guimaraes, A.G. Antitumor effects of carvacrol and thymol: A systematic review. *Front. Pharmacol.* **2021**, *12*, 702487. [CrossRef] [PubMed]

24. Bouhtit, F.; Najar, M.; Moussa Agha, D.; Melki, R.; Najimi, M.; Sadki, K.; Boukhatem, N.; Bron, D.; Meuleman, N.; Hamal, A.; et al. New Anti-Leukemic Effect of Carvacrol and Thymol Combination through Synergistic Induction of Different Cell Death Pathways. *Molecules* **2021**, *26*, 410. [CrossRef]

25. Ahmad, A.; Saeed, M.; Ansari, I.A. Molecular insights on chemopreventive and anticancer potential of carvacrol: Implications from solid carcinomas. *J. Food Biochem.* **2021**, *45*, e14010. [CrossRef]

26. Guimarães, A.G.; Silva, F.V.; Xaviera, M.A.; Santos, M.R.V.; Rita, C.M.; Oliveira, R.C.M.; Oliveira, M.G.B.; Oliveira, A.P.; de Souza, C.C.; Quintans-Júnior, L.J. Orofacial Analgesic-Like Activity of Carvacrol in Rodents. *Z. Naturforsch.* **2012**, *67*, 481–485. [CrossRef]

27. Quintans-Junior, L.J.; Guimaraes, A.G.; Araujo, B.E.S.; Oliveira, G.F.; Santana, M.T.; Moreira, F.V.; Santos, M.R.V.; Cavalcanti, S.C.H.; Junior, W.D.L.; Botelho, M.A. Carvacrol, (−)-borneol and citral reduce convulsant activity in rodents. *Afr. J. Biotechnol.* **2010**, *9*, 6566–6572.

28. Anaeigoudari, A. Hepato-and reno-protective effects of thymoquinone, crocin, and carvacrol: A comprehensive review. *Asian Pac J. Trop. Biomed.* **2022**, *12*, 185. [CrossRef]

29. Khazdair, M.R.; Ghorani, V.; Boskabady, M.H. Experimental and clinical evidence on the effect of carvacrol on respiratory, allergic, and immunologic disorders: A comprehensive review. *BioFactors* **2022**, *48*, 779–794. [CrossRef]

30. Imran, M.; Aslam, M.; Alsagaby, S.A.; Saeed, F.; Ahmad, I.; Afzaal, M.; Arshad, M.U.; Abdelgawad, M.A.; El-Ghorab, A.H.; Khames, A.; et al. Therapeutic application of carvacrol: A comprehensive review. *Food Sci. Nutr.* **2022**, *10*, 3544–3561. [CrossRef]

31. Wang, P.; Wu, Y. A review on colloidal delivery vehicles using carvacrol as a model bioactive compound. *Food Hydrocoll.* **2021**, *120*, 106922. [CrossRef]

32. Domingos, E.L.; Vilhena, R.O.; Santos, J.M.; Fachi, M.M.; Böger, B.; Adam, L.M.; Tonin, F.S.; Pontarolo, R. Comparative efficacy and safety of systemic antifungal agents for candidemia: A systematic review with network meta-analysis and multicriteria acceptability analyses. *Int. J. Antimicrob. Agents* **2022**, *60*, 106614. [CrossRef] [PubMed]

33. Nobile, C.J.; Johnson, A.D. *Candida albicans* biofilms and human disease. *Annu. Rev. Microbiol.* **2015**, *69*, 71. [CrossRef] [PubMed]

34. Lepak, A.; Andes, D. Fungal sepsis: Optimizing antifungal therapy in the critical care setting. *Crit Care Clin.* **2011**, *27*, 123–147. [CrossRef]

35. Jafri, H.; Ahmad, I. *Thymus vulgaris* essential oil and thymol inhibit biofilms and interact synergistically with antifungal drugs against drug resistant strains of *Candida albicans* and *Candida tropicalis*. *J. Mycol. Med.* **2020**, *30*, 100911. [CrossRef] [PubMed]

36. Niu, C.; Wang, C.; Yang, Y.; Chen, R.; Zhang, J.; Chen, H.; Zhuge, Y.; Li, J.; Cheng, J.; Xu, K. Carvacrol induces *Candida albicans* apoptosis associated with Ca^{2+}/calcineurin pathway. *Front. Cell. Infect. Microbiol.* **2020**, *10*, 192. [CrossRef]

37. Miranda-Cadena, K.; Marcos-Arias, C.; Mateo, E.; Aguirre-Urizar, J.M.; Quindós, G.; Eraso, E. In vitro activities of carvacrol, cinnamaldehyde and thymol against *Candida* biofilms. *Biomed. Pharmacother.* **2021**, *143*, 112218. [CrossRef]

38. Ismail, M.; Srivastava, V.; Marimani, M.; Ahmad, A. Carvacrol modulates the expression and activity of antioxidant enzymes in *Candida auris*. *Res. Microbiol.* **2022**, *173*, 103916. [CrossRef]

39. Nóbrega, J.R.; Sousa, P.M.S.; de Lira Mota, K.S.; Cordeiro, L.V.; de Andrade Júnior, F.P.; de Oliveira, W.A. Antifungal activity of carvacrol and antifungal agent combinations against non-albicans *Candida* species. *Sci. Plena* **2019**, *15*, 1–7. [CrossRef]

40. Mauriello, E.; Ferrari, G.; Donsì, F. Effect of formulation on properties, stability, carvacrol release and antimicrobial activity of carvacrol emulsions. *Colloids Surf. B Biointerfaces* **2021**, *197*, 111424. [CrossRef]

41. Fouad, A.M.; Ruan, D.; El-Senousey, H.K.; Chen, W.; Jiang, S.; Zheng, C. Harmful effects and control strategies of aflatoxin b1 produced by *Aspergillus flavus* and *Aspergillus parasiticus* strains on poultry. *Toxins* **2019**, *11*, 176. [CrossRef] [PubMed]

42. Thompson, D.P. Influence of pH on the fungitoxic activity of naturally occurring compounds. *J. Food Protect.* **1990**, *53*, 428–429. [CrossRef] [PubMed]

43. Qu, C.; Li, Z.; Wang, X. UHPLC-HRMS-Based Untargeted Lipidomics Reveal Mechanism of Antifungal Activity of Carvacrol against *Aspergillus flavus*. *Foods* **2022**, *11*, 93. [CrossRef] [PubMed]

44. Rodrigues, M.L. The multifunctional fungal ergosterol. *MBio* **2018**, *9*, e01755-18. [CrossRef]
45. Alcazar-Fuoli, L.; Mellado, E. Ergosterol biosynthesis in *Aspergillus fumigatus*: Its relevance as an antifungal target and role in antifungal drug resistance. *Front. Microbiol.* **2012**, *3*, 439. [CrossRef]
46. Cruz, R.; Wuest, W.M. Beyond ergosterol: Strategies for combatting antifungal resistance in *Aspergillus fumigatus* and *Candida auris*. *Tetrahedron* **2023**, *133*, 133268. [CrossRef]
47. Rodriguez-Cuenca, S.; Pellegrinelli, V.; Campbell, M.; Oresic, M.; Vidal-Puig, A. Sphingolipids and glycerophospholipids—The "ying and yang" of lipotoxicity in metabolic diseases. *Prog. Lipid Res.* **2017**, *66*, 14–29. [CrossRef]
48. Fonseca, L.M.; Souza, E.J.D.; Radünz, M.; Gandra, E.A.; da Rosa Zavareze, E.; Dias, A.R.G. Suitability of starch/carvacrol nanofibers as biopreservatives for minimizing the fungal spoilage of bread. *Carbohydr. Polym.* **2021**, *252*, 117166. [CrossRef]
49. Liu, Q.; Qiao, K.; Zhang, S. Potential of a small molecule carvacrol in management of vegetable diseases. *Molecules* **2019**, *24*, 1932. [CrossRef]
50. Wang, K.; Jiang, S.; Pu, T.; Fan, L.; Su, F.; Ye, M. Antifungal activity of phenolic monoterpenes and structure-related compounds against plant pathogenic fungi. *Nat. Prod. Res.* **2019**, *33*, 1423–1430. [CrossRef]
51. Roca-Couso, R.; Flores-Félix, J.D.; Rivas, R. Mechanisms of action of microbial biocontrol agents against *Botrytis cinerea*. *J. Fungi* **2021**, *7*, 1045. [CrossRef] [PubMed]
52. Zhang, J.; Ma, S.; Du, S.; Chen, S.; Sun, H. Antifungal activity of thymol and carvacrol against postharvest pathogens *Botrytis cinerea*. *J. Food Sci. Technol.* **2019**, *56*, 2611–2620. [CrossRef] [PubMed]
53. Yan, J.; Zhang, J.; Hu, C.; Deng, L.; Ritenour, M.A. Use of carvacrol and thymol in shellac coating to control stem-end rot on 'Ruby Red' grapefruit and maintain fruit quality during simulated storage and marketing. *Sci. Hortic.* **2020**, *272*, 109606. [CrossRef]
54. Xiao, L.; Kang, S.; Lapu, M.; Jiang, P.; Wang, X.; Liu, D.; Li, J.; Liu, M. Preparation and characterization of chitosan/pullulan film loading carvacrol for targeted antibacterial packaging of chilled meat. *Int. J. Biol. Macromol.* **2022**, *211*, 140–149. [CrossRef] [PubMed]
55. Huang, Z.; Nazifi, S.; Hakimian, A.; Firuznia, R.; Ghasemi, H. "Built to Last": Plant-based Eco-friendly Durable Antibacterial Coatings. *ACS Appl. Mater. Interfaces* **2022**, *14*, 43681–43689. [CrossRef]
56. Walczak, M.; Michalska-Sionkowska, M.; Olkiewicz, D.; Tarnawska, P.; Warżyńska, O. Potential of carvacrol and thymol in reducing biofilm formation on technical surfaces. *Molecules* **2021**, *26*, 2723. [CrossRef] [PubMed]
57. Mechmechani, S.; Gharsallaoui, A.; Karam, L.; El Omari, K.; Fadel, A.; Hamze, M.; Chihib, N.E. Pepsin and Trypsin Treatment Combined with Carvacrol: An Efficient Strategy to Fight Pseudomonas aeruginosa and *Enterococcus faecalis* Biofilms. *Microorganisms* **2023**, *11*, 143. [CrossRef]
58. Avire, N.J.; Whiley, H.; Ross, K. A Review of *Streptococcus pyogenes*: Public health risk factors, prevention and control. *Pathogens* **2021**, *10*, 248. [CrossRef]
59. Wijesundara, N.M.; Lee, S.F.; Rupasinghe, H.V. Carvacrol inhibits *Streptococcus pyogenes* biofilms by suppressing the expression of genes associated with quorum-sensing and reducing cell surface hydrophobicity. *Microb. Pathog.* **2022**, *169*, 105684. [CrossRef]
60. Luna, M.; Beltran, O.; Encinas-Basurto, D.A.; Ballesteros-Monrreal, M.G.; Topete, A.; Hassan, N.; López-Mata, M.A.; Reyes-Márquez, V.; Valdez, M.A.; Juarez, J. High antibacterial performance of hydrophobic chitosan-based nanoparticles loaded with Carvacrol. *Colloids Surf. B Biointerfaces* **2022**, *209*, 112191. [CrossRef]
61. Cui, H.; Lu, J.; Li, C.; Rashed, M.M.; Lin, L. Antibacterial and physical effects of cationic starch nanofibers containing carvacrol@ casein nanoparticles against *Bacillus cereus* in soy products. *Int. J. Food Microbiol.* **2022**, *364*, 109530. [CrossRef] [PubMed]
62. Mechmechani, S.; Gharsallaoui, A.; Fadel, A.; El Omari, K.; Khelissa, S.; Hamze, M.; Chihib, N.E. Microencapsulation of carvacrol as an efficient tool to fight *Pseudomonas aeruginosa* and *Enterococcus faecalis* biofilms. *PLoS ONE* **2022**, *17*, e0270200. [CrossRef]
63. Yammine, J.; Gharsallaoui, A.; Fadel, A.; Mechmechani, S.; Karam, L.; Ismail, A.; Chihib, N.E. Enhanced antimicrobial, antibiofilm and ecotoxic activities of nanoencapsulated carvacrol and thymol as compared to their free counterparts. *Food Control* **2023**, *143*, 109317. [CrossRef]
64. Fang, S.; Zhou, Q.; Hu, Y.; Liu, F.; Mei, J.; Xie, J. Antimicrobial carvacrol incorporated in flaxseed gum-sodium alginate active films to improve the quality attributes of Chinese sea bass (*Lateolabrax maculatus*) during cold storage. *Molecules* **2019**, *24*, 3292. [CrossRef] [PubMed]
65. De Souza, G.H.D.A.; dos Santos Radai, J.A.; Mattos Vaz, M.S.; Esther da Silva, K.; Fraga, T.L.; Barbosa, L.S.; Simionatto, S. In vitro and in vivo antibacterial activity assays of carvacrol: A candidate for development of innovative treatments against KPC-producing *Klebsiella pneumoniae*. *PLoS ONE* **2021**, *16*, e0246003. [CrossRef]
66. Khan, I.; Bahuguna, A.; Shukla, S.; Aziz, F.; Chauhan, A.K.; Ansari, M.B.; Bajpai, V.K.; Huh, Y.S.; Kang, S.C. Antimicrobial potential of the food-grade additive carvacrol against uropathogenic *E. coli* based on membrane depolarization, reactive oxygen species generation, and molecular docking analysis. *Microb. Pathog.* **2020**, *142*, 104046. [CrossRef] [PubMed]
67. Jiang, S.; Zhang, J.; Yang, Q.; Sun, D.; Pu, X.; Shen, H.; Li, Q.; Wang, Z.; Lin, B. Antimicrobial activity of natural plant compound carvacrol against soft rot disease agent *Dickeya zeae*. *Curr. Microbiol.* **2021**, *78*, 3453–3463. [CrossRef]
68. Kasthuri, T.; Swetha, T.K.; Bhaskar, J.P.; Pandian, S.K. Rapid-killing efficacy substantiates the antiseptic property of the synergistic combination of carvacrol and nerol against nosocomial pathogens. *Arch. Microbiol.* **2022**, *204*, 590. [CrossRef]
69. Sousa, L.G.V.; Castro, J.; Cavaleiro, C.; Salgueiro, L.; Tomás, M.; Palmeira-Oliveira, R.; Martinez-Oliveira, J.; Cerca, N. Synergistic Effects of Carvacrol, α-Terpinene, γ-Terpinene, p-Cymene and Linalool against *Gardnerella* Species. *Sci. Rep.* **2022**, *12*, 4417. [CrossRef]

70. Li, Q.; Yu, S.; Han, J.; Wu, J.; You, L.; Shi, X.; Wang, S. Synergistic antibacterial activity and mechanism of action of nisin/carvacrol combination against *Staphylococcus aureus* and their application in the infecting pasteurized milk. *Food Chem.* **2022**, *380*, 132009. [CrossRef]

71. Churklam, W.; Chaturongakul, S.; Ngamwongsatit, B.; Aunpad, R. The mechanisms of action of carvacrol and its synergism with nisin against *Listeria monocytogenes* on sliced bologna sausage. *Food Control* **2020**, *108*, 106864. [CrossRef]

72. Wu, M.; Dong, Q.; Ma, Y.; Yang, S.; Aslam, M.Z.; Liu, Y.; Li, Z. Potential antimicrobial activities of probiotics and their derivatives against *Listeria monocytogenes* in food field: A review. *Food Res. Int.* **2022**, *160*, 111733. [CrossRef] [PubMed]

73. Gao, L.; Hu, Y.; Sun, M.L.; Zheng, X.F.; Yang, M.; Rao, S.Q. Synergistic antibacterial effects of carvacrol and ε-polylysine. *Qual. Assur. Saf. Crops Foods* **2021**, *13*, 13–23. [CrossRef]

74. Yoshida, T.; Nagasawa, T. ε-Poly-L-lysine: Microbial production, biodegradation and application potential. *Appl. Microbiol. Biotechnol.* **2003**, *62*, 21–26. [CrossRef] [PubMed]

75. Li, Y.Q.; Han, Q.; Feng, J.L.; Tian, W.L.; Mo, H.Z. Antibacterial characteristics and mechanisms of ε-poly-lysine against *Escherichia coli* and *Staphylococcus aureus*. *Food Control* **2014**, *43*, 22–27. [CrossRef]

76. Addo, K.A.; Li, H.; Yu, Y.; Xiao, X. Unraveling the mechanism of the synergistic antimicrobial effect of cineole and carvacrol on *Escherichia coli* O157: H7 inhibition and its application on fresh-cut cucumbers. *Food Control* **2023**, *144*, 109339. [CrossRef]

77. Fan, L.; Ismail, B.B.; Gao, L.; Liu, D. Comparison of high-and low-frequency thermosonication and carvacrol treatments of carrot juice: Microbial inactivation and quality retention. *Appl. Food Res.* **2022**, *2*, 100162. [CrossRef]

78. Liu, Q.; Zhou, Y.H.; Yang, Z.Q. The cytokine storm of severe influenza and development of immunomodulatory therapy. *Cell. Mol. Immunol.* **2016**, *13*, 3–10. [CrossRef]

79. Nedeva, C.; Menassa, J.; Puthalakath, H. Sepsis: Inflammation is a necessary evil. *Front. Cell Dev. Biol.* **2019**, *7*, 108. [CrossRef]

80. Hafezi, B.; Chan, L.; Knapp, J.P.; Karimi, N.; Alizadeh, K.; Mehrani, Y.; Bridle, B.W.; Karimi, K. Cytokine storm syndrome in SARS-CoV-2 infections: A functional role of mast cells. *Cells* **2021**, *10*, 1761. [CrossRef]

81. Al-Mansori, B.; El-Ageeli, W.H.; Alsagheer, S.H.; Ben-Khayal, F.A. Antioxidant Activity-Synergistic Effects of Thymol and Carvacrol. *Al-Mukhtar J. Sci.* **2020**, *35*, 185–194. [CrossRef]

82. Mahtaj, L.G.; Feizpour, A.; Kianmehr, M.; Soukhtanloo, M.; Boskabady, M.H. The effect of carvacrol on systemic inflammation in Guinea pigs model of {COPD} induced by cigarette smoke exposure. *Pharmacol. Rep.* **2015**, *67*, 140–145. [CrossRef] [PubMed]

83. Del Rio, D.; Stewart, A.J.; Pellegrini, N. A review of recent studies on malondialdehyde as toxic molecule and biological marker of oxidative stress. *Nutr. Metab. Cardiovasc. Dis.* **2005**, *15*, 316–328. [CrossRef]

84. Carvalho, F.O.; Silva, R.; Nunes, P.S.; Felipe, F.A.; Ramos, K.P.P.; Ferreira, L.A.S.; Lima, V.N.B.; Shanmugam, S.; Oliveira, A.S.; Guterres, S.S.; et al. Effects of the solid lipid nanoparticle of carvacrol on rodents with lung injury from smoke inhalation. Naunyn-Schmiedeberg's. *Arch. Pharmacol.* **2019**, *393*, 445–455. [CrossRef] [PubMed]

85. Cicalău, G.; Babes, P.; Calniceanu, H.; Popa, A.; Ciavoi, G.; Iova, G.; Ganea, M.; Scrobotă, I. Anti-Inflammatory and Antioxidant Properties of Carvacrol and Magnolol, in Periodontal Disease and Diabetes Mellitus. *Molecules* **2021**, *26*, 6899. [CrossRef] [PubMed]

86. Shoorei, H.; Khaki, A.; Khaki, A.A.; Hemmati, A.A.; Moghimian, M.; Shokoohi, M. The ameliorative effect of carvacrol on oxidative stress and germ cell apoptosis in testicular tissue of adult diabetic rats. *Biomed. Pharmacother.* **2019**, *111*, 568–578. [CrossRef]

87. Da Silva Lima, M.; Quintans-Júnior, L.J.; de Santana, W.A.; Martins Kaneto, C.; Pereira Soares, M.B.; Villarreal, C.F. Antiinflammatory effects of carvacrol: Evidence for a key role of interleukin-10. *Eur. J. Pharm.* **2013**, *699*, 112–117. [CrossRef]

88. Silva, F.V.; Guimaraes, A.G.; Silva, E.R.; Sousa-Neto, B.P.; Machado, F.D.; Quintans-Junior, L.J.; Arcanjo, D.D.; Oliveira, F.A.; Oliveira, R.C. Anti-inflammatory and anti-ulcer activities of carvacrol, a monoterpene present in the essential oil of oregano. *J. Med. Food* **2012**, *15*, 984–991. [CrossRef]

89. De Santana Souza, M.T.; Teixeira, D.F.; de Oliveira, J.P.; Oliveira, A.S.; Quintans-Junior, L.J.; Correa, C.B.; Camargo, E.A. Protective effect of carvacrol on acetic acid-induced colitis. *Biomed. Pharmacother.* **2017**, *96*, 313–319. [CrossRef]

90. Araruna, M.E.; Serafim, C.; Alves Júnior, E.; Hiruma-Lima, C.; Diniz, M.; Batista, L. Intestinal anti-inflammatory activity of terpenes in experimental models (2010–2020): A review. *Molecules* **2020**, *25*, 5430. [CrossRef]

91. Wijesundara, N.M.; Lee, S.F.; Davidson, R.; Cheng, Z.; Rupasinghe, H.P.V. Carvacrol Suppresses Inflammatory Biomarkers Production by Lipoteichoic Acid- and Peptidoglycan-Stimulated Human Tonsil Epithelial Cells. *Nutrients* **2022**, *14*, 503. [CrossRef] [PubMed]

92. Vecchio, A.J.; Simmons, D.M.; Malkowski, M.G. Structural basis of fatty acid substrate binding to cyclooxygenase-2. *J. Biol. Chem.* **2010**, *285*, 22152–22163. [CrossRef] [PubMed]

93. Jalalvand, M.; Shahsavari, G.; Sheikhian, A.; Ganji, A.; Mosayebi, G. In vitro anti-inflammatory effects of *Satureja khuzestanica* essential oil compared to carvacrol. *Int. J. Basic Sci. Med.* **2020**, *5*, 61–65. [CrossRef]

94. Landa, P.; Kokoska, L.; Pribylova, M.; Vanek, T.; Marsik, P. In vitro Anti-inflammatory Activity of Carvacrol: Inhibitory Effect on COX-2 Catalyzed Prostaglandin E2 Biosynthesis. *Arch. Pharm. Res.* **2009**, *32*, 75–78. [CrossRef]

95. Hotta, M.; Nakata, R.; Katsukawa, M.; Hori, K.; Takahashi, S.; Inoue, H. Carvacrol, a component of thyme oil, activates PPARα and γ and suppresses COX-2 expression. *J. Lipid Res.* **2010**, *51*, 132–139. [CrossRef] [PubMed]

96. Naeem, K.; Al Kury, L.T.; Nasar, F.; Alattar, A.; Alshaman, R.; Shah, F.A.; Khan, A.; Li, S. Natural dietary supplement, carvacrol, alleviates LPS-induced oxidative stress, neurodegeneration, and depressive-like behaviors via the Nrf2/HO-1 pathway. *J. Inflamm. Res.* **2021**, *14*, 1313. [CrossRef] [PubMed]

97. Basauri, A.; González-Fernández, C.; Fallanza, M.; Bringas, E.; Fernandez-Lopez, R.; Giner, L.; Moncalián, G.; De, L.; Ortiz, I. Biochemical interactions between LPS and LPS-binding molecules. *Crit. Rev. Biotechnol.* **2020**, *40*, 292–305. [CrossRef] [PubMed]

98. Liu, T.; Zhang, L.; Joo, D.; Sun, S.C. NF-κB signaling in inflammation. *Signal Transduct. Target. Ther.* **2017**, *2*, 17023. [CrossRef] [PubMed]

99. Kelley, N.; Jeltema, D.; Duan, Y.H.; He, Y. The NLRP3 Inflammasome: An Overview of Mechanisms of Activation and Regulation. *Int. J. Mol. Sci.* **2019**, *20*, 3328. [CrossRef]

100. Kawai, T.; Takeuchi, O.; Fujita, T.; Inoue, J.; Muhlradt, P.F.; Sato, S.; Hoshino, K.; Akira, S. Lipopolysaccharide stimulates the MyD88-independent pathway and results in activation of IFN-regulatory factor 3 and the expression of a subset of lipopolysaccharide-inducible genes. *J. Immunol.* **2001**, *167*, 5887–5894. [CrossRef]

101. Pfalzgraff, A.; Weindl, G. Intracellular lipopolysaccharide sensing as a potential therapeutic target for sepsis. *Trends Pharmacol. Sci.* **2019**, *40*, 187–197. [CrossRef] [PubMed]

102. Marconi, G.D.; della Rocca, Y.; Fonticoli, L.; Guarnieri, S.; Carradori, S.; Rajan, T.S.; Pizzicannella, J.; Diomede, F. The Beneficial Effect of Carvacrol in HL-1 Cardiomyocytes Treated with LPS-G: Anti-Inflammatory Pathway Investigations. *Antioxidants* **2022**, *11*, 386. [CrossRef] [PubMed]

103. Kianmehr, M.; Rezaei, A.; Boskabady, M.H. Effect of carvacrol on various cytokines genes expression in splenocytes of asthmatic mice. *Iran. J. Basic Med. Sci.* **2016**, *19*, 402–410. [PubMed]

104. Somensi, N.; Rabelo, T.K.; Guimaraes, A.G.; Quintans-Junior, L.J.; de Souza Araújo, A.A.; Moreira, J.C.F.; Gelain, D.P. Carvacrol suppresses LPS-induced pro-inflammatory activation in RAW 264.7 macrophages through ERK1/2 and NF-κB pathway. *Int. Immunopharmacol.* **2019**, *75*, 105743. [CrossRef] [PubMed]

105. Cui, J.; Chen, Y.; Wang, H.Y.; Wang, R.F. Mechanisms and pathways of innate immune activation and regulation in health and cancer. *Hum. Vaccines Immunother.* **2014**, *10*, 3270–3285. [CrossRef]

106. Guimarães, A.G.; Oliveira, G.F.; Melo, M.S.; Cavalcanti, S.C.; Antoniolli, A.R.; Bonjardim, L.R.; Quintans-Júnior, L.J. Bioassay-guided evaluation of antioxidant and antinociceptive activities of carvacrol. *Basic Clin. Pharmacol. Toxicol.* **2010**, *107*, 949–957. [CrossRef]

107. Wan, Q.; Song, D.; Li, H.; He, M.L. Stress proteins: The biological functions in virus infection, present and challenges for target-based antiviral drug development. *Signal Transduct. Target. Ther.* **2020**, *5*, 125. [CrossRef]

108. Wieten, L.; van der Zee, R.; Goedemans, R.; Sijtsma, J.; Serafini, M.; Lubsen, N.H.; van Eden, W.; Broere, F. Hsp70 expression and induction as a readout for detection of immune modulatory components in food. *Cell Stress Chaperones* **2010**, *15*, 25–37. [CrossRef]

109. Wieten, L.; van der Zee, R.; Spiering, R.; Wagenaar-Hilbers, J.; van Kooten, P.; Broere, F.; van Eden, W. A novel heat-shock protein coinducer boosts stress protein Hsp70 to activate T cell regulation of inflammation in autoimmune arthritis. *Arthritis Rheum.* **2010**, *62*, 1026–1035. [CrossRef]

110. Ghorani, V.; Alavinezhad, A.; Rajabi, O.; Mohammadpour, A.H.; Boskabady, M.H. Safety and tolerability of carvacrol in healthy subjects: A phase I clinical study. *Drug Chem. Toxicol.* **2021**, *44*, 177–189. [CrossRef]

111. Wang, Q.; Gong, J.; Huang, X.; Yu, H.; Xue, F. In vitro evaluation of the activity of microencapsulated carvacrol against *Escherichia coli* with K88 pili. *J. Appl. Microbiol.* **2009**, *107*, 1781–1788. [CrossRef] [PubMed]

112. Dong, R.H.; Fang, Z.Z.; Zhu, L.L.; Ge, G.B.; Cao, Y.F.; Li, X.B.; Hu, C.M.; Yang, L.; Liu, Z.Y. Identification of CYP isoforms involved in the metabolism of thymol and carvacrol in human liver microsomes (HLMs). *Pharmazie* **2012**, *67*, 1002–1006. [PubMed]

113. Aristatile, B.; Al-Assafa, A.H.; Pugalendi, K.V. Carvacrol ameliorates the Ppar-A and cytochrome P450 expression on d-galactosamine induced hepatotoxicity rats. *Afr. J. Tradit. Complement. Altern. Med.* **2014**, *11*, 118–123. [CrossRef] [PubMed]

114. Hagan, E.C.; Hansen, W.H.; Fitzhugh, O.G.; Jenner, P.M.; Jones, W.I.; Taylor, J.M.; Long, E.L.; Nelson, A.A.; Brouwer, J.B. Food flavourings and compounds of related structure. II. Subacute and chronic toxicity. *Food Cosmet. Toxicol.* **1967**, *5*, 141–157. [CrossRef] [PubMed]

115. Andersen, A. Final report on the safety assessment of sodium *p*-chloro-*m*-cresol, *p*-chloro-*m*-cresol, chlorothymol, mixed cresols, *m*-cresol, *o*-cresol, *p*-cresol, isopropyl cresols, thymol, *o*-cymen-5-ol, and carvacrol. *Int. J. Toxicol.* **2006**, *25*, 29–127. [PubMed]

116. Livingston, A.E. The comparative toxicity of thymol and carvacrol (isothymol). *Public Health Rep.* **1921**, *36*, 1317–1331. [CrossRef]

117. Schroder, V.; Vollmer, H. Über die Ausscheidung von Thymol, Carvacrol, Eugenol und Guajacol und die Verteilung dieser Substanzen im Organismus. *Arch. Exp. Pathol. Pharmak.* **1932**, *168*, 331–353. [CrossRef]

118. Austgulen, L.T.; Solheim, E.; Scheline, R.R. Metabolism in rats of *p*-cymene derivatives: Carvacrol and thymol. *Pharmacol. Toxicol.* **1987**, *61*, 98–102. [CrossRef]

119. De Alvarenga, J.F.R.; Genaro, B.; Costa, B.L.; Purgatto, E.; Manach, C.; Fiamoncini, J. Monoterpenes: Current knowledge on food source, metabolism, and health effects. *Crit. Rev. Food Sci. Nutr.* **2021**, *13*, 1352–1389. [CrossRef]

120. Herber, R.; Lepage, M.; Pierfitte, M.; Villoutreix, J. Metabolism of some phenol derivatives in *Mucor hiemalis*. *Compt. Rend. Sean. Soc. Biol. Filial.* **1972**, *166*, 1087–1090.

121. Numpaque, M.A.; Oviedo, L.A.; Gil, J.H.; García, C.M.; Durango, D.L. Thymol and carvacrol: Biotransformation and antifungal activity against the plant pathogenic fungi *Colletotrichum acutatum* and *Botryodiplodia theobromae. Trop. Plant Pathol.* **2011**, *36*, 3–13. [CrossRef]

122. Noma, Y.; Asakawa, Y. Biotransformation of Monoterpenoids by Microorganisms, Insects, and Mammals. In *Handbook of Essential Oils: Science, Technology, and Applications*; Başer, K.H.C., Buchbauer, G., Eds.; CRC Press, Taylor and Francis Group: London, UK, 2010.

Article

Vernonia polyanthes Less. (Asteraceae Bercht. & Presl), a Natural Source of Bioactive Compounds with Antibiotic Effect against Multidrug-Resistant *Staphylococcus aureus*

Jordana Damasceno Gitirana de Santana [1], Oscar Alejandro Santos-Mayorga [1], Jônatas Rodrigues Florencio [1], Mirella Chrispim Cerqueira de Oliveira [1], Luísa Maria Silveira de Almeida [1], Julianna Oliveira de Lucas Xavier [1], Danielle Cristina Zimmermann-Franco [2], Gilson Costa Macedo [2], Adriana Lúcia Pires Ferreira [3], Orlando Vieira de Sousa [4], Ademar Alves da Silva Filho [4,*] and Maria Silvana Alves [4,*]

[1] Programa de Pós-Graduação em Ciências Farmacêuticas, Universidade Federal de Juiz de Fora, Rua José Lourenço Kelmer s/n, Campus Universitário, Bairro São Pedro, Juiz de Fora 36036-900, MG, Brazil
[2] Centro de Tecnologia Celular e Imunologia Aplicada (IMUNOCET), Departamento de Parasitologia, Microbiologia e Imunologia, Instituto de Ciências Biológicas, Universidade Federal de Juiz de Fora, Rua José Lourenço Kelmer s/n, Campus Universitário, Bairro São Pedro, Juiz de Fora 36036-900, MG, Brazil
[3] Hospital Universitário Clementino Fraga Filho, Universidade Federal do Rio de Janeiro, Rua Professor Rodolpho Paulo Rocco 255, Cidade Universitária, Ilha do Fundão, Rio de Janeiro 21941-913, RJ, Brazil
[4] Departamento de Ciências Farmacêuticas, Faculdade de Farmácia, Universidade Federal de Juiz de Fora, Rua José Lourenço Kelmer s/n, Campus Universitário, Bairro São Pedro, Juiz de Fora 36036-900, MG, Brazil
* Correspondence: ademar.alves@ufjf.br (A.A.d.S.F.); silvana.alves@ufjf.br (M.S.A.); Tel.: +55-32-2102-3893 (A.A.d.S.F. & M.S.A.); Fax: +55-32-2102-3812 (A.A.d.S.F. & M.S.A.)

Abstract: *Vernonia polyanthes* is a medicinal plant used to treat many disorders, including infectious diseases. This study investigated the chemical constituents and the antibacterial activity of *V. polyanthes* leaf rinse extract (Vp-LRE). The chemical characterization of Vp-LRE was established using ultra-high performance liquid chromatography coupled to quadrupole time-of-flight mass spectrometry (UHPLC/Q-TOF-MS), and glaucolide A was identified through ^{1}H and ^{13}C nuclear magnetic resonance (NMR) and mass fragmentation. The cytotoxicity was evaluated using 3-(4,5-dimethylthiazol-2-yl)-2,5-diphenyl tetrazolium bromide (MTT). The antibacterial activity was assessed by minimal inhibitory concentration and minimal bactericidal concentration. Interactions between ligands and beta-lactamase were evaluated via molecular docking. UHPLC/Q-TOF-MS detected acacetin, apigenin, chrysoeriol, isorhamnetin, isorhamnetin isomer, kaempferide, 3′,4′-dimethoxyluteolin, 3,7-dimethoxy-5,3′,4′-trihydroxyflavone, piptocarphin A and glaucolide A. Vp-LRE (30 µg/mL) and glaucolide A (10 and 20 µg/mL) were cytotoxic against RAW 264.7 cells. Glaucolide A was not active, but Vp-LRE inhibited the *Staphylococcus aureus*, methicillin-resistant *S. aureus* (MRSA), *Escherichia coli*, *Salmonella* Choleraesuis and Typhimurium, with a bacteriostatic effect. The compounds (glaucolide A, 3′,4′-dimethoxyluteolin, acacetin and apigenin) were able to interact with beta-lactamase, mainly through hydrogen bonding, with free energy between −6.2 to −7.5 kcal/mol. These results indicate that *V. polyanthes* is a potential natural source of phytochemicals with a significant antibiotic effect against MRSA strains.

Keywords: *Vernonia polyanthes*; flavonoids; glaucolide A; UHPLC/Q-TOF-MS; antibacterial activity; methicillin-resistant *Staphylococcus aureus*

1. Introduction

Infectious diseases are a major threat to human health and are responsible for high rates of morbidity and mortality. The treatment of these diseases is conducted with antibiotics that are often used irrationally, causing the emergence of microbial resistance (in addition to adverse effects) [1]. The declining effectiveness of antibiotics in treating bacterial infections worldwide is evident. The antimicrobial resistance in pathogenic bacteria has become

one of the most serious and complex public health problems of the 21st century [2] with worrying clinical and economic consequences for sanitary and health agencies [3].

In function of this alarming scenario, the World Health Organization (WHO) published the top 20 drug-resistant bacteria list at a global level, with critical (priority 1), high (priority 2) and medium (priority 3) priorities, requiring prompt action from the scientific research community to develop new antibiotics. *Escherichia coli* (carbapenem-resistant, 3rd generation cephalosporin-resistant) (priority 1), *Pseudomonas aeruginosa* (carbapenem resistant) (priority 1), *Staphylococcus aureus* [methicillin-resistant (MRSA), vancomycin intermediate (VISA) and resistant (VRSA)] (priority 2) and *Salmonella* spp. (fluoroquinolone-resistant) (priority 2) strains are major concerns [4]. In this sense, the research of new therapeutic agents represents a relevant strategy in the combat of infections caused by multidrug-resistant bacteria, including MRSA.

The antimicrobial properties of compounds produced by plants have been recognized since antiquity and have been scientifically investigated in the last decades, and several natural products are recognized as antibacterial agents [5–8]. This scientific framework associated with the development of new technologies justifies the renewed interest in the screening of natural products to discovery of new substances with antibacterial potential. Even with the lack of support from major pharmaceutical industries, natural products still show a substantial impact on the remedy discovery process [8]. Nowadays, among all substances approved as new antibacterial chemical entities, a significant percentage of them are natural compounds or their synthetic derivatives [7,8].

Vernonia polyanthes Less. (Asteraceae Bercht. & Presl family), commonly known in Brazil as "assa-peixe", occurs in South America and has been traditionally used mainly to treat infectious and inflammatory processes, as well as wounds, burns, respiratory system disorders, kidney dysfunctions and in an antimycobacterial capacity [9–11]. The therapeutic potential of *V. polyanthes* has been investigated, and its pharmacological activities, such as antihypertensive and diuretic [12], antileishmanial [13], antimycobacterial [11], antiulcerogenic [14], antinociceptive and anti-inflammatory [15], cytotoxic [16] and topical anti-inflammatory [17] effects have been reported. Although some reports about the antibacterial activities of *V. polyanthes* have been published [11,18–20], more investigations are necessary to establish the real antibacterial potential of this plant species, focusing on new antibiotics and new therapeutic approaches mainly to treat "untreatable" infectious diseases. Thus, in function of the medical importance in the last decades, it is relevant to research the antibacterial activity of *V. polyanthes* against multidrug-resistant clinical bacterial strains.

Based on the use of *V. polyanthes* leaves for the treatment of bacterial infectious diseases and the clinical relevance of resistant pathogens, the aim of this study was to evaluate the antibacterial activities of the leaf rinse extract of *V. polyanthes* (Vp-LRE) and its main compound glaucolide A against reference and clinical multidrug-resistant Gram-positive and Gram-negative bacterial strains.

2. Results

2.1. Production of the Extract of V. polyanthes

A crude extract of *V. polyanthes* was prepared by rinsing the leaves with dichloromethane. The rinsed leaves extract of *V. polyanthes* (Vp-LRE) was chosen for analysis since many bioactive compounds in *Vernonia* species (such as flavonoids and sesquiterpene lactones) are localized mainly at the glandular trichomes leaves [21–23].

In this present study, Vp-LRE was prepared and its antibacterial activity against ATCC® and clinical multidrug-resistant Gram-positive and Gram-negative bacterial strains was evaluated, which have not been reported in the literature.

2.2. Total Phenolic and Flavonoid Content Determinations

The total phenolic content of Vp-LRE was spectrophotometrically determined using Folin-Ciocalteu reagent, expressed as gallic acid equivalents (g GAE/100 g) and calculated from the calibrated curve ($r^2 = 0.9970$), while total flavonoid content was estimated using the

aluminum chloride method and expressed as rutin equivalents (g RE/100 g) ($r^2 = 0.9995$). In *V. polyanthes*, the values were 2.53 ± 0.01 g GAE/100 g (Vp-LRE) for phenols and 4.26 ± 0.04 g RE/100 g (Vp-LRE) for flavonoids.

2.3. Evaluation of the Chemical Composition of Vp-LRE by Ultra-High Performance Liquid Chromatography Coupled with Quadrupole Time-of-Flight Mass Spectrometry (UHPLC-MS-QTOF) Analysis

UHPLC-MS-QTOF analysis was applied for the qualitative chemical characterization of different metabolites in Vp-LRE. The components of Vp-LRE were separated and analyzed by UHPLC-MS-QTOF, and a typical UHPLC-MS-QTOF chromatogram of Vp-LRE, at negative ion mode, is shown in Figure 1. Glaucolide A and apigenin were identified and eight compounds were annotated, and detailed information of each peak is listed in Table 1. Peak annotation was based on each compound's molecular ions and its MS/MS studies (Table 1), as well as comparison with the available literature. The options with the lower mass error values and the higher MS scores useful for obtaining better confident formula assignments were preferable. The structures of the proposed compounds were tentatively annotated through studying the fragmentation pattern using MS/MS spectra. In addition, the retention time (Rt) served as criterion of polarity and elution order, which was used for the numbering of the compounds (Figure 1 and Table 1).

2.4. Isolation and Identification of Glaucolide A

As glaucolide A (1; Figure 2) was identified as one of the most representative compounds in Vp-LRE, it was isolated from the extract via chromatographic fractionation and additionally identified by ^{1}H- and ^{13}C-NMR data analysis in comparison to literature [24,25] ^{1}H NMR (500 MHz, CDCl$_3$) δ (ppm): 1.53 (3H; s, H-15); 1.64 (4H, s, H-3b and H-14); 1.92 (3H, q, J = 1.0 Hz, H-4′); 2.04 (3H, s, H-2″); 2.06 (3H, s, H-2″); 2.29 (2H, m, H-2b and H-3a); 2.59 (1H, m, H-9b); 2.79 (2H, m, H-5 and H-9a); 2.93 (1H, m, H-2a); 4.80 (3H, m, H-8, H-13a and H-13b); 4.89 (1H, d, J = 9.5 Hz, H-6); 5.69 (1H, t, J = 1.0 Hz, H-3′); 6.14 (1H, t, J = 1.0 Hz, H-3′). ^{13}C NMR (125 MHz, CDCl$_3$) δ (ppm): 18.0 (C-4′); 18.8 (C-14); 20.7 (C-15); 21.0 (C-2‴); 22.4 (C-2″); 31.8 (C-3); 32.8 (C-2); 40.3 (C-9); 55.0 (C-13); 58.7 (C-5); 61.4 (C-4); 64.4 (C-8); 80.8 (C-6); 84.7 (C-10); 125.0 (C-11); 127.8 (C-3′); 134.7 (C-2′); 163.3 (C-7); 166.2 (C-1′); 169.7 (C-12); 170.2 (C-1‴); 170.9 (C-1″); 206.6 (C-1). The purity of the isolated glaucolide A was estimated to be higher than 95% via HPLC-DAD analysis (Figure 2).
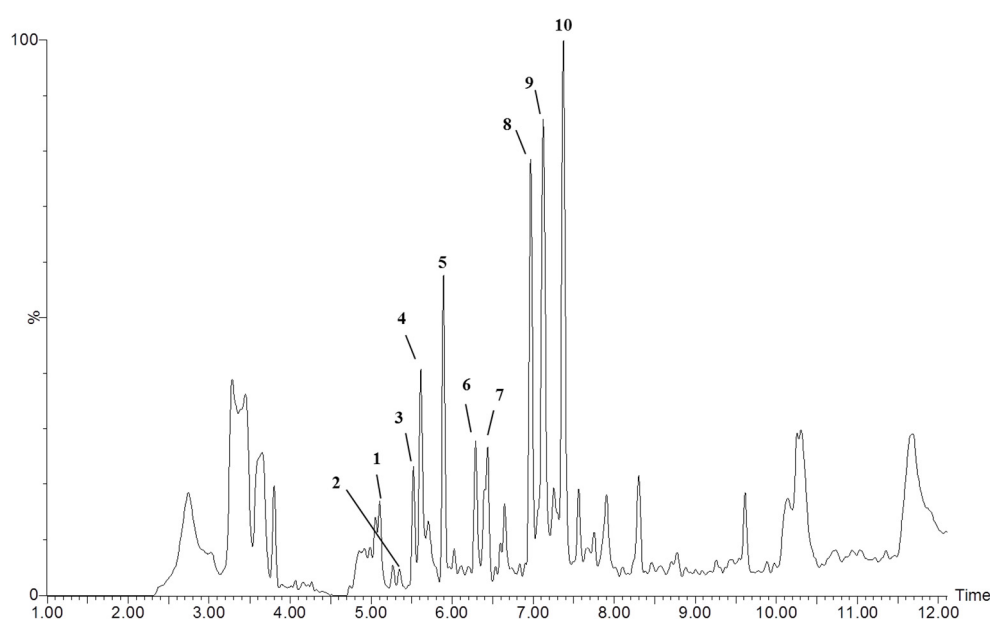

Figure 1. Representative UHPLC-ESI-QTOF-MS chromatogram of *V. polyanthes* leaf rinse extract (Vp-LRE) in the negative mode.

Table 1. Chemical characterization of *V. polyanthes* leaf rinse extract (Vp-LRE) by UHPLC-MS-QTOF.

Peak	Proposed Compound	Rt * (min)	*m/z* ** [M − H]⁻	Main Fragments	Molecular Formula	Score	Error (ppm)
1	Isorhamnetin [a]	5.10	315.0508	299.0956, 197.8085	$C_{16}H_{12}O_7$	99.30	1.0
2	Apigenin [a,b]	5.35	269.0453	197.8080, 162.8410, 116.9287	$C_{15}H_{10}O_5$	100.00	1.1
3	Chrysoeriol	5.52	299.0562	284.0324, 256.0370, 215.1287	$C_{16}H_{12}O_6$	99.64	1.3
4	Isorhamnetin isomer	5.61	315.0497	313.1101, 300.0261, 197.8059	$C_{16}H_{12}O_7$	99.94	−2.5
5	3,7-dimethoxy-5,3′, 4′-trihydroxyflavone [a]	5.89	329.0670	314.0431, 299.0193, 197.8086	$C_{17}H_{13}O_7$	99.80	2.7
6	Kaempferide	6.29	299.0549	284.0324, 197.8066, 116.9282	$C_{16}H_{12}O_6$	99.96	−2.3
7	Piptocarphin A [a]	6.44	457.1261 [M + Cl]⁻	441.1403, 327.1259, 197.8077, 117.9282	$C_{21}H_{26}O_9$	99.52	−0.9
8	Acacetin	6.97	283.0622	268.0374, 239.0346, 197.8082	$C_{16}H_{12}O_5$	99.96	8.1
9	3′,4′-dimethoxyluteolin [a]	7.12	313.0724	298.0485, 255.0300, 197.8088	$C_{17}H_{14}O_6$	98.26	3.8
10	Glaucolide A [a,b]	7.37	499.1384 [M + Cl]⁻	463.1617, 403.1399, 355.1585, 275.0925, 197.8084	$C_{23}H_{28}O_{10}$	99.76	2.6

* Retention time; ** Mass-to-charge Ratio; [a] Compounds previously reported in *Vernonia polyanthes* by Igual et al. (2013) [22]; [b] Confirmation with authentic standards.
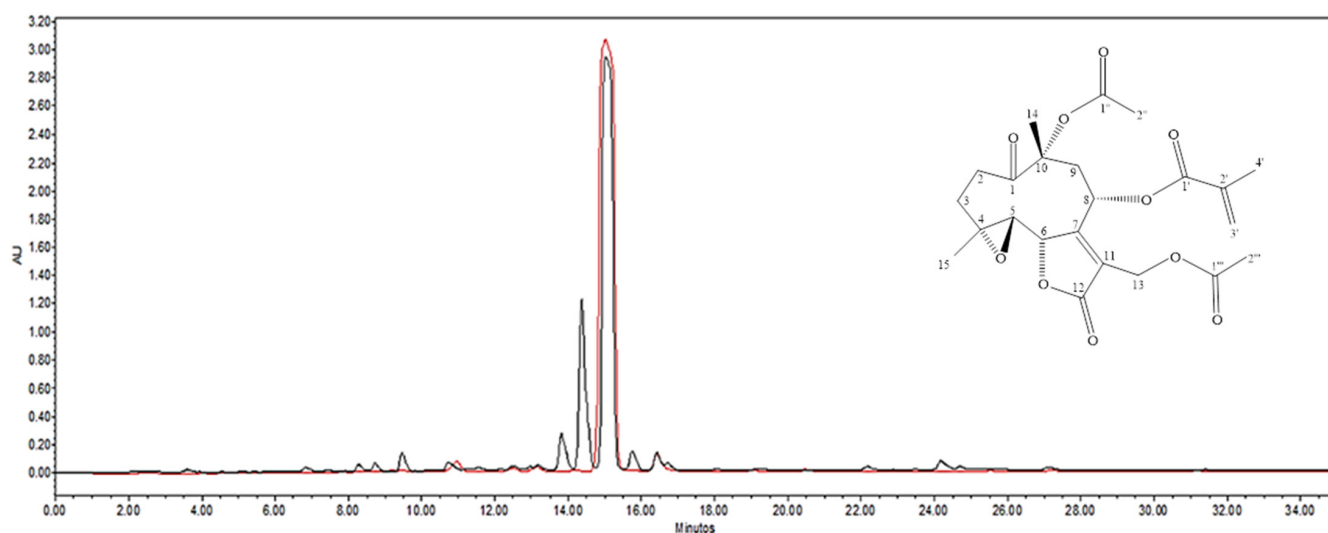
Figure 2. HPLC-DAD chromatograms of Vp-LRE (black line) and isolated glaucolide A (red line), and the chemical structure of glaucolide A.

2.5. HPLC-DAD Analysis of Vp-LRE and Glaucolide A

The chromatographic HPLC-DAD profile of Vp-LRE, at λ 210 nm showed the presence of six major peaks with an intense signal at the Rt of 15.04 min (Figure 2, black line). The isolated glaucolide A, analyzed at the same chromatographic conditions of Vp-LRE showed a high purity peak at Rt = 15.04 in the HPLC-DAD (Figure 2, red line).

2.6. In Vitro Cell Viability/Cytotoxicity Assay

RAW 264.7 cells were selected to evaluate the in vitro cell viability/cytotoxicity because macrophages play a critical role in bacterial infections, as they are responsible for engulfing and destroying invading bacteria as well as producing cytokines, chemokines and reactive oxygen species that help to eliminate bacteria and coordinate the immune response to the infection [26]. This cell line was treated with concentrations ranging from 0.5 to 30 μg/mL of Vp-LRE extract or 0.5 to 20 μg/mL of glaucolide A. After 48 h, the cell viability was determined via MTT assay. As shown in Figure 3, only on the highest concentrations, Vp-LRE (30 μg/mL) and glaucolide A (10 and 20 μg/mL) induced a significant cell viability reduction, compared to the not-treated cells. No significative difference was found between non-treated cells and cells treated with the solvent (DMSO 0.5%). As expected, the positive control (DMSO 5%) reduced the viability by around 90%.

Figure 3. Evaluation of the cytotoxicity of *V. polyanthes* leaf rinse extract (Vp-LRE) and glaucolide A on RAW 264.7 cell line. Cell viability was evaluated via MTT assay and expressed as mean ± SD relative to untreated control (NT) (* $p < 0.05$ vs. NT).

2.7. In Vitro Antibacterial Activity Assessment

The results of the in vitro antibacterial activity by minimal inhibitory concentration (MIC) are presented in Tables 2 and 3. According to these tables, the MIC values showed that Vp-LRE was effective against *Staphylococcus aureus* (ATCC 6538) and (ATCC 292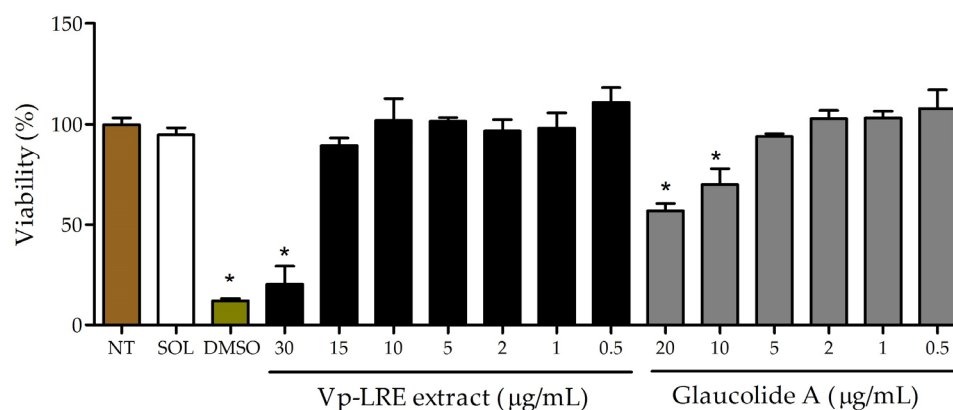13), *Escherichia coli* (ATCC 10536), *Salmonella* Choleraesuis (ATCC 10708), *Salmonella* Typhimurium (ATCC 13311) (Table 2) and MRSA 1485279, MRSA 1605677, MRSA 1664534, MRSA 1688441 and MRSA 1830466 (Table 3). Vp-LRE did not reveal antibacterial effects against the other eight bacterial strains evaluated in this study (three ATCC® and five *Salmonella* clinical strains) at the highest tested concentration (>5000 μg/mL). Glaucolide A showed antibacterial activity against *S. aureus* (ATCC 6538) and *S. aureus* (ATCC 29213) (Table 2). For the other strains, no antibacterial activity was observed in the gradient tested concentration (up to 500 μg/mL).

After the establishment of MIC values (Tables 2 and 3), MBC and the bactericidal or bacteriostatic effects were determined. Vp-LRE revealed a bacteriostatic effect, showing MIC of 5000 μg/mL against *E. coli* (ATCC 10536), *S.* Choleraesuis (ATCC 10708) and *S.* Typhimurium (ATCC 13311). In these cases, MBC was not established because 5000 μg/mL was the highest concentration used in this study, as explained before. Considering the antibacterial action of Vp-LRE under *S. aureus* (ATCC 6538) and *S. aureus* (ATCC 29213) with MIC of 625 μg/mL, the MBC values were 2500 μg/mL and 1250 μg/mL, respectively, with a bacteriostatic effect present for both strains. For MRSA 1485279, MRSA 1605677, MRSA 1664534, MRSA 1688441 and MRSA 1830466, Vp-LRE demonstrated a bacteriostatic effect and the MBC values were 2500 μg/mL against MRSA 1485279, MRSA 1664534 and MRSA 1830466, and 5000 μg/mL for MRSA 1605677 and MRSA 1688441. It is noteworthy that despite the antibacterial activity of Vp-LRE observed against *S.* Choleraesuis (ATCC 10708) (MIC = 5000 μg/mL) and *S.* Typhimurium (ATCC 13311) (MIC = 5000 μg/mL), this extract and glaucolide A were unable to inhibit the five tested clinical strains of *Salmonella*. Based on glaucolide A, it was not possible to determine the MBC values of the two reference strains of *S. aureus* (ATCC 6538 and ATCC 29213) because 500 μg/mL was the highest tested concentration.

2.8. Molecular Docking Interactions

Figure 4 shows the redocking of the cocrystallized ligand [[*N*-(benzyloxycarbonyl) amino]methyl]phosphate (PHOS) at the catalytic site of the β-lactamase of *S. aureus* (PDBid: 1BLH), where the RMSD value was of 1.8929 Å. Thus, it was possible to perform the molecular docking studies in the catalytic site with the proposed ligands.

Table 2. Minimal inhibitory concentration (MIC) values of *V. polyanthes* leaf rinse extract (Vp-LRE) and glaucolide A against ATCC® strains.

Bacterial Strain	MIC (µg/mL)			
	Vp-LRE	**Glaucolide A**	**AMP ***	**CHL ***
S. aureus (ATCC 6538)	625	250	<4	8
S. aureus (ATCC 29213)	625	500	<4 [a]	16 [b]
E. coli (ATCC 10536)	5000	>500	<4	<4
E. coli (ATCC 25922)	>5000	>500	<4 [d]	<4 [d]
S. Choleraesuis (ATCC 10708)	5000	>500	<4	<4
S. Typhimurium (ATCC 13311)	5000	>500	<4	<4
P. aeruginosa (ATCC 9027)	>5000	>500	>500 [c]	64 [c]
P. aeruginosa (ATCC 27853)	>5000	>500	500 [c]	64 [c]

* MIC values of ampicillin (AMP) and chloramphenicol (CHL) were in accordance with the quality control ranges reported for nonfastidious organisms by the Clinical and Laboratory Standards Institute (CLSI), document M100-S24 [27]: [a] 0.5 to 2 µg/mL; [b] 2 to 16 µg/mL; [c] not reported; [d] 2 to 8 µg/mL. These values classify these bacteria as sensitive, with the exception of *P. aeruginosa* (ATCC 9027) and (ATCC 27853).

Table 3. Minimal inhibitory concentration (MIC) values of *V. polyanthes* leaf rinse extract (Vp-LRE) and glaucolide A against clinical strains.

Bacterial Strain	MIC (µg/mL)			
	Vp-LRE	**Glaucolide A**	**AMP ***	**CHL ***
MRSA 1485279	312	>500	250	64
MRSA 1605677	156	>500	250	<4
MRSA 1664534	1250	>500	16	<4
MRSA 1688441	2500	>500	250	<4
MRSA 1830466	1250	>500	64	4
Salmonella spp. 1266695	>5000	>500	<4	<4
S. Enteritidis 1406591	>5000	>500	<4	<4
S. Enteritidis 1418594	>5000	>500	<4	<4
S. Enteritidis 1428260	>5000	>500	<4	<4
Salmonella spp. 1507708	>5000	>500	500	<4

* MIC values of ampicillin (AMP) and chloramphenicol (CHL) were in accordance with the quality control ranges reported for nonfastidious organisms by the Clinical and Laboratory Standards Institute (CLSI), document M100-S24 [27]: These values classify these bacteria as sensitive.
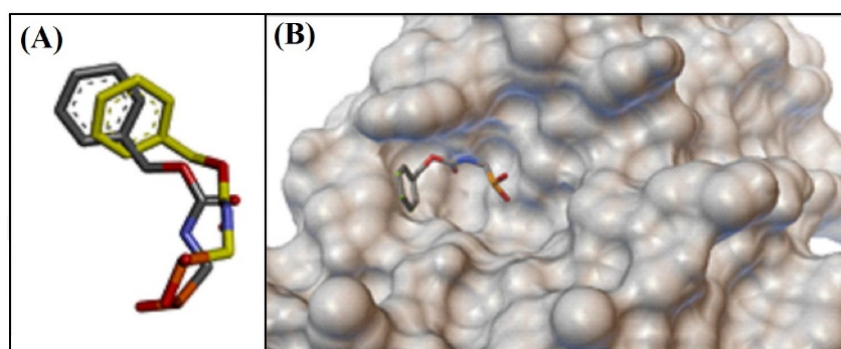
Figure 4. Redocking of the crystallographic ligand at the catalytic site of β-lactamase of *S. aureus*. (**A**) Crystallographic ligand conformation (moss) and conformation obtained by redocking (gray); (**B**) Ligand at the enzyme site.

Clavulanic acid, the reference compound, interacted with the catalytic site of β-lactamase through hydrogen bonding with the Ser70 residue, responsible for the nucleophilic attack on the carbonyl carbon and consequent breakage of the β-lactam ring. Hydrogen bonds with Tyr105, Asn132 and Glu166 residues, dipole–permanent interaction with Gln237 and Van der Waals interactions with the other residues were also established (Figure 5A). The free energy value was −6.6 kcal/mol (Table 4).
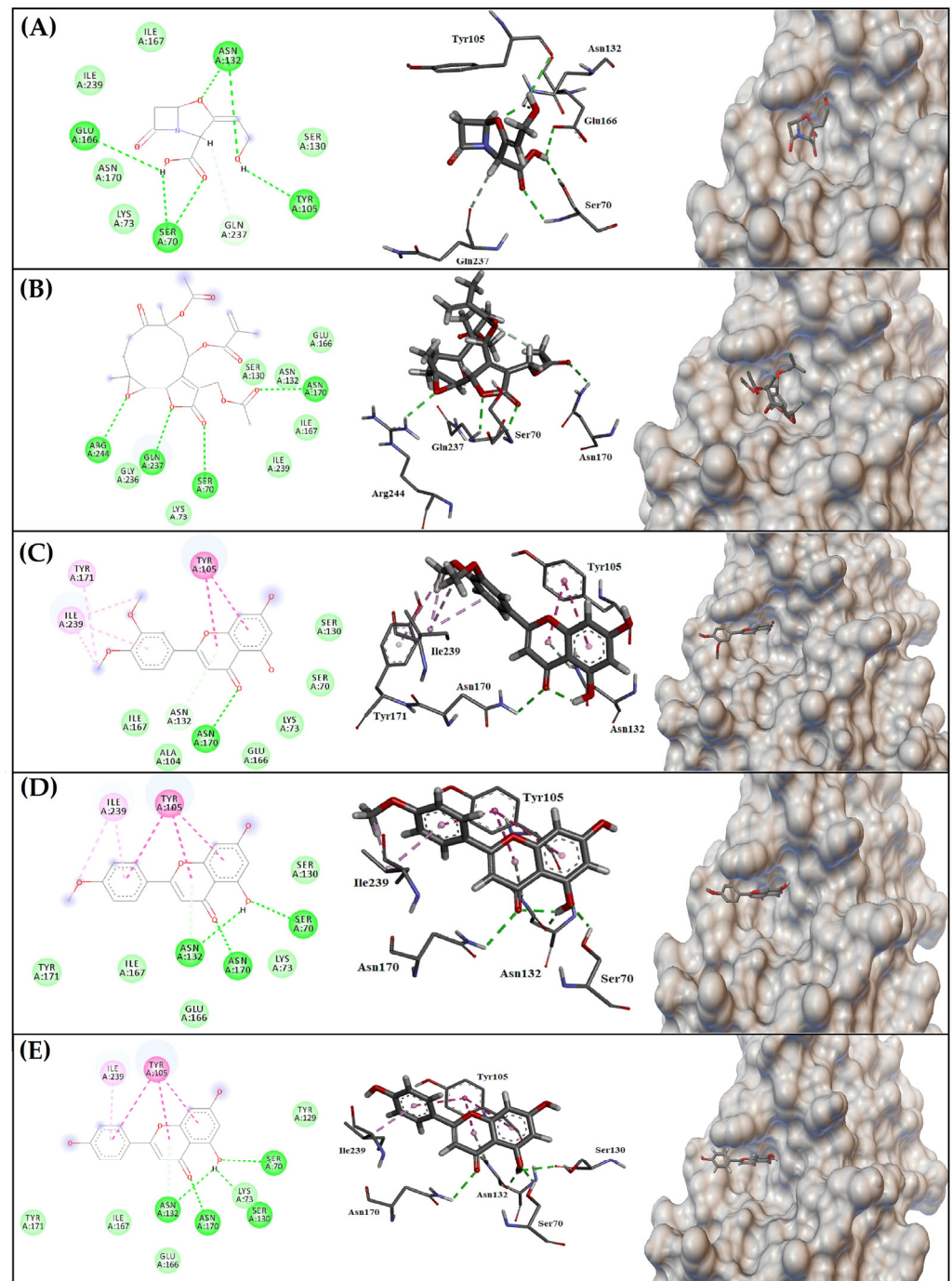
Figure 5. Main molecular interactions between compounds and class β-lactamase catalytic site of *S. aureus*. (**A**) Clavulanic acid. (**B**) Glaucolide A. (**C**) 3′,4′-Dimethoxyluteolin. (**D**) Acacetin. (**E**) Apigenin. Dark green: hydrogen bonding; Light green: Van der Waals; Light pink: alkyl or π-alkyl; Dark pink: π-stacking; Light blue: permanent-dipole. Dashed lines: aromatic ring.

Table 4. Free energy values of ligands.

Ligands	Free Energy (kcal/mol)
Clavulanic acid	−6.6
Glaucolide A	−6.2
3′,4′-Dimethoxyluteolin	−7.1
Acacetin	−7.4
Apigenin	−7.5

Figure 5 presents the conformations and main intermolecular interactions between the ligands and the catalytic site of the *S. aureus* β-lactamase. Glaucolide A (Figure 5B) established hydrogen bonding with residues Ser70, Asn170, Gln237 and Arg244, with a free energy value of −6.2 kcal/mol (Table 4). 3′,4′-Dimethoxyluteolin (Figure 5C) interacted with the Asn170 residue via hydrogen bonding, with the Asn132 residue via dipole-permanence, with the aromatic ring of Tyr105 and Tyr171 and with the Ile239 residue through π-stacking alkyl interactions and π-alkyl, yielding a free energy value of −7.1 kcal/mol (Table 4). Acacetin (Figure 5D) established hydrogen bonds with residues Ser70, Asn132 and Asn170, a π-stacking type interaction with the aromatic ring of Tyr105 and alkyl and π-alkyl interactions with Ile239 residue, and the free energy value was −7.4 kcal/mol (Table 4). The flavonoid apigenin (Figure 5E) established hydrogen bonds with residues Ser70, Ser130, Asn132 and Asn170, a π-stacking type interaction with the aromatic ring of Tyr105 and a π-alkyl interaction with Ile239 residue, and the free energy value was −7.5 kcal/mol (Table 4).

3. Discussion

V. polyanthes leaves are used in Brazilian folk medicine to treat several infectious diseases such as pneumonia, flu, coughs and uterine infections [28]. However, despite the antimicrobial potential of *V. polyanthes* leaves, a correlation between its chemical composition and its antibacterial activity has not been supported by any scientific evidence so far. Additionally, several studies have reported that flavonoids, sesquiterpene lactones and other potentially active compounds of *Vernonia* species are located in the glandular trichomes of the leaves, which are epidermal secretory structures related to the production, storage and secretion of a wide number of compounds associated with plant defense and its antimicrobial and antifeeding effects [21–23]. The locations of these structures on the surfaces of the plant organs allow for the extraction of these compounds by washing the leaves with organic solvents, producing a selective plant extract to obtain the stored compounds in the glandular trichomes called Vp-LRE in the present study [21–23].

First, after preparation of the Vp-LRE, it was analyzed via UHPLC-ESI-QTOF-MS (Figure 1), showing the presence of flavonoids and sesquiterpene lactones in this extract (mainly glaucolide A, which was the major compound as observed through HPLC-DAD analysis (Figure 2)).

Our chemical characterization of Vp-LRE is in accordance with previous studies of metabolites found in *Vernonia* species [29–33]. A discreet number of scientific reports, focusing on the chemical composition of *V. polyanthes*, can be found, showing the presence of mainly caffeoylquinic acids, flavonoids and sesquiterpene lactones (Table 1) [19,20,22,29,30,34]. The structures of the flavonoids acacetin, chrysoeriol, isorhamnetin, isorhamnetin isomer, kaempferide, 3′,4′-dimethoxyluteolin and 3,7-dimethoxy-5,3′,4′-trihydroxyflavone were successfully annotated, with acacetin, chrysoeriol and kaempferide being first detected in *V. polyanthes*. In addition, glaucolide A and apigenin were identified via LC/MS analysis and comparison with authentic compounds (Table 1).

The chemically characterized Vp-LRE was assayed against ATCC® and clinical multidrug-resistant Gram-positive and Gram-negative bacterial strains. From the large panel of evaluated bacteria, our results clearly demonstrated the most active antibacterial action of Vp-LRE against *S. aureus* ATCC® and MRSA clinical tested strains. However, in another investigation, da Costa et al. revealed that these MRSA strains might be heteroresistant (hVISA) or vancomycin intermediate *S. aureus* (VISA), which could have more resistance mechanisms than expected [35]. In this way, the antibacterial potential of *V. polyanthes* as a source of bioactive natural compounds against multidrug-resistant *S. aureus*, as observed with MRSA 1485279 (MIC = 312 μg/mL) and MRSA 1605677 (MIC = 156 μg/mL), is unquestionable. Faced with the possibility of being a hVISA or VISA, these results show that Vp-LRE can present different mode of action related to resistance beyond the presence of the mecA gene (MRSA strains).

Previously published antibacterial data of *V. polyanthes* show some different results that may be due to different methods of extraction and antimicrobial evaluation. Oliveira et al. reported a significant antimycobacterial activity of *V. polyanthes* hydroalcoholic root extract used in the treatment of respiratory diseases [11]. Jorgetto et al. described the hydroalcoholic leaf extract of this plant species bacteriostatic effect against *Bacillus cereus* (ATCC 11778), *Escherichia coli* (ATCC 8739) and *Proteus mirabilis* (ATCC 25933) at MIC of 1.8×10^3, 7.2×10^3 and 1.4×10^3 μg/mL, respectively [18]. Silva et al. demonstrated the antibiotic effect of *V. polyanthes* methanolic extract and essential oil against *S. aureus* ($MIC_{90\%}$ of 3.3×10^3 and 2.8 μg/mL, in this order) and *E. coli* ($MIC_{90\%}$ 26.9×10^3 and 24.1×10^3 μg/mL, respectively) clinical strains [19]. Finally, Waltrich, Hoscheid and Prochnaus evaluated this property of aqueous and methanol extracts, and hexane, dichloromethane and ethyl acetate fractions of *V. polyanthes* flowers against *E. coli* (ATCC 25922), *S. aureus* (ATCC 25923) and *P. aeruginosa* (ATCC 27853) [20]. These authors observed that the ethyl acetate fractions from aqueous and methanol extracts were active against *S. aureus* (ATCC 25923), inhibiting the bacterial growth at concentrations of 6×10^3 and 12×10^3 μg/disk, in this order [20]. In addition, an important aspect is the MIC values obtained with the *S. aureus* reference and clinical strains. According to the Kuete's classification of antimicrobial activity of plant extracts [36], Vp-LRE revealed a moderate antibacterial effect ($100 < MIC \leq 625$ μg/mL) against *S. aureus* (ATCC 6538), *S. aureus* (ATCC 29213), MRSA 1485279 and MRSA 1605677, contributing with the traditional uses of *V. polyanthes* in the treatment of wounds and infectious diseases caused by this microorganism [9–11].

Because glaucolide A was identified as the major compound in Vp-LRE, it was isolated from the extract via chromatographic fractionation, with a purity estimated as higher than 95% by HPLC-DAD data analysis and chemically identified using ^{13}C- and ^{1}H-NMR data analysis in comparison to literature.

The antibacterial activity of glaucolide A was investigated, showing that this sesquiterpene lactone is active against *S. aureus* strains (ATCC 6538) and (ATCC 29213), with MIC values of 250 and 500 μg/mL, respectively. However, glaucolide A showed no activity against *E. coli*, *S. Choleraesuis*, *S. Typhimurium*, and *P. aeruginosa* ATCC® and the others MRSA and *Salmonella* strains tested at the maximum concentration gradient of 500 μg/mL. To our knowledge, glaucolide A has not been yet evaluated against these bacterial strains.

As previously reported by Picman [37], the α-methylene-γ-lactone group may not be essential for the antibacterial activities of sesquiterpene lactones. The antibacterial activity of glaucolide A, which lacks the α-methylene-γ-lactone group, was similar to vernolide, vernodaline, and vernodalol, which have this group in their structures. For instance, despite the α-methylene-γ-lactone group, vernodalol was not active against *S. aureus*, unlike glaucolide A [38,39]. Our results are in agreement with the literature, indicating that the antimicrobial activity of sesquiterpene lactones is related to many chemical characteristics, such as substituent groups, their positions and configuration on the backbone, and that the presence of the α-methylene-γ-lactone moiety or the β-substituted cyclopentenone ring residue are not mandatory for the activity [37].

Regarding cytotoxicity to mammalian cells, Vp-LRE and glaucolide A showed potential toxic effects against macrophages RAW 264.7 at the same range of antibacterial concentrations. Williams et al. [40], who investigated the cytotoxicity of the extract from the leaves of *Vernonia pachyclada* and glaucolides K, L, and M on the human ovarian cancer cell line A2780, found moderate toxic effects for the extract and these compounds, with glaucolide M being the most active. However, the hypothesis that cytotoxic effects of Vp-LRE and glaucolide A may be involved with their antibacterial actions should be further explored in the future.

In addition, many flavonoids such as apigenin have shown direct antibacterial action, synergism with antimicrobial agents and deletion of bacterial virulence [41]. Extracts and fractions with high flavonoid content were reported to exhibit antibacterial activity [42]. In this regard, the total phenolic (2.53 ± 0.01 g GAE/100 g) and flavonoid

(4.26 $\pm$ 0.04 g RE/100 g) contents quantified in the Vp-LRE was higher than those observed in other extracts of *Vernonia* species [43].

One of the strategies to solve bacterial resistance mediated by β-lactamase is the inhibition of this enzyme. Currently, three β-lactamase inhibitors are used in clinical practice in association with β-lactam antibacterial agents: clavulanic acid, tazobactam and sulbactam [44]. Our results showed that 3′,4′-dimethoxyluteolin, acacetin and apigenin (compounds identified in *V. polyanthes*) were able to interact with the catalytic site of the *S. aureus* β-lactamase with free energy values lower than of clavulanic acid (Table 4). Analyzing the chemical structures of the ligands and clavulanic acid, the oxygen atoms seem to be important for establishing hydrogen bonds with the amino acid residues of the catalytic site of the enzyme. According to this data, 3′,4′-dimethoxyluteolin, acacetin and apigenin can be promising inhibitor agents of β-lactamase found in multidrug resistant bacteria.

In conclusion, we have reported, for the first time, the antibacterial effects of the leaf rinse extract of *V. polyanthes* (Vp-LRE) and its major compound glaucolide A against clinical multidrug-resistant Gram-positive and Gram-negative bacterial strains. Flavonoids, such as chrysoeriol, and other sesquiterpene lactones, such as piptocarphin A, were annotated in Vp-LRE after chemical characterization via UHPLC-ESI-QTOF-MS analysis. This study also provides evidence for the traditional use of *V. polyanthes* in the treatment of wounds and bacterial infectious diseases. Considering the antibacterial effects observed using Vp-LRE, although a contribution of glaucolide A may be present, we cannot discard the effects of other active compounds in the extract, such as flavonoids. Further studies are in progress to disclose other important biological effects of this medicinal plant.

4. Materials and Methods

4.1. Plant Material

V. polyanthes was cultivated at the Medicinal Garden of the Faculty of Pharmacy, Federal University of Juiz de Fora, Juiz de Fora city, Minas Gerais State, Southeast region of Brazil (21°46′ S, 43°22′ W), and fresh leaves were collected in January 2014. The species was identified by Dr. Fátima Regina Gonçalves Salimena and a voucher specimen (CESJ number 10329) was deposited in the Herbarium Leopoldo Krieger of this Institution. The plant name *Vernonia polyanthes* Less. has been checked with (http://www.worldfloraonline.org/search?query=Vernonia+polyanthes) (accessed on 16 November 2022) and it is a synonym of *Vernonanthura phosphorica* (Vell.) H. Rob.

4.2. Preparation of Plant Extract

Entire dried leaves (625 g) were rinsed with dichloromethane (5 L) via shaking for 1 min and 30 s at room temperature. The resultant solution was filtered and evaporated in a rotary evaporator at controlled temperature (35–40 °C), resulting in 14 g of the leaf rinse extract of *V. polyanthes* (Vp-LRE).

4.3. Total Phenolic Content Determination

The total phenolic content was determined according to the Folin–Ciocalteu colorimetric method with little adjustments using gallic acid as standard [45]. The absorbance of the resulting blue color solution was measured at 788 nm (Shimadzu®, UV-1800, Tokyo, Japan) after two hours at room temperature. The analyses were performed in triplicate and the results were expressed as g/100 g of gallic acid equivalents (GAE).

4.4. Total Flavonoid Content Determination

Aluminum chloride colorimetric method was carried out according to Sobrinho et al. with few adjustments for total flavonoid content determination using rutin as the standard [45]. Each dilution of Vp-LRE stock solution (5 mg/mL in methanol) after a semi purification was separately mixed with glacial acetic acid P.A., 20% pyridine methanolic solution, 8% aluminum chloride methanolic solution, and distilled water. After 30 min at room temperature, the absorbance of the reaction mixture was measured at 412 nm

(Shimadzu®, UV-1800, Tokyo, Japan). The analyses were performed in triplicate and the results were expressed as g/100 g of rutin equivalents (RE).

4.5. Chemical Composition of Vp-LRE by Ultra-High Performance Liquid Chromatography Coupled to Quadrupole Time-of-Flight Mass Spectrometry (UHPLC/Q-TOF-MS) Analysis

The UHPLC analysis was conducted with an Acquity UHPLC system (Waters Corporation, Milford, MA, USA), supplied with a quaternary pump and an autosampler coupled to an electrospray ionization quadrupole time-of-flight tandem mass spectrometer (ESI-QTOF/MS). Separation was achieved using a BEH C_{18} column (100 mm × 2.1 mm, 1.7 μm) with a flow rate at 0.4 mL/min, and a mobile phase of water with 0.1% formic acid (A) and acetonitrile (B) with a linear gradient of 5% B to 98% B in 12 min. Before the injections (0.5 μL for Vp-LRE and 1.0 μL for the authentic standards), samples were dissolved in methanol (10 mg/mL), centrifuged and filtered in a 0.22 μm filter. ESI-MS spectrometer was operated on negative ionization mode with scan range from *m/z* 100–1000. The ion source temperature was 120 °C with a desolvation temperature of 450 °C, a capillary voltage was 2 kV, a cone voltage was 30 V, and the collision energy was in ramp mode, ranging from 15–30 eV, using nitrogen as desolvation (800 L/h) and cone gas (50 L/h). Data were centroided during acquisition, and leucine-enkephalin (*m/z* 565.2771; 200 pg/mL) (Sigma-Aldrich, Steinheim, Germany) was continuously infused as an external reference into the ESI source with automatic mass correction enabled (LockSpray™). MassLynx™ 4.1 and Chromalynx™ softwares (Waters Corp., Milford, MA, USA) were used to process all data. Moreover, along with the use of authentic standards compounds (apigenin and glaucolide A) for identification, the MS^2 spectra were compared with literature data and online databases, such as MassBank, ChemSpider and Spectral Database for Organic Compounds.

4.6. Isolation and Purification of Glaucolide A from Vp-LRE

Vp-LRE (10 g) was submitted to a vacuum liquid chromatograph system (glass columns with 3–12 cm i.d.) using silica gel (40–63 μm) as stationary phase and combinations of hexane: ethyl acetate as solvents, furnishing 6 fractions (Vp-1 to 6). Fraction Vp-5 (3.5 g, hexane- EtOAc 7:3) was subjected to column chromatography over silica gel, using hexane- EtOAc mixtures as eluent, giving seven subfractions, affording one (0.7 g, from fraction Vp-5.5). The chemical structure of compound 1 was established as glaucolide A using ^{1}H- and ^{13}C-NMR analysis in comparison with literature. ^{1}H- and ^{13}C-NMR spectra (500 MHz for ^{1}H-NMR and 125 MHz for ^{13}C-NMR) were registered in $CDCl_3$ solutions on a Bruker 500 Advance spectrometer with trimethylsilane (TMS) as the internal standard.

4.7. HPLC-DAD Analysis of Vp-LRE and Glaucolide A

Vp-LRE and glaucolide A (isolated from Vp-LRE) were analyzed in a high-performance liquid chromatography (HPLC) system (Waters Corporation, Milford, MA, USA) supplied with a DAD (diode array) detector, binary pumps and an autosampler. As an analytical column, the SunFire C_{18} (5 μm particle size, 4.6 mm × 250 mm, Waters Corporation) was used. The mobile phase was water with 0.5% phosphoric acid (A) and acetonitrile (B) in gradient elution: 40–100% (B) in 0–35 min, with the flow rate of 1 mL/min and detection at 210 nm. Solutions of Vp-LRE and glaucolide A (2 mg/mL) in acetonitrile were filtered through 0.45 μm membrane filters and a volume of 30 μL was injected.

4.8. In Vitro Cell Viability/Cytotoxicity Assay

4.8.1. Cell Line and Cell Culture Conditions

RAW 264.7 macrophage-like cell line (ATCC TIP-71; laboratory's own stock) was cultured in RPMI-1640 supplemented with 10% fetal bovine serum (FBS), 100 U/mL of penicillin and 100 μg/mL of streptomycin at 37 °C in 5% CO_2/95% atmosphere. At 80% confluence, these cells were subjected to the experiment or subculture.

4.8.2. 3-(4,5-Dimethylthiazol-2-yl)-2,5-diphenyl Tetrazolium Bromide (MTT) Assay

The cell viability/cytotoxicity was evaluated by MTT assay [46]. RAW 264.7 cells were plated at density of 2×10^5 cells/well onto 96-well flat bottom plates and incubated at 37 °C and 5% CO_2 for 24 h. The medium was removed and the fresh medium with or without concentrations of Vp-LRE (0.5, 1, 2, 5, 10, 15 and 30 μg/mL) and glaucolide A (1, 2, 5, 10 and 20 μg/mL) were added. After 48 h (37 °C; 5% CO_2), the supernatant was removed and 100 μL of MTT (5 mg/mL) was added to each well and incubated (37 °C; 5% CO_2) for an additional 2 h and 30 min. Subsequently, the supernatant was removed and 100 μL/well of DMSO was added to dissolve any deposited formazan. The optical density was determined at 595 nm using a microplate reader (SpectraMax 190, Molecular Devices, Sunnyvale, CA, USA). DMSO (5%) was used as positive control. All treatments were performed in triplicate.

4.9. In Vitro Antibacterial Activity Assessment

4.9.1. Bacterial Strains

American Type Culture Collection (ATCC®) bacterial strains of *Staphylococcus aureus* subsp. *aureus* ((ATCC 6538), methicillin-sensitive *Staphylococcus aureus* (MSSA)), *Staphylococcus aureus* subsp. *aureus* ((ATCC 29213), MSSA), *Escherichia coli* (ATCC 10536), *Escherichia coli* (ATCC 25922), *Salmonella enterica* subsp. *enterica* serovar Choleraesuis (ATCC 10708), *Salmonella enterica* subsp. *enterica* serovar Typhimurium (ATCC 13311), *Pseudomonas aeruginosa* (ATCC 9027) and *Pseudomonas aeruginosa* (ATCC 27853) were selected for the in vitro antibacterial activity assessment. Five methicillin-resistant *Staphylococcus aureus* (MRSA) 1485279, MRSA 1605677, MRSA 1664534, MRSA 1688441 and MRSA 1830466, two *Salmonella* spp. 1266695 and *Salmonella* spp. 1507708, and three *Salmonella* Enteritidis 1406591, *S.* Enteritidis 1418594 and *S.* Enteritidis 1428260 clinical strains isolated from patients attended at Hospital Universitário Clementino Fraga Filho, Universidade Federal do Rio de Janeiro, Rio de Janeiro, Brazil, kindly donated by MSc. Adriana Lúcia Pires Ferreira, were also tested. These strains were identified via the VITEK 2® automated system (BioMérieux, Durham, NC, USA). All the bacterial strains were stored as suspensions in a 10% (*w/v*) skim milk solution containing 10% (*v/v*) glycerol at −20 °C before use in the bioassays. Prior to use, these strains were aerobically grown in Müeller-Hinton Agar (MHA) at 35 ± 2 °C for 18–24 h. In this article, we used *S. aureus* (ATCC 6538), *S. aureus* (ATCC 29213), *E. coli* (ATCC 10536), *E. coli* (ATCC 25922), *S.* Choleraesuis (ATCC 10708), *S.* Typhimurium (ATCC 13311), *P. aeruginosa* (ATCC 9027) and *P. aeruginosa* (ATCC 27853) to simplify the text.

4.9.2. Minimal Inhibitory Concentration (MIC) Determination

The MIC values of Vp-LRE and glaucolide A (samples) and ampicillin (AMP) and chloramphenicol (CHL) (standard antibiotics) were determined using the broth microdilution method according to the M07-A9 document, with few adjustments [47]. Samples stock solutions were prepared in DMSO (solvent) and water (diluent) at 10 mg/mL (*w/v*) for Vp-LRE and 1 mg/mL for glaucolide A. Antibiotics stock solutions were prepared at 1 mg/mL with solvents and diluents recommended by CLSI [27,47]. In triplicate, two-fold serial dilutions were prepared at concentrations ranging from 5000 to 40 μg/mL (Vp-LRE) and 500 to 4 μg/mL (glaucolide A, AMP and CHL). The appropriate controls were performed. The Vp-LRE concentration gradient was established based on Fabry et al. criteria (MIC < 8000 μg/mL) [48]. Posteriorly, 10 μL of standardized bacteria suspension according to 0.5 McFarland scale were added. After incubation at 35 ± 2 °C for 16–20 h under aerobic conditions, 20 μL of 2,3,5-triphenyl tetrazolium chloride (TTC) solution (1 mg/mL) were used as an indicator of bacterial growth. The system was incubated for further 30 min, and the MIC was determined.

4.9.3. Minimal Bactericidal Concentration (MBC) and Bactericidal or Bacteriostatic Effect Determinations

After determination of MIC values, MBC was established following the Andrews' procedure by spreading of 10 μL of suspensions from wells showing no bacterial growth on MHA Petri dishes [49]. After incubation at $35 \pm 2\,^{\circ}C$ for 16–20 h under aerobic conditions, MBC was determined as the lowest concentration of dilutions that prevented the visible bacterial growth after subculture on MHA Petri dishes. Bacterial growth or no bacterial growth on MHA revealed a bacteriostatic or bactericidal effect, respectively.

4.10. Molecular Docking

The three-dimensional structures of the ligands (glaucolide A, 3′,4′-dimethoxyluteolin, acacetin, apigenin and clavulanic acid) were drawn using the MarvinSketch 20.17 program, which were submitted for geometric optimization in the Avogadro 1.2.0 program to obtain structures that were energetically more stable. The crystallographic coordinates of the three-dimensional structure of β-lactamase from *S. aureus* were obtained from the Protein Data Bank (PDB) (PDBid: 1BLH, resolution 2.3 Å). However, the AutoDock Tools 1.5.6 program was used to prepare this enzyme, where water molecules were removed and polar hydrogens and electrical charges were added for each atom. In addition, this program was used to define the settings of the Grid Box, whose dimension was $14 \times 12 \times 16$ points spaced 1 Å with coordinates x: 5.264, y: -7.758 and z: -6.726. The AutoDock Vina 1.1.2 program was used to perform the molecular docking, and the lowest energy conformations were selected. Then, the results were analyzed using the Discovery Studio v20.1.0.19295 2020 program [50]. The molecular docking protocol was validated by the redocking method with root-mean-square deviation (RMSD) value less than 2.0 Å.

4.11. Statistical Analysis

The results of the cell viability assay were given as mean values ($\pm$SD) and analyzed using GraphPad Prism (version 6.0) software. Significant differences were determined by one-way analysis of variance (ANOVA) and following Tukey's test for multiple comparisons. The significance level in the analysis was $p < 0.05$.

5. Conclusions

In conclusion, we have reported, for the first time, the antibacterial effects of the leaf rinse extract of *V. polyanthes* (Vp-LRE) and its major compound glaucolide A against clinical multidrug-resistant Gram-positive and Gram-negative bacterial strains. Flavonoids, such as chrysoeriol, and other sesquiterpene lactones, such as piptocarphin A, were annotated in Vp-LRE after chemical characterization via UHPLC-ESI-QTOF-MS analysis. The undertaken study provided evidence for the traditional use of *V. polyanthes* in the treatment of wounds and bacterial infectious diseases. Considering the antibacterial effects observed by Vp-LRE, although a contribution of glaucolide A may be present, we cannot discard the effects of other active compounds in the extract, such as flavonoids. Further studies are in progress to disclose other important biological effects of this medicinal plant.

Author Contributions: Conceptualization, M.S.A. and A.A.d.S.F.; methodology, J.D.G.d.S., O.A.S.-M., J.R.F., D.C.Z.-F., L.M.S.d.A. and A.L.P.F.; software, D.C.Z.-F. and G.C.M.; validation, M.S.A., A.A.d.S.F., O.V.d.S and G.C.M.; formal analysis, M.S.A., A.A.d.S.F., O.V.d.S. and G.C.M.; investigation, J.D.G.d.S., O.A.S.-M., J.R.F., M.C.C.d.O., D.C.Z.-F., J.O.d.L.X., L.M.S.d.A. and A.L.P.F.; resources, M.S.A. and A.A.d.S.F.; data curation, M.S.A., A.A.d.S.F., O.V.d.S. and G.C.M.; writing—original draft preparation, J.D.G.d.S., O.A.S.-M., O.V.d.S., M.S.A. and A.A.d.S.F.; writing—review and editing, J.D.G.d.S., O.A.S.-M., J.R.F., D.C.Z.-F., L.M.S.d.A., A.L.P.F., D.C.Z.-F., G.C.M., O.V.d.S., M.S.A. and A.A.d.S.F.; visualization, J.D.G.d.S., O.A.S.-M., J.R.F., D.C.Z.-F., L.M.S.d.A., A.L.P.F., D.C.Z.-F., G.C.M., O.V.d.S., M.S.A. and A.A.d.S.F.; supervision, M.S.A. and A.A.d.S.F.; project administration, M.S.A. and A.A.d.S.F.; funding acquisition, M.S.A. and A.A.d.S.F. All authors have read and agreed to the published version of the manuscript.

References

1. Bloom, D.E.; Cadarette, D. Infectious disease threats in the twenty-first century: Strengthening the global response. *Front. Immunol.* **2019**, *10*, 549. [CrossRef] [PubMed]
2. Laxminarayan, R.; Matsoso, P.; Pant, S.; Brower, C.; Røttingen, J.A.; Klugman, K.; Davies, S. Access to effective antimicrobials: A worldwide challenge. *Lancet* **2015**, *387*, 168–175. [CrossRef] [PubMed]
3. Aslam, B.; Wang, W.; Arshad, M.I.; Khurshid, M.; Muzammil, S.; Rasool, M.H.; Nisar, M.A.; Alvi, R.F.; Aslam, M.A.; Qamar, M.U.; et al. Antibiotic resistance: A rundown of a global crisis. Infect. *Drug Resist.* **2018**, *11*, 1645–1658. [CrossRef] [PubMed]
4. Tacconelli, E.; Carrara, E.; Savoldi, A.; Harbarth, S.; Mendelson, M.; Monnet, D.L.; Pulcini, C.; Kahlmeter, G.; Kluytmans, J.; Carmeli, Y.; et al. Discovery, research, and development of new antibiotics: The WHO priority list of antibiotic-resistant bacteria and tuberculosis. *Lancet Infect. Dis.* **2017**, *18*, 318–327. [CrossRef]
5. Ríos, J.L.; Recio, M.C. Medicinal plants and antimicrobial activity. *J. Ethnopharmacol.* **2005**, *100*, 80–84. [CrossRef]
6. Taylor, P.W. Alternative natural sources for a new generation of antibacterial agents. *Int. J. Antimicrob. Agents* **2013**, *42*, 195–201. [CrossRef]
7. Brown, D.G.; Lister, T.; May-Dracka, T.L. New natural products as new leads for antibacterial drug discovery. *Bioorganic Med. Chem. Lett.* **2014**, *24*, 413–418. [CrossRef]
8. Newman, D.J.; Cragg, G.M. Natural products as sources of new drugs over the nearly four decades from 01/1981 to 09/2019. *J. Nat. Prod.* **2020**, *83*, 770–803. [CrossRef]
9. Kiplimo, J.J. A review on the biological activity and the triterpenoids from the genus *Vernonia* (Asteraceae Family). *Int. Res. J. Pure Appl. Chem.* **2016**, *11*, 1–14. [CrossRef]
10. Alves, V.F.; Neves, L.J. Anatomia foliar de *Vernonia polyanthes* Less. (Asteraceae). *Rev. Univ. Rural Sér. Ciên. Vida* **2003**, *22*, 1–8.
11. Oliveira, D.G.; Prince, K.A.; Higuchi, C.T.; Santos, A.C.B.; Lopes, L.M.X.; Simões, M.J.S.; Leite, C.Q.F. Antimycobacterial activity of some Brazilian indigenous medicinal drinks. *Rev. Ciências Farm. Básicas Apl.* **2007**, *28*, 165–169.
12. da Silveira, R.R.; Foglio, M.A.; Gontijo, J.A.R. Effect of the crude extract of *Vernonia polyanthes* Less. on blood pressure and renal sodium excretion in unanesthetized rats. *Phytomedicine* **2003**, *10*, 127–131. [CrossRef]
13. Braga, F.G.; Bouzada, M.L.M.; Fabri, R.L.; de O. Matos, M.; Moreira, F.O.; Scio, E.; Coimbra, E.S. Antileishmanial and antifungal activity of plants used in traditional medicine in Brazil. *J. Ethnopharmacol.* **2007**, *111*, 396–402. [CrossRef]
14. Barbastefano, V.; Cola, M.; Luiz-Ferreira, A.; Farias-Silva, E.; Hiruma-Lima, C.A.; Rinaldo, D.; Vilegas, W.; Souza-Brito, A.R.M. *Vernonia polyanthes* as a new source of antiulcer drugs. *Fitoterapia* **2007**, *78*, 545–551. [CrossRef]
15. Temponi, V.d.S.; da Silva, J.B.; Alves, M.S.; Ribeiro, A.; de Pinho, J.d.J.R.G.; Yamamoto, C.H.; Pinto, M.A.O.; Del-Vechio-Vieira, G.; de Sousa, O.V. Antinociceptive and anti-inflammatory effects of ethanol extract from *Vernonia polyanthes* leaves in rodents. *Int. J. Mol. Sci.* **2012**, *13*, 3887–3899. [CrossRef] [PubMed]
16. de Carvalho, C.C.; Machado, K.N.; Ferreira, P.M.P.; Pessoa, C.; Fonseca, T.H.S.; Gomes, M.A.; do Nascimento, A.M. Biological screening of extracts of Brazilian Asteraceae plants. *Afr. J. Pharm. Pharmacol.* **2013**, *7*, 2000–2005. [CrossRef]
17. Rodrigues, K.C.M.; Chibli, L.A.; Santos, B.C.S.; Temponi, V.S.; Pinto, N.C.C.; Scio, E.; Del-Vechio-Vieira, G.; Alves, M.S.; Sousa, O.V. Evidence of bioactive compounds from *Vernonia polyanthes* leaves with topical anti-inflammatory potential. *Int. J. Mol. Sci.* **2016**, *17*, 1929. [CrossRef] [PubMed]
18. Jorgetto, G.V.; Fabiano, M.; Boriolo, G.; Silva, L.M.; Nogueira, D.A.; Donizete, T.; Ribeiro, G.E. Analysis on the *in vitro* antimicrobial activity and in vivo mutagenicity by using extract from *Vernonia polyanthes* Less (Assa-peixe). *Rev. Inst. Adolfo Lutz* **2011**, *70*, 53–61.
19. Silva, N.C.C.; Barbosa, L.; Seito, L.N.; Junior, A.F. Antimicrobial activity and phytochemical analysis of crude extracts and essential oils from medicinal plants. *Nat. Prod. Res. Former. Nat. Prod. Lett.* **2012**, *26*, 1510–1514. [CrossRef]
20. Waltrich, K.K.; Hoscheid, J.; Prochnaus, I.S. Antimicrobial activity of crude extracts and fractions of *Vernonia polyanthes* Less (assa-peixe) flowers. *Rev. Bras. Plantas Med.* **2015**, *17*, 909–914. [CrossRef]

21. Appezzato-da-Glória, B.; Batista, F.; Costa, D.; Cristina, V.; Gobbo-Neto, L.; Lucia, V.; Rehder, G.; Hissae, A. Glandular trichomes on aerial and underground organs in *Chrysolaena* species (Vernonieae–Asteraceae): Structure, ultrastructure and chemical composition. *Flora* **2012**, *207*, 878–887. [CrossRef]

22. Igual, M.O.; Elvira, M.; Martucci, P.; Batista, F.; Costa, D.; Gobbo-Neto, L. Sesquiterpene lactones, chlorogenic acids and flavonoids from leaves of *Vernonia polyanthes* Less (Asteraceae). *Biochem. Syst Ecol.* **2013**, *51*, 94–97. [CrossRef]

23. Tissier, A. Glandular trichomes: What comes after expressed sequence tags? *Plant J.* **2012**, *70*, 51–68. [CrossRef] [PubMed]

24. Padolina, W.G.; Yoshioka, H.; Nakatani, N.; Mabry, T.J.; Monti, S.A.; Davis, R.E.; Cox, P.J.; Sim, G.A.; Watson, W.H.; Wu, I.B. Glaucolide-A and -B, new germacranolide-type sesquiterpene from *Vernonia* (Compositae). *Tetrahedron* **1974**, *30*, 1161–1170. [CrossRef]

25. Bardón, A.; Catalán, C.A.N.; Gutiérrez, A.B.; Herz, W. Glaucolides and related sesquiterpene lactones from *Vernonia incana*. *Phytochemistry* **1990**, *29*, 313–315. [CrossRef]

26. Weiss, G.; Schaible, U.E. Macrophage defense mechanisms against intracellular bacteria. *Immunol. Rev.* **2015**, *264*, 182–203. [CrossRef] [PubMed]

27. Clinical and Laboratory Standards Institute. *Performance Standards for Antimicrobial Susceptibility Testing; Twenty-Fourth Informational Supplement*; CLSI document M100-S24; CLSI: Wayne, PA, USA, 2014; ISBN 1562388975.

28. Rocha, J.M.; Gallon, M.E.; de Melo Bisneto, A.V.; Santana Amaral, V.C.; de Almeida, L.M.; Borges, L.L.; Chen-Chen, L.; Gobbo-Neto, L.; Bailão, E.F.L.C. Phytochemical composition and protective effect of *Vernonanthura polyanthes* leaf against in vivo doxorubicin-mediated toxicity. *Molecules* **2022**, *27*, 2553. [CrossRef] [PubMed]

29. Bohlmann, F.; Jakupovic, J.; Gupta, R.K.; King, R.M.; Robinson, H. Allenic germacranolides, bourbonene derived lactones and other constituents from *Vernonia* species. *Phytochemistry* **1981**, *20*, 473–480. [CrossRef]

30. Martucci, M.E.P.; de Vos, R.C.H.; Carollo, C.A.; Gobbo-Neto, L. Metabolomics as a potential chemotaxonomical tool: Application in the genus *Vernonia* Schreb. *PLoS ONE* **2014**, *9*, e93148. [CrossRef]

31. Toyang, N.J.; Verpoorte, R. A review of the medicinal potentials of plants of the genus *Vernonia* (Asteraceae). *J. Ethnopharmacol.* **2013**, *146*, 681–723. [CrossRef]

32. Lopes, J.L.C. Sesquiterpene lactones from *Vernonia*. *Mem. Inst. Oswaldo Cruz* **1991**, *86*, 227–230. [CrossRef] [PubMed]

33. Igile, G.O.; Oleszek, W.; Jurzysta, M.; Burda, S.; Fafunso, M.; Fasanmade, A.A. Flavonoids from *Vernonia amygdalina* and their antioxidant activities. *J. Agric. Food Chem.* **1994**, *42*, 2445–2448. [CrossRef]

34. Bohlmann, F.; Zdero, C.; King, R.M.; Robinson, H. Further hirsutinolides from *Vernonia polyanthes*. *Phytochemistry* **1983**, *22*, 2863–2864. [CrossRef]

35. da Costa, T.M.; Morgado, P.G.M.; Cavalcante, F.S.; Damasco, A.P.; Nouér, S.A.; dos Santos, K.R.N. Clinical and microbiological characteristics of heteroresistant and vancomycin-intermediate *Staphylococcus aureus* from bloodstream infections in a Brazilian teaching hospital. *PLoS ONE* **2016**, *11*, e0160506. [CrossRef] [PubMed]

36. Kuete, V. Potential of Cameroonian plants and derived products against microbial infections: A review. *Planta Med.* **2010**, *76*, 1479–1491. [CrossRef]

37. Picman, A.K. Biological activities of sesquiterpene lactones. *Biochem. Syst. Ecol.* **1986**, *14*, 255–281. [CrossRef]

38. Rabe, T.; Mullholland, D.; Van Staden, J. Isolation and identification of antibacterial compounds from *Vernonia colorata* leaves. *J. Ethnopharmacol.* **2002**, *80*, 91–94. [CrossRef]

39. Erasto, P.; Grierson, D.S.; Afolayan, A.J. Bioactive sesquiterpene lactones from the leaves of *Vernonia amygdalina*. *J. Ethnopharmacol.* **2006**, *106*, 117–120. [CrossRef]

40. Williams, R.B.; Norris, A.; Slebodnick, C.; Merola, J.; Miller, J.S.; Andriantsiferana, R.; Rasamison, V.E.; Kingston, D.G.I. Cytotoxic sesquiterpene lactones from *Vernonia pachyclada* from the Madagascar rainforest. *J. Nat. Prod.* **2005**, *68*, 1371–1374. [CrossRef]

41. Cushnie, T.P.T.; Lamb, A.J. Recent advances in understanding the antibacterial properties of flavonoids. *Int. J. Antimicrob. Agents* **2011**, *38*, 99–107. [CrossRef]

42. Cushnie, T.P.T.; Lamb, A.J. Antimicrobial activity of flavonoids. *Int. J. Antimicrob. Agents* **2005**, *26*, 343–356. [CrossRef] [PubMed]

43. da Silva, J.B.; Temponi, V.D.S.; Gasparetto, C.M.; Fabri, R.L.; Aragão, D.M.D.O.; Pinto, N.D.C.C.; Ribeiro, A.; Scio, E.; Del-Vechio-Vieira, G.; de Sousa, O.V.; et al. *Vernonia condensata* Baker (Asteraceae): A promising source of antioxidants. *Oxid. Med. Cell. Longev.* **2013**, *2013*, 698018. [CrossRef] [PubMed]

44. Safdari, H.; Neshani, A.; Sadeghian, A.; Ebrahimi, M.; Iranshahi, M.; Sadeghian, H. Potent and selective inhibitors of class A β-lactamase: 7-prenyloxy coumarins. *J. Antibiot.* **2014**, *67*, 373–377. [CrossRef] [PubMed]

45. Sobrinho, T.J.D.S.P.; da Silva, C.H.T.P.; do Nascimento, J.E.; Monteiro, J.M.; de Albuquerque, U.P.; de Amorim, E.L.C. Validação de metodologia espectrofotométrica para quantificação dos flavonóides de *Bauhinia cheilantha* (Bongard) Steudel. *Ver. Bras. Cienc. Farm.* **2008**, *44*, 683–689. [CrossRef]

46. Riss, T.L. Cell viability assays. In *Assay Guidance Manual*; Sittampalam, G.S., Markossian, S., Grossman, A., Brimacombe, K., Arkin, K., Auld, D., Austin, C., Baell, J., Chung, T.D.Y., Coussens, N.P., et al., Eds.; Eli Lilly & Company and the National Center for Advancing Translational Sciences: Bethesda, MD, USA, 2016; p. 2016.

47. Clinical and Laboratory Standards Institute. *Methods for Dilution Antimicrobial Susceptibility Tests for Bacteria That Grow Aerobically; Approved Standard—Ninth Edition*, 9th ed.; CLSI document M07-A9; CLSI: Wayne, PA, USA, 2012; Volume 32, ISBN 1562387839.

48. Fabry, W.; Okemo, P.O.; Ansorg, R. Antibacterial activity of East African medicinal plants. *J. Ethnopharmacol.* **1998**, *60*, 79–84. [CrossRef]

49. Andrews, J.M. Determination of minimum inhibitory concentrations. *J. Antimicrob. Chemother.* **2001**, *48*, 5–16. [CrossRef]

50. Oliveira, M.E.; Cenzi, G.; Nunes, R.R.; Andrighetti, C.R.; Valadão, D.M.S.; Reis, C.; Simões, C.M.O.; Nunes, R.J.; Comar Júnior, M.; Taranto, A.G.; et al. Antimalarial activity of 4-metoxychalcones: Docking studies as falcipain/plasmepsin inhibitors, admet and lipophilic efficiency analysis to identify a putative oral lead candidate. *Molecules* **2013**, *18*, 15276–15287. [CrossRef]

Antibacterial and Antibiofilm Efficacy of Thyme (*Thymus vulgaris* L.) Essential Oil against Foodborne Illness Pathogens, *Salmonella enterica* subsp. *enterica* Serovar Typhimurium and *Bacillus cereus*

Daniela Sateriale [1], Giuseppina Forgione [1], Giuseppa Anna De Cristofaro [1], Chiara Pagliuca [2], Roberta Colicchio [2], Paola Salvatore [2,3], Marina Paolucci [1] and Caterina Pagliarulo [1,*]

[1] Department of Science and Technology, University of Sannio, Via F. De Sanctis snc, 82100 Benevento, Italy
[2] Department of Molecular Medicine and Medical Biotechnologies, University of Naples Federico II, Via S. Pansini 5, 80131 Naples, Italy
[3] CEINGE-Biotecnologie Avanzate s.c.ar.l., Via G. Salvatore 486, 80145 Naples, Italy
* Correspondence: caterina.pagliarulo@unisannio.it; Tel.: +39-0824-305141

Abstract: Nowadays, the wide spread of foodborne illness and the growing concerns about the use of synthetic food additives have shifted the focus of researchers towards essential oils (EOs) as possible antimicrobials and preservatives of natural origin. Thanks to their antimicrobial properties against pathogenic and food spoilage microorganisms, EOs have shown good potential for use as alternative food additives, also to counteract biofilm-forming bacterial strains, the spread of which is considered to be among the main causes of the increase in foodborne illness outbreaks. In this context, the aim of this study has been to define the antibacterial and antibiofilm profile of thyme (*Thymus vulgaris* L.) essential oil (TEO) against widespread foodborne pathogens, *Salmonella enterica* subsp. *enterica* serovar Typhimurium and *Bacillus cereus*. TEO chemical composition was analyzed through gas chromatography-mass spectrometry (GC-MS). Preliminary in vitro antibacterial tests allowed to qualitatively verify TEO efficacy against the tested foodborne pathogens. The subsequent determination of minimal inhibitory concentration (MIC) and minimal bactericidal concentration (MBC) values allowed to quantitatively define the bacteriostatic and bactericidal effects of TEO. To evaluate the ability of essential oils to inhibit biofilm formation, a microplate assay was performed for the bacterial biofilm biomass measurement. Results suggest that TEO, rich in bioactive compounds, is able to inhibit the growth of tested foodborne bacteria. In addition, the highlighted in vitro antibiofilm properties of TEO suggest the use of this natural agent as a promising food preservative to counteract biofilm-related infections in the food industry.

Keywords: thyme essential oil; antibacterial agent; antibiofilm activity; natural food preservatives; foodborne illness pathogens

1. Introduction

Foodborne illness encompasses a wide spectrum of illnesses defined by the WHO's Department of Food Safety, Zoonoses and Foodborne Diseases (FOS) as a growing public health problem worldwide [1]. In recent years, most of the foodborne outbreaks in Europe and the United States were related to the consumption of contaminated meat and meat products; fresh processed products of pig meat were the most frequently involved category, along with chicken meat [2]. Meat and meat products contain essential amino acids, B-group vitamins, minerals and other nutrients ideal both for human nutrition and microbial growth [3]. Fresh and transformed meat are rich substrates that strongly support significant microbial growth, since they have nutrients, pH values and water contents generally compatible with the growth of a large number and variety of microorganisms [4].

Therefore, meat and meat products are easily perishable foods and are highly susceptible to the growth of microorganisms, including spoilage microorganisms and foodborne pathogens [5] causing outbreaks which severely affect public health and the economy [6].

The pathogens of great concern for foodborne illness outbreaks mainly include *Salmonella* spp., enterohemorrhagic *Escherichia coli*, *Listeria monocytogenes*, *Bacillus* spp., *Staphylococcus aureus* and *Clostridium* spp. [4,7].

Salmonella spp. is among the most common etiological agents of human gastroenteritis, frequently isolated from both the mammal's gut and environment. Effluents, floors and walls of contaminated abattoir are considered major sources of *Salmonella* species [8,9]. Several serotypes of *Salmonella enterica* such as *Salmonella enterica* subsp. *enterica* serovar Typhimurium are particularly dangerous because they can cause food poisoning and develop biofilms that are difficult to remove [10].

Among other bacterial pathogens causing foodborne illnesses, *Bacillus cereus* is well-known. It is spread both in the environment and in raw foods, such as meat, rice and vegetables. The inadequate cooling after heat treatment is indicated as the main factor contributing to the spread of *B. cereus* in the above-mentioned foods [11]. This microorganism is of particular concern for the food industry, causing food safety issues due to the formation of spores, emetic toxins and biofilms causing diarrhea [12].

The ability of foodborne strains to develop biofilms on different surfaces enhances their persistence in different environments by increasing their physical and chemical resistance [13]. Biofilm-forming bacteria are able to adhere to a wide range of surfaces, including stainless steel, plastic, glass and also food. The adhesion process occurs in a few minutes, until the development of mature biofilms in some hours or days [14], causing major challenges for the food industry [15].

The use of safe and effective preservation methods that allow to counteract the spread of foodborne illness outbreaks and prevent the deterioration of meat products is crucial. Heating, chilling and packaging are some of the current methods for meat and meat product preservation, together with high pressure and ionizing radiation [4]. In addition, the use of chemical preservatives and additives, such as nitrites and nitrates, allow to prevent the spoilage caused by foodborne microorganisms and pathogenic bacteria in meat products [16]. However, the increasing use of synthetic additives in food has raised many carcinogenic and toxic problems and has been related to allergy episodes [4,17–19]. For these reasons, consumers today demand food free of artificial substances, such as antimicrobial and chemically synthesized food preservatives, as they are perceived as harmful to health. Current trends for products without synthetic preservatives have led to the search for natural antimicrobial compounds. There has been thorough research on natural food additives with a broad spectrum of antimicrobial activities, capable of improving the microbiological quality and the shelf-life of perishable foods. Aromatic plants and their derivatives, such as essential oils (EOs), have attracted considerable interest [20–24]. Numerous studies demonstrated that essential oils employed as preservatives possess in vitro antimicrobial properties [25,26]. For instance, results of recent research demonstrated the antimicrobial activity of thyme essential oil against several foodborne pathogens [27–29], thus encouraging their potential use to reduce pathogenic bacteria spread and for the extension of food products' shelf-life [30]. Several studies are underway to evaluate the effectiveness of essential oils when added to foods [31,32], while studies on the application of EOs to prevent biofilm production on food and environmental surfaces have recently increased [33–35].

In this frame, the present study aims to evaluate the in vitro antibacterial effects of thyme essential oil (TEO), form *Thymus vulgaris* L., against important and common causative agents of food infections. Even if TEO is well-known for its ability to inhibit the growth of both Gram negative and Gram positive bacteria [36–38], a significant variability may exist among the in vitro antibacterial effects of the same type of EO, depending both on EO chemical composition and variable susceptibility by tested microbial isolates. In addition, foodborne isolates of the same species could present a different susceptibil-

ity/resistance to natural extracts [39–41]. In this regard, this work aims to confirm the presence of antimicrobial molecules in the tested Italian TEO and to increase the number of scientific evidences demonstrating the sensitivity of important foodborne illness etiological agents to TEO. In particular, the in vitro antibacterial activity of TEO was evaluated against two meat isolates, i.e., *S.* Typhimurium and *Bacillus cereus*. Considering that recent studies showing TEO antibiofilm effects are still few, TEO was tested against foodborne pathogenic isolates both in planktonic and biofilm form, with the future prospect to use it in food preservation to control the safety and quality of meat products along the entire food chain and biofilm formation associated with foodborne pathogens.

2. Results and Discussion

2.1. Chemical Composition of Thyme Essential Oil

The quality and authenticity of thyme essential oil (TEO) tested in this study were evaluated by the manufacturer according to the European Pharmacopoeia (Ph. Eur.) recommendations, by checking the purity of plant raw materials (*Thymus vulgaris* L.) and by measuring quality markers after extraction. In particular, panel sensory analysis allowed the examination of TEO organoleptic properties (odor, color, aspect), while physical analysis (i.e., density and moisture content measuring) allowed to evaluate its purity (>95%), along with the absence of water, and to define TEO as free from foreign bodies or extraneous matter, and from impurities of the raw material itself. These simple, cheap and fast analyses allowed the identification of any adulteration, but chemical characterization analysis by gas chromatography mass spectrometry was necessary to confirm TEO specific fingerprint.

TEO chemical composition is shown in Table 1. Seven main volatile compounds, representing 98.838 ± 0.99% of the total detected constituents, were identified by gas chromatography mass spectrometry analyses in TEO (Figure 1).

Table 1. Chemical composition of thyme essential oil.
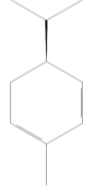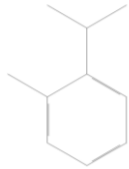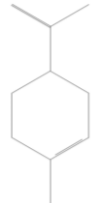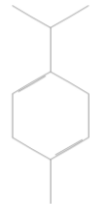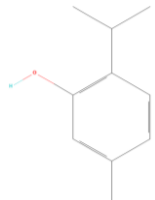
N° Peak	RI	Relative Peak Area %	Identified Compound	Structure
1	973	1.232 ± 0.01	sabinene	
2	978	7.177 ± 0.04	β-pinene	
3	996	0.518 ± 0.00	α-phellandrene	

Table 1. *Cont.*

N° Peak	RI	Relative Peak Area %	Identified Compound	Structure
4	1021	1.680 ± 0.50	o-cymene	
5	1035	39.391 ± 0.20	limonene	
6	1064	4.405 ± 0.02	γ-terpinene	
7	1302	44.435 ± 0.22	thymol	

Results are reported as mean values of relative peak area % (area peak compound/area peak total compounds)×100) ± standard deviation (n = 2). Constituents are presented in the order of elution from the HP-5MS column. NIST MS Search Software (version 2.0) and Wiley 8 mass spectral libraries (USA National Institute of Science and Technology software 2.0) of the GC/MS data system allowed the identification of compounds. The 2D structures were acquired from PubChem Compound Database. RI, retention index.

Thymol (44.435 ± 0.22%), limonene (39.391 ± 0.20%), β-pinene (7.177 ± 0.04%) and γ-terpinene (4.405 ± 0.02%) were identified as the major constituents. The other components, i.e., sabinene, α-phellandrene and o-cymene, were present in a total amount of less than 4% (3.430 ± 0.51%).

Essential oils (EOs) are complex matrices with extremely variable composition and properties. It is known that the chemical constituents of EOs may vary depending on several factors, including harvest season, habitat, drying processes of plant raw material, extraction techniques, storage time and others [42,43]. Due to this variability, the determination of the TEO constituent profile was necessary to confirm the presence of bioactive molecules, including antibacterial compounds. In particular, the chemical composition of TEO in our study is found to be comparable to previous literature studies reporting thymol, limonene, β-pinene and γ-terpinene as major compounds in TEO [44–49]. Similar studies reported that thymol percentage ranging from 12% to 71% for *Thymus vulgaris* EO really contributes to its antimicrobial activity [46,47].
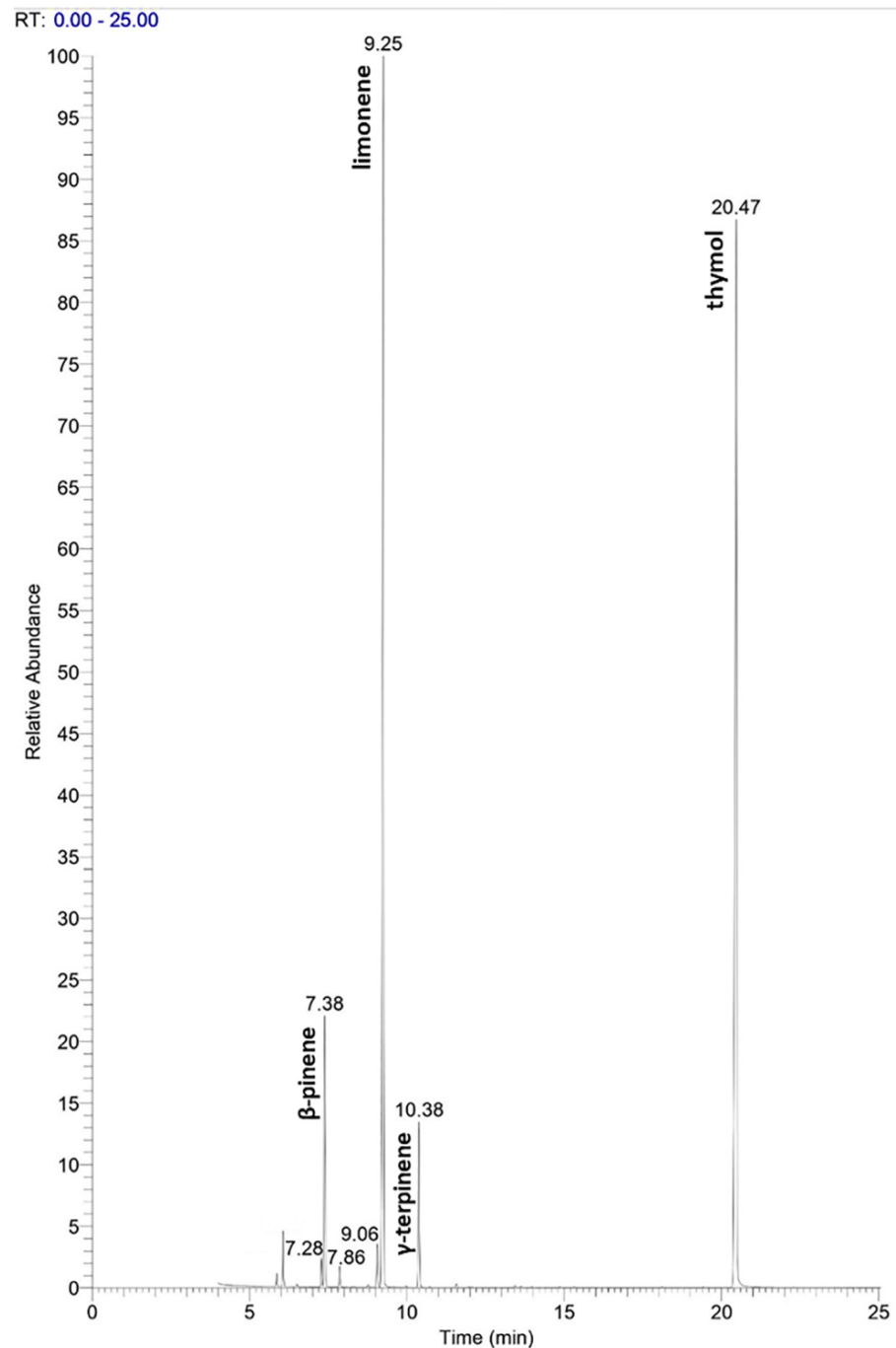
Figure 1. Gas chromatogram of the tested thyme essential oil. The most abundant components were identified through GC-MS analysis by Thermo Scientific TRACE 1310 GC system coupled to an ITQ 900 mass spectrometer and are assigned in the figure. RT, retention time.

2.2. In Vitro Antibacterial Activity of Thyme Essential Oil against Salmonella enterica subsp. Enterica Serovar Typhimurium and Bacillus cereus Food Isolates

TEO exhibited an appreciable inhibitory activity against both *S.* Typhimurium and *B. cereus* bacterial meat isolates, as demonstrated by the inhibition zone of bacterial growth estimated through the agar well diffusion method. Figure 2 shows the mean diameter of the inhibition zone (MDIZ) of bacterial growth exerted by TEO against *S.* Typhimurium ST1 (Figure 2A) and *B. cereus* BC3 (Figure 2B) isolates.
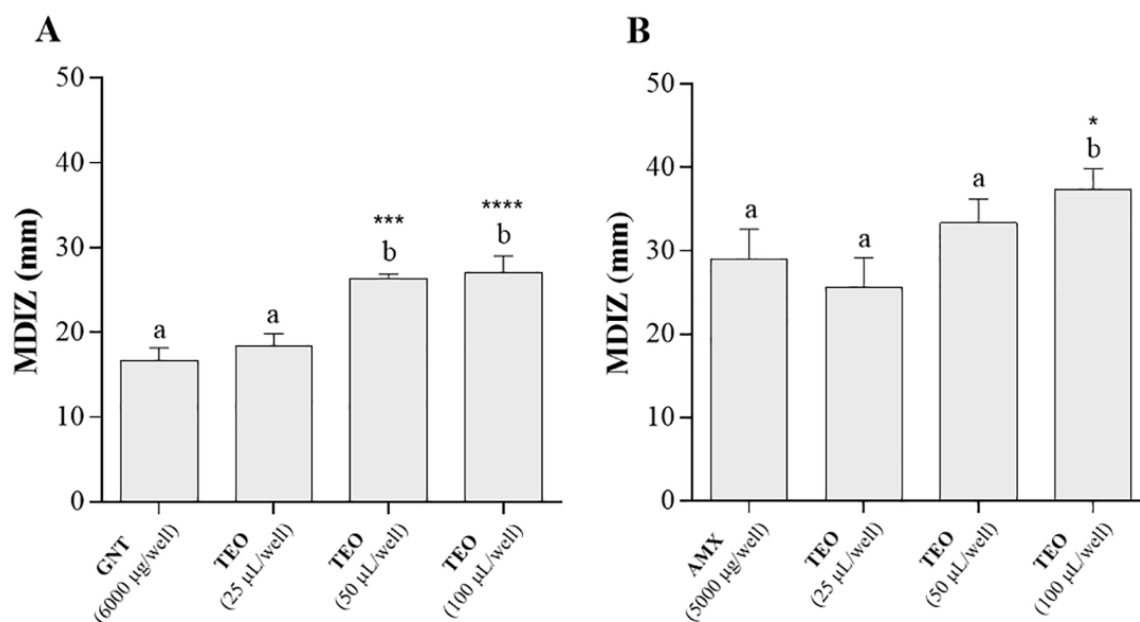
Figure 2. In vitro antibacterial activity of thyme essential oil against *S.* Typhimurium ST1 (**A**) and *B. cereus* BC3 (**B**) food isolates. Results were obtained by agar well diffusion method; triplicate assays with independent cultures. The mean diameters of inhibition zone, reported as mean values ± standard deviation (expressed in mm), are graphically represented. One-way ANOVA test was performed to evaluate statistical significance. Bars comparison with positive control bar (absence of TEO) was analyzed by Dunnett's post hoc test ($p < 0.05$), using asterisks to indicate statistical significance respect to the positive control (**** $p < 0.0001$; *** $p < 0.001$; * $p < 0.05$). Tukey's post hoc test ($p < 0.05$) allowed to examine the statistical significance for multiple comparisons between bars. Different letters (a, b) indicate significant differences between bars; bars with no significant differences receive the same letter. MDIZ, mean diameter of the inhibition zone; TEO, thyme essential oil; GNT, gentamicin; AMX, amoxicillin.

The MDIZ values ranged between 18.33 ± 1.25 mm (vs. *S.* Typhimurium ST1 at the volume of 25 μL/well) and 37.33 ± 2.05 mm (vs. *B. cereus* BC3 at the volume of 100 μL/well). Gentamicin and amoxicillin, tested as positive controls, showed antibacterial efficacy against the isolates, with MDIZ values of 16.67 ± 2.25 mm and 29.00 ± 2.94 mm, respectively; no effects were observed for the negative control. The MDIZ values measured around the wells filled with TEO (at the volumes of 50 μL/well and 100 μL/well against *S.* Typhimurium ST1 and at the volumes of 100 μL/well against *B. cereus* BC3) were significantly higher with respect to MDIZ values measured around the wells filled with the antibiotics gentamicin and amoxicillin. The in vitro antibacterial activity of TEO was also confirmed by quantitative assays. Table 2 shows values of minimum inhibitory concentration (MIC) and minimum bactericidal concentration (MBC).

Table 2. Values of minimal inhibitory concentration and minimal bactericidal concentration of thyme essential oil and positive controls against *S.* Typhimurium ST1 and *B. cereus* BC3 food isolates.

Antibacterial Agent	*S.* Typhimurium ST1		*B. cereus* BC3	
	MIC	MBC	MIC	MBC
TEO	20 μL mL^{-1}	100 μL mL^{-1}	10 μL mL^{-1}	80 μL mL^{-1}
GNT	30 μg mL^{-1}	500 μg mL^{-1}	-	-
AMX	-	-	50 μg mL^{-1}	200 μg mL^{-1}

MIC, minimum inhibitory concentration; MBC, minimum bactericidal concentration; TEO, thyme essential oil; GNT, gentamicin; AMX, amoxicillin.

Tested TEO was able to exert both bacteriostatic and bactericidal effects against *S.* Typhimurium ST1 and *B. cereus* BC3 isolates, with a lower sensitivity of the Gram-negative isolate of *S.* Typhimurium to TEO, compared to the Gram-positive isolate of *B. cereus*. These results are partly in line with recent data in the literature. The significant in vitro antimicrobial activity of TEO has been demonstrated by different studies against various food pathogens, including Gram-positive bacteria, such as *Bacillus cereus* [47], and also against several serotypes of *S.* Typhimurium spp. [50]. In particular, the recent study conducted by Gonzalez et al. (2021) confirmed the in vitro bactericidal activity of TEO against *S.* Typhimurium, an important Gram negative pathogen and causative agent of food outbreaks [51]. In addition, obtained results are particularly significant given that the Italian tested TEO resulted to be more effective compared to other previous studies which tested this essential oil against the same bacterial species. For example, in the study by Valizadeh et al. (2016), the values of the inhibition zone diameter (mm) obtained by testing *Thymus vulgaris* essential oil using the agar well diffusion method were shown to be significantly lower both against *S.* Typhimurium (15 mm) and *B. cereus* (17 mm) isolates [52], compared to Italian TEO tested in this study at the same volume (100 μL) and with the same method. Moreover, MIC for TEO against *S.* Typhimurium ST1 food isolate indicates more significant antimicrobial effects of tested essential oil than those obtained by Penalver et al. (2005); the MIC value (4% *v/v*) for thyme essential oil against *S.* Typhimurium was two-fold higher, indicating lower in vitro antimicrobial effects [53]. In the study of Turgis et al. (2012) no activity was observed for *Thymus vulgaris* essential oil against *S.* Typhimurium at the concentration of 4000 ppm [54]. Finally, another recent study reports a five-fold higher MIC value against *B. cereus* (5% *v/v*) than that obtained by testing TEO against *B. cereus* BC3 isolate [55], thus demonstrating the more significant activity of tested Italian TEO against this foodborne pathogen.

TEO antimicrobial activity depends on its chemical composition. Synergistic interactions between bioactive compounds are responsible for specific antimicrobial mechanisms of action. According to Kang et al. (2018), TEO rich in p-cymene, thymol and γ-terpinene showed the ability to inhibit the growth of *B. cereus* by causing membrane damage, alterations in cell morphology and a decrease in the intracellular pool of ATP [56]. The hyper-permeabilization of the bacterial cell membrane, resulting in the loss of membrane potential and collapse of proton pumps and depletion of ATP, with consequent delays or inhibitions of microbial growth, could be the main mechanism of action of TEO against *Salmonella* spp. [35].

2.3. In Vitro Antibiofilm Activity of Thyme Essential Oil against Salmonella enterica subsp. Enterica Serovar Typhimurium and Bacillus cereus Food Isolates

The anti-biofilm activity of TEO was evaluated against *S.* Typhimurium and *B. cereus* food isolates by the tissue culture plate method to assess the impact of this natural agent upon biofilm formation in the food industry.

In vitro microbiological tests showed that TEO caused a significant inhibition of biofilm biomass of both *S.* Typhimurium and *B. cereus* food isolates compared to untreated controls, as reported in Figures 3A and 4A, respectively.

Optical density (OD_{600nm}) values were measured for biofilms grown in the absence and in the presence of increasing concentrations of TEO (10, 20, 40, 80, 100 μL mL^{-1}). Comparison with the negative control values, represented by sterile broth growth medium, allowed for the determination of the adhesion level for each test condition, enabling the classification of microbial isolates as non-adherent, weakly adherent, moderately adherent and strongly adherent.
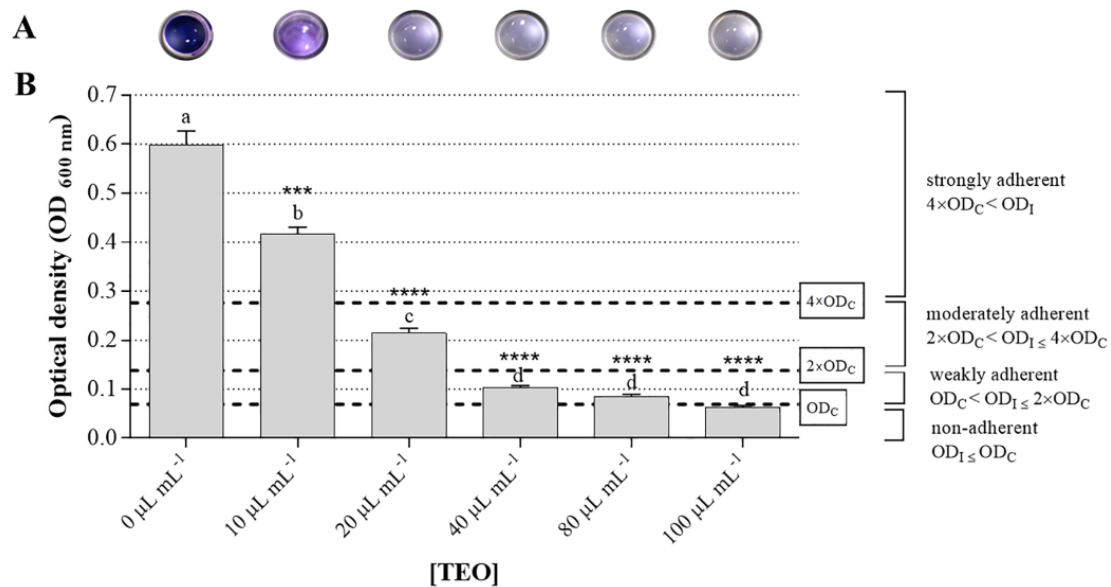
Figure 3. Adherence levels of *S.* Typhimurium ST1 food isolate. (**A**) Biofilm biomass at the bottom of multi-well plates in the presence and absence of increasing concentrations (10, 20, 40, 80, 100 μL mL^{-1}) of TEO. (**B**) Optical density (OD) values, detected by absorbance reading at a wavelength of 600 nm with a microplate reader, of bacterial biofilms developed by *S.* Typhimurium ST1 in absence and in the presence of increasing concentrations (10, 20, 40, 80, 100 μL mL^{-1}) of TEO. The comparison with negative control, represented by the broth medium, allowed to determine the level of adherence for each experimental condition. One-way ANOVA test was performed to evaluate statistical significance. Bars comparison with positive control bar (absence of TEO) was analyzed by Dunnett's post hoc test ($p < 0.05$), using asterisks to indicate statistical significance with respect to the positive control (**** $p < 0.0001$; *** $p < 0.001$). Tukey's post hoc test ($p < 0.05$) allowed to examine the statistical significance for multiple comparisons between bars. Different letters (a–d) indicate significant differences between bars; bars with no significant differences receive the same letter. TEO, thyme essential oil; OD$_I$, isolates optical density, OD$_C$, negative control optical density.
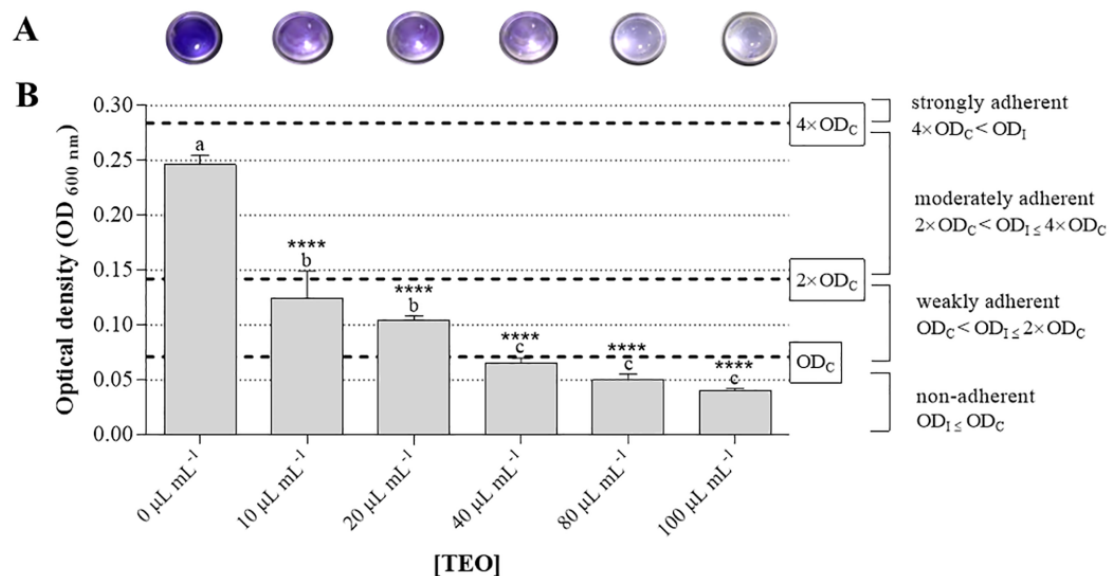
Figure 4. Adherence levels of *B. cereus* BC3 food isolate. (**A**) Biofilm biomass at the bottom of multi-well plates in the presence and absence of increasing concentrations (10, 20, 40, 80, 100 μL mL^{-1}) of TEO. (**B**) Optical density (OD) values, detected by absorbance reading at a wavelength of 600 nm with a microplate reader, of bacterial biofilms developed by *B. cereus* BC3 in the presence and absence

of increasing concentrations (10, 20, 40, 80, 100 $\mu L\ mL^{-1}$) of TEO. The comparison with negative control, represented by the broth medium, allowed to determine the level of adherence for each experimental condition. One-way ANOVA test was performed to evaluate statistical significance. Bars comparison with positive control bar (absence of TEO) was analyzed by Dunnett's post hoc test ($p < 0.05$), using asterisks to indicate statistical significance with respect to the positive control (**** $p < 0.0001$). Tukey's post hoc test ($p < 0.05$) allowed to examine the statistical significance for multiple comparisons between bars. Different letters (a, b, c) indicate significant differences between bars; bars with no significant differences receive the same letter. TEO, thyme essential oil; OD_I, isolates optical density, OD_C, negative control optical density.

In detail, in the absence of TEO (0 $\mu L\ mL^{-1}$), and at the concentration of 10 $\mu L\ mL^{-1}$, *S.* Typhimurium ST1 isolate showed strong adherence ($4 \times OD_C < OD_I$), while in the presence of increasing concentrations of oil, there was a gradual decrease in adhesion, until the absence of adherence at the concentration of 100 $\mu L\ mL^{-1}$ of TEO ($OD_I \leq OD_C$) (Figure 3B), identified as the minimum biofilm inhibition concentration (MBIC) value for the tested oil against *S.* Typhimurium isolate. *B. cereus* BC3 isolate showed strong adherence ($4 \times OD_C < OD_I$) in the absence of thyme essential oil (0 $\mu L\ mL^{-1}$), while in the presence of increasing concentrations of TEO, there was a gradual decrease in adhesion, up to the absence of adhesion at the concentration of 40 $\mu L\ mL^{-1}$ of TEO ($OD_C \leq OD_I$) (Figure 4B). Therefore, the concentration of 40 $\mu L\ mL^{-1}$ can be indicated as the minimum biofilm inhibition concentration (MBIC) for TEO against *B. cereus* meat isolate.

At increasing concentrations of TEO, a progressive increase in the percentage of biofilm inhibition was observed, for both *S.* Typhimurium (Figure 5A) and *B. cereus* (Figure 5B) food isolates.

In particular, TEO was able to inhibit biofilm formation by *S.* Typhimurium ST1 at the concentration of 10 $\mu L\ mL^{-1}$, with an inhibition percentage of 30.03 ± 3.52%, showing a progressive increase in the percentage of biofilm inhibition with increasing TEO concentrations, reaching the inhibition percentage of 89.62 ± 0.32% at the concentration of 100 $\mu L\ mL^{-1}$ (Figure 5A); in the absence of TEO, there was no inhibition of biofilm formation for *S.* Typhimurium food isolate. These results are really promising, compared with results of other studies which demonstrated the antibiofilm effect of thyme essential oil against *Salmonella* spp., with an inhibition percentage of biofilm formation exceeding 60% but generally less than 80% [35,57,58]. This effect could be attributed to the ability of TEO monoterpenes to spread through the exopolysaccharide matrix (EPS) of bacterial biofilms, interfering with key events in the biofilm formation process, such as adhesion protein production [35].

Regarding the tested *B. cereus* meat isolate, there was no inhibition of biofilm formation in the absence of TEO. TEO inhibited the biofilm formation at the concentration of 10 μL mL^{-1} (inhibition percentage of 49.11 ± 9.73%), even if the food isolate was still classifiable as adherent. At the concentration of 100 $\mu L\ mL^{-1}$, the percentage of biofilm inhibition reached the value of 83.85 ± 0.28% (Figure 5B). In the absence of TEO, there was no inhibition of biofilm formation for both *S.* Typhimurium and *B. cereus* food isolates. Other previous studies demonstrated that TEO exerts a significant inhibitory effect on the formation of biofilm by *B. cereus*, although the values of inhibition percentage are lower than those reported in this study and the mechanisms have not yet been fully understood [56,59].
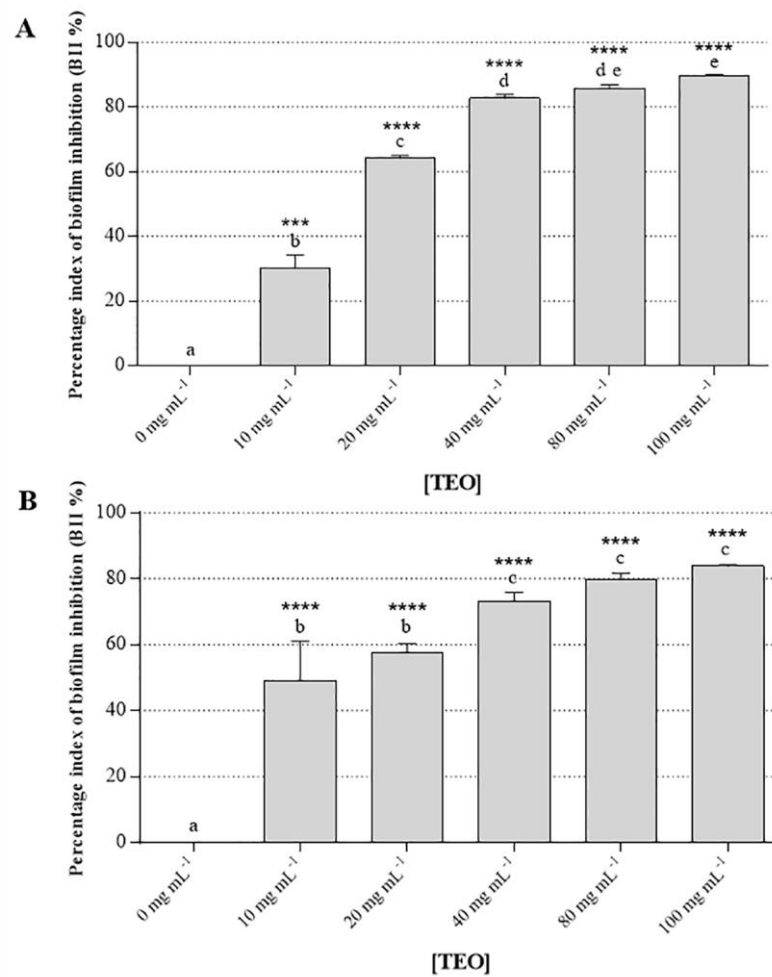
Figure 5. Inhibitory effect of thyme essential oil against biofilm formation by *S.* Typhimurium ST1 (**A**) and *Bacillus cereus* BC3 (**B**) food isolates. Graphs show the percentage inhibition values of biofilms in the presence and absence of increasing concentrations of TEO (10, 20, 40, 80, 100 μL mL^{-1}). One-way ANOVA test was performed to evaluate statistical significance. Bars comparison with positive control bar (absence of TEO) was analyzed by Dunnett's post hoc test ($p < 0.05$), using asterisks to indicate statistical significance with respect to the positive control (**** $p < 0.0001$; *** $p < 0.001$). Tukey's post hoc test ($p < 0.05$) allowed to examine the statistical significance for multiple comparisons between bars. Different letters (a, b, c, d, e) indicate significant differences between bars; bars with no significant differences receive the same letter. TEO, thyme essential oil.

3. Materials and Methods

3.1. Thyme Essential Oil (TEO)

Thyme essential oil (TEO) was provided by the Italian manufacturing company Alta Profumeria S.r.l. (Durazzano, Benevento, Italy) in collaboration with the University of Sannio for several scientific research projects. It was obtained from plant aerial parts (leaves and flowers) of *Thumus vulgaris* L. by the steam distillation method and it was stored at 0–4 °C in the dark until further use.

3.2. Gas Chromatography-Mass Spectrometry Analysis of TEO

GC-MS analysis was carried out by Thermo Scientific TRACE 1310 GC system coupled to an ITQ 900 mass spectrometer (Thermo Fisher Scientific, Waltham, MA, USA). An HP-5MS capillary column (30 m × 0.25 mm, 0.25 μm film thickness) was used. Analyses were performed according to Alsaraf et al. (2020) [60], with slight modifications. The maximum elution temperature was 350 °C, with helium as the carrier gas (flow rate of 1 mL min^{-1}).

Injection temperature was set to 290 °C, while 270 °C was the set temperature for the ion source. The chemical ionization energy of 70 eV was used for MS. Mass spectral data collection in full-scan mass was carried out between 40 and 550 amu. TEO was diluted in hexane (1:10 dilution ratio) and an aliquot of sample (2 μL) was injected (150:1 split ratio). Oven temperature was programmed at 60 °C, with a constant gradually increasing rate of 3 °C min^{-1} until 280 °C. Compounds were identified using NIST MS Search Software (version 2.0). Identification was based on retention indices relatives to n-alkanes and computer matching by comparing query mass spectra with reference mass spectra in the Wiley 8 mass spectral libraries (USA National Institute of Science and Technology software 2.0) of the GC/MS data system. Analyses were performed in duplicate and the percentage of each identified compound was estimated by dividing its mean area by the total chromatogram area.

3.3. Meat Bacterial Isolates and Growth Conditions

TEO was tested for its antibacterial effects against *Salmonella enterica* subsp. *enterica* serovar Typhimurium and *Bacillus cereus* meat isolates in the Laboratory of Microbiology of the Department of Science and Technology, University of Sannio. Bacterial isolates used in this study were denominated *S.* Typhimurium ST1 and *B. cereus* BC3. They were isolated from samples of minced chicken meat (*S.* Typhimurium ST1) and minced pig meat (*B. cereus* BC3) and identified by differential and chromogenic selective media. In particular, the selective and chromogenic and differential media Xylose Lysine Desoxycholate Agar (CONDA, Madrid, Spain) and *Bacillus* ChromoSelect Agar (Sigma-Aldrich S.r.l., Milano, Italy), with the addition of Polymyxin B Selektiv-Supplement (Cat. No. P9602, Sigma-Aldrich S.r.l., Milano, Italy), were used for in vitro growth and identification of *S.* Typhimurium and *B. cereus* isolates, respectively. After Gram staining (Gram staining kit, Sigma-Aldrich S.r.l., Milano, Italy), the observation by microscopy Motic B1-223 (Thermo Fisher Scientific, Waltham, MA, USA) allowed to complete the phenotypic identification. *S.* Typhimurium ST1 isolate was shown to be susceptible to β-lactam antibiotics (amoxicillin and ampicillin) and chloramphenicol, as well as gentamicin, chosen as the positive control (Supplemenatry Material Table S1). The sensitivity profile of *B. cereus* BC3 isolate (Table S1) shows its susceptibility to chloramphenicol, gentamicin and β-lactam antibiotics, especially to amoxicillin, selected as the control for following antimicrobial tests. Meat bacterial isolates were grown at 37 °C for 24 h in aerobic conditions, on the non-selective medium Luria Bertani (LB) (CONDA, Madrid, Spain), in order to revitalize them before use for microbiological assay.

3.4. In Vitro Antibacterial Assays

3.4.1. Agar Well Diffusion Method

A preliminary in vitro antimicrobial assay was performed in order to qualitatively evaluate the TEO antibacterial activity against tested foodborne isolates. Specifically, the agar well diffusion method was carried out, similar to Perez (1990) [61]. Briefly, bacterial meat isolates were grown in LB broth. After reaching an optical density (O.D.) of 0.5 OD$_{600nm}$, aliquots (200 μL) of each microbial suspension were spread on LB agar. Then, wells of 6 mm diameter were punched with sterilized glass Pasteur into agar media and were filled up with TEO aliquots (25, 50, 100 μL) and with selected test controls. In particular, gentamicin (Sigma-Aldrich S.r.l., Milano, Italy) and amoxicillin (Sigma-Aldrich S.r.l., Milano, Italy) were used as positive controls for *S.* Typhimurium ST1 and *B. cereus* BC3 isolates, respectively; distilled water was used as a negative control. After plates incubation at 37 °C for 24 h, in aerobic conditions, the mean diameter of the inhibition zone (MDIZ) (expressed in mm) produced by TEO around the wells was measured in order to evaluate the TEO in vitro antibacterial activity against the selected bacterial foodborne pathogens.

3.4.2. Tube Dilution Method

Tube dilution method with standard bacterial inoculum 1×10^5 CFU/mL (Colonies Forming Units/mL) in LB broth was performed, according to the Clinical and Laboratory Standards Institute (CLSI) 2022 guidelines [62], in order to quantitatively determine the susceptibility of *S.* Typhimurium ST1 and *B. cereus* BC3 foodborne isolates to different concentrations of TEO. In brief, TEO was directly added to the broth medium reaching increasing final concentrations (0, 5, 10, 20, 40, 60, 80, 100, 120, 140 µL mL^{-1}). After a vigorous stirring by vortex mixer, tubes were incubated at 37 °C for 24 h in aerobic conditions, with constant shaking to maintain homogenous TEO micelle aggregates in the broth medium. After incubation, the values of minimum inhibitory concentration (MIC) were determined through the observation of tube turbidity. In addition, for the determination of the minimum bactericidal concentration (MBC) values, aliquots of serial dilutions of the bacterial suspensions were spread on LB agar and viable bacterial counts were performed after plate incubation under appropriate growth conditions. MIC was assigned to the lowest concentration of TEO that prevented the bacterial growth. MBC was defined as the minimum concentration of TEO that killed 99% of bacteria from the initial inoculum. Gentamicin (Sigma-Aldrich S.r.l., Milano, Italy) and amoxicillin (Sigma-Aldrich S.r.l., Milano, Italy) were used as positive controls for *S.* Typhimurium ST1 and *B. cereus* BC3 isolates, respectively, while distilled water was used as the negative control.

3.5. In Vitro Antibiofilm Assays

3.5.1. Tissue Culture Plate Method (TCPM)

The so-called Tissue culture plate method (TCPM) was carried out to measure biofilm biomass of tested foodborne bacteria, as described in Sateriale et al. (2020) [63]. After growing overnight cultures of selected microorganisms at 37 °C for 24 h in LB broth, with aerobic incubation, the OD$_{600nm}$ of fresh cultures were further adjusted until 0.5 OD. Then, aliquots of starter cultures (200 µL) were dispensed into wells of a 96-well flat-bottomed microplate (Nunc™ MicroWell 96-well microplates, Thermo Scientific, Roskilde, Denmark) in six replicates, using sterile LB broth as the negative control. The incubation at 37 °C for 24 h without shaking allowed the adhesion of bacterial cells to the microplate surface. Each bacterial culture was removed after incubation, and free-floating bacterial cells were removed by washing wells with phosphate buffer saline ($1\times$ PBS, pH 7.3) three times. Then, adherent biofilms were fixed with 85% ethanol (Sigma-Aldrich, Merck KGaA, Darmstadt, Germany) for 15 min and stained with 0.2% crystal violet (Sigma-Aldrich, Merck KGaA, Darmstadt, Germany) for 5 min. After washing with deionized water to remove the stain excess, plates were dried upside down in a thermostat at the temperature of 30 °C for 10 min. After the addition of 85% ethanol (Sigma-Aldrich, Merck KGaA, Darmstadt, Germany) in crystal violet-stained biofilms, the OD values were recorded at 600 nm wavelength by a microplate reader (Bio-Rad Microplate reader, Model 680). The measurement of the optical density of bacterial isolates (OD$_I$), and the comparison with values measured for sterile LB broth used as the negative control (OD$_C$), allowed to classify the bacterial isolates as non-adherent (OD$_I \leq$ OD$_C$), weakly adherent (OD$_C <$ OD$_I \leq 2 \times$ OD$_C$), moderately adherent ($2 \times$ OD$_C <$ OD$_I \leq 4 \times$ OD$_C$) and strongly adherent ($4 \times$ OD$_C <$ OD$_I$).

3.5.2. Biofilm Formation Inhibition Assay

To evaluate the ability of TEO to inhibit biofilm formation, some modifications to the tissue culture plate method were carried out. In particular, increasing concentrations of TEO (0, 10, 20, 40, 80, 100 µg mL^{-1}) were added to each 96-well microplate well. Sterile LB broth was added to the negative control wells. Finally, 0.1 mL of each bacterial culture, with 0.5 OD A$_{600nm}$ wavelength, was pipetted to each well, reaching the final volume of 0.2 mL. LB (0.2 mL) broth was added into the wells without bacterial culture as the blank. The plates were wrapped loosely and aerobically incubated at 37 °C for 24 h without shaking. After incubation, the staining step of the TCPM method with crystal violet was performed, followed by microplate reading at the wavelength of 600 nm. According to

Bakkiyaraj et al. (2013) [64], results were indicated as the percentage of biofilm formation inhibition, as follows:

$$\text{Biofilm formation inhibition \%} = \left(\frac{OD_{control} - OD_{assay}}{OD_{control}} \right) \times 100$$

where $OD_{control}$ corresponds to the mean optical density measured for bacterial biofilms grown in the absence of TEO, while OD_{assay} is the mean optical density measured for bacterial biofilms grown in the presence of TEO. Minimum Biofilm Inhibition Concentration (MBIC) was defined as the lowest concentration of TEO able to produce bacterial biofilm inhibition.

3.6. Statistical Data Analysis

Antimicrobial assays were performed against three independent bacterial cultures. Obtained results have been graphically reported by 'GraphPad Prism 7.00' software and statistical significance has been validated by one-way ANOVA test, with Dunnett's and Tukey's corrections. *p* values < 0.05 have been considered statistically significant.

4. Conclusions

In this study, we demonstrated that thyme essential oil (TEO) has an excellent antibacterial activity against important food pathogens, *Salmonella enterica* subsp. *enterica* serovar Typhimurium and *Bacillus cereus*, in planktonic form. The bacteriostatic and bactericidal activities of TEO were higher against the Gram-positive pathogens than the Gram-negative ones. TEO was also active in counteracting the biofilm formation by *S.* Typhimurium and *B. cereus*. Altogether, the results of this study suggest that TEO may be a viable candidate as a natural food additive to be employed in the food industry, as an alternative to synthetic preservatives, to control foodborne contamination and biofilm formation associated with *S.* Typhimurium and *B. cereus* pathogens. The antibacterial and antibiofilm activities of TEO against meat pathogen isolates stimulate further research to assess TEO ability to prolong the shelf-life of meat food.

Author Contributions: Conceptualization, C.P. (Caterina Pagliarulo) and D.S.; methodology, D.S., G.F. and G.A.D.C.; data curation, D.S. and C.P. (Caterina Pagliarulo); writing—original draft preparation, D.S. and C.P. (Caterina Pagliarulo); writing—review and editing, D.S., C.P. (Caterina Pagliarulo) and M.P.; visualization, R.C., C.P. (Chiara Pagliuca) and P.S.; supervision, C.P. (Caterina Pagliarulo), M.P., R.C. and P.S.; project administration, C.P. (Caterina Pagliarulo); funding acquisition, C.P. (Caterina Pagliarulo) and M.P. All authors have read and agreed to the published version of the manuscript.

References

1. WHO. *The Global Burden of Foodborne Diseases: Taking Stock and Charting the Way Forward: WHO Consultation to Develop a Strategy to Estimate the Global Burden of Foodborne Diseases*; WHO: Geneva, Switzerland, 2007; pp. 25–27.
2. Omer, M.K.; Álvarez-Ordoñez, A.; Prieto, M.; Skjerve, E.; Asehun, T.; Alvseike, O.A. A Systematic Review of Bacterial Foodborne Outbreaks Related to Red Meat and Meat Products. *Foodborne Pathog. Dis.* **2018**, *15*, 598–611. [CrossRef] [PubMed]

3. Pateiro, M.; Munekata, P.E.S.; Sant'Ana, A.S.; Domínguez, R.; Rodríguez-Lázaro, D.; Lorenzo, J.M. Application of Essential Oils as Antimicrobial Agents against Spoilage and Pathogenic Microorganisms in Meat Products. *Int. J. Food Microbiol.* **2021**, *337*, 108966. [CrossRef] [PubMed]

4. Jayasena, D.D.; Jo, C. Essential Oils as Potential Antimicrobial Agents in Meat and Meat Products: A Review. *Trends Food Sci. Technol.* **2013**, *34*, 96–108. [CrossRef]

5. Casaburi, A.; Piombino, P.; Nychas, G.J.; Villani, F.; Ercolini, D. Bacterial Populations and the Volatilome Associated to Meat Spoilage. *Food Microbiol.* **2015**, *45*, 83–102. [CrossRef] [PubMed]

6. Li, H.; Sun, X.; Liao, X.; Gänzle, M. Control of Pathogenic and Spoilage Bacteria in Meat and Meat Products by High Pressure: Challenges and Future Perspectives. *Compr. Rev. Food Sci. Food Saf.* **2020**, *19*, 3476–3500. [CrossRef]

7. Kalogianni, A.I.; Lazou, T.; Bossis, I.; Gelasakis, A.I. Natural Phenolic Compounds for the Control of Oxidation, Bacterial Spoilage, and Foodborne Pathogens in Meat. *Foods* **2020**, *9*, 794. [CrossRef]

8. Allerberger, F.; Liesegang, A.; Grif, K.; Khaschabi, D.; Prager, R.; Danzl, J.; Höck, F.; Öttl, J.; Dierich, M.P.; Berghold, C.; et al. Occurrence of *Salmonella enterica* Serovar Dublin in Austria. *Wien. Med. Wochenschr.* **2003**, *153*, 148–152. [CrossRef]

9. Miranda, J.M.; Mondragon, A.C.; Martinez, B.; Guarddon, M.; Rodriguez, J.A. Prevalence and Antimicrobial Resistance Patterns of *Salmonella* from Different Raw Foods in Mexico. *J. Food Prot.* **2009**, *72*, 966–971. [CrossRef]

10. Srey, S.; Jahid, I.K.; Ha, S. Do Biofilm Formation in Food Industries: A Food Safety Concern. *Food Control* **2013**, *31*, 572–585. [CrossRef]

11. Nortjé, G.L.; Vorster, S.M.; Greebe, R.P.; Steyn, P.L. Occurrence of *Bacillus cereus* and *Yersinia enterocolitica* in South African Retail Meats. *Food Microbiol.* **1999**, *16*, 213–217. [CrossRef]

12. Huang, Y.; Flint, S.H.; Palmer, J.S. *Bacillus cereus* Spores and Toxins–The Potential Role of Biofilms. *Food Microbiol.* **2020**, *90*, 103493. [CrossRef] [PubMed]

13. Steenackers, H.; Hermans, K.; Vanderleyden, J.; De Keersmaecker, S.C.J. *Salmonella* Biofilms: An Overview on Occurrence, Structure, Regulation and Eradication. *Food Res. Int.* **2012**, *45*, 502–531. [CrossRef]

14. Hall-Stoodley, L.; Costerton, J.W.; Stoodley, P. Bacterial Biofilms: From the Natural Environment to Infectious Diseases. *Nat. Rev. Microbiol.* **2004**, *2*, 95–108. [CrossRef] [PubMed]

15. Alvarez-Ordóñez, A.; Coughlan, L.M.; Briandet, R.; Cotter, P.D. Biofilms in Food Processing Environments: Challenges and Opportunities. *Annu. Rev. Food Sci. Technol.* **2019**, *10*, 173–195. [CrossRef]

16. Sindelar, J.J.; Milkowski, A.L. Sodium Nitrite in Processed Meat and Poultry Meats: A Review of Curing and Examining the Risk/Benefit of Its Use. *Am. Meat Sci. Assoc.* **2011**, *3*, 1–14.

17. El-Wahab, H.M.F.A.; Moram, G.S.E.D. Toxic Effects of Some Synthetic Food Colorants and/or Flavor Additives on Male Rats. *Toxicol. Ind. Health* **2013**, *29*, 224–232. [CrossRef] [PubMed]

18. Sweis, I.E.; Cressey, B.C. Potential role of the common food additive manufactured citric acid in eliciting significant inflammatory reactions contributing to serious disease states: A series of four case reports. *Toxicol. Rep.* **2018**, *5*, 808–812. [CrossRef]

19. Rath, D. A critical review on food adulteration and its risk on health. *IJNRD* **2022**, *7*, 353–356.

20. Calo, J.R.; Crandall, P.G.; O'Bryan, C.A.; Ricke, S.C. Essential Oils as Antimicrobials in Food Systems—A Review. *Food Control* **2015**, *54*, 111–119. [CrossRef]

21. Al-Maqtari, Q.A.; Rehman, A.; Mahdi, A.A.; Al-Ansi, W.; Wei, M.; Yanyu, Z.; Yao, W. Application of essential oils as preservatives in food systems: Challenges and future prospectives—A review. *Phytochem. Rev.* **2022**, *21*, 1209–1246. [CrossRef]

22. Zang, E.; Jiang, L.; Cui, H.; Li, X.; Yan, Y.; Liu, Q.; Li, M. Only Plant-based Food Additives: An Overview on Application, Safety, and Key Challenges in the Food Industry. *Food Rev. Int.* **2022**, 1–32. [CrossRef]

23. Jafarzadeh, S.; Abdolmaleki, K.; Javanmardi, F.; Hadidi, M.; Mousavi Khaneghah, A. Recent advances in plant-based compounds for mitigation of mycotoxin contamination in food products: Current status, challenges and perspectives. *Int. J. Food Sci.* **2022**, *57*, 2159–2170. [CrossRef]

24. Balasubramaniam, V.G.; Ramakrishnan, S.R.; Antony, U. Opportunities and Challenges of Plant Extracts in Food Industry. In *Plant Extracts: Applications in the Food Industry*, 1st ed.; Academic Press; Elsevier: London, UK, 2021; pp. 295–315. ISBN 9780128224939.

25. Ballester-Costa, C.; Sendra, E.; Fernández-López, J.; Pérez-Álvarez, J.A.; Viuda-Martos, M. Chemical Composition and In Vitro Antibacterial Properties of Essential Oils of Four Thymus Species from Organic Growth. *Ind. Crops Prod.* **2013**, *50*, 304–311. [CrossRef]

26. Ruiz-Navajas, Y.; Viuda-Martos, M.; Sendra, E.; Perez-Alvarez, J.A.; Fernandez-Lopez, J. In Vitro Antioxidant and Antifungal Properties of Essential Oils Obtained from Aromatic Herbs Endemic to the Southeast of Spain. *J. Food Prot.* **2013**, *76*, 1218–1225. [CrossRef] [PubMed]

27. Ed-Dra, A.; Nalbone, L.; Filali, F.R.; Trabelsi, N.; El Majdoub, Y.O.; Bouchrif, B.; Giarratana, F.; Giuffrida, A. Comprehensive Evaluation on the Use of *Thymus vulgaris* Essential Oil as Natural Additive against Different Serotypes of *Salmonella enterica*. *Sustainability* **2021**, *13*, 4594. [CrossRef]

28. Sadekuzzaman, M.; Mizan, M.F.R.; Kim, H.S.; Yang, S.; Ha, S. Do Activity of Thyme and Tea Tree Essential Oils against Selected Foodborne Pathogens in Biofilms on Abiotic Surfaces. *LWT* **2018**, *89*, 134–139. [CrossRef]

29. Thielmann, J.; Muranyi, P.; Kazman, P. Screening Essential Oils for Their Antimicrobial Activities against the Foodborne Pathogenic Bacteria *Escherichia coli* and *Staphylococcus aureus*. *Heliyon* **2019**, *5*, e01860. [CrossRef]

30. Sharma, S.; Barkauskaite, S.; Duffy, B.; Jaiswal, A.K.; Swarna, J. Characterization and Antimicrobial Activity of Biodegradable Active Packaging Enriched with Clove and Thyme Essential Oil for Food Packaging Application. *Foods* **2020**, *9*, 1117. [CrossRef]
31. Rafiq, R.; Hayek, S.A.; Anyanwu, U.; Hardy, B.I.; Giddings, V.L.; Ibrahim, S.A.; Tahergorabi, R.; Kang, H.W. Antibacterial and Antioxidant Activities of Essential Oils from *Artemisia herba-alba Asso.*, *Pelargonium Capitatum × Radens* and *Laurus nobilis* L. *Foods* **2016**, *5*, 28. [CrossRef]
32. Ruiz-Navajas, Y.; Viuda-Martos, M.; Barber, X.; Sendra, E.; Perez-Alvarez, J.A.; Fernández-López, J. Effect of Chitosan Edible Films Added with Thymus Moroderi and Thymus Piperella Essential Oil on Shelf-Life of Cooked Cured Ham. *J. Food Sci. Technol.* **2015**, *52*, 6493–6501. [CrossRef]
33. Trevisan, D.A.C.; Campanerut-Sá, P.A.Z.; da Silva, A.F.; Batista, A.F.P.; Seixas, F.A.V.; Peralta, R.M.; de Sá-Nakanishi, A.B.; de Abreu Filho, B.A.; Junior, M.M.; Mikcha, J.M.G. Action of Carvacrol in *Salmonella typhimurium* Biofilm: A Proteomic Study. *J. Appl. Biomed.* **2020**, *18*, 106–114. [CrossRef]
34. Basavegowda, N.; Patra, J.K.; Baek, K.H. Essential Oils and Mono/Bi/Tri-Metallic Nanocomposites as Alternative Sources of Antimicrobial Agents to Combat Multidrug-Resistant Pathogenic Microorganisms: An Overview. *Molecules* **2020**, *25*, 1058. [CrossRef]
35. Guillín, Y.; Cáceres, M.; Torres, R.; Stashenko, E.; Ortiz, C. Effect of Essential Oils on the Inhibition of Biofilm and Quorum Sensing in *Salmonella enteritidis* 13076 and *Salmonella typhimurium* 14028. *Antibiotics* **2021**, *10*, 1191. [CrossRef] [PubMed]
36. Vunnava, A. Review on *Thymus vulgaris* Traditional Uses and Pharmacological Properties. *Med. Aromat. Plants* **2014**, *3*, 1000167.
37. Benameur, Q.; Gervasi, T.; Pellizzeri, V.; Pľuchtová, M.; Tali-Maama, H.; Assaous, F.; Guettou, B.; Rahal, K.; Gruľová, D.; Dugo, G.; et al. Antibacterial Activity of *Thymus vulgaris* Essential Oil Alone and in Combination with Cefotaxime against BlaESBL Producing Multidrug Resistant Enterobacteriaceae Isolates. *Nat. Prod. Res.* **2019**, *33*, 2647–2654. [CrossRef] [PubMed]
38. Mohammed, R.K.; Musa, F.H.; Mehdi, B.Y.; Al-Rawe, A.M. Impacts of the Alcoholic Extract and Essential Oil of *Thymus vulgaris* L. against the Causative Agent of Acne Formation (*Staphylococcus aureus*). *Syst. Rev. Pharm.* **2020**, *11*, 495–498. [CrossRef]
39. Lemos, M.F.; Lemos, M.F.; Pacheco, H.P.; Guimarães, A.C.; Fronza, M.; Endringer, D.C.; Scherer, R. Seasonal variation affects the composition and antibacterial and antioxidant activities of *Thymus vulgaris*. *Ind. Crops. Prod.* **2017**, *95*, 543–548. [CrossRef]
40. Kabdal, T.; Kumar, R.; Prakash, O.; Nagarkoti, K.; Rawat, D.S.; Srivastava, R.M.; Dubey, S.K. Seasonal variation in the essential oil composition and biological activities of *Thymus linearis* Benth. Collected from the Kumaun region of Uttarakhand, India. *Biochem. Syst. Ecol.* **2022**, *103*, 104449. [CrossRef]
41. Kim, M.; Sowndhararajan, K.; Kim, S. The Chemical Composition and Biological Activities of Essential Oil from Korean Native Thyme Bak-Ri-Hyang (*Thymus quinquecostatus Celak.*). *Molecules* **2022**, *27*, 4251. [CrossRef]
42. Hudaib, M.; Aburjai, T. Volatile Components of *Thymus vulgaris* L. from Wild-Growing and Cultivated Plants in Jordan. *Flavour Fragr. J.* **2007**, *22*, 322–327. [CrossRef]
43. Do, T.K.T.; Hadji-Minaglou, F.; Antoniotti, S.; Fernandez, X. Authenticity of essential oils. *TrAC Trends Anal. Chem.* **2015**, *66*, 146–157. [CrossRef]
44. Rota, M.C.; Herrera, A.; Martínez, R.M.; Sotomayor, J.A.; Jordán, M.J. Antimicrobial Activity and Chemical Composition of *Thymus vulgaris*, *Thymus zygis* and *Thymus hyemalis* Essential Oils. *Food Control* **2008**, *19*, 681–687. [CrossRef]
45. Pirbalouti, A.G.; Hashemi, M.; Ghahfarokhi, F.T. Essential Oil and Chemical Compositions of Wild and Cultivated Thymus Daenensis Celak and *Thymus vulgaris* L. *Ind. Crops Prod.* **2013**, *48*, 43–48. [CrossRef]
46. Shabnum, S.; Wagay, M.G. Essential Oil Composition of *Thymus vulgaris* L. and Their Uses. *J. Res. Dev.* **2011**, *11*, 83–94.
47. Kowalczyk, A.; Przychodna, M.; Sopata, S.; Bodalska, A.; Fecka, I. Thymol and Thyme Essential Oil—New Insights into Selected Therapeutic Applications. *Molecules* **2020**, *25*, 4125. [CrossRef]
48. Jordán, M.J.; Martínez, R.M.; Goodner, K.L.; Baldwin, E.A.; Sotomayor, J.A. Seasonal Variation of Thymus Hyemalis Lange and Spanish *Thymus vulgaris* L. Essential Oils Composition. *Ind. Crops Prod.* **2006**, *24*, 253–263. [CrossRef]
49. Quynh, C.T.T.; Trang, V.T. Volatile Composition, Antioxidant Property and Antimicrobial Activities against Food-Borne Bacteria of Vietnamese Thyme (*Thymus vulgaris* L.) Essential Oil. *Vietnam J. Sci. Technol.* **2019**, *57*, 127. [CrossRef]
50. Boskovic, M.; Djordjevic, J.; Ivanovic, J.; Janjic, J.; Zdravkovic, N.; Glisic, M.; Glamoclija, N.; Baltic, B.; Djordjevic, V.; Baltic, M. Inhibition of *Salmonella* by Thyme Essential Oil and Its Effect on Microbiological and Sensory Properties of Minced Pork Meat Packaged under Vacuum and Modified Atmosphere. *Int. J. Food Microbiol.* **2017**, *258*, 58–67. [CrossRef]
51. Gonzalez, K.; Johnson, A.; Gonsalves, V.; Santos, A. Antimicrobial Properties of Thyme Essential Oil on *Salmonella typhimurium*. *FASEB J.* **2021**, *35*. [CrossRef]
52. Valizadeh, S.; Mahmodi, R.; Fakheri, T.; Katiraie, F.; Rahmani, V. Investigating the phytochemical, antibacterial and antifungal effects of *Thymus vulgaris* and *Cuminum cyminum* essential oils. *Med. Lab. J.* **2016**, *10*, 36–43. [CrossRef]
53. Penalver, P.; Huerta, B.; Borge, C.; Astorga, R.; Romero, R.; Perea, A. Antimicrobial activity of five essential oils against origin strains of the Enterobacteriaceae family. *APMIS* **2005**, *113*, 1–6.
54. Turgis, M.; Vu, K.D.; Dupont, C.; Lacroix, M. Combined antimicrobial effect of essential oils and bacteriocins against foodborne pathogens and food spoilage bacteria. *Int. Food Res. J.* **2012**, *48*, 696–702. [CrossRef]
55. Sotelo-Boyás, M.; Correa-Pacheco, Z.; Bautista-Baños, S.; y Gómez, Y.G. Release study and inhibitory activity of thyme essential oil-loaded chitosan nanoparticles and nanocapsules against foodborne bacteria. *Int. J. Biol. Macromol.* **2017**, *103*, 409–414. [CrossRef] [PubMed]

56. Kang, J.; Liu, L.; Wu, X.; Sun, Y.; Liu, Z. Effect of Thyme Essential Oil against *Bacillus cereus* Planktonic Growth and Biofilm Formation. *Appl. Microbiol. Biotechnol.* **2018**, *102*, 10209–10218. [CrossRef]

57. Čabarkapa, I.; Čolović, R.; Đuragić, O.; Popović, S.; Kokić, B.; Milanov, D.; Pezo, L. Anti-Biofilm Activities of Essential Oils Rich in Carvacrol and Thymol against *Salmonella enteritidis*. *Biofouling* **2019**, *35*, 361–375. [CrossRef]

58. Grigore-Gurgu, L.; Ionela Bucur, F.; Borda, D.; Alexa, E.-A.; Neagu, C.; Ioana Nicolau, A. Biofilms Formed by Pathogens in Food and Food Processing Environments. In *Bacterial Biofilms*; IntechOpen: London, UK, 2020; pp. 1–32.

59. Soni, K.A.; Oladunjoye, A.; Nannapaneni, R.; Schilling, M.W.; Silva, J.L.; Mikel, B.; Bailey, R.H. Inhibition and Inactivation of *Salmonella typhimurium* Biofilms from Polystyrene and Stainless Steel Surfaces by Essential Oils and Phenolic Constituent Carvacrol. *J. Food Prot.* **2013**, *76*, 205–212. [CrossRef] [PubMed]

60. Alsaraf, S.; Hadi, Z.; Al-Lawati, W.M.; Al Lawati, A.A.; Khan, S.A. Chemical Composition, in Vitro Antibacterial and Antioxidant Potential of Omani Thyme Essential Oil along with in Silico Studies of Its Major Constituent. *J. King Saud Univ.-Sci.* **2020**, *32*, 1021–1028. [CrossRef]

61. Perez, C.; Pauli, M.; Bazerque, P. An Antibiotic Assay by the Agar Well Diffusion Method. *Acta Biol. Med. Exp.* **1990**, *15*, 113–115.

62. Clinical and Laboratory Standards Institute (CLSI). *Performance Standards for Antimicrobial Susceptibility Testing*, 32nd ed.; CLSI Supplement M100; Clinical and Laboratory Standards Institute (CLSI): Wayne, PA, USA, 2022; ISBN 978-1-68440-134-5.

63. Sateriale, D.; Imperatore, R.; Colicchio, R.; Pagliuca, C.; Varricchio, E.; Volpe, M.G.; Salvatore, P.; Paolucci, M.; Pagliarulo, C. Phytocompounds vs. Dental Plaque Bacteria: In Vitro Effects of Myrtle and Pomegranate Polyphenolic Extracts Against Single-Species and Multispecies Oral Biofilms. *Front. Microbiol.* **2020**, *11*, 592265. [CrossRef]

64. Bakkiyaraj, D.; Nandhini, J.R.; Malathy, B.; Pandian, S.K. The Anti-Biofilm Potential of Pomegranate (*Punica granatum* L.) Extract against Human Bacterial and Fungal Pathogens. *Biofouling* **2013**, *29*, 929–937. [CrossRef]

Article

Evaluation of the Antimicrobial Capacity of Bacteria Isolated from Stingless Bee (*Scaptotrigona aff. postica*) Honey Cultivated in Açai (*Euterpe oleracea*) Monoculture

Iago Castro da Silva [1], **Eveson Oscar Almeida Conceição** [1], **Daniel Santiago Pereira** [2], **Hervé Rogez** [1] and **Nilton Akio Muto** [1,*]

[1] Centre for Valorization of Amazonian Bioactive Compounds & Biological Science Institute, Federal University of Pará, Belém 6075-110, PA, Brazil

[2] Embrapa Amazônia Oriental, Belém 66095-903, PA, Brazil

* Correspondence: niltonmuto@ufpa.br

Abstract: Many antimicrobial compounds have been seeking to protect the human body against pathogenic microbial infections. In recent times, there has been considerable growth of pathogens resistant to existing drugs due to the inappropriate use of antibiotics. In the present study, bacteria isolated from the honey of stingless bees native to the Amazon called *Scaptotrigona aff. postica* and *Apis mellifera* were used to determine their potential antimicrobial properties and characterize the medium cultivated with isolated bacteria. The results showed inhibition of nine isolates. Among these isolates, SCA12, SCA13, and SCA15 showed inhibitory activity similar to that of vancomycin, which was used as a positive control. The SCA13 strain obtained the best results with antimicrobial extract against the tested pathogens; the species was identified as *Enterococcus faecalis*, and its lyophilized extract was characterized by temperature, pH, and trypsin, in which they showed antimicrobial activity. This work shows that bacteria isolated from the stingless bee honey, *Scaptotrigona aff. postica*, have the potential to produce antimicrobial substances.

Keywords: plant-derived compounds; stingless bee honey; pathogenic strains; antimicrobial activity

1. Introduction

Bee honey has been studied for centuries, from classical antiquity to the present day. In this context, honey has been used for various purposes, ranging from food supplements to wound healing. Honey, along with other bee products, is associated with the image of a natural, healthy, and clean product [1]; its medicinal properties and antimicrobial activity are generally related to its physical and chemical characteristics [2]. Gonçalves et al. [3] mentioned that in addition to its nutritional properties, the use of honey in folk medicine is also due to its pharmacological properties. Among these properties, antimicrobial activity has attracted interest among researchers because of its potential applicability in clinical cases [4–6].

The honey of stingless bees, known as meliponines, is used in popular therapies, mainly in rural areas [7] and among indigenous peoples, who believe that different types of honey have specific healing properties and are used to cure a wide range of diseases [8]. Understanding the antibacterial potential of bee honey and its microorganisms can be an attractive and low-cost alternative for the treatment of clinical conditions, in addition to leveraging the production chain of the stingless bee product, *Scaptotrigona aff. postica* [9]. Bees of the Meliponini tribe comprise approximately 60 genera distributed throughout the tropical and subtropical regions of the world. They are important insects in the maintenance of ecosystems, acting as a source of food, in addition to dispersing seeds and pollen through pollination. This last function gives bees the name of pollinating insects, and among these is the species *Scaptotrigona depilis*, common in neotropical regions such as Argentina, Bolivia,

Paraguay, and Brazil, with prevalence in the states of Mato Grosso do Sul, Minas Gerais, Paraná, Rio Grande do Sul, and São Paulo [10].

Among the pharmacological properties of honey, its antimicrobial activity, such as healing and antioxidant capacity, has aroused interest among researchers because of its potential applicability in clinical cases. Therefore, the use of honey as a therapeutic agent has shown promising results. However, therapeutic effects vary according to the constituents and compound varieties. Honey has been reported to have an inhibitory effect on approximately 60 species of bacteria, 3 including aerobic and anaerobic gram-positive and gram-negative bacteria, such as *Staphylococcus aureus* and *Pseudomonas aeruginosa*, which are considered opportunistic pathogens [11–17].

In general, honey produced by the meliponine species presents several differences in physicochemical terms compared to honey produced by *A. mellifera*. For instance, honey from stingless bees has higher acidity, which can be detected by its taste and sensorial properties [18]. Acidity is important for maintaining stability and reducing the risk of the development of pathogenic microorganisms. Physicochemical factors (such as pH and acidity) are considered important antimicrobial factors, providing greater stability to the product, since the optimal pH for the growth of several pathogens in animals ranging from 7.2 to 7.4. Thus, antimicrobial activity can be caused by several physicochemical factors, such as pH, humidity, and sugars present in its composition. In addition to physicochemical factors, the presence of symbiotic bacteria in honey detains mechanisms that produce peptides and other molecules with antimicrobial properties, such as organic acids [19].

It is now recognized that most honey has proven antibacterial activity, which is dependent on a variety of factors. These factors include hydrogen peroxide generation, osmosis, acidity, limited availability of water molecules, and the presence of antimicrobial molecules, such as flavonoids and phenolic acids. In addition to their proven antibacterial activity, flavonoids are powerful antioxidants with an incredible ability to scavenge free radicals [20]. Regarding microorganisms with antimicrobial properties found in honey, several bioactive molecules such as potential antibiotics are the results of secondary metabolites of bacterial fermentation processes, with other compounds that may present antioxidant activity [19,20].

Honey from açai (*Euterpe oleracea*) produced in Pará has different qualities from other wild floral nectar honey because the açai bioactive compounds are not only found in the fruit, but also in different vegetal organs of the plant, such as the floral nectar. Well-known bioactive compounds present in açai, such as anthocyanins, flavonoids, non-anthocyanin flavonoids, amino acids, fatty acids, and minerals, have important anti-inflammatory and antioxidative properties. In addition, açai fruits have high levels of total mesophilic bacteria with high diversity, some of them being probiotic candidates and antagonistic potential against pathogens [21].

Given the importance of studies cited on physicochemical factors and microbial composition of honey from stingless bees, the objective of the present study was to detect in vitro antimicrobial activity from bacteria isolated from the honey of the native Amazonian stingless bee *Scaptotrigona aff. postica* against pathogenic bacteria. In addition, we characterized the compounds produced by these bacteria in relation to oxygen concentration, temperature, pH, and enzymatic activity.

2. Results

2.1. Sample Isolation

Twenty-eight strains were obtained from 9 honey samples (5 of *A. mellifera* and 4 of *S. aff. postica*), 22 strains of which were isolated from *S. aff. postica* honey and 6 strains of which were isolated from *A. mellifera* honey. Microbial growth occurred on plates that were anaerobically inoculated with *A. mellifera* honey in MRS agar culture medium. The first honey concentration of 100% was pure, the second was a concentration diluted in 50% saline solution, and the third corresponded to a concentration diluted in 25% of honey in

saline solution to evaluate whether the concentration of honey is a parameter that influences the number of colonies obtained. Preliminary results confirmed that there was growth only in the anaerobic plates in the spread plate (50% and 25%) and pour plate (100% and 50%) techniques, as shown in Table 1.

Table 1. Microbial growth of *A. mellifera* honey samples on MRS Agar for aerobic and anaerobic processes.

Presence of Oxygen	Honey Concentration	Spread Plate	Pour Plate
Aerobiosis	100%	−	−
Aerobiosis	50%	−	−
Aerobiosis	25%	−	−
Anaerobiosis	100%	−	+
Anaerobiosis	50%	+	+
Anaerobiosis	25%	+	−

In the procedure performed with honey from *S. aff. postica*, many plates showed microbial growth, with high bacterial content which grew in 10^{-1}, 10^{-2}, and 10^{-3} dilutions of samples.

Figure 1 shows the antimicrobial test performed on samples of *S. aff. postica* honey at three concentrations (25%, 50%, and 100%) against *E. coli*. The results showed that the antimicrobial capacity of honey from *S. aff. postica* was higher at the highest concentration used. As can be seen in Figure 1, the inhibition halos are higher according to the honey concentration used. Based on these results, it was observed that the smallest halos were observed as the samples were diluted. The lower the concentration, the lower the antimicrobial activity of the honey, a natural hygroscopic characteristic of honey (dehydration of the bacteria by hyperosmolar properties) for *E.coli*, inhibition is related to physicochemical characteristics of honey and not necessarily to antimicrobial compounds.

Figure 1. Antimicrobial test with different concentrations (25%, 50%, and 100%) of *S. aff. postica* honey against *E. coli*.

2.2. Screening of Strains with Antimicrobial Activity

The 28 isolated strains of *S. aff. postica* and *A. mellifera* grew under anaerobic conditions in the absence of oxygen. With a concentration of less than 0.1% Oxygen. The strains were coded according to the bee species and the number of colonies isolated from the Petri dishes. Isolated strains of *S. aff. postica* were coded as SCA, and the isolated strains of *A.*

mellifera were coded as API. The 28 isolated strains underwent an antimicrobial selection test, in which their ability to inhibit pathogenic bacteria *B. cereus* (Biomedh 11778, Itapoa, Belo Horizonte, *E. coli* (Laborclin 25922, Pinhais, Brazil), *S. aureus* (Laborclin 25923, Pinhais, Brazil) and *Salmonella* sp. (Biomedh 14028, Itapoa, Belo Horizonte) was tested. The tests were performed in triplicate and the interactions were analyzed according to the presence or absence of halos. Table 2 shows the results of the presence or absence of inhibition by the isolated strain, classified into low (<11 mm), medium (12–14 mm) and high (>15 mm) activity, respectively, according to the size growth inhibition halo in the antimicrobial test. From a qualitative analysis, halos with small diameters showed low antimicrobial activity, as well as halos with large diameters, showed high antimicrobial activity.

Table 2. Antimicrobial selection test of strains isolated from the honey of *S. aff. postica* (SCA) and *A. mellifera* (API). (−) No activity, (+) Low activity, (++) Medium activity, (+++) High activity.

Isolated Strain	Inhibitory Activity			
	B. cereus	*E. coli*	*S. aureus*	*Salmonella* sp.
SCA01	−	−	−	−
SCA02	−	−	−	−
SCA03	−	−	−	−
SCA04	−	−	−	+
SCA05	−	−	−	+
SCA06	−	−	−	++
SCA07	++	+	++	++
SCA08	−	−	+	−
SCA09	−	−	−	−
SCA10	−	−	−	−
SCA11	++	++	−	+++
SCA12	+	++	−	++
SCA13	+++	++	+	+
SCA14	+	+	−	−
SCA15	+	++	+	++
SCA16	++	−	++	−
SCA17	++	+	−	++
SCA18	+	−	−	++
SCA19	+	−	−	−
SCA20	−	−	−	−
SCA21	−	−	−	−
SCA22	−	−	−	−
API01	−	−	−	−
API02	+	−	−	−
API03	++	+	−	−
API04	−	−	−	−
API05	+	−	+	−
API06	++	−	+	−
Streptomycin	++	++	+++	+++

Bacillus cereus was inhibited by 14 isolates, highlighting the SCA13 strain, which showed greater inhibition than the positive control. *E. coli* was inhibited by eight strains, and *S. aureus* showed fewer strains with antimicrobial capacity, totaling seven isolates. *Salmonella* sp. was inhibited by ten honey isolates. The SCA-07, SCA-13, and SCA-15 strains showed the highest antimicrobial spectrum among those isolated from *S. aff. postica* honey.

From the results obtained, seven strains were selected from *S. aff. postica* and two from *A. mellifera*: SCA-07, SCA-11, SCA-12, SCA-13, SCA-15, SCA-16, SCA-17, API03, and API-06 according to the potential inhibitory activity against pathogenic bacteria (*B. cereus*, *E. coli*, *S. aureus*, and *Salmonella* sp.).

2.3. Morphological Identification and Molecular Identification

In the morphological identification step, a Gram stain was performed. The strains SCA-07, SCA-11, SCA-12, SCA-15, SCA-17, API-03, and API-06 were classified as Gram-variable because they contain Gram-positive bacilli at the top and Gram-negative cocci at the bottom. The SCA-13 strain was classified as a Gram-positive coccus. The SCA-16 strain was classified as a Gram-positive bacillus.

The SCA13 strain was selected according to the best results obtained by screening for strains with antimicrobial activity for molecular identification. Its total DNA was extracted using phenol/chloroform and characterized via a comparison of homology to the 16S gene. The DNA sequences obtained from the ACTGene Molecular Analysis were compared with existing sequences using the Basic Local Alignment Search Tool (BLAST) of the National Center of Biotechnology Information (NCBI), which resulted in a 98% match to the species *Enterococcus faecalis.* The result of the analysis of sequence similarities is in Supplementary Materials Data S1.

2.4. Antagonist Activity

The bacteria isolated from honey selected in the inhibitory potential test underwent antagonist analysis and were tested with the spot-on-lawn assay to determine whether they had antagonistic activity against indicator bacteria, *B. cereus* and *L. monocytogenes* (Figure 2). Selected strains were tested, and antagonist activity was detected by the formation of a growth inhibition halo. In Figure 2, it is possible to observe inhibition halos against the indicator bacteria to select the antimicrobial-producing bacteria.

(A) **(B)** **(C)**
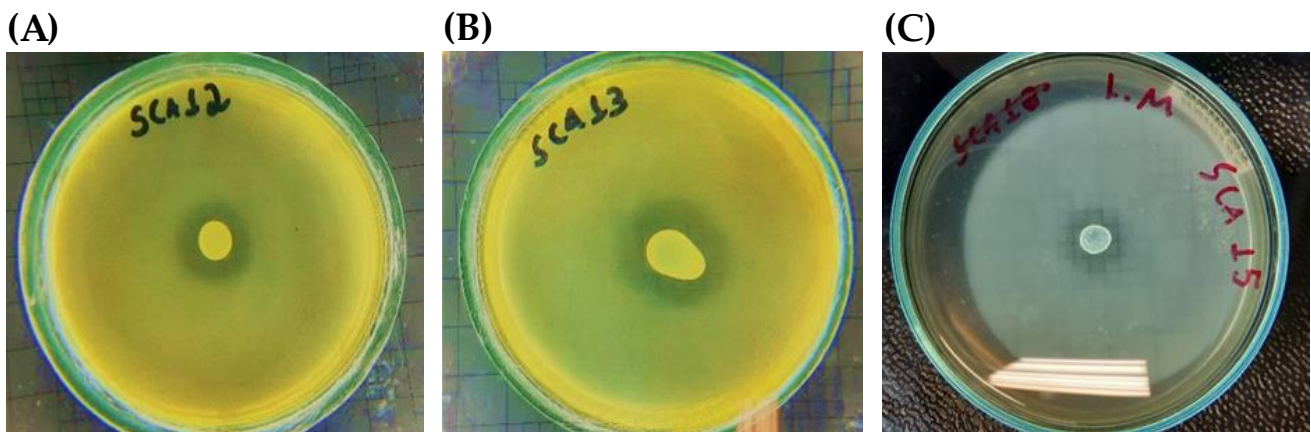
Figure 2. Spot-on-lawn assay results. (**A**) SCA12 bacterium showing growth inhibition halo against the indicator bacterium, *B. cereus*; (**B**) SCA13 bacterium showing growth inhibition halo against the indicator bacterium, *B. cereus*; (**C**) SCA15 bacterium showing a halo of inhibition against the indicator bacterium, *L. monocytogenes*.

Strains SCA07, SCA16, SCA17, API03, and API06 were not significantly different from the control ($p > 0.05$) and strain SCA11 ($p \leq 0.05$), that is, they showed lower inhibition than vancomycin, in relation to the indicator. The SCA12, SCA13, and SCA15 strains were statistically significant ($p < 0.00001$). Therefore, they had an inhibitory action similar to that of vancomycin, used as a positive control (Figure 3).
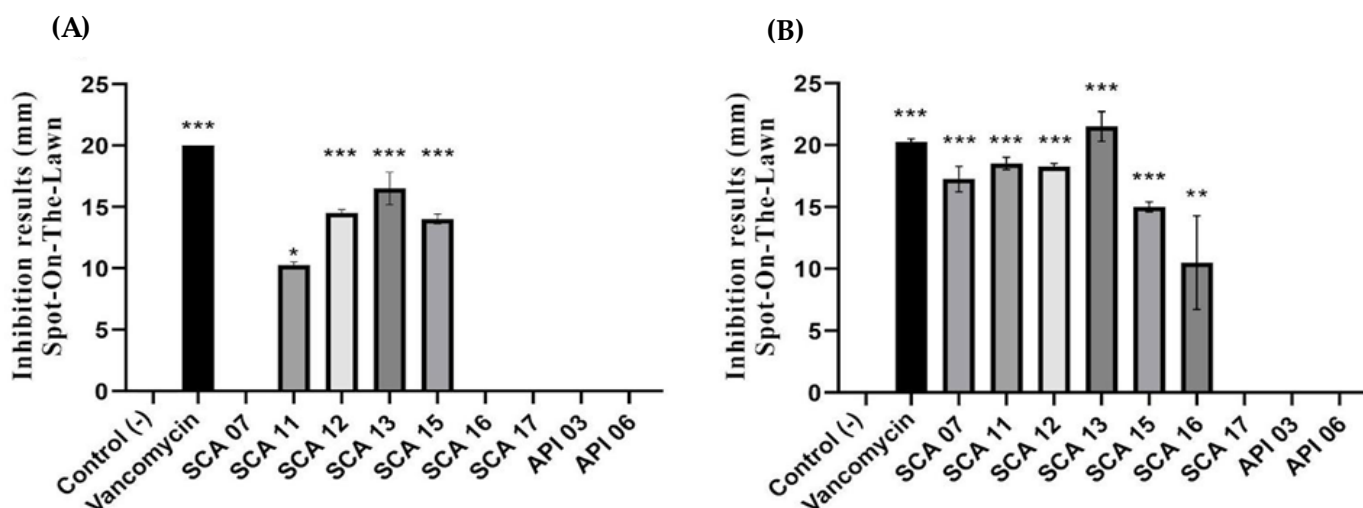
Figure 3. Antimicrobial activity of strains isolated from different kinds of honey against (**A**) *L. monocytogenes*, and (**B**) *B. cereus*. * $p < 0.05$; ** $p < 0.01$; *** $p < 0.00001$.

Later, lyophilized extracts isolated from SCA12, SCA13, and SCA15 were tested in wells by diffusion to determine whether the substances produced by the bacteria isolated from honey were produced extracellularly or intracellularly. SCA13 and SCA15 were able to inhibit both pathogenic bacteria, whereas the SCA12 strain was not able to inhibit *L. monocytogenes*. The SCA13 strain exhibited a higher inhibition halo, as shown in Table 3.

Table 3. Well-Diffusion test results of lyophilized isolated extracts. ($-$) No activity, (+) Low activity (<11 mm), (++) Medium activity (12–14 mm) and (+++) High (>15 mm) activity.

Isolated Strain	Inhibitory Activity	
	B. cereus	*L. monocytogenes*
SCA12	++	−
SCA13	+++	++
SCA15	+	+

2.5. Extract Characterization

The exposed strain SCA13, which is facultative aerobic, showed an extract with higher inhibitory activity under anaerobic conditions against both pathogens (*B. cereus* and *L. monocytogenes*) than under aerobic conditions.

The inhibitory activity of SCA-13, a facultative anaerobic Gram-positive coccus (*E. faecalis*) showed higher inhibition at anaerobiosis treatment. Excess oxygen and oxidative stress can disrupt the growth of most organisms, but the underlying mechanisms of damage have proved difficult to unravel. For instance, O_2^- and H_2O_2 can oxidize the exposed Fe–S clusters of a family of dehydratases. This event destabilizes the clusters, and their consequent disintegration eliminates enzyme activity. SCA-13 had to be able to overcome a number of barriers including anaerobiosis, pH shifts, and high osmolarity. The isolated bacteria from honey also had to develop successful strategies to be able to compete with other organisms for substrate found in these environments. In addition, SCA-13 must also assimilate nutrient substrates as well as survive under the harsh conditions presented to it in honey and in the gastrointestinal tract of bees.

With the metabolites of the inoculum growth of the SCA13 strain having been more favorable in anaerobiosis, the lyophilized anaerobic extract underwent three types of treatments (thermostability, sensitivity to neutral pH, and sensitivity to proteolytic enzymes).

In relation to temperature sensitivity, the extract of strain SCA13 was autoclaved at 121 °C for 15 min. The extracts obtained after autoclaving did not show statistical differences from vancomycin. The supernatant extract of the SCA13 strain was incubated

for 72 h to inhibit the growth of the indicator bacteria from the thermostability treatment at 121 °C. From Table 4, it can be inferred that the proteins were not denatured during heat treatment, as they did not present statistical significance ($p > 0.05$) for the two indicator bacteria; that is, the extract of the SCA13 strain was not altered in the thermostability test at 121 °C, which shows the resistance of antimicrobial peptides to high temperatures.

Table 4. Treatment results. Mean and standard deviation of growth inhibition halos (with 10 mm). * SCA13 without Treatment.

Strain SCA13	Inhibitory Activity	
(Treatment)	*B. cereus*	*L. monocytogenes*
Control wT *	10.25 ± 0.4	10.25 ± 0.5
Autoclaved	11.50 ± 0.5	11.00 ± 0.0
Neutral pH	10.25 ± 0.4	08.50 ± 0.5
Trypsin	08.00 ± 0.0	08.00 ± 0.0

Inhibition halos formed in the neutral pH (pH 7.0) characterization of SCA13 strain extracts. The extract of the SCA13 strain did not show statistical significance ($p > 0.05$) against either pathogen, so it can be stated that the neutralization of the extract was not able to reduce the antimicrobial activity of the peptides.

As for sensitivity to the proteolytic enzyme trypsin, the extract did not show a significant difference ($p > 0.05$) between *B. cereus* and *L. monocytogenes*, showing that it was not inactivated after a possible inactivation with the enzyme trypsin in relation to the control without any type of treatment. The inactivation of antimicrobial peptides in the presence of trypsin and other proteolytic enzymes would be an indication that the substance is a protein in nature.

The lyophilized extract of the SCA13 strain that showed inhibitory activity in the well diffusion test was tested with the application of treatments to determine its characteristics and spectrum of action under different conditions. Table 4 presents the results.

3. Discussion

Every day, new antimicrobials are sought to evade antimicrobial resistance generated by the abusive and inappropriate use of antibiotics. Honey is a natural, healthy product with medicinal properties and antimicrobial activity, closely related to its physicochemical characteristics and, more recently, to the gut microbiota of honeybees. In the present study, we found that the higher the concentration of honey, the greater the inhibition of pathogenic bacteria. It is important to emphasize that the initial results were not able to verify the hypothesis that the bacteria present in the honey were responsible for the inhibition owing to the chemical and nutritional composition of the honey, which contains other compounds capable of inhibiting it. The water content of honey is undoubtedly one of the most important characteristics, as it influences its viscosity, specific weight, maturity, crystallization, flavor, conservation, and palatability [22].

Many species of microorganism are found in the intestines of bees; of these 1% yeast (*W. anomalus*), 29% are gram positive bacteria, including *Bacillus*, *Bacterium*, *Streptococcus* and *Clostridium* species, and 70% are gram-negative or gram-positive bacteria, including *Achromobacter*, *Citrobacter*, *Enterobacter*, *Erwinia*, *E. coli*, *Flavobacterium*, *Klebsiella*, *Proteus* and *Pseudomonas*. [23]. These insects need to defend themselves against pathogens, but they also need to protect their food sources from attacks by microorganisms. According to Menegatti [24], one of the defense strategies acquired during the evolution of insects is symbiotic association with bacteria capable of biosynthesizing natural products (antibiotics and antifungals) against pathogens. Therefore, most of the bacteria found in both the honey of *A. mellifera* and stingless bees have antimicrobial capacity as a function of the bees' defense against pathogens found in their natural habitat.

The SCA13 strain resulted from the molecular identification of *Enterococcus faecalis*, a species of bacteria that is abundant in food sources of animal origin such as cheese, chicken,

and cassava [25]. In addition, it survives under adverse conditions such as extreme pH, temperature, and salinity [26]. They can produce substances with antagonistic potential, such as organic acids (lactic acid), hydrogen peroxide, lytic bacteriophages, proteolytic enzymes, and antimicrobial substances of a protein nature, called bacteriocins [27,28]. Studies have been developed on the antibacterial activity of honey on antibiotic-resistant pathogens, pathogenic bacteria involved in some diseases, pathogenic bacterial food and bacteria responsible for the deterioration of food (spoilage bacteria), and their different levels of sensitivity to honey. Bacteria such as *Staphylococcus aureus*, *Staphylococcus epidermidis*, *Bacillus stearothermophilus* are extremely sensitive, while *Staphylococcus uberis*, *Escherichia coli*, *Klebsiella pneumoniae*, *Bacillus cereus*, *Alcaligenes faecalis*, *Lactobacillus acidophilus*, *Helicobacter pylori*, *Bacillus subtilis* are moderately sensitive and the growth of *Micrococcus luteus*, *Enterococcus faecalis* and *Pseudomonas aeruginosa* appear to be unaffected by honey [29].

Using the spot-on-lawn assay, Nardi [30] observed a better comparison of antimicrobial activity, according to Çadick and Çitak [31], these metabolites can be produced during the test period, which can increase the diffusion capacity of the substances produced by the bacteria and the concentration of these substances in the culture medium with three strains that showed inhibitory activity against the two indicator bacteria.

These extracts were tested by diffusion in wells to determine whether the substances produced by the bacteria isolated from honey were produced extracellularly or intracellularly. Studies carried out on *Solanum trilobatum* leaves resulted in a protein with antibacterial potential against *V. cholerae* and *S. aureus* evaluated by well diffusion method and Minimum Inhibitory Concentration (MIC) by microdilution assay. In addition, the protein was identified by peptide mass fingerprinting, and morphology by the three-dimensional structure [32]. In a study by Salles [9], many strains isolated from açai showed growth inhibition halos using the spot-on-lawn technique against *B. cereus* and *L. monocytogenes*. These results agree with those of the honey strains, in which the extract of the SCA13 strain showed the highest inhibitory rates in the well-diffusion test through growth inhibition halos among others, as shown in Figure 2. According to Dimitrieva-Moats and Unlu [33], lyophilized extract promotes more stable activity. Thus, inhibition was observed due to an increase in the concentration of the extract produced. Using the well-diffusion technique, it was possible to verify that the metabolites produced by the bacteria isolated from honey were produced extracellularly. Table 3 shows that the selected producing bacteria were able to inhibit the two indicator bacteria, except for the SCA12 strain, which was not able to inhibit *L. monocytogenes*.

The characterization tests of the bacterial extract were carried out because some physicochemical factors (such as pH and acidity) are considered important antimicrobial factors, providing greater stability to the product regarding the development of microorganisms. According to studies by Nogueira-Neto [34], the optimal pH for the growth range of several pathogenic microorganisms in animals is between 7.2 to 7.4. Melipona honey has high acidity, which is an indicator of the tested antimicrobial properties. Many authors have claimed that some bacterial strains increase the production of metabolites when they are subjected to a certain level of stress. This explains the increased production of peptides due to oxidative stress or in a microaerophilic environment. According to Ochner [35], several proteins are produced by bacteria in the defense against oxidative stress, many of which are related to the response to this stress have already been identified, although there is a lack of studies that explain their mechanisms of action in a more complex way.

Regarding the concept of sensitivity to the proteolytic enzyme trypsin, some studies, such as that conducted by Salles [9], showed resistance to the trypsin enzyme in two types of treatment times: 2 h and 18 h. In contrast to the work by Bromberg [36], the bacteriocin produced by CTC 484 culture showed saline sensitivity to trypsin. These results are in concordance with the extract of the SCA13 strain subjected to trypsin treatment, which showed growth inhibition. Govan and Harris [37] stated that extracts that were reactive in the presence of trypsin might be new types of peptides that have not yet been studied.

Breeding native stingless bees is a prominent activity in the state of Pará, with many species indicating potential for management and breeding in the Amazon biome [38]. The breeding of "straw bees" (*S. aff. postica*) has recently gained prominence because of its potential use in directed pollination of the açai palm tree (*Euterpe oleracea*) crop, and productivity could be increased by up to 2.5 times with the pollination service [39]. The results of this study allow us to infer the importance of honey in the creation of this bee species, and this product may become a future tool for bioactive compounds with potential uses in the pharmaceutical industry.

4. Materials and Methods

4.1. Collection, Asepsis, and Isolation of Strains

Honey samples from *S. aff. postica* and *A. mellifera* were collected from the municipality of Santa Maria do Pará in 2018. The honey samples from both species used in this study, *A. mellifera* and *S. aff. postica*, showed floral predominance in açai (*Euterpe oleracea*) cultures. It was found that the honey was monofloral for açai in *S. aff. postica* honey. Four samples (A, B, C, and D) were collected from *S. aff. postica* and five samples (A, B, C, D, and E) were collected from *A. mellifera*. Honey was collected using a syringe and stored in 50 mL falcon tubes. The samples were stored at the Center for Valorization of Bioactive Compounds of the Amazon (CVACBA). Nine samples were used: four (A, B, C, and D) of honey from *S. aff. postica* and five samples (A, B, C, D, and E) of honey from *A. mellifera.*

From these samples, 30 g of honey was used in three concentrations: the first pure reference to a concentration of 100%, the second was a concentration diluted in 50% saline solution (FUJIFILM Irvine Scientific 0.85%, Santa Ana, CA, USA), and the third corresponded to a concentration diluted in 25% of honey in saline solution (FUJIFILM Irvine Scientific 0.85%, Santa Ana, USA) to evaluate whether the concentration of honey is a parameter that influences the number of colonies obtained. Subsequently, the techniques of spread plate and pour plate of the concentrations obtained in Petri dishes containing culture medium agar of Man Rogosa Sharpe (MRS agar) were performed to verify whether the bacteria present in the honey had aerobic or anaerobic characteristics. The procedure was carried out in 12 plates, divided into spread plates (100%, 50%, and 25%) for aerobiosis, spread plates (100%, 50%, and 25%) for anaerobiosis, pour plates (100%, 50%, and 25%) for aerobic, and pour plates (100%, 50%, and 25%) for anaerobic conditions. The plates were then incubated at 37 °C for 72 h.

With the acquisition of four samples of honey from *S. aff. postica*, serial dilutions were performed in up to 10 units of honey in peptone saline solution (HIMEDIA, Model AG-7013/SP, West Chester, PA, USA) for each sample, totaling 20 plates. Soon after dilution, the honey solutions were placed in Petri dishes containing Man Rogosa and Sharpe (MRS agar) using the spread plate technique. The solutions were spread over the culture medium using a Drigalski spatula. The plates were then incubated at 37 °C for 72 h under anaerobic conditions.

4.2. Screening—Antimicrobial Test

To perform the antimicrobial test, different concentrations of honey were initially used (100%, 50%, and 25%) against the pathogenic bacteria, *Escherichia coli* (Laborclin 25922, Pinhais, Brazil). This technique was carried out as follows: plates containing Mueller-Hinton agar prepared in advance were removed from the refrigerator until they reached room temperature. Wells (4 mm in diameter) were made on an agar plate. Using a sterile swab, the bacterial inoculum with 0.5 turbidites on the MacFarland scale was evenly distributed over the agar surface and left to rest at 27 °C for approximately 3 min. Fifty microliters of the concentrations obtained from honey from *A. mellifera* and *S. aff. postica* were dispensed into each properly identified well. After this procedure, the plates were incubated in a bacteriological oven at 37 °C for 24 h in aerobiosis with opening jar and anaerobic environment using a sealable jar with the BD GasPak™ EZ Anaerobe Container System (Sparks, USA).

To screen for candidate bacteria, another antimicrobial test was performed according to the methodology adapted from Patel [40], which consisted of filtering the metabolites produced by the honey isolates. The procedure consisted of applying a bacterial inoculum with a turbidity of 0.5 on the MacFarland scale using the turbidimetric method to standardize the pathogenic bacteria used in the test (*S. aureus*, *E. coli*, *B. cereus*, and *Salmonella* sp.). The inoculum was distributed over the surfaces of Petri dishes containing Mueller-Hinton agar medium. Wells were made on the surface of the agar, 4 mm in diameter, and agar was removed from the wells with sterile forceps. The wells were properly identified, and 25 µL of bacterial filtrate from colonies isolated and cultivated from honey from *A. mellifera* and *S. aff. postica* was dispensed into the wells according to the strains isolated. The plates were then incubated in an oven at 37 °C for 24 h. The antibiotic was Streptomycin (10 µg) (Laborclin 640623, Pinhais, Brazil). All selected positive samples were analyzed in triplicate.

4.3. Identification of the Genera of Microorganisms

The identification was based on physicochemical tests following the methodology of ANVISA [41] for the detection and identification of bacteria of medical importance.

4.3.1. Genomic DNA Extraction

Total DNA was extracted from the bacterial DNA extraction as described by Seldin and Dubnau [42] using phenol-chloroform. After extraction, the DNA sample was mixed with blue juice dye in a proportion of 1:2 of the total volume of the mixture and subjected to horizontal electrophoresis in 1 % (w/v) agarose gel. Ethidium bromide (0.1%) was added to $10\times$ diluted Tris-acetate-EDTA (TAE) buffer for 30 min at a constant voltage of 90 V. The molecular weight marker used was the "1 Kb Plus DNA Ladder" (Promega®, Madison, USA). The gel was observed and photographed under UV light using a UV light transilluminator (model) to analyze the purity and quality of the genetic material.

4.3.2. Molecular Identification

The bacterial strain was molecularly identified by amplifying the entire 16S rRNA gene fragment using universal primers 8F (5′-AGAGTTTGATCCTGGCTCAG-3′) [43] and 1492R (5′-GGTTACCTTGTTACGACTT-3′) [44]. PCR was performed in a final volume of 70µL containing 5X Green GoTaq® Flexi Buffer (1X) from Promega®, 1 mM MgCl$_2$, 0.2 mM dNTPs, 1.5 µM of each primer, 5 U/µL of GoTaq® DNA polymerase, DNA at concentrations between 50 and 100 ng/µL, and sterile filtered water (all reagents from Sigma-Aldrich®). The cycle applied was: $35\times$ (1 min at 95 °C; 1 min at 55 °C; 1 min at 72 °C); $1\times$ (10 min at 72 °C); 4 °C. Sequencing of the DNA sample was performed through outsourced services of the company ACTGene Molecular Analysis using the Sanger method [45]. The obtained sequences were compared with those present in GenBank using the Basic Local Alignment Search Tool (BLAST) of the National Center of Biotechnology Information (NCBI) using the BLAST nucleotide tool (BLASTn) [46].

4.4. The Antagonist Activity
4.4.1. Spot-on-Lawn Assay

The bacteria that showed antimicrobial activity and were consequently selected for the screening process underwent an antagonist test against other microorganisms called indicator cultures (*Bacillus cereus* and *Listeria monocytogenes*).

According to the method described by Nardi [30], bacterial samples were activated in test tubes containing MRS broth (Man, Rogosa, and Sharpe) and incubated at 37 °C for 24 h under aerobic conditions, shaking the tubes in the Shaker TOS20 orbital shaker at 200 rpm. After activation, 5 µL of each sample was deposited in the center of a petri dish containing MRS agar and incubated in an anaerobic chamber at 37 °C for 24 h. After this period, chloroform was added to the lids of the Petri dishes with sterilized cotton under UV light for 30 min to eliminate microorganisms. Immediately after UV exposure, the plates were closed under laminar flow. The indicator cultures underwent activation and were

grown in brain-heart infusion (BHI) broth. Soon after, 10 μL of the indicator culture was added to tubes containing 3.5 mL of semi-solid agar. Then, the tubes with semi-solid agar containing the indicator bacteria were poured into Petri dishes, with 3.5 mL of semi-solid agar in 15 mL Falcon tubes added to the plates. Vancomycin-640630-Laborclin (30 μg) was used as the positive control. The plates were then incubated at 37 °C for 48 h under aerobic conditions. Inhibition zones were based on the Clinical and Laboratory Standards Institute— Performance Standards for Antimicrobial Susceptibility Testing method [47]. From the measurement of the size of the zone of inhibition with a halometer and the classification of strains into sensitive, moderately sensitive, intermediate, or resistant according to the diameter of the standard zone established for each antimicrobial drug. The analysis was performed in triplicate.

4.4.2. Diffusion Test in Wells

The well diffusion test was carried out with the aim of determining whether the compounds produced by the bacteria isolated from honey present intra-or extracellular activity to facilitate the characterization process that was carried out later, as mentioned in the work performed by Salles [9]. Patel's study [40] was used as a reference for the development of the analysis. Producing bacteria that showed inhibitory activity were activated in MRS broth and incubated at 37 °C for 24 h under aerobic conditions. The isolated bacteria were centrifuged at 5000 rpm for 5 min, and the supernatants were collected. The supernatant extracts of each producer bacterium were filtered through whatmann paper n° 2 with the help of a vacuum pump (Prismatec 132, Itu, Brazil) and then frozen at −20 °C for 24 h to be lyophilized (JJ cientifica, São Carlos, Brazil) for 72 h. After this process, the lyophilized content of each tube was resuspended in 500 μL of ultrapure water, and it was inoculated in wells made in BHI agar with 3.5 mL of semi-solid BHI medium and 40 μL of the indicator culture (*B. cereus* and *L. monocytogenes).* The plates were then incubated at 37 °C for 24 h under aerobic conditions. Extracts with activity were selected for characterization. The analysis was performed in triplicate.

4.5. Extract Characterization

The extracts produced by the bacteria that showed antimicrobial activity were characterized in their spectrum of action through four types of treatments [48].

4.5.1. Oxygen Concentration

The extract of the bacterium that showed antimicrobial activity in the analysis of antagonist activity was tested to determine if the concentration of oxygen in the culture medium could interfere with the inhibition potential of the extract and subsequently optimize the production process of the lyophilized extract. For this, two different cultivations were carried out, one cultivation under aerobic conditions using agitator equipment to control the distribution of oxygen in the jars, and the method used to generate an anaerobic environment was the BD GasPak™ EZ Anaerobe Container System (Sparks, USA).

4.5.2. Thermal Stability

Regarding thermal stability, the first step involved autoclaving the supernatant extracts at 121 °C for 15 min, after which the extracts were frozen and lyophilized. The next step consisted of resuspending the extract in 1000 μL of ultrapure water and then inoculating it into wells made in BHI agar culture medium with the addition of 3.5 mL of semi-solid BHI medium and 40 μL of the indicator bacteria (*B. cereus* and *L. monocytogenes*).

4.5.3. Proteolytic Enzyme Sensitivity

Sensitivity to proteolytic enzymes was determined according to the method adapted [9]. The lyophilized extracts were resuspended in 1 mL of Tris-HCl buffer (50 mM, pH 7.6) plus calcium chloride (1 mM), with the proteolytic enzyme trypsin (Sequencing Grade Modified 9PIV511-PROMEGA modified) added to the medium at a ratio of 1:100 (12.5 ng/μL) and

it was diluted in 100 μL of acetic acid buffer. The samples were then placed in a water bath at 37 °C overnight. Subsequently, it was inoculated into wells made in BHI agar with 3.5 mL of semi-solid BHI medium and 40 μL of the indicator (*B. cereus* and *L. monocytogenes*) culture. The plates were then incubated at 37 °C for 24 h under aerobic conditions [49].

4.5.4. pH Effect

For pH characterization, the extracts were neutralized to pH 7.0, using sodium hydroxide (20%). The pH measurements were performed using pH indicator strips. After neutralization of the extracts, they were resuspended in 1000 μL of ultrapure water and later were inoculated in wells made in BHI agar added to 3.5 mL of semi-solid BHI medium with 40 μL of the indicator culture (*B. cereus* and *L. monocytogenes*).

4.6. Statistical Analysis

Statistical analyses were performed using the BioEstat® software (version 5.0). Analysis of variance was performed using the Kruskal-Wallis test to verify whether the isolated strains had superior or inferior inhibitory action compared to the control (antibiotic). In all tests, a significant level of 0.05 ($\alpha = 0.05$) was considered.

5. Conclusions

This study shows that bacteria isolated from the stingless bee honey, *Scaptotrigona aff. postica*, have the potential to produce antimicrobial substances. Of the twenty-eight bacteria isolated, three showed extracellular activity in the well-diffusion test after the lyophilization process, including SCA13 (which was identified as *Enterococcus faecalis*). Characterization tests are fundamental to defining the characteristics that differentiate antimicrobial peptides from others. The extract of the characterized bacteria showed a small decrease in activity in the presence of trypsin compared with the indicator bacteria. The results demonstrate the possibility of the substance contained in the supernatant extract being of a protein-like nature. The extracts showed activity after autoclaving at 121 °C, indicating that they may be class I and II bacteriocins. The neutralized extracts showed the same activity as that of the control extract, a factor that indicates better activity of the extract at acidic pH.

References

1. Bogdanov, S.; Jurendic, T.; Sieber, R.; Gallmann, P. Honey for nutrition and health: A review. *J. Am. Coll. Nutr.* **2008**, *27*, 677–689. [CrossRef] [PubMed]
2. Molan, P.C. Why honey is effective as a medicine. 1 Its use in modern medicine. *Bee World* **1999**, *80*, 80–92. [CrossRef]
3. Gonçalves, A.L.; Filho, A.A.; Menezes, H. Antimicrobial activity of honey from the native stingless bee nannotrigona testaceicornis (Hymenoptera: Apidae, Meliponini). *Arch. Inst. Biol.* **2005**, *4*, 455–459. [CrossRef]
4. Ephem, S.E.E. Clinical observations on the wound healing properties of honey. *Br. J. Surg.* **1988**, *75*, 679–681.
5. Zumla, A.; Lulat, A. Honey-a remedy rediscovered. *J. R. Soc. Med.* **1989**, *82*, 384. [CrossRef]
6. Willix, D.J.; Molan, P.C.; Harfoot, C.G. A comparison of the sensitivity of wound-infecting species of bacteria to the antibacterial activity of manuka honey and other honey. *J. Appl. Bacteriol.* **1992**, *73*, 388–394. [CrossRef]
7. Cortopassi-Laurino, M.; Gelli, D.S. Analyze pollinique, physical-chimiques properties and antibacterial action des miels d'abeilles africanisées Apis mellifera et de Méliponinés du Brésil. *Apidology* **1991**, *22*, 61–73. [CrossRef]
8. Posey, D.A. Ethnoentomology of indigenous tribes in the Amazon. In *Brazilian Ethnological Summary: 1. Ethnobiology*, 2nd ed.; Ribeiro, D., Ed.; FINEP: Petrópolis, Brazil, 1987; Volume 1, pp. 251–271.
9. Salles, M.L.O.C. Antimicrobial Production Potential from Bacteria Isolated from açaí (*Euterpe oleracea*). Belém. Master's Dissertation, Biotechnology Course, Federal University of Pará, Belém, Brazil, 2015. Available online: http://bdtd.ibict.br/vufind/Record/UFPA_8b8e9d74001447adb55fcdd7c8002dcc/Details (accessed on 7 February 2020).
10. Pedro, S.R.d.M. The stingless bee fauna in Brazil (Hymenoptera: Apidae). *Sociobiology* **2014**, *61*, 348–354. [CrossRef]
11. Alves, D.F.S.; Cabral, F.d.C.; Cabral, P.P.d.A.C.; de Oliveira, R.M.; do Rego, A.C.M.; Medeiros, A.C. Effects of topical application of *Melipona subnitida* honey on infected wounds of rats. *Rev. Col. Bras. Cir.* **2008**, *35*, 188–193. [CrossRef]
12. Olaitan, P.B.; Adeleke, O.E.; Ola, I.O. Honey: A reservoir for microorganisms and an inhibitory agent for microbes. *Afr. Health Sci.* **2007**, *7*, 159–165.
13. Lee, H.; Churey, J.J.; Worobo, R.W. Antimicrobial activity of bacterial isolates from different floral sources of honey. *Int. J. Food Microbiol.* **2008**, *126*, 240–244. [CrossRef] [PubMed]
14. de Castro, A.U.; Neto, N.M.A.; Viana, J.A. Topical use of bee honey, oxytetracycline and hydrocortisone, in the repair of skin wounds, by second intention, in rabbits. *Ceres Mag.* **2009**, *56*, 38–44.
15. Iurlina, M.O.; Fritz, R. Characterization of microorganisms in Argentinean honey from different sources. *Int. J. Food Microbiol.* **2005**, *105*, 297–304. [CrossRef] [PubMed]
16. Lerrer, B.; Zinger-Yosovich, K.D.; Avrahami, B.; Gilboa-Garber, N. Honey and royal jelly, like human milk, abrogate lectin-dependent infection-preceding *Pseudomonas aeruginosa* adhesion. *ISME J.* **2007**, *1*, 149–155. [CrossRef]
17. Kwakman, P.H.S.; Velde, A.A.t.; Boer, L.; Speijer, D.; Vandenbroucke-Grauls, M.J.C.; Zaat, S.A.J. How honey kills bacteria. *FASEB J.* **2010**, *24*, 2576–2582. [CrossRef]
18. Souza, B.; Roubik, D.; Barth, O.; Heard, T.; Enríquez, E.; Carvalho, C.; Villas-Bôas, J.; Marchini, L.; Locatelli, J.; Persano-Oddo, L.; et al. Composition of honey from stingless bees: Establishing quality requirements. *Interscience* **2006**, *31*, 867–875.
19. Kolter, R.; Van Wezel, G.P. Goodbye to brute force in antibiotic discovery? *Nat. Microbiol.* **2016**, *1*, 15020. [CrossRef]
20. Pereira, L.R.d.L. Characterization and Biological Activities of Propolis from Native Bees. Master's Dissertation, Institute of Biosciences of the University of São Paulo, São Paulo, Brazil, 2021.
21. Abe Sato, S.T.; Marques, J.M.; Freitas, A.L.; Progênio, R.C.S.; Nunes, M.R.T.; Massafra, J.M.V.; Moura, F.G.; Rogez, H. Isolation and genetic identification of endophytic lactic acid bacteria from the Amazonian açaí fruits: Probiotics features of selected strains and their potential to inhibit pathogens. *Front. Microbiol.* **2021**, *11*, 610524. [CrossRef]
22. Seemann, P.; Neira, M. *Tecnología de la Producción Apícola*; Universidad Austral de Chile/Facultad de Ciencias Agrarias Empaste: Valdivia, Chile, 1988; 202p.
23. Tysset, C.; Durand, C.; Taliergio, Y.P. Contribution to the study of microbial contamination and hygiene of commercial honey. *J. Hell. Vet. Med. Soc. Rev. de Med. Vet.* **1970**, *146*, 1471–1492.
24. Menegatti, C. Bacterial Symbionts Associated with the Stingless Bee Melipona Scutellaris as Sources of Bioactive Natural Products. Master's Thesis, Faculty of Pharmaceutical Scienses, University of São Paulo, Ribeirão Preto, Brazil, 2016.
25. Costa, L.D.F.X.; Falcão, D.A.; Grassotti, T.T.; Christiano, F.D.P.; Frazzon, J.; Frazzon, A.P.G. Antimicrobial resistance of enterococci isolated from food in South Brazil: Comparing pre- and post-RDC 20/2011. *An Acad. Bras. Cienc.* **2022**, *94*, 20201765. [CrossRef]
26. Caridi, A.; Micari, P.; Foti, F.; Ramondino, D.; Sarullo, V. Ripening and seasonal changes in microbiological and chemical parameters of the artisanal cheese Caprino d'Aspromonte produced from raw or thermized goat's milk. *Food Microbiol.* **2003**, *20*, 201–209. [CrossRef]
27. Giraffa, G. Functionality of enterococci in dairy products. *Int. J. Food Microbiol.* **2003**, *88*, 215–222. [CrossRef] [PubMed]
28. Hajikhani, R.; Beyatli, Y.; Aslim, B. Antimicrobial activity of enterococci strains isolated from white cheese. *Int. J. Dairy Technol.* **2007**, *60*, 105–108. [CrossRef]
29. Pereira, A.P. Characterization of Honey for the Production of Mead. Master's Dissertation, Agrarian School of Bragança, Bragança, Portugal, 2008.
30. Nardi, F.; Carapelli, A.; Dallai, R.; Roderick, G.K.; Frati, F. Population structure and colonization history of the olive fly, Bactrocera oleae (Diptera, Tephritidae). *Mol. Ecol.* **2005**, *14*, 2729–2738. [CrossRef] [PubMed]

31. Çadirci, B.H.; Çitak, S. A Comparison of Two Methods Used for Measuring Antagonistic Activity of Lactic Acid Bacteria. *Pakistan J. Nutr.* **2005**, *4*, 237–241.

32. Radhakrishnan, M.; Palayam, M.; Altemimi, A.B.; Karthik, L.; Krishnasamy, G.; Cacciola, F.; Govindan, L. Leucine-Rich, Potent Anti-Bacterial Protein against Vibrio cholerae, *Staphylococcus aureus* from *Solanum trilobatum* Leaves. *Molecules* **2022**, *27*, 1167. [CrossRef]

33. Dimitrieva-Moats, G.Y.; Ünlü, G. Development of Freeze-Dried Bacteriocin-Containing Preparations from Lactic Acid Bacteria to Inhibit Listeria monocytogenes and Staphylococcus aureus. *Probiotics Antimicrob. Prot.* **2012**, *4*, 27–38. [CrossRef]

34. Nogueira-Neto, P. *Life and Breeding of Indigenous Stingless Bees*; Nogueirapis: São Paulo, Brazil, 1997; 445p.

35. Ochsner, U.A.; Vasil, M.L.; Alsabbagh, E.; Parvatiyar, K.; Hassett, D.J. Role of the Pseudomonas aeruginosa oxyR-recG operon in oxidative stress defense and DNA repair: OxyR-dependent regulation of katB-ankB, ahpB, and ahpC-ahpF. *J. Bacteriol.* **2000**, *182*, 4533–4544. [CrossRef]

36. Bromberg, R.; Moreno, I.; Delboni, R.R.; Cintra, H.C. Characteristics of bacteriocin produced by *Lactococcus lactis* ssp. hordniae CTC 484 and its effect on Listeria monocytogenes in beef. *Food Sci. Technol.* **2006**, *26*, 135–144. [CrossRef]

37. Govan, J.R.W.; Harris, G. Typing of *Pseudomonas cepacia* by bacteriocin susceptibility and production. *J. Clin. Microbiol.* **1985**, *22*, 490–494. [CrossRef]

38. Venturieri, G.C. *Breeding Indigenous Stingless Bees*, 2nd ed. rev.; Embrapa Eastern Amazon: Belém, PA, Brazil, 2008; 60p.

39. Muto, N.A.; de Sousa Leite, R.O.; Pereira, D.S.; Louis, H.; Rogez, G.; Venturieri, G.C. Impact of the introduction of stingless bee colonies (Scaptotrigona aff. postica) on the productivity of acai (*Euterpe oleracea*) Impacto da introdução de colônias de abelhas sem ferrão (Scaptotrigona aff. postica) na produtividade de açaí (*Euterpe oleracea*). *Rev. Verde* **2020**, *15*, 265–273.

40. Patel, A.; Shah, N.; Ambalam, P.; Prajapati, J.B.; Holst, O.; Ljungh, A. Antimicrobial profile of lactic acid bacteria isolated from vegetables and indigenous fermented foods of India against clinical pathogens using microdilution method. *Biomed. Environ. Sci.* **2013**, *26*, 759–764. [PubMed]

41. Anvisa—National Health Surveillance Agency. Ministry of Health. 2004. Available online: https://bvsms.saude.gov.br/bvs/saudelegis/anvisa/2004/res0306_07_12_2004.html (accessed on 7 February 2020).

42. Seldin, L.D. Deoxyribonucleic acid homology between *Bacillus polymyxa*, *Bacillus macerans*, *Bacillus azotofixans*, and other nitrogen-614 fixing strains of Bacillus. *Syst. Bacteriol.* **1985**, *35*, 151–154. [CrossRef]

43. Turner, S.; Pryer, K.M.; Miao, V.P.W.; Palmer, J.D. Investigating deep phylogenetic relationships among cyanobacteria and plastids by small subunit rRNA sequence analysis. *J. Eukaryot. Microbiol.* **1999**, *46*, 327–338. [CrossRef]

44. Lane, D.J. 16S/23S rRNA sequencing. In *Nucleic Acid Techniques in Bacterial Systematics*; Stackebrandt, E., Goodfellow, M., Eds.; John Wiley & Sons: Nova Iorque, Brazil, 1991; pp. 115–147.

45. Sanger, F.; Nicklen, S.; Coulson, A.R. DNA sequencing with chain-terminating inhibitors. *Proc. Natl. Acad. Sci. USA* **1977**, *74*, 5463. [CrossRef] [PubMed]

46. Altschul, S.F.; Madden, T.L.; Schäffer, A.A.; Zhang, J.; Zhang, Z.; Miller, W.; Lipman, D.J. Gapped BLAST and PSI-BLAST: A new generation of protein database search programs. *Nucleic Acids Res.* **1997**, *25*, 3389–3402. [CrossRef]

47. Clinical and Laboratory Standards Institute, NCCLS. Performance Standards for Antimicrobial Susceptibility Testing. Pensylvania: Clinical and Laboratory Standards Institute, 2015. 15o Informational Supplement. CLSI/ NCCLS Document M100-515. Available online: https://clsi.org/standards/products/microbiology/documents/m100/ (accessed on 7 February 2020).

48. Sankar, M.; Dimitratos, N.; Miedziak, P.J.; Wells, P.P.; Kiely, C.J.; Hutchings, G.J. Designing bimetallic catalysts for a green and sustainable future. *Chem. Soc. Ver.* **2012**, *41*, 8099–8139. [CrossRef]

49. Carvalho, F.T.; Velini, E.D.; Martins, D. Aquatic plants and infestation level of species present in the bariri reservoir, on the tietê river. Aquatic Plants and Infestation Level at the Bariri Reservoir in Tietê River. *Planta Daninha* **2005**, *23*, 371–374. [CrossRef]

Article

An In Vitro and In Silico Investigation about *Monteverdia ilicifolia* Activity against *Helicobacter pylori*

Mariana Nascimento de Paula [1], Taísa Dalla Valle Rörig Ribeiro [1], Raquel Isolani [1], Daniela Cristina de Medeiros Araújo [2], Augusto Santos Borges [3], Gisele Strieder Philippsen [4], Rita de Cássia Ribeiro Gonçalves [3], Rodrigo Rezende Kitagawa [3], Flavio Augusto Vicente Seixas [5] and João Carlos Palazzo de Mello [1,*]

1 Laboratory of Pharmaceutical Biology, Department of Pharmacy, State University of Maringá, Maringá 87020-900, Brazil
2 Ingá University Center, Maringá 87035-510, Brazil
3 Department of Pharmaceutical Science, Federal University of Espirito Santo, Vitória 29047-105, Brazil
4 Federal University of Paraná, Jandaia do Sul 86900-000, Brazil
5 Department of Technology, State University of Maringá, Umuarama 87501-390, Brazil
* Correspondence: mello@uem.br; Tel.: +55-44-3011-4627

Abstract: *Monteverdia ilicifolia* is a Brazilian native plant, traditionally used to treat gastric diseases that are now associated with *Helicobacter pylori* and are commonly associated with several human diseases. We point out the *M. ilicifolia* extract as active against *H. pylori*. The crude extract produced with acetone:water presented the best *H. pylori* inhibitory activity of all five extracts (MIC 64 μg/mL). The ethyl-acetate fractions from crude extracts produced with ethanol and acetone showed a MIC of 64 μg/mL. Both ethyl-acetate fractions and the crude extract produced with acetone showed an antioxidant capacity of between 14.51 and 19.48 μg/mL in the DPPH assay. In the FRAP assay, two ethyl-acetate fractions (EAF2 and EAF4) presented the antioxidant capacity of 5.40 and 5.15 mM Trolox/g of extract. According to the results obtained from the antioxidant and antibacterial assays, two fractions (EAF2 and nBF5) were analyzed by mass spectrometry and confirmed the presence of monomeric, dimeric, trimeric tannins, and glycosylated flavonoids. Some compounds were tested using bioinformatics to evaluate the best enzyme inhibitors and the molecular interaction between the enzyme and the tested ligands. The presence of these polyphenol compounds could play an important role in antioxidant and inhibitory capacities against *H. pylori* and can be used to assist in the treatment or prevention of infection by *H. pylori*.

Keywords: *Monteverdia ilicifolia*; Maytenus ilicifolia; antioxidant capacity; condensed tannins; glycosylated flavonoids; bioinformatics

1. Introduction

Helicobacter pylori is a Gram-negative bacillus that can contribute to the development of human diseases, such as gastric ulcers, gastritis, gastric adenocarcinoma, and lymphoma. The bacteria express some virulence factors that expand the possibilities of the bacteria interacting with the host cells. One of those factors allows the bacteria to neutralize the acidity of gastric secretion, hydrolyzing urea to ammonium and CO_2, promoting the adjustment of pH in the stomach to neutral, and producing a cytopathic effect in the stomach cells. This mechanism allows the bacteria to survive in stomach conditions [1,2].

In 2015 approximately 50% of the world's population (4.4 billion) was estimated to be infected with *H. pylori*. In developing and newly industrialized countries, the prevalence is higher than in developed countries. This difference reflects the level of urbanization, sanitation, access to clean water, and varied socioeconomic statuses. Brazil has one of the highest infection prevalences in Latin America and the Caribbean (71.2%) [3].

The first-line treatment for *H. pylori* infection is one proton pump inhibitor, amoxicillin, and clarithromycin for 14 days. As an alternative, treatment can be used in quadruple

therapy with bismuth for 10–14 days and concomitant therapy for 14 days [4]. Several therapeutic strategies have been proposed to increase bacteria eradication rates. *H. pylori* infection is a unique therapeutic challenge. The infection eradication failure rate remains as high as 5–20%, along with frequent relapses in gastric ulcers even after the discerned complete healing. Natural products have great potential to serve as alternative sources of bioactive compounds and can be used to treat infectious diseases. The rapid growth of bacterial resistance to antimicrobials is occurring worldwide, putting the effectiveness of these drugs at risk, and making the treatment of bacterial infections a major challenge [5].

Time and effort have been spent to find effective alternative treatments against the bacterium and to intervene in the initial infection phase, which is becoming very popular in the search for alternative therapies, including medicinal plants that are active against the bacterium, to improve the effectiveness of bacteria eradication [6].

Monteverdia ilicifolia (Mart. ex Reissek) Biral, previously known as *Maytenus ilicifolia* Mart. ex Reissek Celastraceae is an Atlantic Forest native plant. In Brazil it is popularly known as espinheira-santa, cancerosa, and cancorosa-de-sete-espinhos [7,8]. *M. ilicifolia* is popularly used due to its analgesic, antiulcer, antitumor, aphrodisiac, antispasmodic, contraceptive, antiulcerogenic, diuretic, and healing properties. In 1988 the medicinal properties of *M. ilicifolia* were proven to treat gastrointestinal diseases, especially gastritis and ulcers, and in 2009 the plant was included in the National List of Medicinal Plants of Interest to the Unified Health System, associated with the Health Ministry, in Brazil [9].

M. ilicifolia ethnopharmacological information is well documented, with pharmacological, microbiological, and phytochemistry studies. The leaves of *M. ilicifolia* are rich in triterpenes, chromones, alkaloids, essential oils, and polyphenols, as well as tannins and flavonoids. The identified compounds in the vegetal specie have shown antiulcerogenic, antioxidant, gastroprotection, antifungal, anticarcinogenic, anti-leishmanicidal, trypanomicide, and anti-inflammatory properties [10–16].

Polyphenol extracts from medicinal plants have been studied for their antimicrobial activity. The results have been positive, showing their ability to inhibit the growth of *Vibrio cholerae*, *Streptococcus mutans*, *Campylobacter jejuni*, *Escherichia coli*, *Candida albicans*, *Staphylococcus aureus*, *Porphyromonas gingivalis*, and *Helicobacter pylori*, among others [17,18].

This study aimed to evaluate the antibacterial (*H. pylori*) and antioxidant activity, as well as identify compounds from *M. ilicifolia* extracts and fractions.

2. Results and Discussion

2.1. Epicatechin Determination Using HPLC

According to the Brazilian Pharmacopeia [19], the *M. ilicifolia* plant drug must present at least 2.8 mg/g in the extract of epicatechin. All extracts prepared showed an epicatechin concentration higher than the preconized limit. The profile for the five extracts is presented in Figure 1. The CE1 presented the lower epicatechin concentration (mg/g of extract) of 3.6 ± 0.02, followed by the CE2 at 15.54 ± 0.14, CE4 at 16.77 ± 2.14, and CE3 at 19.63 ± 2.04. The CE5 presented a higher epicatechin concentration of 20.66 ± 1.99.

2.2. Antibacterial Activities of Extracts and Semi-Purified Fractions against H. pylori

Initially, the effect of the crude extracts, ethyl-acetate, *n*-butanolic, and aqueous fractions was investigated at different concentrations (32–1024 µg/mL), as shown in Table 1.

Table 1. The MIC_{50} of *Monteverdia ilicifolia* extracts and fractions against *Helicobacter pylori*.

MIC_{50} (µg/mL $\pm$ SD)	CE1	CE2	CE3	CE4	CE5
CE	1024 ± 2.1	1024 ± 5.1	512 ± 5.6	512 ± 2.2	64 ± 9.8
EAF	$>1024 \pm 17.3$	64 ± 5.4	256 ± 1.3	256 ± 3.5	64 ± 16.1
*n*BF	$>1024 \pm 4.7$	256 ± 1.3	1024 ± 2.7	1024 ± 3.2	128 ± 4.0
AQF	$>1024 \pm 4.5$	$>1024 \pm 0.7$	512 ± 1.9	512 ± 5.1	256 ± 8.7

CE1 = crude extract aqueous; CE2 = crude extract ethanol: water 50:50; CE3 = crude extract ethanol: water 70:30; CE4 = crude extract ethanol: water 96:4; CE5 = crude extract acetone:water 7:3; EAF: ethyl-acetate fraction; *n*BF: *n*-butanolic fraction; AQF: aqueous fraction.
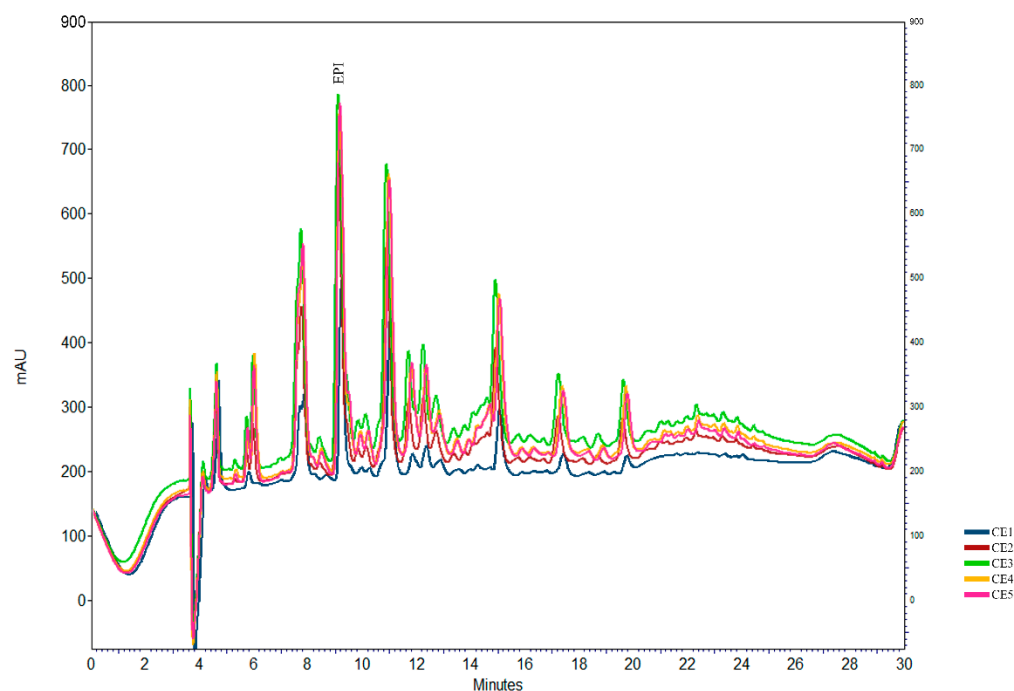
Figure 1. Chromatographic profile at 210 nm of the purified extract of *Monteverdia ilicifolia*. Chromatographic conditions: column Phenomenex®, Gemini C-18 (250 mm × 4.6 mm i.d., 5 µm), SecurityGuard (RP-cartridge) (20 mm × 4.6 mm i.d., 5 µm). Mobile phase: water (formic acid 0.1%) A and acetonitrile (formic acid 0.1%) B: 0 min 18% B; 13 min 25% B; 16 min 34% B; 20 min 42% B; 23 min 65% B; 25 min 18% B; flow-rate, 0.8 mL/min (CE1 = crude extract aqueous; CE2 = crude extract ethanol: water 50:50; CE3 = crude extract ethanol: water 70:30; CE4 = crude extract ethanol: water 96:4; CE5 = crude extract acetone: water 7:3).

The best inhibitory activity corresponded to the CE5, EAF2, and EAF5 with an MIC_{50} of 64 µg/mL and nBF5 of 128 µg/mL. It was observed that partition with ethyl acetate demonstrated better MIC in comparison with other fractions.

The antibacterial result obtained is concordant with the result found in a previous study using *Plumbago zeylanica* L. The extract produced with acetone presented the lowest MICs when compared with the ethanol:water extract. In another study performed with *Sclerocarya birrea* (A.Rich.) Hochst, the result was similar, where the extract produced with acetone:water showed a MIC comparable with amoxicillin and metronidazole [20,21].

The fractions produced with the ethyl acetate and n-butanol for the ethanol:water 50:50 (v/v) and acetone:water 7:3 (v/v) extracts showed to be MIC between 64 and 256 µg/mL. This can be explained because when a crude extract is prepared using the mixture of acetone:water or when a fraction is obtained by the partition of crude extracts with ethyl acetate, the compounds that are mostly obtained in both cases are phenolic compounds [22].

The result obtained for the nBF inhibitory activity (128 µg/mL) can be compared with the result shown in the study using *Rosa hybrida* Colorado extract that is, it is rich in polyphenols compounds when the MIC was 10 µg/mL to the butanolic fraction and 100 µg/mL to the ethanolic fraction [23].

One of *H. pylori*'s virulence factors is the presence of the urease enzyme. This enzyme is responsible for allowing the bacteria to stay alive in the acid stomach environment [1,2]. The ability of *M. ilicifolia* extracts and fractions to inhibit the bacterial urease enzyme was evaluated. The results (Table S1) showed that nBF5 presented the best inhibition (47.08%), followed by EAF2 (40.50%). nBF2 and EAF5 showed an enzyme inhibition of 37.27% and 37.51%, respectively.

The anti-*H. pylori* activity was tested for several traditional herbs in past studies and showed that *Cimicifuga heracleifolia* Kom could inhibit the urease enzyme by 42% [24]. It

was related to the ability of several phenolic compounds to inhibit the urease enzyme. Compounds that had catechol as a skeleton showed the most potent inhibitory activities, ranging from 38 to 94%. This activity is attributed to the two ortho-hydroxyl groups that are presented in the aromatic ring of polyphenols molecules [25]. According to Pessuto [11], the number of polyphenolic hydroxyls present in the compound structure and the stereochemistry of the compounds are directly related to the ability to scavenge free radicals.

M. ilicifolia is a plant rich in polyphenols compounds, such as (epi)catechin (**I**), (epi)gallocatechin (**II**), procyanidins B1 and B2 (**III** and **IV**), quercetin-3-*O*-α-L-rhamnopyranosyl(1→6)-*O*-[β-D-glucopyranosyl(1→3)-*O*-α-L-rhamnopyranosyl(1→2)]-*O*-β-D-galactopyranoside (**V**), and kaempferol-3-*O*-α-L-rhamnopyranosyl(1→6)-*O*-[β-D-glucopyranosyl(1→3)-*O*-α-L-rhamnopyranosyl(1→2)]-O-β-Dgalactopyranoside (**VI**) maytefolins A and B (**VII** and **VIII**), (Figure 2). Due to the well-known presence of phenolic compounds in the specie, we can suggest that the anti-*H. pylori* activity observed is a result of their presence [11,26,27].
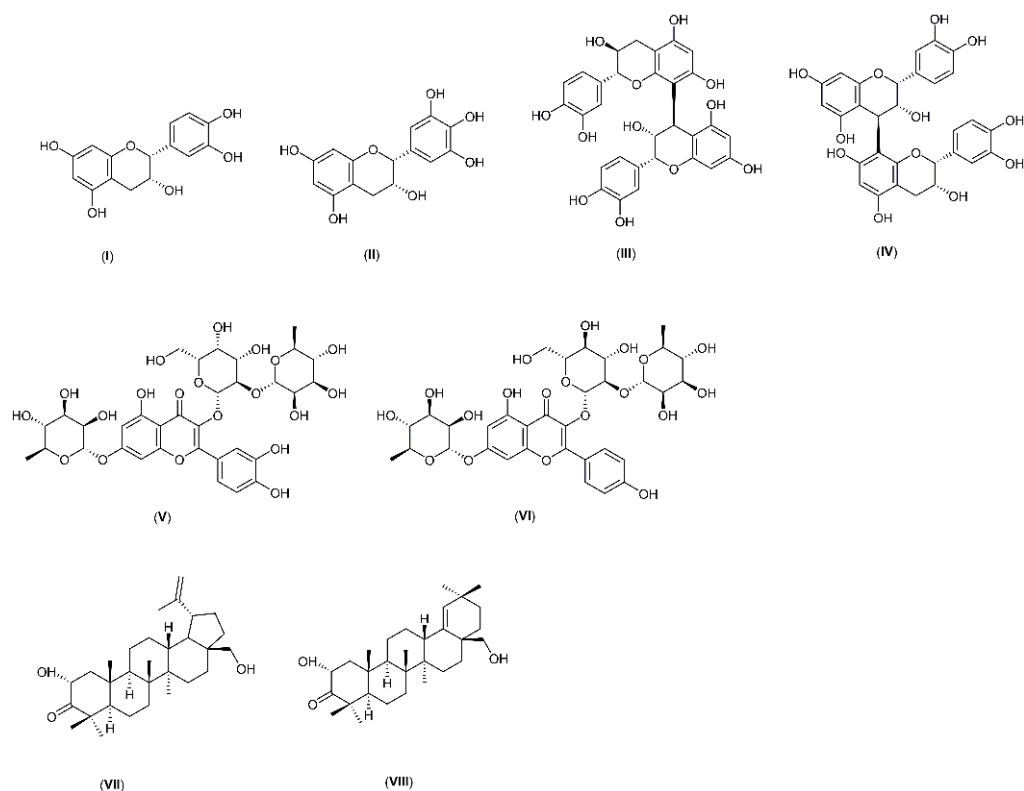
Figure 2. Chemical structures of compounds from *Monteverdia ilicifolia* (**I–VIII**) (Chem Draw v.14.0.0.118).

2.3. UPLC-MS Profiles of M. ilicifolia Extracts

Based on the anti-*H. pylori* assays, two fractions were chosen to follow the chemistry characterization. EAF2 and *n*BF5 were used in the UPLC-MS analysis.

Table 2 shows the retention time of the compounds separated for chromatography from EAF2, as well as the ion and correspondent fragment in the negative mode.

In the *n*BF5 fraction, it was characterized by glycosylated flavonoids such as kaempferol-galactoside-rhamnoside-rhamnoside and quercetin-rhamnopiranosyl-glucopiranoside-rhamonoside; besides this, the fraction presents some compounds that could not be identified (Table S2).

Several studies have shown the presence of tannins and flavonoids in *M. ilicifolia* extracts that are considered responsible for their biological activity. Monomeric and dimeric flavonoids, such as epicatechin and procyanidins B1 and B2, were isolated and charac-

terized in studies over the years from aqueous, hexanic, and acetonic extracts [11,28,29]. Glycosylated flavonoids are also present in the leaves extracted from *M. aquifolium* and *M. ilicifolia* and are composed of quercetin and kaempferol 3-*O*-glycosides [27,28,30,31]. Some authors have already demonstrated that procyanidins, catechin, and gallic acid isolated from natural products can have activity against *H. pylori* with reference strain and antibiotic-sensitive and resistant clinical isolates [32–36].

Table 2. Compound identification of EAF2 (ethanol: water 50:50 *v/v*) detected by UHPLC-HRMS negative mode.

Identification	Retention Time (Min)	[M-H]⁻ (*m/z*)	Main Fragments
(epi)gallocatechin	8.83	305	109, 125, 139, 165, 219, 237, 261
procyanidin B2	10.63	577	125, 151, 245, 289, 407, 425, 451
(epi)catechin	12.29	289	109, 179, 203, 245
(epi)afzelechin-(epi)catechin	13.70	561	125, 289, 435
(epi)afzelechin-(epi)catechin-(epi)catechin	14.77	849	125, 289, 407, 559, 679
(epi)afzelechin-(epi)afzelechin-(epi)catechin	15.31	833	125, 239, 407, 543
kaempferol-galactoside-rhamnoside-rhamnoside	15.51	739	284
(epi)catechin-(epi)catechin	17.17	577	125, 161, 289, 407
(epi)afzelechin-(epi)catechin	21.31	561	289, 435
kaempferol-rhamnopentoside	21.71	563	284

All these studies support the characterization proposed in the present work, considering that the same substances were isolated and characterized in those studies carried out with the specie. With the results obtained in the activity assays conducted with the fractions, we can presume that the phenolic compounds are responsible for the activity, as several authors demonstrated [11,27,28,30,31].

2.4. Antioxidant Capacity of Extracts and Semi-Purified Fractions

For the antioxidant capacity assays, seven extracts and fractions were selected that showed the best activity against *H. pylori*. The DPPH results are shown in Figure S1; the antioxidant capacity is present as IC_{50}, which means that the extract concentration is needed to promote 50% of the antioxidant activity.

The antioxidant capacity for the tested extracts varies between 14.51 and 98.35 μg/mL. The more pronounced antioxidant capacity was observed in EAF4 with an IC_{50} 14.51 μg/mL followed by CE5 (IC_{50} 19.08 μg/mL) and EAF2 (IC_{50} 19.48 μg/mL), with no significant statistical difference. The worst antioxidant capacity in the DPPH assay was observed for *n*BF5 with an IC_{50} 98.35 μg/mL and the AQF3 (IC_{50} 94.72 μg/mL). The quercetin, used as a positive control, presented an IC_{50} of 2.99 μg/mL. It is known that the antioxidant capacity is more pronounced in the presence of polyphenols [11]. This can explain why the extract obtained with acetone and water was rich in phenolic compounds and had a more notable result.

A previous study tested the antioxidant capacity using the DPPH radical scavenging method of the ethyl-acetate and *n*-butanolic fraction from *M. royleana* (Wall. ex M.A. Lawson) Cufod, both rich in polyphenols. The ethyl-acetate fraction showed an IC_{50} of 55.01 μg/mL, while the *n*-butanolic fraction was 58.01 μg/mL. The antioxidant capacity was evaluated for the ethyl-acetate fraction from an acetonic crude extract by the DPPH radical scavenging method and showed a result of 25.39 μg/mL [11,37].

For the FRAP assay, the values of the antioxidant capacity were expressed as an mM Trolox/g extract equivalent (Figure S2). In this assay, the absorbance variance found was linearly proportional to the antioxidant concentration.

The FRAP assay showed results varying from 0.77 to 5.40 mM Trolox/g of the extract. The EAF2 and EAF4 showed the result of 5.40 and 5.15 mM Trolox/g of the extract,

respectively, with no significant statistical difference. The quercetin was used as the positive control, and the antioxidant capacity was 15.41 mM Trolox/g of the extract.

Some species from the Celastraceae family were tested to determine the antioxidant capacity using the FRAP assay. They found *Cassine orientalis* (Jacq.) Kuntze e *M. pyria* (Willemet) N. Robson has an antioxidant capacity of 584 ± 5.24 e 190 ± 0.87 μM trolox/g in the extract [38].

Polyphenols have a great chemical structure for the removal of free radicals. For the best activity, these compounds must present some specific structural characteristics with the hydroxyl groups and in the ring substitution. Some structural specifications were tested previously, and it was confirmed that the presence of the ortho-hydroxyl group in the ring B increases the antioxidant capacity [39,40].

The compounds present in the extracts produced with organic solvents can eliminate free radicals more effectively than those compounds with more polarity present in aqueous extracts or fractions; the explanation could be the higher presence of phenolic compounds in the extracts produced using organic solvents.

The fact that FAE2 showed the best antioxidant capacity over the *n*BF could be explained by the fact that EAF2 is richer in phenolic compounds. These results are according to the conclusions of [11], who said that phenolic hydroxyl present in the phenolic compounds, as the fraction with the best antioxidant capacity and the one rich in phenolic compounds with orto-hydroxyl in the structure, are more capable of scavenging free radicals.

In summary, the present study demonstrated the anti-*H. pylori* activity of *M. ilicifolia* extracts and fractions represents a strong potential for use in the treatment or even more strongly acting in the prevention of *H. pylori* infection. The antioxidant capacity was confirmed for the specie using two different methods. Both activities can be attributed to the presence of phenolic compounds, such as monomeric, dimeric, and glycosylated flavonoids, which can be found in higher amounts in the extracts and fractions produced with organic solvents.

2.5. Virtual Screening

To identify the compound most likely to act as the *H. pylori* urease inhibitor from those present in the *M. ilicifolia* extract, four molecular docking simulations for each compound in the library using two different programs were carried out. In this way, the mean scores obtained from each program were used in the calculation of the mean relative score expressed by Equation (1). The compound kaempferol-3-galactoside-6-rhamnoside-3-rhamnoside, named CID 44258967, had the highest mean relative score, followed by the compound (epi)afzelechin-(epi)catechin-(epi)catechin, named AFZ-CAT-CAT (Figure 3). For these compounds, the best pose obtained in each docking simulation in the Gold program showed a recurrent conformation pattern in the urease active site (Figure S3), which suggests a site-specific interaction profile with the enzyme, which is characteristic of compounds with a drug-like behavior. Together, these data suggest that the compounds CID 44258967 and AFZ-CAT-CAT are the most likely urease inhibitors presented in the *M. ilicifolia* extract.

To describe the molecular interactions that occur between urease and the best MRS ligands, the PoseView program [41] was used. For the compound CID44258967 (Figure 4A), the program predicts the hydrogen bonds with residues His221, Glu222, Thr251, Ala278, and Arg338, hydrophobic contacts with the residues Met317, Leu318, Cys321, and Phe334, a π-π stacking with residue Phe334, and a charge-dipole interaction with one of the Ni^{2+} cofactors. For the compound AFZ-CAT-CAT (Figure 4B), hydrogen bonds are predicted with the residues Ala169, Glu222, Asp223, and Asp362, a hydrophobic contact with Met366 and charge-dipole interaction with the two Ni^{2+} cofactors.

There are no reports in the literature citing the activity of kaempferol-3-galactoside-6-rhamnoside-3-rhamnoside or (epi)afzelechin-(epi)catechin-(epi)catechin as urease inhibitors, which makes this work the first one to associate anti-ureolytic activity with these two compounds.
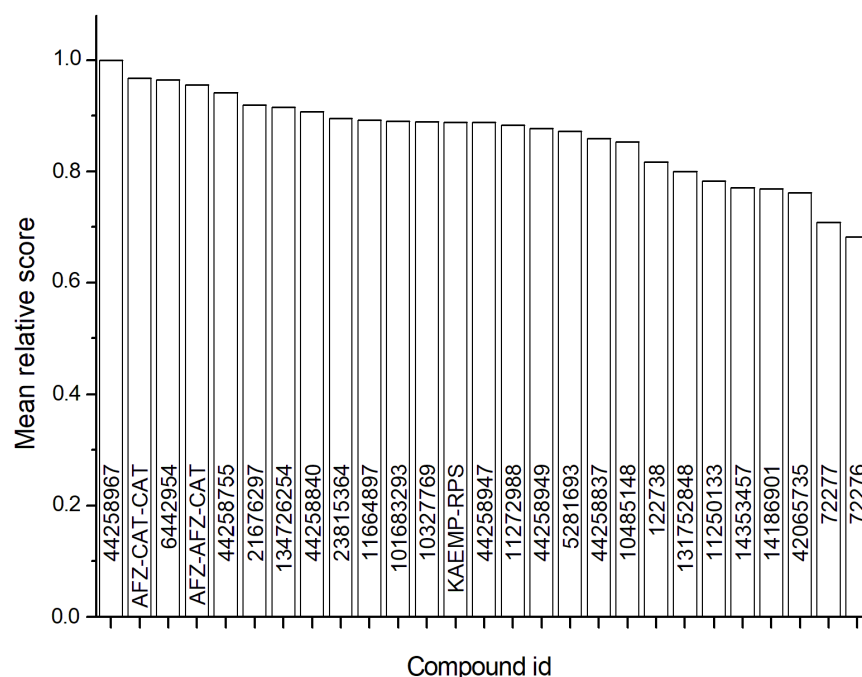
Figure 3. Mean relative docking scores of the compounds of the *Monteverdia ilicifolia* extract. The reference crystallographic ligand DJM (CID42065735) was used as reference.

Regarding toxicity, as far as we know, there are no reports in the literature describing the possible toxic effects of these two compounds, which leads us to evaluate their toxicity in silico by the SwissADME server. As a result, the AFZ-CAT-CAT compound showed three violations of Lipinski's rules, MW > 500, the number of N or O > 10, and the number of NH or OH > 5. In addition, it has an alert as a possible pan assay interference compound (PAIN). The compound CID44258967 presented the same three violations of Lipinski's rules but no alert as PAIN. However, Lipinsky's rules assess the usability of the compounds as oral drugs, not regarding their toxic effects. In this way, the extract, and fractions of *M. ilicifolia* used in this work, have already been evaluated for toxicity and showed no relevant effect on the mitochondrial activity of human stomach AGS cells (AGS, ATCC CRL-1739) [42].
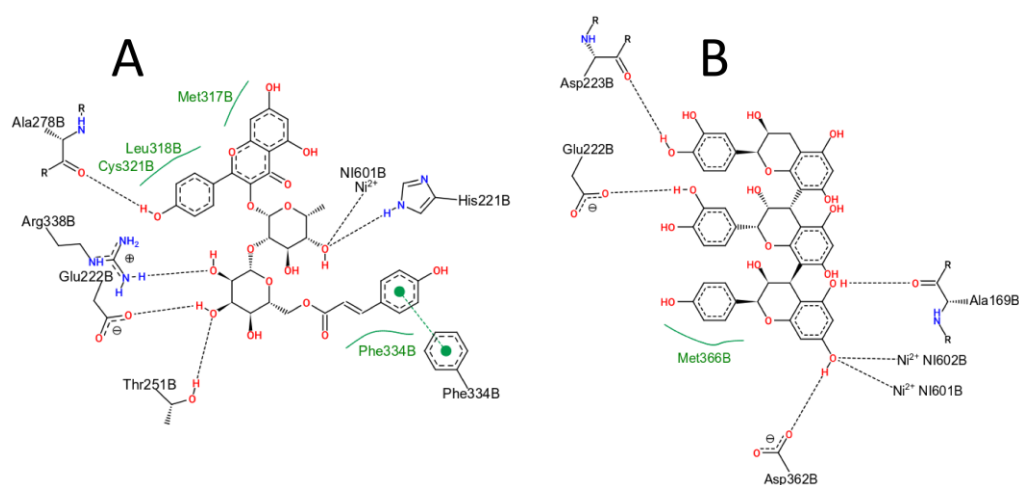
Figure 4. Intermolecular interactions between ligands Kaempferol-3-galactoside-6-rhamnoside-3-rhamnoside, CID44258967 (**A**) and (epi)afzelechin-(epi)catechin-(epi)catechin, AFZ-CAT-CAT (**B**), evaluated by the PoseView program.

3. Materials and Methods

3.1. Plant Material

The leaves of *M. ilicifolia* were collected in Marialva, Brazil (23°28′43″ S; 51°47′39″ W; 622 m altitude) on 16 February 2016. The plant material was identified and deposited in the State University of Maringa herbarium under registration number 29221. The material was collected with the permission of IBAMA-SISBIO and registered under the number 11995-3. Access to the botanical material was registered by the Sistema Nacional de Gestão do Patrimônio Genético e do Conhecimento Tradicional Associado, SisGen, under #AB65084.

3.2. Extracts and Fractions Preparation

The pulverized leaves were macerated with *n*-hexane (10%, *w/v*) for 10 days to decrease. Afterward, five extracts of 10% (*w/v*) were produced by turbo extraction (Ultra-turrax®—UTC115KT) using in *v/v* proportion:water (CE1); ethanol:water 50:50 (CE2); ethanol:water 70:30 (CE3); ethanol:water 96:4 (CE4), and acetone:water 7:3 (CE5). The solutions were filtered, evaporated on a rotary evaporator under reduced pressure at 40 °C, and lyophilized. The extracts were further partitioned in water with ethyl acetate and *n*-butanol. The fractios solutions were evaporated and lyophilized, resulting in ethyl-acetate (EAF), *n*-butanolic (*n*BF), and aqueous fractions (AQF) [11]. The crude extracts and fractions yield are presented in Table S3.

3.3. Epicatechin Determination Using HPLC Method

The analyses were carried out using a Thermo® HPLC (Thermo Electron, Waltham, MA, USA), with a PDA (photo diode array) spectrophotometry detector module (Model Finnigan™ Surveyor PDA Plus Detector-Thermo Electron, Waltham, MA, USA), integral pumps, and degasser (Finnigan™ Surveyor LC Pump Plus - Thermo Electron, Waltham, MA, USA) and autosampler (Finnigan™ Surveyor Autosampler Plus-Thermo Electron, Waltham, MA, USA) equipped with a 10 µL loop and controller software (Chromquest™, version 4.2, Thermo Electron, Waltham, MA, USA), a Phenomenex® Gemini C-18 (250 × 4.6 mm, 5 µm) (Phenomenex®, Torrance, CA, USA), and a guard column (Phenomenex® SecurityGuard™-RP C-18 cartridge) (Phenomenex®, Torrance, CA, USA). It was used as a mobile phase water:formic acid (pH 2.5) (phase A) and acetonitrile:formic acid (pH 2.5) (phase B). It used a linear gradient of 0 min 18% B; 13 min 25% B; 16 min 34% B; 20 min 42% B; 23 min 65% B; 25 min 18% B, with a flow of 0.8 mL/min, and 100 µL injection volume. Detection was performed at 210 nm [29].

The sample preparation was carried out following a previous study using 1 g of each crude extract instead the pulverized leaves. The standard solution's preparation and obtention of the calibration curve were conducted according to the previous study (Epicatechin calibration curve: y = 151,061x + 2,726,000) [29].

3.4. Bacteria Strain

It used *H. pylori* strain ATCC® 43504, amoxicillin sensitive, and metronidazole resistance. Bacteria were grown in the Columbia Agar supplemented with sheep blood (5%) in a 10.0% CO_2 atmosphere at 37.0 °C for 72 h [43].

3.4.1. Minimum Inhibitory Concentration (MIC) and Minimum Bactericidal Concentration (MBC)

The anti-*H. pylori* assay was conducted by the microdilution method [44]. As a positive control, amoxicillin and metronidazole (Sigma Chemical Co., St. Louis, MO, USA) were used. In each well, 100 µL of the sample solutions (32–1024 µg/mL) and 100 µL *H. pylori* suspension ($\approx 10^6$–10^7 bacteria/mL) were added both in supplemented BHI. The absorbance was measured at 620 nm and then incubated (37.0 °C/72 h/10.0% CO_2). After incubation, the plate was homogenized, and a new measurement was performed to determine the MIC.

The MBC assay was performed for samples that presented MIC. The sample corresponding to the microplate well without apparent growth in BHI was harvested in a

Columbia Agar plate (5% sheep blood) and incubated at 37.0 °C, 10.0% CO_2, 72 h. The assay was determined by the lowest sample concentration able to inhibit colony formation.

3.4.2. Urease Inhibition Assay

Urease inhibition activity was determined based on the production of ammonia catalyzed by the enzyme urease, according to the method described by [44]. The reaction microplate contained a mixture of 25 μL of urease 4 UI (Sigma Jack Bean urease type III) and 25 μL of the sample at varying concentrations, and it was incubated at room temperature for two hours. Then, 25 μL of phenol red (0.02%) and 200 μL of urea (50 mM) in 100 mM phosphate buffer (pH 6.8) were added to the microplate. After 20 min, the mixture absorbance was read at 540 mm using a microplate reader (iMark®, BioRad, Washington, DC, USA). Boric acid was used as the standard positive control for urease inhibition.

3.5. UHPLC-MS Conditions

UHPLC-MS analysis was performed on a Nexera X2 liquid chromatography system with an LC-30AD pump and Phenomenex® Gemini C-18 column (250 mm × 4.6 mm) coupled with a Q-TOF Impact II (Bruker Daltonics, Bremen, Germany), with electrospray ionization source. The column was maintained at 40 °C with a linear elution gradient of water 0.1% formic acid (eluent A) and acetonitrile 0.1% formic acid (eluent B). The elution procedure follows 0–13 min 18% B; 13–16 min 25% B; 16–20 min 34% B; 20–23 min 42% B; 23–25 min 65% B; 25–28 min 18% B. The flow rate was 0.4 mL/min, and a 20 μL aliquot of each sample was injected.

The ESI was set in the Auto MS/MS acquisition mode, with an acquisition rate of 5 Hz (MS and MS/MS). The scans were acquired using the mass analyzer at 70–1500 *m/z*. The analyses were performed in a positive and negative ionization mode, with a capillary voltage of 4.00 kV, supply temperature of 220 °C, and desolvation gas flow of 8.0 L/min. Daughter-scan experiments were performed using the collision-induced dissociation (CID) obtained using a collision energy ramp in the range of 15–50 eV and collision gas pressure of 3.06×10^{-3} mBar in the collision chamber.

3.6. Antioxidant Capacity Assay
3.6.1. Determination of DPPH (2,2-diphenyl-1-picrylhydrazyl) Radical Levels

M. ilicifolia extracts and fractions were diluted in methanol and prepared at final concentrations of 3.1–100.0 μg/mL. A total of 100 μL of freshly prepared 130 μM DPPH was added to 100 μL of the sample at different concentrations. The microplates were kept at room temperature and protected from light. After 30 min, the absorbances were measured at 517 nm in a microplate spectrophotometer (Biochrom Asys UVM 340-Cambridge, Cambridgeshire, England). Negative (methanol added to DPPH), white (methanol only), and positive (Trolox standard) controls were used [45].

3.6.2. Ferric Reducing Antioxidant Power (FRAP) Assay

The FRAP assay method was described previously [45]. Trolox and samples (20–100 μg/mL) were diluted in ethanol. Absorbance values were measured using a microplate spectrophotometer (Biochrom Asys UVM 340 - Cambridge, Cambridgeshire, England) at 595 nm. To determine the total antioxidant capacity, it was used in the Trolox calibration curve equation (20–600 μM; y = 0.0028x + 0.0199 R^2 = 0.9993) from the sample's absorbances. The results were expressed as Trolox equivalent antioxidant capacity (TEAC).

3.7. Virtual Screening

One of the beta subunits of the hetero 24-mer urease from *H. pylori* and bonded to the inhibitor 2-{[1-(3,5-dimethylphenyl)-1H-imidazol-2-yl]sulfanyl}-N-hydroxyacetamide (named DJM; CID 42065735) (PDB id: 6ZJA) was used in the virtual screening of compounds described in the *M. ilicifolia* extract (Table S4). The programs and respective protocols were defined based on the redocking of the ligand in the urease. The AutoDock-Vina (Vina)

program [46] used the standard search and ranking algorithms, with the search space defined by the box centered on the ligand, with dimensions of 30, 20, and 30 Å at x, y, and z, respectively. The uff force field [47] was used to minimize the ligands. The program Gold [48] uses the search space with a 15 Å radius centered on the ligand. The search algorithm employed a 200% efficiency, with 30 runs, and the ASP scoring and the 'Allow early termination' option was disabled.

The compounds described in the *M. ilicifolia* extract plus the reference ligand CID 42065735 were in the library for the virtual screening. The 2D or 3D structures of the compounds were obtained from the PubChem database or drawn by the ChemDraw® program. Different isomers were used when necessary, and the OpenBabel program [49] was used to add hydrogens and convert them to 3D.

The mean relative score (*MRS*) was calculated from the mean docking score of each compound after four simulations using each program (Equation (1)). In this equation, *Vina* represents the average score of the compound obtained from four simulations using the *Vina* program, and *Vina*$_{max}$ expresses the maximum average score observed for the given compounds of the library; the same concept was applied to the results from the Gold program (*Gold* and *Gold*$_{max}$). The *MRS* allows the ranking of compounds with the ligand CID42065735 as a reference.

$$MRS = \frac{1}{2}\left(\frac{Vina}{Vina_{max}} + \frac{Gold}{Gold_{max}}\right) \tag{1}$$

The in-silico toxicity was estimated by the SwissADME server [50].

3.8. Statistical Analysis

Numerical data were presented as the means ± standard deviation (SD). The number of repetitions of individual assays was different and was present in the description of each of them. One-way ANOVA with Bonferroni post-test was performed considering values of $p \leq 0.05$ as statistically significant.

4. Conclusions

The EAF2 and *n*BF5 presented the best in vitro anti-*H. pylori* activity among all the extracts and fractions tested. In the urease enzyme inhibition test, the highest percentage of inhibition was observed in the *n*BF5 and EAF2. The antioxidant capacity was better observed in the ethyl acetate fractions tested and for the CE5. The in silico assays demonstrated that kaempferol-3-galactoside-6-rhamnoside-3-rhamnoside and (epi)afzelechin-(epi)catechin-(epi)catechin presented in the fractions EAF2 and *n*BF5 and have an anti-ureolytic activity. The anti-*H. pylori* and antioxidant activity observed can be attributed to the phenolic compounds present in EAF2 and *n*BF5.

the same conformation for each pose in all simulations indicates a pattern of drug-like behaviour; Table S4: Compounds identification of EAF2 and nBF5.

Abbreviations

CE1	Crude extract aqueous
EAF1	Ethyl-acetate fraction from crude extract aqueous
nBF1	n-Butanolic fraction from crude extract aqueous
AQF1	Aqueous fraction from crude extract aqueous
CE2	Crude extract ethanol: water 50:50 (*v/v*)
EAF2	Ethyl-acetate fraction from crude extract ethanol: water 50:50 (*v/v*)
nBF2	n-Butanolic fraction from crude extract ethanol: water 50:50 (*v/v*)
AQF2	Aqueous fraction from crude extract ethanol: water 50:50 (*v/v*)
CE3	Crude extract ethanol: water 70:30 (*v/v*)
EAF3	Ethyl-acetate fraction from crude extract ethanol: water 70:30 (*v/v*)
nBF3	n-Butanolic fraction from crude extract ethanol: water 70:30 (*v/v*)
AQF3	Aqueous fraction from crude extract ethanol: water 70:30 (*v/v*)
CE4	Crude extract ethanol: water 96:4 (*v/v*)
EAF4	Ethyl-acetate fraction from crude extract ethanol: water 96:4 (*v/v*)
nBF4	n-Butanolic fraction from crude extract ethanol: water 96:4 (*v/v*)
AQF4	Aqueous fraction from crude extract ethanol: water 96:4 (*v/v*)
CE5	Crude extract acetone: water 70:30 (*v/v*)
EAF5	Ethyl-acetate fraction from crude extract acetone: water 70:30 (*v/v*)
nBF5	n-Butanolic fraction from crude extract acetone: water 70:30 (*v/v*)
AQF5	Aqueous fraction from crude extract acetone: water 70:30 (*v/v*)

References

1. Wroblewski, L.E.; Peek, R.M.; Wilson, K.T. Helicobacter pylori and gastric cancer: Factors that modulate disease risk. *Clin. Microbiol. Rev.* **2010**, *23*, 713–739. [CrossRef] [PubMed]
2. Kao, C.-Y.; Sheu, B.-S.; Wu, J.-J. Helicobacter pylori infection: An overview of bacterial virulence factors and pathogenesis. *Biomed. J.* **2016**, *39*, 14–23. [CrossRef] [PubMed]
3. Hooi, J.K.; Lai, W.Y.; Ng, W.K.; Suen, M.M.; Underwood, F.E.; Tanyingoh, D.; Malfertheiner, P.; Graham, D.Y.; Wong, V.W.; Wu, J.C. Global Prevalence of Helicobacter pylori Infection: Systematic Review and Meta-analysis. *Gastroenterology* **2017**, *153*, 420–429. [CrossRef] [PubMed]
4. Coelho, L.G.V.; Marinho, J.R.; Genta, R.; Ribeiro, L.T.; Passos, M.d.C.F.; Zaterka, S.; Assumpção, P.P.; Barbosa, A.J.A.; Barbuti, R.; Braga, L.L.J.A.d.g. IVth Brazilian Consensus Conference on Helicobacter pylori Infection. *Arq. Gastroenterol.* **2018**, *55*, 97–121. [CrossRef] [PubMed]

5.   Hunt, R.; Xiao, S.; Megraud, F.; Leon-Barua, R.; Bazzoli, F.; Van der Merwe, S.; Vaz Coelho, L.; Fock, M.; Fedail, S.; Cohen, H. Helicobacter pylori in developing countries. World gastroenterology organisation global guideline. *J. Gastrointest. Liver Dis.* **2011**, *20*, 299–304.

6.   Kusters, J.G.; van Vliet, A.H.; Kuipers, E.J. Pathogenesis of Helicobacter pylori infection. *Clin. Microbiol. Rev.* **2006**, *19*, 449–490. [CrossRef] [PubMed]

7.   Jorge, R.; Leite, J.; Oliveira, A.; Tagliati, C. Evaluation of antinociceptive, anti-inflammatory and antiulcerogenic activities of Maytenus ilicifolia. *J. Ethnopharmacol.* **2004**, *94*, 93–100. [CrossRef]

8.   Biral, L.; Simmons, M.P.; Smidt, E.C.; Tembrock, L.R.; Bolson, M.; Archer, R.H.; Lombardi, J.A. Systematics of New World Maytenus (Celastraceae) and a New Delimitation of the Genus. *Syst. Bot.* **2017**, *42*, 680–693. [CrossRef]

9.   Mazza, M.; dos Santos, J.; Mazza, C.d.S. Fenologia reprodutiva de Maytenus ilicifolia (Celastraceae) na Floresta Nacional de Irati, Paraná, Brasil. *Braz. J. Bot.* **2011**, *34*, 565–574. [CrossRef]

10. Souza-Formigoni, M.L.O.; Oliveira, M.G.M.; Monteiro, M.G.; da Silveira-Filho, N.G.; Braz, S.; Carlini, E. Antiulcerogenic effects of two Maytenus species in laboratory animals. *J. Ethnopharmacol.* **1991**, *34*, 21–27. [CrossRef]

11. Pessuto, M.B.; Costa, I.C.d.; Souza, A.B.d.; Nicoli, F.M.; Petereit, F.; Luftmann, H.; Mello, J.C.P. Atividade antioxidante de extratos e taninos condensados das folhas de Maytenus ilicifolia Mart. ex Reiss. *Química Nova* **2009**, *32*, 412–416. [CrossRef]

12. Gullo, F.P.; Sardi, J.C.; Santos, V.A.; Sangalli-Leite, F.; Pitangui, N.S.; Rossi, S.A.; de Paula e Silva, A.C.; Soares, L.A.; Silva, J.F.; Oliveira, H.C. Antifungal activity of maytenin and pristimerin. *Evid.-Based Complement. Altern. Med.* **2012**, *2012*, 340787. [CrossRef]

13. Araújo Júnior, R.F.d.; Oliveira, A.L.C.d.S.L.; Pessoa, J.B.; Garcia, V.B.; Guerra, G.C.B.; Soares, L.A.L.; de Souza, T.P.; Petrovick, P.R.; de Araújo, A.A. Maytenus ilicifolia dry extract protects normal cells, induces apoptosis and regulates Bcl-2 in human cancer cells. *Exp. Biol. Med.* **2013**, *238*, 1251–1258. [CrossRef]

14. Dos Santos, V.A.; Leite, K.M.; da Costa Siqueira, M.; Regasini, L.O.; Martinez, I.; Nogueira, C.T.; Galuppo, M.K.; Stolf, B.S.; Pereira, A.M.S.; Cicarelli, R. Antiprotozoal activity of quinonemethide triterpenes from Maytenus ilicifolia (Celastraceae). *Molecules* **2013**, *18*, 1053–1062. [CrossRef]

15. Wonfor, R.; Natoli, M.; Parveen, I.; Beckman, M.; Nash, R.; Nash, D. Anti-inflammatory properties of an extract of M. ilicifolia in the human intestinal epithelial Caco-2 cell line. *J. Ethnopharmacol.* **2017**, *209*, 283–287. [CrossRef]

16. Tanaka, N.; Kashiwada, Y.J.J.o.n.m. Characteristic metabolites of Hypericum plants: Their chemical structures and biological activities. *J. Nat. Med.* **2021**, *75*, 423–433. [CrossRef]

17. Taguri, T.; Tanaka, T.; Kouno, I. Antimicrobial activity of 10 different plant polyphenols against bacteria causing food-borne disease. *Biol. Pharm. Bull.* **2004**, *27*, 1965–1969. [CrossRef]

18. Daglia, M. Polyphenols as antimicrobial agents. *Curr. Opin. Biotechnol.* **2012**, *23*, 174–181. [CrossRef]

19. Anvisa. *Farmacopeia Brasileira*, 5th ed.; Agência Nacional de Vigilância Sanitária: Brasília, Brazil; Volume 2, pp. 922–927.

20. Wang, Y.C.; Huang, T.L. Anti-Helicobacter pylori activity of *Plumbago zeylanica* L. *Pathog. Dis.* **2005**, *43*, 407–412. [CrossRef]

21. Njume, C.; Afolayan, A.J.; Ndip, R.N. Preliminary phytochemical screening and in vitro anti-Helicobacter pylori activity of acetone and aqueous extracts of the stem bark of Sclerocarya birrea (Anacardiaceae). *Arch. Med. Res.* **2011**, *42*, 252–257. [CrossRef]

22. Santos, S.d.c.; Mello, J.C.P.d. Taninos. In *Farmacognosia: Da planta ao medicamento*; Simões, C.M.O., Schenkel, E.P., Gosmann, G., Mello, J.C.P.d., Mentz, L.A., Petrovick, P.R., Eds.; Editora da UFRGS; Editora da UFSC: Porto Alegre, Florianópolis, 2007; pp. 615–656.

23. Park, D.; Shin, K.; Choi, Y.; Guo, H.; Cha, Y.; Kim, S.-H.; Han, N.S.; Joo, S.S.; Choi, J.K.; Lee, Y.B. Antimicrobial activities of ethanol and butanol fractions of white rose petal extract. *Regul. Toxicol. Pharmacol.* **2016**, *76*, 57–62. [CrossRef]

24. Bae, E.-A.; Han, M.J.; Kim, N.-J.; Kim, D.-H. Anti-Helicobacter pylori Activity of Hearbal Medicines. *Biol. Pharm. Bull.* **1998**, *21*, 990–992. [CrossRef] [PubMed]

25. Xiao, Z.-P.; Shi, D.-H.; Li, H.-Q.; Zhang, L.-N.; Xu, C.; Zhu, H.-L. Polyphenols based on isoflavones as inhibitors of Helicobacter pylori urease. *Bioorganic Med. Chem.* **2007**, *15*, 3703–3710. [CrossRef] [PubMed]

26. Ohsaki, A.; Imai, Y.; Naruse, M.; Ayabe, S.; Komiyama, K.; Takashima, J. Four new triterpenoids from Maytenus ilicifolia. *J. Nat. Prod.* **2004**, *67*, 469–471. [CrossRef]

27. Leite, J.P.V.; Rastrelli, L.; Romussi, G.; Oliveira, A.B.; Vilegas, J.H.; Vilegas, W.; Pizza, C. Isolation and HPLC quantitative analysis of flavonoid glycosides from Brazilian beverages (Maytenus ilicifolia and M. aquifolium). *J. Agric. Food Chem.* **2001**, *49*, 3796–3801. [CrossRef] [PubMed]

28. Leite, J.P.V.; Braga, F.C.; Romussi, G.; Persoli, R.M.; Tabach, R.; Carlini, E.A.; Oliveira, A.B. Constituents from Maytenus ilicifolia leaves and bioguided fractionation for gastroprotective activity. *J. Braz. Chem. Soc.* **2010**, *21*, 248–254. [CrossRef]

29. Lopes, G.C.; Blainski, A.; Santos, P.V.P.d.; Diciaula, M.C.; Mello, J.C.P.d. Development and validation of an HPLC method for the determination of epicatechin in Maytenus ilicifolia (Schrad.) Planch., Celastraceae. *Rev. Bras. De Farmacogn.* **2010**, *20*, 781–788. [CrossRef]

30. Sannomiya, M.; Vilegas, W.; Rastrelli, L.; Pizza, C. A flavonoid glycoside from Maytenus aquifolium. *Phytochemistry* **1998**, *49*, 237–239. [CrossRef]

31. Vilegas, W.; Sanommiya, M.; Rastrelli, L.; Pizza, C. Isolation and structure elucidation of two new flavonoid glycosides from the infusion of Maytenus aquifolium leaves. Evaluation of the antiulcer activity of the infusion. *J. Agric. Food Chem.* **1999**, *47*, 403–406. [CrossRef]

32. Silvan, J.M.; Gutiérrez-Docio, A.; Moreno-Fernandez, S.; Alarcón-Cavero, T.; Prodanov, M.; Martinez-Rodriguez, A.J.J.F. Procyanidin-rich extract from grape seeds as a putative tool against Helicobacter pylori. *Foods* **2020**, *9*, 1370. [CrossRef]

33. Pastene, E.; Parada, V.; Avello, M.; Ruiz, A.; Garcia, A. Catechin-based procyanidins from Peumus boldus Mol. aqueous extract inhibit Helicobacter pylori urease and adherence to adenocarcinoma gastric cells. *Phytother. Res.* **2014**, *28*, 1637–1645. [CrossRef] [PubMed]

34. Mabe, K.; Yamada, M.; Oguni, I.; Takahashi, T. In vitro and in vivo activities of tea catechins against Helicobacter pylori. *Antimicrob. Agents Chemother.* **1999**, *43*, 1788–1791. [CrossRef] [PubMed]

35. Díaz-Gómez, R.; López-Solís, R.; Obreque-Slier, E.; Toledo-Araya, H. Comparative antibacterial effect of gallic acid and catechin against Helicobacter pylori. *LWT Food Sci. Technol.* **2013**, *54*, 331–335. [CrossRef]

36. Yanagawa, Y.; Yamamoto, Y.; Hara, Y.; Shimamura, T. A combination effect of epigallocatechin gallate, a major compound of green tea catechins, with antibiotics on Helicobacter pylori growth in vitro. *Curr. Microbiol.* **2003**, *47*, 244–249. [CrossRef]

37. Shabbir, M.; Khan, M.R.; Saeed, N. Assessment of phytochemicals, antioxidant, anti-lipid peroxidation and anti-hemolytic activity of extract and various fractions of Maytenus royleanus leaves. *BMC Complement. Altern. Med.* **2013**, *13*, 143. [CrossRef]

38. Soobrattee, M.A.; Bahorun, T.; Neergheen, V.S.; Googoolye, K.; Aruoma, O.I. Assessment of the content of phenolics and antioxidant actions of the Rubiaceae, Ebenaceae, Celastraceae, Erythroxylaceae and Sterculaceae families of Mauritian endemic plants. *Toxicol. Vitr.* **2008**, *22*, 45–56. [CrossRef]

39. Resende, F.O.; Rodrigues-Filho, E.; Luftmann, H.; Petereit, F.; Mello, J.C.J.J.o.t.B.C.S. Phenylpropanoid substituted flavan-3-ols from Trichilia catigua and their in vitro antioxidative activity. *J. Braz. Chem. Soc.* **2011**, *22*, 2087–2093. [CrossRef]

40. Van Acker, S.A.; Tromp, M.N.; Griffioen, D.H.; Van Bennekom, W.P.; Van Der Vijgh, W.J.; Bast, A. Structural aspects of antioxidant activity of flavonoids. *Free Radic. Biol. Med.* **1996**, *20*, 331–342. [CrossRef]

41. Stierand, K.; Maaß, P.C.; Rarey, M.J.B. Molecular complexes at a glance: Automated generation of two-dimensional complex diagrams. *Bioinformatics* **2006**, *22*, 1710–1716. [CrossRef]

42. de Paula, M.N.; Kelm, M.; Symma, N.; Isolani, R.G.; da Silva, F.P.; Sendker, J.; Hensel, A.; de Mello, J.C.P.J.R.B.d.F. Anti-adhesive Activity of Maytenus ilicifolia Against Helicobacter pylori. *Braz. J. Pharmacogn.* **2021**, *31*, 726–731. [CrossRef]

43. Chierrito, D.; Villas-Boas, C.B.; Tonin, F.S.; Fernandez-Llimos, F.; Sanches, A.C.; de Mello, J.C.J.C.n. Using cell cultures for the investigation of treatments for attention deficit hyperactivity disorder: A systematic review. *Curr. Neuropharmacol.* **2019**, *17*, 916–925. [CrossRef] [PubMed]

44. Borges, A.S.; Minozzo, B.R.; Santos, H.; Santa Ardisson, J.; Rodrigues, R.P.; Romão, W.; de Souza Borges, W.; Gonçalves, R.d.C.R.; Beltrame, F.L.; Kitagawa, R.R. Plectranthus barbatus Andrews as anti-Helicobacter pylori agent with activity against adenocarcinoma gastric cells. *Ind. Crops Prod.* **2020**, *146*, 112207. [CrossRef]

45. Sereia, A.L.; de Oliveira, M.T.; Baranoski, A.; Marques, L.L.M.; Ribeiro, F.M.; Isolani, R.G.; de Medeiros, D.C.; Chierrito, D.; Lazarin-Bidóia, D.; Zielinski, A.A.F. In vitro evaluation of the protective effects of plant extracts against amyloid-beta peptide-induced toxicity in human neuroblastoma SH-SY5Y cells. *PLoS ONE* **2019**, *14*, e0212089. [CrossRef]

46. Trott, O.; Olson, A.J. AutoDock Vina: Improving the speed and accuracy of docking with a new scoring function, efficient optimization, and multithreading. *J. Comp. Chem.* **2010**, *31*, 455–461. [CrossRef] [PubMed]

47. Rappé, A.K.; Casewit, C.J.; Colwell, K.; Goddard III, W.A.; Skiff, W.M.J.J.o.t.A.c.s. UFF, a full periodic table force field for molecular mechanics and molecular dynamics simulations. *J. Am. Chem. Soc.* **1992**, *114*, 10024–10035. [CrossRef]

48. Jones, G.; Willett, P.; Glen, R.C.; Leach, A.R.; Taylor, R.J.J.o.m.b. Development and validation of a genetic algorithm for flexible docking. *J. Mol. Biol.* **1997**, *267*, 727–748. [CrossRef]

49. O'Boyle, N.M.; Banck, M.; James, C.A.; Morley, C.; Vandermeersch, T.; Hutchison, G.R.J.J.o.c. Open Babel: An open chemical toolbox. *J. Cheminform.* **2011**, *3*, 1–14. [CrossRef]

50. Daina, A.; Michielin, O.; Zoete, V.J.S.r. SwissADME: A free web tool to evaluate pharmacokinetics, drug-likeness and medicinal chemistry friendliness of small molecules. *Sci. Rep.* **2017**, *7*, 1–13. [CrossRef]

Article

Essential Oils of Aromatic Plant Species from the Atlantic Rainforest Exhibit Extensive Chemical Diversity and Antimicrobial Activity

Crislene V. Perigo [1], Lenita L. Haber [2], Roselaine Facanali [1], Maria A. R. Vieira [1], Roseli B. Torres [1], Luís C. Bernacci [1], Elsie F. Guimarães [3], João B. Baitello [4], Marcos E. G. Sobral [5], Vera Quecini [6,*] and Marcia Ortiz M. Marques [1,*]

1   Instituto Agronômico, Campinas 13075-630, Brazil
2   Vegetables Research Center, Brazilian Agricultural Research Corporation, Brasília 70351-970, Brazil
3   Instituto de Pesquisas Jardim Botânico do Rio de Janeiro, Rio de Janeiro 22460-030, Brazil
4   Instituto Florestal do Estado de São Paulo, São Paulo 02377-000, Brazil
5   Natural Sciences Department, Campus Dom Bosco, Universidade Federal de São João del-Rei, São João del Reio 36301-160, Brazil
6   Grape and Wine Research Center, Brazilian Agricultural Research Corporation, Bento Gonçalves 95701-008, Brazil
*   Correspondence: vera.quecini@embrapa.br (V.Q.); marcia.marques@sp.gov.br (M.O.M.M.); Tel.: +55-(54)-3455-8000 (V.Q.); +55-(19)-3202-1700 (M.O.M.M.)

Abstract: Microbial resistance, caused by the overuse or inadequate application of antibiotics, is a worldwide crisis, increasing the risk of treatment failure and healthcare costs. Plant essential oils (EOs) consist of hydrophobic metabolites with antimicrobial activity. The antimicrobial potential of the chemical diversity of plants from the Atlantic Rainforest remains scarcely characterized. In the current work, we determined the metabolite profile of the EOs from aromatic plants from nine locations and accessed their antimicrobial and biocidal activity by agar diffusion assays, minimum inhibitory concentration, time-kill and cell-component leakage assays. The pharmacokinetic properties of the EO compounds were investigated by in silico tools. More than a hundred metabolites were identified, mainly consisting of sesqui and monoterpenes. Individual plants and botanical families exhibited extensive chemical variations in their EO composition. Probabilistic models demonstrated that qualitative and quantitative differences contribute to chemical diversity, depending on the botanical family. The EOs exhibited antimicrobial biocidal activity against pathogenic bacteria, fungi and multiple predicted pharmacological targets. Our results demonstrate the antimicrobial potential of EOs from rainforest plants, indicate novel macromolecular targets, and contribute to highlighting the chemical diversity of native species.

Keywords: ADME; biological activity; GC-MS; network analyses; terpene; volatiles

1. Introduction

Antimicrobial resistance is the main cause of relapsing infections and treatment failure in microbe-induced pathogenesis, leading to higher rates of patient morbidity and mortality, but also imposing increased costs to healthcare [1]. The selective pressure enforced by the overuse and/or misuse of antimicrobials triggers genetic and metabolic modifications in pathogenic microorganisms that allow them to extrude or detoxify multiple drugs, giving rise to Multidrug-Resistant (MDR) pathogens [1]. The molecular mechanisms underlying drug resistance are classified into three main groups: (i) reduction in the intracellular concentration of the antimicrobial agent; (ii) molecular modifications of the antimicrobial target; and (iii) inactivation of the antimicrobial molecule [2]. The evolution of pathogenic microorganisms shuffles and combines these general mechanisms to overcome the mode of

action of several classes of antimicrobial compounds. Thus, new therapeutic molecules are continuously sought after to combat MDR pathogens.

Several plant compounds and mixtures of compounds exhibit antimicrobial potential, including Essential Oils (EOs) [3]. EOs are an important part of the volatile organic metabolites, produced by four major biosynthetic routes: the shikimate/phenylalanine, the mevalonic acid, the methylerythritol phosphate and lipoxygenase pathways [4–7]. EOs consist of hydrophobic metabolites stored in and released by specialized secretory structures of the plants, involved in a wide range of biotic interactions in the natural environment, including with herbivores and their parasitoids, pollinators, and other plants [4,6,7]. Chemically, EOs consist of complex blends of terpenoids, benzenoids/phenylpropanoids, volatile carotenoid derivatives, and methylated volatiles [6,7]. The hydrophobicity and variable degree of reactivity of EO metabolites make them interesting therapeutic products to be used against pathogenic microorganisms, alone or in combination with traditional antibiotics [8–10]. However, a large portion of the plants' chemical diversity remains unexplored, as most studies have focused on domesticated species. The flora in the Brazilian portion of the Atlantic Rainforest is considered one of the richest in the world, consisting of more than forty-thousand species, with nearly half of them being endemic [11]. The biome is also one of the primary biodiversity hotspots in the world, with approximately twenty-thousand species [11]. The plants in the Atlantic Rainforest exhibit high inter- and intra-specific genetic variation, which, coupled with the distinct environmental conditions, allows them to produce hundreds of thousands of distinct specialized metabolites [12]. The chemical diversity of the EOs from rainforest plants remains scarcely characterized. Comprehensive chemical characterization of the EOs from undomesticated species may discover novel aspects of the plants metabolic diversity and contribute alternative compounds for green chemistry applications, including the design of novel pharmaceuticals.

The current work aimed at investigating the chemical composition and antimicrobial potential of the EOs from plant species found in the Atlantic Rainforest. The results demonstrate expressive inter- and intra-specific chemical variation, significant antimicrobial activity and interesting pharmacokinetic characteristics and macromolecular pharmacological targets of the EO compounds. These findings can contribute to their use in pharmaceutical applications.

2. Results

2.1. Botanical and Chemical Characterization

Fifty distinct aromatic plant species, belonging to fifteen botanical families, were identified in nine locations of the Atlantic rainforest in the State of São Paulo (Table S1, Figure S1). The number of families with associated traditional use were found in coastal locations (Ubatuba and Pariquera-Açu) and the transition region in Votuporanga (Figures S1 and S2). The metabolite profile of 63 EO samples was determined by GC-MS (Figure 1, Table 1). The oil yield was highly variable, ranging between 0.004 and 2.88%, with shrubs producing approximately 1.6 times higher contents than trees (Figure S3). The highest EO contents were found in Pipearaceae shrubs (Figure S3). The biological metabolite variation ranged between trace amounts ($\leq$0.05) and 94.46%. The complete chemical data and their associated metadata are deposited at the National Metabolomics Repository, under identifier ST000606.

A total of 113 metabolites were identified, consisting mostly of monoterpenes (MT) (29%) and sesquiterpenes (ST) (56%), along with phenylpropanoids (PP) (7.5%), benzyl alcohols (BA) (3%) and ketones (MK) (3%) (Figure 1). More than 50% (63/113) of the metabolites were present as major components (Table 1) and most metabolites in the EOs chemical composition ($\geq$80%) were identified in all samples (50 out of 63, 79.4%) (Table 1, Figures 1 and 2). The percentage of unidentified metabolites ranged between 1.12% (Lp6101606, *Piper aduncum*) and 44.2% (Lp6101714, *Eugenia myrcianthes*) of the total (Figure 1). The number of metabolites per sample ranged between 2 (Lp051901, *Myrcia spectabilis*) and 28 (Lp6101822, *Campomanesia guavirota*) (Figure 1).
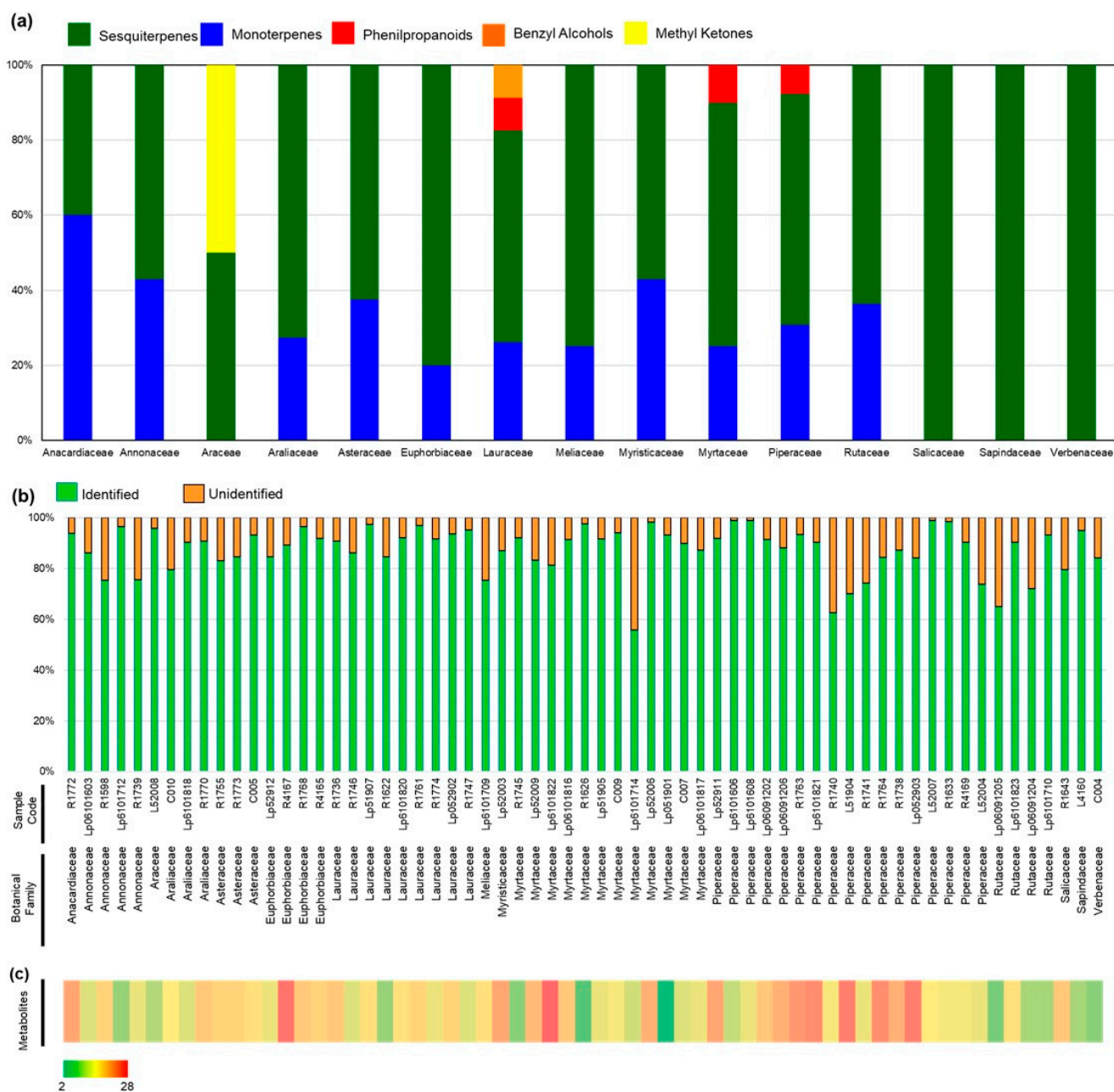
Figure 1. Summary of the metabolite profiles of aromatic plants from the Atlantic Rainforest. (**a**) Percentage of identified metabolites per chemical class for each botanical family. (**b**) Percentage of unidentified features per EO. (**c**) Chemical complexity of EO samples represented as heatmap.

The identified metabolites were classified in monoterpenes (MT) (29%), sesquiterpenes (ST) (56%), phenylpropanoids (PP) (7.5%), benzenoids (BA) (3%), and ketones (MK) (3%) (Table 1, Figures S4–S6). The most frequent compound was α-pinene, followed by bicyclogermacrene, germacrene D and *trans*-caryophyllene (Table 1). The least frequent metabolites, present above trace levels, were geraniol and methyl-geranate (Table S1). Coastal locations (Pariquera-Açu and Ubatuba) exhibited higher botanical diversity of aromatic species, alongside the plateau sites in Campinas and Votuporanga (Figures S1 and S2).

Table 1. Main components (≥10%) of the essential oil extracted from plant species from the Atlantic rainforest. Plant species are presented within botanical families. Latitude and longitude coordinates are represented as decimal values. Essential oil yield is presented as dry weight (*w/w*) percentages. Complete chemical profile, literature, and calculated retention indices (RI) and experiment metadata are deposited at the National Metabolomics Repository under identifier ST000606.

Family/Species	Sample/Herbarium Code	Location (Coordinates, Elevation)	Yield (%)	Major Components (%)
Anacardiaceae				
Schinus terebinthifolius Raddi	R1772/IAC 47521	Ribeirão Preto (47°51′58.72″ S, 21°12′52.36″ W, 570 m)	0.26	α-phellandrene (23.2); α-pinene (18.2); β-phellandrene (16.8)
Annonaceae				
Annona dioica A.St.-Hil.	Lp06101603/IAC 47955	Votuporanga (50°3′55.60″ S, 20°27′41.20″ W, 463 m)	0.37	bicyclogermacrene (30.1); germacrene D (21.0); *trans*-caryophyllene (12.2)
Guatteria australis A.St.-Hil.	R1598/ IAC 46831	Ubatuba (45°7′39.30″ S, 23°25′18.60″ W, 26 m)	0.14	spathulenol (27.4); caryophyllene oxide (18.8)
Xylopia aromatica (Lam.) Mart.	Lp6101712/ IAC 47969	Votuporanga (50°3′34.99″ S, 20°27′15.20″ W, 4 m)	0.16	limonene (71.7)
Xylopia brasiliensis Spreng.	R1739/IAC 47266	Pariquera-Açu (47°52′48.76″ S, 24°36′48.42″ W, 25 m)	0.17	1,8-cineole (11.1); spathulenol (28.3)
Araceae				
Monstera cf. *adansonii* Schott	L52008/IAC 47079	Ubatuba (45°7′47.57″ S, 23°24′49.97″ W, 180 m)	0.14	β-phellandrene (36.7), α-pinene (17.2), 2 tridecanone (17.0)
Araliaceae				
Dendropanax cuneatus (DC.) Decne. & Planch.	C010/IAC 47099	Jundiai (46°55′40.69″ S, 23°6′42.70″ W, 770 m)	0.12	caryophyllene oxide (15.6), trans caryophyllene (13.2), β pinene (10.9)
Dendropanax cuneatus (DC.) Decne. & Planch.	Lp6101818/IAC 47975	Adamantina (51°9′6.80″ S, 21°39′47.01″ W, 380 m)	0.004	spathulenol (22.1), trans caryophyllene (18.4), bicyclogermacrene (15.7), δ-3-carene (12.5)
Dendropanax cuneatus (DC.) Decne. & Planch.	R1770/IAC 47519	Mococa (46°59′55.30″ S, 21°25′24.56″ W, 568 m)	0.21	bicyclogermacrene (32.8)
Asteraceae				
Baccharis dracunculifolia DC.	R1755/IAC 47282	Pariquera-Açu (46°59′44.79″ S, 24°37′15.32″ W, 25 m)	0.42	*trans*-nerolidol (30.5), β-copaen-4-α-ol (12.0), limonene (11.6)
Baccharis dracunculifolia DC.	R1773/IAC 47522	Ribeirão Preto (47°52′12.64″ S, 21°11′27.63″ W, 557 m)	0.54	*trans*-nerolidol (27.3), limonene (17.4)
Cyrtocymura scorpioides (Lam.) H. Rob.	C005/IAC 47097	Jundiai (46°55′40.69″ S, 23°6′42.70″ W, 770 m)	0.32	germacrene D (36.1), β-pinene (26.6)
Euphorbiacae				
Croton celtidifolius Baill.	Lp52912/IAC 29030	Monte Alegre do Sul (46°40′30.18″ S, 22°41′58.52″ W, 743 m)	0.16	cis-β-guaiene (15.8), germacrene D (11.7), *trans*-nerolidol (11.1)
Croton floribundus Spreng.	R4167/IAC 46976	Campinas (47°4′3.36″ S, 22°51′45.72″ W, 670 m)	0.09	*trans*-caryophyllene (21.9), caryophyllene oxide (13.7)
Croton urucurana Baill.	R1768/IAC 47517	Mococa (46°59′55.30″ S, 21°25′24.56″ W, 568 m)	0.11	bicyclogermagrene (43.4), germacrene D (24.0)
Croton warmingii Müll. Arg.	R4165/IAC 46974	Campinas (47°4′3.57″ S, 22°51′45.79″ W, 670 m)	0.15	bicyclogermacrene (17.4), *trans*-caryophyllene (16.8)

Family/Species	Sample/Herbarium Code	Location (Coordinates, Elevation)	Yield (%)	Major Components (%)
Lauraceae				
Aiouea sp.	R1736/IAC 47263	Pariquera-Açu (46°59′44.79″ S, 24°37′15.32″ W, 25 m)	0.28	α-phellandrene (24.5), *trans*-nerolidol (19.4)
Aniba viridis Mez	R1746/IAC 47273	Pariquera-Açu (47°52′48.76″ S, 24°36′48.42″ W, 25 m)	0.59	benzyl salicylate (23.4), benzyl benzoate (14.1)
Aniba viridis Mez	Lp51907/ AC 47071	Ubatuba (45°7′39.29″ S, 23°25′18.59″ W, 29 m)	0.42	linalool (11.1), *trans*-nerolidol (73.1)
Endlicheria paniculata (Spreng.) J.F.Macbr.	R1622/IAC 46801	Campinas (47°4′3.30″ S, 22°51′50.00″ W, 652 m)	0.05	α-selinene (34.5), spathulenol (15.3), γ-muurolene (11.8)
Nectandra megapotamica (Spreng.) Mez	Lp6101820/IAC 47986	Adamantina (51°9′7.50″ S, 21°39′47.00″ W, 349 m)	0.13	*cis*-β-guaiene (23.4), spathulenol (15.6)
Nectandra megapotamica (Spreng.) Mez	R1761/IAC 47510	Mococa (46°58′51.65″ S, 21°26′53.71″ W, 600 m)	0.27	α-pinene (27.1), β-pinene (28.2), bicyclogermagrene (16.4)
Nectandra megapotamica (Spreng.) Mez	R1774/IAC 47523	Ribeirão Preto (47°52′12.64″ S, 21°11′27.63″ W, 557 m)	0.10	oxygenated sesquiterpene (28.1), α-pinene (18.7), β-pinene (17.3)
Nectranda megapotamica (Spreng.) Mez	Lp052902/IAC 47084	Monte Alegre do Sul (46°39′57.60″ S, 22°42′15.12″ W, 778 m)	0.07	*cis*-β-guaiene (22.7), α-pinene (21.2), β-pinene (18.5)
Ocotea odorifera (Vell.) Rohwer	R1747/IAC 47274	Pariquera-Açu (47°52′48.76″ S, 24°36′48.42″ W, 25 m)	2.88	camphor (50.5), methyl-eugenol (20.0)
Meliaceae				
Trichilia elegans A.Juss.	Lp6101709/IAC 47961	Votuporanga (50°3′30.60″ S, 20°27′27.50″ W, 479 m)	0.28	germacrene B (44.3)
Myristicaceae				
Virola bicuhyba (Schott ex Spreng.) Warb.	Lp52003/IAC 49465	Ubatuba (45°7′20.86″ S, 23°24′34.06″ W, 50 m)	0.14	*cis*-β-guaiene (21.4), *trans*-caryophyllene (18.1)
Myrtaceae				
Calyptranthes lanceolata O.Berg	R1745/IAC 47272	Pariquera-Açu (47°52′48.76″ S, 24°36′48.42″ W, 25 m)	0.12	methyl eugenol (80.4)
Calyptranthes lucida Mart. ex DC.	Lp52009/IAC 47080	Ubatuba (45°7′39.29″ S, 23°25′18.59″ W, 30 m)	0.19	caryophyllene oxide (17.3), *trans*-caryophyllene (16.9), bicyclogermacrene (12.4)
Campomanesia guavirota (DC.) Kiaersk.	Lp6101822/IAC 47988	Adamantina (51°9′8.20″ S, 21°39′46.50″ W, 355 m)	0.33	α-pinene (12.3), linalool (11.8)
Eugenia moraviana O.Berg.	Lp06101816/ IAC 47973	Adamantina (51°9′6.19″ S, 21°39′47.80″ W, 373 m)	0.04	β-pinene (16.2), *trans*-caryophyllene (14.2), β elemene (11.0)
Eugenia neoverrucosa Sobral	R1626/IAC 46825	Campinas (47°4′0.30″ S, 22°51′52.03″ W, 650 m)	0.42	α-pinene (94.5)
Eugenia prasina O.Berg	Lp51905/IAC 47069	Ubatuba (45°7′39.29″ S, 23°25′18.59″ W, 29 m)	0.28	limonene (61.4), α-pinene (12.6)
Eugenia pyriformis Cambess.	C009/IAC 34660	Jundiai (46°55′40.69″ S, 23°6′42.69″ W, 770 m)	0.17	β-pinene (39.7), α-pinene (31.5)
Eugenia myrcianthes Nied.	Lp6101714/ IAC 47971	Votuporanga (50°3′30.10″ S, 20°27′20.99″ W, 488 m)	0.06	β-copaen-4-α-ol (31.7)
Marlierea exocoriata Mart.	Lp52006/IAC 47077	Ubatuba (45°7′8.70″ S, 23°24′32.52″ W, 38 m)	0.28	α-pinene (37.6), β-pinene (18.2), sabinene (11.2)
Myrcia spectabilis DC.	Lp051901/IAC 47045	Ubatuba (45°7′39.29″ S, 23°25′18.59″ W, 29 m)	0.41	*trans-cis*-farnesol (52.1), *cis-cis*-farnesol (41.1)
Myrcia splendens (Sw.) DC.	C007/IAC 37365	Jundiai (46°55′40.51″ S, 23°6′42.52″ W, 770 m)	0.21	α-pinene (28.1), germacrene D (20.9)
Myrcia tomentosa (Aubl.) DC.	Lp06101817/IAC 47974	Adamantina (51°9′6.40″ S, 21°39′46.70″ W, 370 m)	0.15	germacrene D (33.09%), *trans*-caryophyllene (20.41%),

Table 1. *Cont.*

Piperaceae				
Piper aduncum L.	Lp52911/IAC 47090	Monte Alegre do Sul (46°40′20.99″ S, 22°42′0.36″ W, 743 m)	0.51	spathulenol (10.6), valencene (9.7), α-pinene (6.4), asaricin (14.9), safrole (13.3)
Piper aduncum L.	Lp6101606/IAC 47958	Votuporanga (50°3′53.10″ S, 20°27′46.30″ W, 458 m)	1.52	asaricin (80.1), safrole (10.8)
Piper aduncum L.	Lp6101608/IAC 47960	Votuporanga (50°3′53.10″ S, 20°27′46.60″ W, 465 m)	1.55	asaricin (73.4), safrole (10.5)
Piper amalago L.	Lp06091202/IAC 32056	Campinas (47°4′2.30″ S, 22°51′53.70″ W, 664 m)	0.20	β-phellandrene (39.3), α-pinene (14.8), germacrene D (11.7)
Piper amalago L.	Lp06091206/IAC 46823	Campinas (50°3′53.09″ S, 20°27′46.30″ W, 458 m)	0.36	β-phellandrene (15.9), α-pinene (6.7), sabinene (6.3), bicyclogermagrene (20.8), spathulenol (9.1)
Piper amalago L.	R1763/IAC 47512	Mococa (46°58′51.65″ S, 21°26′53.71″ W, 600 m)	0.26	β-phellandrene (33.1), α-pinene (11.7), bicyclogermagrene (15.0)
Piper amalago L.	Lp6101821/IAC 47987	Adamantina (51°9′7.89″ S, 21°39′47.19″ W, 349 m)	0.23	β-phellandrene (12.3), sabinene (8.2), myrcene (6.8), bicyclogermagrene (19.4); γ-muurolene (5.9), spathulenol (5.6)
Piper amplum Kunth.	R1740/IAC 7267	Pariquera-Açu (47°52′48.76″ S, 24°36′48.42″ W, 25 m)	0.38	α-pinene (18.1), *cis*-β-ocimene (10.5), limonene (8.6), *trans*-caryophyllene (8.8), germacrene D (5,5)
Piper cernuum Vell.	L51904/IAC 7068	Ubatuba (45°7′39.04″ S, 23°25′18.52″ W, 30 m)	0.32	α-pinene (10.0), camphene (6.3), dihydro-β-agarofuran (28.7), 10-epi γ-eudesmol (13.5), 4-epi-*cis*-dihydro-agarofuran (10.8)
Piper cernuum Vell.	R1741/IAC 7268	Pariquera-Açu (47°52′48.76″ S, 24°36′48.42″ W, 25 m)	1.84	dihydro-β-agarofuran (33.8), 10-epi-γ-eudesmol (12.2), α-pinene (11.8), camphene (8.7)
Piper crassinervium Kunth.	R1764/IAC 7513	Mococa (46°59′55.30″ S, 21°25′24.56″ W, 568 m)	0.53	β-pinene (11.6), α-pinene (11.5), germacrene D (9,2), *trans*-caryophyllene (7.8), guaiol (5.5), bicyclogermacrene (5.1)
Piper gaudichaudianum Kunth.	R1738/IAC 7265	Pariquera-Açu (47°52′48.76″ S, 24°36′48.42″ W, 25 m)	0.16	*trans*-nerolidol (17.5), α-pinene (12.2), caryophyllene oxide (8.5), *trans*-caryophyllene (8.2), β-pinene (7.0), *trans*-β-guaiene (6.9)
Piper leptorum Kunth.	Lp052903/IAC 7085	Monte Alegre do Sul (46°39′53.99″ S, 22°42′13.32″ W, 778 m)	0.60	seychellene (34.7), caryophyllene oxide (12.5)
Piper rivinoides Kunth.	L52007/IAC 47078	Ubatuba (45°7′16.03″ S, 23°25′16.36″ W, 30 m)	0.63	α-pinene (73.2), β-pinene (5.2)
Piper solmsianum C.DC.	R1633/IAC 46832	Ubatuba (45°7′8.79″ S, 23°24′32.47″ W, 40 m)	0.39	δ-3-carene (66.9), myrcene (26.1), α-pinene (22.7), α-selinene (5.5)
Piper umbellatum (L.)	R4169/IAC 46978	Campinas (47°4′4.69″ S, 22°51′54.60″ W, 667 m)	0.18	germacrene D (55.8), bicyclogermacrene (11.8), *trans*-caryophyllene (6.3)
Piper xylosteoides (Kunth.) Steud.	L52004/IAC 47075	Ubatuba (45°7′37.64″ S, 23°25′16.03″ W, 30 m)	1.04	spathulenol (12.3), germacrene B (10.6), β-copaen-4-α-ol (9.4), *trans*-nerolidol (8.2), *trans*-β-guaiene; (7.8)
Rutaceae				
Esenbeckia febrifuga (A.St.-Hil.) A.Juss. ex Mart	Lp06091205/IAC 44591	Campinas (47°4′3.49″ S, 22°51′47.19″ W, 672 m)	0.14	caryophyllene oxide (46.7)
Helietta apiculata Benth.	Lp6101823/IAC 47989	Adamantina (51°9′12.19″ S, 21°39′41.90″ W, 365 m)	0.16	limonene (42.3)
Metrodorea nigra A.St.-Hil.	Lp06091204/IAC 46826	Campinas (47°4′0.52″ S, 22°51′52.24″ W, 650 m)	0.05	spathulenol (23.6), bicyclogermacrene (16.6), germacrene D (15.3)
Zanthoxylum petiolare A.St.-Hil. & Tul.	Lp6101710/IAC 47962	Votuporanga (50°3′29.80″ S, 20°27′27.40″ W, 479 m)	0.18	β-phellandrene (40.7), germacrene D (22.0)

Table 1. *Cont.*

Salicaceae				
Casearia sylvestris Sw.	R1643/IAC 46842	Ubatuba (45°7′26.44″ S, 23°24′37.87″ W, 50 m)	0.16	*trans*-β-guaiene (12.2), 1,10-di-epi-cubenol (12.1)
Sapindaceae				
Cupania vernalis Cambess.	L4160/IAC 46969	Campinas (47°4′1.63″ S, 22°51′47.24″ W, 670 m)	0.20	bicyclogermacrene (35.9), germacrene D (21.4), *trans*-caryophyllene (16.1)
Verbenaceae				
Aloysia virgata (Ruiz & Pav.) Juss.	C004/IAC 4614	Jundiai (46°55′40.45″ S, 23°6′42.48″ W, 770 m)	0.22	γ-muurolene (32.7), *trans*-β-guaiene (24.6)
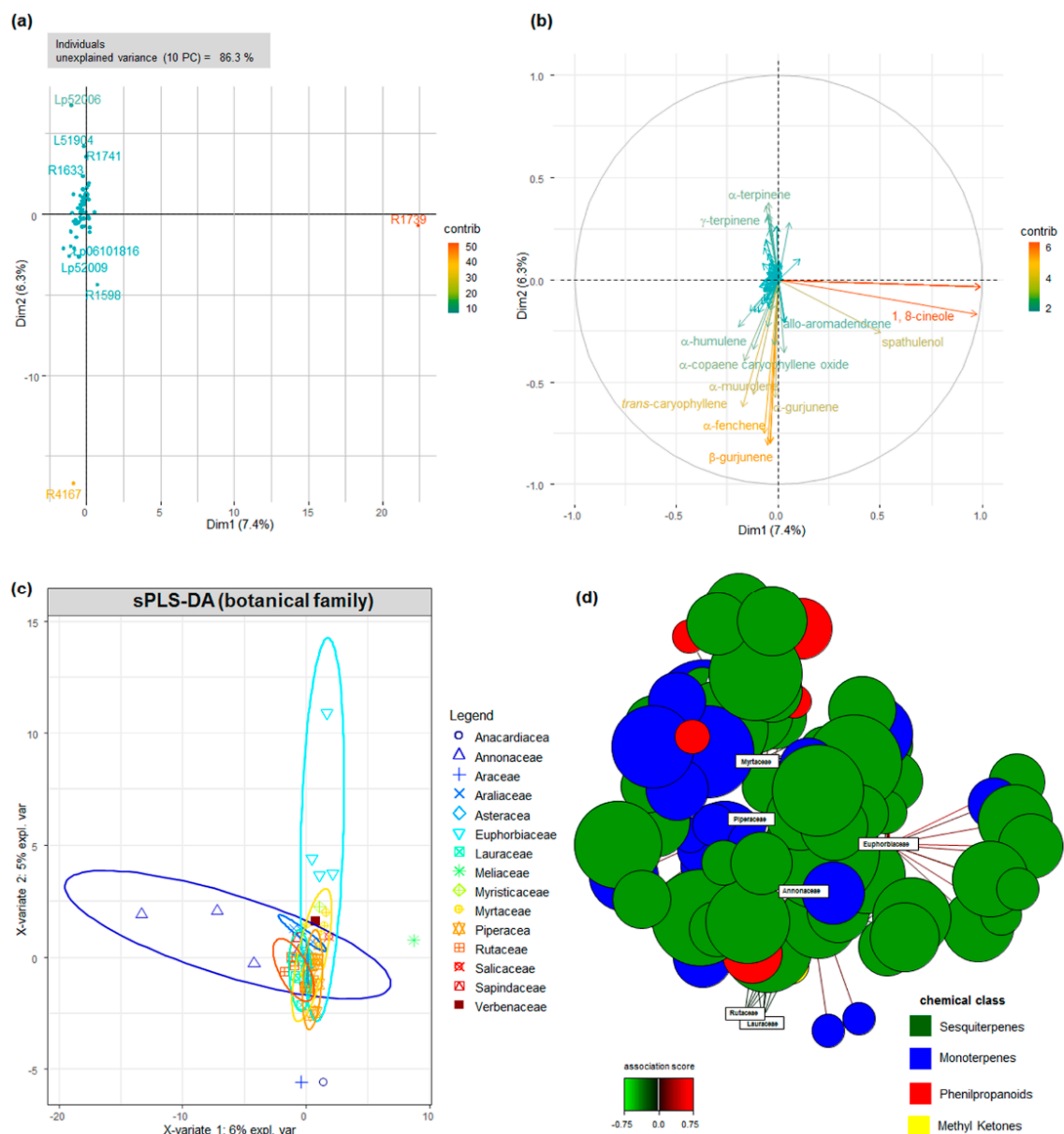
Figure 2. Multivariate analyses of the chemical composition of the Eos. Principal Component Analysis (PCA) of the chemical profile of the Eos, represented as (**a**) individual (EO sample) and

(**b**) variable (metabolite contents) contributions to the total variance. Contribution is a variable scaled version of the squared correlation between individual profiles/variables and component axes, represented as color scale. (**c**) Sparse Partial Least Square (sPLS) classification of the EO chemical profiles using the botanical families as discriminant (DA). Confidence ellipses at 95% were generated by 100 times bootstrapping and are color-coded. (**d**) Relevance network for metabolite and botanical family association at 75% threshold. Chemical classes and sPLS−DA association are represented by colors.

Multivariate analyses demonstrated that a large portion (86.3%) of the variation in the chemical composition of the EOs remained unexplained, even when considering ten principal components (Figures 2 and S4). A sparse Partial Least Squares Regression (sPLS) approach, using the botanical families as discriminant variables (DA, discriminant analysis), was employed to reduce data dimensionality (Figure 2). The supervised classification was not enough to clearly attribute the EOs' chemical composition to a given botanical family, as a wide range of metabolites was shared by the investigated individuals. We hypothesized that the unbalanced nature of the data—that is, the uneven frequency of botanical families among the locations—could have contributed to the poor prediction performance of the method. Therefore, simulations with balanced data were carried out (Figure S4), although they were not sufficient in increasing the classification performance of the method, suggesting the existence of high intra-specific chemical variation. The presence of family-specific compounds, such as geraniol in Annonaceae and *n*-octane in Euphorbiaceae, contributed to group separation.

The significant intra-group variation prompted us to investigate the chemical diversity among the individuals within the most frequent botanical families, applying Gaussian Mixture (GMM) modelling to the EO chemical profiles (Figures 3 and S6). The agreement between the model and the actual data classification, estimated by the adjusted Rand index (ARI), was higher than 65% for all botanical families, with the exception of Annonaceae (Figure 3). The best-fit GMM models demonstrated that quantitative differences in the chemical composition were the principal contributors to sample separation in Asteraceae and Piperaceae (model VII) and Myrtaceae and Lauraceae (model VEI), whereas, in Euphorbiaceae and Rutaceae (model VEV), qualitative chemical differences also contributed to the within-group covariance (Figures 3 and S6). The groups of chemical profiles in the EOs from Euphorbiaceae were highly variable, although the number of identified metabolites was approximately 1.7-fold smaller than in Myrtaceae and Piperaceae (Figures 3 and S6). The relative contribution of mono and sesquiterpenes to the best-fit GM model of the EOs' composition was investigated and the qualitative (n) and quantitative (q) differences between the contribution of mono and sesquiterpenes to the EO models is shown (Figure 3). Monoterpenes had the most significant contribution to the composition of Piperaceae EOs, and sesquiterpenes to Myrtaceae, whereas benzyl alcohols are relevant metabolites in Lauraceae (Figure 3).

The metabolic models were associated with the phylogenetic classification at the genus-level for Lauraceae and Myrtaceae, and at the species-level for Piperaceae; these were the botanical families with the highest agreement between the theoretical model and the observed chemical composition. In Lauraceae, relevance networks demonstrated that benzyl alcohols were strongly associated with the genus *Aniba*, whereas allo-aromadendrene, germacrene D and δ-cadinene were more intricately linked to *Nectandra*. Myrcene, *trans*-β-guaiene and bicyclogermacrene were relevant to the EO composition of all of the investigated genera in Myrtaceae, although the relevance network analyses differentiated the chemical profile of EOs from the genera *Myrcia*, *Eugenia* and *Calyptranthes* (Figure 3). Germancre B was relevant to *Myrcia* and *Eugenia*, whereas spathulenol and aromadendrene were significant to *Eugenia* and *Calyptranthes* (Figure 3). In Piperaceae, the metabolic profile of *Piper amalago* EOs was the most divergent, with contributions from α-phellandrene, β-bourbonene and 1-epi-cubenol, whereas several metabolites were shared with *P. aduncum* and *P. cernuum* EOs, although high camphene levels and the presence of dihydro-agarofuran sesquiterpenes were exclusive to the latter (Figure 3).
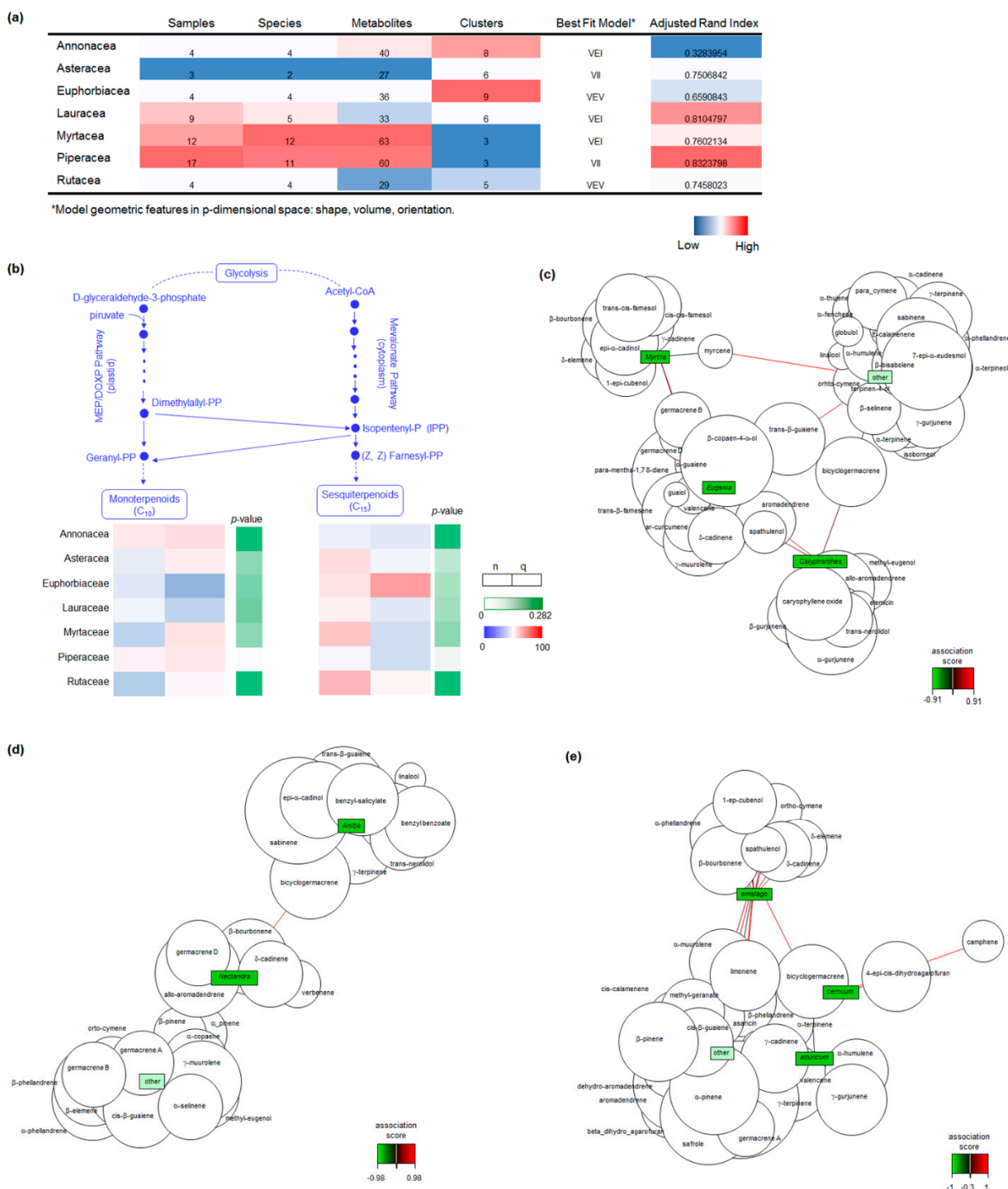
Figure 3. Chemical diversity of the EO composition within the most frequent botanical families. (**a**) Heatmap summary of GMMs of the EO chemical profiles of the most frequent botanical families. (**b**) Contribution of MT and ST metabolites to the qualitative (n) and quantitative (q) EO profile in the most frequently sampled aromatic families. Contribution is represented as a percentage of the composition in each botanical family. Relevance network for the identified metabolites in Myrtaceae (**c**) and Lauraceae (**d**) genera, and Piperaceae species (**e**). Association scores are represented as gradient for each network.

Simultaneous hierarchical clustering of the samples based on the PLS similarity matrix and relevance network analyses demonstrated that the significant associations were

caused by the presence or absence of specific metabolites, such as dihydro-agarofuran sesquiterpenes in *Piper cernuum* and benzyl alcohols in Lauraceae, and the absence of monoterpenes in Salicaceae and Sapindaceae (Figures 1–3). Among the distinct metabolite profiles, monoterpenes were not detected in Eos from *Casearea sylvestris* (Salicaceae) and *Cupania vernalis* (Sapindaceae).

2.2. Chemical Composition and Antimicrobial Activity

Certified tea tree (*Melaleuca alternifolia* (Maiden and Betche) Cheel) EO and four pathogenic bacteria were used to determine the working concentration for the growth inhibition assays (Figure 4). The dilution medium (mineral oil) did not interfere with bacterial growth, whereas, the broad-spectrum antibiotics (cefotaxime) prevented bacterial growth at 100 $\mu g.mL^{-1}$ (Figure 4). Concentrated EO completely inhibited *Staphylococcus epidermidis* growth and caused 35%, 51%, and 78% reduction in the propagation of *Escherichia coli*, *S. aureus*, and *Corynebacterium xerosis*, respectively (Figure 4). The growth inhibition of the frequent skin and mucous membrane colonizers *S. epidermidis* and *C. xerosis* were the most responsive to EO treatment (Figure 4), whereas *E. coli* and *S. aureus* were less affected by EO-induced growth inhibition (Figure 4). The tea tree EO concentration at 5% (v/v) allowed us to clearly identify growth inhibition for the investigated pathogens and was employed in the large-scale disk diffusion agar assays of the antimicrobial potential of the EOs from the rainforest species.
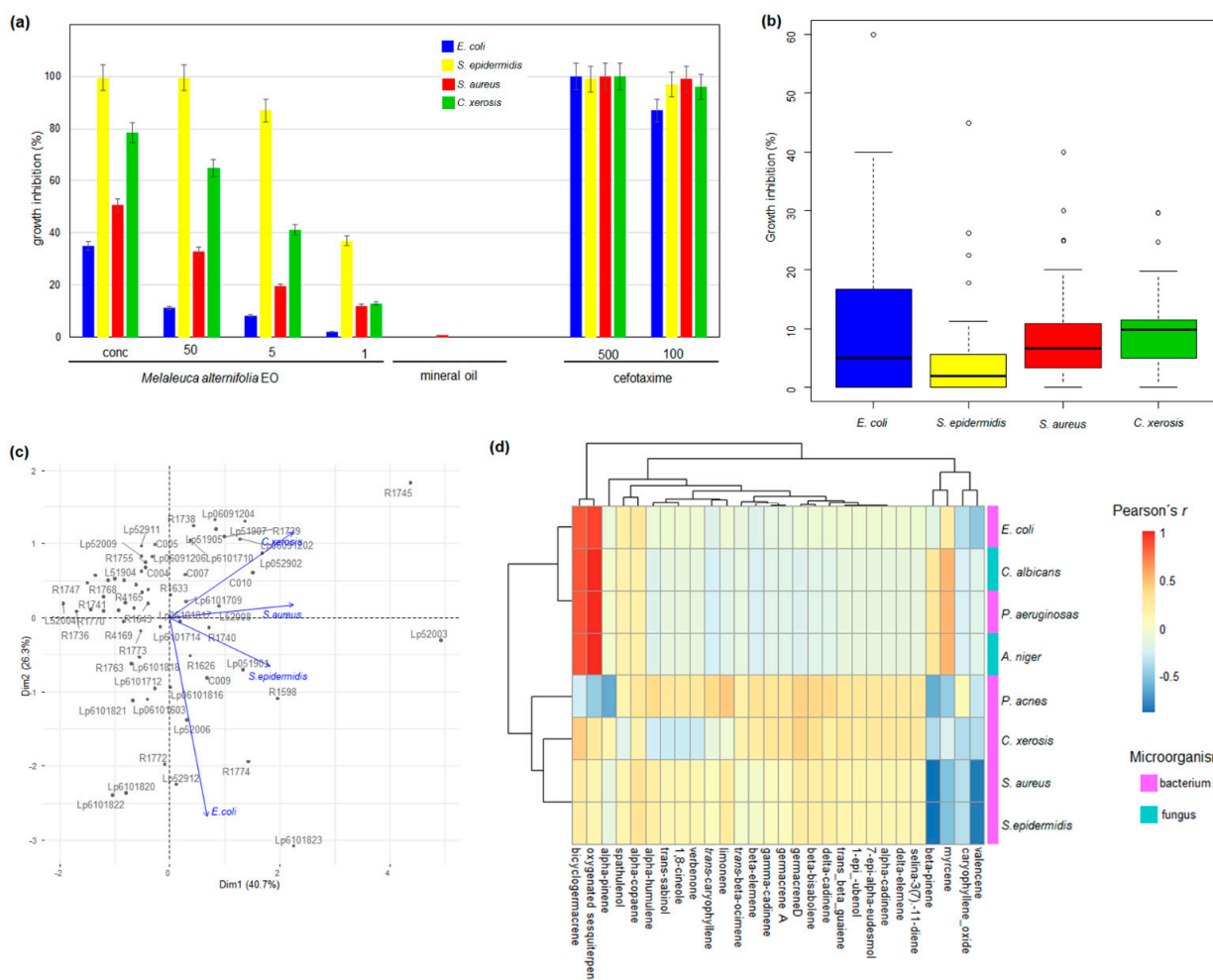
Figure 4. Biological activity of the EOs against pathogenic bacteria. (**a**) Dose-response estimation with positive and negative controls. (**b**) Growth inhibition amplitude for *E. coli*, *S. aureus*, *S. epidermidis* and

C. xerosis. (**c**) PCA biplot of bacterial growth inhibition by the individual EOs. (**d**) Heatmap representation of the correlation between EO composition and minimum inhibitory concentration for pathogenic fungi and bacteria. Pearson's correlation coefficients and their corresponding *p*-values are shown in Table S2.

Most of the EOs from the rainforest plants exhibited antibacterial activity, although individual EO antibacterial activity was highly variable (Figures 4 and S7). The maximum growth inhibition reached up to 60% against *E. coli* (Lp6101823, from *Helietta apiculata*, Rutaceae) (Figures 4 and S7). Other EOs also exhibited a high potential to impair bacterial growth, such as 45% against *S. epidermidis* (R1598, *Guatteria australis*, Annonaceae), 40% against *S. aureus* (R1745, *Calyptranthes lanceolata*, Myrtaceae) and 30% against *C. xerosis* (Lp52006, *Marlierea exocoriata*, Myrtaceae), representing 2.4-, 1.6-, 3.7- and 1.6-fold the inhibitory effect of certified *M. alternifolia* EO at the same concentration (Figures 4 and S7). The composition of the bacteria cell wall influenced the susceptibility to EO activity, contributing to approximately 41% of the variation in the PC analyses (Figure 4). The weight of the Gram-negative type of cell wall (*E. coli*) most strongly affected the first component, whereas the Gram-positive wall assembly (staphylococci and *C. xerosis*) exerted greater influence on the first component (Figure 4). The capacity to inhibit bacterial growth by the EO from native rainforest species was often higher or equivalent to certified *Melaleuca alternifolia* oil (Figure S7).

Ten EOs were selected for Minimum Inhibitory Concentration (MIC) assays against the previously investigated bacteria, plus the opportunistic pathogen *Pseudomonas aeruginosas*, the skin pathogen *Propionibacterium acnes*, the filamentous fungus *Aspergillus niger*, and the infective yeast *Candida albicans* (Table 2). The antibacterial activity was confirmed for concentrations as low as 0.124 μL/mL (Lp6101712, *Xylopia aromatica*, Annonaceae) against *C. xerosis*. *Aspergillus niger* and *Candida albicans* growth was impaired by all tested EOs at 0.5 μL/mL (Table 2). The correlation between the contents of the major metabolites in the essential oils and their antibacterial activity was investigated and are represented as a heatmap (Figure 4), and the statistical significance is presented in Table S2. The contents of oxygenated sesquiterpenes and bicyclogermacrene were positively correlated with the inhibition of *E. coli*, *C. albicans*, *P. aeruginosa*, and *A. niger* (Figure 4, Table S2). The myrcene contents were also positively correlated with the impairment of *C. albicans*, *P. aeruginosa*, and *A. niger* propagation, whereas the levels of limonene were positively correlated with the inhibition of *P. acnes* (Figure 4, Table S2). The contents of several major metabolites exhibited weak correlation with the antimicrobial activity against the tested pathogens (Figure 4).

To investigate the mechanism of action of the EOs against the tested pathogenic bacteria, we employed time-kill and cell component leakage assays (Figure 5). The bacterial kinetics of the EOs demonstrated that complete killing was reached 2 h after treatment at MIC with the EOs from Myrtaceae and Annonaceae against *E. coli*, Rutaceae, Myrtaceae, Salicaceae, Annonaceae, and Lauraceae against *S. epidermidis* and *S. aureus* (Figure 5). None of the tested EOs were able to induce the complete killing of *C. xerosis* at MIC, although most of them were able to reduce propagation up to 8 h after treatment (Figure 5). The investigated EOs induced cell component leakage at MIC for all of the tested bacterial species (Figure 5). The loss of nucleic acid and protein was detected, suggesting that EO treatment caused the formation of non-selective pores. The investigated EOs caused a greater loss of intracellular nucleic acids to *S. aureus* and *C. xerosis*, whereas protein leakage was higher in *E. coli*, *S. aureus*, and *C. xerosis* (Figure 5). As shown in the growth inhibition, MIC and time-kill assays, the most effective EOs for inducing bacterial intracellular component losses were from *Helietta apiculata* (Rutaceae, Lp6101823), *Xylopia brasiliensis* (Annonaceae, R1739), and *Nectandra megapotamica* (Lauraceae, R1774) (Figure 5). Correlation analyses demonstrated that growth inhibition was positively correlated to nucleic acid leakage for *E. coli* and, to a lesser extent, *S. epidermidis* (Figure 5, Table S3). In contrast, for *S. aureus*, growth impairment was positively associated with protein loss (Figure 5, Table S3).

Table 2. Minimum inhibitory concentrations (MIC) of selected EOs. Growth inhibition is presented in μg mL^{-1} in comparison to normalized positive and negative controls plus/minus standard errors.

Botanical Family		Microorganism							Filamentous Fungus	Yeast
		Bacteria								
Plant Species (Location)	Sample Code	*C. xerosis*	*E. coli*	*P. acnes*	*P. aeruginosa*	*S. aureus*	*S. epidermidis*	*A. niger*	*C. albicans*	
Annonaceae										
Xylopia brasiliensis (Pariquera-Açu)	R1739	50 ± 2.2	50 ± 2.5	25 ± 1.3	25 ± 1.1	50 ± 2.5	50 ± 2.4	25 ± 1.2	25 ± 1.3	
Xylopia aromatica (Votuporanga)	Lp6101712	6.2 ± 0.1	25 ± 1.2	12.5 ± 0.6	25 ± 1.2	25 ± 1.3	25 ± 1.2	25 ± 1.2	25 ± 1.2	
Lauraceae										
Nectandra megapotamica (Ribeirão Preto)	R1774	6.2 ± 0.1	12.5 ± 0.6	25 ± 1.2	25 ± 1.1	25 ± 1.2	25 ± 1.2	25 ± 1.1	25 ± 1.2	
Myrtaceae										
Eugenia neoverrucosa (Campinas)	R1626	6.2 ± 0.1	25 ± 1.2	25 ±1.2	25 ± 1.2	25 ± 1.1	25 ± 1.2	25 ± 1.2	25 ± 1.2	
Eugenia prasina (Ubatuba)	Lp51905	12.5 ± 0.6	25 ± 1.2	25 ± 1.2	12.5 ± 0.6	25 ± 1.1	25 ± 1.1	25 ± 1.2	25 ± 1.2	
Eugenia pyriformis (Jundiai)	C009	50 ± 2.3	50 ± 2.2	25 ± 1.2	25 ± 1.2	50 ± 2.2	50 ± 2.3	25 ± 1.2	25 ± 1.2	
Myrcia splendens (Jundiai)	C007	12.5 ± 0.6	25 ± 1.2	12.5 ± 0.6	25 ± 1.2	25 ± 1.2	25 ± 1.2	25 ± 1.2	25 ± 1.2	
Rutaceae										
Helietta apiculata (Adamantina)	Lp6101823	12.5 ± 0.6	25 ± 1.2	12.5 ± 0.6	25 ± 1.2	25 ± 1.2	25 ± 1.2	25 ± 1.2	25 ± 1.2	
Salicaceae										
Casearia sylvestris (Ubatuba)	R1643	12.5 ± 0.6	25 ± 1.2	12.5 ± 0.5	25 ± 1.2	25 ± 1.3	25 ± 1.2	25 ± 1.2	25 ± 1.2	

The performance of the EOs from the rainforest plants against pathogenic microorganisms prompted us to investigate the pharmacokinetic properties of their major components using in silico tools (Figure 6). The Absorption, Distribution, Metabolism, and Excretion (ADME) properties, such as the number of heavy atoms, number of aromatic heavy atoms, fraction Csp3, number of rotatable bonds, H-bond acceptors and donors, molecule predicted solubility, absorption, CYP inhibition prediction, violation of Lipinski, Ghose, Veber, Egan, and Muegge parameters, bioavailability score, PAINS and Brenk alerts, Lead-likeness violations and predicted synthetic accessibility, were investigated for 27 major EO components (Table S4). Most of the metabolites present in the EOs exhibited adequate drug-like predicted properties, individually (Table S4), indicating their medicinal potential alone or in combination with other metabolites found in EOs. The complexity of EO composition was not reflected in the number of predicted macromolecular targets, as EOs with a greater number of major metabolites, such as R1643 from *Casearia sylvestris* (Salicaceae), exhibited a similar number of predicted targets than those with a simpler composition, such as Lp6101712, from *Xylopia aromatica* (Annonaceae), where limonene represented more than 71% of the EO metabolites (Table 1, Figure 6). The EOs from Annonaceae (R1739 and Lp6101712, from *Xylopia brasiliensis* and *X. aromatica*) had the most divergent number of predicted macromolecular targets, with 12 exclusive categories including the classes Eraser, Primary active transporter, Other nuclear protein, Lyase, Reader, Transferase, and Ligase (Figure 6, Table S5). The majority of the EO metabolites displayed the predicted macromolecular targets of pharmacological interest (Figure 6).
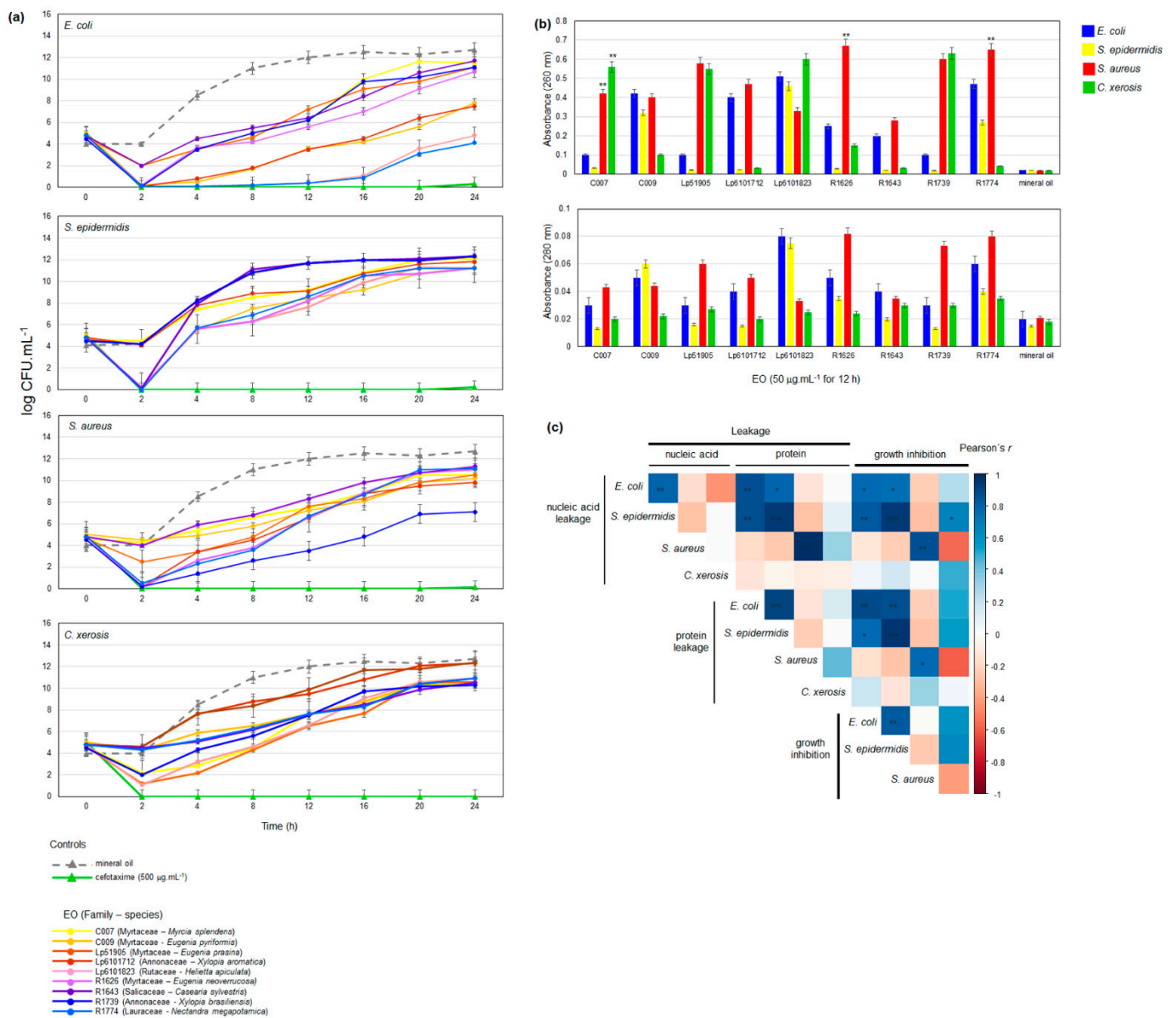
Figure 5. Eos antibacterial activity mode of action investigation. (**a**) Time-kill kinetics against pathogenic bacteria. Positive and negative control curves are represented by triangle and EO by circle markers and colors. (**b**) Cell component leakage assay, for nucleic acid (absorbance at 260 nm) and protein (absorbance at 280 nm). (**c**) Heatmap representation of the correlation between cell component leakage and inhibition of bacterial growth. Significance levels are represented as: '***' 0.001, '**' 0.01, and '*' 0.1. Pearson's correlation coefficients and their corresponding *p*-values are shown in Table S3.
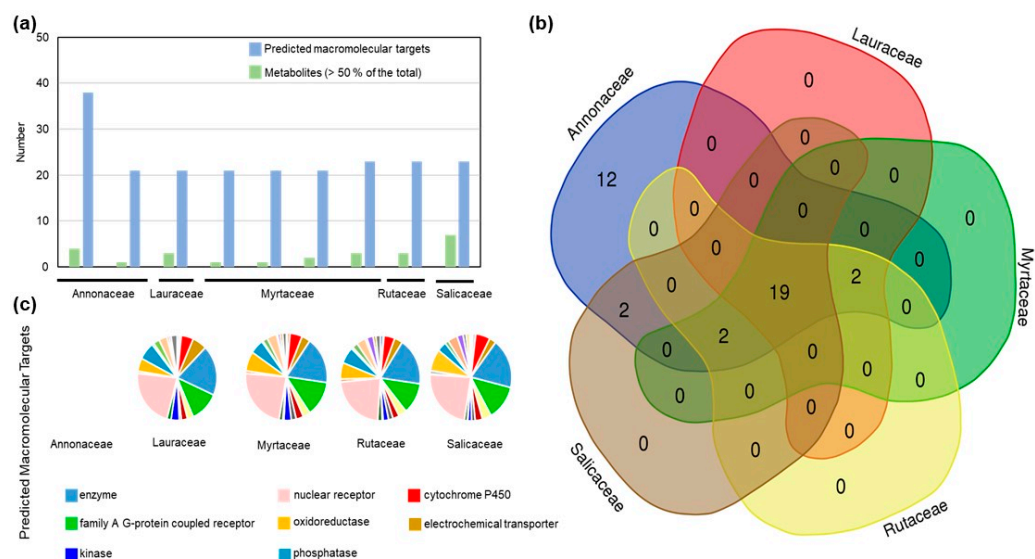
Figure 6. Pharmacokinetics properties of the EOs. (**a**) Number of metabolites and predicted macromolecular targets in the EOs per botanical family. Venn diagram (**b**) and pie chart (**c**) of the predicted ADME class targets of the metabolites in the EOs per botanical family. The complete list of predicted targets aggregated for each botanical family is shown in Table S5.

3. Discussion

Essential oils are among the most studied plant extracts for treating infectious diseases and controlling microbial growth, primarily due to the antimicrobial activity of terpenes, phenylpropanoids, and flavonoids [3,8,10,13]. The antimicrobial mechanisms and molecular target sites of the metabolites in plant EOs are distinct from those of traditional antimicrobial agents, making them important elements in combinatorial strategies against infectious microorganisms [10,13]. To address the knowledge gap in the antimicrobial potential of EOs from the highly diverse rainforest, we have botanically classified and chemically characterized the EOs of plant species from nine areas. The isolated EOS were further characterized for antimicrobial and biocidal activity through agar diffusion assays, minimum inhibitory concentration, time-kill, and cell-component leakage assays. Subsequently, we investigated the pharmacokinetic properties of the EO compounds using in silico tools.

The chemical profiling of the EOs confirmed the roles of inter- and intra-specific genetic variation and environmental conditions in determining the metabolic diversity of rainforest plants [12]. In the EOs from 50 species, we identified 113 distinct metabolites. In contrast, the chemical characterization of the EOs from 48 Lamiaceae species, including basil, rosemary, lavender, and peppermint, revealed 83 compounds [14], although a review work demonstrated that 150 compounds have been identified in EOs from *Rosmarinus officinalis* L. alone [15]. In two commercial cultivars of lavender and lavandin, the chemical characterization revealed 50 compounds in the EOs [16]. Fruits from the native African *Xylopia aethiopica* produced EOs with 14 identified metabolites in GC-MS analyses [17]. Employing high-speed countercurrent GC, 15 compounds were identified in the EOs from the rainforest native *Piper mollicomum* [18,19]. The genus *Piper* is widely distributed throughout the tropics and more than 250 compounds were identified in the EOs from its species [20]. Thus, the resolution of the chemical profiles identified in our study are comparable to those reported for EOs from cultivated and wild aromatic plants. As observed in the cultivated and model plants [4,21,22], the investigated rainforest species also exhibited high intra-specific chemical variation, although family-specific compounds were also present, such as geraniol in Annonaceae and η-octane in Euphorbiaceae. Among the distinct metabolite profiles, monoterpenes were not detected in the EOs from *Casearea sylvestris* (Salicacea) and *Cupania vernalis* (Sapindaceae). Although known as a sesquiterpene-rich species, monoter-

penes have been identified in the Eos of *C. sylvestris* [23,24]. The metabolite profile of *C. vernalis* remains poorly characterized, although several extracts were demonstrated to exhibit biological activity [25]. The significant intra-group variation in their EO chemical composition was further investigated by applying Gaussian Mixture (GM) modelling. GM clustering has a probabilistic nature and does not assume independence between adjacent measures, making it suitable to study metabolites synthesized by the same or shared pathways [26,27]. The chemical profiles of the EOs from Euphorbiacea were highly variable, mostly due to quantitative differences [28,29], as shown for the *Croton* species. The relative contribution of the chemical classes to EO composition was variable, with a predominance of monoterpenes in Piperaceae, sesquiterpenes in Myrtaceae, and benzyl alcohols in Lauraceae. The principal biosynthetic pathway of monoterpenes in plants is the MEP/DOPX localized in plastids, whereas sesquiterpenes are synthesized from precursors of the mevalonate pathway in the cytosol, although interaction between the pathways are known [6,30]. The scaffold of sesquiterpenes in plants is catalyzed by Terpene Synthases (TPS), which produce structurally distinct acyclic, mono-, bi- and tri-cyclic ST from common prenyl diphosphate precursors [31]. Genomic studies have associated the transcription of TPS genes to the ST profile in Myrtaceae [32,33], Lauraceae [34,35], and Piperaceae [36]. The shikimate pathway and phenylalanine biosynthesis from chorismate produce volatile benzenoids, although the information is from plant reproductive structures and does not include Lauraceae [37]. The extensive intra-specific chemical diversity of aromatic and medicinal plant species is challenging for several steps required for their widespread use, including yield, cultivation, and extraction conditions [38]. Similarly, the chemical variation within a given species reinforces the need for genetic and chemical profiling of the individuals of interest [39,40].

The antibacterial activity of the isolated EOs was initially investigated by agar diffusion assays against the frequent skin and mucous membrane colonizers *Staphylococcus epidermidis* and *Corynebacterium xerosis* [41,42], as well as the leading bacterial pathogens in healthcare-associated infections, *Escherichia coli* and *S. aureus* [43]. *S. aureus*, along with *Enterococcus* spp., *Klebsiella* spp., *Acinetobacter baumannii*, *Pseudomonas aeruginosa*, and *Enterobacter* spp., constitutes the "ESKAPE" group of multi-drug resistant pathogens [8]. Antibacterial activity was observed for most of the EOs from the rainforest, at higher levels than that observed for certified *Melaleuca alternifolia* oil. The composition of the bacterial cell wall determined the susceptibility to EO activity, as shown previously [8,13,44]. The antimicrobial activity of the EOs was more variable for the Gram-negative type of cell wall (*E. coli*), whereas the Gram-positive wall assembly (staphylococci and *C. xerosis*), consisting of glycopolymers and proteins, associated with teichoic acids, polysaccharides, and proteins, was less affected by the investigated EOs. These observations agree with the roles of EO compounds in the destabilization of bacterial cellular architecture, due to the disruption of the membrane's integrity, leading to the impairment of cellular activities, such as energy production and membrane transport, and the loss of cellular components and ions [44]. These observations suggest a potential harmful effect of the EOs to non-target cells; however, their use in cosmetics and household products has been shown to be safe and able to impair bacterial growth. Moreover, combinatory therapeutic alternatives and topic applications may contribute to reducing mutagenic, cyto- and geno-toxic, effects.

The metabolite profile and synergistic interactions among the compounds are critical to EO antimicrobial activity [9,44,45]. The reactivity of the metabolites is associated with their antimicrobial potential, as oxygenate and cyclic molecules have higher inhibitory effect on microorganisms than hydrocarbons in mixtures or isolated [9,44]. The interactions among the EO metabolites responsible for antimicrobial properties may lead to the enhanced activity or attenuation of negative effects [44,45]. Moreover, the distinct molecular structure of the EO compounds allow them to display a broader spectrum of action in comparison to isolated substances [44,45].

The ability to inhibit bacterial growth allowed us to choose ten EOs for the MIC assays, using the "ESKAPE" opportunistic pathogen *Pseudomonas aeruginosas*, the skin pathogen

Propionibacterium acnes, in addition to the previously investigated bacteria, along with the filamentous fungus *Aspergillus niger* and the infectious yeast *Candida albicans*. The MIC assays confirmed the antimicrobial potential of the EOs, at levels similar to those reported for oils from commercially cultivated plants, such as rosemary and thyme [8,46]. The contents of oxygenated sesquiterpenes, bicyclogermacrene and myrcene were positively correlated to microbial growth inhibition. Recent studies have demonstrated that phenolic terpenoids display higher antibacterial activity against Gram-negative and Gram-positive bacteria [47]. The author observed that treatment with phenolic terpenoids carvacrol and thymol immediately caused the loss of cell membrane integrity and ion leakage. The importance of the hydroxyl group of the phenol moiety was also highlighted in the work, as O-methyl derivatives and benzylic partners were shown to be ineffective [47]. These observations agree with the correlation results in our study. However, the contents of several major metabolites exhibit weak correlation with the antimicrobial activity against the tested pathogens, indicating a synergistic effect among the EO metabolites [8,48]. The combination of carvacrol, thymol, eugenol and nootkatone was shown to exert the bacteriostatic and bactericidal effects, even at low concentrations, highlighting the complementary effect of the different compounds in the EO [48].

The mechanism of the EOs' action against the pathogenic bacteria was investigated by time-kill and cell component leakage assays. The kill kinetics assays confirmed fast bactericidal action, as shown previously for EOs from cultivated *Origanum vulgare* [49–51] and tea tree [52]. However, viable cells were detectable at later stages for all treatments, including broad-spectrum commercial antibiotics. Treatment with the EOs at MIC induced the loss of nucleic acid and protein, suggesting the formation of non-selective pores. The time-kill and cell component leakage results agree with the proposed modes of action of EOs against bacterial pathogens, functioning to destabilize the cell structure, then leading to perturbations in the integrity of the membrane system, disrupting several cellular activities, such as energy production and cellular transport [44,51,52]. The disruption of bacterial membranes by EOs appears to be non-selective and to induce a general leakage of the cellular components and the loss of ions [44], although our indirect evidence from correlation analyses indicate that EO-induced nucleic acid leakage is more prejudicial to *E. coli* and *S. epidermidis* than to *S. aureus* and *C. xerosis*.

The use of plant-derived compounds in pharmaceutical applications is dependent on their pharmacokinetic properties, Absorption, Distribution, Metabolism, and Excretion (ADME), which is, in turn, dependent on the chemical structure of its individual components [38,45]. In silico predictive tools demonstrated that the individual metabolites found in the investigated EOs exhibit adequate drug-like predicted properties. Moreover, the predicted macromolecular targets of the individual metabolites include several classes of pharmacological interest, such as kinases, phosphatases, nuclear receptors and cytochrome P450. The complexity of EO composition did not reflect the number of predicted macromolecular targets, but was associated with the molecular structure of its metabolites. The EOs isolated from *Xylopia brasiliensis* and *X. aromatica* (Annonaceae) were predicted to have 12 exclusive classes of macromolecular targets. The identification of macromolecular targets of pharmacological interest suggests that the EOs may have further applications in drug composition.

4. Materials and Methods

4.1. Biological Samples Collection and Environmental Data

Aromatic plants were sampled from nine Atlantic rainforest reserves at experimental stations managed by Agência Paulista de Tecnologia dos Agronegócios (APTA) (Figure S1) for botanical identification, herbarium mounts and chemical analyses. The families of aromatic plants were selected based on their reported biological activity, aroma emission and plant distribution (Table S6).

Plants were tagged and the coordinate reference determined by Global Positioning System (GPS). Voucher specimens were deposited at the Herbarium of Instituto Agronômico

(IAC) (http://herbario.iac.sp.gov.br/ (accessed on 7 December 2022)), under the given accession numbers (Table 1) and classified according to the list of species of Brazilian flora [53].

4.2. Essential Oil Extraction

As this was a study of native aromatic plants, in order to preserve the species, only the vegetative aerial parts were sampled, and the essential oils were extracted exclusively from the leaves. The leaves were detached from the stalks and air-dried at room temperature, in the absence of direct light. The EOs were extracted from 54 to 1870 g of dry material, depending on availability, for two hours, by hydrodistillation in Clevenger-type apparatus, according to the Brazilian Pharmacopeia [54]. The oils were stored in hermetically closed vials at $-20\,^{\circ}C$ before chemical profiling. Yield is represented as oil weight (g) per dry material weight (g).

4.3. Chemical Characterization and Quantification of Essential Oils

The chemical composition of the EOs was determined by gas chromatography coupled with mass spectrometry (GC-MS Shimadzu, model QP-5000, Kyoto, Japan), equipped with fused silica capillary column OV—5 (30 m $\times$ 0.25 mm $\times$ 0.25 μm, Ohio Valley Specialty Chemical, Inc., Marietta, OH, USA), using Helium as a carrier gas (1.0 mL min^{-1}); operating with injector temperature of 220 $^{\circ}C$, the transfer line was kept at 230 $^{\circ}C$, a split ratio of 1:20, and an injection volume of 1.0 μL of EO solution (1 μL essential oil/1 mL ethyl-acetate, chromatography grade) was employed using the auto-sampler. The GC was operated under temperature-programmed conditions, between 60 $^{\circ}C$ and 240 $^{\circ}C$, by 3 $^{\circ}C$ per min^{-1}. The MS data were acquired in the full-scan mode (m/z 40–450) using the electron ionization (EI), with an ionization voltage of 70 eV. The quantitative analyses were performed by the area normalization method, as triplicate readings, by gas chromatography with a flame ionization detector (GC–FID Shimadzu, model GC-2010). The analyses were conducted under the same oven operating conditions used in GC-MS. The metabolites were identified by the comparative analyses of mass spectra against the system database (Nist 62.lib) and by retention indices [55] obtained from the injection of a mixture of *n*-alkanes (C_9H_{20}-$C_{25}H_{52}$, Sigma Aldrich, St. Louis, MO, USA, 99%), applying the equation described by Van den Dool and Kratz [56]. The metabolites were considered as major components when representing $\geq$ 10%. The complete chemical data and their associated metadata are deposited at the National Metabolomics Repository (https://www.metabolomicsworkbench.org/data/index.php (accessed on 7 December 2022)), under identifier ST000606.

4.4. Microbial Strains

Certified cultures of *Escherichia coli* (ATCC 8739), *Staphylococcus aureus* (ATCC 6538), *S. epidermidis* (ATCC 12228), *Corynebacterium xerosis* (ATCC 373), *Pseudomonas aeruginosa* (ATCC 9027), *Propionibacterium acnes* (ATCC 11827), *Candida albicans* (ATCC 10231) and *Aspergillus niger* (ATCC 16404) were provided by Instituto Adolfo Lutz (São Paulo, SP, Brazil). Bacterial cultures were started from isolated colonies, and fungal cultures, from single spores. The bacterial concentration was estimated based on spectrophotometric absorbance readings at 600 nm for *E. coli* and *P. aeruginosa*, 490 nm for *S. epidermidis* and *P. aeruginosa*, 530 nm for *S. aureus* and 578 nm for *C. xerosis*, for McFarland turbidity standard.

4.5. Estimation of EO Effective Concentration for Antimicrobial Activity

Certified commercial essential oil from tea tree (*Melaleuca alternifolia*, (Maiden and Betche) Cheel) was used to estimate the effective concentration for antimicrobial activity analyses. Serial EO dilutions were prepared in sterile mineral oil in a volume/volume basis up to a total of 200 μL. The bacterial cultures were diluted to 0.5 McFarland standards in Tryptone Soy Broth (TSB, Oxoid Thermo Scientific, Loughborough, UK) liquid medium and supplemented with serial dilutions of tea tree EO. The suspensions were incubated

at 37 ± 2 °C, with continuous agitation at 200 rpm for 36 h. Absorbance readings of 1 mL aliquots were used to calculate growth inhibition, in comparison to the negative control consisting of TSB supplemented with 200 μL of sterile mineral oil. Broad-spectrum antibiotics cefotaxime (Merck/Sigma-Aldrich, St. Louis, MO, USA) was used as the positive control at 500 μg mL^{-1}. The minimum estimated concentration of tea tree EO impairing bacterial growth (5% *v/v*) was used in further analyses with the 63 EO samples from the rainforest plants.

4.6. Antimicrobial Activity Analyses

Antibacterial activity was investigated by growth inhibition in agar diffusion assays for four bacterial species, and minimum inhibitory concentration (MIC) analyses were used for the bacteria and fungi. For both assays, bacterial suspensions were initiated from inoculating a single colony to 20 mL of TSB (Oxoid ThermoScientific, UK) and grown to saturation at 28 °C, for approximately 14 h, with 200 rpm shaking. An aliquot of 1 mL was transferred to 20 mL of fresh medium, and the procedure was repeated twice. Bacterial concentrations on the final saturated suspension were corrected to 10^{-8} colony forming unit (CFU) per mL^{-1} by absorbance readings at 600 nm for *E. coli* and *P. aeruginosa*, 490 nm for *S. epidermidis*, 530 nm for *S. aureus*, and 578 nm for *C. xerosis*, to prepare the adjusted inocula. For the agar diffusion assays, 1 mL of the saturated bacterial culture was added to 400 mL of cooled, fused Nutrient Agar medium (Oxoid ThermoScientific, UK) and supplemented with 1.5 mL of a 2% (*w/v*) solution of 2,3,5-triphenyl tetrazolium chloride (TTC). The mixture was poured into 9 mm sterile Petri dishes containing five, evenly distributed, sterile aluminum rings with a diameter of 6 mm. The rings were removed from the solidified medium and 300 μL of essential oil at 5% (*w/v*) in sterile mineral oil were added to the wells. The plates were incubated horizontally in a bacteriological oven at 37 ± 2 °C for 48 h, and after growth, the abaxial surface of the plates was digitalized, and inhibition halos were measure in ImageJ2 [57], by applying the *Measure* function from the *Analyze* menu. *Melaleuca* EO (absolute and 5% (*w/v*)) and cefotaxime (500 μg mL^{-1}) and the sterile mineral oils were used as positive and negative controls, respectively.

The minimal inhibitory concentration (MIC) was determined for nine EO samples using the broth microdilution method, according to CLSI guidelines [58]. The EO samples were diluted at 1% (*v/v*) in propylene glycol and submitted to serial dilutions (1:2) in sterile 96-well microplates containing 100 μL of TBS. Actively growing microorganisms from the adjusted cultures were diluted an optical density of 0.5 McFarland, equivalent to 2×10^6 colony forming units (CFU).mL^{-1} in TSB and 20 μL of the diluted culture were added to the wells to give a final inoculum of approximately 1×10^5 CFU.mL^{-1}. The microplates were incubated at 37 ± 2 °C for 48 h for bacteria or at 25 ± 2 °C for 72 h for fungal and yeast cultures. The MIC values were determined by monitoring the microorganism growth at the adequate optical density in the presence of multiple concentrations of the EOs. After the incubation period, the plates were scanned for turbidity in an Enzyme Linked Immunosorbent Assay (ELISA) reader. The negative controls consisted of TS broth and TS broth inoculated with propylene glycol, without EO. The MIC values are presented as the smallest concentration inhibiting microorganism growth in μg of EO per mL ± standard error.

4.7. Mode of Action Investigations

The antimicrobial mode of action of the nine selected EO samples was investigated for bactericidal activity and cell-component leakage analyses, as described in the Clinical and Laboratory Standards Institute M26A approved guidelines [58]. In the time-kill kinetics analyses, bacterial suspensions were grown in the TSBup to mid logarithmic phase, as described. Dilutions corresponding to 0.5 McFarland (~10^{-8} CFU mL^{-1}) were prepared in 10 mM PBS buffer at pH 7.4, and added to 20 mL TBS supplemented with 200 μL of EO at 50 μg mL^{-1}. Aliquots were taken at 0, 2, 4, 8, 12, 16, 20 and 24 h after inoculation and plated on TBS agar in triplicate. The plates were incubated overnight at 37 °C and the

bacterial colonies were counted. Cefotaxime and sterile mineral oil were used as positive and negative control, respectively.

The membrane permeability was investigated by cell-component leakage analyses, as described [59]. Bacterial suspensions at 0.5 McFarland turbidity ($\sim 10^8$ CFU mL^{-1}) were supplemented with 50 μg.mL^{-1} of EO, incubated at 37 °C with continuous agitation at 200 rpm for 12 h. Intact bacterial cells were precipitated by centrifugation at $9000 \times g$ for 10 min at 4 °C and the contents of extracellular nucleic acids and proteins were determined by absorbance readings of the supernatant at 260 nm and 280 nm, respectively.

4.8. EO Metabolite Physicochemical and Pharmacokinetic Properties

The major metabolites of the nine selected EOs were compiled, their canonical Simplified Molecular-Input Line-Entry System (SMILES) format were obtained and their molecular structures were used for in silico prediction of physicochemical, drug-likeness, pharmacokinetics, medicinal chemistry friendliness, and Absorption, Distribution, Metabolism and Excretion (ADME) properties, using the SwissADME algorithm [60]. Macromolecular target prediction was carried out using SwissTargetPrediction algorithm [60].

4.9. Data Analyses

Data preprocessing and analyses were performed using R [61]. The oil yield and chemical composition data were averaged, centered and Pareto-scaled. Supervised and unsupervised multivariate and modelling analyses were performed using mixOmics [62] and mclust [63]. The best fitting model for the chemical data was determined by Bayesian Information Criterion (BIC) and Integrated Complete-data Likelihood (ICL) and include the number of mixing components and covariance parametrization [63]. For each component, several parameters were computed, including the mean and the variance, as well as the density mixing probabilities and the total number of gene pairs. Pearson coefficients and correlation significance levels were obtained in Hmisc [64] and represented graphically using corrplot [65].

This article does not contain any studies with human and/or animal participants performed by any of the authors. The sampling of native plants for research purposes is authorized under permit AD0077F, issued by Sistema Nacional de Gestão do Patrimônio Genético e do Conhecimento Tradicional Associado (SisGen).

The metabolomics and metadata reported in this paper are available at Metabolomics Workbench (https://www.metabolomicsworkbench.org/data/index.php (accessed on 7 December 2022)), study identifier ST000606.

5. Conclusions

In the current study, we have investigated the antimicrobial potential of the EOs from aromatic plants from the Atlantic rainforest. EOs were isolated from 63 plants, comprising 15 botanical families. The EOs' chemical compositions consisted of 113 distinct metabolites, primarily mono and sesquiterpenes. Multivariate analyses detected extensive inter- and intra-specific variation in the chemical profiles of the EOs. These observations were confirmed by Gaussian models, which revealed distinct contributions of quantitative and qualitative differences within the botanical families. Relevance networks allowed the identification of genera-specific metabolites for Lauraceae and Myrtaceae, and species-specific profiles for Piperaceae. The EOs exhibited extensive antimicrobial potential against pathogenic bacteria and fungi, and the biocidal capacity was demonstrated for a selected group of EOs. The EOs' treatment of pathogenic bacteria promoted a fast reduction in the number of viable, colony-forming cells, and caused the loss of cellular components. In silico analyses demonstrated that the major metabolites in the EOs have adequate pharmacokinetic properties and interesting predicted pharmacological targets. Our results may contribute to the development of new plant-based antimicrobial products.

Supplementary Materials: The following supporting information can be downloaded at: https://www.mdpi.com/article/10.3390/antibiotics11121844/s1, Figure S1: Biogeographically defined domain of the Atlantic rainforest in Brazil and plant collection sites in the state of São Paulo; Figure S2: Distribution of plants from botanical families in the Rainforest locations; Figure S3: Essential oil yield per botanical family, location, season, and plant growth habit; Figure S4: PCA of the chemical composition of the EOs; Figure S5: Performance of sPLS-DA of the EO chemical composition using botanical families as discriminant; Figure S6: Bayesian Information Criterion (BIC) and Gaussian Mixture Model (GMM) classification of the metabolic profile of EOs; Figure S7: Growth inhibition (%) of the EOs in agar diffusion assays; Table S1: Chemical composition and metabolite identification for the EOs from 63 plants from the Atlantic Rainforest; Table S2: Correlation analyses between the contents of the most abundant metabolites from the isolated EOs and growth inhibition; Table S3: Correlation analyses between cell component loss and growth inhibition; Table S4: Prediction of pharmacokinetic properties of 27 major components of the EOs. Table S5. Agglomerate macromolecular target prediction for the major metabolites of the EOs from the Annonaceae, Lauraceae, Myrtacea, Rutaceae, and Salicaceae botanical families. Table S6. Botanical classification, biome of occurrence, aroma description, antimicrobial action, and reported EO toxicity of the plants sampled in Atlantic Rainforest locations.

Institutional Review Board Statement: The sampling and analyses of native plants in the current work is authorized by Sistema Nacional de Gestão do Patrimônio Genético e do Conhecimento Tradicional Associado (SisGen), under license permit AD0077F [66–125].

Informed Consent Statement: Not applicable.

Data Availability Statement: The metabolomics and metadata reported in this paper are available at Metabolomics Workbench (https://www.metabolomicsworkbench.org/data/index.php (accessed on 7 December 2022)), study identifier ST000606.

Conflicts of Interest: The authors declare no conflict of interest. The funders had no role in the design of the study; in the collection, analyses, or interpretation of data; in the writing of the manuscript; or in the decision to publish the results.

References

1. Huemer, M.; Shambat, S.M.; Brugger, S.D.; Zinkernagel, A.S. Antibiotic resistance and persistence—Implications for human health and treatment perspectives. *EMBO Rep.* **2020**, *21*, e51034. [CrossRef] [PubMed]
2. Blair, J.M.A.; Webber, M.A.; Baylay, A.J.; Ogbolu, D.O.; Piddock, L.J.V. Molecular mechanisms of antibiotic resistance. *Nat. Rev. Microbiol.* **2015**, *13*, 42–51. [CrossRef] [PubMed]
3. Pormohammad, A.; Hansen, D.; Turner, R.J. Antibacterial, Antibiofilm, and Antioxidant Activity of 15 Different Plant-Based Natural Compounds in Comparison with Ciprofloxacin and Gentamicin. *Antibiotics* **2022**, *11*, 1099. [CrossRef] [PubMed]
4. Erb, M.; Kliebenstein, D.J. Plant Secondary Metabolites as Defenses, Regulators, and Primary Metabolites: The Blurred Functional Trichotomy. *Plant Physiol.* **2020**, *184*, 39–52. [CrossRef] [PubMed]
5. Lange, B.M. The Evolution of Plant Secretory Structures and Emergence of Terpenoid Chemical Diversity. *Annu. Rev. Plant Biol.* **2015**, *66*, 139–159. [CrossRef]
6. Tholl, D. Biosynthesis and biological functions of terpenoids in plants. *Adv. Biochem. Eng. Biotechnol.* **2015**, *148*, 63–106. [CrossRef]
7. Dudareva, N.; Klempien, A.; Muhlemann, J.K.; Kaplan, I. Biosynthesis, function and metabolic engineering of plant volatile organic compounds. *New Phytol.* **2013**, *198*, 16–32. [CrossRef]

8. Trifan, A.; Luca, S.V.; Greige-Gerges, H.; Miron, A.; Gille, E.; Aprotosoaie, A.C. Recent advances in tackling microbial multidrug resistance with essential oils: Combinatorial and nano-based strategies. *Crit. Rev. Microbiol.* **2020**, *46*, 338–357. [CrossRef]

9. Raut, J.S.; Karuppayil, S.M. A status review on the medicinal properties of essential oils. *Ind. Crops Prod.* **2014**, *62*, 250–264. [CrossRef]

10. Solórzano-Santos, F.; Miranda-Novales, M.G. Essential oils from aromatic herbs as antimicrobial agents. *Curr. Opin. Biotechnol.* **2012**, *23*, 136–141. [CrossRef]

11. Máthé, Á.; de Sales Silva, J.C. Introduction to medicinal and aromatic plants in Brazil. In *Medicinal and Aromatic Plants of South America. Medicinal and Aromatic Plants of the World*; Albuquerque, U., Patil, U., Máthé, Á., Eds.; Springer: Dordrecht, The Netherlands, 2018; Volume 5, pp. 47–69. [CrossRef]

12. Massad, T.J.; Richards, L.A.; Philbin, C.; Yamaguchi, L.F.; Kato, M.J.; Jeffrey, C.S.; Oliveira, C., Jr.; Ochsenrider, K.; de Moraes, M.M.; Tepe, E.J.; et al. The chemical ecology of tropical forest diversity: Environmental variation, chemical similarity, herbivory, and richness. *Ecology* **2022**, *20*, e3762. [CrossRef]

13. Álvarez-Martínez, F.; Barrajón-Catalán, E.; Herranz-López, M.; Micol, V. Antibacterial plant compounds, extracts and essential oils: An updated review on their effects and putative mechanisms of action. *Phytomedicine* **2021**, *90*, 153626. [CrossRef]

14. Mint Evolutionary Genomics Consortium. Phylogenomic Mining of the Mints Reveals Multiple Mechanisms Contributing to the Evolution of Chemical Diversity in Lamiaceae. *Mol. Plant* **2018**, *11*, 1084–1096. [CrossRef]

15. Borges, R.S.; Ortiz, B.L.S.; Pereira, A.C.M.; Keita, H.; Carvalho, J.C.T. Rosmarinus officinalis essential oil: A review of its phytochemistry, anti-inflammatory activity, and mechanisms of action involved. *J. Ethnopharmacol.* **2019**, *229*, 29–45. [CrossRef]

16. Stierlin, É.; Nicolè, F.; Costes, T.; Fernandez, X.; Michel, T. Metabolomic study of volatile compounds emitted by lavender grown under open-field conditions: A potential approach to investigate the yellow decline disease. *Metabolomics* **2020**, *16*, 31. [CrossRef]

17. Alolga, R.N.; León, M.A.S.C.C.; Osei-Adjei, G.; Onoja, V. GC-MS-based metabolomics, antibacterial and anti-inflammatory investigations to characterize the quality of essential oil obtained from dried Xylopia aethiopica fruits from Ghana and Nigeria. *J. Pharm. Pharmacol.* **2019**, *71*, 1544–1552. [CrossRef]

18. Perigo, C.V.; Torres, R.B.; Bernacci, L.C.; Guimarães, E.F.; Haber, L.L.; Facanali, R.; Vieira, M.A.; Quecini, V.; Marques, M.O.M. The chemical composition and antibacterial activity of eleven Piper species from distinct rainforest areas in Southeastern Brazil. *Ind. Crops Prod.* **2016**, *94*, 528–539. [CrossRef]

19. Marques, M.O.; Perigo, C.V.; Haber, L.L.; Vieira, M.A.; Facanali, R.; Torres, R.B.; Bernacci, L.C.; Quecini, V. Composition and antimicrobial activity of the essential oils from a wide range of species from the Atlantic Rainforest in Brazil. *Facta Univ. Ser. Phys. Chem. Technol.* **2018**, *16*, 77.

20. Salehi, B.; Zakaria, Z.A.; Gyawali, R.; Ibrahim, S.A.; Rajkovic, J.; Shinwari, Z.K.; Khan, T.; Sharifi-Rad, J.; Ozleyen, A.; Turkdonmez, E.; et al. Piper Species: A Comprehensive Review on Their Phytochemistry, Biological Activities and Applications. *Molecules* **2019**, *24*, 1364. [CrossRef]

21. Lee, S.; Oh, D.-G.; Singh, D.; Lee, J.S.; Lee, S.; Lee, C.H. Exploring the metabolomic diversity of plant species across spatial (leaf and stem) components and phylogenic groups. *BMC Plant Biol.* **2020**, *20*, 39. [CrossRef]

22. Li, D.; Gaquerel, E. Next-Generation Mass Spectrometry Metabolomics Revives the Functional Analysis of Plant Metabolic Diversity. *Annu. Rev. Plant Biol.* **2021**, *72*, 867–891. [CrossRef] [PubMed]

23. Pereira, F.G.; Marquete, R.; Cruz, L.O.; Caldeira-de-Arujo, A.; Mansur, E.; de Lima Moreira, D. DNA damages promoted by the essential oil from leaves of *Casearia sylvestris* Sw. (Salicaceae). *J. Med. Plants Res.* **2016**, *10*, 818–822. [CrossRef]

24. Spósito, L.; Oda, F.B.; Vieira, J.H.; Carvalho, F.A.; Ramos, M.A.D.S.; de Castro, R.C.; Crevelin, E.J.; Crotti, A.E.M.; Santos, A.G.; da Silva, P.B.; et al. In vitro and in vivo anti-*Helicobacter pylori* activity of *Casearia sylvestris* leaf derivatives. *J. Ethnopharmacol.* **2018**, *233*, 1–12. [CrossRef] [PubMed]

25. de Mesquita, M.; Grellier, P.; Mambu, L.; de Paula, J.; Espindola, L. In vitro antiplasmodial activity of Brazilian Cerrado plants used as traditional remedies. *J. Ethnopharmacol.* **2007**, *110*, 165–170. [CrossRef] [PubMed]

26. Laursen, T.; Møller, B.L.; Bassard, J.-E. Plasticity of specialized metabolism as mediated by dynamic metabolons. *Trends Plant Sci.* **2015**, *20*, 20–32. [CrossRef]

27. Knudsen, C.; Gallage, N.J.; Hansen, C.C.; Møller, B.L.; Laursen, T. Dynamic metabolic solutions to the sessile life style of plants. *Nat. Prod. Rep.* **2018**, *35*, 1140–1155. [CrossRef]

28. Valarezo, E.; Gaona-Granda, G.; Morocho, V.; Cartuche, L.; Calva, J.; Meneses, M. Chemical Constituents of the Essential Oil from Ecuadorian Endemic Species *Croton ferrugineus* and Its Antimicrobial, Antioxidant and α-Glucosidase Inhibitory Activity. *Molecules* **2021**, *26*, 4608. [CrossRef]

29. El-Din, M.I.G.; Youssef, F.S.; Altyar, A.E.; Ashour, M.L. GC/MS Analyses of the Essential Oils Obtained from Different *Jatropha* Species, Their Discrimination Using Chemometric Analysis and Assessment of Their Antibacterial and Anti-Biofilm Activities. *Plants* **2022**, *11*, 1268. [CrossRef]

30. Fang, C.; Luo, J.; Wang, S. The Diversity of Nutritional Metabolites: Origin, Dissection, and Application in Crop Breeding. *Front. Plant Sci.* **2019**, *10*, 1028. [CrossRef]

31. Karunanithi, P.S.; Zerbe, P. Terpene Synthases as Metabolic Gatekeepers in the Evolution of Plant Terpenoid Chemical Diversity. *Front. Plant Sci.* **2019**, *10*, 1166. [CrossRef]

32. Bustos-Segura, C.; Padovan, A.; Kainer, D.; Foley, W.J.; Külheim, C. Transcriptome analysis of terpene chemotypes of *Melaleuca alternifolia* across different tissues. *Plant Cell Environ.* **2017**, *40*, 2406–2425. [CrossRef]

33. Padovan, A.; Keszei, A.; Hassan, Y.; Krause, S.T.; Köllner, T.G.; Degenhardt, J.; Gershenzon, J.; Külheim, C.; Foley, W.J. Four terpene synthases contribute to the generation of chemotypes in tea tree (*Melaleuca alternifolia*). *BMC Plant Biol.* **2017**, *17*, 160. [CrossRef]

34. Chen, C.; Zheng, Y.; Zhong, Y.; Wu, Y.; Li, Z.; Xu, L.-A.; Xu, M. Transcriptome analysis and identification of genes related to terpenoid biosynthesis in *Cinnamomum camphora*. *BMC Genom.* **2018**, *19*, 550. [CrossRef]

35. Chaw, S.-M.; Liu, Y.-C.; Wu, Y.-W.; Wang, H.-Y.; Lin, C.-Y.I.; Wu, C.-S.; Ke, H.-M.; Chang, L.-Y.; Hsu, C.-Y.; Yang, H.-T.; et al. Stout camphor tree genome fills gaps in understanding of flowering plant genome evolution. *Nat. Plants* **2019**, *5*, 63–73. [CrossRef]

36. Jin, Z.; Kwon, M.; Lee, A.-R.; Ro, D.-K.; Wungsintaweekul, J.; Kim, S.-U. Molecular cloning and functional characterization of three terpene synthases from unripe fruit of black pepper (*Piper nigrum*). *Arch. Biochem. Biophys.* **2018**, *638*, 35–40. [CrossRef]

37. Sun, P.; Schuurink, R.C.; Caissard, J.-C.; Hugueney, P.; Baudino, S. My Way: Noncanonical Biosynthesis Pathways for Plant Volatiles. *Trends Plant Sci.* **2016**, *21*, 884–894. [CrossRef]

38. Lautié, E.; Russo, O.; Ducrot, P.; Boutin, J.A. Unraveling Plant Natural Chemical Diversity for Drug Discovery Purposes. *Front. Pharmacol.* **2020**, *11*, 397. [CrossRef]

39. Mugula, B.B.; Kiboi, S.K.; Kanya, J.I.; Egeru, A.; Okullo, P.; Curto, M.; Meimberg, H. Knowledge Gaps in Taxonomy, Ecology, Population Distribution Drivers and Genetic Diversity of African Sandalwood (*Osyris lanceolata* Hochst. & Steud.): A Scoping Review for Conservation. *Plants* **2021**, *10*, 1780. [CrossRef]

40. Gros-Balthazard, M.; Battesti, V.; Ivorra, S.; Paradis, L.; Aberlenc, F.; Zango, O.; Zehdi-Azouzi, S.; Moussouni, S.; Naqvi, S.A.; Newton, C.; et al. On the necessity of combining ethnobotany and genetics to assess agrobiodiversity and its evolution in crops: A case study on date palms (*Phoenix dactylifera* L.) in Siwa Oasis, Egypt. *Evol. Appl.* **2020**, *13*, 1818–1840. [CrossRef]

41. Funke, G.; von Graevenitz, A.; Clarridge, J.E., 3rd; Bernard, K.A. Clinical microbiology of coryneform bacteria. *Clin. Microbiol. Rev.* **1997**, *10*, 125–159. [CrossRef]

42. Otto, M. Staphylococcus epidermidis—The 'accidental' pathogen. *Nat Rev Microbiol.* **2009**, *7*, 555–567. [CrossRef] [PubMed]

43. Poolman, J.T.; Anderson, A.S. *Escherichia coli* and *Staphylococcus aureus*: Leading bacterial pathogens of healthcare associated infections and bacteremia in older-age populations. *Expert Rev. Vaccines* **2018**, *17*, 607–618. [CrossRef] [PubMed]

44. Tariq, S.; Wani, S.; Rasool, W.; Shafi, K.; Bhat, M.A.; Prabhakar, A.; Shalla, A.H.; Rather, M.A. A comprehensive review of the antibacterial, antifungal and antiviral potential of essential oils and their chemical constituents against drug-resistant microbial pathogens. *Microb. Pathog.* **2019**, *134*, 103580. [CrossRef] [PubMed]

45. Leigh-de Rapper, S.; Viljoen, A.; van Vuuren, S. Essential Oil Blends: The Potential of Combined Use for Respiratory Tract Infections. *Antibiotics* **2021**, *10*, 1517. [CrossRef]

46. Abers, M.; Schroeder, S.; Goelz, L.; Sulser, A.; Rose, T.S.; Puchalski, K.; Langland, J. Antimicrobial activity of the volatile substances from essential oils. *BMC Complement. Med. Ther.* **2021**, *21*, 124. [CrossRef]

47. Ergüden, B. Phenol group of terpenoids is crucial for antibacterial activity upon ion leakage. *Lett. Appl. Microbiol.* **2021**, *73*, 438–445. [CrossRef]

48. Yamaguchi, T. Antibacterial effect of the combination of terpenoids. *Arch. Microbiol.* **2022**, *204*, 520. [CrossRef]

49. Wijesundara, N.M.; Rupasinghe, H. Essential oils from *Origanum vulgare* and *Salvia officinalis* exhibit antibacterial and anti-biofilm activities against *Streptococcus pyogenes*. *Microb. Pathog.* **2018**, *117*, 118–127. [CrossRef]

50. Sim, J.X.F.; Khazandi, M.; Chan, W.Y.; Trott, D.J.; Deo, P. Antimicrobial activity of thyme oil, oregano oil, thymol and carvacrol against sensitive and resistant microbial isolates from dogs with otitis externa. *Vet. Dermatol.* **2019**, *30*, 524-e159. [CrossRef]

51. Scandorieiro, S.; Rodrigues, B.C.D.; Nishio, E.K.; Panagio, L.A.; de Oliveira, A.G.; Durán, N.; Nakazato, G.; Kobayashi, R.K.T. Biogenic Silver Nanoparticles Strategically Combined With Origanum vulgare Derivatives: Antibacterial Mechanism of Action and Effect on Multidrug-Resistant Strains. *Front. Microbiol.* **2022**, *13*, 842600. [CrossRef]

52. Carson, C.F.; Mee, B.J.; Riley, T.V. Mechanism of Action of *Melaleuca alternifolia* (Tea Tree) Oil on *Staphylococcus aureus* Determined by Time-Kill, Lysis, Leakage, and Salt Tolerance Assays and Electron Microscopy. *Antimicrob. Agents Chemother.* **2002**, *46*, 1914–1920. [CrossRef]

53. Jardim Botânico do Rio de Janeiro; Lista de Espécies da Flora do Brasil. REFLORA. (In Portuguese). 2015. Available online: http://floradobrasil.jbrj.gov.br (accessed on 26 February 2022).

54. Brazilian Pharmacopeia. *Farmacopeia Brasileira*, 6th ed.; ANVISA: Brasília, Brazil, 2019.

55. Adams, R.P. *Identification of Essential Oil Components by Gas Cromatography/Mass Spectroscopy*, 4th ed.; Allured Publishing Corporation: Carol Stream, IL, USA, 2007; 811p.

56. Van den Dool, E.; Kratz, P. A generalization of the retention index system including linear temperature programmed gas-liquid partition chromatography. *J. Chromatog.* **1963**, *11*, 463–471. [CrossRef]

57. Rueden, C.T.; Schindelin, J.; Hiner, M.C.; Dezonia, B.E.; Walter, A.E.; Arena, E.T.; Eliceiri, K.W. ImageJ2: ImageJ for the next generation of scientific image data. *BMC Bioinform.* **2017**, *18*, 529. [CrossRef]

58. Clinical and Laboratory Standards Institute (CLSI). *Methods for Determining Bactericidal Activity of Antimicrobial Agents*; Approved Guideline; CLSI Document M26-A; CLSI: Wayne, PA, USA, 1999.

59. Turgis, M.; Han, J.; Caillet, S.; Lacroix, M. Antimicrobial activity of mustard essential oil against *Escherichia coli* O157:H7 and Salmonella typhi. *Food Control* **2009**, *20*, 1073–1079. [CrossRef]

60. Daina, A.; Michielin, O.; Zoete, V. SwissADME: A free web tool to evaluate pharmacokinetics, drug-likeness and medicinal chemistry friendliness of small molecules. *Sci. Rep.* **2017**, *7*, 42717. [CrossRef]

61. R Core Team. *A Language and Environment for Statistical Computing*; R Foundation for Statistical Computing: Vienna, Austria, 2021; ISBN 3-900051-07-0. Available online: http://www.R-project.org/ (accessed on 10 June 2022).

62. Rohart, F.; Gautier, B.; Singh, A.; Lê Cao, K.-A. mixOmics: An R package for 'omics feature selection and multiple data integration. *PLoS Comput. Biol.* **2017**, *13*, e1005752. [CrossRef]

63. Scrucca, L.; Fop, M.; Murphy, T.B.; Raftery, A.E. mclust 5: Clustering, Classification and Density Estimation Using Gaussian Finite Mixture Models. *R J.* **2016**, *8*, 289–317. [CrossRef]

64. Harrell, F., Jr. Package 'Hmisc'. 2019. Available online: https://cran.r-project.org/web/packages/Hmisc/Hmisc.pdf (accessed on 10 June 2022).

65. Wei, T.; Simko, V. R Package "Corrplot": Visualization of a Correlation Matrix. Version 0.84. 2017. Available online: https://github.com/taiyun/corrplot (accessed on 10 June 2022).

66. Mattar, V.T.; Borioni, J.L.; Hollmann, A.; Rodriguez, S.A. Insecticidal activity of the essential oil of Schinus areira against Rhipibruchus picturatus (F.) (Coleoptera: Bruchinae), and its inhibitory effects on acetylcholinesterase. *Pestic. Biochem. Physiol.* **2022**, *185*. [CrossRef]

67. De Groot, A.C.; Schmidt, E. Tea tree oil: Contact allergy and chemical composition. *Contact Dermat.* **2016**, *75*, 129–143. [CrossRef]

68. Moura-Costa, G.F.; Nocchi, S.R.; Ceole, L.F.; de Mello, J.C.P.; Nakamura, C.V.; Filho, B.P.D.; Temponi, L.G.; Ueda-Nakamura, T. Antimicrobial activity of plants used as medicinals on an indigenous reserve in Rio das Cobras, Paraná, Brazil. *J. Ethnopharmacol.* **2012**, *143*, 631–638. [CrossRef]

69. Gehrke, I.T.; Neto, A.T.; Pedroso, M.; Mostardeiro, C.P.; Da Cruz, I.B.; Silva, U.F.; Ilha, V.; Dalcol, I.I.; Morel, A.F. Antimicrobial activity of Schinus lentiscifolius (Anacardiaceae). *J. Ethnopharmacol.* **2013**, *148*, 486–491. [CrossRef] [PubMed]

70. Uliana, M.P.; Fronza, M.; da Silva, A.G.; Vargas, T.S.; Andrade, T.; Scherer, R. Composition and biological activity of Brazilian rose pepper (Schinus terebinthifolius Raddi) leaves. *Ind. Crops Prod.* **2016**, *83*, 235–240. [CrossRef]

71. Lima, I.M.D.S.F.; Zagmignan, A.; Santos, D.M.; Maia, H.S.; Silva, L.D.S.; Cutrim, B.D.S.; Vieira, S.L.; Filho, C.M.B.; de Sousa, E.M.; Napoleão, T.H.; et al. Schinus terebinthifolia leaf lectin (SteLL) has anti-infective action and modulates the response of Staphylococcus aureus-infected macrophages. *Sci. Rep.* **2019**, *9*, 18159. [CrossRef]

72. Cascaes, M.M.; De Moraes, A.B.; Cruz, J.N.; Franco, C.D.J.P.; E Silva, R.C.; Nascimento, L.D.D.; Ferreira, O.O.; dos Anjos, T.O.; de Oliveira, M.S.; Guilhon, G.M.S.P.; et al. Phytochemical Profile, Antioxidant Potential and Toxicity Evaluation of the Essential Oils from *Duguetia* and *Xylopia* Species (*Annonaceae*) from the Brazilian Amazon. *Antioxidants* **2022**, *11*, 1709. [CrossRef] [PubMed]

73. Pereira, T.S.; Esquissato, G.N.M.; Costa, E.V.; Nogueira, P.C.D.L.; de Castro-Prado, M.A.A. Mutagenic and cytostatic activities of the *Xylopia laevigata* essential oil in human lymphocytes. *Nat. Prod. Res.* **2019**, *35*, 1682–1685. [CrossRef]

74. Moura, A.P.G.; Beltrão, D.M.; Pita, J.C.L.R.; Xavier, A.L.; Brito, M.T.; de Sousa, T.K.G.; Batista, L.M.; de Carvalho, J.E.; Ruiz, A.L.T.G.; Della Torre, A.; et al. Essential oil from fruit of *Xylopia langsdorffiana*: Antitumour activity and toxicity. *Pharm. Biol.* **2016**, *54*, 3093–3102. [CrossRef]

75. Nascimento, M.N.G.D.; Junqueira, J.G.M.; Terezan, A.P.; Severino, R.; Silva, T.; Martins, C.H.G.; Severino, V.G.P.; Cacuro, T.A.; Waldman, W. Chemical Composition and Antimicrobial Activity of Essential Oils from Xylopia aromatica (Annonaceae) Flowers and Leaves. *Rev. Virtual Quim* **2018**, *10*, 1578–1590. [CrossRef]

76. Ricardo, L.M.; de Paula-Souza, J.; Andrade, A.; Brandão, M.G. Plants from the Brazilian Traditional Medicine: Species from the books of the Polish physician Piotr Czerniewicz (Pedro Luiz Napoleão Chernoviz, 1812–1881). *Rev. Bras. de Farm.* **2017**, *27*, 388–400. [CrossRef]

77. Meneguelli, A.Z.; Camargo, E.E.S.; Buccini, D.F.; Roriz, B.C.; Cerqueira, G.R.; Moreno, S.E. Ethnopharmacological and botanical evaluation of medicinal plants used by Brazilian Amazon Indian community. *Interações (Campo Grande)* **2020**. [CrossRef]

78. Cruz-Galvez, A.M.; Gómez-Aldapa, C.A.; Villagómez-Ibarra, J.R.; Chavarría-Hernández, N.; Rodríguez-Baños, J.; Rangel-Vargas, E.; Castro-Rosas, J. Antibacterial effect against foodborne bacteria of plants used in traditional medicine in central Mexico: Studies in vitro and in raw beef. *Food Control* **2013**, *32*, 289–295. [CrossRef]

79. Balakrishnan, R.; Cho, D.-Y.; Su-Kim, I.; Choi, D.-K. Dendropanax Morbiferus and Other Species from the Genus Dendropanax: Therapeutic Potential of Its Traditional Uses, Phytochemistry, and Pharmacology. *Antioxidants* **2020**, *9*, 962. [CrossRef]

80. Bueno, G.; Rico, S.L.C.; Périco, L.L.; Ohara, R.; Rodrigues, V.P.; Emílio-Silva, M.T.; Assunção, R.; da Rocha, L.R.M.; Nunes, D.S.; Besten, M.A.; et al. The essential oil from Baccharis trimera (Less.) DC improves gastric ulcer healing in rats through modulation of VEGF and MMP-2 activity. *J. Ethnopharmacol.* **2021**, *271*, 113832. [CrossRef]

81. Cazella, L.N.; Glamoclija, J.; Soković, M.; Gonçalves, J.E.; Linde, G.A.; Colauto, N.B.; Gazim, Z.C. Antimicrobial Activity of Essential Oil of Baccharis dracunculifolia DC (Asteraceae) Aerial Parts at Flowering Period. *Front. Plant Sci.* **2019**, *10*, 27. [CrossRef]

82. Zuccolotto, T.; Bressan, J.; Lourenço, A.V.F.; Bruginski, E.; Veiga, A.; Marinho, J.V.N.; Raeski, P.A.; Heiden, G.; Salvador, M.J.; Murakami, F.S.; et al. Chemical, Antioxidant, and Antimicrobial Evaluation of Essential Oils and an Anatomical Study of the Aerial Parts from *Baccharis* Species (Asteraceae). *Chem. Biodivers.* **2019**, *16*, e1800547. [CrossRef]

83. Camargo, J.G.S.D. Desreplicação dos Extratosativos de Cyrtocymurascorpioides (Asteraceae) contra *Candida* spp. e *Trichomonas vaginalis*. 2020. MSc. Dissertation, Instituto de Biociências, Letras e CiênciasExatas (IBILCE), UNESP, São José do Rio Preto, SP, Brazil. Available online: http://hdl.handle.net/11449/194314 (accessed on 7 December 2022).

84. Santos, N.C.; da Silva, J.E.; Santos, A.C.C.; Dantas, J.D.O.; Tavares, S.R.S.A.; Andrade, V.S.; Oliveira, S.D.D.S.; Blank, A.F.; Araújo, A.P.A.; Bacci, L. Bioactivity of essential oils from Croton grewioides and its major compounds: Toxicity to soybean looper Chrysodeixis includens and selectivity to the predatory stink bug Podisus nigrispinus. *Environ. Sci. Pollut. Res.* **2022**, 1–12. [CrossRef]

85. Silva, K.; Peruchetti, D.; Sirtoli, G.; Takiya, C.; Pinheiro, A.; Leal-Cardoso, J.; Caruso-Neves, C. High Doses of Essential Oil of *Croton Zehntneri* Induces Renal Tubular Damage. *Plants* **2021**, *10*, 1400. [CrossRef]

86. Almeida-Pereira, C.S.; Nogueira, P.C.D.L.; Barbosa, A.A.T.; Nizio, D.A.D.C.; Arrigoni-Blank, M.D.F.; Sampaio, T.S.; Alves, R.P.; de Araujo-Couto, H.G.S.; Feitosa-Alcantara, R.B.; de Melo, J.O.; et al. Chemical composition and antimicrobial activity of essential oils of a *Croton tetradenius* Baill. germplasm. *J. Essent. Oil Res.* **2019**, *31*, 379–389. [CrossRef]

87. Rocha, A.R.d.S.; Sousa, H.G.; Júnior, E.P.D.V.; de Lima, F.L.; Costa, A.S.; de Araújo, A.R.; Leite, J.R.S.; Martins, F.A.; Oliveira, M.B.P.; Plácido, A.; et al. Extracts and fractions of *Croton* L. (Euphorbiaceae) species with antimicrobial activity and antioxidant potential. *LWT* **2021**, *139*. [CrossRef]

88. Silva, N.N.S.; Silva, J.R.A.; Alves, C.N.; Andrade, E.H.A.; da Silva, J.K.R.; Maia, J.G.S. Acetylcholinesterase Inhibitory Activity and Molecular Docking Study of 1-Nitro-2-Phenylethane, the Main Constituent of *Aniba canelilla* Essential Oil. *Chem. Biol. Drug Des.* **2014**, *84*, 192–198. [CrossRef]

89. da Silva, J.K.R.; da Trindade, R.C.S.; Maia, J.G.S.; Setzer, W.N. Chemical Composition, Antioxidant, and Antimicrobial Activities of Essential Oils of *Endlicheria arenosa* (Lauraceae) from the Amazon. *Nat. Prod. Commun.* **2016**, *11*, 1934578X1601100537. [CrossRef]

90. de Moura, V.M.; Guimarães, N.D.C.; Batista, L.T.; Freitas-De-Sousa, L.A.; Martins, J.D.S.; de Souza, M.C.S.; de Almeida, P.D.O.; Monteiro, W.M.; de Oliveira, R.B.; Dos-Santos, M.C.; et al. Assessment of the anti-snakebite properties of extracts of Aniba fragrans Ducke (Lauraceae) used in folk medicine as complementary treatment in cases of envenomation by Bothrops atrox. *J. Ethnopharmacol.* **2018**, *213*, 350–358. [CrossRef] [PubMed]

91. da Silva, Y.C.; Silva, E.M.S.; Fernandes, N.; Lopes, N.L.; Orlandi, P.P.; Nakamura, C.V.; Costa, E.; Júnior, V.F.D.V. Antimicrobial substances from Amazonian Aniba (Lauraceae) species. *Nat. Prod. Res.* **2019**, *35*, 849–852. [CrossRef] [PubMed]

92. Longhini, R.; Lonni, A.A.; Sereia, A.L.; Krzyzaniak, L.M.; Lopes, G.C.; de Mello, J.C.P. Trichilia catigua: Therapeutic and cosmetic values. *Rev. Bras. de Farm.* **2017**, *27*, 254–271. [CrossRef]

93. da Silva, L.L.; de Almeida, R.; e Silva, F.T.; Verícimo, M.A. Review on the therapeutic activities of the genus Trichilia. *Res. Soc. Dev.* **2021**, *10*. [CrossRef]

94. Cordeiro, R.M.; Silva, A.P.D.S.E.; Pinto, R.H.H.; da Costa, W.A.; da Silva, S.H.M.; Pinheiro, W.B.D.S.; Arruda, M.S.P.; Junior, R.N.C. Supercritical CO_2 extraction of ucuúba (*Virola surinamensis*) seed oil: Global yield, kinetic data, fatty acid profile, and antimicrobial activities. *Chem. Eng. Commun.* **2018**, *206*, 86–97. [CrossRef]

95. González-Rodríguez, M.; Ruiz-Fernández, C.; Francisco, V.; Eldjoudi, D.A.; Ramadan, F.Y.; Cordero-Barreal, A.; Pino, J.; Lago, F.; Campos-Toimil, M.; Carvalho, G.R.; et al. Pharmacological Extracts and Molecules from *Virola* Species: Traditional Uses, Phytochemistry, and Biological Activity. *Molecules* **2021**, *26*, 792. [CrossRef]

96. Ribeiro, C.L.; Silva, R.M.; Fernandes, R.D.M.N.; Araújo, M.R.; Soares, I.M.; da Silva, J.F.M.; Nascimento, G.N.L.D.; Pimenta, R.S.; Scapin, E. Chemical assessment, antioxidant and antimicrobial of leafs extracts of Virola sebifera, an Amazonian medicinal plant. *Res. Soc. Dev.* **2021**, *10*. [CrossRef]

97. de Moraes, A.B.; Ferreira, O.O.; da Costa, L.S.; Almeida, L.Q.; Varela, E.L.P.; Cascaes, M.M.; Franco, C.D.J.P.; Percário, S.; Nascimento, L.D.D.; de Oliveira, M.S.; et al. Phytochemical Profile, Preliminary Toxicity, and Antioxidant Capacity of the Essential Oils of *Myrciaria floribunda* (H. West ex Willd.) O. Berg. and *Myrcia sylvatica* (G. Mey) DC. (Myrtaceae). *Antioxidants* **2022**, *11*, 2076. [CrossRef]

98. Magalhães, B.Q.; Machado, F.P.; Sanches, P.S.; Lima, B.; Falcão, D.Q.; von Ranke, N.; Bello, M.L.; Rodrigues, C.R.; Santos, M.G.; Rocha, L.; et al. *Eugenia sulcata* (Myrtaceae) Nanoemulsion Enhances the Inhibitory Activity of the Essential Oil on P2X7R and Inflammatory Response In Vivo. *Pharmaceutics* **2022**, *14*, 911. [CrossRef]

99. de Araújo, F.F.; Neri-Numa, I.A.; Farias, D.D.P.; da Cunha, G.R.M.C.; Pastore, G.M. Wild Brazilian species of Eugenia genera (Myrtaceae) as an innovation hotspot for food and pharmacological purposes. *Food Res. Int.* **2019**, *121*, 57–72. [CrossRef]

100. Macedo, J.G.F.; Rangel, J.M.L.; Santos, M.D.O.; Camilo, C.J.; da Costa, J.G.M.; Souza, M.M.D.A. Therapeutic indications, chemical composition and biological activity of native Brazilian species from Psidium genus (Myrtaceae): A review. *J. Ethnopharmacol.* **2021**, *278*, 114248. [CrossRef]

101. Vechi, G.; Tenfen, A.; Capusiri, E.S.; Gimenez, A.; Cechinel-Filho, V. Antiparasitic activity of two Brazilian plants: Eugenia mattosii and Marlierea eugeniopsoides. *Nat. Prod. Res.* **2020**, *35*, 4876–4880. [CrossRef]

102. Maiolini, T.C.S.; Rosa, W.; Miranda, D.D.O.; Costa-Silva, T.A.; Tempone, A.G.; Bueno, P.C.P.; Dias, D.F.; de Paula, D.A.C.; Sartorelli, P.; Lago, J.H.G.; et al. Essential Oils from Different Myrtaceae Species from Brazilian Atlantic Forest Biome–Chemical Dereplication and Evaluation of Antitrypanosomal Activity. *Chem. Biodivers.* **2022**, *19*. [CrossRef]

103. de Oliveira, A.C.; Simões, R.C.; Lima, C.A.P.; da Silva, F.M.A.; Nunomura, S.M.; Roque, R.A.; Tadei, W.P.; Nunomura, R.C.S. Essential oil of Piper purusanum C.DC (Piperaceae) and its main sesquiterpenes: Biodefensives against malaria and dengue vectors, without lethal effect on non-target aquatic fauna. *Environ. Sci. Pollut. Res.* **2022**, *29*, 47242–47253. [CrossRef]

104. Zhang, C.; Zhao, J.; Famous, E.; Pan, S.; Peng, X.; Tian, J. Antioxidant, hepatoprotective and antifungal activities of black pepper (*Piper nigrum* L.) essential oil. *Food Chem.* **2020**, *346*, 128845. [CrossRef]

105. Da Silva, J.K.; da Trindade, R.; Alves, N.S.; Figueiredo, P.L.; Maia, J.G.S.; Setzer, W.N. Essential Oils from Neotropical Piper Species and Their Biological Activities. *Int. J. Mol. Sci.* **2017**, *18*, 2571. [CrossRef]

106. de Pascoli, I.C.; dos Anjos, M.M.; da Silva, A.A.; Lorenzetti, F.B.; Cortez, D.A.G.; Mikcha, J.M.G.; Nakamura, T.U.; Nakamura, C.V.; Filho, B.A.D.A. Piperaceae extracts for controlling Alicyclobacillus acidoterrestris growth in commercial orange juice. *Ind. Crops Prod.* **2018**, *116*, 224–230. [CrossRef]

107. Majolo, C.; Monteiro, P.C.; Nascimento, A.V.P.D.; Chaves, F.C.M.; Gama, P.E.; Bizzo, H.R.; Chagas, E.C. Essential Oils from Five Brazilian *Piper* Species as Antimicrobials Against Strains of *Aeromonas hydrophila*. *J. Essent. Oil Bear. Plants* **2019**, *22*, 746–761. [CrossRef]

108. dos Santos, A.L.M.; Araújo, F.A.M.; Matisui, D.S.; da Costa, L.A.M.A.; Macêdo, A.J.; de Lucena, J.M.V.M. Antimicrobial and antibiofilm properties of essential oils from Piper marginatum Jacq. *Res. Soc. Dev.* **2021**, *10*. [CrossRef]

109. Shoorvarzi, S.N.; Shahraki, F.; Shafaei, N.; Karimi, E.; Oskoueian, E. *Citrus aurantium* L. bloom essential oil nanoemulsion: Synthesis, characterization, cytotoxicity, and its potential health impacts on mice. *J. Food Biochem.* **2020**, *44*, e13181. [CrossRef]

110. Volpato, G.T.; Francia-Farje, L.A.; Damasceno, D.C.; Oliveira, R.V.; Hiruma-Lima, C.A.; Kempinas, W.G. Effect of essential oil from Citrus aurantium in maternal reproductive outcome and fetal anomaly frequency in rats. *An. Da Acad. Bras. De Ciências* **2015**, *87*, 407–415. [CrossRef] [PubMed]

111. Orlanda, J.F.; Nascimento, A. Chemical composition and antibacterial activity of Ruta graveolens L. (Rutaceae) volatile oils, from São Luís, Maranhão, Brazil. *S. Afr. J. Bot.* **2015**, *99*, 103–106. [CrossRef]

112. Fernandes, T.S.; Copetti, D.; Carmo, G.D.; Neto, A.T.; Pedroso, M.; Silva, U.F.; Mostardeiro, M.A.; Burrow, R.E.; Dalcol, I.I.; Morel, A.F. Phytochemical analysis of bark from Helietta apiculata Benth and antimicrobial activities. *Phytochemistry* **2017**, *141*, 131–139. [CrossRef] [PubMed]

113. Da Silva, F.B.; Dos Santos, N.O.; Pascon, R.C.; Vallim, M.; Figueiredo, C.R.; Martins, R.C.C.; Sartorelli, P. Chemical Composition and In Vitro Cytotoxic and Antimicrobial Activities of the Essential Oil from Leaves of *Zanthoxylum monogynum* St. Hill (Rutaceae). *Medicines* **2017**, *4*, 31. [CrossRef] [PubMed]

114. de Paula, R.C.; da Silva, S.M.; Faria, K.F.; Frézard, F.; Moreira, C.P.D.S.; Foubert, K.; Lopes, J.C.D.; Campana, P.R.V.; Rocha, M.P.; Silva, A.F.; et al. In vitro antileishmanial activity of leaf and stem extracts of seven Brazilian plant species. *J. Ethnopharmacol.* **2018**, *232*, 155–164. [CrossRef]

115. Filho, D.E.S.; De Sousa, J.B.; Dos Santos, H.S.; Fontenelle, R.O.D.S. Compostos químicos isolados de extratos e óleos essenciais do gênero *Zanthoxylum* Linnaeus (Rutaceae) e seu potencial antimicrobiano. *Hoehnea* **2020**, *47*. [CrossRef]

116. Silva, S.L.D.; Chaar, J.D.S.; Figueiredo, P.D.M.S.; Yano, T. Cytotoxic evaluation of essential oil from CaseariasylvestrisSw on human cancer cells and erythrocytes. *ActaAmazonica* **2008**, *38*, 107–112.

117. Flaviane, G.P.; Ronaldo, M.; Letícia, O.C.; Adriano, C.-D.; Elisabeth, M.; Davyson, D.L.M.; Pereira, F.G.; Marquete, R.; Cruz, L.O.; Caldeira-De-Arujo, A.; et al. DNA damages promoted by the essential oil from leaves of *Casearia sylvestris* Sw. (Salicaceae). *J. Med. Plants Res.* **2016**, *10*, 818–822. [CrossRef]

118. Ribeiro, S.M.; Fratucelli, D.O.; Bueno, P.C.P.; De Castro, M.K.V.; Francisco, A.A.; Cavalheiro, A.J.; Klein, M.I. Antimicrobial and antibiofilm activities of Casearia sylvestris extracts from distinct Brazilian biomes against *Streptococcus mutans* and *Candida albicans*. *BMC Complement. Altern. Med.* **2019**, *19*, 308. [CrossRef]

119. Ribeiro, I.C.D.O.; Mariano, E.G.A.; Careli, R.T.; Morais-Costa, F.; De Sant'Anna, F.M.; Pinto, M.S.; De Souza, M.R.; Duarte, E.R. Plants of the Cerrado with antimicrobial effects against *Staphylococcus* spp. and Escherichia coli from cattle. *BMC Vet. Res.* **2018**, *14*, 32. [CrossRef]

120. da Cruz, J.E.R.; Saldanha, H.C.; e Freitas, G.R.O.; Morais, E.R. A review of medicinal plants used in the Brazilian Cerrado for the treatment of fungal and bacterial infections. *J. Herb. Med.* **2021**, *31*, 100523. [CrossRef]

121. Barros, L.M.; Duarte, A.E.; Morais-Braga, M.F.B.; Waczuk, E.P.; Vega, C.; Leite, N.F.; De Menezes, I.R.A.; Coutinho, H.D.M.; Rocha, J.B.T.; Kamdem, J.P. Chemical Characterization and Trypanocidal, Leishmanicidal and Cytotoxicity Potential of *Lantana camara* L. (Verbenaceae) Essential Oil. *Molecules* **2016**, *21*, 209. [CrossRef]

122. Postay, L.F.; Cabral, D.S.; Heringer, O.A.; Vieira, L.V.; de Moraes, L.R.; Freitas, G.; Gomes, L.C. The effectiveness of surfactants applied with essential oil of Lippia alba in the anesthesia of Nile tilapia (*Oreochromis niloticus*) and their toxicity assessment for fish and mammals. *Environ. Sci. Pollut. Res.* **2020**, *28*, 10224–10233. [CrossRef]

123. de Souza, R.C.; da Costa, M.M.; Baldisserotto, B.; Heinzmann, B.M.; Schmidt, D.; Caron, B.O.; Copatti, C.E. Antimicrobial and synergistic activity of essential oils of Aloysia triphylla and Lippia alba against Aeromonas spp. *Microb. Pathog.* **2017**, *113*, 29–33. [CrossRef]

124. Zamora, C.M.P.; Torres, C.A.; Nuñez, M.B. Antimicrobial Activity and Chemical Composition of Essential Oils from Verbenaceae Species Growing in South America. *Molecules* **2018**, *23*, 544. [CrossRef]

125. Nader, T.T.; Leonel, A.H.; Henrique, C.Y.; Contini, S.H.T.; Crevelin, E.J.; França, S.D.C.; Berton, B.W.; Pereira, A.M.S. Dynamized Aloysia Polystachya (Griseb.) Essential Oil: A Promising Antimicrobial Product. *Homeopathy* **2022**. [CrossRef]

Antifungal Activity of Essential Oil and Plant-Derived Natural Compounds against *Aspergillus flavus*

Fei Tian, So Young Woo, Sang Yoo Lee, Su Been Park, Yaxin Zheng and Hyang Sook Chun *

Food Toxicology Laboratory, School of Food Science and Technology, Chung-Ang University, Anseong 17546, Republic of Korea
* Correspondence: hschun@cau.ac.kr

Abstract: *Aspergillus flavus* is a facultative parasite that contaminates several important food crops at both the pre- and post-harvest stages. Moreover, it is an opportunistic animal and human pathogen that causes aspergillosis diseases. *A. flavus* also produces the polyketide-derived carcinogenic and mutagenic secondary metabolite aflatoxin, which negatively impacts global food security and threatens human and livestock health. Recently, plant-derived natural compounds and essential oils (EOs) have shown great potential in combatting *A. flavus* spoilage and aflatoxin contamination. In this review, the in situ antifungal and antiaflatoxigenic properties of EOs are discussed. The mechanisms through which EOs affect *A. flavus* growth and aflatoxin biosynthesis are then reviewed. Indeed, several involve physical, chemical, or biochemical changes to the cell wall, cell membrane, mitochondria, and related metabolic enzymes and genes. Finally, the future perspectives towards the application of plant-derived natural compounds and EOs in food protection and novel antifungal agent development are discussed. The present review highlights the great potential of plant-derived natural compounds and EOs to protect agricultural commodities and food items from *A. flavus* spoilage and aflatoxin contamination, along with reducing the threat of aspergillosis diseases.

Keywords: natural compounds; essential oil; antifungal agent; *Aspergillus flavus*; aflatoxin; mechanism of action

1. Introduction

Aspergillus flavus is a facultative parasite that naturally exists as a saprophytic soil fungus and contaminates several important food crops at both the pre- and post-harvest stages. The fungus causes diseases in agricultural crops, such as cottonseed, maize, peanuts, and tree nuts, alongside being an opportunistic animal and human pathogen that causes aspergillosis diseases (Figure 1) [1]. *A. flavus* produces aflatoxin, which is a carcinogenic and mutagenic polyketide secondary metabolite. Aflatoxin contamination represents a worldwide food safety concern that impacts both the marketability and safety of multiple food crops [2]. The global economic losses due to their contamination have been estimated to be in the hundreds of millions of dollars, while maize and peanuts are the most affected food crops. For example, the US Food and Drug Administration (FDA) estimates that aflatoxin contamination in maize alone could cause annual losses to the food industry ranging from 52.1 million USD to 1.68 billion USD. Although most aflatoxigenic fungi commonly grow in tropical and subtropical climates (35° N–35° S), zones with a perennial aflatoxin contamination risk have expanded due to global climate changes. *A. flavus* and aflatoxin contaminations are predicted to pose serious threats to many countries and regions in the near future [3].
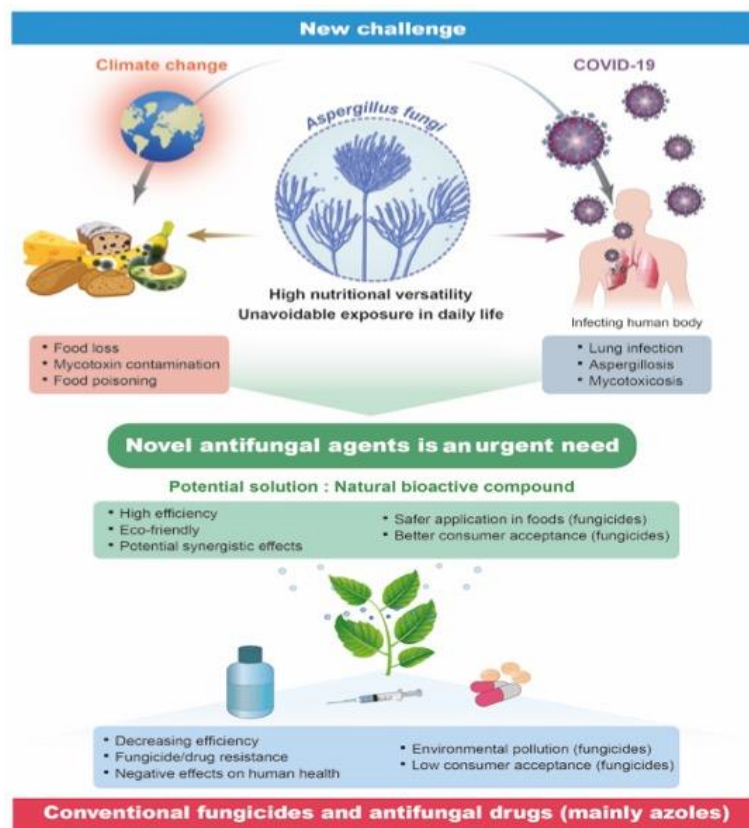
Figure 1. A schematic of the threat posed by *Aspergillus flavus* and the current measures available to combat it.

A. flavus also colonizes the soil and decays vegetation, which makes avoiding exposure to this fungus at home, at the workplace, or even during hospitalizations almost impossible [2]. Indeed, *A. flavus* is also isolated comparatively at a higher frequency from aspergillosis infections in humans, especially in developing countries. According to the US Centers for Disease Control and Prevention (CDC), the number of hospitalizations related to aspergillosis in the United States increased by an average of 3% per year during 2000–2013. Moreover, nearly 15,000 aspergillosis-associated hospitalizations occurred in the United States in 2014, at an estimated cost of 1.2 billion USD. Interestingly, most people breathe in *Aspergillus* spores every day without becoming ill. However, people with weakened immune systems or lung diseases are at a higher risk of developing health problems due to *Aspergillus*. For example, recent studies on ventilated patients with COVID-19 have reported a higher incidence of aspergillosis, affecting up to 30% of intubated patients [4].

The control of *A. flavus* and aflatoxin contamination usually focuses on inhibiting the development of spores and mycelia and/or the inactivation of aflatoxins by their transformation into nontoxic compounds. These processes depend primarily on chemical and physical approaches, including the use of synthetic fungicides, ozone fumigation, irradiation, dehulling or cooking processes, and manipulating environmental factors during harvests and storage. Most of the current strategies are expensive, time-consuming, and inefficient, while some even fail to protect the food without causing major changes in its physical properties and a serious loss of nutritive value. The continued application of synthetic fungicides is still the most effective and widely used recourse to control *A. flavus* and aflatoxin contamination. Synthetic fungicides, represented by azoles, which act by inhibiting the fungal cell membrane synthesis, are currently the major recourse for preventing *Aspergillus* contamination in food. However, despite the strict regulations on the application of chemical compounds in food, the use of synthetic fungicides can induce notable side effects, including toxicity to humans and animals, environmental pollution,

and the development of drug-resistant fungal pathogens [5,6]. For example, triazole fungicides are one of the most widely used broad-spectrum fungicides. Human exposure to triazole fungicides induces various adverse health effects, including developmental and hepatic toxicities, liver carcinogenicity, and reproductive toxicities. Recent studies also suggest that many triazole fungicides are potential endocrine disruptors and could interfere with steroid hormone biosynthesis in mammals [7]. Strobilurin fungicides are another group of fungicides that have been widely used in agriculture for decades. Studies have confirmed the cytotoxicity and genotoxicity of strobilurin fungicides to human peripheral blood lymphocytes [8]. Aspergillosis treatments also depend on the use of azole antifungal drugs (e.g., voriconazole and itraconazole), to which an increasing number of fungal species have developed resistance. Meanwhile, consumers' demand for healthier and more sustainable food products is also increasing. In response, the food industry is reformulating its products to replace artificial food additives and preservatives with natural, label-friendly alternatives [9]. Therefore, the development of novel antifungal agents that effectively inhibit the growth, mycotoxin biosynthesis, and pathogenicity of *A. flavus* is in urgent need.

Most plants produce natural antimicrobial agents, either as part of their normal growth and development or in response to microbial infections or environmental stresses. Many plant-derived natural compounds and herbal extracts, such as phenols, terpenes, and terpenoids, have great potential for utilization in the combat of both foodborne and human pathogens [9]. Besides being highly effective, many plant-derived natural compounds are safe for human health and biodegradable, which makes them attractive substitutes for synthetic preservatives. Although plant-derived natural compounds seem promising for the development of novel antifungal and antiaflatoxigenic strategies against *A. flavus*, the lack of in situ and in vivo studies regarding their activities and the limited understanding of their mechanisms of action, as well as the lack of cost-benefit and ecotoxicity assessments, have largely deterred their application in the development of novel antifungal agents. Furthermore, standardized commercial productions require the consideration of multiple factors, including plant varieties, plant nutrition, geographic location, seasonal variation, surrounding climate, agronomic practices, and methods of extraction and storage [10]. Therefore, further studies are required to understand their physicochemical properties and possible mechanisms of action. Hence, this review aims to provide an overview of the published data on these issues. Moreover, the information provided here can facilitate the implementation of plant-derived natural compounds as natural antifungal agents in food preservation and human health protection.

2. Antifungal and Antiaflatoxigenic Activities of Plant-Derived Natural Compounds against *A. flavus*

Plant-derived natural compounds are known to have broad-spectrum antimicrobial activities and diverse effects on microbial physiological and metabolic activities. Many studies have demonstrated that plant-derived natural compounds or essential oils (EOs) exhibit antifungal and antiaflatoxigenic activities against *A. flavus*. Many previous studies were conducted in vitro using direct-contact antimicrobial assays [10–15]. Some plant-derived natural compounds have been similarly tested on food materials, such as corn, wheat, soybean, chickpea, pistachio, peanut, and rice (Table 1). The most widely invested plant-derived natural compounds or EOs against *A. flavus* and aflatoxin contamination in food materials are isolated from food-flavoring plants, such as clove (*Syzygium aromaticum* L.), cinnamon (*Cinnamomum zeglanicum*, *C. verum*), oregano (*Origanum vulgare* L.), and thyme (*Thymus vulgaris* L.). These plants and their EOs or extracts have been used in food preparation for centuries and are categorized as "generally recognized as safe" (GRAS) by the U.S. FDA. Moreover, many of them possess beneficial effects on the human body, which, combined, makes them the ideal sources of safe, natural, antifungal, and antiaflatoxigenic agents.

Table 1. In situ antifungal and antiaflatoxigenic activities of plant-derived natural compounds against *A. flavus* in different food systems.

Name of the Plant	Major Components	Food Systems	Antifungal Activity	Antiaflatoxigenic Activity	References
Ageratum conyzoides	β-Caryophyllene; germacrene-D; dimetoxy ageratocromene	Wheat; corn; soybean	80.8% inhibition at 1 μL/mL (vapor) in wheat grain (12 months); 79.5% and 100% inhibition in corn and soybeans, respectively, with 5 μL EO (disk diffusion assay, 5 days)	93.7% reduction with 50 μL in 60 g corn (direct contact) (10 days); >75% reduction with 50 μL in 60 g in soybeans (direct contact) (10 days)	[16,17]
Ajowan (*Trachyspermum ammi* L.)	*p*-Cymene; thymol	Wheat; chickpea	46.2% and 65.2% inhibition at 0.8 μL/mL (vapor) in wheat and chickpea, respectively (12 months)	100% inhibition at 0.8 μL/mL (vapor) in wheat and chickpea (12 months)	[18]
Anise (*Pimpinella anisum* L.)	Anethol	Corn; wheat	MIC: 1000–3000 μg/g (dependent on aw) in corn (11 days); 100% inhibition at 1% (*v/w*) in wheat (14 days)	100% inhibition at 1000 → 3000 μg/g (dependent on aw) in corn (11 days); 100% inhibition at 1% (*v/w*) in wheat (8 weeks)	[6,19]
Boldo (*Pëumus boldus* Mol)	α-Terpinolene; α-terperpine; *p*-cimene	Corn	MIC: 500–2000 μg/g (dependent on aw) (11 days)	100% inhibition at 500–2000 μg/g (dependent on aw) (11 days)	[6]
Boswellia carterii Birdw	Phenylethyl alcohol; benzyl acetate	Pepper fruits (*Piper nigrum* L.)	65.4% inhibition at 1.75 μL/mL (vapor) (6 months)	No record	[20]
Boswellia serrata	3-Carene; β-ocimene	Corn	No record	95.6% inhibition at 10 μL/g (10 days)	[21]
Cananga odorata	β-Caryophyllene	Chickpea	77.4% inhibition at 2 μL/mL (vapor) (6 months)	No record	[22]
Caraway (*Carum carvi*)	Limonene; carvone	Bread; polenta	90% inhibition at 636.47 μL/L (vapor) in bread (14 days)	100% inhibition in bread requires > 500 μL/L of EO (vapor) (14 days); 100% inhibition at 4.5 μg/g in polenta (14 days)	[23,24]
Carum copticum	*p*-Cymene; γ-terpinene; thymol	Cherry tomato	58.0% inhibition at 100 μL/mL (vapor) (30 days)	No record	[25]
Chenopodium ambrosioides Linn.	α-Terpinene; *p*-cymene; Ascaridole	Pigeon pea	100% inhibition at 0.29 μL/mL (vapor) (6 months)	No record	[26]
Cicuta virosa L. var. *latisecta* Celak	*p*-Cymene; γ-terpinene; cuminaldehyde	Cherry tomato	89.9% inhibition at 200 μg/mL (vapor) (9 days)	No record	[27]
Cinnamomum glaucescens	1,8-Cineole; 2-propenoic acid	Chickpea	71.1% inhibition at 4.5 μL/mL (vapor) (12 months)	No record	[28]
Cinnamon (*Cinnamomum verum*)	Cinnamaldehyde; eugenol	Maize extract medium; bread	90% inhibition at 820 → 1000 mg/L (depending on temperature and water activity) in maize extract medium (12 days); 90% inhibition at 558.44 μL/L (vapor) in bread (14 days)	500–1000 mg/L (depending on temperature and water activity) in maize extract medium (12 days); 100% inhibition at 500 μL/L (vapor) in bread (14 days)	[23,29]
Cinnamon (*Cinnamomum zeglanicum*)	Cinnamaldehyde; eugenol; phenol, 2-methoxy-4-(2-propenyl)phenol	Pistachio; finger millet (*Eleusine coracana*); wheat	60–83% inhibition at 0.5 μL/mL (vapor) in finger millet (up to 6 months); 100% inhibition at 2% (*v/w*) in wheat (14 days)	100% inhibition with 25 mL of 9% (vol/vol) EO solution in 500 g pistachio (3 months); 100% inhibition at 2% (*v/w*) in wheat (8 weeks)	[19,30,31]
Citrus reticulata	Limonene; geranial; neral	Tuberous roots of *Asparagus racemosus*	68.6% inhibition at 500 ppm (*v/v*) (12 months)	61.76% inhibition at 500 ppm (*v/v*) (12 months)	[32]

Table 1. *Cont.*

Name of the Plant	Major Components	Food Systems	Antifungal Activity	Antiaflatoxigenic Activity	References
Clausena pentaphylla	Sabinene; α-terpinolene; methyl eugenol	Pigeon pea seed	100% inhibition at 0.29 μL/mL (vapor) (6 months)	No record	[33]
Clove (*Caryophyllus aromaticus*)	eugenol	Pistachio	No record	100% inhibition with 25 mL of 9% (vol/vol) EO in 500 g pistachio (3 months).	[30]
Clove (*Syzygium aromaticum* L.)	Benzenemethanol; eugenol; eugeyl acetate; β-caryophyllene	Corn; Iranian white cheese; bread; tomato paste	100% inhibition at 500–3000 μg/g (dependent on water activity) in corn (11 days); 100% inhibition at 10 μL/L (vapor) in corn (5 days); 100% inhibition at 150 ppm in Iranian white cheese (up to 40 days); 90% inhibition at 674.49 μL/L (vapor) in bread (14 days); 48% inhibition at 500 ppm in tomato paste (2 months)	100% inhibition at 1000–2000 μg/g (dependent on water activity) in corn (11 days); 100% inhibition at 10 μL/L (vapor) in corn (5 days); 100% inhibition at 50–150 ppm in Iranian white cheese (up to 40 days); 100% inhibition at 500 μL/L (vapor) in bread (14 days);	[6,23,34–36]
Coleus aromaticus	Thymol; γ-terpinene; *p*-cymene	Wheat	87.37% inhibition at 0.1 μL/mL (vapor) (12 months);	No record	[16]
Commiphora myrrha	α–Elemene; curzerene; furanoeudesma-1,3-diene	Chickpea	55.4% inhibition at 3 μL/mL (vapor) (6 months)	No record	[22]
Coriander (*Coriandrum sativum* L.)	Linalool; λ-terpinene	Chickpea	65.5% inhibition at 2.5 μL/mL (vapor) (6 months)	No record	[22]
Cymbopogon citratus	Geranial; neral; myrcene	Tuberous root of *Asparagus racemosus*	78.4% inhibition at 500 ppm (*v/v*) (12 months)	100% inhibition at 500 ppm (*v/v*) on (12 months)	[32]
Dill (*Anethum graveolens* L.)	Carvone; limonene; apiol	Cherry tomato	88.9% inhibition at 120 μg/mL (vapor) (9 days)	No record	[37]
Fennel (*Foeniculum vulgare*)	Estragole; anethole	Tobacco leave	51.20–55.35% inhibition at 1.25 μL/mL (vapor) (6 months);	100% inhibition at 1.25 μL/mL (vapor) (6 months);	[38]
Fingerroot (*Boesenbergia rotunda*)	Nerol; L-camphor	In-shell peanut	No record	98.3% and 18.0% inhibition at 16% (*v/v*, in mineral oil) when applied via direct exposure and vapor exposure, respectively (10 days).	[39]
Hedychium spicatum	1,8-Cineole	Chickpea	72.0% inhibition at 2.5 μL/mL (vapor)	No record	[22]
Holy basil (*Ocimum sanctum*)	Eugenol; β-caryophyllene	Apocynaceae (*Rauvolfia serpentina* L., medicinal plant)	74.0% inhibition at 1 μL/mL (vapor) (6 months)	No record	[40]
Hyptis suaveolens	β-Caryophyllene; caryophyllene oxide; sabinene	Wheat	83.3% inhibition at 1.2 μL/mL (vapor) (12 months)	No record	[16]
Juniper (*Juniperus communis* L.)	α-Pinene	Polenta	No record	100% inhibition at 50 μg/g (14 days)	[24]
Lemongrass (*Cymbopogon citrati* [DC] Stapf.)	Neral; geranial	Bread	90% inhibition at 134.12 μL/L (vapor) (14 days)	100% inhibition at 125 μL/L (vapor) (14 days)	[23]
Lippia alba	Myrcene; neral; geranial	Green gram seed	92.5% inhibition at 80 μL/0.25 L (vapor) (6 months)	100% inhibition at 80 μL/0.25 L (vapor) (6 months)	[41]
Litsea cubeba	D-Limonene; (Z)-limonene oxide; (E)-limonene oxide	Licorice	100% inhibition at 5 μL/g (vapor) (20 days);	100% inhibition at 5 μL/g (vapor) (20 days);	[42]
Marjoram (*Origanum majorana* L.)	Terpinen-4-ol; cis-sabinene hydrate; *p*-cymene	Chickpea	67.9% inhibition at 3 μL/mL (vapor) (6 months)	No record	[22]

Table 1. *Cont.*

Name of the Plant	Major Components	Food Systems	Antifungal Activity	Antiaflatoxigenic Activity	References
Mentha spicata L.	Carvone; limonene	Chickpea	52.2% inhibition at 1 µL/mL (vapor) (12 months);	100% inhibition at 1 µL/mL (vapor) (12 months);	[43]
Michelia alba	Linalool	Brown rice	100% inhibition at 300 µL/L (vapor) (12 weeks)	No record	[44]
Mint (*Mentha viridis*)	Menthone; carvone	Wheat; corn	100% inhibition at 200 mL/100 g in corn (21 days); 92% inhibition at 2% (*v/w*) in wheat (14 days)	100% inhibition at 300 mL/100 g in corn (21 days); >99% inhibition at 2% (*v/w*) in wheat (8 weeks)	[19,45]
Mountain thyme (*Hedeoma multiflora* Benth)	α-Terpinolene; *p*-cymene; carvacrol	Corn	100% inhibition at 500–2000 µg/g (dependent on water activity) (11 days);	100% inhibition at 1000 µg/g (11 days);	[6]
Ocimum basilicum L.	Methyl eugenol	Dry fruits (cashew nut, almond, grapes, chironji, groundnut, date palm, and coconut)	53.8–65.5% inhibition at 1 µg/mL (vapor) (6 months)	No record	[46]
Oregano (*Origanum vulgare* L.)	Carvacrol; linalool; 4-terpineol	Maize extract medium; bread; corn; soybean	90% inhibition at 820 → 1000 mg/L (depending on temperature and water activity) in maize extract medium (12 days); 90% inhibition at 319.85 µL/L (vapor) in bread (14 days); 100% inhibition with 5 µL EO in corn and soybean (disk diffusion assay, 5 days)	100% inhibition at >1000 mg/L in maize extract medium (12 days); 100% inhibition at 125 µL/L (vapor) in bread (14 days); >90% and 88.16% inhibition with 200 µL EO in 60 g corn and soybean, respectively (direct contact) (10 days)	[17,23,29]
Pine (*Pinus pinaster*)	β-Caryophyllene; β-selinene	In-shell peanut	No record	98.1% and 12.9% inhibition at 16% (*v/v*, in mineral oil) when applied via direct exposure and vapor exposure, respectively (10 days)	[39]
Poleo (*Lippia turbinate* var. integrifolia (griseb))	Peperitenone oxide; limonene	Corn	100% inhibition at 500–2000 µg/g (depending on water active) (11 days)	100% inhibition at 500–2000 µg/g (depending on water active) (11 days)	[6]
Rosewood (*Aniba rosaeodora*)	Linalool	In-shell peanut	No record	98.5% and 17.2% inhibition at 16% (*v/v*, in mineral oil) when applied via direct exposure and vapor exposure, respectively (10 days)	[39]
Rosmarinus officinalis L.	α-Pinene; 1, 8-cineole; camphor	Black pepper (*Piper nigrum*)	73.5% inhibition at 1.5 µL/mL (vapor) (6 months);	No record	[47]
Styrax tonkinensis	Benzoic acid; 6-phenyl-tetrahydro-naphthaline	In-shell peanut	No record	95.8% and 20.2% inhibition at 16% (*v/v*, in mineral oil) when applied via direct exposure and vapor exposure, respectively (10 days).	[39]
Summer savory (*Satureja hortensis*)	γ-terpinene; carvacrol; thymol	Tomato paste	59% inhibition at 500 ppm (2 months)	No record	[36]
Thyme (*Thymus vulgaris* L.)	Carvacrol; a-terpinolene; thymol; *p*-cymene; β-phellandrene; linalool	Bread; tomato paste; wheat; brown rice; white rice	90% inhibition at 474.2 µL/L (vapor) in bread (14 days); 87% inhibition at 500 ppm in tomato paste (2 months); 100% inhibition at 1% (*v/w*) in wheat (14 days)	100% inhibition at 250 µL/L (vapor) in bread (14 days); 100% inhibition at 1% (*v/w*) on wheat (8 weeks); 72.7% inhibition at 10 µg/mL (vapor) in brown rice; 18.0% inhibition at 10 µg/mL (vapor) in white rice	[19,23,36,48]

Table 1. *Cont.*

Name of the Plant	Major Components	Food Systems	Antifungal Activity	Antiaflatoxigenic Activity	References
Thyme (*Zataria multiflora*)	Thymol; carvacrol	Iranian white cheese	89.0% inhibition at 600 ppm (up to 40 days)	92.9% inhibition at 600 ppm (up to 40 days)	[35]
Thymus daenensis Celak	Thymol; carvacrol	Pistachio	No record	100% inhibition with 25 ml of 9% (vol/vol) EO solution in 500 g pistachio (3 months)	[30]
Turmeric (*Curcuma longa* L.)	Tumerone; ar-turmerone; β-sesquiphellandrene; zingiberene; cycloisolongifolene	Corn	~90% inhibition at 4 µg/mL (5 days)	~93% inhibition at 4 µg/mL (5 days)	[49]
Vatica (*Vatica diospyroides* Symington)	Benzyl acetate	Corn	100% inhibition at 50 µL/L (vapor) (5 days)	100% inhibition at 50 µL/L (vapor) (5 days)	[34]
Ylang ylang (*Cananga odorata*)	Linalool; benzyl acetate; tetradecane; germacrene D	In-shell peanut	No record	96.4% and 25.1% inhibition at 16% (*v/v*, in mineral oil) when applied via direct exposure and vapor exposure, respectively (10 days).	[39]
Zanthoxylum alatum	Linalool; methyl cinnamate	Black pepper (*Piper nigrum*)	87.6% inhibition at 2.5 µL/mL (vapor) (6 months)	No record	[50]
Zanthoxylum molle Rehd	Limonene; terpinen-4-ol; 2-undecanone	Cherry tomato	91.7% inhibition at 0.2 µg/mL (vapor) (9 days)	No record	[51]
Zingiber zerumbet	α-Caryophyllene; zerumbone	Corn	100% inhibition at 200 ppm (15 days)	100% inhibition at 100 ppm (direct contact) (15 days)	[52]
Ziziphora clinopodioides	Pulegone; piperitenone; *p*-menth-3-en-8-ol	Corn	No record	99.8% inhibition at 6250 µg/mL (29 days)	[53]

The antifungal agents extracted from different plants are highly diverse [54,55]. Most of the plant-derived natural compounds that exhibit antifungal activity are phenols, terpenes, and terpenoids [9]. The antimicrobial activity of phenols is closely connected with their hydroxyl group, which is bonded directly to a benzene ring. The presence of a free hydroxyl group enables phenols to exchange their proton, thus, promoting their ability to modify the cell membrane integrity of microbes [56]. Meanwhile, the hydroxyl group's relative position on the benzene ring can potentially affect their antimicrobial efficacy. Tian et al. investigated the structure–activity relationships of plant-derived flavonoids against *A. flavus* growth and aflatoxin biosynthesis. Flavonoids represent the largest group of naturally occurring phenolic compounds, and Tian et al. identified that the [–OH] or [–O–CH$_3$] groups at position 6 of ring A and position 4′ of ring B are closely associated with the antifungal and antiaflatoxigenic activities of natural flavonoids [57]. Regarding terpenes, the connection between their structure and functional groups and their antimicrobial activities remains unclear. Previously, the number of double bonds and acyclic, monocyclic, and bicyclic structures in terpenes has been shown to limit their antimicrobial activities [9,58]. Terpenoids are suggested to possess greater antimicrobial activities than most terpenes, and these activities are mainly determined by their functional groups, such as alcohols and aldehydes [59]. Furthermore, their hydrogen-bonding capacity and relative solubility could potentially affect their antimicrobial activities.

The efficiency of plant-derived natural compounds against fungal growth and mycotoxin production is affected by environmental factors, including light, oxygen, pH, temperature, and water activity. Light exposure and high amounts of oxygen in packaging generally decrease the antimicrobial efficiency of plant-derived natural compounds, probably through oxidation [60]. Passone et al. reported that exposing boldo (Pëumus boldus Mol.) to UV light and sunlight for 30 min reduced the EOs' antifungal activity by 29.1% and 29.6%, respectively [61]. The antimicrobial effects of plant-derived natural compounds tend to increase as environmental pH levels decrease [62]. The hydrophobicity of plant-derived natural compounds has been reported to increase at low pH levels since these

dissolve in the lipids of microbial cell membranes more easily. Temperature is a key factor in the growth and mycotoxin production of *A. flavus*. The susceptibility of microbials to plant-derived natural compounds generally increases as storage temperatures decrease [60]. Meanwhile, the antifungal ability of plant-derived natural compounds is usually stable against alterations in temperature. Passone et al. evaluated the antifungal activity of EOs in boldo (*P. boldus* Mol.) and poleo (*Lippia turbinata*) following exposure to various temperatures (40, 60, and 80 °C). They observed the same level of inhibition against *A. flavus* [61]. Sharma and Tripathi tested the thermostability of *Citrus sinensis* L. EOs against *A. niger* following exposure to temperatures of 40, 60, 80, 100, and 121 °C and found that the activity of *C. sinensis* EOs did not change after any of the treatments [62]. Furthermore, the antifungal and antiaflatoxigenic efficiencies of EOs are closely dependent on the water activity of the substrate. Generally, as the water activity decreases, the fungal growth is unfavored, and the antifungal activity of the EOs is promoted. The antiaflatoxigenic effects of EOs increase at relatively low water activities [61].

The interactions between individual plant-derived natural compounds may cause synergistic or antagonistic effects. For example, several studies report that a mixture of the major components of an essential oil exhibits weaker antibacterial activity than the whole EO, most likely due to the remaining missing components [63,64]. Currently, the majority of studies regarding the synergistic antifungal effects of plant-derived natural compounds have focused on the interactions of phenols, terpenes, and terpenoids. Songsamoe et al. tested the synergistic effect of linalool and caryophyllene and found that a 10:1 ratio was key to enhancing the antifungal activity of M. alba EOs against *A. flavus* [44]. Stević et al. likewise demonstrated that the synergistic activity between thymol and carvacrol plays an important role in the overall antifungal activity of thyme and oregano EOs [65]. The synergistic antifungal effects of different EOs have been further reported. For example, a combination of oregano and thyme EOs resulted in a synergistic antifungal effect against a variety of food pathogens, including *A. flavus*, *A. parasiticus*, and *P. chrysogenum*. Moreover, mixtures of peppermint and tea tree EOs exhibited synergistic effects against *A. niger* [66]. However, it remains extremely difficult to predict the antimicrobial efficacy of EO mixtures since each EO is a complex mixture of different chemical compounds, and interactions between the individual components can produce both synergistic and antagonistic antimicrobial effects [67]. The interaction between EO compounds and those in the food matrix could potentially affect the antifungal and antiaflatoxigenic efficiencies of EOs. Tian et al. evaluated the antiaflatoxigenic activity of thyme EOs in brown and white rice [48]. Here, thyme EOs reduced aflatoxin accumulation by up to 72.7% in brown rice but by only 18.0% in white rice. Brown rice contains higher levels of fiber, minerals, phenolic compounds, protein, and vitamins compared with white rice [68], which may partly contribute to its resistance to aflatoxin contamination. Further suggestions include a potential interaction between the EO's phenolic compounds and those in white rice, while the possible synergistic effects between these bioactive constituents can promote the antiaflatoxigenic activity of this EO.

The synergistic antifungal effects of plant-derived natural compounds with fungicides and antifungal drugs have also been reported. For example, baicalein, a flavonoid originally isolated from *Scutellaria baicalensis* and *Scutellaria lateriflora*, showed no antifungal effects against *A. flavus* when tested at a concentration of 4 μg/mL in an in vitro test. However, at the same concentration, baicalein was able to reduce the 80% effective concentrations of strobilurins (azoxystrobin and pyraclostrobin) from 4 μg/mL and 0.125 μg/mL to 0.5 μg/mL and 0.016 μg/mL, respectively [69,70]. Cinnamaldehyde was reported to show strong synergy with fluconazole antifungal drugs against the human pathogenic fungus *A. fumigatus* by reducing the minimum inhibitory concentration of fluconazole from 200 μg/mL to 25 μg/mL in vitro [71]. Plant-derived natural compounds are suggested to promote the antifungal activity of fungicides and drugs by increasing the bioavailability of co-administered drugs in fungal cells through the inhibition of metabolizing enzymes, such as cytochrome P450 isoforms and multi-drug or efflux transporters [72–74]. Plant-

derived natural compounds are able to boost the antifungal efficiency of commonly used antifungal agents while reducing their required amounts for the effective inhibition of fungal contamination and infections, and, hence, they may lower the potential toxic effects on humans. Therefore, plant-derived natural compounds represent a good source of combined agents for antifungal treatments or therapies. Further studies on the in vivo and in situ synergistic effects of plant-derived natural compounds with fungicides and antifungal drugs are of great significance.

3. Antifungal Mechanisms of Plant-Derived Natural Compounds and EOs against *A. flavus*

3.1. Acting on the Cell Wall of A. flavus

Different plant-derived natural compounds may target various kinds of microbes and execute their antimicrobial activity through numerous mechanisms. Meanwhile, the antifungal effects of natural compounds often have multiple targets, including the cell wall, cell membrane, mitochondria, and metabolic enzymes. Accordingly, their antifungal mechanisms of action may be due to physical, chemical, or biochemical changes in these cell components. Fungi have a unique cell wall structure that is absent in humans. It is comprised of a complex and dynamic structure of chitin, glycans, and glycoproteins, which fulfills several essential functions connected with the interaction between the cell and its environment. Indeed, the fungal cell wall is involved in the morphogenesis of fungal cells, the protection of the protoplasts from physical damage and osmotic stress, cell recognition in various interactions, and the exchange of nutrients and metabolic products, alongside drug resistance against antifungal agents [75]. Cumulatively, these properties make the fungal cell wall a promising target for antifungal agents. Chitin and glucan are mainly located in the inner layer of the fungal cell wall. In most filamentous fungi, chitin consists of β-1,4-linked N-acetylglucosamine and is covalently linked to β-1,3-glucan, which provides the structural integrity and physical strength of the cell wall [28,29]. Therefore, the disruption of chitin biosynthesis causes disorder in the fungal cell wall, which leads to cell lysis and death [26]. Many successful antifungal agents, such as nikkomycin and polyoxin, perform their antifungal activity by specifically inhibiting fungal chitin synthase (Figure 2). Another major cell wall polysaccharide in filamentous fungi is β-1,3-glucan, which is essential for proper cell wall formation and normal cellular development [27]. Antifungal agents, such as caspofungin, micafungin, and anidulafungin, inhibit β-1,3-glucan synthase and, consequently, can disrupt the fungal cell wall formation, preventing fungal growth. In the outer layer of the fungal cell wall, cell wall-associated proteins are covalently bound to mannan and form mannosylated glycoproteins [34–36]. These proteins perform a wide range of functions and are involved in various cellular activities, including cell-to-cell interactions, trafficking of nutrition and macromolecules, providing protection against toxic substances, and cell surface adhesion.
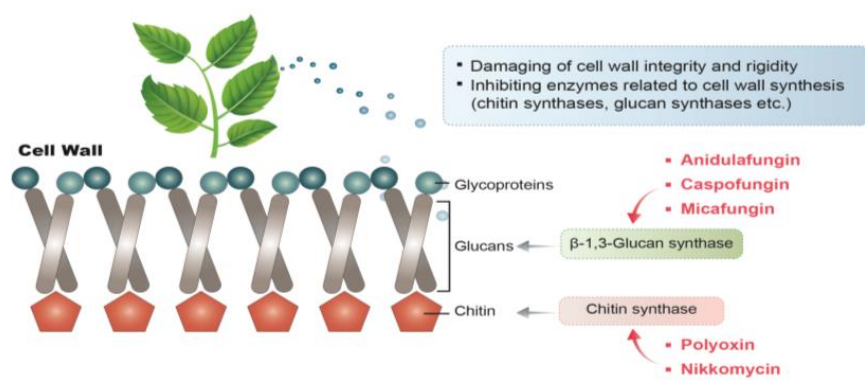

Figure 2. Mechanisms of action of plant-derived natural compounds and antifungal agents acting on the cell wall of *A. flavus*.

The antifungal activity of numerous plant-derived natural compounds and EOs was reported to damage the integrity and rigidity of the *A. flavus* cell wall. For example, paeonol (2-hydroxy-4-methoxyacetone), which is an active component commonly isolated from *Cynanchum paniculatum*, is reported to alter the cell wall ultrastructure and reduce the content of both β-1,3-glucan and chitin in *A. flavus* [76]. Similarly, extracts of *Tulbaghia violacea* were found to reduce the content of β-1,3-glucan and chitin in the *A. flavus* cell wall [77]. Indeed, da Silva and co-workers tested the antifungal effects of *R. officinalis* L. EOs and observed significant microscopic morphological changes, including cell wall rupturing and cytoplasmic leakage [78]. Such modifications are potentially associated with plant-derived natural compounds interfering with the enzymes related to cell wall synthesis. The building blocks of the fungal cell wall, such as chitins, glucans, and pectins, are continuously remodeled to cope with fungal growth and development by different enzymes, such as chitin and glucan synthases, glycohydrolases, and transglycosidases [79]. Fungicides have been developed by targeting the related enzymes, including polyoxins (which inhibit chitin synthesis), echinocandins (which inhibit β-1,3-glucan synthase), and tricyclazole (which inhibits melanin synthesis). Several plant-based natural compounds are known to inhibit cell wall synthases. Indeed, Marei et al. found that thymol and limonene had inhibitory effects on fungal cellulase and pectin methyl esterase [80]. Additionally, Bang et al. reported that cinnamaldehyde inhibits chitin synthase and β-1,3-glucan synthase [81].

3.2. Acting on the Cell Membrane of A. flavus

Fungal membranes have been proposed as the major targets for the antifungal activity of plant-based natural compounds (Figure 3). The ability to pass through the cell wall and penetrate the cell membrane is fundamental for their antifungal activity. Natural compounds may affect fungal membranes through several mechanisms of action, including: (1) altering membrane fluidity and permeability; (2) reducing the proton motive force; (3) damaging membrane proteins; (4) inhibiting enzymes related to membrane synthesis; (5) inducing cytoplasmic membrane degradation [82–84]. These alterations in the cell membrane result in the loss of cell homeostasis, leakage of cell components, and, ultimately, cell death. Plant-based natural compounds, such as thymol, carvacrol, and eugenol, have been reported to cause ion imbalance across the cell membrane by dissipating H+ and K+ ion gradients, thus, facilitating the leakage of vital cellular components and inducing water stress, alongside intracellular ATP depletion [85]. Numerous plant-based natural compounds act by binding to membrane ergosterol or inhibiting its biosynthesis. Ergosterol is the main sterol derivative of fungi and is essential for preserving cell membrane functionality and maintaining the cell's integrity, viability, and normal growth functions [86]. Since ergosterol is essential to fungal cells, antifungal drugs and fungicides have been developed and widely applied to act through the same mechanism in both clinical and agricultural antifungal practices. Among them, polyenes (which bind to ergosterol) and azoles (which inhibit ergosterol synthesis) are the most successful. Freires and co-workers found that coriander (*C. sativum* L.) EO could bind to the fungal membrane ergosterol and increase ionic permeability to cause membrane damage, leading to cell death [87]. Tian et al. reported that *C. jensenianum* EOs inhibited ergosterol biosynthesis in *A. flavus* [88]. A similar effect was also detected with natural compounds extracted from dill (*A. graveolens* L.), thyme (*T. vulgaris* L.), and turmeric (*C. longa* L.) [49,89,90]. Moreover, treatments with the plant-derived natural monoterpene citral downregulated ergosterol biosynthetic genes (e.g., *erg7*, *erg11*, *erg6*, *erg3*, and *erg5*) [91]. Lipophilic natural compounds, such as phenols and aldehydes, can pass through the double phospholipid bilayer and interact with ergosterol or enter the nucleus and regulate its biosynthetic genes. Ultimately, this causes cell membrane modification, fatty acid profile alterations, and osmotic imbalances, which lead to irreversible damage to the membrane and morphological alteration in hyphae, conidiophores, and conidia and, finally, cell death [9]. The attachment or penetration of the natural compounds via the fungal membranes may prompt the cell structures to disintegrate, causing the fungal cells to become more permeable to the compounds. Phenols, such as thymol,

carvacrol, and eugenol, possess a system of delocalized electrons and may also reduce the pH gradient across the cytoplasmic membrane by acting as proton exchangers. The collapse of the proton motive force and the depletion of the ATP pool, resulting from such an effect, can lead to the leakage of iron and intracellular cell constituents and, eventually, cause cell death [92]. Terpenoids also execute their antimicrobial activity at the cell membrane level. It has been reported that terpenoids disrupt the membrane permeability by altering the membrane fatty acid composition and ergosterol content, which results in leakage of the cell contents [93].
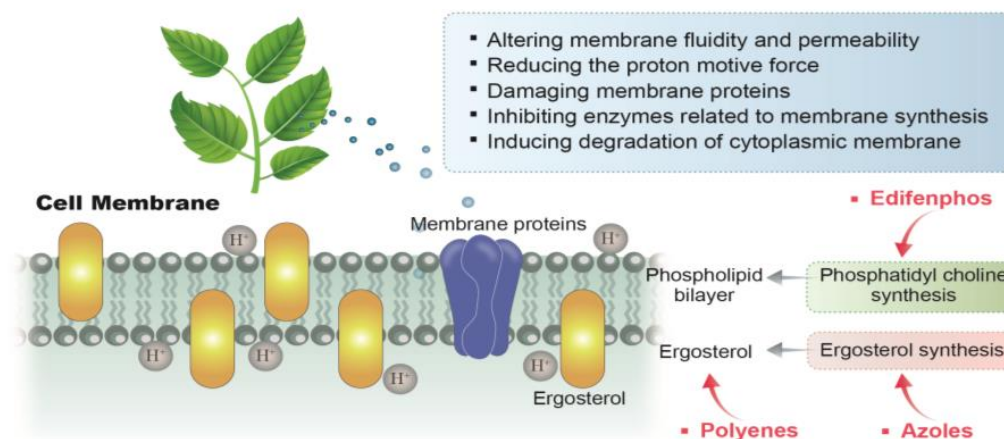

Figure 3. Mechanisms of action of plant-derived natural compounds and antifungal agents acting on the cell membrane of *A. flavus*.

3.3. Acting on the Mitochondria of A. flavus

Mitochondria play wide-ranging roles in fungal cells. Mostly known for their role in cellular respiration, mitochondria are also associated with other important cellular functions related to virulence, developmental and morphogenetic transitions, drug resistance, ergosterol biosynthesis, and cell wall maintenance [94]. The respiratory chain has been proven to be an effective target for fungicides to control fungal contamination in food crops. Quinone outside-inhibiting (QoI) fungicides, represented by strobilurins, are the most important group of fungicides developed for respiration inhibition (Figure 4). QoI fungicides inhibit fungal pathogens by blocking the transfer of electrons at the quinone outer binding site of the mitochondrial complex III, thus, reducing the production of ATP, which leads to a reduction in the normal metabolic functions and, eventually, cell death. Plant-derived natural compounds and EOs also appear to inhibit fungal growth by damaging mitochondria. For example, (E)-2-hexenal, a leaf volatile produced naturally by green plants as a defense response, was found to inhibit the mitochondrial dehydrogenases and disrupt the mitochondrial energy metabolism of *A. flavus* [95,96]. Honokiol, a phenolic compound isolated from the plant *Magnolia officinalis*, caused mitochondrial hyperpolarization and dysfunction and led to ATP depletion in *A. flavus* [97]. Dill (A. graveolens L.) EOs were reported to reduce *A. flavus* growth by promoting mitochondrial dysfunction and the accumulation of reactive oxygen species (ROS) [90]. Tea tree EO was also found to damage the mitochondria of *Botrytis cinerea* [98]. However, the exact mechanisms through which dill and tea tree EOs function are not fully understood. It has been suggested that these EOs may contain natural compounds that can modulate mitochondrial functions by (1) disrupting the mitochondrial membrane, (2) inhibiting mitochondrial enzymes, (3) suppressing oxidative phosphorylation, and (4) altering the mitochondrial redox balance. Li et al. reported that tee tree EOs can destroy the mitochondrial morphology and function in *B. cinerea* by increasing the mitochondrial membrane permeability and decreasing the enzymatic activities related to the tricarboxylic acid (TCA) cycle (malic dehydrogenase, succinate dehydrogenase, ATPase, citrate synthetase, isocitrate dehydrogenase, and α-ketoglutarate dehydrogenase). These alterations subsequently result in matrix loss, accumulation of

ROS, and increased mitochondrial irregularity [98]. Zheng et al. determined that citral exerted antifungal activity by altering the mitochondrial morphology, which resulted in the loss of the mitochondrial matrix and mitochondrial collapse [99]. Tian et al. also detected mitochondrial morphological alterations in *A. flavus* treated with dill EOs and suggested that these are caused by an increase in the mitochondrial membrane permeability, malfunctions in the cellular metabolism, and a breakdown of the mitochondrial matrix [90]. Additionally, plant-based natural compounds may be able to damage fungal mitochondria by disrupting the osmotic balance, causing calcium and protons to leak, and, consequently, altering the electrochemical potentials. For example, Rao and co-workers reported that carvacrol was able to induce calcium stress in yeast's mitochondria through the activation of the target of rapamycin (TOR) signaling pathway [100]. Some EOs contain natural compounds that can induce mitochondrial dysfunction via the inhibition of mitochondrial enzymes. For example, turmeric (*C. longa* L.) EOs were found to inhibit ATPase, malate dehydrogenase, and succinate dehydrogenase in *A. flavus* mitochondria, thus, suppressing its contamination in maize [49]. Dill EOs were also found to inhibit fungal ATPase [101]. Phenols and aldehydes in plants have been suggested to be the major natural compounds that interact with mitochondrial enzymes [102].
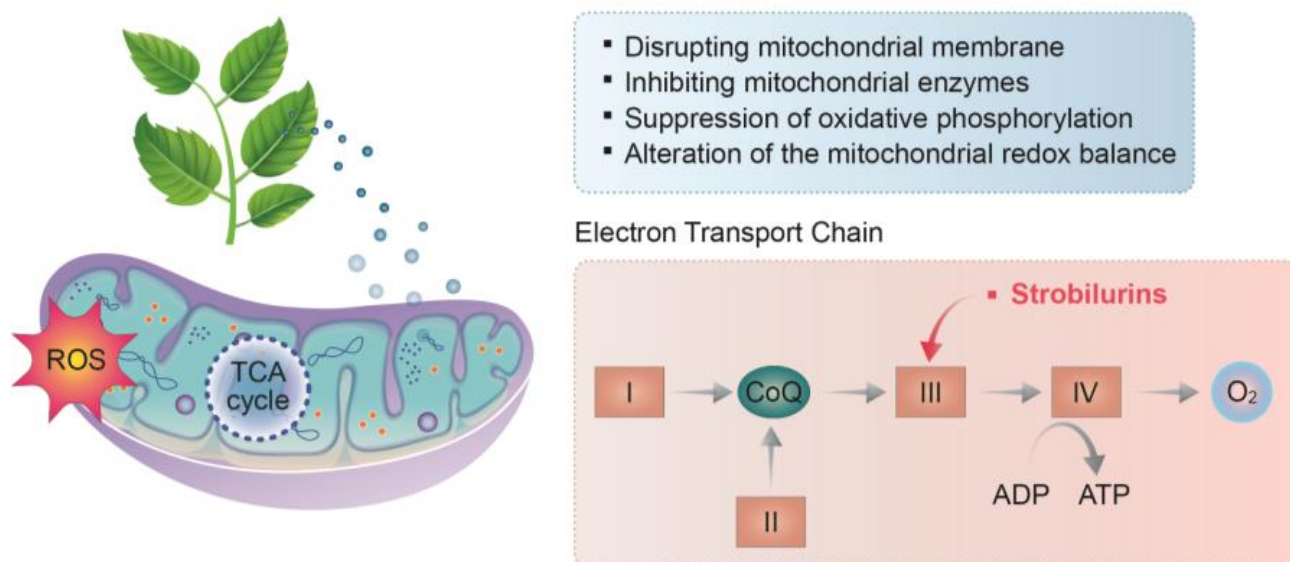
Figure 4. Mechanism of action of plant-derived natural compounds and antifungal agents acting on the mitochondria of *A. flavus*. I, II, III, IV, mitochondrial complex I, II, III, IV.

4. Antiaflatoxigenic Mechanisms of Plant-Derived Natural Compounds and EOs against *A. flavus*

Aflatoxin is a polyketide-derived furanocoumarin; a type of carcinogenic and mutagenic secondary metabolite that threatens global food security. Many studies suggest that reduced fungal growth is not solely responsible for the inhibition of aflatoxin production by plant-based natural compounds. Instead, the specific inhibition of aflatoxin biosynthesis is also thought to play a role. Different plant-derived natural compounds have been proven to inhibit the production of aflatoxin at lower concentrations than those that inhibit mycelial growth. For example, Tian et al. tested the antiaflatoxigenic activity of 36 structurally related natural flavonoids isolated from plants. Baicalein, flavone, hispidulin, kaempferol, and liquiritigenin were found to exclusively exhibit significant antiaflatoxigenic activity (>80% inhibition compared to the control), despite having none or very low antifungal activity [57]. Aflatoxin production inhibitors that do not affect fungal growth may also be useful as selective aflatoxin control agents without significantly interrupting the microbial environment or incurring the rapid spread of resistant strains.

Currently, the antiaflatoxigenic modes of action of plant-based natural compounds are not clearly understood. However, over the last few decades, it has been hypothesized that natural compounds may inhibit aflatoxin biosynthesis through: (1) modulating extracellular and intracellular factors affecting aflatoxin biosynthesis; (2) interrupting the cell signaling upstream of the aflatoxin biosynthetic pathway; (3) inhibiting carbohydrate catabolism, which is connected to aflatoxin biosynthesis; (4) inhibiting specific genes or enzymes in the aflatoxin biosynthetic pathway (Figure 5) [103]. In addition, the antiaflatoxigenic activity of natural compounds is potentially related to the transduction and perception of signals involved in the switch of fungal cells from vegetative to reproductive development. The correlation between secondary metabolism and fungal sporulation has been highlighted in many studies [22,104].
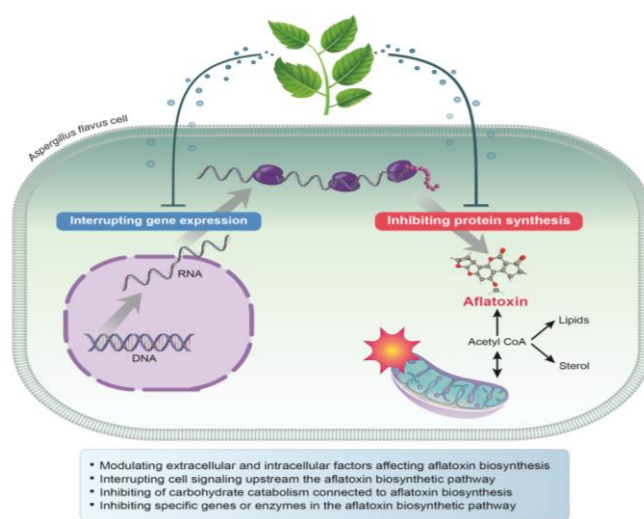
Figure 5. Mechanisms of action of plant-derived natural compounds against aflatoxin biosynthesis of *A. flavus*.

In particular, the mitochondria in *A. flavus* also play critical roles in the biosynthesis of aflatoxin. Mitochondria are responsible for providing ATP, NADPH, and acetyl-CoA for aflatoxin biosynthesis. Plant-based natural components may disrupt the mitochondria and cease the formation of acetyl-CoA that feeds the aflatoxin biosynthesis pathway, ultimately leading to the inhibition of aflatoxin biosynthesis. Mitochondria are also involved in many important fungal cellular activities that affect aflatoxin production, such as regulating fungal development, directing cellular metabolism, and maintaining cellular ROS levels. Many secondary fungal metabolites, including aflatoxin, are synthesized when the fungus finishes its initial growth phase and begins its development stage, which is represented by sporulation [22,104]. Moreover, mitochondria have been suggested to contribute to the regulation of both the physiological and morphological developments of fungal cells [105]. Mitochondria also regulate the lipid metabolism in fungal cells. It has been suggested that on initiation of aflatoxin biosynthesis, the external carbon source was greatly consumed, thus, resulting in aflatoxin production from the breakdown of reserve carbon sources, mostly lipids and fatty acids [106]. Additionally, some natural compounds' antiaflatoxigenic activities may be related to the inhibition of lipid peroxidation and oxygenation, which are processes involved in aflatoxin biosynthesis [107]. Studies on *A. flavus* have revealed the importance of oxylipins in the regulation of aflatoxin biosynthesis, conidia production, and sclerotia formation [108]. Mitochondria may also affect aflatoxin synthesis via a ROS-related mechanism. Studies have shown that aflatoxin biosynthesis involves a boost in the oxygen uptake of fungal cells, followed by an increase in ROS generation. This change occurs when fungal cells switch from trophophase to idiophase, at which point different secondary metabolic pathways become active [109]. The stimulation of aflatoxin biosynthesis by ROS-induced oxidative stress has also been previously reported [110,111].

The presence of multiple cytochrome p450 monooxygenases and monooxygenases in the aflatoxin biosynthesis pathway also indicates the involvement of both oxygen consumption and ROS production in this system. Many natural compounds possess strong antioxidant activities that can scavenge the ROS inside the fungal cells. The antiaflatoxigenic mechanism of natural compounds may be associated with their antioxidant activity and ROS scavenging ability, which attenuates the fungal oxidative stress responses and reduces aflatoxin production [112].

Additional reports have also suggested that the antiaflatoxigenic activity of some natural compounds occurs via the inhibition of the carbohydrate metabolism by inhibiting some key enzymes [27]. Alternatively, it could occur by inhibiting the aflatoxin biosynthetic pathway by suppressing the expression of the aflatoxin biosynthetic genes. Indeed, the expression of internal transcriptional regulators (*aflR* and *aflS*) in the aflatoxin biosynthetic pathway is inhibited by natural phenols and terpenoids [113,114]. Furthermore, the expression of structural genes, such as *aflD*, *aflK*, *aflE*, *aflM*, *aflO*, *aflP*, *aflO*, and *aflQ*, is reported to be suppressed by different plant-derived natural components [49,113–115]. However, the mechanisms through which they exert their actions at the molecular level still need to be deciphered fully.

5. Future Perspective

Recently, consumers' demands for healthier and more sustainable food products have required the food industry to reformulate their products by replacing artificial additives with natural, label-friendly alternatives [9]. Many plant-derived natural compounds and EOs have exhibited great potential against fungal propagation and mycotoxin production. Many present either no mammalian toxicity or a lower one than synthetic fungicides, which had a higher lethal dose of 50 values during toxicological testing using oral administration in mice [116–118]. Presently, natural compound-based fungicides are being developed and are available in European countries and the USA, e.g., Fungastop^{TM} and Armorex^{TM} II (Soil Technologies Corp., Fairfield, IA, USA). Future studies may focus on improving the stability and performance of plant-derived natural antifungal compounds and EOs to allow for their application in foods and complex biological systems, in addition to an in-depth investigation into their antifungal mechanisms (Figure 6).
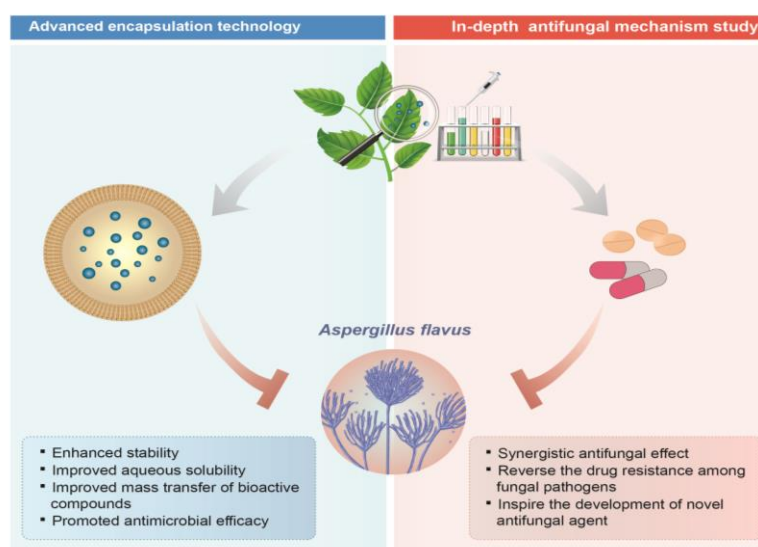

Figure 6. Future perspectives towards the application of plant-derived natural compounds against *A. flavus*.

The extraction process for plant-derived bioactive compounds and EOs plays an important role in both their yield and quality. Considering their low amounts in plants, it is desirable to use methodologies that can result in maximum yields with a minimum

loss in functional properties. Plant-derived bioactive compounds encompass a wide range of natural metabolites with different physiochemical qualities. The extraction of these compounds is strongly dependent on the hydrophobic or lipophilic characters of the target molecules. Currently, various innovative extraction methods have been proposed for the extraction of bioactive compounds and EOs from plant materials, including high pressure extraction, high voltage electrical discharges, microwave-assisted extraction, pressurized liquid extraction, pulsed electric fields-assisted extraction, sub- and supercritical fluid extraction, and ultrasound-assisted extraction [119–121]. These techniques are able to reduce the usage of chemical solvents and energy during the extraction process and improve the yields and quality of EOs.

Despite the great interest in the exploitation of natural compound-based food preservatives, their large-scale utilization is currently limited, as are their antifungal and antimycotoxigenic activities [122]. The major limitations regarding the application of plant-derived natural compounds in food commodities include low water solubility, instability, susceptibility to oxidation, volatilization, and rapid degradation in different environmental conditions [123]. Meanwhile, due to the low stability of many natural components, their antifungal and antimycotoxigenic effects tend to be compromised following long-term storage. One way to mitigate this effect is to develop suitable structural barriers to enclose the natural compounds. In this regard, modern encapsulation techniques that use different physical, physicochemical, and mechanical methods with the assistance of carrier matrices have been tested for the formulation of natural compounds or EO-based preservatives. The encapsulation of plant-derived natural compounds and EOs can reduce the loss of bioactivity and offer the possibility of controlling the release in treated foods [124]. Thus, emulsion-based delivery systems and active packaging materials, formulated with the incorporation of natural compounds, have been tested to improve the aqueous solubility and mass transfer of natural antimicrobial compounds in foods. In particular, nanotechnology, as a quickly growing field, has been applied to a variety of marketable products around the world. Nanoencapsulation of bioactive compounds and nanoemulsified EOs have demonstrated the advantages of more efficient and targeted use of antifungal agents in a safer and environmentally friendly way [125–128]. Such advantages were associated with their distinct physicochemical and functional characteristics and enhanced ability to transport bioactive constituents through biological membranes. Therefore, nanotechnology has the potential to significantly improve the antifungal efficiency of plant-derived natural compounds and EOs in practical applications.

Currently, the primarily used antifungal drugs and fungicides exert their antifungal activities by targeting the fungal cell wall, cell membrane, mitochondria, or important metabolic enzymes. Plant-derived natural antifungal compounds that act on either the same or connected cellular structures can potentially enhance the antifungal effects of the fungicides. Natural compounds that disrupt cell membrane functions or ATP production may also inhibit the activity of drug efflux pumps, thus, decreasing the drug resistance of fungal cells. Natural compounds that interact with the cellular redox system may improve the antifungal effects of mitochondria-targeting antifungal agents [129]. In these cases, the natural compounds function by attenuating the ability of the fungal cells to activate the defense response against fungicides. Hence, these do not necessarily require a great degree of antifungal potency to be effective. The application of these natural compounds, in combination with conventional fungicides, can lower the dosage levels required to control the pathogens and reduce the costs and risks of negative side effects. Such natural compounds could make the use of conventional fungicides safer and more effective, while also overcoming the development of drug resistance in both food and human fungal pathogens.

References

1. Fountain, J.; Scully, B.; Ni, X.; Kemerait, R.; Lee, D.; Chen, Z.-Y.; Guo, B. Environmental influences on maize-*Aspergillus flavus* interactions and aflatoxin production. *Front. Microbiol.* **2014**, *5*, 40. [CrossRef] [PubMed]

2. Amaike, S.; Keller, N.P. *Aspergillus flavus*. *Annu. Rev. Phytopathol.* **2011**, *49*, 107–133. [CrossRef]

3. Baranyi, N.; Kocsubé, S.; Varga, J. Aflatoxins: Climate change and biodegradation. *Curr. Opin. Food Sci.* **2015**, *5*, 60–66. [CrossRef]

4. Bartoletti, M.; Pascale, R.; Cricca, M.; Rinaldi, M.; Maccaro, A.; Bussini, L.; Fornaro, G.; Tonetti, T.; Pizzilli, G.; Francalanci, E.; et al. Epidemiology of invasive pulmonary aspergillosis among intubated patients with COVID-19: A prospective study. *Clin. Infect. Dis* **2021**, *73*, e3606–e3614. [CrossRef] [PubMed]

5. Prakash, B.; Shukla, R.; Singh, P.; Kumar, A.; Mishra, P.K.; Dubey, N.K. Efficacy of chemically characterized *Piper betle* L. essential oil against fungal and aflatoxin contamination of some edible commodities and its antioxidant activity. *Int. J. Food Microbiol.* **2010**, *142*, 114–119. [CrossRef]

6. Bluma, R.V.; Etcheverry, M.G. Application of essential oils in maize grain: Impact on *Aspergillus* section *Flavi* growth parameters and aflatoxin accumulation. *Food Microbiol.* **2008**, *25*, 324–334. [CrossRef]

7. Lv, X.; Pan, L.; Wang, J.; Lu, L.; Yan, W.; Zhu, Y.; Xu, Y.; Guo, M.; Zhuang, S. Effects of triazole fungicides on androgenic disruption and CYP3A4 enzyme activity. *Environ. Pollut.* **2017**, *222*, 504–512. [CrossRef]

8. Feng, Y.; Huang, Y.; Zhan, H.; Bhatt, P.; Chen, S. An overview of strobilurin fungicide degradation: Current status and future perspective. *Front. Microbiol.* **2020**, *11*, 389. [CrossRef]

9. Rao, J.; Chen, B.; McClements, D.J. Improving the efficacy of essential oils as antimicrobials in foods: Mechanisms of action. *Annu. Rev. Food Sci. Technol.* **2019**, *10*, 365–387. [CrossRef]

10. Khan, F.A.; Khan, N.M.; Ahmad, S.; Nasruddin; Aziz, R.; Ullah, I.; Almehmadi, M.; Allahyani, M.; Alsaiari, A.A.; Aljuaid, A. Phytochemical profiling, antioxidant, antimicrobial and cholinesterase inhibitory effects of essential oils isolated from the leaves of *Artemisia scoparia* and *Artemisia absinthium*. *Pharmaceuticals* **2022**, *15*, 1221. [CrossRef]

11. Khan, F.A.; Khan, S.; Khan, N.M.; Khan, H.; Khan, S.; Ahmad, S.; Rehman, N.; Aziz, R. Antimicrobial and antioxidant role of the aerial parts of *Aconitum violaceum*. *J. Mex. Chem. Soc.* **2021**, *65*, 84–93. [CrossRef]

12. Ali, F.; Jan, A.K.; Khan, N.M.; Ali, R.; Mukhtiar, M.; Khan, S.; Khan, S.A.; Aziz, R. Selective biological activities and phytochemical profiling of two wild plant species, *Teucrium polium* and *Capsicum annum* from Sheringal, Pakistan. *Chiang Mai J. Sci.* **2018**, *45*, 881–887.

13. Khan, H.; Ali, F.; Khan, N.M.; Shah, A.; Rahman, S.U. GC-MS Analysis of fixed oil from *Nelumbo nucifera* Gaertn seeds: Evaluation of antimicrobial, antileishmanial and urease inhibitory activities. *J. Chem. Soc. Pak.* **2016**, *38*, 1168–1173.

14. Hu, Z.Y.; Yuan, K.; Zhou, Q.; Lu, C.; Du, L.H.; Liu, F. Mechanism of antifungal activity of *Perilla frutescens* essential oil against *Aspergillus flavus* by transcriptomic analysis. *Food Control* **2021**, *123*, 107703. [CrossRef]

15. Oliveira, R.C.; Carvajal-Moreno, M.; Correa, B.; Rojo-Callejas, F. Cellular, physiological and molecular approaches to investigate the antifungal and anti-aflatoxigenic effects of thyme essential oil on *Aspergillus flavus*. *Food Chem.* **2020**, *315*, 126096. [CrossRef]

16. Prakash, B.; Dubey, N.K. Evaluation of chemically characterised essential oils of *Coleus aromaticus*, *Hyptis suaveolens* and *Ageratum conyzoides* against storage fungi and aflatoxin contamination of food commodities. *Int. J. Food Sci. Technol.* **2011**, *46*, 754–760. [CrossRef]

17. Esper, R.H.; Goncalez, E.; Marques, M.O.; Felicio, R.C.; Felicio, J.D. Potential of essential oils for protection of grains contaminated by aflatoxin produced by *Aspergillus flavus*. *Front. Microbiol.* **2014**, *5*, 269. [CrossRef]

18. Kedia, A.; Prakash, B.; Mishra, P.K.; Dwivedy, A.K.; Dubey, N. *Trachyspermum ammi* L. essential oil as plant based preservative in food system. *Ind. Crops Prod.* **2015**, *69*, 104–109. [CrossRef]

19. Soliman, K.M.; Badeaa, R. Effect of oil extracted from some medicinal plants on different mycotoxigenic fungi. *Food Chem. Toxicol.* **2002**, *40*, 1669–1675. [CrossRef]

20. Prakash, B.; Mishra, P.K.; Kedia, A.; Dubey, N. Antifungal, antiaflatoxin and antioxidant potential of chemically characterized *Boswellia carterii* Birdw essential oil and its *in vivo* practical applicability in preservation of *Piper nigrum* L. fruits. *LWT Food Sci. Technol.* **2014**, *56*, 240–247. [CrossRef]

21. Venkatesh, H.N.; Sudharshana, T.N.; Abhishek, R.U.; Thippeswamy, S.; Manjunath, K.; Mohana, D.C. Antifungal and antimycotoxigenic properties of chemically characterised essential oil of *Boswellia serrata* Roxb. ex Colebr. *Int. J. Food Prop.* **2017**, *20*, 1856–1868. [CrossRef]

22. Prakash, B.; Singh, P.; Kedia, A.; Dubey, N. Assessment of some essential oils as food preservatives based on antifungal, antiaflatoxin, antioxidant activities and in vivo efficacy in food system. *Food Res. Int.* **2012**, *49*, 201–208. [CrossRef]

23. Císarová, M.; Hleba, L.; Medo, J.; Tančinová, D.; Mašková, Z.; Čuboň, J.; Kováčik, A.; Foltinová, D.; Božik, M.; Klouček, P. The *in vitro* and *in situ* effect of selected essential oils in vapour phase against bread spoilage toxicogenic aspergilli. *Food Control* **2020**, *110*, 107007. [CrossRef]

24. Kocić-Tanackov, S.; Dimić, G.; Jakšić, S.; Mojović, L.; Djukić-Vuković, A.; Mladenović, D.; Pejin, J. Effects of caraway and juniper essential oils on aflatoxigenic fungi growth and aflatoxins secretion in polenta. *J. Food Process. Preserv.* **2019**, *43*, e14224. [CrossRef]

25. Kazemi, M. Effect of *Carum copticum* essential oil on growth and aflatoxin formation by *Aspergillus* strains. *Nat. Prod. Res.* **2015**, *29*, 1065–1068. [CrossRef]

26. Pandey, A.K.; Singh, P.; Palni, U.T.; Tripathi, N. Application of *Chenopodium ambrosioides* Linn. essential oil as botanical fungicide for the management of fungal deterioration in pulses. *Biol. Agric. Hortic.* **2013**, *29*, 197–208. [CrossRef]

27. Tian, J.; Ban, X.; Zeng, H.; He, J.; Huang, B.; Wang, Y. Chemical composition and antifungal activity of essential oil from *Cicuta virosa* L. var. *latisecta Celak. Int. J. Food Microbiol.* **2011**, *145*, 464–470. [CrossRef]

28. Prakash, B.; Singh, P.; Yadav, S.; Singh, S.C.; Dubey, N.K. Safety profile assessment and efficacy of chemically characterized *Cinnamomum glaucescens* essential oil against storage fungi, insect, aflatoxin secretion and as antioxidant. *Food Chem. Toxicol.* **2013**, *53*, 160–167. [CrossRef]

29. Gómez, J.V.; Tarazona, A.; Mateo-Castro, R.; Gimeno-Adelantado, J.V.; Jiménez, M.; Mateo, E.M. Selected plant essential oils and their main active components, a promising approach to inhibit aflatoxigenic fungi and aflatoxin production in food. *Food Addit. Contam. Chem. Anal. Control Expo. Risk Assess.* **2018**, *35*, 1581–1595. [CrossRef]

30. Khorasani, S.; Azizi, M.H.; Barzegar, M.; Hamidi-Esfahani, Z.; Kalbasi-Ashtari, A. Inhibitory effects of cinnamon, clove and celak extracts on growth of *Aspergillus flavus* and its aflatoxins after spraying on pistachio nuts before cold storage. *J. Food Saf.* **2017**, *37*, e12383. [CrossRef]

31. Kiran, S.; Kujur, A.; Prakash, B. Assessment of preservative potential of *Cinnamomum zeylanicum* Blume essential oil against food borne molds, aflatoxin B$_1$ synthesis, its functional properties and mode of action. *Innov. Food Sci. Emerg. Technol.* **2016**, *37*, 184–191. [CrossRef]

32. Singh, P.; Shukla, R.; Kumar, A.; Prakash, B.; Singh, S.; Dubey, N.K. Effect of *Citrus reticulata* and *Cymbopogon citratus* essential oils on *Aspergillus flavus* growth and aflatoxin production on *Asparagus racemosus*. *Mycopathologia* **2010**, *170*, 195–202. [CrossRef]

33. Pandey, A.K.; Palni, U.T.; Tripathi, N.N. Evaluation of *Clausena pentaphylla* (Roxb.) DC oil as a fungitoxicant against storage mycoflora of pigeon pea seeds. *J. Sci. Food Agric.* **2013**, *93*, 1680–1686. [CrossRef] [PubMed]

34. Boukaew, S.; Prasertsan, P.; Sattayasamitsathit, S. Evaluation of antifungal activity of essential oils against aflatoxigenic *Aspergillus flavus* and their allelopathic activity from fumigation to protect maize seeds during storage. *Ind. Crops Prod.* **2017**, *97*, 558–566. [CrossRef]

35. Moosavi-Nasab, M.; Jamalian, J.; Heshmati, H.; Haghighi-Manesh, S. The inhibitory potential of *Zataria multiflora* and *Syzygium aromaticum* essential oil on growth and aflatoxin production by *Aspergillus flavus* in culture media and Iranian white cheese. *Food Sci. Nutr.* **2018**, *6*, 318–324. [CrossRef] [PubMed]

36. Omidbeygi, M.; Barzegar, M.; Hamidi, Z.; Naghdibadi, H. Antifungal activity of thyme, summer savory and clove essential oils against *Aspergillus flavus* in liquid medium and tomato paste. *Food Control* **2007**, *18*, 1518–1523. [CrossRef]

37. Tian, J.; Ban, X.; Zeng, H.; Huang, B.; He, J.; Wang, Y. *In vitro* and *in vivo* activity of essential oil from dill (*Anethum graveolens* L.) against fungal spoilage of cherry tomatoes. *Food Control* **2011**, *22*, 1992–1999. [CrossRef]

38. Kedia, A.; Dwivedy, A.K.; Pandey, A.K.; Kumar, R.R.; Regmi, P.; Dubey, N.K. Efficacy of chemically characterized *Foeniculum vulgare* Mill seed essential oil in protection of raw tobacco leaves during storage against fungal and aflatoxin contamination. *J. Appl. Microbiol.* **2015**, *119*, 991–998. [CrossRef]

39. Jantapan, K.; Poapolathep, A.; Imsilp, K.; Poapolathep, S.; Tanhan, P.; Kumagai, S.; Jermnak, U. Inhibitory Effects of Thai essential oils on potentially aflatoxigenic *Aspergillus parasiticus* and *Aspergillus flavus*. *Biocontrol. Sci.* **2017**, *22*, 31–40. [CrossRef]

40. Kumar, A.; Dubey, N.K.; Srivastava, S. Antifungal evaluation of *Ocimum sanctum* essential oil against fungal deterioration of raw materials of *Rauvolfia serpentina* during storage. *Ind. Crops Prod.* **2013**, *45*, 30–35. [CrossRef]

41. Pandey, A.K.; Sonker, N.; Singh, P. Efficacy of some essential oils against *Aspergillus flavus* with special reference to *Lippia alba* oil an inhibitor of fungal proliferation and aflatoxin B$_1$ production in green gram seeds during storage. *J. Food Sci.* **2016**, *81*, M928–M934. [CrossRef] [PubMed]

42. Li, Y.; Kong, W.; Li, M.; Liu, H.; Zhao, X.; Yang, S.; Yang, M. *Litsea cubeba* essential oil as the potential natural fumigant: Inhibition of *Aspergillus flavus* and AFB$_1$ production in licorice. *Ind. Crops Prod.* **2016**, *80*, 186–193. [CrossRef]

43. Kedia, A.; Dwivedy, A.K.; Jha, D.K.; Dubey, N.K. Efficacy of *Mentha spicata* essential oil in suppression of *Aspergillus flavus* and aflatoxin contamination in chickpea with particular emphasis to mode of antifungal action. *Protoplasma* **2016**, *253*, 647–653. [CrossRef] [PubMed]

44. Songsamoe, S.; Matan, N.; Matan, N. Antifungal activity of *Michelia alba* oil in the vapor phase and the synergistic effect of major essential oil components against *Aspergillus flavus* on brown rice. *Food Control* **2017**, *77*, 150–157. [CrossRef]

45. Gibriel, Y.; Hamza, A.; Gibriel, A.; Mohsen, S. In Vivo effect of mint (*Mentha viridis*) essential oil on growth and aflatoxin production by *Aspergillus flavus* isolated from stored corn. *J. Food Saf.* **2011**, *31*, 445–451. [CrossRef]

46. Kumar, A.; Shukla, R.; Singh, P.; Prakash, B.; Dubey, N.K. Chemical composition of *Ocimum basilicum* L. essential oil and its efficacy as a preservative against fungal and aflatoxin contamination of dry fruits. *Int. J. Food Sci. Technol.* **2011**, *46*, 1840–1846. [CrossRef]

47. Prakash, B.; Kedia, A.; Mishra, P.K.; Dwivedy, A.K.; Dubey, N.K. Assessment of chemically characterised *Rosmarinus officinalis* L. essential oil and its major compounds as plant-based preservative in food system based on their efficacy against food-borne moulds and aflatoxin secretion and as antioxidant. *Int. J. Food Sci. Technol.* **2015**, *50*, 1792–1798. [CrossRef]

48. Tian, F.; Lee, S.Y.; Chun, H.S. Comparison of the antifungal and antiaflatoxigenic potential of liquid and vapor phase of *Thymus vulgaris* essential oil against *Aspergillus flavus*. *J. Food Prot.* **2019**, *82*, 2044–2048. [CrossRef]

49. Hu, Y.; Zhang, J.; Kong, W.; Zhao, G.; Yang, M. Mechanisms of antifungal and anti-aflatoxigenic properties of essential oil derived from turmeric (*Curcuma longa* L.) on *Aspergillus flavus*. *Food Chem.* **2017**, *220*, 1–8. [CrossRef]

50. Prakash, B.; Singh, P.; Mishra, P.K.; Dubey, N.K. Safety assessment of *Zanthoxylum alatum* Roxb. essential oil, its antifungal, antiaflatoxin, antioxidant activity and efficacy as antimicrobial in preservation of *Piper nigrum* L. fruits. *Int. J. Food Microbiol.* **2012**, *153*, 183–191. [CrossRef]

51. Tian, J.; Zeng, X.; Feng, Z.; Miao, X.; Peng, X.; Wang, Y. *Zanthoxylum molle* Rehd. essential oil as a potential natural preservative in management of *Aspergillus flavus*. *Ind. Crops Prod.* **2014**, *60*, 151–159. [CrossRef]

52. Madegowda, B.H.; Rameshwaran, P.; Nagaraju, N.P.; Murthy, P.S. *In-vitro* Mycological activity of essential oil from *Zingiber zerumbet* rhizomes. *J. Essent. Oil Res.* **2016**, *28*, 81–88. [CrossRef]

53. Moghadam, H.D.; Sani, A.M.; Sangatash, M.M. Antifungal activity of essential oil of *Ziziphora clinopodioides* and the inhibition of aflatoxin B$_1$ production in maize grain. *Toxicol. Ind. Health* **2016**, *32*, 493–499. [CrossRef]

54. Hu, Y.; Kong, W.; Yang, X.; Xie, L.; Wen, J.; Yang, M. GC-MS combined with chemometric techniques for the quality control and original discrimination of *Curcumae longae* rhizome: Analysis of essential oils. *J. Sep. Sci.* **2014**, *37*, 404–411. [CrossRef] [PubMed]

55. Ojeda-Amador, R.M.; Fregapane, G.; Salvador, M.D. Influence of cultivar and technological conditions on the volatile profile of virgin pistachio oils. *Food Chem.* **2020**, *311*, 125957. [CrossRef]

56. Ben Arfa, A.; Combes, S.; Preziosi-Belloy, L.; Gontard, N.; Chalier, P. Antimicrobial activity of carvacrol related to its chemical structure. *Lett. Appl. Microbiol.* **2006**, *43*, 149–154. [CrossRef]

57. Tian, F.; Woo, S.Y.; Lee, S.Y.; Park, S.B.; Im, J.H.; Chun, H.S. Plant-based natural flavonoids show strong inhibition of aflatoxin production and related gene expressions correlated with chemical structure. *Food Microbiol.* **2023**, *109*, 104141. [CrossRef]

58. Cox, S.D.; Mann, C.M.; Markham, J.L.; Gustafson, J.E.; Warmington, J.R.; Wyllie, S.G. Determining the antimicrobial actions of tea tree oil. *Molecules* **2001**, *6*, 87–91. [CrossRef]

59. Dorman, H.J.; Deans, S.G. Antimicrobial agents from plants: Antibacterial activity of plant volatile oils. *J. Appl. Microbiol.* **2000**, *88*, 308–316. [CrossRef]

60. Burt, S. Essential oils: Their antibacterial properties and potential applications in foods—A review. *Int. J. Food Microbiol.* **2004**, *94*, 223–253. [CrossRef]

61. Passone, M.A.; Girardi, N.S.; Etcheverry, M. Antifungal and antiaflatoxigenic activity by vapor contact of three essential oils, and effects of environmental factors on their efficacy. *LWT Food Sci. Technol.* **2013**, *53*, 434–444. [CrossRef]

62. Skandamis, P.N.; Nychas, G.J. Development and evaluation of a model predicting the survival of *Escherichia coli* O157:H7 NCTC 12900 in homemade eggplant salad at various temperatures, pHs, and oregano essential oil concentrations. *Appl. Environ. Microbiol.* **2000**, *66*, 1646–1653. [CrossRef] [PubMed]

63. Rota, M.C.; Herrera, A.; Martínez, R.M.; Sotomayor, J.A.; Jordán, M.J. Antimicrobial activity and chemical composition of *Thymus vulgaris*, *Thymus zygis* and *Thymus hyemalis* essential oils. *Food Control* **2008**, *19*, 681–687. [CrossRef]

64. Sarrazin, S.L.; Oliveira, R.B.; Barata, L.E.; Mourao, R.H. Chemical composition and antimicrobial activity of the essential oil of *Lippia grandis* Schauer (Verbenaceae) from the western Amazon. *Food Chem.* **2012**, *134*, 1474–1478. [CrossRef] [PubMed]

65. Stević, T.; Berić, T.; Šavikin, K.; Soković, M.; Gođevac, D.; Dimkić, I.; Stanković, S. Antifungal activity of selected essential oils against fungi isolated from medicinal plant. *Ind. Crops Prod.* **2014**, *55*, 116–122. [CrossRef]

66. Hossain, F.; Follett, P.; Dang Vu, K.; Harich, M.; Salmieri, S.; Lacroix, M. Evidence for synergistic activity of plant-derived essential oils against fungal pathogens of food. *Food Microbiol.* **2016**, *53*, 24–30. [CrossRef]

67. Goni, P.; López, P.; Sánchez, C.; Gómez-Lus, R.; Becerril, R.; Nerín, C. Antimicrobial activity in the vapour phase of a combination of cinnamon and clove essential oils. *Food Chem.* **2009**, *116*, 982–989. [CrossRef]

68. Lamberts, L.; De Bie, E.; Vandeputte, G.E.; Veraverbeke, W.S.; Derycke, V.; De Man, W.; Delcour, J.A. Effect of milling on colour and nutritional properties of rice. *Food Chem.* **2007**, *100*, 1496–1503. [CrossRef]

69. Tang, J.D.; Ciaramitaro, T.; Tomaso-Peterson, M.; Diehl, S.V. Activity of two strobilurin fungicides against three species of decay fungi in agar plate tests. In Proceedings of the International Research Group on Wood Protection, Section 3, Wood Protecting Chemicals: Paper Prepared for the IRG48 Scientific Conference on Wood Protection, Ghent, Belgium, 4–8 June 2017; pp. 2–13.

70. Tian, F.; Lee, S.Y.; Woo, S.Y.; Choi, H.Y.; Park, S.B.; Chun, H.S. Effect of plant-based compounds on the antifungal and antiaflatoxigenic efficiency of strobilurins against *Aspergillus flavus*. *J. Hazard. Mater.* **2021**, *415*, 125663. [CrossRef]

71. Khan, M.S.A.; Ahmad, I. Antifungal activity of essential oils and their synergy with fluconazole against drug-resistant strains of *Aspergillus fumigatus* and *Trichophyton rubrum*. *Appl. Microbiol. Biotechnol.* **2011**, *90*, 1083–1094. [CrossRef]

72. Belofsky, G.; Kolaczkowski, M.; Adams, E.; Schreiber, J.; Eisenberg, V.; Coleman, C.M.; Zou, Y.; Ferreira, D. Fungal ABC transporter-associated activity of isoflavonoids from the root extract of *Dalea formosa*. *J. Nat. Prod.* **2013**, *76*, 915–925. [CrossRef]

73. Fukuda, I.; Ashida, H. Modulation of drug-metabolizing enzymes and transporters by polyphenols as an anticarcinogenic effect. In *Polyphenols in Human Health and Disease*; Watson, R.R., Preedy, V.R., Zibadi, S., Eds.; Academic Press: Cambridge, MA, USA, 2014; pp. 1127–1135. [CrossRef]

74. Ziberna, L.; Fornasaro, S.; Čvorović, J.; Tramer, F.; Passamonti, S. Bioavailability of flavonoids: The role of cell membrane transporters. In *Polyphenols in Human Health and Disease*; Watson, R.R., Preedy, V.R., Zibadi, S., Eds.; Academic Press: Cambridge, MA, USA, 2014; pp. 489–511. [CrossRef]

75. Bowman, S.M.; Free, S.J. The structure and synthesis of the fungal cell wall. *Bioessays* **2006**, *28*, 799–808. [CrossRef] [PubMed]

76. Li, Q.; Zhao, Y.; Zhu, X.M.; Xie, Y.L. Antifungal efficacy of paeonol on *Aspergillus flavus* and its mode of action on cell walls and cell membranes. *LWT-Food Sci. Technol.* **2021**, *149*, 111985. [CrossRef]

77. Belewa, V.; Baijnath, H.; Frost, C.; Somai, B.M. *Tulbaghia violacea* Harv. plant extract affects cell wall synthesis in *Aspergillus flavus*. *J. Appl. Microbiol.* **2017**, *122*, 921–931. [CrossRef] [PubMed]

78. da Silva Bomfim, N.; Nakassugi, L.P.; Faggion Pinheiro Oliveira, J.; Kohiyama, C.Y.; Mossini, S.A.; Grespan, R.; Nerilo, S.B.; Mallmann, C.A.; Alves Abreu Filho, B.; Machinski, M., Jr. Antifungal activity and inhibition of fumonisin production by *Rosmarinus officinalis* L. essential oil in *Fusarium verticillioides* (Sacc.) Nirenberg. *Food Chem.* **2015**, *166*, 330–336. [CrossRef]

79. Gow, N.A.R.; Latge, J.P.; Munro, C.A. The fungal cell wall: Structure, biosynthesis, and function. *Microbiol. Spectr.* **2017**, *5*. [CrossRef]

80. Marei, G.I.K.; Rasoul, M.A.A.; Abdelgaleil, S.A. Comparative antifungal activities and biochemical effects of monoterpenes on plant pathogenic fungi. *Pestic. Biochem. Physiol.* **2012**, *103*, 56–61. [CrossRef]

81. Bang, K.H.; Lee, D.W.; Park, H.M.; Rhee, Y.H. Inhibition of fungal cell wall synthesizing enzymes by trans-cinnamaldehyde. *Biosci. Biotechnol. Biochem.* **2000**, *64*, 1061–1063. [CrossRef]

82. Bakkali, F.; Averbeck, S.; Averbeck, D.; Idaomar, M. Biological effects of essential oils—A review. *Food Chem. Toxicol.* **2008**, *46*, 446–475. [CrossRef]

83. Di Pasqua, R.; Betts, G.; Hoskins, N.; Edwards, M.; Ercolini, D.; Mauriello, G. Membrane toxicity of antimicrobial compounds from essential oils. *J. Agric. Food Chem.* **2007**, *55*, 4863–4870. [CrossRef]

84. Pauli, A. Anticandidal low molecular compounds from higher plants with special reference to compounds from essential oils. *Med. Res. Rev.* **2006**, *26*, 223–268. [CrossRef] [PubMed]

85. Dwivedy, A.K.; Kumar, M.; Upadhyay, N.; Prakash, B.; Dubey, N.K. Plant essential oils against food borne fungi and mycotoxins. *Curr. Opin. Food Sci.* **2016**, *11*, 16–21. [CrossRef]

86. Ghannoum, M.A.; Rice, L.B. Antifungal agents: Mode of action, mechanisms of resistance, and correlation of these mechanisms with bacterial resistance. *Clin. Microbiol. Rev.* **1999**, *12*, 501–517. [CrossRef] [PubMed]

87. Freires Ide, A.; Murata, R.M.; Furletti, V.F.; Sartoratto, A.; Alencar, S.M.; Figueira, G.M.; de Oliveira Rodrigues, J.A.; Duarte, M.C.; Rosalen, P.L. *Coriandrum sativum* L. (Coriander) essential oil: Antifungal activity and mode of action on *Candida* spp., and molecular targets affected in human whole-genome expression. *PLoS ONE* **2014**, *9*, e99086. [CrossRef] [PubMed]

88. Tian, J.; Huang, B.; Luo, X.; Zeng, H.; Ban, X.; He, J.; Wang, Y. The control of *Aspergillus flavus* with *Cinnamomum jensenianum* Hand.-Mazz essential oil and its potential use as a food preservative. *Food Chem.* **2012**, *130*, 520–527. [CrossRef]

89. Kohiyama, C.Y.; Ribeiro, M.M.Y.; Mossini, S.A.G.; Bando, E.; da Silva Bomfim, N.; Nerilo, S.B.; Rocha, G.H.O.; Grespan, R.; Mikcha, J.M.G.; Machinski Jr, M. Antifungal properties and inhibitory effects upon aflatoxin production of *Thymus vulgaris* L. by *Aspergillus flavus* Link. *Food Chem.* **2015**, *173*, 1006–1010. [CrossRef]

90. Tian, J.; Ban, X.; Zeng, H.; He, J.; Chen, Y.; Wang, Y. The mechanism of antifungal action of essential oil from dill (*Anethum graveolens* L.) on *Aspergillus flavus*. *PLoS ONE* **2012**, *7*, e30147. [CrossRef]

91. OuYang, Q.; Tao, N.; Jing, G. Transcriptional profiling analysis of *Penicillium digitatum*, the causal agent of citrus green mold, unravels an inhibited ergosterol biosynthesis pathway in response to citral. *BMC Genom.* **2016**, *17*, 599. [CrossRef]

92. Ultee, A.; Bennik, M.; Moezelaar, R. The phenolic hydroxyl group of carvacrol is essential for action against the food-borne pathogen *Bacillus cereus*. *Appl. Environ. Microbiol.* **2002**, *68*, 1561–1568. [CrossRef]

93. Trombetta, D.; Castelli, F.; Sarpietro, M.G.; Venuti, V.; Cristani, M.; Daniele, C.; Saija, A.; Mazzanti, G.; Bisignano, G. Mechanisms of antibacterial action of three monoterpenes. *Antimicrob. Agents Chemother.* **2005**, *49*, 2474–2478. [CrossRef]

94. Dagley, M.J.; Gentle, I.E.; Beilharz, T.H.; Pettolino, F.A.; Djordjevic, J.T.; Lo, T.L.; Uwamahoro, N.; Rupasinghe, T.; Tull, D.L.; McConville, M. Cell wall integrity is linked to mitochondria and phospholipid homeostasis in *Candida albicans* through the activity of the post-transcriptional regulator Ccr4-Pop2. *Mol. Microbiol.* **2011**, *79*, 968–989. [CrossRef] [PubMed]

95. Ma, W.; Zhao, L.; Zhao, W.; Xie, Y. (E)-2-Hexenal, as a potential natural antifungal compound, inhibits *Aspergillus flavus* spore germination by disrupting mitochondrial energy metabolism. *J. Agric. Food Chem.* **2019**, *67*, 1138–1145. [CrossRef]

96. Ma, W.B.; Zhao, L.L.; Johnson, E.T.; Xie, Y.L.; Zhang, M.M. Natural food flavour (E)-2-hexenal, a potential antifungal agent, induces mitochondria-mediated apoptosis in *Aspergillus flavus* conidia via a ROS-dependent pathway. *Int. J. Food Microbiol.* **2022**, *370*, 109633. [CrossRef] [PubMed]

97. Zhang, W.; Li, B.; Lv, Y.; Wei, S.; Zhang, S.; Hu, Y. Transcriptomic analysis shows the antifungal mechanism of honokiol against *Aspergillus flavus*. *Int. J. Food Microbiol.* **2022**, *384*, 109972. [CrossRef] [PubMed]

98. Li, Y.; Shao, X.; Xu, J.; Wei, Y.; Xu, F.; Wang, H. Tea tree oil exhibits antifungal activity against *Botrytis cinerea* by affecting mitochondria. *Food Chem.* **2017**, *234*, 62–67. [CrossRef] [PubMed]

99. Zheng, S.; Jing, G.; Wang, X.; Ouyang, Q.; Jia, L.; Tao, N. Citral exerts its antifungal activity against *Penicillium digitatum* by affecting the mitochondrial morphology and function. *Food Chem.* **2015**, *178*, 76–81. [CrossRef]

100. Rao, A.; Zhang, Y.; Muend, S.; Rao, R. Mechanism of antifungal activity of terpenoid phenols resembles calcium stress and inhibition of the TOR pathway. *Antimicrob. Agents Chemother.* **2010**, *54*, 5062–5069. [CrossRef]

101. Pinto, E.; Hrimpeng, K.; Lopes, G.; Vaz, S.; Goncalves, M.J.; Cavaleiro, C.; Salgueiro, L. Antifungal activity of *Ferulago capillaris* essential oil against *Candida*, *Cryptococcus*, *Aspergillus* and dermatophyte species. *Eur. J. Clin. Microbiol. Infect. Dis.* **2013**, *32*, 1311–1320. [CrossRef]

102. Loi, M.; Paciolla, C.; Logrieco, A.F.; Mule, G. Plant bioactive compounds in pre- and postharvest management for aflatoxins reduction. *Front. Microbiol.* **2020**, *11*, 243. [CrossRef]

103. Chaudhari, A.K.; Dwivedy, A.K.; Singh, V.K.; Das, S.; Singh, A.; Dubey, N.K. Essential oils and their bioactive compounds as green preservatives against fungal and mycotoxin contamination of food commodities with special reference to their nanoencapsulation. *Environ. Sci. Pollut. Res.* **2019**, *26*, 25414–25431. [CrossRef]

104. Calvo, A.M.; Wilson, R.A.; Bok, J.W.; Keller, N.P. Relationship between secondary metabolism and fungal development. *Microbiol. Mol. Biol. Rev.* **2002**, *66*, 447–459. [CrossRef] [PubMed]

105. Osiewacz, H.D. Mitochondrial quality control in aging and lifespan control of the fungal aging model *Podospora anserina*. *Biochem. Soc. Trans.* **2011**, *39*, 1488–1492. [CrossRef] [PubMed]

106. Molnár, A.P.; Nemeth, Z.; Fekete, E.; Flipphi, M.; Keller, N.P.; Karaffa, L. Analysis of the relationship between alternative respiration and sterigmatocystin formation in *Aspergillus nidulans*. *Toxins* **2018**, *10*, 168. [CrossRef] [PubMed]

107. Bluma, R.; Amaiden, M.R.; Daghero, J.; Etcheverry, M. Control of *Aspergillus* section *Flavi* growth and aflatoxin accumulation by plant essential oils. *J. Appl. Microbiol.* **2008**, *105*, 203–214. [CrossRef] [PubMed]

108. Scarpari, M.; Punelli, M.; Scala, V.; Zaccaria, M.; Nobili, C.; Ludovici, M.; Camera, E.; Fabbri, A.A.; Reverberi, M.; Fanelli, C. Lipids in *Aspergillus flavus*-maize interaction. *Front. Microbiol.* **2014**, *5*, 74. [CrossRef]

109. Zaccaria, M.; Ludovici, M.; Sanzani, S.M.; Ippolito, A.; Cigliano, R.A.; Sanseverino, W.; Scarpari, M.; Scala, V.; Fanelli, C.; Reverberi, M. Menadione-induced oxidative stress re-shapes the oxylipin profile of *Aspergillus flavus* and its lifestyle. *Toxins* **2015**, *7*, 4315–4329. [CrossRef]

110. Roze, L.V.; Laivenieks, M.; Hong, S.Y.; Wee, J.; Wong, S.S.; Vanos, B.; Awad, D.; Ehrlich, K.C.; Linz, J.E. Aflatoxin biosynthesis is a novel source of reactive oxygen species-a potential redox signal to initiate resistance to oxidative stress? *Toxins* **2015**, *7*, 1411–1430. [CrossRef]

111. Umesha, S.; Manukumar, H.M.; Chandrasekhar, B.; Shivakumara, P.; Shiva Kumar, J.; Raghava, S.; Avinash, P.; Shirin, M.; Bharathi, T.R.; Rajini, S.B.; et al. Aflatoxins and food pathogens: Impact of biologically active aflatoxins and their control strategies. *J. Sci. Food Agric.* **2017**, *97*, 1698–1707. [CrossRef]

112. Kim, J.H.; Campbell, B.C.; Yu, J.; Mahoney, N.; Chan, K.L.; Molyneux, R.J.; Bhatnagar, D.; Cleveland, T.E. Examination of fungal stress response genes using *Saccharomyces cerevisiae* as a model system: Targeting genes affecting aflatoxin biosynthesis by *Aspergillus flavus* Link. *Appl. Microbiol. Biotechnol.* **2005**, *67*, 807–815. [CrossRef]

113. Jahanshiri, Z.; Shams-Ghahfarokhi, M.; Allameh, A.; Razzaghi-Abyaneh, M. Inhibitory effect of eugenol on aflatoxin B$_1$ production in *Aspergillus parasiticus* by downregulating the expression of major genes in the toxin biosynthetic pathway. *World J. Microbiol. Biotechnol.* **2015**, *31*, 1071–1078. [CrossRef]

114. Moon, Y.S.; Lee, H.S.; Lee, S.E. Inhibitory effects of three monoterpenes from ginger essential oil on growth and aflatoxin production of *Aspergillus flavus* and their gene regulation in aflatoxin biosynthesis. *Appl. Biol. Chem.* **2018**, *61*, 243–250. [CrossRef]

115. Lv, C.; Wang, P.; Ma, L.; Zheng, M.; Liu, Y.; Xing, F. Large-scale comparative analysis of eugenol-induced/repressed genes expression in *Aspergillus flavus* using RNA-seq. *Front. Microbiol.* **2018**, *9*, 1116. [CrossRef] [PubMed]

116. Prakash, B.; Shukla, R.; Singh, P.; Mishra, P.K.; Dubey, N.K.; Kharwar, R.N. Efficacy of chemically characterized *Ocimum gratissimum* L. essential oil as an antioxidant and a safe plant based antimicrobial against fungal and aflatoxin B$_1$ contamination of spices. *Food Res. Int.* **2011**, *44*, 385–390. [CrossRef]

117. Shukla, R.; Singh, P.; Prakash, B.; Dubey, N.K. Efficacy of *Acorus calamus* L. essential oil as a safe plant-based antioxidant, aflatoxin B$_1$ suppressor and broad spectrum antimicrobial against food-infesting fungi. *Int. J. Food Sci. Technol.* **2013**, *48*, 128–135. [CrossRef]

118. Singh, H.P.; Mittal, S.; Kaur, S.; Batish, D.R.; Kohli, R.K. Chemical composition and antioxidant activity of essential oil from residues of *Artemisia scoparia*. *Food Chem.* **2009**, *114*, 642–645. [CrossRef]

119. Ahmad-Qasem, M.H.; Canovas, J.; Barrajon-Catalan, E.; Micol, V.; Carcel, J.A.; Garcia-Perez, J.V. Kinetic and compositional study of phenolic extraction from olive leaves (var. Serrana) by using power ultrasound. *Innov. Food Sci. Emerg. Technol.* **2013**, *17*, 120–129. [CrossRef]

120. Barba, F.J.; Terefe, N.S.; Buckow, R.; Knorr, D.; Orlien, V. New opportunities and perspectives of high pressure treatment to improve health and safety attributes of foods. A review. *Food Res. Int.* **2015**, *77*, 725–742. [CrossRef]

121. Giacometti, J.; Kovacevic, D.B.; Putnik, P.; Gabric, D.; Bilusic, T.; Kresic, G.; Stulic, V.; Barba, F.J.; Chemat, F.; Barbosa-Canovas, G.; et al. Extraction of bioactive compounds and essential oils from mediterranean herbs by conventional and green innovative techniques: A review. *Food Res. Int.* **2018**, *113*, 245–262. [CrossRef]

122. Singh, A.; Dwivedy, A.K.; Singh, V.K.; Upadhyay, N.; Chaudhari, A.K.; Das, S.; Dubey, N.K. Essential oils based formulations as safe preservatives for stored plant masticatories against fungal and mycotoxin contamination: A review. *Biocatal. Agric. Biotechnol.* **2019**, *17*, 313–317. [CrossRef]

123. El Asbahani, A.; Miladi, K.; Badri, W.; Sala, M.; Ait Addi, E.H.; Casabianca, H.; El Mousadik, A.; Hartmann, D.; Jilale, A.; Renaud, F.N.; et al. Essential oils: From extraction to encapsulation. *Int. J. Pharm* **2015**, *483*, 220–243. [CrossRef]

124. Moretti, M.D.; Sanna-Passino, G.; Demontis, S.; Bazzoni, E. Essential oil formulations useful as a new tool for insect pest control. *AAPS PharmSciTech* **2002**, *3*, E13. [CrossRef] [PubMed]

125. Das, S.; Singh, V.K.; Dwivedy, A.K.; Chaudhari, A.K.; Upadhyay, N.; Singh, A.; Deepika; Dubey, N.K. Fabrication, characterization and practical efficacy of *Myristica fragrans* essential oil nanoemulsion delivery system against postharvest biodeterioration. *Ecotoxicol. Environ. Saf.* **2020**, *189*, 110000. [CrossRef] [PubMed]

126. Gundewadi, G.; Sarkar, D.J.; Rudra, S.G.; Singh, D. Preparation of basil oil nanoemulsion using *Sapindus mukorossi* pericarp extract: Physico-chemical properties and antifungal activity against food spoilage pathogens. *Ind. Crops Prod.* **2018**, *125*, 95–104. [CrossRef]

127. Dávila-Rodríguez, M.; López-Malo, A.; Palou, E.; Ramírez-Corona, N.; Jiménez-Munguía, M.T. Antimicrobial activity of nanoemulsions of cinnamon, rosemary, and oregano essential oils on fresh celery. *LWT* **2019**, *112*, 108247. [CrossRef]

128. Wan, J.; Zhong, S.; Schwarz, P.; Chen, B.; Rao, J. Physical properties, antifungal and mycotoxin inhibitory activities of five essential oil nanoemulsions: Impact of oil compositions and processing parameters. *Food Chem.* **2019**, *291*, 199–206. [CrossRef]

129. Sies, H.; Jones, D.P. Reactive oxygen species (ROS) as pleiotropic physiological signalling agents. *Nat. Rev. Mol. Cell Biol.* **2020**, *21*, 363–383. [CrossRef]

Naringenin and Its Derivatives—Health-Promoting Phytobiotic against Resistant Bacteria and Fungi in Humans

Anna Duda-Madej [1,*], Jakub Stecko [2], Jakub Sobieraj [2], Natalia Szymańska [2] and Joanna Kozłowska [3,*]

1   Department of Microbiology, Faculty of Medicine, Wroclaw Medical University, Chałubińskiego 4, 50-368 Wrocław, Poland
2   Faculty of Medicine, Wroclaw Medical University, Ludwika Pasteura 1, 50-367 Wrocław, Poland
3   Department of Food Chemistry and Biocatalysis, Faculty of Biotechnology and Food Science, Wrocław University of Environmental and Life Sciences, C.K. Norwida 25, 50-375 Wrocław, Poland
*   Correspondence: anna.duda-madej@umw.edu.pl (A.D.-M.); joanna.kozlowska@upwr.edu.pl (J.K.)

Abstract: Naringenin is a trihydroxyflavanone present in large amount in different citrus fruits, e.g., oranges, pomelos, grapefruits, but also in tomatoes, fenugreek and coffee. It has a wide range of pharmacological and biological effects beneficial to human health. Its antioxidant, anti-cancer, anti-inflammatory, antifungal and antimicrobial activity is frequently reported in scientific literature. In this review we presented the current state of knowledge on the antimicrobial activity of naringenin and its natural and synthetic derivatives as a phytobiotic against resistant Gram-positive and Gram-negative bacteria as well as fungi in humans. Most of the data reported here have been obtained from in vitro or in vivo studies. Over the past few years, due to the overuse of antibiotics, the occurrence of bacteria resistant to all available antibiotics has been growing. Therefore, the main focus here is on antibiotic resistant strains, which are a significant, worldwide problem in the treatment of infectious diseases. The situation is so alarming that the WHO has listed microbial resistance to drugs on the list of the 10 most important health problems facing humanity. In addition, based on scientific reports from recent years, we described the potential molecular mechanism of action of these bioflavonoids against pathogenic strains of microorganisms. As plant-derived substances have been pushed out of use with the beginning of the antibiotic era, we hope that this review will contribute to their return as alternative methods of preventing and treating infections in the epoch of drug resistance.

Keywords: naringenin; naringenin derivatives; antimicrobial activity; anti-inflammatory activity; antioxidant activity; antifungal activity

1. Introduction

Naringenin (5,7,4′-trihydroxyflavanone) is an aglycone, which is a derivative of hydrogenated flavone, belonging to the group of flavonoid compounds, which are a part of a huge group of polyphenols. It is also produced by the cyclization of 2′,4′,6′,4-tetrahydroxychalcone (naringenin chalcone) (Figure 1). This bioflavanone occurs naturally in an inactive form as naringin and is converted into its active form, naringenin, by bacteria belonging to the gut microbiome [1]. This, one of the most important representatives of flavonoid compounds, is a component of the everyday human diet, where it is responsible for the color and bitter-sour taste of food. The best sources of it are grapefruit, sour orange, tart cherries, tomatoes, grapes and Greek oregano. It is also found in smaller amounts in bergamot, beans, fenugreek, milk thistle, tea, coffee, cocoa and red wine [2]. Although almost all citrus fruits are source of flavonoids for humans, their concentration varies and depends on the type, variety, harvest time and environmental conditions in which they grow.

Naringenin has a wide range of positive effects on human health. It promotes carbohydrate metabolism, increases antioxidant defense, scavenges reactive oxygen species, modulates the activity of the immune system and also has anti-cancer, anti-inflammatory

and anti-atherosclerotic effects [3]. It also has the ability to cross the blood-brain barrier, and therefore exerts a variety of positive neuronal effects [4]. These versatile properties of naringenin can be helpful in the prevention and combating of such disorders as obesity, hyperlipidemia, hypertension, atherosclerosis, diabetes and even Alzheimer's disease.
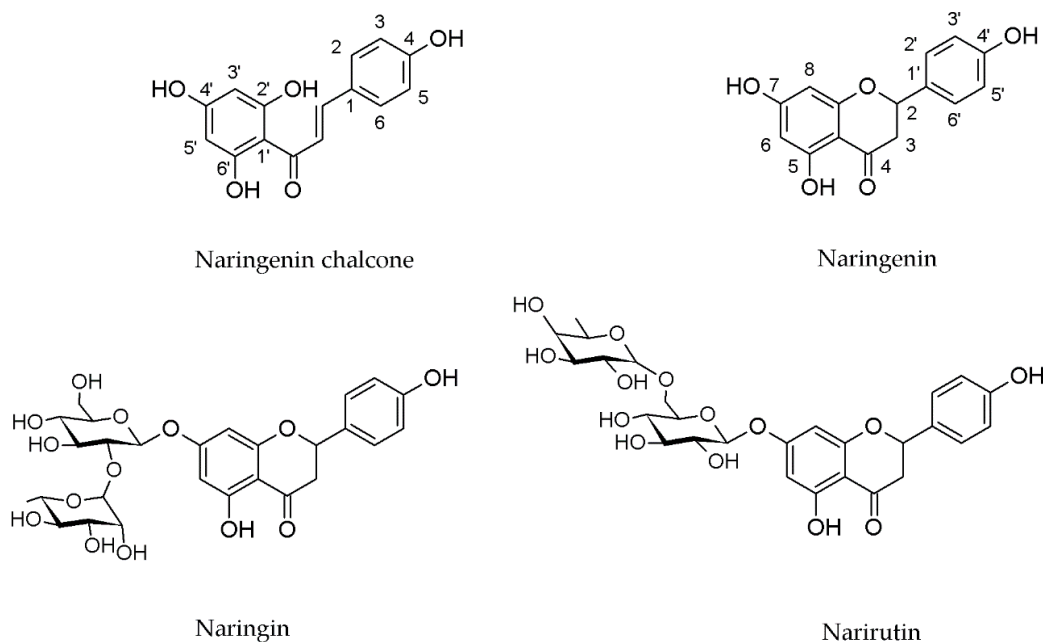

Figure 1. Structures of naringenin chalcone, naringenin, naringin and narirutin.

The last decade has enriched world literature with reviews about naringenin and its natural derivatives in terms of their biological properties, e.g., anti-cancer [5], antioxidant, anti-hyperlipidemic, anti-obesity, hepatoprotective [6,7], anti-inflammatory, anti-diabetic and anti-neurodegenerative activities [8,9]. This paper summarizes the current knowledge on the antimicrobial activity of this bioflavonoid and its natural but also synthetic derivatives. The analysis considers clinical strains of both bacteria—Gram-positive and Gram-negative—characterized by a wide panel of resistance, but also non-pathogenic strains. Furthermore, we collected information about antifungal activity of these substances. In addition, we presented detailed information explaining the mechanism of action of these compounds based on the world literature of recent years.

2. Content of Naringenin and its Glycosides in Plants and Products of Plant Origin

Naringenin is widespread in various citrus fruits (grapefruits, lemons, limes, oranges, mandarins, pomelos and bergamots), but also in vegetables, herbs and products of plant origin such as juices or wine. The content in plants is different and depends on the variety and part (flavedo, albedo, pith, seeds, membranes) of fruits, and the diversity of the composition in products of plant origin results from the way of preparation of the final product [10,11]. In plants, naringenin usually occurs as glycoside form: naringin (naringenin-7-rhamnoglucoside) and narirutin (naringenin-7-glucoside) (Figure 1).

Grapefruit (*Citrus paradisi*) is a fruit known for its abundant content of naringenin and its derivatives. The comparison of the content of flavonoids in different varieties of grapefruit proved that naringin is a dominant compound. Its content in white grapefruit was 16.90 mg/100 mg, and in pink/red grapefruit 13.87 mg/100 mg. Moreover, the second flavonoid occurring in the greatest amount was narirutin, with an amount of 5.36 mg/100mg and 3.34 mg/100 mg in white and pink/red variety, respectively [12]. McIntosh et al. also determined the content of naringin in three varieties (Duncan, Marsh and Thompson) of grapefruit in different parts of the fruit. Their research, conducted on different plant tissues, showed the highest amount of naringin in the back membrane, which is

near albedo (17,994–27,330 ppm) in all tested varieties. The lowest content of this glucoside form of naringenin has been found in juice vesicles (295–377 ppm) [10]. Additionally, Victor et al. searched for the best extraction method of naringin from grapefruit peel. As a result of their research, scientists obtained the highest amount of naringenin glycoside from wet albedo using hot methanol (0.7375 g of naringin/69.84 g fresh albedo) [11]. Among ready-to-eat products of plant origin characterized by a high content of naringenin and its derivatives, grapefruit juices are distinguished. Ho and co-workers determined the content of naringenin and naringin in grapefruit juices obtained from four different varieties of grapefruits by squeezing the fruits by hand or by squeezer. In more than half the results, the amount of naringin in juices obtained by squeezer was two times higher than by hand (141–656 mg/L grapefruit juice). Furthermore, the concentration of aglycon–naringenin in both types of squeezing was definitely lower, in range of 2.2–80 mg/L grapefruit juice [13].

Naringin is also observed in pomelo fruits (*Citrus grandis*). Sudto et al. performed different types of extraction on pomelo peels, which confirmed the content of naringenin-7-rhamnoglucoside up to 2.4% [14]. Moreover, Lin and co-workers tested three different cultivars of pomelo, and each of them were fragmented to exocarp, mesocarp, lamella, WBW (waste blanching water) and WBE (waste blanching water from exocarps). The naringin concentration was highest in the WBW part of fruit in every variation and amounted to 25.53 mg/g [15].

Another citrus fruit especially abundant in naringin is sweet orange (*Citrus sinensis*). High performance liquid chromatography (HPLC) is an effective and frequently used method to evaluate the content of compounds. Ni et al. using this method determined the amount of flavonoids in citrus juice from *Citrus sinensis*. Authors reported the naringin was present in a concentration of 22.06 ± 0.50 μg/mL. However, naringenin was not detected in the tested concentration range [16]. It is also interesting that in citrus juices tested by Silva et al., naringenin and naringin were present in low concentrations of 0.11–0.176 mg/100 mg and 0.011–0.030 mg/100 mg, respectively [17]. Yalim and co-workers also evaluated the naringin content of sweet orange juices obtained from three different varieties of oranges from four various regions. One type of juice was received by squeezing fruits by hand and second one by blending the orange peels (albedo and flavedo) and mixed with deionized water. The concentration of naringin in orange peel juice was about 2–20 times higher than in orange juice [18].

A scientific group from Spain determined the content of flavonoids in citrus juice obtained from four *Citrus* species: *C. paradisi*, *C. aurantium*, *C. reticulata* and *C. sinensis*. The concentration of naringin and naringenin were 338.36 mg/100 g and 2.35 mg/100 g, respectively [19]. Also, Dhuique-Mayer et al. evaluated the amount of naringenin glycoside from citrus juices from eight varieties of sweet oranges and also from clementine (*Citrus clementina*) and mandarin (*Citrus deliciosa*). The concentration of narirutin in tested juices was in the range of 37.2–98.4 mg/L [20].

Besides citrus fruits, the presence of naringenin was observed in *Musa paradisiaca* L. Behiry et al. determined the concentration of naringenin in banana peel methanolic extract at the level of 8.47 mg/100 g dry extract [21]. Naringenin and its derivatives were also detected at a much lower concentration by Dębski et al. in seven-day-old sprouts of fenugreek (*Trigonella foenum-graecum* L.). Scientists specified the concentration of naringenin and esters of naringenin at the level of 1.4 μg/100 g DW (dry weight). However, glycosides of naringenin were observed in a concentration of 6.3 μg/100 g DW [22]. In the case of green beans of coffee, Alkaltham et al. reported the concentration of naringenin at the level of 1.7 mg/100 g. Furthermore, beans roasted in a microwave or in a conventional oven contained a three-fold higher amount of naringenin with concentrations of 6.04 mg/100 g and 6.05 mg/100 g, respectively [23].

Naringenin also occurs in vegetables, e.g., in tomatoes. Paganga and co-workers determined the concentration of naringenin in Spanish tomatoes at a level of 282 mg/kg DW [24]. Interesting work was conducted by Bugianesi et al., which determined the blood content of naringenin after consumption of cooked tomato paste by men. Their results showed that

the test meal containing 150 mg of cooked tomatoes contained 3.8 mg of naringenin and the content of naringenin in plasma after 2 h was 0.12 μmol/L [25].

3. Other Derivatives of Naringenin

Among naringenin derivatives, one of the most described compounds are ether derivatives of naringenin. *O*-alkyl derivatives of naringenin also occur naturally in plants of the Boraginaceae family, e.g., 5-*O*-methylnaringenin, 7,4′-di-*O*-methylnaringenin, 7-*O*-methylnaringenin (sakuranetin) and isosakuranetin (4′-*O*-methylnaringenin) (Figure 2) [26–28]. Sakuranetin is a phytoalexin present in rice, which is biosynthesized in plants as an effect of biotic or abiotic stress by naringenin 7-*O*-methyltransferase [29]. There is also a chemical method to obtain 7-*O*-methylnaringenin in a simple reaction of naringenin with methyl iodide or methyl bromide in short time with a high yield [30]. Furthermore, 7-*O*-butylnaringenin is well-known for high activity against *Staphylococcus aureus* MRSA (methicillin-resistant *S. aureus*) [31], but also against *Helicobacter pylori* [32]. The elongation of the alkyl chain attached to naringenin at the C-7 position, and also at the C-4′ position, is a popular reaction in the last decade [30,33,34].
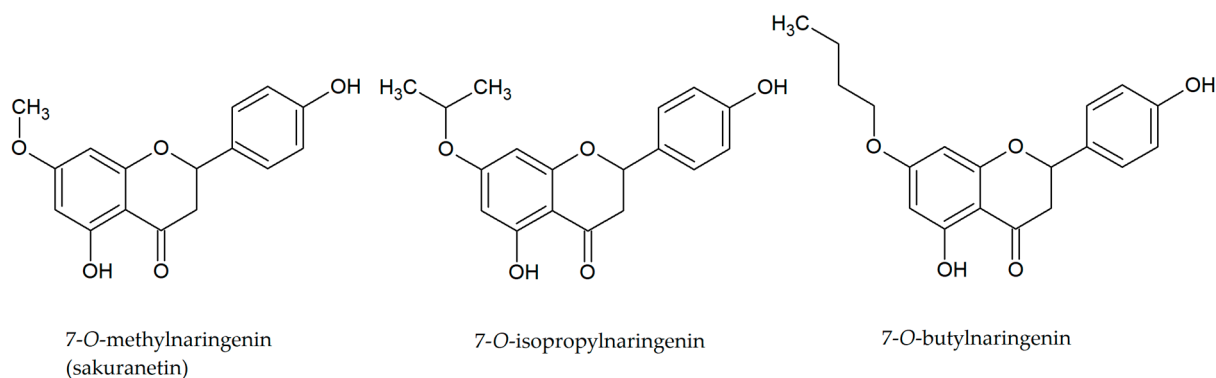

Figure 2. Structures of *O*-alkyl derivatives of naringenin.

4. Properties of Naringenin

4.1. Anti-Cancer Activity

The anti-cancer, anti-proliferative and anti-tumor activity of naringenin is primarily related to its ability to repair DNA. Its anti-tumor activity has been demonstrated against breast cancer cells [35], liver cancer [36,37], prostate cancer [38], melanoma [39] and glioblastoma of the brain and spinal cord [40].

Naringenin has been shown to affect both the internal (mitochondrial) and the external (receptor) pathway of apoptosis activation. This bioflavonoid acts in multiple ways at different steps in these pathways. First of all, it blocks the G0/G1 and G2/M phases, and therefore prevents the proliferation of neoplastic cells. It influences the accumulation of the p53 protein, which in turn binds to anti-apoptotic proteins (e.g., Bcl-2), promotes the action of the Bax protein and leads to the formation of pores in the mitochondrial membrane. In this way, it contributes to the loss of the mitochondrial membrane potential, and through this it releases apoptogenic factors, e.g., AIF, cytochrome c [41,42]. It induces apoptosis by damaging the cell nucleus or increasing the ratio of Bax/Bcl-2 cells, i.e., key regulators of apoptosis that control ion flow (K^+, H^+, Cl^-, Ca^{2+}) and reactive oxygen species. Thus, it acts as the "death factor" of the neoplastic cell. Under the influence of naringenin, there is also an intracellular accumulation of TGF-β1 (a factor involved in tumorigenesis), and thus reduced secretion and inhibition of the neoplastic process [36].

Recent studies have shown that naringenin, in addition to its effect on apoptosis, also has an inhibitory effect on proliferation (inhibits the phosphorylation of ERK1/2—extracellular signal-regulated kinase 1/2 and JNK—Jun N-terminal kinase) and angiogenesis (inhibits the expression of Tie2—tyrosine-protein kinase receptor-2 and enhances the expression of Ang2—angiopoietin-2) in murine and human melanoma cells (B16F10 and SK-MEL-28 cell lines, respectively) [43].

4.2. Anti-Inflammatory Activity

Naringenin inhibits leukocyte recruitment, thus preventing the action of resident macrophages, which produce chemotactic molecules to attract leukocytes to the focus of inflammation (mainly neutrophils). It also acts directly on macrophages by inducing the activation of Nfr2, a factor that initiates the anti-inflammatory response [44]. In addition, naringenin stops the activation of NF-κB, thus contributing to the inhibition of the secretion of pro-inflammatory cytokines, e.g., IL-33, TNFα, IL-1β and IL-6 [8]. It has been shown that this bioflavonoid can suppress the TLR4 receptor, necessary to recognizing bacterial lipopolysaccharide and initiating an inflammatory response in the body [6,8]. Other intracellular proteins (e.g., MyD88—myeloid differentation primary response protein 88; TIRAP/Mal—Tir domain-containing adapter protein; TRIF/TICAM1—TIR domain containing adapter including INF-β; TRAM/TICAM2—Trif-related adapter molecule) are also involved in the recruitment of inflammation, leading to the activation of a cascade of proteins necessary in various conventional pathways (e.g., NO secretion or NF-κB activation). This allows the activated macrophage to participate in inflammation, for example by synthesizing nitric oxide, oxygen free radicals or pro-inflammatory cytokines. However, in the presence of naringenin, it becomes impossible, forasmuch as this bioflavonoid also inhibits nitric oxide synthase (iNOS), preventing the release of NO. It also has an inhibitory effect on the mitogen-activated protein kinase, MAPK, the cascade of which plays an important role in the expression of pro-inflammatory cytokines. In addition, naringenin inhibits the production of superoxide anion and other reactive oxygen species (ROS) while increasing antioxidant capacity [45].

4.3. Antioxidant Activity

Naringenin is a powerful antioxidant. It can scavenge free radicals and affect the activity of antioxidant enzymes. Jung et al. reported an increase in the activity of superoxide dismutase (SOD) and catalase (CAT) after the administration of this bioflavonoid in the studied group of people with hypercholesterolemia [46]. On the other hand, in animal studies, the administration of this bioflavonoid decreased lipid peroxidation and increased the level of antioxidants. In addition, it has been shown to effectively neutralize hydroxyl (•OH), superoxide (O^{2-}), hydrogen peroxide (H_2O_2) radicals, nitric oxide (NO^-) and DPPH radicals, thereby alleviating liver complications caused by the administration of streptozotocin (STZ) [47]. The same authors, using in vivo studies on mice, showed an increase in the activity of SOD, CAT, glutathione peroxidase (GPx), glutathione S-transferase (GST) and glutathione (GSH), i.e., enzymes that are the body's defense strategy under unfavorable conditions. Naringenin's antioxidant abilities are most likely due to its ability to chelate trace amounts of metals, such as iron and copper, which contribute to enhancing ROS production [48]. In addition, naringenin has the ability to donate electrons or a hydrogen atom, leading to the oxidation of superoxide and hydroxyl radicals generated by hydrogen peroxide, therefore causing an enhancement of antigenotoxic activity [49].

4.4. Effects on the Nervous System

Naringenin inhibits pain induced by inflammatory stimuli, such as phenyl-β-benzoquinone, acetic acid, formalin, complete Freud's adjuvant, capsaicin, carrageenan, superoxide anion and LPS [50].

It has been shown that this bioflavonoid has an antinociceptive effect and enhances the pain tolerance of the nervous system in vivo [4]. Inflammatory cells released by pro-hyperalgesic cytokines (such as IL-33, TNF-α, IL-1β and IL-6), activate the nociceptor neurons and induce pain sensitization, leading to pain [51]. The ability of naringenin to inhibit NF-κB activity and induce Nfr2 activation indicates its indirect influence on the activity of nociceptor neuron. It has been shown that naringenin inhibits NF-κB-dependent production of TNF-α and IL-1β, i.e., cytokines that induce nociception by sensitizing neurons through p38 MAPK phosphorylation [50]. Moreover, naringenin regulates TRP

channels, expressed by nociceptor neurons such as TRPV1, TRPM3 and TRPM8. In this way, it contributes to the induction of analgesia, i.e., the phenomenon of pain relief [52].

4.5. Antidiabetic Activity

In vitro and in vivo studies prove the role of naringenin in the prevention and treatment of insulin resistance and type 2 diabetes. This bioflavonoid can reduce glucose adsorption by the intestinal brush border, and also reduces the level of this sugar in the kidneys. The in vivo research of Li and co-workers on albino rabbits provides evidence that naringenin, by inhibiting intestinal glucose absorption as well as renal reabsorption, directly contributes to the attenuation of hyperglycemia. Furthermore, in vitro studies concerning isolation of the brush border membrane vesicles (BBMV) of the intestines and the renal cortex revealed reduced activity of glucose uptake [53].

Moreover, it has been shown that naringenin also contributes to reabsorption, increased uptake and use of glucose by muscle and adipose tissues. Using primary porcine myotubes confirmed increased glucose uptake by naringenin while reducing intracellular ROS [54,55]. That indicates this bioflavonoid is counteracting insulin resistance. In turn, adipocytes 3T3-L1, treated with naringenin, showed significant reduction of insulin-stimulated glucose levels [56]. Moreover, the signaling cascades, i.e., NF-κB and JNK, inhibited by this aglycone, have suppressed TNF-α induction and adipocyte expression induced by co-culture of macrophages, TLR2. This action directly contributes to the inhibitory involvement in obesity-induced cellulitis [57].

Naringenin has also been shown to have a productive effect on pancreatic β-cells. By "teaching" them, it increases their ability to detect glucose. Bhattacharya et al. proved in their study that β-cells from rat pancreas', exposed to this bioflavonoid, upregulate insulin-stimulated glucose secretion and, in addition, increase the expression of several genes of these cells: *Glut2; Gck; Ins1,2; Beta2; Act1,2; Pdx1* and *Bcl2*. This suggests that naringenin has a pro-apoptotic effect on pancreatic cells, increasing their sensitivity to glucose [58].

4.6. Hepatoprotective Properties

Naringenin reduces triglyceride production and affects gluconeogenesis, contributing to the attenuation of hyperglycemia and hyperlipidemia. The in vivo studies of Ortiz-Andrade et al. confirm this effect. They showed that this bioflavonoid increases the concentration of high-density lipoproteins (HDL) in the serum of Wistar albino rats. In addition, it contributes to the reduction of the activity of enzymes necessary in the process of gluconeogenesis: glucose-6-phosphatase and fructose-1,6-bisphosphatase in the liver [59]. In turn, in vivo studies performed by Sharma et al. confirm that naringin significantly improves the lipid profile in the same animal model on a high-fat diet. Rat serum shows decreased levels of triglycerides, triacylglycerol, LDL cholesterol and non-esterified fatty acids (NEFA), while elevated levels of HDL cholesterol are observed [60].

4.7. Antimicrobial Activity of Naringenin

The increasing resistance of bacteria to antimicrobial drugs is a global trend, comparable to an eruption of a sleeping volcano. Currently, for every group of antibiotics, there can be found strains of bacteria which are resistant. This ever-growing problem is due to the intensive use of antibiotics in many areas including food production, veterinary medicine and medicine. Their excessive administration during the COVID-19 pandemic, the treatment of asymptomatic patients and the increasing use of broad-spectrum antibiotics (in the absence of narrow-spectrum ones) promotes this phenomenon and facilitates its propagation [61–63]. This overuse leads to the development of multidrug-resistant phenotypes: VRE (vancomycin-resistant *Enterococcus*), MRSA, ESBLs (extended-spectrum beta-lactamases), KPC (*Klebsiella pneumoniae* carbapenemase) and NDM-1 (New Delhi metallo-β-lactamase-1). Naringenin and its derivatives have antimicrobial properties, especially against Gram-positive bacteria, such as *S. aureus*, including antibiotic resistant strain MRSA. At the moment, the results of clinical trials of this bioflavonoid as an antimicrobial

agent are poor, and there are no registered clinical trials in the databases of both the U.S. and E.U. However, its pharmacological safety was proven for doses as high as 900 mg (escalated safe total dose) [64], so its usage as an antimicrobial drug can be explored in future.

## 5. Antimicrobial Activity against Gram-Positive Bacteria

Multidrug-resistant (MDR) strains of bacteria are increasingly being isolated mainly in hospital treatment, but also in non-hospital treatment. The prevalence of CA-MRSA (community-associated MRSA) strains is becoming particularly alarming. The Center for Disease Control and Prevention (CDC) listed MRSA as a "serious threat". This growing resistance brings the need to search for new therapeutic options. Naringenin activity against MRSA is confirmed by number of laboratory investigations and is probably stronger against Gram-positive bacteria than Gram-negative, as shown in a study comparing naringenin activity and mechanism of action against *S. aureus* and *Escherichia coli*. In both species, maximum growth rate was decreasing with increasing concentration of naringenin. However, for *S. aureus*, the inhibition was much more significant, because for a concentration of 1.47 mM, an almost three-fold decrease in viability of this strain was shown. Also, time to reach the stationary phase of growth for *S. aureus* was elongated by naringenin solution. Complete growth inhibition of this strain was observed up to 14 h in the presence of this bioflavonoid at a concentration of 2.20 mM. In the same study, membrane fluidity and fatty acid profiles were investigated, showing that submission to naringenin altered membrane composition in favor of anteiso-branched fatty acids, resulting in increased membrane fluidity. This mechanism of action can suggest that difference in naringenin activity against Gram-positive and Gram-negative bacteria can emerge from differences in their membrane structure [65]. Also, Wang and co-workers, in their other studies, showed that naringenin can interact with the bacterial cell in a variety of ways. This bioflavonoid has an effect on both membrane fatty acids and proteins, and also can bind to the DNA of *S. aureus* [66].

A mechanism of action different than that of standard antibiotics can explain why naringenin and its derivatives are active against antibiotic-resistant pathogens such as MRSA. The results of research in this direction are very promising. In a study from 2013, MIC of this bioflavonoid against MRSA (bovine isolate) was measured to be 20 mM, while for its derivative, 7-*O*-butylnaringenin, it was only 0.625 mM [31]. In a more complex study on human isolates, MIC of 12 various naringenin derivatives ranged between 4 and 64 μg/mL. The substances with the greatest potential against MRSA (clinical isolate from blood infections) were: 7-*O*-butylonaringenin oxime and 7-*O*-hexylnaringenin oxime with MIC value of 4 μg/mL; 7-*O*-butylnaringenin, 7-*O*-pentylnaringenin oxime and 7,4′-di-*O*-isopropylnaringenin oxime with MIC value of 8 μg/mL; 7-*O*-ethylnaringenin oxime and 7-*O*-isopropylnaringenin oxime with MIC value of 16 μg/mL. Of these compounds, 7-*O*-isopropylnaringenin oxime showed the lowest MBC value at 32 μg/mL. The same study investigated interactions between the actions of bioflavonoid-based substances and antibiotics against MRSA, showing a synergistic effect between particular naringenin derivatives, such as 7-*O*-isopropylnaringenin oxime and 7-*O*-hexylnaringenin oxime, which lowered MIC for gentamicin eight-fold, MIC for erythromycin (four-fold) and MIC for gentamycin/erythromycin (eight-fold) for 1 and 2 derivative, respectively [67]. In another study, the addition of naringenin and its fluorinated derivatives proved to decrease MIC of ciprofloxacin for MRSA (hospital isolate) by up to 50-fold [68]. Scheme 1a,b show the results of both authors discussed above. However, one study suggested antagonistic interaction between β-lactam antibiotics and naringenin. In this study, bioflavonoid inhibited growth of both MRSA and MSSA (methicillin-sensitive *S. aureus*), but the growth was visible around penicillin and oxacillin discs and methicillin strips [69]. In contrary, another study revealed synergistic interaction between naringenin and oxacillin against MRSA, resulting in lesser cell growth measured as cell density [70].

a) Antimicrobial activity of naringenin derivatives against Gram+ bacteria
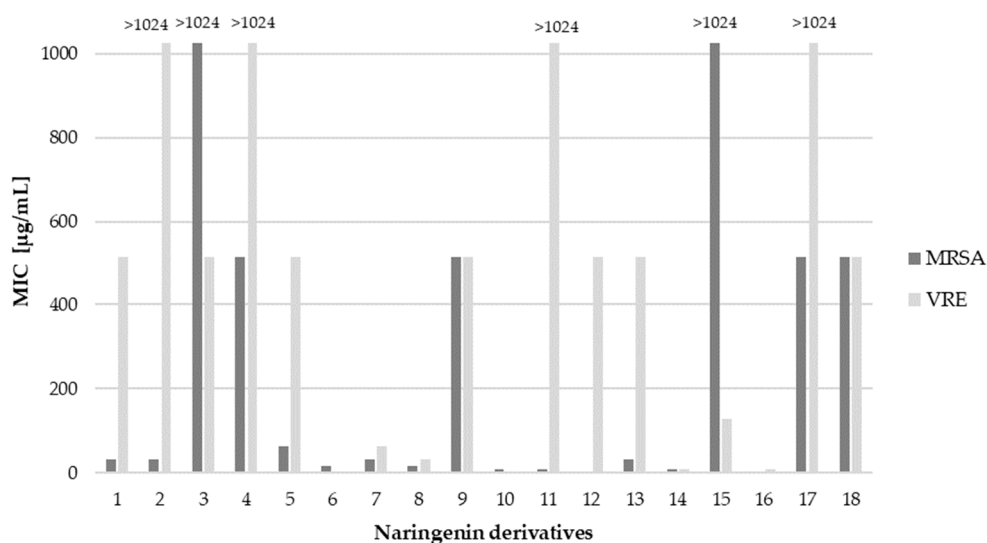
b) Activity of naringenin and its derivatives against MRSA
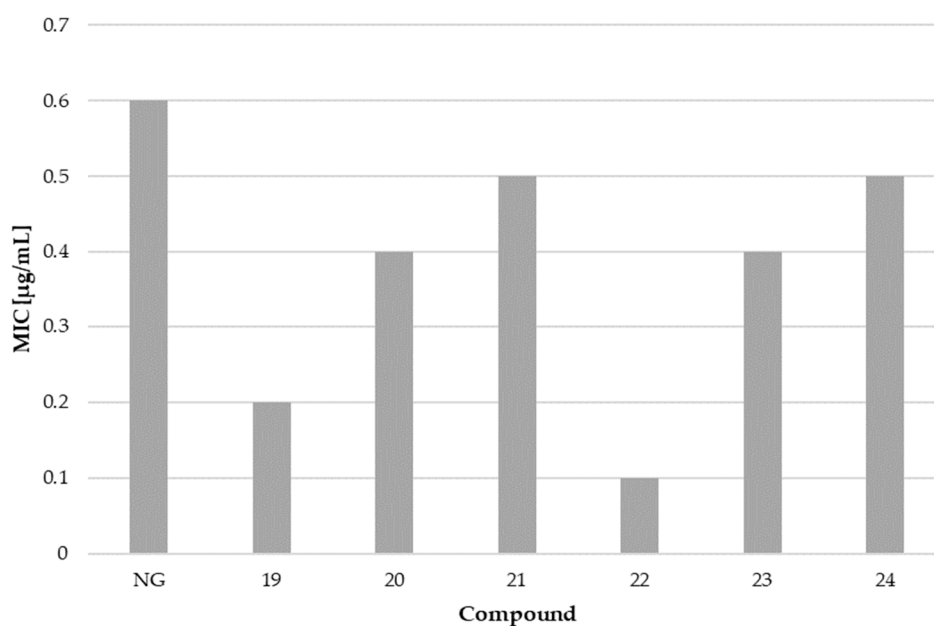
Scheme 1. In vitro activity of naringenin and its derivatives against Gram-positive bacteria. (**a**) 1—7-*O*-methylnaringenin; 2—7-*O*-methylnaringenin oxime; 3—7,4′-di-*O*-methylnaringenin; 4—7,4′-di-*O*-methylnaringenin oxime; 5—7-*O*-ethylnaringenin; 6—7-*O*-ethylnaringenin oxime; 7—7-*O*-isopropylnaringenin; 8—7-*O*-isopropylnaringenin oxime; 9—7,4′-di-*O*-isopropylnaringenin; 10—7,4′-di-*O*-isopropylnaringenin oxime; 11—7-*O*-butylnaringenin; 12—7-*O*-butylnaringenin oxime; 13—7-*O*-pentylnaringenin; 14—7-*O*-pentylnaringenin oxime; 15—7-*O*-hexylnaringenin; 16—7-*O*-hexylnaringenin oxime; 17—7,4′-di-*O*-hexylnaringenin; 18—7,4′-di-*O*-hexylnaringenin oxime (based on Duda-Madej et al. [67]). (**b**) NG—naringenin; 19—6-fluoronaringenin; 20—6-chloronaringenin; 21—6-iodonaringenin; 22—6,8-difluoronaringenin; 23—6,8-dichloronaringenin; 24—6,8-diiodonaringenin (based on Mohammed et al. [68]).

Since biofilm formation by pathogenic bacteria is considered a major virulence factor (it protects against immune response mechanisms and the targeted action of antimicrobial

agents), fighting is a key step in infection control. The useful property of naringenin in this field is its ability to inhibit the formation of biofilm. Such action was proven in the case of *Streptococcus mutans*. In this study, naringenin solution with a concentration of 200 μg/mL almost totally inhibited the formation of biofilm, while 100 μg/mL had about 70% effect and 50 μg/mL was effective at 50%, respectively. Not only growth of bacteria was inhibited, but also their surface hydrophobicity was increased and aggregation reduced. The same study used PCR to determine expression of genes related with biofilm formation: *gtfB*, *gtfC*, *comD*, *comE*, and *luxS*. Those were proven to be suppressed by this bioflavonoid [71]. An analogical study was performed for MRSA and Δ*agr* mutant (mutation inserted in the accessory gene regulator quorum sensing (QS) system), revealing lower expression of *icaAD* gene and thus lower levels of biofilm formation after incubation in naringenin [70].

One more characteristic of naringenin is that it inhibits production of α-toxin, one of the *S. aureus* cytotoxins. This property was confirmed for three different *S. aureus* strains (ATCC 29213, ATCC 10832, and 8325-4) by measurement of haemolytic activity, which decreased to 5.79%, 9.27% and 4.91% compared to the control group. The α-toxin-reduced expression was confirmed using western blot analysis. Interestingly, for one of the tested *S. aureus* strains, USA 300, no α-toxin antigen was detected after treatment with naringenin solution at a dose as low as 2 μg/mL. Zhang and co-workers treated, with naringenin solutions, both lung carcinoma epithelial cells (A549 cell line) and *S. aureus* co-culture system, which simulated pneumonia. They showed that this bioflavonoid had the ability to damage cancer cells, as well as cells changed by the disease process, at levels as high as 50%. They determined the cytotoxic dose for a concentration of 9.22 μg/mL of naringenin by measuring lactate dehydrogenase (LDH) activity. Furthermore, the authors tested with in vivo studies the effect of this bioflavonoid on mice infected with an *S. aureus* strain that caused pneumonia. A dose of 100 mg/kg was administered, which corresponded to 26.04 μg/mL maximum plasma concentration. In histological analysis, the lungs of treated mice had only few focal inflammation areas, while in the control group there were extreme signs of injury [72]. Such effects of naringenin may be due to its effects on the immune response and the levels of secreted cytokines, as evidenced by the research of Yao et al. A study conducted on children with bronchial pneumonia showed that bioflavonoid lowers plasma concentration of pro-inflammatory cytokines such as IL-6, IL-8 and TNF-α and increases the level of anti-inflammatory IL-10, with even greater efficiency than azithromycin [73]. Administration of naringenin turned out to be beneficial for children due to reduction of inflammation, shortening disappearance time of clinical symptoms and reducing complications after therapy. This gives positive insight on naringenin as a potent drug for infections; however, no cultures were done, hence MIC/MBC were not measured. Given these optimistic data, we cannot be sure whether the improvement of the patients is a result of the antimicrobial or anti-inflammatory properties of naringenin.

Naringenin and naringin antimicrobial properties can be used in many ways. One of the investigated areas is usage of naringin in orthopedy, as an element of titanium implant coating. Controlled release of bioflavonoid from a metal-organic framework allowed it to both induce osseointegration and prevent *S. aureus* infection [74]. Another way to use naringin to treat infections caused by Gram-positive bacteria is in a complex with gold nanoparticles stabilized by gum tragacanth. Naringenin encapsulated in a gold nanoparticle showed an MIC of 21.98 μg/mL against *Bacillus subtilis* ATCC 11774. This value is significantly lower (more than three-fold) than for the pure bioflavonoid, for which the MIC was 68.43 μg/mL [75]. In the case of *Micrococcus luteus* ATCC 10240 MIC values were similar for pure bioflavonoid and that complexed with gold nanoparticles (25 μg/mL), but the IC_{50} (the concentration at which 50% growth inhibition was observed) was lower for the complex, with values of 371.66 μg/mL and 253.93 μg/mL, respectively. Therefore, flavonoids such as naringenin or naringin and their derivatives can be used in fighting against infectious diseases not only by direct action but also using carriers such as the described gold nanoparticles, or as a component of biomaterials.

In conclusion, naringenin and its derivatives have the potential to be used against Gram-positive bacteria due to number of different properties. They inhibit not only the growth of pathogenic bacteria, including those resistant to classic antibiotics (MRSA), but also reduce biofilm formation and toxin production. Therapeutic use must still be tested in clinical trials, but taking into consideration all these properties, its pharmacological safety and possible synergistic interaction with antibiotics, naringenin and its derivatives have considerable potential to be used in therapy, especially in treatment of infections caused by antibiotic-resistant pathogens such as MRSA.

6. Antimicrobial Activity against Gram-Negative Bacteria

Resistance among Gram-negative bacteria appears to be a bigger problem due to easy spreading by plasmid transfer [76]. The second reason is lack of new antibiotics targeting Gram-negative bacteria or the existing ones being very harmful for the patients. Searching for compounds with promising MIC values is of primary interest to many scientist; often they seek novelties among natural components. The activity of naturally derived compounds against Gram-negative bacteria is usually lower, probably due to the presence of negatively charged lipids in the outer layer of the membrane, which acts like the lipid barrier [77,78]. Despite the fact that naringenin is not a new substance—it was the object of research in the late 80s and early 90s—the compound has been undergoing a renaissance in recent years [79]. Naringenin derivatives have become an object of particular interest. There are many scientific studies describing the activity of plant extracts containing naringenin, but there is not much research on the pure compound, which is the focus of this review. The MIC of naringenin and naringin against Gram-negative bacteria were measured by many authors and are summarized by us in the table below (Table 1). The most frequently tested species were *E. coli*, *H. pylori*, *Pseudomonas aeruginosa* and *K. pneumoniae*. Authors determined the antibacterial activity against different strains of these bacteria, which were either purchased or isolated from patients. The MIC values of naringenin ranged from 0.5–1 up to 2000 µg/mL; however usually 1000 µg/mL was the highest concentration tested. There were similarly good results for *H. pylori*, ranging from 40 µg/mL to 100 µg/mL. The values for *E. coli* heavily differed (12.5–1000 µg/mL). Results of naringin were significantly worse comparing to naringenin. Some close derivatives of naringenin tested by Murti et al. and Duda-Madej et al. had surprisingly satisfying values (MIC ≤ 50 µg/mL) shown in the Scheme 2a,b [67,80]. Beside in vitro measurements of MICs, there are a number of molecular and biochemical studies demonstrating the effect of this bioflavonoid on the Gram-negative bacterial cell. Indeed, it has been shown that naringenin could affect the expression of genes involved in QS (e.g., *lasI, lasR, rhlI, rhlR, lasA, lasB, phzA1* and *rhlA)*, thus reducing the production of pyocyanin and elastin of *P. aeruginosa* PAO1 [81]. It is also known that naringenin exhibits 34% inhibition on the urease of *H. pylori,* although in concentration of 300 µg/mL, which is 3–7.5 times higher than its MIC against *H. pylori* strains [82].

Vikram and co-workers suggested that naringenin attenuates virulence and mobility of *Salmonella enterica* subsp. *enterica* serovar Typhimurium owing to repressing 24 genes of pathogenicity island 1 and down-regulating 17 genes of mobility [83]. The same research team, in another of their studies, demonstrated the inhibitory effect of naringenin on biofilm formation of *Vibrio harveyi* and *E. coli* O157:H7 strains. The bioflavonoid directly disrupted the type III secretion system (T3SSs) of these strains [84]. Other researchers have shown a direct effect of naringenin on the bacterial cell. In the presence of this compound some spectacular changes occurred in the composition of the outer cell membrane of *E. coli* strains. This was due to influence on the expression of fatty acid biosynthesis-associated genes, including *fabG, fabI, fabD, cfa* (decrease), and *fabA* (up-regulates) [65]. Although naringenin appears to be a promising substance in the fight against Gram-negative bacteria, similar to current antibiotics it can be neutralized by microbes. *Herbaspirillum seropedicae* has the ability to degrade naringenin, probably owing to SmR1 operon, whose expression is induced by naringenin. Mutation of *fdeA* gene, belonging to SmR1 operon, results in a decline of the ability to degrade naringenin [85]. Complementing the effective fight against

Gram-negative bacteria is the search for different forms of naringenin delivery into the body. It has been shown that only 15% of this bioflavonoid is absorbed after oral administration, so treatment by this route is not very promising, and new solutions are required [8,73].
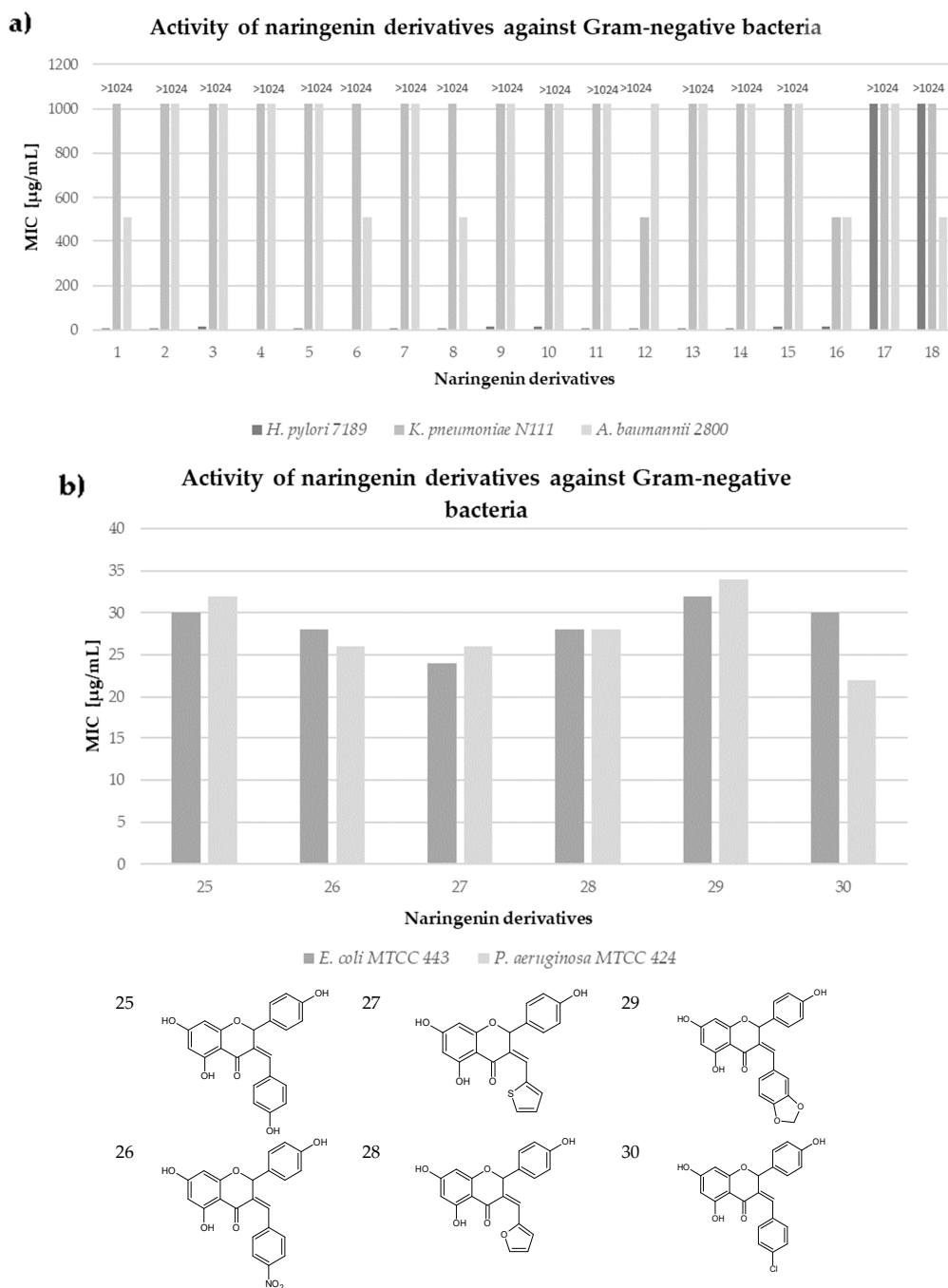
Scheme 2. In vitro activity of naringenin derivatives against Gram-negative bacteria. (**a**) 1—7-*O*-methylnaringenin; 2—7-*O*-methylnaringenin oxime; 3—7,4′-di-*O*-methylnaringenin; 4—7,4′-di-*O*-methylnaringenin oxime; 5—7-*O*-ethylnaringenin; 6—7-*O*-ethylnaringenin oxime; 7—7-*O*-isopropylnaringenin; 8—7-*O*-isopropylnaringenin oxime; 9—7,4′-di-*O*-isopropylnaringenin; 10—7,4′-di-*O*-isopropylnaringenin oxime; 11—7-*O*-butylnaringenin; 12—7-*O*-butylnaringenin oxime; 13—7-*O*-pentylnaringenin; 14—7-*O*-pentylnaringenin oxime; 15—7-*O*-hexylnaringenin; 16—7-*O*-hexylnaringenin oxime; 17—7,4′-di-*O*-hexylnaringenin; 18—7,4′-di-*O*-hexylnaringenin oxime (based on Duda-Madej et al. [67]). (**b**) based on Murti et al. [80].

Table 1. In vitro activity of naringenin and naringin against Gram-negative bacteria.

Strain	Activity of Naringenin	Reference
P. aeruginosa c.i.	128 μg/mL	[86]
E. coli ATCC 8739	1000 μg/mL	[87]
E. coli ATCC 11775	1000 μg/mL	
H. pylori ATCC43504	80 μg/mL	[82]
H. pylori NCTC11637	40 μg/mL	
H. pylori NCTC11638	40 μg/mL	
H. pylori 82516 c.i.g	40 μg/mL	
H. pylori 82548 c.i.g	40 μg/mL	
H. pylori 4 c.i.g	100 μg/mL	
E. coli ATCC 25922	1000 μg/mL	[65]
E. cloacae DMST 21394	>512 μg/mL	[88]
E. cloacae DMST 21549	>512 μg/mL	
E. cloacae DMST 19719	>512 μg/mL	
E. coli ATCC 25922	>512 μg/mL	
K. pneumoniae ATCC 13883	0.5–1 μg/mL	[89]
H. pylori ATCC 43504	100 μg/mL	[90]
H. pylori ATCC 51932	100 μg/mL	
H. pylori OX.22 c.i.	100 μg/mL	
H. pylori OX. 63 c.i.	100 μg/mL	
H. pylori OX.64 c.i.	100 μg/mL	
H. pylori OX.67 c.i.	100 μg/mL	
H. pylori OX.83 c.i.	100 μg/mL	
Bacteroides galacturonicus DSM 3978	250 μg/mL	[91]
Escherichia coli DSM 1116	>250 μg/mL	
H. pylori ATCC 43 504	100 μg/mL	[92]
E. coli ATCC 31030	550 μg/mL	[79]
P. mirabilis ATCC 25933	550 μg/mL	
P. aeruginosa ATCC 10145	500 μg/mL	
S. enterica subsp. *enterica* serovar Paratyphi B(S-3)	600 μg/mL	
S. enterica subsp. *enterica* serovar Typhi D(S-58)	400 μg/mL	
S. enterica subsp. *enterica* serovar Typhimurium ATCC 14028	600 μg/mL	
S. sonnei D1, L1, S2 ATCC 9290	450 μg/mL	
S. marcescens ATCC 11105	500 μg/mL	
S. boydii C2, L1, S2 ATCC 8700	100 μg/mL	
S. marcescens ATCC 27117	400 μg/mL	[93]
E. coli ATCC 25922	>2000 μg/mL	[94]
K. pneumoniae ATCC 13883	2000 μg/mL	
P. mirabilis ATCC 43071	2000 μg/mL	
P. aeruginosa ATCC 27857	>2000 μg/mL	
S. enterica subsp. *enterica* serovar Typhimurium ATCC 14028	>2000 μg/mL	

Table 1. *Cont.*

Strain	Activity of Naringenin	Reference
E. coli MTCC 1652	12.5 µg/mL	[95]
P. aeruginosa MTCC 424	23.5 µg/mL	
E. coli K-12 MG1655	800 µg/mL	[96]
S. enterica subsp. *enterica* serovar Typhimurium LT2	1000 µg/mL	
P. putida ATCC 795	1000 µg/mL	
S. enterica subsp. *enterica* serovar Typhimurium ATCC 14028	250 µg/mL	[97]
E. coli 916 c.i.g	125 µg/mL	[98]
S. enterica subsp. *enterica* serovar Typhimurium 450 c.i.g	125 µg/mL	
E. coli ATCC 25922	400 µg/mL	[99]
Strain	**Activity of Naringin**	**Reference**
P. aeruginosa ATCC 9027	1000 µg/mL	[87]
H. pylori ATCC43504	>100 µg/mL	[82]
H. pylori NCTC11637	>100 µg/mL	
H. pylori NCTC11638	>100 µg/mL	
H. pylori 82516 c.i.g	>100 µg/mL	
H. pylori 82548 c.i.g	>100 µg/mL	
H. pylori 4 c.i.g	>100 µg/mL	
H. pylori ATCC 43 504	>100 µg/mL	[92]
E. coli c.i.	500 µg/mL	[100]
P. aeruginosa c.i.	500 µg/mL	
E. coli ATCC 31030	900 µg/mL	[93]
P. mirabilis ATCC 25933	700 µg/mL	
P. aeruginosa ATCC 10145	600 µg/mL	
S. enterica subsp. *enterica* serovar Typhimurium ATCC 14028	800 µg/mL	
S. marcescens ATCC 27117	600 µg/mL	
E. coli ATCC 25922	>2000 µg/mL	[101]
E. coli K-12 MG1655	>1000 µg/mL	[96]
S. enterica subsp. *enterica* serovar Typhimurium LT2	>1000 µg/mL	
P. putida ATCC 795	>1000 µg/mL	

Legend: c.i.—clinical isolates; c.i.g—clinical isolates from gastroscopic samples; OX—clinical isolates obtained from the Microbiology Lab at OUCRU (Oxford University Clinical Research Unit, Ho Chi Minh City, Vietnam) from patients with duodenal and stomach ulcers.

7. Antifungal Activity

According to the CDC, in 2021 in the United Stated there were about 7000 deaths from fungal diseases (*CDC*, n.d.). However, this is only an estimated number as many infections were undiagnosed. Fungal diseases may be really serious and life-threatening, especially in immunosuppressed patients, because they usually suffer from invasive fungal infections (IFIs).

The burden of fungal diseases is the trigger point for searching for new antifungal agents. Many studies are focused on naringenin and its derivatives, as among many properties, they exhibit antifungal effects. In the table below, there are gathered MICs of naringenin and its derivatives that reflect their activity against selected fungi (Table 2).
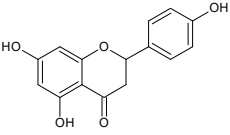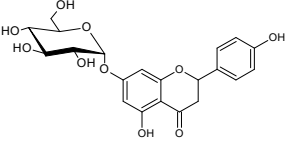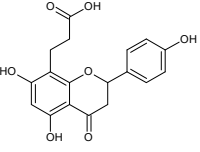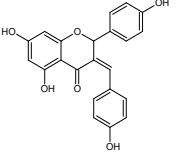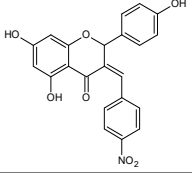
Soberón and co-workers pointed out that *Candida albicans* is a pathogen that frequently causes hospital infections and may be resistant to many antifungal agents. Inspired by Argentinean folk medicine, the authors obtained naringenin from *Tessaria dodoneifolia* ethanolic extract and examined its antifungal activity on two *C. albicans* strains: ATCC 10231 (sensitive to fluconazole) and 12–99 (resistant to fluconazole). Naringenin was active against both tested strains, and—the main conclusion of the experiment—the results obtained suggested that the combination of this bioflavonoid with fluconazole showed a synergistic effect against resistant strains. Naringenin's MIC value is marked as 40 μg/mL against both *C. albicans* ATCC 10231 and 12–99 (Table 2) [102]. However, when naringenin was used in concentration 83 μg/mL, it had no antifungal activity on *C. albicans* ATCC 10231 or on *Candida* spp. [103].

Moreover, according to Rauha et al., naringenin fails to inhibit growth of *C. albicans* ATCC 10231, *Aspergillus niger* ATCC 16404 and *Saccharomyces cerevisiae* FOMK [84]. Also, naringin showed no antimicrobial activity against these fungi with its MIC value of 1250 μg/mL against *C. albicans* from clinical isolates (Table 2) [101].

Another group of compounds which possess antifungal properties are ether derivatives of naringenin. *O*-Alkyl derivatives of naringenin and their oximes were tested for activity against bacteria and fungi. It turns out that the strongest effect against *Fusarium linii* KB-F1 showed not only naringenin, but also 7-*O*-dodecylnaringenin oxime, 7,4′-di-*O*-dodecylnaringenin and its oxime. These compounds caused complete growth inh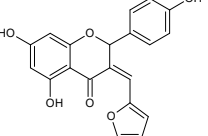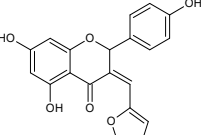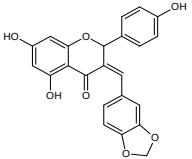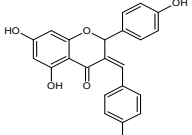ibition of this fungal strain. The same effect was observed for naringenin oxime and 7,4′-di-*O*-pentylnaringenin against *A. niger* DSM1957. Based on these results, elongation of the *O*-alkyl chains attached at positions C-7 and C-4′ in naringenin increased the antimicrobial activity. In the case of *C. albicans* DSM1386, oximes of *O*-alkyl derivatives exhibited a stronger effect than just *O*-alkyl derivatives. This is an important observation, which suggest that introducing the oxime group amplified biological properties [30]. The enhancing of the antifungal properties of naringenin is caused also by introducing heterocyclic nuclei. In the study of Murti Y., twelve naringenin derivatives, substituted at C-3 position, were tested for activity against two fungal strains: *A. niger* MTCC 9687 and *C. albicans* MTCC 183. All of these compounds had an antifungal effect, but the 4′-chlorophenyl-substituted naringenin molecule at the C-3 position had the strongest antifungal activity, and its MIC value was 16 μg/mL against both fungal strains (Table 2). Although all of the derivatives showed antifungal activity, there are also moieties that may reduce it. The methoxy-substituted phenyl ring decreased the antifungal effect of naringenin [80]. According to the above-mentioned studies, different naringenin derivatives also have significant biological properties, some of them even greater than naringenin. This knowledge can open up new possibilities in searching for new antifungal agents.

Flavonoids are also examined for their activity against major rice pathogens. The main cause of much plantation damage and food losses are fungal diseases—the most destructive fungus species appears to be *Magnaporthe oryzae (Pyricularia oryzae)*. Rice is a staple food for over 50% of the world's population, so such crop damage may lead to tragic consequences [104]. The influence of naringenin on this strain was associated with an inhibitory effect on the spore germination with as low as 7 μg of this bioflavonoid [105]. What is more, rice plants actually use naringenin to produce sakuranetin, which have better antifungal properties. On the other hand, *M. oryzae* metabolizes sakuranetin into naringenin, so it lowers the resistance of rice plants [106]. Being aware of this process may be a starting point for further examination of activity against rice pathogens of naringenin.

Table 2. In vitro activity of naringenin and its derivatives against selected fungi strains.

Compound	Strain	Activity	Reference
	Candida albicans ATCC 90028	5 μM	[107]
	Candida parapsilosis ATCC 22019	5 μM	
	Trichosporon beigelii KCTC 7707	2,5 μM	
	Malassezia furfur KCTC 7743	10 μM	
	Trichophyton rubrum KCTC 6345	5 μM	
	Aspergillus flavus KCTC 6905	10 μM	
	Saccharomyces cerevisiae KCTC 7296	5 μM	
	Candida albicans ATCC 10231	40 μg/mL	[102]
	Candida albicans 19–22	40 μg/mL	
	Candida albicans ATCC 10231	16 mg/mL	[108]
	Candida kruzei ATCC 6258	32 mg/mL	
	Aspergillus niger 439	100 μg/mL	[109]
	Fusarium oxysporum (M42)	n.i.e.	
	Candida albicans (N/A)	n.i.e.	
	Saccharomyces cerevisiae (N/A)	n.i.e.	
	Candida albicans MTCC 183	22 μg/mL	[80]
	Aspergillus niger MTCC9687	20 μg/mL	
	Candida albicans MTCC 183	18 μg/mL	[80]
	Aspergillus niger MTCC9687	18 μg/mL	
	Candida albicans MTCC 183	24 μg/mL	[80]
	Aspergillus niger MTCC9687	20 μg/mL	
	Candida albicans MTCC 183	22 μg/mL	[80]
	Aspergillus niger MTCC9687	22 μg/mL	
	Candida albicans MTCC 183	22 μg/mL	[80]
	Aspergillus niger MTCC9687	24 μg/mL	
	Candida albicans MTCC 183	16 μg/mL	[80]
	Aspergillus niger MTCC9687	16 μg/mL	

Legend: N/A—not available; n.i.e.—no inhibitory effect.

8. The Mechanism of Action of Naringenin on Bacteria and Fungi

Naringenin, like all flavonoids, blocks the respiratory chain, fatty acid synthesis, gyrase activity, QS molecules and increases membrane permeability [110].

Song and co-workers showed in their research that the presence of naringenin not only influences the distribution of fatty acids in the bacterial cell, but also reduces the expression of genes involved in biofilm formation. This situation contributes to a change in the structure of the biofilm and an increase in the sensitivity of the *S. aureus* strain showing MR resistance to antibiotics [70]. Other studies have also shown that naringenin is an antagonist of cell-to-cell signaling, an important regulatory factor in biofilm production in some bacteria [84]. The results obtained by Paczkowski et al. provide additional facts in this regard. They showed that this bioflavonoid has the ability to simultaneously inhibit the pairs LasI/R and RhlI/R, i.e., two synthetases with their receptors, which are responsible for the synthesis of two autoinducers in QS in *P. aeruginosa* [111].

It is significant that flavonoids, including the naringenin discussed in this review, have been shown to use different antimicrobial mechanisms than the antibiotics available on the market [112]. Thus, they can play a huge role in amplifying the synergism of antimicrobial therapy. The available literature data clearly indicate that naringenin interacting with antibiotics enhanced both the synergistic and additive effect. Hyperadditional synergism has been demonstrated in the interaction of this flavonoid with oxacillin, a β-lactam antibiotic [70]. An additive and synergistic effect was also observed in the combination of *O*-alkyl naringenin derivatives with antibiotics from the groups macrolides, fluoroquinolones, nitroimidazoles, aminoglycosides, glycopeptides and polypeptides. Duda-Madej and co-workers speculate that this phenomenon occurs most likely because naringenin and its derivatives must act on the same target sites as the antibiotics used, namely the cell wall, genetic material and/or protein synthesis [67]. Given the fact of the confirmed synergistic effect of naringenin in combination with antibiotics and the ability of this bioflavonoid to increase the activity of liver enzymes (ALT—alanine aminotransaminase; AST—aspartate aminotransferase) [36,113], due caution should be exercised during antibiotic therapy, remembering that these enzymes are responsible for metabolizing drugs. Therefore, the administration of this bioflavonoid at the same time as an antibiotic may contribute to a significant decrease or a dangerous increase (depending on the antibiotic used) in its concentration in the body. Ultimately, this can result in the failure of the antimicrobial therapy or the occurrence of various side effects.

Tsuchiya et al., conducting research on the MRSA strain, proved that the antimicrobial effect of naringenin consists of reduced fluidity in the hydrophilic and hydrophobic regions of both the inner and outer cell membranes [114]. The bacterial plasma membrane is responsible for the processes of self-regulation, respiration, transport, biosynthesis and cross-linking of peptidoglycan, as well as lipid biosynthesis. Thus, disruption of its integrity may directly or indirectly affect metabolic processes and lead to the death of the bacterial cell. Moreover, the ability of the bioflavonoid to block the synthesis of the cell envelope by inhibiting the effect on 3-hydroxylacyl-ACP dehydratase in *H. pylori* and 3-ketoacyl-ACP synthase in *E. faecalis* has been proven [115,116]. These enzymes are necessary for the synthesis of, inter alia, lipoproteins, phospholipids and lipopolysaccharides, i.e., components of the cell membrane. The inhibitory effect on these pathways disrupts the proper functioning of the bacterial cell and represents the hook for disrupting their proliferation. This ability of naringenin is very important as it is desirable in the development of new antibacterial drugs.

Studies on the antimicrobial mechanism of naringenin indicate its active participation in the inhibition of the efflux pumps, i.e., proteins involved in pumping out the antibiotic from the bacterial cell [117]. This bioflavonoid ability has the potential to be developed in the future as a phytobiotic in the fight against microbial resistance. Additionally, the studies by Oh et al. confirm this fact, as they have shown that phenolic compounds (including naringenin) reduce the expression level of CmeABC, a multi-drug efflux pump that is important in antibiotic resistance in *Campylobacter jejuni* strains [118].

9. Conclusions

Naringenin, commonly found in large amounts in citrus fruits, is known for many biological activities, e.g., the antioxidant, anti-inflammatory, anti-cancer, but also antimicrobial. Naringenin itself is characterized by a much lower activity against Gram-negative bacteria, in contrast to Gram-positive bacteria, where this activity is much more satisfactory. In turn, its antifungal activity is at a moderate level against both filamentous and sporulation fungi. Very promising results in antimicrobial activity are given by naringenin derivatives, which emphatically improve the antimicrobial activity. The incorporation of the oxime group in place of the carbonyl moiety at the C-4 position significantly increases the activity against pathogenic microorganisms, both Gram-positive (e.g., *S. aureus*, *E. faecalis*) and Gram-negative (e.g., *H. pylori*, *E. coli*, *P. aeruginosa*). A similar relationship was observed in studies on antifungal activity. Pure naringenin showed even more than two times lower activity than its derivatives (containing, among others: *O*-alkyl chains; 4′-hydroxyphenyl, 4′-nitrophenyl, 4′-chlorophenyl, thiophene, furfural or piperonal rings). The comprehensive action of naringenin, which we focus on in this review, suggests the need for further research on this bioflavonoid and its derivatives and their relationship with pathogenic microorganisms and, consequently, their effects on the human body.

References

1. Shakeel, S.; Rehman, M.U.; Tabassum, N.; Amin, U.; Mir, M. Effect of Naringenin (A Naturally Occurring Flavanone) against Pilocarpine-Induced Status Epilepticus and Oxidative Stress in Mice. *Pharmacogn. Mag.* **2017**, *13*, S154–S160. [CrossRef] [PubMed]
2. Amin, I.; Majid, S.; Farooq, A.; Wani, H.A.; Noor, F.; Khan, R.; Shakeel, S.; Bhat, S.A.; Ahmad, A.; Madkhali, H.; et al. *Naringenin (4,5,7-Trihydroxyflavanone) as a Potent Neuroprotective Agent: From Chemistry to Medicine*, 1st ed.; Elsevier B.V.: Amsterdam, The Netherlands, 2020; Volume 65, ISBN 9780128179055.
3. Rashed, K. International Journal of Biomedical and Advance Research Biological Properties of Naringenin: A Review QR Code. *Int. J. Biomed. Adv. Res.* **2021**, *12*, 12. [CrossRef]
4. Chung, T.W.; Li, S.; Lin, C.C.; Tsai, S.W. Antinociceptive and Anti-Inflammatory Effects of the Citrus Flavanone Naringenin. *Tzu Chi Med. J.* **2019**, *31*, 81–85. [CrossRef]
5. Rauf, A.; Shariati, M.A.; Imran, M.; Bashir, K.; Khan, S.A.; Mitra, S.; Bin Emran, T.; Badalova, K.; Uddin, M.S.; Mubarak, M.S.; et al. Comprehensive Review on Naringenin and Naringin Polyphenols as a Potent Anticancer Agent. *Environ. Sci. Pollut. Res.* **2022**, *29*, 31025–31041. [CrossRef] [PubMed]
6. Naeini, F.; Namkhah, Z.; Ostadrahimi, A.; Tutunchi, H.; Hosseinzadeh-Attar, M.J. A Comprehensive Systematic Review of the Effects of Naringenin, a Citrus-Derived Flavonoid, on Risk Factors for Nonalcoholic Fatty Liver Disease. *Adv. Nutr.* **2021**, *12*, 413–428. [CrossRef]
7. Karim, N.; Jia, Z.; Zheng, X.; Cui, S.; Chen, W. A Recent Review of Citrus Flavanone Naringenin on Metabolic Diseases and Its Potential Sources for High Yield-Production. *Trends Food Sci. Technol.* **2018**, *79*, 35–54. [CrossRef]
8. Salehi, B.; Fokou, P.V.T.; Sharifi-Rad, M.; Zucca, P.; Pezzani, R.; Martins, N.; Sharifi-Rad, J. The Therapeutic Potential of Naringenin: A Review of Clinical Trials. *Pharmaceuticals* **2019**, *12*, 11. [CrossRef]
9. Hartogh, D.J.D.; Tsiani, E. Antidiabetic Properties of Naringenin: A Citrus Fruit Polyphenol. *Biomolecules* **2019**, *9*, 99. [CrossRef]
10. McIntosh, C.A.; Mansell, R.L. Three-Dimensional Distribution of Limonin, Limonoate A-Ring Monolactone, and Naringin in the Fruit Tissues of Three Varieties of Citrus Paradisi. *J. Agric. Food Chem.* **1997**, *45*, 2876–2883. [CrossRef]
11. Victor, M.M.; David, J.M.; Sakukuma, M.C.K.; França, E.L.; Nunes, A.V.J. A Simple and Efficient Process for the Extraction of Naringin from Grapefruit Peel Waste. *Green Process. Synth.* **2018**, *7*, 524–529. [CrossRef]

12. Peterson, J.J.; Beecher, G.R.; Bhagwat, S.A.; Dwyer, J.T.; Gebhardt, S.E.; Haytowitz, D.B.; Holden, J.M. Flavanones in Grapefruit, Lemons, and Limes: A Compilation and Review of the Data from the Analytical Literature. *J. Food Compos. Anal.* **2006**, *19*, 74–80. [CrossRef]

13. Ho, P.C.; Saville, D.J.; Coville, P.F.; Wanwimolruk, S. Content of CYP3A4 Inhibitors, Naringin, Naringenin and Bergapten in Grapefruit and Grapefruit Juice Products. *Pharm. Acta Helv.* **2000**, *74*, 379–385. [CrossRef] [PubMed]

14. Sudto, K.; Pornpakakul, S.; Wanichwecharungruang, S. An Efficient Method for the Large Scale Isolation of Naringin from Pomelo (*Citrus grandis*) Peel. *Int. J. Food Sci. Technol.* **2009**, *44*, 1737–1742. [CrossRef]

15. Lin, L.Y.; Huang, C.Y.; Chen, K.C.; Peng, R.Y. Pomelo Fruit Wastes Are Potentially Valuable Antioxidants, Anti-Inflammatories, Antihypertensives, and Antihyperglycemics. *Hortic. Environ. Biotechnol.* **2021**, *62*, 377–395. [CrossRef]

16. Ni, H.; Zhang, S.F.; Gao, Q.F.; Hu, Y.; Jiang, Z.D.; Chen, F. Development and Evaluation of Simultaneous Quantification of Naringin, Prunin, Naringenin, and Limonin in Citrus Juice. *Food Sci. Biotechnol.* **2015**, *24*, 1239–1247. [CrossRef]

17. Cerqueira, E.; Silva, L.C.R.; David, J.M.; Borges, R.D.S.Q.; Ferreira, S.L.C.; David, J.P.; Reis, P.S.D.; Bruns, R.E. Determination of Flavanones in Orange Juices Obtained from Different Sources by HPLC/DAD. *J. Anal. Methods Chem.* **2014**, *2014*, 13–18. [CrossRef]

18. Yalim, S.; Özdemir, Y.; Ekiz, H.I. Naringin in Turkish Orange Juices and Its Reduction by Naringinase. *J. Food Drug Anal.* **2004**, *12*, 273–276. [CrossRef]

19. de Lourdes Mata Bilbao, M.; Andrés-Lacueva, C.; Jáuregui, O.; Lamuela-Raventós, R.M. Determination of Flavonoids in a Citrus Fruit Extract by LC-DAD and LC-MS. *Food Chem.* **2007**, *101*, 1742–1747. [CrossRef]

20. Dhuique-Mayer, C.; Caris-Veyrat, C.; Ollitrault, P.; Curk, F.; Amiot, M.J. Varietal and Interspecific Influence on Micronutrient Contents in Citrus from the Mediterranean Area. *J. Agric. Food Chem.* **2005**, *53*, 2140–2145. [CrossRef]

21. Behiry, S.I.; Okla, M.K.; Alamri, S.A.; El-Hefny, M.; Salem, M.Z.; Alaraidh, I.A.; Ali, H.M.; Al-Ghtani, S.M.; Monroy, J.C.; Salem, A.Z. Antifungal and Antibacterial Activities of *Musa paradisiaca*, L. Peel Extract: HPLC Analysis of Phenolic and Flavonoid Contents. *Processes* **2019**, *11*, 215. [CrossRef]

22. Dębski, H.; Wiczkowski, W.; Horbowicz, M. Effect of Elicitation with Iron Chelate and Sodium Metasilicate on Phenolic Compounds in Legume Sprouts. *Molecules* **2021**, *26*, 1345. [CrossRef] [PubMed]

23. Saeed Alkaltham, M.; Musa Özcan, M.; Uslu, N.; Salamatullah, A.M.; Hayat, K. Effect of Microwave and Oven Roasting Methods on Total Phenol, Antioxidant Activity, Phenolic Compounds, and Fatty Acid Compositions of Coffee Beans. *J. Food Process. Preserv.* **2020**, *44*, e14874. [CrossRef]

24. Paganga, G.; Miller, N.; Rice-Evans, C.A. The Polyphenolic Content of Fruit and Vegetables and Their Antioxidant Activities. What Does a Serving Constitute? *Free Radic. Res.* **1999**, *30*, 153–162. [CrossRef] [PubMed]

25. Bugianesi, R.; Catasta, G.; Spigno, P.; D'Uva, A.; Maiani, G. Naringenin from Cooked Tomato Paste Is Bioavailable in Men. *J. Nutr.* **2002**, *132*, 3349–3352. [CrossRef] [PubMed]

26. Sâmia Andricia, S.; da Silva, M.D.F.A.; Tavares, J.F.; Emídio, V.L. da-Cunha, J.M.B.-F.; Silva, M.S.D. Flavanones from Aerial Parts of Cordia Globosa (Jacq.) Kunth, Boraginaceae. *Rev. Bras. Farmacogn.* **2010**, *20*, 675–681. [CrossRef]

27. Nobakht, M.; Grkovic, T.; Trueman, S.J.; Wallace, H.M.; Katouli, M.; Quinn, R.J.; Brooks, P.R. Chemical Constituents of Kino Extract from Corymbia Torelliana. *Molecules* **2014**, *19*, 17862–17871. [CrossRef]

28. Suksamrarn, A.; Chotipong, A.; Suavansri, T.; Boongird, S.; Timsuksai, P.; Vimuttipong, S.; Chuaynugul, A. Antimycobacterial Activity and Cytotoxicity of Flavonoids from the Flowers of Chromolaena Odorata. *Arch. Pharm. Res.* **2004**, *27*, 507–511. [CrossRef] [PubMed]

29. Shimizu, T.; Lin, F.; Hasegawa, M.; Okada, K.; Nojiri, H.; Yamane, H. Purification and Identification of Naringenin 7-O-Methyltransferase, a Key Enzyme in Biosynthesis of Flavonoid Phytoalexin Sakuranetin in Rice. *J. Biol. Chem.* **2012**, *287*, 19315–19325. [CrossRef]

30. Kozłowska, J.; Potaniec, B.; Zarowska, B.; Anioł, M. Synthesis and Biological Activity of Novel O-Alkyl Derivatives of Naringenin and Their Oximes. *Molecules* **2017**, *22*, 1485. [CrossRef]

31. Lee, K.A.; Moon, S.H.; Lee, J.Y.; Kim, K.T.; Park, Y.S.; Paik, H.D. Antibacterial Activity of a Novel Flavonoid, 7-O-Butyl Naringenin, against Methicillin-Resistant Staphylococcus Aureus (MRSA). *Food Sci. Biotechnol.* **2013**, *22*, 1725–1728. [CrossRef]

32. Moon, S.H.; Lee, J.H.; Kim, K.T.; Park, Y.S.; Nah, S.Y.; Ahn, D.U.; Paik, H.D. Antimicrobial Effect of 7-O-Butylnaringenin, a Novel Flavonoid, and Various Natural Flavonoids against Helicobacter Pylori Strains. *Int. J. Environ. Res. Public Health* **2013**, *10*, 5459–5469. [CrossRef] [PubMed]

33. Albuquerque de Oliveira Mendes, L.; Ponciano, C.S.; Depieri Cataneo, A.H.; Wowk, P.F.; Bordignon, J.; Silva, H.; Vieira de Almeida, M. The Anti-Zika Virus and Anti-Tumoral Activity of the Citrus Flavanone Lipophilic Naringenin-Based Compounds. *Chem. Biol. Interact.* **2020**, *331*, 109218. [CrossRef] [PubMed]

34. Kozłowska, J.; Grela, E.; Baczynska, D.; Grabowiecka, A.; Anioł, M. Novel O-Alkyl Derivatives of Naringenin and Their Oximes with Antimicrobial and Anticancer Activity. *Molecules* **2019**, *24*, 679. [CrossRef] [PubMed]

35. Chandrika, B.B.; Steephan, M.; Kumar, T.R.S.; Sabu, A.; Haridas, M. Hesperetin and Naringenin Sensitize HER2 Positive Cancer Cells to Death by Serving as HER2 Tyrosine Kinase Inhibitors. *Life Sci.* **2016**, *160*, 47–56. [CrossRef] [PubMed]

36. Hernández-Aquino, E.; Muriel, P. Beneficial Effects of Naringenin in Liver Diseases: Molecular Mechanisms. *World J. Gastroenterol.* **2018**, *24*, 1679–1707. [CrossRef]

37. Arul, D.; Subramanian, P. Naringenin (Citrus Flavonone) Induces Growth Inhibition, Cell Cycle Arrest and Apoptosis in Human Hepatocellular Carcinoma Cells. *Pathol. Oncol. Res.* **2013**, *19*, 763–770. [CrossRef]

38. Lim, W.; Park, S.; Bazer, F.W.; Song, G. Naringenin-Induced Apoptotic Cell Death in Prostate Cancer Cells Is Mediated via the PI3K/AKT and MAPK Signaling Pathways. *J. Cell. Biochem.* **2017**, *118*, 1118–1131. [CrossRef]

39. Nasr Bouzaiene, N.; Chaabane, F.; Sassi, A.; Chekir-Ghedira, L.; Ghedira, K. Effect of Apigenin-7-Glucoside, Genkwanin and Naringenin on Tyrosinase Activity and Melanin Synthesis in B16F10 Melanoma Cells. *Life Sci.* **2016**, *144*, 80–85. [CrossRef]

40. Stompor, M.; Uram, Ł.; Podgórski, R. In Vitro Effect of 8-Prenylnaringenin and Naringenin on Fibroblasts and Glioblastoma Cells-Cellular Accumulation and Cytotoxicity. *Molecules* **2017**, *22*, 1092. [CrossRef]

41. Lu, W.L.; Yu, C.T.R.; Lien, H.M.; Sheu, G.T.; Cherng, S.H. Cytotoxicity of Naringenin Induces Bax-Mediated Mitochondrial Apoptosis in Human Lung Adenocarcinoma A549 Cells. *Environ. Toxicol.* **2020**, *35*, 1386–1394. [CrossRef]

42. Shi, X.; Luo, X.; Chen, T.; Guo, W.; Liang, C.; Tang, S.; Mo, J. Naringenin Inhibits Migration, Invasion, Induces Apoptosis in Human Lung Cancer Cells and Arrests Tumour Progression in Vitro. *J. Cell. Mol. Med.* **2021**, *25*, 2563–2571. [CrossRef] [PubMed]

43. Choi, J.; Lee, D.H.; Jang, H.; Park, S.Y.; Seol, J.W. Naringenin Exerts Anticancer Effects by Inducing Tumor Cell Death and Inhibiting Angiogenesis in Malignant Melanoma. *Int. J. Med. Sci.* **2020**, *17*, 3049–3057. [CrossRef] [PubMed]

44. Manchope, M.F.; Calixto-Campos, C.; Coelho-Silva, L.; Zarpelon, A.C.; Pinho-Ribeiro, F.A.; Georgetti, S.R.; Baracat, M.M.; Casagrande, R.; Verri, W.A. Naringenin Inhibits Superoxide Anion-Induced Inflammatory Pain: Role of Oxidative Stress, Cytokines, Nrf-2 and the No-CGMP-PKG-KATP Channel Signaling Pathway. *PLoS ONE* **2016**, *11*, e0153015. [CrossRef]

45. Liu, X.; Wang, N.; Fan, S.; Zheng, X.; Yang, Y.; Zhu, Y.; Lu, Y.; Chen, Q.; Zhou, H.; Zheng, J. The Citrus Flavonoid Naringenin Confers Protection in a Murine Endotoxaemia Model through AMPK-ATF3-Dependent Negative Regulation of the TLR4 Signalling Pathway. *Sci. Rep.* **2016**, *6*, 39735. [CrossRef] [PubMed]

46. Jung, U.J.; Kim, H.J.; Lee, J.S.; Lee, M.K.; Kim, H.O.; Park, E.J.; Kim, H.K.; Jeong, T.S.; Choi, M.S. Naringin Supplementation Lowers Plasma Lipids and Enhances Erythrocyte Antioxidant Enzyme Activities in Hypercholesterolemic Subjects. *Clin. Nutr.* **2003**, *22*, 561–568. [CrossRef]

47. Rashmi, R.; Bojan Magesh, S.; Mohanram Ramkumar, K.; Suryanarayanan, S.; Venkata SubbaRao, M. Antioxidant Potential of Naringenin Helps to Protect Liver Tissue from Streptozotocin-Induced Damage. *Rep. Biochem. Mol. Biol.* **2018**, *7*, 76–84.

48. Rahman, K. Studies on Free Radicals, Antioxidants, and Co-Factors. *Clin. Interv. Aging* **2007**, *2*, 219–236.

49. Sakihama, Y.; Mano, J.; Sano, S.; Asada, K.; Yamasaki, H. Reduction of Phenoxyl Radicals Mediated by Monodehydroascorbate Reductase. *Biochem. Biophys. Res. Commun.* **2000**, *279*, 949–954. [CrossRef]

50. Pinho-Ribeiro, F.A.; Zarpelon, A.C.; Mizokami, S.S.; Borghi, S.M.; Bordignon, J.; Silva, R.L.; Cunha, T.M.; Alves-Filho, J.C.; Cunha, F.Q.; Casagrande, R.; et al. The Citrus Flavonone Naringenin Reduces Lipopolysaccharide-Induced Inflammatory Pain and Leukocyte Recruitment by Inhibiting NF-KB Activation. *J. Nutr. Biochem.* **2016**, *33*, 8–14. [CrossRef]

51. Pinho-Ribeiro, F.A.; Verri, W.A.; Chiu, I.M. Nociceptor Sensory Neuron–Immune Interactions in Pain and Inflammation. *Trends Immunol.* **2017**, *38*, 5–19. [CrossRef]

52. Straub, I.; Mohr, F.; Stab, J.; Konrad, M.; Philipp, S.E.; Oberwinkler, J.; Schaefer, M. Citrus Fruit and Fabacea Secondary Metabolites Potently and Selectively Block TRPM3. *Br. J. Pharmacol.* **2013**, *168*, 1835–1850. [CrossRef]

53. Li, J.M.; Che, C.T.; Lau, C.B.S.; Leung, P.S.; Cheng, C.H.K. Inhibition of Intestinal and Renal Na+-Glucose Cotransporter by Naringenin. *Int. J. Biochem. Cell Biol.* **2006**, *38*, 985–995. [CrossRef] [PubMed]

54. Andrew Haber, C.; Lam, T.K.T.; Yu, Z.; Gupta, N.; Goh, T.; Bogdanovic, E.; Giacca, A.; George Fantus, I.; Andrew, C.; Gupta, N.; et al. N-Acetylcysteine and Taurine Prevent Hyperglycemia-Induced Insulin Resistance in Vivo: Possible Role of Oxidative Stress. *Am. J. Physiol. Endocrinol. Metab.* **2003**, *285*, E744–E753. [CrossRef] [PubMed]

55. Bhattacharya, S.; Christensen, K.B.; Cathrine, L.; Olsen, B.; Christensen, L.P.; Grevsen, K.; Faergeman, N.J.; Kristiansen, K.; Young, J.F.; Oksbjerg, N. Bioactive Components from Flowers of *Sambucus nigra* L. Increase Glucose Uptake in Primary Porcine Myotube Cultures and Reduce Fat Accumulation in *Caenorhabditis elegans*. *J. Agric. Food Chem.* **2013**, *61*, 11033–11040. [CrossRef] [PubMed]

56. Claussnitzer, M.; Skurk, T.; Hauner, H.; Daniel, H.; Rist, M.J. Effect of Flavonoids on Basal and Insulin-Stimulated 2-Deoxyglucose Uptake in Adipocytes. *Mol. Nutr. Food Res.* **2011**, *55*, S26–S34. [CrossRef]

57. Yoshida, H.; Watanabe, W.; Oomagari, H.; Tsuruta, E.; Shida, M.; Kurokawa, M. Citrus Flavonoid Naringenin Inhibits TLR2 Expression in Adipocytes. *J. Nutr. Biochem.* **2013**, *24*, 1276–1284. [CrossRef]

58. Bhattacharya, S.; Oksbjerg, N.; Young, J.F.; Jeppesen, P.B. Caffeic Acid, Naringenin and Quercetin Enhance Glucose-Stimulated Insulin Secretion and Glucose Sensitivity in INS-1E Cells. *Diabetes, Obes. Metab.* **2014**, *16*, 602–612. [CrossRef]

59. Ortiz-Andrade, R.R.; Sánchez-Salgado, J.C.; Navarrete-Vázquez, G.; Webster, S.P.; Binnie, M.; García-Jiménez, S.; León-Rivera, I.; Cigarroa-Vázquez, P.; Villalobos-Molina, R.; Estrada-Soto, S. Antidiabetic and Toxicological Evaluations of Naringenin in Normoglycaemic and NIDDM Rat Models and Its Implications on Extra-Pancreatic Glucose Regulation. *Diabetes, Obes. Metab.* **2008**, *10*, 1097–1104. [CrossRef]

60. Sharma, A.K.; Bharti, S.; Ojha, S.; Bhatia, J.; Kumar, N.; Ray, R.; Kumari, S.; Arya, D.S. Up-Regulation of PPARγ, Heat Shock Protein-27 and -72 by Naringin Attenuates Insulin Resistance, β-Cell Dysfunction, Hepatic Steatosis and Kidney Damage in a Rat Model of Type 2 Diabetes. *Br. J. Nutr.* **2011**, *106*, 1713–1723. [CrossRef]

61. Dodds, D.R. Antibiotic Resistance: A Current Epilogue. *Biochem. Pharmacol.* **2017**, *134*, 139–146. [CrossRef]

62. Gross, P.A.; Patel, B. Reducing Antibiotic Overuse: A Call for a National Performance Measure for Not Treating Asymptomatic Bacteriuria. *Clin. Infect. Dis.* **2007**, *45*, 1335–1337. [CrossRef] [PubMed]

63. Davies, J.; Davies, D. Origins and Evolution of Antibiotic Resistance. *Microbiol. Mol. Biol. Rev.* **2010**, *74*, 9–16. [CrossRef] [PubMed]

64. Rebello, C.J.; Beyl, R.A.; Lertora, J.J.L.; Greenway, F.L.; Ravussin, E.; Ribnicky, D.M.; Poulev, A.; Kennedy, B.J.; Castro, H.F.; Campagna, S.R.; et al. Safety and Pharmacokinetics of Naringenin: A Randomized, Controlled, Single-Ascending-Dose Clinical Trial. *Diabetes, Obes. Metab.* **2020**, *22*, 91–98. [CrossRef] [PubMed]

65. Wang, L.H.; Zeng, X.A.; Wang, M.S.; Brennan, C.S.; Gong, D. Modification of Membrane Properties and Fatty Acids Biosynthesis-Related Genes in Escherichia Coli and Staphylococcus aureus: Implications for the Antibacterial Mechanism of Naringenin. *Biochim. Biophys. Acta-Biomembr.* **2018**, *1860*, 481–490. [CrossRef] [PubMed]

66. Wang, L.H.; Wang, M.S.; Zeng, X.A.; Xu, X.M.; Brennan, C.S. Membrane and Genomic DNA Dual-Targeting of Citrus Flavonoid Naringenin against: Staphylococcus Aureus. *Integr. Biol. (UK)* **2017**, *9*, 820–829. [CrossRef] [PubMed]

67. Duda-Madej, A.; Kozłowska, J.; Krzyzek, P.; Anioł, M.; Seniuk, A.; Jermakow, K.; Dworniczek, E. Antimicrobial O -Alkyl Derivatives of Naringenin and Their Oximes against Multidrug-Resistant Bacteria. *Molecules* **2020**, *25*, 174–183. [CrossRef] [PubMed]

68. Mohammed, N.H.; Mostafa, M.I.; Al-Taher, A.Y. Augmentation Effects of Novel Naringenin Analogues and Ciprofloxacin as Inhibitors for Nora Efflux Pump (EPIs) and Pyruvate Kinase (PK) against MRSA. *J. Anim. Vet. Adv.* **2015**, *14*, 386–392.

69. Denny, B.J.; West, P.W.J.; Mathew, T.C. Antagonistic Interactions between the Flavonoids Hesperetin and Naringenin and β-Lactam Antibiotics against Staphylococcus Aureus. *Br. J. Biomed. Sci.* **2008**, *65*, 145–147. [CrossRef]

70. Song, H.-S.; Kant Bhatia, S.; Gurav, R.; Choi, T.-R.; Joong Kim, H.; Park, L.; Han, Y.-H.; Young Park, J.; Mi Lee, S.; Lee Park, S.; et al. Naringenin as an Antibacterial Reagent Controlling of Biofilm Formation 1 and Fatty Acid Metabolism in MRSA. *bioRxiv* **2020**. [CrossRef]

71. Yue, J.; Yang, H.; Liu, S.; Song, F.; Guo, J.; Huang, C. Influence of Naringenin on the Biofilm Formation of Streptococcus Mutans. *J. Dent.* **2018**, *76*, 24–31. [CrossRef]

72. Zhang, Y.; Wang, J.F.; Dong, J.; Wei, J.Y.; Wang, Y.N.; Dai, X.H.; Wang, X.; Luo, M.J.; Tan, W.; Deng, X.M.; et al. Inhibition of α-Toxin Production by Subinhibitory Concentrations of Naringenin Controls Staphylococcus Aureus Pneumonia. *Fitoterapia* **2013**, *86*, 92–99. [CrossRef] [PubMed]

73. Yao, W.; Zhang, X.; Xu, F.; Cao, C.; Liu, T.; Xue, Y. The Therapeutic Effects of Naringenin on Bronchial Pneumonia in Children. *Pharmacol. Res. Perspect.* **2021**, *9*, e00825. [CrossRef] [PubMed]

74. Yu, M.; You, D.; Zhuang, J.; Lin, S.; Dong, L.; Weng, S.; Zhang, B.; Cheng, K.; Weng, W.; Wang, H. Controlled Release of Naringin in Metal-Organic Framework-Loaded Mineralized Collagen Coating to Simultaneously Enhance Osseointegration and Antibacterial Activity. *ACS Appl. Mater. Interfaces* **2017**, *9*, 19698–19705. [CrossRef] [PubMed]

75. Rao, K.; Imran, M.; Jabri, T.; Ali, I.; Perveen, S.; Shafiullah; Ahmed, S.; Shah, M.R. Gum Tragacanth Stabilized Green Gold Nanoparticles as Cargos for Naringin Loading: A Morphological Investigation through AFM. *Carbohydr. Polym.* **2017**, *174*, 243–252. [CrossRef] [PubMed]

76. Virolle, C.; Goldlust, K.; Djermoun, S.; Bigot, S.; Lesterlin, C. Plasmid Transfer by Conjugation in Gram-Negative Bacteria: From the Cellular to the Community Level. *Genes* **2020**, *11*, 1239. [CrossRef]

77. Ikigai, H.; Nakae, T.; Hara, Y.; Shimamura, T. Bactericidal Catechins Damage the Lipid Bilayer. *Biochim. Biophys. Acta* **1993**, *1147*, 132–136. [CrossRef]

78. Céliz, G.; Daz, M.; Audisio, M.C. Antibacterial Activity of Naringin Derivatives against Pathogenic Strains. *J. Appl. Microbiol.* **2011**, *111*, 731–738. [CrossRef]

79. Han, S.-S.; Lee, C.-K.; Kim, Y.-S. Antimicrobial Effects of Naringenin Alone and in Combination with Related Flavonoids. *Yakhak Hoeji* **1992**, *36*, 407–411.

80. Murti, Y. Biological Evaluation of Synthesized Naringenin Derivatives as Antimicrobial Agents. *Anti-Infective Agents* **2020**, *19*, 192–199. [CrossRef]

81. Vandeputte, O.M.; Kiendrebeogo, M.; Rasamiravaka, T.; Stévigny, C.; Duez, P.; Rajaonson, S.; Diallo, B.; Mol, A.; Baucher, M.; el Jaziri, M. The Flavanone Naringenin Reduces the Production of Quorum Sensing-Controlled Virulence Factors in Pseudomonas Aeruginosa PAO1. *Microbiology* **2011**, *157*, 2120–2132. [CrossRef]

82. Bae, E.A.; Han, M.J.; Kim, D.H. In Vitro Anti-Helicobacter Pylori Activity of Some Flavonoids and Their Metabolites. *Planta Med.* **1999**, *65*, 442–443. [CrossRef] [PubMed]

83. Vikram, A.; Jesudhasan, P.R.; Jayaprakasha, G.K.; Pillai, S.D.; Jayaraman, A.; Patil, B.S. Citrus Flavonoid Represses Salmonella Pathogenicity Island 1 and Motility in S. Typhimurium LT2. *Int. J. Food Microbiol.* **2011**, *145*, 28–36. [CrossRef] [PubMed]

84. Vikram, A.; Jayaprakasha, G.K.; Jesudhasan, P.R.; Pillai, S.D.; Patil, B.S. Suppression of Bacterial Cell-Cell Signalling, Biofilm Formation and Type III Secretion System by Citrus Flavonoids. *J. Appl. Microbiol.* **2010**, *109*, 515–527. [CrossRef]

85. Marin, A.M.; Souza, E.M.; Pedrosa, F.O.; Souza, L.M.; Sassaki, G.L.; Baura, V.A.; Yates, M.G.; Wassem, R.; Monteiro, R.A. Naringenin Degradation by the Endophytic Diazotroph Herbaspirillum Seropedicae SmR1. *Microbiology* **2013**, *159*, 167–175. [CrossRef] [PubMed]

86. Ng, T.B.; Ling, J.M.L.; Wang, Z.T.; Cai, J.N.; Xu, G.J. Examination of Coumarins, Flavonoids and Polysaccharopeptide for Antibacterial Activity. *Gen. Pharmacol.* **1996**, *27*, 1237–1240. [CrossRef]

87. Rauha, J.P.; Remes, S.; Heinonen, M.; Hopia, A.; Kähkönen, M.; Kujala, T.; Pihlaja, K.; Vuorela, H.; Vuorela, P. Antimicrobial Effects of Finnish Plant Extracts Containing Flavonoids and Other Phenolic Compounds. *Int. J. Food Microbiol.* **2000**, *56*, 3–12. [CrossRef]

88. Eumkeb, G.; Chukrathok, S. Synergistic Activity and Mechanism of Action of Ceftazidime and Apigenin Combination against Ceftazidime-Resistant Enterobacter Cloacae. *Phytomedicine* **2013**, *20*, 262–269. [CrossRef]

89. Negm, W.A.; El-aasr, M.; Kamer, A.A.; Elekhnawy, E. Investigation of the Antibacterial Activity and Efflux Pump Inhibitory Effect of Cycas Thouarsii r.Br. Extract against Klebsiella Pneumoniae Clinical Isolates. *Pharmaceuticals* **2021**, *14*, 756. [CrossRef]

90. Tran Trung, H.; Truong Thi Huynh, H.; Nguyen Thi Thuy, L.; Nguyen Van Minh, H.; Thi Nguyen, M.N.; Luong Thi, M.N. Growth-Inhibiting, Bactericidal, Antibiofilm, and Urease Inhibitory Activities of Hibiscus *Rosa sinensis* L. Flower Constituents toward Antibiotic Sensitive- And Resistant-Strains of Helicobacter Pylori. *ACS Omega* **2020**, *5*, 20080–20089. [CrossRef]

91. Duda-Chodak. A Polyphenols and the Gut Microbiota. *J. Physiol. Pharmacol.* **2012**, *63*, 497–503.

92. Shin, J.E.; Kim, J.M.; Bae, E.A.; Hyun, Y.J.; Kim, D.H. In Vitro Inhibitory Effect of Flavonoids on Growth, Infection and Vacuolation of Helicobacter Pylori. *Planta Med.* **2005**, *71*, 197–201. [CrossRef] [PubMed]

93. Seong Sun Han, I.J.Y. Studies on Antimicrobial Activities and Safety of Natural Naringin in Korea. *Korean J. Mycol.* **1988**, *16*, 33–44.

94. de Andrade, C.A.; de S. Carvalho, J.L.; Cunico, M.M.; Lordello, A.L.L.; Higaskino, C.E.K.; Almeida, S.C.D.C.; Dias, J.D.F.G.; Kerber, V.A.; Miguel, M.D.; Miguel, O.G. Antioxidant and Antibacterial Activity of Extracts, Fractions and Isolated Substances from the Flowers of *Acacia podalyriifolia* A. Cunn. Ex G. Don. *Brazilian J. Pharm. Sci.* **2010**, *46*, 715–721. [CrossRef]

95. Mundlia, J.; Ahuja, M.; Kumar, P.; Pillay, V. Improved Antioxidant, Antimicrobial and Anticancer Activity of Naringenin on Conjugation with Pectin. *3 Biotech* **2019**, *9*, 312. [CrossRef] [PubMed]

96. Mandalari, G.; Bennett, R.N.; Bisignano, G.; Trombetta, D.; Saija, A.; Faulds, C.B.; Gasson, M.J.; Narbad, A. Antimicrobial Activity of Flavonoids Extracted from Bergamot (*Citrus bergamia* Risso) Peel, a Byproduct of the Essential Oil Industry. *J. Appl. Microbiol.* **2007**, *103*, 2056–2064. [CrossRef]

97. Mandalari, G.; Bisignano, C.; D'Arrigo, M.; Ginestra, G.; Arena, A.; Tomaino, A.; Wickham, M.S.J. Antimicrobial Potential of Polyphenols Extracted from Almond Skins. *Lett. Appl. Microbiol.* **2010**, *51*, 83–89. [CrossRef]

98. Parkar, S.G.; Stevenson, D.E.; Skinner, M.A. The Potential Influence of Fruit Polyphenols on Colonic Microflora and Human Gut Health. *Int. J. Food Microbiol.* **2008**, *124*, 295–298. [CrossRef]

99. Rastogi, N.; Domadia, P.; Shetty, S.; Dasgupta, D. Screening of Natural Phenolic Compounds for Potential to Inhibit Bacterial Cell Division Protein FtsZ. *Indian J. Exp. Biol.* **2008**, *46*, 783–787.

100. Adamczak, A.; Ożarowski, M.; Karpiński, T.M. Antibacterial Activity of Some Flavonoids and Organic Acids Widely Distributed in Plants. *J. Clin. Med.* **2020**, *9*, 109. [CrossRef]

101. Pereira, R.M.S.; Andrades, N.E.D.; Paulino, N.; Sawaya, A.C.H.F.; Eberlin, M.N.; Marcucci, M.C.; Favero, G.M.; Novak, E.M.; Bydlowski, S.P. Synthesis and Characterization of a Metal Complex Containing Naringin and Cu, and Its Antioxidant, Antimicrobial, Antiinflammatory and Tumor Cell Cytotoxicity. *Molecules* **2007**, *12*, 1352–1366. [CrossRef]

102. Soberón, J.R.; Sgariglia, M.A.; Carabajal Torrez, J.A.; Aguilar, F.A.; Pero, E.J.I.; Sampietro, D.A.; Fernández de Luco, J.; Labadie, G.R. Antifungal Activity and Toxicity Studies of Flavanones Isolated from Tessaria Dodoneifolia Aerial Parts. *Heliyon* **2020**, *6*, e05174. [CrossRef] [PubMed]

103. Salazar-Aranda, R.; Granados-Guzmán, G.; Pérez-Meseguer, J.; González, G.M.; De Torres, N.W. Activity of Polyphenolic Compounds against Candida Glabrata. *Molecules* **2015**, *20*, 17903. [CrossRef] [PubMed]

104. Dean, R.; Van Kan, J.A.L.; Pretorius, Z.A.; Hammond-Kosack, K.E.; Di Pietro, A.; Spanu, P.D.; Rudd, J.J.; Dickman, M.; Kahmann, R.; Ellis, J.; et al. The Top 10 Fungal Pathogens in Molecular Plant Pathology. *Mol. Plant Pathol.* **2012**, *13*, 414–430. [CrossRef] [PubMed]

105. Padmavati, M.; Sakthivel, N.; Thara, K.V.; Reddy, A.R. Differential Sensitivity of Rice Pathogens to Growth Inhibition by Flavonoids. *Phytochemistry* **1997**, *46*, 499–502. [CrossRef]

106. Katsumata, S.; Hamana, K.; Horie, K.; Toshima, H.; Hasegawa, M. Identification of Sternbin and Naringenin as Detoxified Metabolites from the Rice Flavanone Phytoalexin Sakuranetin by Pyricularia Oryzae. *Chem. Biodivers.* **2017**, *14*, e1600240. [CrossRef]

107. Kim, H.; Lee, D.G. Naringin-Generated ROS Promotes Mitochondria-Mediated Apoptosis in Candida Albicans. *IUBMB Life* **2021**, *73*, 953–967. [CrossRef]

108. Orhan, D.D.; Özçelik, B.; Özgen, S.; Ergun, F. Antibacterial, Antifungal, and Antiviral Activities of Some Flavonoids. *Microbiol. Res.* **2010**, *165*, 496–504. [CrossRef]

109. Son, N.T.; Harada, K.; Cuong, N.M.; Fukuyama, Y. Two New Carboxyethylflavanones from the Heartwood of Dalbergia Tonkinensis and Their Antimicrobial Activities. *Nat. Prod. Commun.* **2017**, *12*, 1721–1723. [CrossRef]

110. Górniak, I.; Bartoszewski, R.; Króliczewski, J. Comprehensive Review of Antimicrobial Activities of Plant Flavonoids. *Phytochem. Rev.* **2019**, *18*, 241–272. [CrossRef]

111. Paczkowski, J.E.; Mukherjee, S.; McCready, A.R.; Cong, J.P.; Aquino, C.J.; Kim, H.; Henke, B.R.; Smith, C.D.; Bassler, B.L. Flavonoids Suppress Pseudomonas Aeruginosa Virulence through Allosteric Inhibition of Quorum-Sensing Receptors. *J. Biol. Chem.* **2017**, *292*, 4064–4076. [CrossRef]

112. Pandey, A.K. Shashank Kumar Perspective on Plant Products as Antimicrobials Agents: A Review. *Pharmacologia* **2013**, *4*, 469–480. [CrossRef]

113. Ammar, N.M.; Hassan, H.A.; Abdallah, H.M.I.; Afifi, S.M.; Elgamal, A.M.; Farrag, A.R.H.; El-Gendy, A.E.N.G.; Farag, M.A.; Elshamy, A.I. Protective Effects of Naringenin from Citrus Sinensis (Var. Valencia) Peels against CCl4-Induced Hepatic and Renal Injuries in Rats Assessed by Metabolomics, Histological and Biochemical Analyses. *Nutrients* **2022**, *14*, 841. [CrossRef] [PubMed]

114. Tsuchiya, H.; Iinuma, M. Reduction of Membrane Fluidity by Antibacterial Sophoraflavanone G Isolated from Sophora Exigua. *Phytomedicine* **2000**, *7*, 161–165. [CrossRef]

115. Jeong, K.W.; Lee, J.Y.; Kang, D., II; Lee, J.U.; Shin, S.Y.; Kim, Y. Screening of Flavonoids as Candidate Antibiotics against Enterococcus Faecalis. *J. Nat. Prod.* **2009**, *72*, 719–724. [CrossRef]

116. Zhang, L.; Kong, Y.; Wu, D.; Zhang, H.; Wu, J.; Chen, J.; Ding, J.; Hu, L.; Jiang, H.; Shen, X. Three Flavonoids Targeting the β-Hydroxyacyl-Acyl Carrier Protein Dehydratase from Helicobacter Pylori: Crystal Structure Characterization with Enzymatic Inhibition Assay. *Protein Sci.* **2008**, *17*, 1971–1978. [CrossRef] [PubMed]

117. Xiao, Z.P.; Wang, X.D.; Wang, P.F.; Zhou, Y.; Zhang, J.W.; Zhang, L.; Zhou, J.; Zhou, S.S.; Hui, O.; Lin, X.Y.; et al. Design, Synthesis, and Evaluation of Novel Fluoroquinolone-Flavonoid Hybrids as Potent Antibiotics against Drug-Resistant Microorganisms. *Eur. J. Med. Chem.* **2014**, *80*, 92–100. [CrossRef]

118. Oh, E.; Jeon, B. Synergistic Anti-Campylobacter Jejuni Activity of Fluoroquinolone and Macrolide Antibiotics with Phenolic Compounds. *Front. Microbiol.* **2015**, *6*, 1129. [CrossRef]

Article

Antifungal Effect of Brassica Tissues on the Mycotoxigenic Cereal Pathogen *Fusarium graminearum*

Samina Ashiq *, Simon Edwards [ID], Andrew Watson, Emma Blundell † and Matthew Back [ID]

Agriculture and Environment Department, Harper Adams University, Newport, Shropshire TF10 8NB, UK
* Correspondence: sashiq@harper-adams.ac.uk
† Current address: Circular1 Health, Waterfront Business Park, Michaelson Rd, Barrow-in-Furness, Cumbria LA14 2TF, UK.

Abstract: *Fusarium graminearum* is a globally important cereal pathogen, causing head blight in wheat, resulting in yield losses and mycotoxin contamination. Currently, triazole fungicides are used to suppress *Fusarium graminearum*, however, the declining effectiveness of triazoles and concerns over the safety of pesticides have led to the pursuit of safe alternative crop protection strategies such as biofumigation. In the present study, species belonging to Brassicaceae (*Brassica juncea*, *Raphanus sativus*, *Eruca sativa*) were assessed for their biofumigation potential against *F. graminearum* and the glucosinolate profile of the brassicas was determined. In Petri dishes, mycelial plugs of *Fusarium graminearum* were exposed to frozen/defrosted leaf discs of brassicas collected at early-leaf, stem-extension, and early-bud stages. Additionally, *F. graminearum* inoculum was incubated in soil amended with chopped tissues of brassicas in a closed jar experiment. Glucosinolate analysis of the leaf tissue of brassicas revealed that the total glucosinolate concentration of *B. juncea* 'Brons' increased with advancing growth stage (24.5–51.9 μmol g^{-1}). *Brassica juncea* leaf discs were effective against mycelial growth, while the sinigrin content in the leaf tissue corresponded to the level of suppression. At the stem-extension and early-bud stages, *B. juncea* 'Brons' showed 87–90% suppression with four leaf discs, and 100% suppression with eight leaf discs. *Brassica juncea* 'Caliente Rojo' leaf discs collected at the stem-extension stage showed 94% inhibition with eight discs. In the closed jar experiment, each brassica species significantly suppressed *F. graminearum* inoculum by 41–55%. The findings suggest that the brassica species investigated in the present study could be effective in reducing the inoculum of *F. graminearum* in soil prior to cereal production.

Keywords: biofumigant; sinigrin; head blight; *Brassica juncea*; *Eruca sativa*; *Raphanus sativus*

1. Introduction

Fusarium graminearum, an ascomycete fungus, is the most prevalent and important pathogen of head blight in wheat and has been reported in all continents except Antarctica [1]. It is also an important causal agent of ear rot and stalk rot in maize [2]. Fusarium head blight can result in yield losses as high as 50% in cereals [3,4], although >70% yield losses were recorded in Argentina in 2012 [5]. In 2015/16, Fusarium head blight caused yield losses valued at $1.176 billion in the U.S. [6]. *Fusarium graminearum* not only causes yield losses but also economic and health losses due to mycotoxin production in cereals. The major mycotoxins produced by *F. graminearum* are deoxynivalenol and zearalenone. Deoxynivalenol induces vomiting, anorexia, reduces food intake, and causes hepatotoxic, immunotoxic, and neurovirulent effects [7]. Zearalenone, a mycoestrogen, has adverse effects on the reproductive system and is associated with the early onset of puberty in young children [8,9]. Contamination with concentrations exceeding the EU legal limits of 100 μg kg^{-1} zearalenone and 1250 μg kg^{-1} deoxynivalenol in wheat for human consumption were detected in 29% and 13% of wheat samples, respectively, in England in 2008 [10]. Moreover, 83% of durum wheat samples from Tunisia in 2007 [11] and 12.5% of maize

samples from Serbia in 2011 [12] were found to be contaminated with deoxynivalenol at concentrations higher than the EU legal limit of 1750 µg kg^{-1} for these foodstuffs.

The use of fungicides, particularly triazoles, has been the main method of *F. graminearum* management. However, there are serious concerns due to their declining effectiveness and the high selection pressure for fungicide resistance [13–15]. Thus, the use of triazole fungicides may potentially be reduced due to a decrease in *Fusarium* sensitivity. Additionally, evidence concerning the endocrine-disrupting potential of triazoles [16,17] has prompted the quest to find alternative safer management strategies. Currently, control strategies such as biopesticides have been gaining interest due to their safer effect on the environment and health. One such approach, "biofumigation", which was first coined in the 1990s, uses brassica crops such as mustard and radish, which are rich in glucosinolates (GSLs). The method involves growing brassica crops between cash crops, followed by shredding and incorporation into the soil. The tissue disruption allows for the physical contact of GSL and myrosinase enzymes, which are present separately in intact cells [18]. Myrosinase enzymes are located primarily in specialised cells known as myrosin cells, which are dispersed throughout the brassica tissues [19]. Within the myrosin cells, myrosinase enzymes are present in protein containing vacuoles: the myrosin grains [20]. On the other hand, GSLs are distributed throughout the plant organs and are located in translucent vacuoles or moved for long-term storage in sulphur-rich cells called the S-cells [21,22]. Glucosinolates are non-toxic unless they are hydrolysed upon tissue disruption. The interaction of GSL and myrosinases leads to the catalysis of GSL into a range of biologically active substances including toxic isothiocyanates (ITC) [23,24]. These volatile substances are known to have toxic effects on nematodes [25], weed [26], and fungi [27,28].

Although the term biofumigation was introduced in the 1990s, the suppression of soil-borne pathogens by volatile organic compounds from brassica tissues was reported in the 1970/80s. Lewis and Papavizas [29] reported the suppression of *Rhizoctonia solani* using cabbage tissues in the laboratory experiments. Colonisation of buckwheat stem segments in the *R. solani*-infested soil was reduced by 75% when exposed to vapours from decomposing cabbage tissues. Since these initial studies, biofumigation has been investigated for its suppressive effects against fungal pathogens, nematodes, and weeds. In an in vitro study [30], leaf tissues of the *Brassica* species were tested against *Pythium* and *Rhizoctonia* species. Radial growth of *Pythium ultimum* and *Rhizoctonia solani* in Petri dishes were reduced by 100% and 73%, respectively, 48 h after being placed inverted over the neck of a 500 mL jar containing 10 g of macerated leaves of *B. juncea*. In another study [31], where freeze-dried, macerated shoot tissues of brassica cultivars were mixed with 200 g of artificially infested sterile quartz sand (200 *Verticillium dahliae* microsclerotia g^{-1} sand) in sealed flasks, *B. juncea* tissue (0.6 g) proved to be the most inhibitive with up to 80% suppression. Handiseni et al. [32] also successfully demonstrated the suppressive effect of brassica tissues against *R. solani*; in this study, macerated shoot tissue of *B. juncea* (3 g in Petri dish) was found to be the most effective, causing >90% inhibition of mycelial growth.

Whilst biofumigation has attracted significant interest, research on its potential application for reducing the inoculum of *Fusarium* species affecting cereals is scarce. *Fusarium graminearum* produces ascospores (sexual spores) and conidia (asexual spores) and mainly overwinters as mycelium in infected crop debris, which serves as the primary inoculum for head blight disease in cereals [33]. Previously, ITC were tested against mycelial radial growth and conidial germination of *F. graminearum* under in vitro conditions [34]. Among the tested ITC, allyl and methyl ITC were overall more efficient, showing a lower effective dose resulting in 50% inhibition (ED$_{50}$) (35–150 mg L^{-1}), suggesting volatiles released from the damaged brassica tissues could have a suppressive effect on *F. graminearum*. Thus, the present study was performed to investigate the potential of brassicas to suppress *F. graminearum*. The aim of this study was to evaluate the effect of the leaf tissue of brassicas on mycelial growth of *F. graminearum* in vitro and to investigate the effect of shredded brassica tissues on the *F. graminearum* inoculum in a closed jar experiment.

2. Results

2.1. Glucosinolate Content of Brassica Leaf Tissue

The concentrations of the GSLs occurring in the leaf tissue of the brassicas are shown in Table 1. The GSL profile found in the leaves varied both qualitatively and quantitatively among the cultivars. The predominant GSL of *B. juncea* was sinigrin (allyl ITC-precursor) and that of *Raphanus sativus* was glucoraphanin (sulforaphane-precursor). The total GSL concentration of *B. juncea* 'Brons' increased with advancing growth stage (24.5–51.9 μmol g^{-1}). However, in the other three brassicas tested, the total GSL concentrations in leaf tissue were lower at the early-bud stage compared to stem-extension. Sinigrin comprised 91–94% of the total GSL content of the leaf tissue of *B. juncea* 'Caliente Rojo', occurring in the highest concentration (59.5 μmol g^{-1}) at the stem-extension stage, while the total GSL concentration ranged from 25.0 to 63.5 μmol g^{-1}. The total GSL concentration of *Eruca sativa* 'Trio 'and *R. sativus* 'Bokito' ranged from 12.9 to 17.2 μmol g^{-1} and 8.7 to 39.6 μmol g^{-1}, respectively.

Table 1. The type and concentration of glucosinolates in freeze-dried leaf tissue of brassica plants used in the leaf disc assay to investigate the effect of volatiles released from defrosted leaf discs of brassicas on the mycelial growth of *Fusarium graminearum* in vitro.

Glucosinolate	*Brassica juncea* Brons			*Brassica juncea* Caliente Rojo			*Raphanus sativus* Bokito			*Eruca sativa* Trio		
	I [a]	II [b]	III [c]	I	II	III	I	II	III	I	II	III
Glucoberin	2.47 (0.6) [d]	3.15 (0.49)	2.01 (0.41)	1.29 (0.2)	1.81 (0.3)	1.33 (0.37)	2.28 (0.4)	1.16 (0.18)	2.15 (0.6)	2.54 (0.6)	2.55 (0.33)	2.37 (0.75)
Progoitrin	0.38 (0.1)	0.34 (0.02)	0.30 (0.10)	0.25 (0.04)	0.23 (0.11)	0.26 (0.09)	0.35 (0.08)	0.37 (0.12)	0.46 (0.08)	0.30 (0.1)	0.00	0.00
Sinigrin	21.44 (1.7)	24.02 (2.94)	48.52 (3.03)	22.72 (1.88)	59.54 (2.32)	50.9 (3.8)	-	-	-	-	-	-
Gluconapin	0.00	0.00	0.35 (0.09)	0.27 (0.07)	0.35 (0.03)	0.25 (0.09)	-	-	-	-	-	-
Glucobrassicin	0.14 (0.04)	0.03 (0.01)	0.11 (0.02)	0.11 (0.02)	0.14 (0.02)	0.23 (0.12)	1.62 (0.26)	3.87 (1.9)	2.62 (0.6)	0.22 (0.03)	0.54 (0.08)	0.58 (0.08)
Gluconasturtiin	0.11 (0.01)	0.39 (0.05)	0.58 (0.08)	0.24 (0.08)	0.97 (0.19)	0.76 (0.12)	0.32 (0.13)	1.13 (0.2)	0.96 (0.2)	0.77 (0.12)	0.42 (0.15)	0.24 (0.10)
Neoglucobrassicin	0.00	0.00	0.00	0.05 (0.01)	0.04 (0.01)	0.01 (0.007)	0.00	0.00	0.00	0.00	0.06 (0.02)	0.00
Glucoraphanin	-	-	-	-	-	-	2.90 (0.5)	23.56 (3.2)	7.29 (2.1)	2.42 (0.51)	2.84 (0.64)	2.75 (0.6)
Glucoraphenin	-	-	-	-	-	-	0.18 (0.05)	1.34 (0.4)	0.44 (0.07)	-	-	-
4 hydroxy glucobrassicin	-	-	-	0.05 (0.01)	0.37 (0.1)	0.4 (0.15)	0.00	0.04 (0.01)	0.03 (0.01)	-	-	-
Glucoraphasatin	-	-	-	-	-	-	1.02 (0.03)	8.10 (1.1)	11.09 (3.1)	-	-	-
Glucoalyssin	-	-	-	-	-	-	-	-	-	0.86 (0.18)	0.51 (0.2)	0.45 (0.14)
Glucoerucin	-	-	-	-	-	-	-	-	-	0.57 (0.14)	1.20 (0.01)	1.50 (0.28)
4-mercaptobutyl	-	-	-	-	-	-	-	-	-	3.58 (0.72)	5.70 (0.44)	3.21 (0.58)
unknown	-	-	-	-	-	-	-	-	-	0.61 (0.2)	0.83 (0.23)	0.69 (0.19)
unknown	-	-	-	-	-	-	-	-	-	1.04 (0.12)	2.59 (0.66)	2.83 (0.74)
Total glucosinolates	24.54 (2.26)	27.94 (4.18)	51.87 (3.34)	24.98 (4.59)	63.45 (3.46)	54.15 (2.94)	8.67 (2.33)	39.56 (1.25)	25.05 (3.69)	12.90 (1.20)	17.23 (2.47)	14.63 (2.57)

[a] I = early-leaf growth stage (4 to 5 true leaves unfolded); [b] II = stem-extension stage; [c] III = early-bud stage; [d] GSL conc. μmol g^{-1} freeze-dried leaf tissue, mean (SE) values from two replicates.

2.2. Effect of Brassica Leaf Discs on Fusarium graminearum

The effect of *B. juncea* 'Brons' on *F. graminearum* varied slightly between the first experiment (with three brassicas; Supplementary Table S1) and the second experiment (with four brassicas). For example, *F. graminearum*, when exposed to two leaf discs collected at the stem-extension stage of *B. juncea* 'Brons', showed a 9% reduction in the first experiment in contrast to the 60% reduction in the second experiment. *Raphanus sativus* 'Bokito' and *E. sativa* 'Trio' showed similar effects in both experiments. Results of the second experiment are presented here.

Different responses of *F. graminearum* were observed according to the brassica species, dosage of leaf discs, and growth stage (Figures 1 and 2). The interaction between the brassica growth stage, brassica species, and number of leaf discs was very highly significant ($p < 0.001$). The fungal growth measured five days after exposure to the *B. juncea* leaf discs indicated a decline in the mycelial growth of *F. graminearum*. At the early-leaf stage experiment, the highest dosage of *B. juncea* 'Brons' (eight leaf discs) inhibited the radial growth by 41%. At the stem-extension and early-bud stages, the efficacy of *B. juncea* 'Brons' showed 87–90% suppression with four leaf discs, and complete suppression with eight leaf discs. The suppressive effect of all doses at the early-bud stage of *B. juncea* 'Brons' was significantly higher ($p < 0.05$) than the control (untreated). *Brassica juncea* 'Caliente Rojo' leaf discs collected at the stem-extension stage showed 20% inhibition with the lowest dose (one disc) and 94% inhibition with eight discs. When compared to the untreated control, no significant difference in the radial growth of *F. graminearum* was observed when exposed to leaf discs of *R. sativus* 'Bokito' collected at each of the growth stages. In the case of *E. sativa* 'Trio' (early-bud stage), the radial growth with one, two, and eight leaf discs was almost similar to that of the untreated, whereas the radial growth with four leaf discs was 15% higher than that of the untreated. At the stem-extension stage, the radial growth with two, four, and eight leaf discs (~20% higher than the untreated) was greater than the radial growth with one leaf disc (15% higher than the untreated). However, the differences in all treatments for *E. sativa* 'Trio' were insignificant.

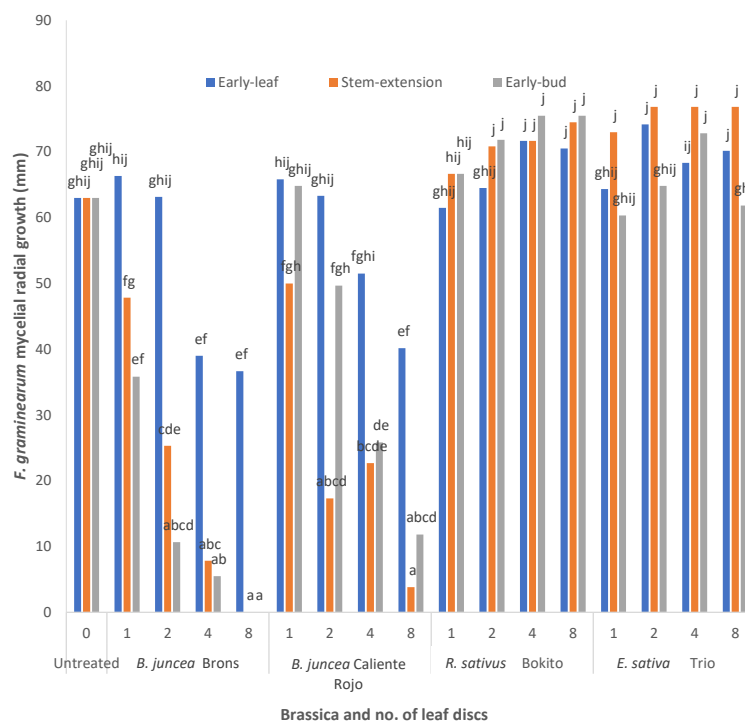**Figure 1.** The mycelial colony growth of *Fusarium graminearum* FG2502 in Petri dishes after 5 days untreated and exposed to 1, 2, 4, 8 leaf discs collected at three growth stages of *Brassica juncea* 'Brons', *B. juncea* 'Caliente Rojo', *Raphanus sativus* 'Bokito', and *Eruca sativa* 'Trio'. Different letters indicate significant differences according to the post hoc Tukey's test ($p = 0.05$, CV% = 10, SED = 4.276).
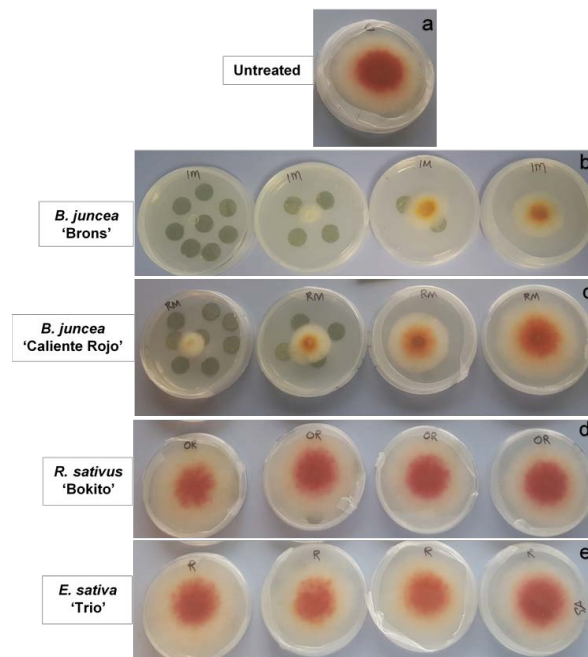
Figure 2. *Fusarium graminearum* FG2502 agar plugs exposed to (**a**) 0 (untreated), 1, 2, 4 and 8 leaf discs (right to left) collected at the early-bud stage of (**b**) *Brassica juncea* 'Brons', (**c**) *Brassica juncea* 'Caliente Rojo', (**d**) *Raphanus sativus* 'Bokito', and (**e**) *Eruca sativa* 'Trio', incubated at room temperature (ca. 20 °C) after 5 days.

2.3. Biofumigation Effect of Brassicas in Closed Jar Experiment

Data on the three brassica species (*B. juncea* 'Brons', *R. sativus* 'Bokito', *E. sativa* 'Trio') was consistent between the first (Supplementary Table S2) and second experiments and the results of the second experiment are presented here.

There was no significant interaction between the brassica species, biomass quantity, or inoculum type. The suppressive effect of the chopped shoots of brassicas on the *F. graminearum* inoculum was very highly significant ($p < 0.001$) (Figure 3). On average, inhibition efficiency between 41 and 55% was determined for the brassica treatments tested. The effect of biomass quantity at the two doses (15 g and 65 g) was not significant.
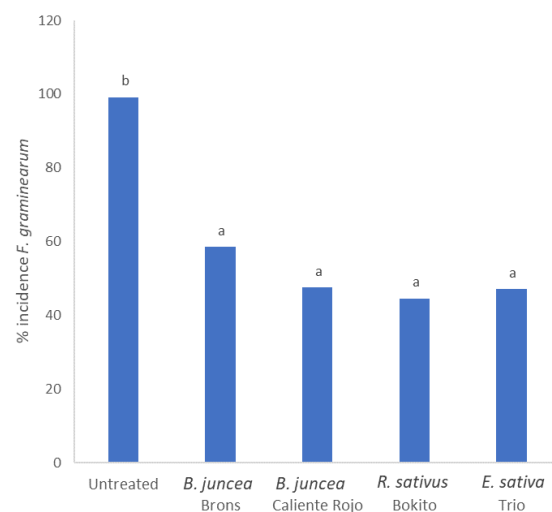

Figure 3. Percentage incidence of *Fusarium graminearum* FG2502 recovered in inoculum incubated for 8 weeks in jars filled with chopped brassica shoots and soil. Different letters indicate significant differences according to the post hoc Tukey's test ($p = 0.05$, CV% = 60.3, SED = 9.93).

3. Discussion

Variation in the efficacy of Brassicaceae plants in inhibiting *F. graminearum* mycelium in the leaf disc assay could be associated with the respective GSL profile. Results highlight that the defrosted leaves of *Brassica juncea* 'Brons', collected at the three development stages, caused significant inhibition of the mycelial growth of *F. graminearum*. Meanwhile, the results of the GSL analysis indicate that sinigrin content increases with advanced stages in this cultivar. This could be related to the inhibition of *F. graminearum*, as the level of suppression increased with the advancing growth stage of *B. juncea* 'Brons'. Similarly, the effect of *B. juncea* 'Caliente Rojo' could be related to the sinigrin content detected in the leaf tissue, with the greatest suppression of *F. graminearum* observed with leaves collected at the stem-extension stage. Hence, the effective inhibition of *F. graminearum* mycelium by *B. juncea* leaf discs could be attributed to high levels of sinigrin. Sinigrin is the parent-GSL of allyl ITC and this GSL comprises about 98–99% of the total GSL content of some *Brassica* species such as *B. juncea* and *B. nigra* [35,36]. Allyl ITC has been found to be the predominating compound (>90%) in volatiles released from the macerated leaves of *B. juncea* [30]. Correlations of mycelial inhibition with the release of allyl ITC from brassica leaf tissues have been observed [37]. In a previous study [38], *B. juncea* was found to be the most effective in inhibiting *Sclerotinia sclerotiorum* radial growth by 74–90% when agar plugs were exposed to the fresh macerated tissues of *B. juncea*, *B. campestris*, and *B. napus*. An in vitro assay [39] showed that macerated leaf tissues of *B. juncea* resulted in 73% and 100% inhibition of *F. oxysporum* and *Rhizoctonia solani*, respectively. Conversely, Kirkegaard et al. [40] reported up to 50% suppression of *F. graminearum* mycelial growth by ground freeze-dried tissue of the *B. juncea* shoots (10–500 mg per Petri dish). However, in this study, intact plants were initially frozen at −20 °C before separating into roots and shoots followed by freeze-drying. Hence, the comparatively lower suppression of *F. graminearum* may have resulted from the loss of volatiles by GSL hydrolysis during storage at −20 °C and the processing of samples, in contrast to the present study where leaf discs were immediately flash frozen in liquid nitrogen and stored at −80 °C. Nevertheless, the two studies cannot be directly compared due to the difference in the type of tissue material used.

If we assume a sinigrin content of 48.5 μmol g^{-1} leaf tissue (Table 1) and an ITC release efficiency of 1% [41], eight leaf discs would yield allyl ITC concentrations of 49 mg kg^{-1}, suggesting that this concentration is sufficient to completely inhibit *F. graminearum* mycelial growth as shown by the *B. juncea* 'Brons' leaves from the early-bud stage. Morra and Kirkegaard [41] recorded 14–26% efficiency of ITC release from *B. juncea* leaf discs frozen at −19 °C prior to incubation with the soil in bottles, whereas a <1% release efficiency was noticed using fresh leaf discs. The higher efficiency was attributed to extreme membrane disruption due to the freezing and thawing of tissues, allowing for greater contact between GSL and myrosinase. Hence, the allyl ITC release efficiency from the frozen leaf discs in the present assay might be higher than 1% due to a greater GSL/ITC conversion. Previous in vitro work has shown the suppressive effect of allyl ITC on *F. graminearum* at ED$_{50}$ concentrations of 62–135 mg L^{-1} [34]. Studies on *Alternaria* spp. suggest that ITC promotes the production of reactive oxygen species and disrupts mitochondrial function [42] and the plasma membrane [43,44] in fungal cells. In our previous study [34], the sensitivity of five strains of *F. graminearum* (FG2556, FG2498, FG2560, FG2502, FG2481—from UK wheat isolated in 2016) to ITC associated with these brassicas was found to be broadly similar. Therefore, in the present study, one strain, FG2502, was assessed.

In the leaf disc assay, *F. graminearum* mycelial plugs, which were completely inhibited by *B. juncea* 'Brons' treatments, showed no subsequent growth when transferred to fresh potato dextrose agar (PDA) media, indicating that the effect was fungicidal rather than fungistatic (data not shown). This is consistent with Charron and Sams [30], who reported a fungicidal effect of *B. juncea* macerated leaves on the radial growth of *Pythium ultimum*. The radial growth of *P. ultimum* exposed to macerated leaves was completely inhibited after 48 h, and the *P. ultimum* plugs, when transferred to fresh PDA, did not grow. The lowest dose (one leaf disc) of *B. juncea* showed a slight stimulation in colony growth, although this

was not significantly different to the control. *Raphanus sativus* 'Bokito' and *E. sativa* 'Trio' also appeared to insignificantly stimulate colony growth. Such stimulation is consistent with a previous report by Kirkegaard et al. [40] where the colony growth of *Bipolaris sorokiniana* was stimulated when exposed to lower quantities of *B. juncea* and *B. napus* tissues. A slightly higher inhibition in the *B. juncea* 'Brons' treatment was seen in the second experiment in comparison to the first leaf disc assay, as above-mentioned. This could be due to plants grown at different times of the year (experiment 1: October–January; experiment 2: September–November). Slightly longer daylight hours and higher temperatures during the time period of the second experiment may have resulted in higher GSL concentrations, as these factors are known to increase the production of GSL in brassica tissues [45].

The two cultivars of *B. juncea* were effective in both the leaf disc and closed jar experiments, however, *R. sativus* and *E. sativa*, despite being ineffective in the leaf disc assay, showed significant suppression in the closed jar experiment. In addition to ITC, other less toxic compounds such as nitriles and thiocyanates are also produced as a result of GSL hydrolysis, and these compounds are known to have biocidal properties [46,47]. Moreover, other toxic compounds such as dimethyl disulphide and carbon disulphide are released during the decomposition of plant material, which may also contribute to the biofumigation effect [48,49]. These factors may have contributed to the suppressive activity seen by *R. sativus* and *E. sativa* in the present closed jar study.

In the closed jar experiment, the two quantities of the chopped tissue added, 65 g and 15 g, were calculated as equivalent to 50 t fresh wt. ha^{-1} and 12 t fresh wt. ha^{-1}, respectively. The rationale behind these rates was to mimic the biofumigation potential of brassica plants with an achievable high biomass (50 t fresh wt. ha^{-1}) in the field [50] and a relatively low biomass (25% of a high yield). Previously, Handiseni et al. [32] exposed *R. solani* mycelial plugs to *B. juncea*-amended soil in sealed bags. A dose dependent response was reported with inhibition ranging from <5% inhibition at a 0.4% (wt/wt) incorporation rate to approximately 50% inhibition at the 3.2% (wt/wt) incorporation rate. This was in contrast to findings from the closed jar experiment where the dose effect was not significant. As the present experiment was carried out in airtight jars, volatiles released from even the lower dose (15 g) were sufficient to effectively suppress *F. graminearum*. However, in agreement with the present findings, Mayton et al. [37] reported a >50% radial growth inhibition of *F. sambucinum* in Petri dishes inverted onto jars containing the macerated leaf tissue of *B. nigra* and *B. juncea*, which was not affected by the quantity of tissue (10–40 g).

Using a cut-and-carry approach, brassica mulch was applied to *F. graminearum* infected wheat plots in field experiments performed over two years [51]. Fusarium head blight incidence was significantly reduced by 58% in the first year by *Sinapis alba* and 18% by *B. juncea* in the second year. The two types of mulch also reduced deoxynivalenol content in the wheat grain by 40–50%. Crop debris, particularly that of maize, is a primary source of inoculum for Fusarium head blight in wheat [52,53]. Crop debris is present in all shapes and sizes, and to reduce the variability within an experimental system, it is beneficial to have an artificial crop debris model system. Two types of substrates were used in the present study, chaff represented natural crop residue and blind oat spikes represented an artificial crop debris that is uniform in size and nutritional status, and were uniformly infected with *F. graminearum*. The volatiles from the chopped brassica tissue appeared to have inhibited *F. graminearum* inoculum, irrespective of the inoculum type. This suggests that biofumigation could prove to be effective in reducing the *F. graminearum* inoculum present in a variety of crop residues such as chaff, seed, and straw under field conditions. However, it would be useful to identify whether biofumigation is equally effective against inoculum of various sizes, as *F. graminearum* within larger pieces of inoculum may be protected from contact with the inhibitory compounds released during the process.

Brassica juncea 'Caliente Rojo', which is a fairly new cultivar, was not available at the time period of the first experiments. The suppressive effect of *B. juncea* 'Caliente Rojo' seen in the present study suggests that this cultivar could be a promising biofumigant for managing *F. graminearum* in the field. The cultivar could be sown following the harvest of

wheat in summer, and incorporated in autumn followed by subsequent cereal production. Glucosinolate analysis of this cultivar showed that concentrations of the dominant GSL, sinigrin, were highest at the stem-extension stage compared to the other two stages. A balance between the biomass and GSL concentration could be achieved by identifying an appropriate growth stage between stem-extension and flowering to maximize the GSL content for incorporation. The biofumigant, when chopped and incorporated, is then likely to produce ITC at sufficiently effective concentrations. Glucosinolate concentrations recorded in the present study could be achievable in field situations. Total GSL concentrations of up to 50, 69, and 61 μmol g^{-1} biomass have been detected in *B. juncea*, *R. sativus*, and *E. sativa*, respectively under field conditions [54]. Biofumigation, if applied in a cereal rotation, may therefore be useful in the reduction of *F. graminearum* inoculum in the field, thus suppressing infection in the subsequent cereal crop. However, it should be considered that the present experiments were carried out under controlled conditions. In the field, various factors such as soil pH, temperature, moisture, and organic content as well as the biofumigant crop establishment and growth should be considered, as these factors can affect the outcome of biofumigation. Moreover, weather conditions such as temperature, daylight hours, and rainfall also influence the efficacy of biofumigation.

4. Materials and Methods

4.1. Brassicas and Fungal Culture

Seeds of *B. juncea* 'Brons' (Indian mustard), *R. sativus* 'Bokito' (oilseed radish), and *E. sativa* 'Trio' (rocket) were supplied by RAGT Seeds (Essex, UK) and *B. juncea* 'Caliente Rojo' (Indian mustard) by Tozer Seeds (Surrey, UK). The four cultivars were grown in a glasshouse in 10 cm pots with mean temperatures of 12 °C (night) and 17 °C (day). For first experiment, plants were grown between October 2019–January 2020 and for second experiment, plants were grown between September–November 2020. *Fusarium graminearum* strain FG2502 from UK wheat isolated in 2016 was provided by Fera Science Ltd. (York, UK). The strain was confirmed as *F. graminearum* by species-specific PCR using a previously published assay [55].

4.2. Leaf Disc Assay

Leaves of three cultivars (*B. juncea* 'Brons', *R. sativus* 'Bokito', *E. sativa* 'Trio') were sampled at the early-leaf stage (4–5 true leaves unfolded). Using a 15 mm (diameter) cork borer, 45 discs were cut from the leaves of each cultivar. The leaf discs, separated by Miracloth (EMD Millipore Corp., Billerica, MA, USA) in stacks of fives and held together by a paper clip, were immediately flash frozen in liquid nitrogen and stored at −80 °C until required for the assay. Agar plugs with a 7 mm diameter were cut from the outer margin of actively growing *F. graminearum* (FG2502) on PDA (Merck, KGaA, Darmstadt, Germany) media. These were transferred to the centre of 9 cm Petri dishes containing PDA with the mycelium facedown. The frozen leaf discs were transferred in dry ice from the freezer to the work-station to prevent the discs from defrosting prematurely. Leaf discs at doses of one, two, four, and eight discs were placed with forceps onto the upturned lids of the Petri dishes while the inverted bottom containing the fungal plug was held aside. The plates in the inverted position were immediately sealed with parafilm. The control plates did not contain leaf discs. Three replicates were used per treatment. The plates were incubated at room temperature (ca. 20 °C) and radial colony growth was measured after 5–6 days, just before the untreated mycelia had reached the edge of the plates. Experiments to investigate the effect of brassica leaves at the stem-extension and early-bud stages were performed as above.

The assay was repeated independently using *B. juncea* 'Caliente Rojo', in addition to the other brassica species tested in the first experiment.

4.3. Closed Jar Experiment

4.3.1. Preparation of Inoculum Bags

Conidial suspensions were prepared following a previous method [56] with some modifications. *Fusarium graminearum* (FG2502) was sub-cultured on PDA using 20 plates and incubated at room temperature (ca. 20 °C). After 14 days, conidia were harvested by the addition of 20–25 mL sterile distilled water to each plate and conidia were dislodged using a sterile spreader. The suspension was filtered through Miracloth to remove the mycelium. The filtrate was centrifuged at $3000\times g$ for 10 min. The supernatant was removed and conidia re-suspended in 15 mL sterile distilled water and centrifuged at $3000\times g$ for 10 min. Conidia were washed twice and re-suspended in 15 mL sterile distilled water. Conidia were counted using an Improved Neubauer counting chamber (Weber 99, Scientific International, Teddington, UK) and the concentration adjusted to 3×10^4 spores mL^{-1}.

A kilogram of oat screenings (Morning Foods, Crewe, UK), which were predominantly blind oat spikes, were soaked in distilled water for 12 h before autoclaving for 15 min in a 78 cm × 40 cm autoclavable bag [VWR (129–0581), UK]. The oats were re-autoclaved for 15 min after 24 h and allowed to cool. A total of 100 mL (3×10^6 spores) of the above prepared spore suspension was added to the bag, mixed well, and incubated for 10–12 days in the dark at ca. 18 °C. Five pieces of inoculum (blind oat spikes) were added to perforated nylon sachets (7 cm × 5.5 cm) and sealed with a plastic bag sealing machine (Impulse heat sealer, 200 mm). Additionally, wheat chaff was randomly collected post-harvest from a *F. graminearum*-inoculated wheat experiment at the research facilities of Harper Adams University, Newport, Shropshire, UK. Five pieces of chaff were added to nylon bags and sealed as described above. Both types of inoculum (Figure 4a) were confirmed for *F. graminearum* infection on PDA prior to use in the experiment.
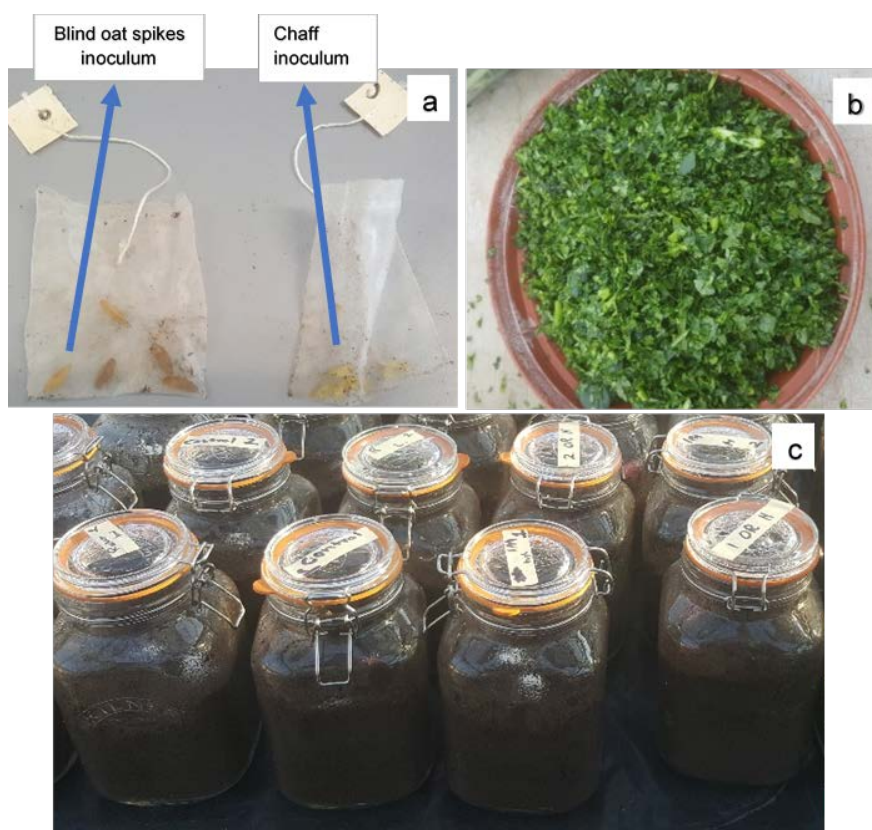

Figure 4. The experimental setup of the closed jar biofumigation experiment. (**a**) Blind oat spikes inoculated with *Fusarium graminearum* and chaff from the *F. graminearum*-inoculated wheat in nylon sachets. (**b**) Brassica shoots chopped in food processor. (**c**) Sealed jars containing the two types of inoculum sachets buried in loam-based compost incorporated with chopped brassica tissue.

4.3.2. Evaluating Effect of Biofumigants on Inoculum

Two litre glass jars with rubber seal clips (22 cm × 12 cm × 12 cm) were filled with John Innes No. 2 loam-based compost [composition: loam, peat, coarse sand, hoof and horn meal, superphosphate, potassium sulphate, calcium carbonate; pH: 5.5–6 (provided by supplier); 46% moisture] to a depth of 10 cm. At the early-bud stage, shoots of *B. juncea* 'Brons', *R. sativus* 'Bokito', and *E. sativa* 'Trio' were harvested and chopped in a food processer for 15 s. Chopped tissue (Figure 4b) at two quantities, 65 g and 15 g, were added to soil-filled jars and mixed well. Jars without brassica amendments served as the controls. One inoculum bag (blind oat spikes) was buried in each jar and the lid closed hermetically. Five replicates were used per treatment and the jars were incubated in a glasshouse with mean temperatures of 12 °C (night) and 17 °C (day) (Figure 4c). After eight weeks, the bags were extracted, and the inoculum substrates were tested for *F. graminearum* growth on Petri dishes containing modified Czapek Dox iprodione agar media [57]. Briefly, the selective media were prepared by adding dichloran solution (0.2% in ethanol), chloramphenicol solution (5% in ethanol), and trace metal solution (1% $ZnSO_4 \cdot 7H_2O$ + 0.5% $CuSO_4 \cdot 5H_2O$) each 1 mL L^{-1} of Czapek Dox agar (Sigma-Aldrich, Switzerland) media. Once autoclaved and cooled down to 55 °C, 10 mL of chlortetracycline solution (0.5%) and 1 mL of Bumper® suspension (0.3%) containing 750 µg propiconazole were added per L of media before pouring into plates. The five inoculum pieces were removed from each bag, placed on a media plate, and incubated at room temperature (ca. 20 °C) for 12–15 days. *Fusarium graminearum* incidence in the inoculum pieces was recorded as the presence of *F. graminearum* colony growth based on the characteristic reddish pigmentation. For confirmation, the assumed *F. graminearum* colonies were sub-cultured on PDA and incubated at room temperature (ca. 20 °C) for 14 days. The conidia were harvested as described above and identified according to the morphological characteristics [58].

The experiment was independently repeated using *B. juncea* 'Caliente Rojo', in addition to the other brassicas tested in the first experiment. Additionally, a bag of the chaff inoculum (five pieces per bag) was also buried in each jar.

4.4. Glucosinolate Analysis

Approximately 10 g of leaf tissue of the brassica plants was collected at the three developmental stages (early-leaf, stem-extension, early-bud), flash frozen in liquid nitrogen, and stored at −80 °C until freeze dried. Freeze-dried (GVD6/13 MKI freeze dryer; GIROVAC Ltd., North Walsham, UK) samples were milled (IKA®M 20 Universal Mill, Staufen, Germany) and stored at −18 °C before sending to the NIAB Labtest, Cambridge, UK, where the samples were analysed following the ISO 9167 "Rapeseed and rapeseed meals—Determination of glucosinolates content—Method using HPLC" [59].

4.5. Statistical Analysis

Data were subjected to general analysis of variance using Genstat® (20th edition) statistical software. The closed jar experiments were arranged in the glasshouse in a completely randomised design. In the leaf disc assay, there were three factors—brassica species, brassica growth stage, number of leaf discs. In the closed jar experiment, the three factors were brassica species, biomass quantity, and inoculum type. Where necessary, data were angular transformed to improve the normality of the residuals. Significant differences between treatments were determined using the post hoc Tukey test (p = 0.05).

References

1. Backhouse, D. Global distribution of *Fusarium graminearum, F. asiaticum* and *F. boothii* from wheat in relation to climate. *Eur. J. Plant Pathol.* **2014**, *139*, 161–173. [CrossRef]
2. McMullen, M.; Bergstrom, G.; De Wolf, E.; Dill-Macky, R.; Hershman, D.; Shaner, G.; Van Sanford, D. A unified effort to fight an enemy of wheat and barley: Fusarium head blight. *Plant Dis.* **2012**, *96*, 1712–1728. [CrossRef] [PubMed]
3. Gilchrist, L.; Dubin, H.J. Fusarium head blight. In *Bread Wheat Improvement and Production, Plant Production and Protection*; Curtis, B.C., Rajaram, S., Macpherson, H.G., Eds.; Series 30; FAO: Rome, Italy, 2002.
4. Mielniczuk, E.; Skwaryło-Bednarz, B. Fusarium Head Blight, mycotoxins and strategies for their reduction. *Agronomy* **2020**, *10*, 509. [CrossRef]
5. Palazzini, J.; Fumero, V.; Yerkovich, N.; Barros, G.; Cuniberti, M.; Chulze, S. Correlation between *Fusarium graminearum* and deoxynivalenol during the 2012/13 wheat Fusarium head blight outbreak in Argentina. *Cereal Res. Commun.* **2015**, *43*, 627–637. [CrossRef]
6. Wilson, W.; Dahl, B.; Nganje, W. Economic costs of Fusarium Head Blight, scab and deoxynivalenol. *World Mycotoxin J.* **2018**, *11*, 291–302. [CrossRef]
7. Guo, H.; Ji, J.; Wang, J.S.; Sun, X. Deoxynivalenol: Masked forms, fate during food processing, and potential biological remedies. *Compr. Rev. Food Sci. Food Saf.* **2020**, *19*, 895–926. [CrossRef] [PubMed]
8. Szuets, P.; Mesterhazy, A.; Falkay, G.Y.; Bartok, T. Early telarche symptoms in children and their relations to zearalenon contamination in foodstuffs. *Cereal Res. Commun.* **1997**, *25*, 429–436. [CrossRef]
9. Zhao, F.; Li, R.; Xiao, S.; Diao, H.; Viveiros, M.M.; Song, X.; Ye, X. Postweaning exposure to dietary zearalenone, a mycotoxin, promotes premature onset of puberty and disrupts early pregnancy events in female mice. *Toxicol. Sci.* **2013**, *132*, 431–442. [CrossRef]
10. Edwards, S.G.; Jennings, P. Impact of agronomic factors on Fusarium mycotoxins in harvested wheat. *Food Addit. Contam. Part A* **2018**, *35*, 2443–2454. [CrossRef]
11. Bensassi, F.; Zaied, C.; Abid, S.; Hajlaoui, M.R.; Bacha, H. Occurrence of deoxynivalenol in durum wheat in Tunisia. *Food Control.* **2010**, *21*, 281–285. [CrossRef]
12. Jakšić, S.; Abramović, B.; Jajić, I.; Baloš, M.Ž.; Mihaljev, Ž.; Despotović, V.; Šojić, D. Co-occurrence of fumonisins and deoxynivalenol in wheat and maize harvested in Serbia. *Bull. Environ. Contam. Toxicol.* **2012**, *89*, 615–619. [CrossRef] [PubMed]
13. Becher, R.; Hettwer, U.; Karlovsky, P.; Deising, H.B.; Wirsel, S.G.R. Adaptation of *Fusarium graminearum* to tebuconazole yielded descendants diverging for levels of fitness, fungicide resistance, virulence, and mycotoxin production. *Phytopathology* **2010**, *100*, 444–453. [CrossRef] [PubMed]
14. Klix, M.B.; Verreet, J.-A.; Beyer, M. Comparison of the declining triazole sensitivity of *Gibberella zeae* and increased sensitivity achieved by advances in triazole fungicide development. *Crop Prot.* **2007**, *26*, 683–690. [CrossRef]
15. Yerkovich, N.; Cantoro, R.; Palazzini, J.M.; Torres, A.; Chulze, S.N. Fusarium head blight in Argentina: Pathogen aggressiveness, triazole tolerance and biocontrol-cultivar combined strategy to reduce disease and deoxynivalenol in wheat. *Crop Prot.* **2020**, *137*, 105300. [CrossRef]

16. Poulsen, R.; Luong, X.; Hansen, M.; Styrishave, B.; Hayes, T. Tebuconazole disrupts steroidogenesis in *Xenopus laevis*. *Aquat. Toxicol.* **2015**, *168*, 28–37. [CrossRef]

17. Lv, X.; Pan, L.; Wang, J.; Lu, L.; Yan, W.; Zhu, Y.; Xu, Y.; Guo, M.; Zhuang, S. Effects of triazole fungicides on androgenic disruption and CYP3A4 enzyme activity. *Environ. Pollut.* **2017**, *222*, 504–512. [CrossRef]

18. Kirkegaard, J.A.; Gardner, P.A.; Desmarchelier, J.M.; Angus, J.F. Biofumigation using *Brassica* species to control pests and diseases in horticulture and agriculture. In *9th Australian Research Assembly on Brassicas*; Wratten, M., Mailer, R.J., Eds.; British Society for Plant Pathology, Agricultural Research Institute: Wagga Wagga, NSW, Australia, 1993; pp. 77–82.

19. Andréasson, E.; Jørgensen, L.B.; Höglund, A.-S.; Rask, L.; Meijer, J. Different myrosinase and idioblast distribution in *Arabidopsis* and *Brassica napus*. *Plant Physiol.* **2001**, *127*, 1750–1763. [CrossRef]

20. Thangstad, O.P.; Iversen, T.H.; Slupphaug, G.; Bones, A. Immunocytochemical localization of myrosinase in *Brassica napus* L. *Planta* **1990**, *180*, 245–248. [CrossRef]

21. Koroleva, O.A.; Gibson, T.M.; Cramer, R.; Stain, C. Glucosinolate-accumulating S-cells in *Arabidopsis* leaves and flower stalks undergo programmed cell death at early stages of differentiation. *Plant J.* **2010**, *64*, 456–469. [CrossRef]

22. Jørgensen, M.E.; Nour-Eldin, H.H.; Halkier, B.A. Transport of defense compounds from source to sink: Lessons learned from glucosinolates. *Trends Plant Sci.* **2015**, *20*, 508–514. [CrossRef]

23. Bones, A.M.; Rossiter, J.T. The myrosinase-glucosinolate system, its organisation and biochemistry. *Physiol. Plant* **1996**, *97*, 194–208. [CrossRef]

24. Wittstock, U.; Burow, M. Glucosinolate breakdown in *Arabidopsis*: Mechanism, regulation and biological significance. *Arab. Book* **2010**, *8*, e0134. [CrossRef]

25. Dahlin, P.; Hallmann, J. New insights on the role of allyl isothiocyanate in controlling the root knot nematode *Meloidogyne hapla*. *Plants* **2020**, *9*, 603. [CrossRef] [PubMed]

26. Norsworthy, J.K.; Meehan, J.T. Use of isothiocyanates for suppression of Palmer amaranth (*Amaranthus palmeri*), pitted morning-glory (*Ipomoea lacunosa*), and yellow nutsedge (*Cyperus esculentus*). *Weed Sci.* **2005**, *53*, 884–890. [CrossRef]

27. Sarwar, M.; Kirkegaard, J.A.; Wong, P.T.W.; Desmarchelier, J.M. Biofumigation potential of brassicas. 3. In vitro toxicity of isothiocyanates to soil-borne fungal pathogens. *Plant Soil* **1998**, *201*, 71–89.

28. Smolinska, U.; Morra, M.J.; Knudsen, G.R.; James, R.L. Isothiocyanates produced by Brassicaceae species as inhibitors of *Fusarium oxysporum*. *Plant Dis.* **2003**, *87*, 407–412. [CrossRef]

29. Lewis, J.A.; Papavizas, G.C. Effect of volatiles from decomposing plant tissues on pigmentation, growth, and survival of Rhizoctonia solani. *Soil Sci.* **1974**, *118*, 156–163. [CrossRef]

30. Charron, C.S.; Sams, C.E. Inhibition of *Pythium ultimum* and *Rhizoctonia solani* by shredded leaves of Brassica species. *J. Am. Soc. Hortic. Sci.* **1999**, *124*, 462–467. [CrossRef]

31. Neubauer, C.; Heitmann, B.; Müller, C. Biofumigation potential of Brassicaceae cultivars to *Verticillium dahliae*. *Eur. J. Plant Pathol.* **2014**, *140*, 341–352. [CrossRef]

32. Handiseni, M.; Jo, Y.-K.; Lee, K.-M.; Zhou, X.-G. Screening brassicaceous plants as biofumigants for management of *Rhizoctonia solani* AG1-IA. *Plant Dis.* **2016**, *100*, 758–763. [CrossRef]

33. Leplat, J.; Friberg, H.; Abid, M.; Steinberg, C. Survival of *Fusarium graminearum*, the causal agent of Fusarium head blight. A review. *Agron. Sustainable Dev.* **2013**, *33*, 97–111. [CrossRef]

34. Ashiq, S.; Edwards, S.G.; Fatukasi, O.; Watson, A.; Back, M.A. In vitro activity of isothiocyanates against *Fusarium graminearum*. *Plant Pathol.* **2022**, *71*, 594–601. [CrossRef]

35. Matteo, R. Non-Food Brassicas for Green Chemistry Purposes through a Biorefinery Approach. Master's Thesis, University of Bologna, Bologna, Italy, 2017.

36. Ngala, B.M.; Woods, S.R.; Back, M.A. In vitro assessment of the effects of *Brassica juncea* and *Raphanus sativus* leaf and root extracts on the viability of *Globodera pallida* encysted eggs. *Nematology* **2015**, *17*, 543–556. [CrossRef]

37. Mayton, H.S.; Olivier, C.; Vaughn, S.F.; Loria, R. Correlation of fungicidal activity of Brassica species with allyl isothiocyanate production in macerated leaf tissue. *Phytopathology* **1996**, *86*, 267–271. [CrossRef]

38. Ojaghian, M.R.; Jiang, H.; Xie, G.-L.; Cui, Z.-Q.; Zhang, J.; Li, B. In vitro biofumigation of Brassica tissues against potato stem rot caused by *Sclerotinia sclerotiorum*. *Plant Pathol. J.* **2012**, *28*, 185–190. [CrossRef]

39. Larkin, R.P.; Griffin, T.S. Control of soilborne potato diseases using Brassica green manures. *Crop Prot.* **2007**, *26*, 1067–1077. [CrossRef]

40. Kirkegaard, J.A.; Wong, P.T.W.; Desmarchelier, J.M. In vitro suppression of fungal root pathogens of cereals by Brassica tissues. *Plant Pathol.* **1996**, *45*, 593–603. [CrossRef]

41. Morra, M.J.; Kirkegaard, J.A. Isothiocyanate release from soil-incorporated Brassica tissues. *Soil Biol. Biochem.* **2002**, *34*, 1683–1690. [CrossRef]

42. Calmes, B.; N'Guyen, G.; Dumur, J.; Brisach, C.A.; Campion, C.; Iacomi, B.; Pigné, S.; Dias, E.; Macherel, D.; Guillemette, T. Glucosinolate-derived isothiocyanates impact mitochondrial function in fungal cells and elicit an oxidative stress response necessary for growth recovery. *Front. Plant Sci.* **2015**, *6*, 414. [CrossRef]

43. Wang, T.; Li, Y.; Bi, Y.; Zhang, M.; Zhang, T.; Zheng, X.; Dong, Y.; Huang, Y. Benzyl isothiocyanate fumigation inhibits growth, membrane integrity and mycotoxin production in *Alternaria alternata*. *RSC Adv.* **2020**, *10*, 1829–1837. [CrossRef]

44. Zhang, M.; Li, Y.; Bi, Y.; Wang, T.; Dong, Y.; Yang, Q.; Zhang, T. 2-Phenylethyl isothiocyanate exerts antifungal activity against *Alternaria alternata* by affecting membrane integrity and mycotoxin production. *Toxins* **2020**, *12*, 124. [CrossRef] [PubMed]

45. Björkman, M.; Klingen, I.; Birch, A.N.E.; Bones, A.M.; Bruce, T.J.A.; Johansen, T.J.; Meadow, R.; Mølmann, J.; Seljåsen, R.; Smart, L.E. Phytochemicals of Brassicaceae in plant protection and human health–Influences of climate, environment and agronomic practice. *Phytochem.* **2011**, *72*, 538–556. [CrossRef] [PubMed]

46. Peterson, C.J.; Cosse, A.; Coats, J.R. Insecticidal components in the meal of *Crambe abyssinica. J. Agric. Urban Entomol.* **2000**, *17*, 27.

47. Tsao, R.; Peterson, C.J.; Coats, J.R. Glucosinolate breakdown products as insect fumigants and their effect on carbon dioxide emission of insects. *BMC Ecol.* **2002**, *2*, 5. [CrossRef]

48. Bending, G.D.; Lincoln, S.D. Characterisation of volatile sulphur-containing compounds produced during decomposition of *Brassica juncea* tissues in soil. *Soil Biol. Biochem.* **1999**, *31*, 695–703. [CrossRef]

49. Motisi, N.; Doré, T.; Lucas, P.; Montfort, F. Dealing with the variability in biofumigation efficacy through an epidemiological framework. *Soil Biol. Biochem.* **2010**, *42*, 2044–2057. [CrossRef]

50. Lazzeri, L.; Leoni, O.; Bernardi, R.; Malaguti, L.; Cinti, S. Plants, techniques and products for optimising biofumigation in full field. *Agroindustria* **2004**, *3*, 281–288.

51. Drakopoulos, D.; Kägi, A.; Gimeno, A.; Six, J.; Jenny, E.; Forrer, H.-R.; Musa, T.; Meca, G.; Vogelgsang, S. Prevention of Fusarium head blight infection and mycotoxins in wheat with cut-and-carry biofumigation and botanicals. *Field Crops Res.* **2020**, *246*, 107681. [CrossRef]

52. Champeil, A.; Fourbet, J.-F.; Doré, T.; Rossignol, L. Influence of cropping system on Fusarium head blight and mycotoxin levels in winter wheat. *Crop Prot.* **2004**, *23*, 531–537. [CrossRef]

53. Vogelgsang, S.; Beyer, M.; Pasquali, M.; Jenny, E.; Musa, T.; Bucheli, T.D.; Wettstein, F.E.; Forrer, H.-R. An eight-year survey of wheat shows distinctive effects of cropping factors on different Fusarium species and associated mycotoxins. *Eur. J. Agron.* **2019**, *105*, 62–77. [CrossRef]

54. Ngala, B.M.; Haydock, P.P.J.; Woods, S.; Back, M.A. Biofumigation with *Brassica juncea, Raphanus sativus* and *Eruca sativa* for the management of field populations of the potato cyst nematode *Globodera pallida. Pest Manag. Sci.* **2015**, *71*, 759–769. [CrossRef] [PubMed]

55. Waalwijk, C.; van der Heide, R.; de Vries, I.; van der Lee, T.; Schoen, C.; Costrel-de Corainville, G.; Häuser-Hahn, I.; Kastelein, P.; Köhl, J.; Lonnet, P. Quantitative detection of *Fusarium* species in wheat using TaqMan. *Eur. J. Plant Pathol.* **2004**, *110*, 481–494. [CrossRef]

56. Edwards, S.G.; Seddon, B. Selective media for the specific isolation and enumeration of *Botrytis cinerea* conidia. *Lett. Appl. Microbiol.* **2001**, *32*, 63–66. [CrossRef] [PubMed]

57. Hofgaard, I.S.; Seehusen, T.; Aamot, H.U.; Riley, H.; Razzaghian, J.; Le, V.H.; Hjelkrem, A.-G.R.; Dill-Macky, R.; Brodal, G. Inoculum potential of *Fusarium* spp. relates to tillage and straw management in Norwegian fields of spring oats. *Front. Microbiol.* **2016**, *7*, 556. [CrossRef] [PubMed]

58. Leslie, J.F.; Summerell, B.A. *The Fusarium Laboratory Manual*; Blackwell Publishing: Ames, IA, USA, 2006.

59. ISO 9167 Rapeseed and Rapeseed Meals—Determination of Glucosinolates Content—Method Using HPLC. Available online: https://www.iso.org/standard/72207.html (accessed on 21 March 2022).

Rhodiola rosea Reduces Intercellular Signaling in *Campylobacter jejuni*

Ajda Kunčič [1], **Franz Bucar** [2] and **Sonja Smole Možina** [1,*]

1   Department of Food Science and Technology, Biotechnical Faculty, University of Ljubljana, Jamnikarjeva ulica 101, 1000 Ljubljana, Slovenia
2   Department of Pharmacognosy, Institute of Pharmaceutical Sciences, University of Graz, Beethovenstraße 8, 8010 Graz, Austria
*   Correspondence: sonja.smole-mozina@bf.uni-lj.si; Tel.: +386-1-320-3751

Abstract: *Campylobacter jejuni* is a major foodborne pathogen and the leading cause of bacterial gastroenteritis, i.e., campylobacteriosis. Besides searching for novel antimicrobials, identification of new targets for their action is becoming increasingly important. *Rhodiola rosea* has long been used in traditional medicine. Ethanolic extracts from the roots and rhizomes of the plant contain a wide range of bioactive compounds with various pharmacological activities. In this study, cultivated plant materials have been used, i.e., "Mattmark" and "Rosavine". Through optimized protocols, we obtained fractions of the initial ethanolic extracts rich in most important bioactive compounds from *R. rosea*, including salidroside, rosavins, proanthocyanidins (PACs), and flavonoids. The antimicrobial activity in relation to the chemical composition of the extracts and their fractions was studied with an emphasis on *C. jejuni* AI-2-mediated intercellular signaling. At concentration 15.625 mg/L, bioluminescence reduction rates varied from 27% to 72%, and the membrane remained intact. Fractions rich in PACs had the strongest antimicrobial effect against *C. jejuni*, with the lowest minimal inhibitory concentrations (MICs) (M F3 40%: 62.5 mg/L; R F3 40%: 250 mg/L) and the highest intercellular signaling reduction rates (M F3 40%: 72%; R F3 40%: 65%). On the other hand, fractions without PACs were less effective (MICs: M F5 PVP: 250 mg/L; R F5 PVP: 1000 mg/L and bioluminescence reduction rates: M F5 PVP: 27%; R F5 PVP: 43%). Additionally, fractions rich in flavonoids had strong antimicrobial activity (MICs: M F4 70%: 125 mg/L; R F4 70%: 250 mg/L and bioluminescence reduction rates: M F4 70%: 68%; R F4 70%: 50%). We conclude that PACs and flavonoids are crucial compound groups responsible for the antimicrobial activity of *R. rosea* roots and rhizomes in *C. jejuni*.

Keywords: *Rhodiola rosea*; proanthocyanidins; flavonoids; *Campylobacter jejuni*; LuxS; intercellular signaling

1. Introduction

Overuse of antibiotics in veterinary and human medicine is responsible for the development of antibiotic-resistant strains. Due to increased antimicrobial resistance, the search for novel antimicrobial agents and their potential targets is of utmost importance. Antibiotic resistance has also been recorded for *Campylobacter jejuni*, a major foodborne pathogen and the leading cause of bacterial gastroenteritis, also known as campylobacteriosis. This infection occurs very commonly in European countries. With over 120,000 confirmed human cases of illness in 2020, it has been the most commonly reported zoonosis, representing over 60% of all reported cases in 2020 [1].

There are different potential targets that can be affected by antimicrobials. Among them are bacterial intercellular communication systems, collectively termed quorum sensing (QS) [2]. QS is a bacterial cell-to-cell communication and it refers to the ability of bacteria to sense information from other cells in the population [3]. Bacteria communicate through small molecules also known as autoinducers (AIs) [4]. The autoinducer-2 (AI-2) signaling molecule regulates interspecies communication as it is present in both Gram-positive and

Gram-negative bacteria [5,6]. Elvers and Park [7] described the role of the *luxS* gene in the production of the AI-2 signal and AI-2-mediated signaling in *C. jejuni*. The LuxS enzyme has a central role as a metabolic enzyme in the methyl cycle, responsible for the generation of S-adenosyl-L-methionine (SAM). The enzyme has its role in the two-step reaction of homocysteine formation, where AI-2 is formed as a by-product [8]. As LuxS-deficient *C. jejuni* shows critical differences in colonization and virulence [9], AI-2-mediated signaling can be considered as a potential target for the control of that pathogen.

Natural compounds with anti-QS potential can be found in medicinal plants and their extracts [10]. Various phytochemicals inhibit *C. jejuni* intercellular signaling. Examples of this include citrus ethanolic extracts [11], epigallocatechin gallate (EGCG) [12], resveratrol inclusion complexes [13], coriander essential oil, linalool [14], *Euodia ruticarpa* ethanolic extract [15], carvacrol [16], curcumin, allyl sulfide, garlic oil, and ginger oil [17]. Šimunović et al. [9] investigated the correlation of QS inhibition with changes in *C. jejuni* motility, adhesion to polystyrene surfaces, and adhesion to and invasion of INT407 cells. A positive correlation was reported between *C. jejuni* QS reduction and reduced motility, adhesion to polystyrene surfaces, and invasion. In their screening, among 20 natural extracts, essential oils, and pure compounds, *Rhodiola rosea* ethanolic extract showed the best overall antimicrobial activity against *C. jejuni*.

Rhodiola rosea L. (*Sedum roseum* (L.) Scop.) is an herbaceous plant belonging to the family Crassulaceae. Vernacular names by which we can recognize the plant include roseroot, golden root, and arctic root [18]. The plant grows up to 70 cm in height and has fleshy, succulent leaves. The flowers form a compact whorled inflorescence on top of the halms. The root system forms thick rhizomes [19].

R. rosea has long been used in traditional medicine. A key factor determining the quality of its formulations is the quantification of salidroside, rosavin, and rosarin [20]. In Northern Europe, Russia, and North America, *R. rosea* extracts are standardized to contain at least 3% rosavins and from 0.8% to 1% salidroside [21,22]. The majority of these extracts are derived from wild plants harvested in Russia and Mongolia, which threatens the long-term conservation of natural populations. In addition, fraudulent material containing non-*R. rosea* plant material is suspected to be on the market. In order to preserve the natural sources of *R. rosea* plant material (the collection of which is prohibited in many countries), and to ensure the quality and authenticity of the plant material, domestication and cultivation of the plant seems to be the most appropriate solution [23].

Extracts of the plant's underground organs contain various compounds, including monoterpene alcohols and their glycosides, cyanogenic glycosides, aryl glycosides, phenylethanoids (salidroside, p-tyrosol), phenylpropanoids and their glycosides (rosavins), flavonoids, flavonolignans, proanthocyanidins (PACs), and gallic acid derivatives [24]. According to Ma et al. [25], salidroside, p-tyrosol, rosarin, rosavin, rosin, and rosiridin are responsible for the biological activity of *R. rosea*. Besides being used in pharmaceutical preparations, the plant is popular as a food additive and dietary supplement. The plant's underground organs can be used as a crude drug (dried and powdered) or as an extract [26].

Due to its wide range of biologically active compounds, the plant has various pharmacological activities. Among them are antioxidative, anti-inflammatory, anti-fatigue, anti-depressive, anxiolytic, anti-tumor, antimicrobial, neuroprotective, cardioprotective, and normalizing endocrine and immune activities [24,27–29].

In the present study, ethanolic extracts were prepared from *R. rosea* cultivated plant material, i.e., "Mattmark" and "Rosavine", of which "Mattmark" is the first synthetic *R. rosea* cultivar [23]. For the first time, biologically active compounds or compound groups from *R. rosea* were separated into different fractions, and antimicrobial activity, with an emphasis on AI-2-mediated intercellular signaling in relation to the chemical composition of the extracts and their fractions, was studied. Due to great antimicrobial activity having been previously reported for the ethanolic extract from *R. rosea* in *C. jejuni*, the aim of the study was to evaluate whether certain compounds or compound groups are crucial for this activity.

2. Material and Methods

2.1. Bacterial Strains and Growth Conditions

C. jejuni NCTC 11168, *C. jejuni* 11168Δ*luxS*, and *Vibrio harveyi* MM30 are part of Chair of Biotechnology, Microbiology and Food Safety (Biotechnical Faculty, University of Ljubljana, Ljubljana, Slovenia) strain collection and were stored at −80 °C. *C. jejuni* strains were stored in a 20% glycerol (Kemika, Zagreb, Croatia) and an 80% Muller-Hinton broth (MHB) (Oxoid, Hampshire, UK) solution. *V. harveyi* MM30 was stored in a 20% glycerol and an 80% AI bioassay (AB) liquid medium solution (composed as described in [9]). A reference strain, *C. jejuni* NCTC 11168, was revitalized by cultivating on Karmali selective media (Oxoid, Hampshire, UK), followed by cultivating on Mueller–Hinton agar (MHA) (Oxoid, Hampshire, UK) at 42 °C in microaerophilic conditions (85% N_2, 10% CO_2 and 5% O_2). A mutant strain, *C. jejuni* 11168Δ*luxS*, which does not produce the AI-2 signal [2], was cultivated on MHA with the addition of 30 mg/L kanamycin (Merck, Darmstadt, Germany). A reporter strain, *V. harveyi* MM30, with eliminated AI-2 production [30], was used for AI-2 bioassays and was directly inoculated into 5 mL of AB liquid medium and incubated at 30 °C in aerobic conditions.

2.2. Plant Material

R. rosea roots and rhizomes from cultivated plant material were provided by Dr. Christoph Carlen and Mr. Claude-Alain Carron (Agroscope, Conthey, Switzerland). Two types of plant material were used: "Mattmark", harvested in April 2017 in Conthey at an altitude of 460 m, and "Rosavine", harvested in June 2012 in Bruson at an altitude of 1050 m. Voucher specimens were kept at the Institute of Pharmaceutical Sciences, Department of Pharmacognosy, University of Graz.

2.3. Extracts Preparation

Ethanolic extracts were prepared from the roots and rhizomes of the plant. Sliced dried plant material was ground and about 50 g was used for the extraction. The lipophilic compounds were removed by pre-extraction with hexane (Carl Roth, Karlsruhe, Germany). Ethanolic extraction with 96% ethanol (Carl Roth, Karlsruhe, Germany) took place in an ultrasonic bath (Elma, Singen, Germany) for 10 min at room temperature, followed by centrifugation at 4000 RPM for 10 min. Ethanolic extraction was repeated three times, the supernatants were collected, and the solvent was evaporated using a rotary evaporator (Heidolph, Schwabach, Germany), followed by freeze drying using a VirTis Sentury freeze dryer (SP Scientific, Buena, CA, USA) resulting in 28.52% ("Mattmark") and 32.47% ("Rosavine") extraction yields. The ethanolic extracts, designated as M/R 96% EtOH, were stored in dark glass flasks in a fridge at 4 °C.

2.4. Fractionation of the Extracts: Fractions Preparation

Five fractions, enriched with different compounds or compound groups, were obtained from each crude ethanolic extract. Fractionation was performed on DIAION HP-20 adsorbent resin (Sigma-Aldrich, Steinheim, Germany) or using Polyclar AT (polyvinylpyrrolidone, or PVP) (Serva, Heidelberg, Germany). For the elution of compounds from the column, we used micropure water (MW; Barnstead Easypure RF) and different concentrations of methanol (Carl Roth, Karlsruhe, Germany).

The separation protocol described by Sun et al. [31] for the purification of salidroside and p-tyrosol was modified to obtain fractions of the ethanolic extracts as follows. DIAION HP-20 adsorbent resin was pre-treated by soaking it in 70% methanol/MW solution at 4 °C overnight, followed by washing with MW in a Buchner funnel until no alcohol remained. Then, 100 mg of crude ethanolic extract was dissolved in 10 mL of MW and centrifuged at 4000 RPM for 10 min at room temperature. The dissolved extract was mixed with 15 g of pre-treated DIAION HP-20 adsorbent resin. After full adsorption of substances to the adsorbent, it was loaded into a glass column and the bed volume (BV) was determined as 24 mL. Subsequently, the column was eluted with two BV of MW and two

BV of a 20%, 40%, and 70% methanol/MW solution. The eluents were collected and their composition was determined directly by UHPLC-PDA-ESI-MS analysis. The optimized elution protocol was scaled up by a factor of 12 in order to obtain enough material for further microbiological analysis, resulting in fractions of M/R F1 0%, M/R F2 20%, M/R F3 40%, and M/R F4 70%.

The fifth fraction of each crude ethanolic extract was prepared using PVP, which mainly binds compounds with phenolic OH groups, e.g., tannins, PACs, and many flavonoids. Therefore, 50 mg of crude ethanolic extract was dissolved in 15 mL of 50% methanol/MW solution, followed by centrifugation at 4000 RPM for 10 min at room temperature. The supernatant was added to 1.25 g of PVP, mixed, and again centrifuged at 4000 RPM for 10 min at room temperature. The supernatant was filtered through a filter paper (Carl Roth, Karlsruhe, Germany) and the solvent was evaporated using a rotary evaporator, followed by freeze drying. In this case, the optimized protocol was scaled up by a factor of 20 to obtain enough material for further microbiological analysis, resulting in fractions M/R F5 PVP.

2.5. Chemical Characterization (UHPLC-PDA-ESI-MS Analysis)

Analysis of crude extracts and their fractions was carried out on two Dionex UltiMate 3000 UHPLC systems (Thermo Fisher Scientific, Waltham, CA, USA). The first system was coupled to a linear ion-trap mass spectrometer (MS), LTQ XL, equipped with an electrospray ionization (ESI) ion source (Thermo Fisher Scientific, Waltham, California, USA). Both systems were equipped with a photodiode array detector (PDA) (Thermo Fisher Scientific, Waltham, California, USA). Separation was undertaken on a Zorbax SB-C18 rapid resolution HD column (Agilent, Santa Clara, California, USA), 100 × 2.1 mm, 1.8 μm particle size. The mobile phase consisted of MW + 0.1% formic acid (A) (Honeywell Fluka, Seelze, Germany) and acetonitrile (VWR International, Rosny-sous-Bois-cedex, France) + 0.1% formic acid (B). A gradient elution was performed, starting with 2% B, increasing to 22% B at 13.33 min, 70% B at 22.22 min, then dropping back to 2% B at 22.67 min and keeping this composition until the end (28 min). The column temperature was set to 40 °C. Flow rate was set to 0.450 mL/min. Injection volume was 2 μL. Samples of crude ethanolic extracts were prepared using 20% ethanol/MW (2:8) in a concentration of 5 mg/mL and centrifuged at 13,000 RPM for 10 min at room temperature before analysis. Fractions were prepared using MW and different concentrations of ethanol/MW or methanol/MW. Therefore, we analyzed the fractions directly, after centrifugation at 13,000 RPM for 10 min at room temperature. PDA detection was performed in the 190 nm to 500 nm wavelength range. The mass spectra were recorded in negative and positive ion mode in the m/z range of 50 to 2000 amu. Mass spectral conditions were set as follows: source voltage 5.0 kV (ESI positive), 3.5 kV (ESI negative); capillary temperature 350 °C; source temperature 300 °C; sheath gas flow 40 arb, auxiliary gas flow 10 arb.

2.6. Determination of Minimal Inhibitory Concentrations (MICs)

The MICs of preparations against *C. jejuni* NCTC 11168 and *C. jejuni* 11168Δ*luxS* were determined by the broth microdilution method previously described [32] with some modifications. Stock solutions were prepared in dimethyl sulfoxide (DMSO) (Merck, Germany) and later diluted in MHB to a final concentration of 1000 mg/L and 2.5% of DMSO. The bacterial inoculum contained approximately 5×10^5 colony-forming units (CFU)/mL. Cell viability was determined using resazurin fluorescent dye solution, prepared as previously described [9]. The fluorescence intensity was measured using the microplate reader Varioskan LUX (Thermo Fischer Scientific, Waltham, CA, USA) at an excitation wavelength of 560 nm and an emission wavelength of 590 nm. The MIC represents the lowest concentration where fluorescence, expressed in relative fluorescence units (RFU), reached the value of the negative control. The MICs were determined in triplicate.

2.7. AI-2 Bioassay

AI-2 bioassays were performed to evaluate the influence of the preparations on *C. jejuni* AI-2-mediated intercellular signaling. The cell-free spent media (SMs) were prepared and AI-2 bioassays were performed as described in [9]. Briefly, *C. jejuni* NCTC 11168 (*C. j.* 11168-Tr.) and *C. jejuni* 11168Δ*luxS* (*C. j.* 11168Δ*luxS*-Tr.) cultures with approximately 5×10^5 CFU/mL were treated separately with sub-inhibitory concentrations of preparations (i.e., 0.25× MIC or lower). Stock solutions were prepared in DMSO and were further diluted in MHB to a final 1% of DMSO. After 24 h incubation, SMs were prepared by filter-sterilization through 0.2 μm syringe filters (Sartorius, Göttingen, Germany). The SMs were stored in a freezer at −20 °C.

For AI-2 bioassays, *V. harveyi* MM30 was used as a reporter strain because it does not produce the AI-2 signal itself [30,33]. The bacterial culture was prepared with approximately 5×10^3 CFU/mL. Bioluminescence was measured using a microplate reader (Varioskan LUX) at 30 min intervals over 22.5 h. An impact of preparations in sub-inhibitory concentrations on *C. jejuni* intercellular signaling was determined indirectly from the reported bioluminescence of *V. harveyi* MM30 expressed in relative light units (RLU) and compared with the non-treated control (*C. j.* 11168-C+). To confirm that LuxS-deficient *C. jejuni* does not produce an AI-2 signal, we added *V. harveyi* MM30 culture to 5% of *C. jejuni* 11168Δ*luxS* (*C. j.* 11168Δ*luxS*-C+) SM and measured the bioluminescence of the reporter strain. By measuring the bioluminescence of *V. harveyi* MM30 without the addition of *C. jejuni* SM, we proved that the strain does not produce the AI-2 signal itself. Bioluminescence reduction rates (%) were calculated using equation 1. They indicate how *C. jejuni* AI-2-mediated intercellular signaling is reduced due to the exposure of bacteria to the preparations in comparison with the non-treated control.

$$\text{Bioluminescence reduction rate } [\%] = 100 - \left(\left(\frac{(C.\ j.\ 11168 - \text{Tr.} - C.\ j.\ 11168\Delta luxS - \text{Tr.})}{(C.\ j.\ 11168 - \text{C} + -C.\ j.\ 11168\Delta luxS - \text{C+})} \right) \times 100 \right) \quad (1)$$

To examine whether compounds of the most active fractions (i.e., PACs from Fractions 3) bind to AI-2 signal molecule, additional AI-2 bioassays were performed. In this case, we added preparations in sub-inhibitory concentrations to the initial SMs, and after 1 h incubation we measured bioluminescence of the *V. harveyi* MM30 reporter strain. The signals were compared with the ones from the original SMs, and bioluminescence reduction rates were calculated again. All the experiments were carried out in triplicate.

2.8. Membrane Integrity

The influence of preparations on *C. jejuni* membrane integrity was determined using a LIVE/DEAD BacLight Bacterial Viability kit (L-7012; Molecular Probes, Eugene, CA, USA).

The membrane disruption assays were performed according to Kovač et al. [34]. A mixture of green fluorescent dye SYTO 9 and propidium iodide (PI) was prepared according to the manufacturer instructions. Stock solutions of the extracts and their fractions were prepared in DMSO at 100-fold higher concentrations and were further diluted in MHB to the final 1% of DMSO. The dye mixture was added to 100 μL of the treated or non-treated *C. jejune* cultures with approximately 5×10^5 CFU/mL (1:1, *v/v*). The kinetics of PI intracellular penetration was measured in RFU by a microplate reader (Varioskan LUX) in terms of the SYTO 9 fluorescence at an excitation wavelength of 481 nm and an emission wavelength of 510 nm. Kinetic measurements over the last 10 min of the assays were used to calculate the membrane disruption (%). The experiment was carried out in triplicate.

2.9. Statistical Analysis

Before statistical tests, normality was tested for all the data using Shapiro–Wilk and Kolmogorov–Smirnov tests. Based on the normality test, we determined statistical significance between treatments and control using the Mann–Whitney U test in the case of non-normal distribution of the data, and using one-way ANOVA in case the data were

normally distributed. At a 95% confidence interval, the results were statistically significant at value $p < 0.05$. The analyses were performed using IBM SPSS Statistics software, version 23 (IBM Corp., Armonk, CA, USA).

3. Results

3.1. Chemical Characterization of the Extracts and Fractions

The composition of the ethanolic extracts was qualitatively analyzed by comparing the retention time, mass spectrometric fragmentation, and UV spectra from UHPLC-PDA-ESI-MS data analysis with data from the literature [35–39]. Eighteen compounds were identified in the "Mattmark" ethanolic extract (Table S1, Figure S1) and seventeen in the "Rosavine" ethanolic extract (Table S2, Figure S1). Aside from typical salidroside (phenylethanoid) and rosavins (cinnamyl alcohol glycosides), chromatograms recorded at UV 270 nm indicated significant amounts of PACs as a complex mixture, of which only a few compounds could be assigned to epigallocatechin-3-O-gallate (EGCG), and two dimers containing EGCG and epigallocatechin (EGC), respectively. Two flavonoid glycosides could be assigned to the herbacetin-7-O-glycosides rhodiosin and rhodionin. The main difference between the "Mattmark" and "Rosavine" plant material is in the quantity of certain compounds or compound groups. Thus, "Mattmark" (Figure S2) contains more PACs, rosavins, and flavonoids than "Rosavine". On the other hand, "Rosavine" (Figure S2) has higher amounts of salidroside, based on peak area comparison in UV chromatograms.

Five fractions were prepared from each crude ethanolic extract of the plant material. The main compounds or compound groups of each fraction are listed in Table 1. The composition of each fraction obtained from the "Mattmark" ethanolic extract is shown on Figure 1, and a comparison of peak areas of selected compounds is presented in Figure S3. By the adsorption of the crude ethanolic extracts to DIAION HP-20 adsorbent resin and the stepwise elution of compounds by increasing methanol concentrations, the separation of compound groups could be obtained, although salidroside could be found in Fractions F2 and Fractions F3, and rosavins could be found in Fractions F2 (trace amounts), Fractions F3, and Fractions F4. After adsorption of the crude ethanolic extracts to PVP, UHPLC analysis indicated that PACs and flavonoids, as well as gallic acid, were almost quantitatively removed from the extracts (Fractions F5).

Table 1. Fractions obtained from "Mattmark" and "Rosavine" ethanolic extracts and their main compounds.

| No.	Label	Solvent	Main Compounds/Compound Groups
1	M/R F1 0%	MW, 0% methanol	Rich in gallic acid (Figure 1A)
2	M/R F2 20%	20% methanol	Rich in salidroside (Figure 1B)
3	M/R F3 40%	40% methanol	Rich in salidroside, rosavins, and PACs (Figure 1C)
4	M/R F4 70%	70% methanol	Rich in rosavins and flavonoids (Figure 1D)
5	M/R F5 PVP	50% methanol	Rich in salidroside and rosavins (contains almost no PACs or flavonoids) (Figure 1E)
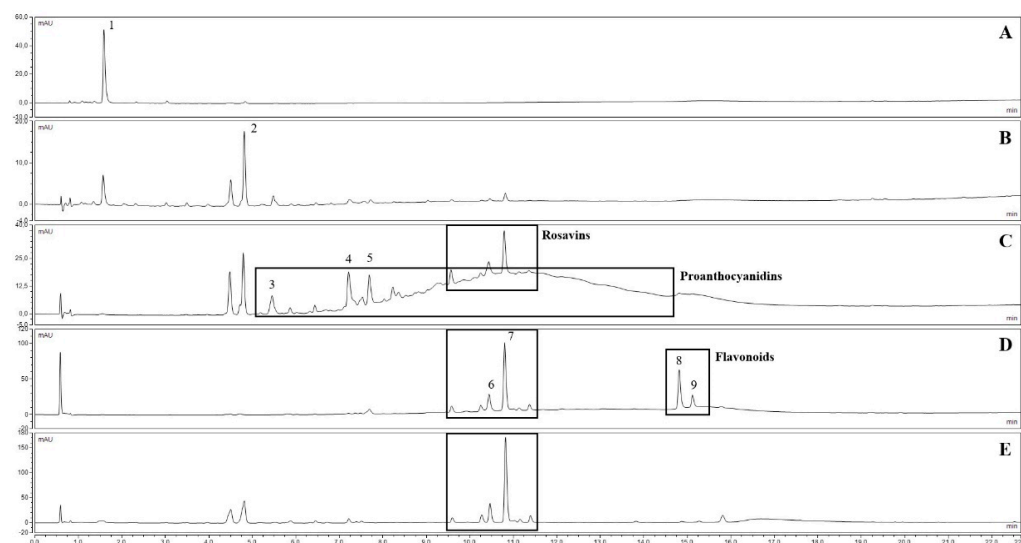
Figure 1. UV chromatograms at 270 nm of "Mattmark" fractions (**A**): Fraction 1 (M F1 0%); (**B**): Fraction 2 (M F2 20%); (**C**): Fraction 3 (M F3 40%); (**D**): Fraction 4 (M F4 70%); (**E**): Fraction 5 (M F5 PVP)). Compounds: 1 = gallic acid, 2 = salidroside, 3 = EGC-EGCG dimer, 4 = EGCG-EGCG dimer, 5 = EGCG, 6 = rosarin, 7 = rosavin, 8 = rhodiosin, 9 = rhodionin; for details see Table S1.

3.2. Determination of MICs

The MICs were determined by the broth microdilution method for the reference strain *C. jejuni* NCTC 11168 and for the mutant strain *C. jejuni* 11168Δ*luxS* (Table 2). Preparations with MICs under 1000 mg/L were tested further in sub-inhibitory concentrations, i.e., 0.25× MICs or lower, to avoid an impact on cell growth.

For *C. jejuni* NCTC 11168, the MIC of the "Mattmark" ethanolic extract was 125 mg/L, while the MICs of its fractions varied from 62.5 to 500 mg/L. The MIC of the "Rosavine' ethanolic extract was 500 mg/L, while the MICs of its fractions varied from over 1000 to 250 mg/L. In general, Fractions 3 and Fractions 4 showed better or the same antimicrobial activity than the ethanolic extracts, while Fractions 1, Fractions 2, and Fractions 5 were less or equally effective. The MICs of the "Mattmark" ethanolic extract and its fractions were lower compared with the MICs of the "Rosavine" ethanolic extract and its fractions.

Table 2. Determined MICs of ethanolic extracts and their fractions for *C. jejuni* NCTC 11168; *C. jejuni* 11168Δ*luxS*.

Extracts/Fractions	*C. jejuni* **NCTC 11168**	*C. jejuni* **11168Δ***luxS*
	MIC (mg/L)	
	"Mattmark" Plant Material	
M 96% EtOH	125	125
M F1 0%	250	250
M F2 20%	125	125
M F3 40%	62.5	62.5
M F4 70%	125	125
M F5 PVP	250	250
	"Rosavine" Plant Material	
R 96% EtOH	500	250
R F1 0%	>1000	1000
R F2 20%	>1000	500
R F3 40%	250	62.5
R F4 70%	250	125
R F5 PVP	1000	500

3.3. Inhibition of Intercellular Signaling

AI-2 bioassays were performed to evaluate whether the ethanolic extracts and their fractions, in sub-inhibitory concentrations, affected *C. jejuni* AI-2-mediated intercellular signaling.

First, the impact of the ethanolic extracts and their fractions on AI-2 production in *C. jejuni* was tested in sub-inhibitory concentrations of $0.25\times$ MICs. In this case, all the preparations significantly inhibited *C. jejuni* signaling ($p < 0.05$), with bioluminescence reduction rates from 54% to 91% (Figure 2A). The "Mattmark" ethanolic extract and its fractions were more effective in intercellular signaling reduction, although they were tested in lower concentrations than the "Rosavine" ethanolic extract and its fractions. Overall, *R. rosea* preparations showed a high impact on *C. jejuni* signaling but, due to the variation in tested concentrations, it was not possible to assign specific compounds or compound groups to the observed effect.

Consequently, the reduction in *C. jejuni* AI-2-mediated intercellular signaling by the preparations was tested at the same concentration, i.e., 15.625 mg/L, which corresponds to $0.25\times$ MIC of "Mattmark" Fraction 3. By testing preparations at the same concentration, we aimed to find out if some extracts/fractions were more effective in reducing intercellular signaling. Both ethanolic extracts, as well as almost all their fractions, significantly affected *C. jejuni* signaling, even if present at such a low concentration ($p < 0.05$). Only "Mattmark" Fraction 5 did not have a significant impact ($p > 0.05$). Bioluminescence reduction rates varied from 27% to 72% (Figure 2B). Both Fractions 3 most effectively reduced *C. jejuni* signaling when tested at the same concentration. Additionally, Fractions 4 had a great impact. On the other hand, Fractions 5, which were devoid of PACs and flavonoids, were less effective (Figure 2B).
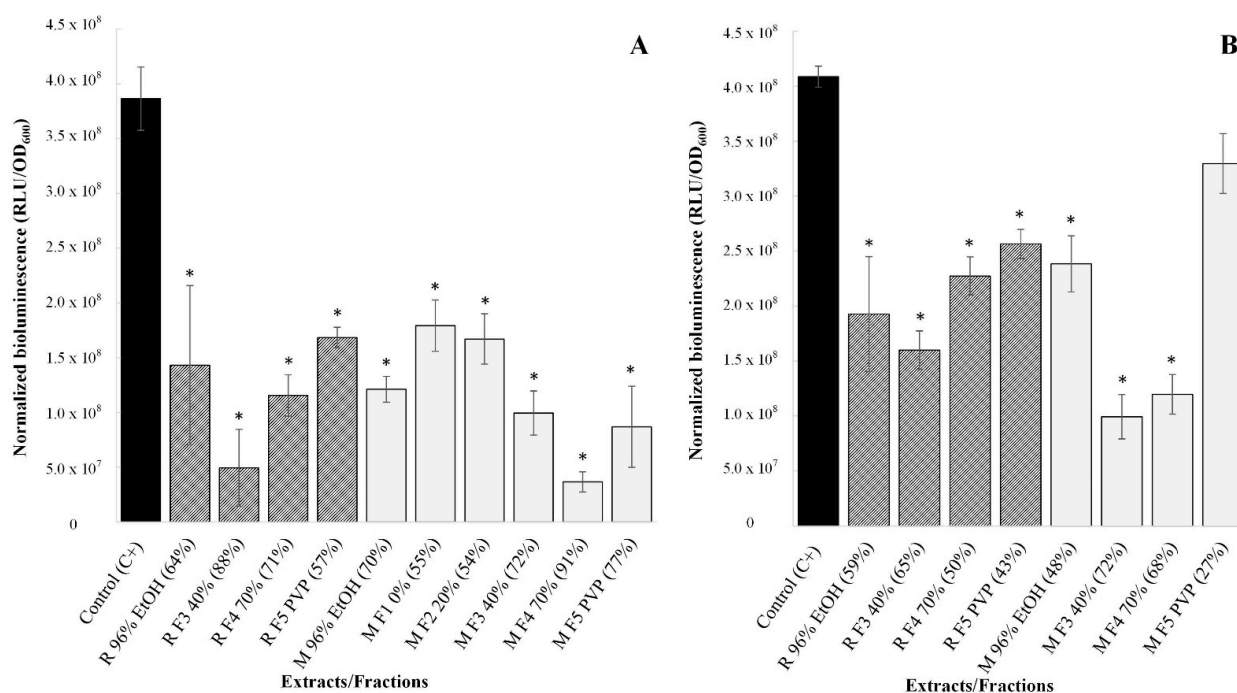
Figure 2. Bioluminescence reported after the addition of *V. harveyi* MM30 to 5% of SM obtained from non-treated control (C+) or to 5% of SMs obtained after treating *C. jejuni* NCTC 11168 with different preparations in sub-inhibitory concentrations ((**A**): $0.25\times$ MIC; (**B**): 15.625 mg/L). Average bioluminescence in RLU with deducted background and normalized to OD_{600} are presented $\pm$ standard deviations. In addition, the bioluminescence reduction rate is presented in brackets. * represents statistically significant values.

3.4. Disruption of Membrane Integrity

Membrane integrity assays were performed to determine if the disruption of *C. jejuni* membrane is also involved in the antimicrobial activity of *R. rosea* preparations. As in previous experiments, preparations were first tested at sub-inhibitory concentrations of 0.25× MICs, followed by testing at the same concentration, i.e., 15.625 mg/L.

At 0.25× MICs, the disruptive impact on membrane integrity varied from 3% to 31% (Figure 3(A1,A2)). In this case, the disruption of membrane integrity is likely to contribute to the antimicrobial activity of at least some of the preparations. On the other hand, when tested at the same concentration of 15.625 mg/L, the disruptive impact on membrane integrity was very low and varied from 2% to 6% (Figure 3(B1,B2)). We assume that such an effect does not contribute to the antimicrobial activity of the preparations.

Figure 3. Influence of the extracts and their fractions on *C. jejuni* NCTC 11168 membrane integrity ((**A1**/**A2**): preparations tested at 0.25× MICs; (**B1**/**B2**): preparations tested in the same concentration, i.e., 15.625 mg/L). An impact on membrane integrity in RFU is presented ± standard deviations. In addition, the decrease in membrane integrity is presented in brackets. * represents statistically significant values.

4. Discussion

QS represents an important mechanism for modulating *C. jejuni* behavior within its population [40]. In the present study, ethanolic extracts of cultivated plant material, i.e., "Mattmark" and "Rosavine", were prepared and fractionated by optimized protocols in order to obtain five fractions rich in salidroside, rosavins, PACs, and/or flavonoids. The fifth fractions, with almost no gallic acid, PACs, or flavonoids, were prepared from the initial ethanolic extracts to determine whether this group of compounds could play the most important role in the antimicrobial activity of *R. rosea* ethanolic extract.

According to the MICs, Fractions 1—rich in mainly simple gallic acid (M/R F1 0%)—and Fractions 5—without gallic acid, PACs, or flavonoids (M/R F5 PVP)—have lower antimicrobial activity, corresponding to higher MICs than the ethanolic extracts (R/M 96% EtOH). Moreover, Fractions 5 have lower antimicrobial activity than Fractions 3 (M/R F3 40%), which are rich in PACs. This indicates that PACs, including the monomeric EGCG, could be one of the crucial compound groups responsible for the antimicrobial activity of *R. rosea* ethanolic extract. Furthermore, flavonoids (herbacetin glycosides) might also contribute to anti-*Campylobacter* activity when comparing Fractions 4 and Fractions 5.

AI-2 bioassays were performed to determine the effect of the ethanolic extracts and their fractions on *C. jejuni* AI-2-mediated signaling. At concentrations of $0.25 \times$ MICs, both ethanolic extracts and their fractions showed a statistically significant impact ($p < 0.05$), with bioluminescence reduction rates ranging from 54 to 91%. Due to the variation in tested concentrations of the preparations, it was not possible to refer to the compounds or groups of compounds that play the most important role in this. Therefore, the preparations were tested at the same concentration, i.e., 15.625 mg/L, which also represents the $0.25 \times$ MIC of M F3 40%. All preparations, except R F5 PVP, significantly affected *C. jejuni* signaling ($p < 0.05$), even at such a low concentration. Here, it is important to note that M F3 40% showed a greater reduction in intercellular signaling than R F3 40%. Besides this, M F5 PVP showed much lower impact than R F5 PVP. It is also important that "Mattmark" plant material contained a higher amount of PACs and flavonoid than "Rosavine" plant material. In addition, Fractions 3 were enriched in PACs, including EGCG, while Fractions 5 had the PACs removed. These results suggest that PACs may be one of the crucial compounds in *R. rosea* with the potential to reduce *C. jejuni* signaling. High bioluminescence reduction rates (from 65% to 72%) were achieved in the case of treating *C. jejuni* with a sub-inhibitory concentration of Fractions 3, compared with lower impact (from 27% to 43%) when *C. jejuni* was treated with sub-inhibitory concentration of Fractions 5. Because M F3 40% contains more PACs than R F3 40%, a greater loss of activity was observed for "Mattmark" when we removed those compounds, as we did in Fractions 5. Similarly to MIC determination, the herbacetin glycosides rhodionin and rhodiosin could also be relevant for intercellular signaling reduction. This can be deduced from the significant reduction in bioluminescence by Fractions 4 (which were rich in these flavonoids) and the decrease in the respective effects in Fractions 5 (which were also devoid of flavonoid glycosides). The stronger intercellular signaling reduction by M F4 70% compared with R F4 70%, showing a lower concentration of flavonoids, supports the assumption that the herbacetin glycosides contribute to the observed intercellular signaling reduction of the crude extract. A high QS reduction rate (>90%) had previously been reported when *C. jejuni* was treated with sub-inhibitory concentrations of, e.g., *C. limon* [11] and *R. rosea* [9] ethanolic extracts. Strong anti-QS activity of EGCG from green tea against *C. jejuni* NCTC 11168 was previously reported by the authors of [12]. In their case, EGCG decreased the bioluminescence reported for *V. harveyi* BB152 of 96% when tested at a sub-inhibitory concentration of $0.75 \times$ MBC or 65.25 mg/L. Our study supports the conclusion of Šimunović et al. [9] that QS or AI-2-mediated intercellular signaling is a potential target in the control of *C. jejuni* and that various natural plant-based preparations act as true intercellular signaling modulators. As an upgrade to their research, we can see from our results that PACs, including EGCG and the herbacetin glycosides, are the most important compound groups of *R. rosea* crude ethanolic extract responsible for AI-2-mediated signaling reduction in *C. jejuni*.

This study also demonstrated that the antimicrobial activity of the extracts and their fractions was due to the reduction in *C. jejuni* signaling without affecting the membrane integrity. Even though preparations at $0.25\times$ MICs did not affect cell growth, the membrane integrity was significantly disrupted ($p > 0.05$) by "Rosavine" ethanolic extract and its Fractions 3 and Fractions 4. Nevertheless, no significant effect ($p < 0.05$) on membrane integrity was observed compared with the non-treated control when the extracts and their fractions were tested at a concentration of 15.625 mg/L. The study also excluded that PACs affect *C. jejuni* signaling by binding to the AI-2 signaling molecule which was released to the growth medium. The AI-2 bioassays have shown that the reported bioluminescence of the reporter strain *V. harveyi* MM30 did not vary significantly ($p < 0.05$) between the initial SMs and the SMs to which we once again added Fractions 3, rich in PACs, at a concentration of 15.625 mg/L. For example, the bioluminescence reduction rates varied from 1% to 2% between the initial SMs obtained after treating *C. jejuni* with sub-inhibitory concentrations of Fractions 3 and the same SMs to which preparations were again added in sub-inhibitory concentrations (data not shown).

PACs are the most abundant plant-derived polyphenols belonging to one of the tannin groups (condensed tannins). They are among the most commonly consumed dietary polyphenols. Condensed tannins are able to form insoluble complexes with carbohydrates and proteins [41]. Studies have shown that mucosal immunity to pathogen infection can be enhanced by PACs [42]. In addition, our study supports the fact that PACs, in this case from *R. rosea* underground organs, represent natural compounds with the ability to reduce intercellular signaling in order to fight *C. jejuni*. This is in agreement with a recent publication of Hao et al. [43]: this confirmed EGCG with significant inhibitory effects on the development of biofilm, protease, elastase activity, swimming, and swarming motility, which were also positively related to the production of C4-AHL signaling molecules in *Pseudomonas aeruginosa*. In addition, herbacetin glycosides of *R. rosea* might also contribute to *C. jejuni* signaling reduction. Interestingly, a study by the authors of [44] showed that herbacetin has a high affinity to LuxR-type protein *Shewanella baltica* in a virtual screening.

5. Conclusions

In this study, we provided a protocol for the separation of bioactive compounds or compound groups from *R. rosea* roots and rhizomes. Our results suggest PACs and flavonoids are the most important compound groups from *R. rosea*, with great potential for *C. jejuni* AI-2-mediated signaling reduction. Nevertheless, it is still unclear whether AI-2 in *C. jejuni* represents a true QS signaling molecule or whether it is a metabolic by-product of a crucial central metabolic methyl cycle pathway [45]. To date, AI-2 receptors have still not been identified [46], and mechanisms by which bioactive compounds affect *C. jejuni* signaling should be further investigated.

Institutional Review Board Statement: Not applicable.

Informed Consent Statement: Not applicable.

Data Availability Statement: The data are available in the Supplementary Materials.

Conflicts of Interest: The authors declare no conflict of interest.

References

1. EFSA and ECDC. The European Union one health 2020 zoonoses report. *EFSA J.* **2021**, *19*, 6971.
2. Plummer, P.J. *LuxS* and quorum-sensing in *Campylobacter*. *Front. Cell. Infect. Microbiol.* **2012**, *2*, 9. [CrossRef]
3. Vasil, M.L. DNA microarrays in analysis of quorum sensing: Strengths and limitations. *J. Bacteriol.* **2003**, *185*, 2061–2065. [CrossRef]
4. Deep, A.; Chaudhary, U.; Gupta, V. Quorum sensing and bacterial pathogenicity: From molecules to disease. *J. Lab. Physicians.* **2011**, *3*, 4–11. [CrossRef]
5. Federle, M.J.; Bassler, B.L. Interspecies communication in bacteria. *J. Clin. Investig.* **2003**, *112*, 1291–1299. [CrossRef]
6. Ng, W.L.; Bassler, B.L. Bacterial quorum-sensing network architectures. *Annu. Rev. Genet.* **2009**, *43*, 197–222. [CrossRef]
7. Elvers, K.T.; Park, S.F. Quorum sensing in *Campylobacter jejuni*: Detection of a *luxS* encoded signaling molecule. *Microbiology* **2002**, *148*, 1475–1481. [CrossRef]
8. Winzer, K.; Hardie, K.R.; Burgess, N.; Doherty, N.; Kirke, D.; Holden, M.T.G.; Linforth, R.; Cornell, K.A.; Taylor, A.J.; Hill, P.J.; et al. LuxS: Its role in central metabolism and the in vitro synthesis of 4-hydroxy-5-methyl-3(2H)-furanone. *Microbiology* **2002**, *148*, 909–922. [CrossRef]
9. Šimunović, K.; Ramić, D.; Xu, C.; Smole Možina, S. Modulation of *Campylobacter jejuni* motility, adhesion to polystyrene surfaces, and invasion of INT407 cells by quorum-sensing inhibition. *Microorganisms* **2020**, *8*, 104. [CrossRef]
10. Asfour, H.Z. Anti-quorum sensing natural compounds. *J. Microsc. Ultrastruct.* **2018**, *6*, 1–10. [CrossRef]
11. Castillo, S.; Heredia, N.; Arechiga-Carvajal, E.; García, S. Citrus extracts as inhibitors of quorum sensing, biofilm formation and motility of *Campylobacter jejuni*. *Food Biotechnol.* **2014**, *28*, 106–122. [CrossRef]
12. Castillo, S.; Heredia, N.; García, S. 2(5H)-Furanone, epigallocatechin gallate, and a citric-based disinfectant disturb quorum-sensing activity and reduce motility and biofilm formation of *Campylobacter jejuni*. *Folia Microbiol.* **2014**, *60*, 89–95. [CrossRef]
13. Duarte, A.; Alves, A.C.; Ferreira, S.; Silva, F.; Domingues, F.C. Resveratrol inclusion complexes: Antibacterial and anti-biofilm activity against *Campylobacter* spp. and *Arcobacter butzleri*. *Food Res. Int.* **2015**, *77*, 244–250. [CrossRef]
14. Duarte, A.; Luís, Â.; Oleastro, M.; Domingues, F.C. Antioxidant properties of coriander essential oil and linalool and their potential to control *Campylobacter* spp. *Food Control* **2016**, *61*, 115–122. [CrossRef]
15. Bezek, K.; Kurinčič, M.; Knauder, E.; Klančnik, A.; Raspor, P.; Bucar, F.; Smole Možina, S. Attenuation of adhesion, biofilm formation and quorum sensing of *Campylobacter jejuni* by *Euodia ruticarpa*. *Phytother. Res.* **2016**, *30*, 1527–1532. [CrossRef]
16. Wagle, B.R.; Donoghue, A.M.; Shrestha, S.; Upadhyaya, I.; Arsi, K.; Gupta, A.; Liyanage, R.; Rath, N.C.; Donoghue, D.J.; Upadhyay, A. Carvacrol attenuates *Campylobacter jejuni* colonization factors and proteome critical for persistence in the chicken gut. *Poult. Sci.* **2020**, *99*, 4566–4577. [CrossRef]
17. Wagle, B.R.; Donoghue, A.M.; Jesudhasan, P.R. Select phytochemicals reduce *Campylobacter jejuni* in postharvest poultry and modulate the virulence attributes of *C. jejuni*. *Front. Microbiol.* **2021**, *12*, 725087. [CrossRef]
18. Ganzera, M.; Yayla, Y.; Khan, I.A. Analysis of the marker compounds of *Rhodiola rosea* L. (golden root) by reversed phase high performance liquid chromatography. *Chem. Pharm. Bull.* **2001**, *49*, 465–467. [CrossRef]
19. Bykov, V.A.; Zapesochnaya, G.G.; Kurkin, V.A. Traditional and biotechnological aspects of obtaining medicinal preparations from *Rhodiola Rosea*, L. (A review). *Pharm. Chem. J.* **1999**, *33*, 29–40. [CrossRef]
20. Rodin, I.A.; Stavrianidi, A.N.; Braun, A.V.; Shpigun, O.A.; Popik, M.V. Simultaneous determination of salidroside, rosavin, and rosarin in extracts from *Rhodiola rosea* by high performance liquid chromatography with tandem mass spectrometry detection. *J. Anal. Chem.* **2012**, *67*, 1026–1030. [CrossRef]
21. Khanum, F.; Singh Bawa, A.; Singh, B. *Rhodiola rosea*: A versatile adaptogen. *Compr. Rev. Food Sci. Food Saf.* **2005**, *4*, 55–62. [CrossRef]
22. Perfumi, M.; Mattioli, L. Adaptogenic and central nervous system effects of single doses of 3% rosavin and 1% salidroside *Rhodiola rosea* L. extract in mice. *Phytother. Res.* **2007**, *21*, 37–43. [CrossRef]
23. Vouillamoz, J.F.; Carron, C.A.; Malnoë, P.; Baroffio, C.A.; Carlen, C. *Rhodiola rosea* Mattmark, the first synthetic cultivar is launched in Switzerland. *Acta Hortic.* **2012**, *955*, 185–189. [CrossRef]
24. Panossian, A.; Wikman, G.; Sarris, J. Rosenroot (*Rhodiola rosea*): Traditional use, chemical composition, pharmacology and clinical efficacy. *Phytomedicine* **2010**, *17*, 481–493. [CrossRef]
25. Ma, C.Y.; Tang, J.; Wang, H.; Gu, X.; Tao, G.J. Simultaneous determination of six active compounds in *Rhodiola*, L. by RP-LC. *Chromatographia* **2008**, *67*, 383–388. [CrossRef]

26. Kosakowska, O.; Bączek, K.; Przybył, J.L.; Pióro-Jabrucka, W.; Czupa, W.; Synowiec, A.; Gniewosz, M.; Costa, R.; Mondello, L.; Węglarz, Z. Antioxidant and antibacterial activity of roseroot (*Rhodiola rosea* L.) dry extracts. *Molecules.* **2018**, *23*, 1767. [CrossRef]
27. Brown, R.P.; Gerbarg, P.L.; Ramazanov, Z. *Rhodiola rosea*: A phytomedicinal overview. *Reliab. Herb. Med. Inf.* **2002**, *56*, 40–52.
28. Chiang, H.M.; Chen, H.C.; Wu, C.S.; Wu, P.Y.; Wen, K.C. *Rhodiola* plants: Chemistry and biological activity. *J. Food Drug Anal.* **2015**, *23*, 359–369. [CrossRef]
29. Kelly, G.S. *Rhodiola rosea*: A possible plant adaptogen. *Altern. Med. Rev.* **2001**, *6*, 293–302.
30. Surette, M.G.; Miller, M.B.; Bassler, B.L. Quorum sensing in *Escherichia coli*, *Salmonella typhimurium*, and *Vibrio harveyi*: A new family of genes responsible for autoinducer production. *Proc. Natl. Acad. Sci. USA* **1999**, *96*, 1639–1644. [CrossRef]
31. Sun, L.; Zhou, R.; Sui, J.; Liu, Y. Simultaneous preparation of Salidroside and p-Tyrosol from *Rhodiola crenulata* by DIAION HP-20 macroporous resin chromatography combined with silica gel chromatography. *Molecules* **2018**, *23*, 1602. [CrossRef]
32. Klančnik, A.; Piskernik, S.; Jeršek, B.; Smole Možina, S. Evaluation of diffusion and dilution methods to determine the antibacterial activity of plant extracts. *J. Microbiol. Methods* **2010**, *81*, 121–126. [CrossRef]
33. Bassler, B.L.; Greenberg, E.P.; Stevens, A.M. Cross-species induction of luminescence on the quorum-sensing bacterium *Vibrio harveyi*. *J. Bacteriol.* **1997**, *179*, 4043–4045. [CrossRef]
34. Kovač, J.; Šimunović, K.; Wu, Z.; Klančnik, A.; Bucar, F.; Zhang, Q.; Smole Možina, S. Antibiotic resistance modulation and modes of action of (-)-α-pinene in *Campylobacter jejuni*. *PLoS ONE* **2015**, *10*, e0122871.
35. Alperth, F.; Turek, I.; Weiss, S.; Vogt, D.; Bucar, F. Qualitative and quantitative analysis of different *Rhodiola rosea* rhizome extracts by UHPLC-DAD-ESI-MSn. *Sci. Pharm.* **2019**, *87*, 8. [CrossRef]
36. Olennikov, D.N.; Chirikova, N.K.; Vasilieva, A.G.; Fedorov, I.A. LC-MS profile, gastrointestinal and gut microbiota stability and antioxidant activity of *Rhodiola rosea* herb metabolites: A comparative study with subterranean organs. *Antioxidants* **2020**, *9*, 526. [CrossRef]
37. Petsalo, A.; Jalonen, J.; Tolonen, A. Identification of flavonoids of *Rhodiola rosea* by liquid chromatography-tandem mass spectrometry. *J. Chromatogr. A* **2006**, *1112*, 224–231. [CrossRef]
38. Zapesochnaya, G.G.; Kurkin, V.A. The flavonoids of the rhizomes of *Rhodiola rosea*. *Plenum Publ. Corp.* **1983**, *19*, 21–29.
39. Zomborszki, Z.P.; Kúsz, N.; Csupor, D.; Peschel, W. Rhodiosin and herbacetin in *Rhodiola rosea* preparations: Additional markers for quality control? *Pharm. Biol.* **2019**, *57*, 295–305. [CrossRef]
40. Teren, M.; Turonova Michova, H.; Vondrakova, L.; Demnerova, K. Molecules autoinducer 2 and cjA and their impact on gene expression in *Campylobacter jejuni*. *J. Mol. Microbiol. Biotechnol.* **2019**, *28*, 207–215. [CrossRef]
41. Balalaie, A.; Rezvani, M.B.; Mohammadi Basir, M. Dual function of proanthocyanidins as both MMP inhibitor and crosslinker in dentin biomodification: A literature review. *Dent. Mater. J.* **2018**, *37*, 173–182. [CrossRef]
42. Andersen-Civil, A.I.S.; Arora, P.; Williams, A.R. Regulation of enteric infection and immunity by dietary proanthocyanidins. *Front. Immunol.* **2021**, *12*, 637603. [CrossRef]
43. Hao, S.; Yang, D.; Zhao, L.; Shi, F.; Ye, G.; Fu, H.; Lin, J.; Guo, H.; He, R.; Li, J.; et al. EGCG-mediated potential inhibition of biofilm development and quorum sensing in *Pseudomonas aeruginosa*. *Int. J. Mol. Sci.* **2021**, *22*, 4946. [CrossRef]
44. Wang, Y.; Wang, Y.; Chen, J.; Koseki, S.; Yang, Q.; Yu, H.; Fu, L. Screening and preservation application of quorum sensing inhibitors of *Pseudomonas fluorescens* and *Shewanella baltica* in seafood products. *LWT* **2021**, *149*, 111749. [CrossRef]
45. Ramić, D.; Ogrizek, J.; Bucar, F.; Jeršek, B.; Jeršek, M.; Smole Možina, S. *Campylobacter jejuni* biofilm control with *Lavandin* essential oils and by-products. *Antibiotics* **2022**, *11*, 854. [CrossRef]
46. Püning, C.; Su, Y.; Lu, X.; Gölz, G. Molecular mechanisms of *Campylobacter* biofilm formation and quorum sensing. In *Fighting Campylobacter Infections.* Current Topics in Microbiology and Immunology; Backert, S., Ed.; Springer: Cham, Switzerland, 2021; Volume 431, pp. 293–319.

Campylobacter jejuni Biofilm Control with Lavandin Essential Oils and By-Products

Dina Ramić [1], Janja Ogrizek [1], Franz Bucar [2], Barbka Jeršek [1], Miha Jeršek [3] and Sonja Smole Možina [1,*]

[1] Department of Food Science and Technology, Biotechnical Faculty, University of Ljubljana, Jamnikarjeva 101, 1000 Ljubljana, Slovenia; dina.ramic@bf.uni-lj.si (D.R.); ogrizek.janja@gmail.com (J.O.); barbka.jersek@bf.uni-lj.si (B.J.)
[2] Department of Pharmacognosy, Institute for Pharmaceutical Sciences, University of Graz, A-8010 Graz, Austria; franz.bucar@uni-graz.at
[3] Slovenian Museum of Natural History, Prešernova Cesta 20, 1001 Ljubljana, Slovenia; mjersek@pms-lj.si
* Correspondence: sonja.smole-mozina@bf.uni-lj.si; Tel.: +386-1-320-3751

Abstract: The food industry is constantly struggling with one of the most prevalent biofilm-forming and food-borne pathogenic bacteria, *Campylobacter jejuni*. Different approaches are used to control biofilms in the food production chain, but none is fully effective. In this study, we aim to produce and determine the chemical profile of essential oils (EOs), ethanolic extracts of flowers prior to distillation (EFs), and ethanolic extracts of post-distillation waste material (EWMs) from *Lavandula × intermedia* 'Bila', 'Budrovka' St Nicholas and 'Budrovka', which were further used to reduce *C. jejuni* intercellular signaling, adhesion, and biofilm formation, as well as to test their antioxidant activity. Glycosides of hydroxycinnamic acids were the major constituents of both types of lavandin ethanolic extract, while linalool, linalyl acetate, 1,8-cineol, and camphor were the major compounds found in lavandin EOs. Tested EOs showed the best antibacterial activity with a minimal inhibitory concentration of 0.25 mg/mL. Lavandin EFs proved more effective in reducing *C. jejuni* intercellular signaling and adhesion compared to lavandin EOs and EWMs, while lavandin EOs showed a slightly better effect against biofilm formation. Interestingly, the best antioxidant activity was determined for lavandin EWMs. A positive and moderate correlation was found between the reduction of *C. jejuni* intercellular signaling and adhesion, as well as between adhesion and biofilm formation. These findings mean novel bacterial targets are of interest for biofilm control with alternative natural agents throughout the whole food production chain.

Keywords: *Campylobacter jejuni*; biofilm; adhesion; intercellular signaling; lavandin formulations

1. Introduction

Microbial biofilms are the predominant form of bacterial lifestyle in industrial environments and protect bacteria from physical trauma, desiccation, and antimicrobial agents [1]. Numerous reports have found that food-borne pathogens persist on food contact surfaces (e.g., plastic, steel, glass, rubber, and wood) in the form of biofilms and affect the quality, quantity, and safety of food products. Moreover, their control is a serious challenge in the food production chain because they cause huge economic and energy losses, damage surfaces and equipment, and lead to continuous contamination of food, posing a major ongoing public health risk [2].

Pathogenic bacteria *Campylobacter jejuni* are one of the most common bacterial agents of self-limiting gastrointestinal diseases in humans, but they can also cause more serious neurological disorders, such as Guillain–Barré syndrome [3]. Contaminated surfaces and undercooked poultry meat are the most common vectors of pathogen transmission to humans. Campylobacters represent a severe public health burden in the European Union, where they caused approximately 121.000 intestinal infections in 2020, leading to huge

economic losses [4]. A global concern is also the increasing prevalence of antibiotic-resistant and biocide-resistant strains of *C. jejuni*, isolated mainly from poultry [5,6].

Although Campylobacters are considered susceptible bacteria, they survive in environments outside their natural habitat, i.e., intestines. Properties such as intercellular signaling with AI-2 signaling molecule, motility, and chemotaxis allow them to form biofilms or colonize existing biofilms on abiotic surfaces such as polystyrene, glass, and stainless steel. Within biofilms, Campylobacters are protected from antimicrobial agents that penetrate the biofilm matrix slowly and poorly [7]. Various approaches are used to control Campylobacters in the food production chain, but none is fully effective [8]. Therefore, the right approach is needed to control Campylobacters and their biofilm formation in the food production chain at all stages, from primary production to slaughter, processing, and sale of meat. With increasing concerns about antibiotic resistance and environmental impacts, conventional antibiotics, biocides, and preservation methods are being replaced with naturally occurring alternatives that are recognized as safe (GRAS) and have a broad spectrum of antimicrobial activity, including prevention of intercellular signaling, adhesion, and biofilm formation (interrelated bacterial characteristics that are necessary for biofilm establishment) [9–12].

The plants from the *Lamiaceae* family, genus *Lavandula*, are an inexhaustible source of biologically active phytochemicals with great antimicrobial, anti-biofilm, and antioxidant properties. The genus *Lavandula* includes 39 species, numerous hybrids, and about 400 registered cultivars grown generally in the Mediterranean region [13]. Three *Lavandula* species are used for commercial essential oil (EO) production: *Lavandula angustifolia* Mill. (true lavender), *Lavandula × intermedia* Emeric ex Loisel syn. *L. hybrida* L. (lavandin) and *Lavandula latifolia* Medicus (spike lavender) [14]. Nowadays, the cultivation of lavandin, a natural sterile hybrid derived from a cross between *L. angustifolia* and *L. latifolia*, has become increasingly popular because of higher EO yields in comparison to true lavender (120 kg/ha compared to 40 kg/ha). It is preferred for personal care and hygiene products, industrial and household cleaners, as well as for antiseptics, antifungals, and insecticides [15,16]. In this study, flowers of indigenous Croatian cultivars *Lavandula × intermedia* 'Bila', 'Budrovka' St Nicholas (SN), and 'Budrovka' were used for the first time to prepare EOs and ethanolic extracts in order to test their anti-biofilm and antioxidant activity, features important for ensuring food safety and quality.

Higher production of EO consequently resulted in increased accumulation of by-products, i.e., waste materials and hydrolates gained after EO distillation [17,18]. These by-products remain a potentially important source of potent phytochemicals, as shown by the results for spike lavender (which have great antioxidant properties) and lavender hydrolates (which have antifungal and antibacterial properties) [19,20]. The reuse of such natural waste material is environmentally friendly, which makes it more popular than synthetic disinfectants that are often used in the food industry and can lead to additional unnecessary chemicals in the environment [21]. Our previous study has shown that *L. angustifolia* waste material had a promising anti-biofilm effect against pre-established *C. jejuni* biofilms [22], but in this study, lavandin waste materials were used to target *C. jejuni* properties, i.e., intercellular signaling, adhesion, and biofilm formation to prevent *C. jejuni* biofilm establishment.

The aim of this study was to find potential antimicrobials that will be able to prevent or reduce *C. jejuni* National Collection of Type Culture (NCTC) 11168 biofilm formation on an abiotic surface. For that purpose, dried flowers of *Lavandula × intermedia* 'Bila', 'Budrovka' SN, and 'Budrovka' were used to produce EOs, ethanolic extracts of flowers prior to distillation (EFs), and ethanolic extracts of post-distillation waste material (EWMs). Afterward, their chemical characterization was performed. *C. jejuni* intercellular signaling and adhesion were used as targets to prevent or reduce biofilm formation in its early stages. Further, *C. jejuni* biofilm formation, with the addition of lavandin formulations at subinhibitory concentration, was monitored in order to determine how preventive measures affect *C. jejuni* biofilm establishment. A correlation between intercellular signaling, adhesion

and biofilm formation was determined. Finally, the antioxidant activity of *L. × intermedia* formulations was also explored.

2. Results

2.1. Chemical Composition of Lavandin Ethanolic Extracts and EOs

The lavandin ethanolic extracts (EFs and EWMs) were analyzed for their phenolic compounds using LC-PDA-ESI-MS analysis. Glycosides of hydroxycinnamic acids were the major constituents of both types of lavandin ethanolic extract. Rosmarinic acid was found in both types of ethanolic extracts; salvianolic A and 3-(3,4-dihydroxyphenyl) lactic acid were only detected in the EWMs. The latter can be easily derived from rosmarinic acid by ester hydrolysis. In addition, flavones apigenin-7-O-glucoside and ladanein were detected. Flavonoids only had a minor role in the composition of the lavandin ethanolic extracts (EFs and EWMs). Table 1 summarizes the peaks that were identified for both types of lavandin ethanolic extract. It is interesting to note that the yield of ethanol extraction was higher for waste materials (EWMs) than for dried flowers (EFs) (Figure S1). Supplementary Figures S2 and S3 illustrate representative UV chromatograms for EFs and EWMs, respectively. To see the difference in composition between both types of extracts, EF and EWM, a comparison of peak areas of individual compounds, i.e., quantification of their relative amounts, is presented in Supplementary Figure S4.

Table 1. Identification of the main common phenolic compounds in the lavandin ethanolic extract (EF) and lavandin (EWM).

No.	Rt	Compound Identified	Full Scan MS (*m/z*)	Fragment Ions (MS^2; *m/z*)	UV Maximum (nm)
1	4.97	3-(3,4-Dihydroxyphenyl)lactic acid *	395 [M+HCOOH-H]$^-$, 197 [M-H]$^-$	197 (100)	225 sh, 281
2	8.34	Coumaric acid hexoside I	325 [M-H]$^-$	163 (100), 119 (25)	263, 290 sh
3	10.23	Ferulic acid hexoside I	355 [M-H]$^-$	193 (100), 149 (20)	302
4	10.23	Caffeic acid hexoside	387 [M+HCOOH-H]$^-$	341 (100), 207 (25)	302
5	12.13	Coumaric acid hexoside II	371 [M+HCOOH-H]$^-$, 325 [M-H]$^-$	325 (100)	277, 290 sh
6	14.21	Ferulic acid hexoside II	401 [M+HCOOH-H]$^-$, 355 [M-H]$^-$	355 (100)	295, 319
7	18.87	Apigenin-7-O-glucoside	431 [M-H]$^-$	269 (100)	268, 334
8	19.60	Rosmarinic acid	359 [M-H]$^-$	161 (100), 179 (30), 223 (10)	292 sh, 328
9	23.96	Salvianolic acid A *	493 [M-H]$^-$	295 (100), 313 (10)	287, 340 sh
10	30.24	Ladanein (5,6-di-OH-7,4'-dimethoxy flavone)	315 [M-H]$^-$	300 (100)	284, 333

* Not detected in lavandin ethanolic extract (EF).

According to the gas chromatography–mass spectrometry (GC–MS) analysis, used lavandin EOs belong to *Lavandula × intermedia* 'Bila', L. × intermedia 'Budrovka' SN, and L. × intermedia 'Budrovka' (Table 2). Linalool was the most represented terpene alcohol in the chemical composition of tested EOs, where lavandin EO 'Bila' contained 40.4%, lavandin EO 'Budrovka' SN 43.1%, and lavandin EO 'Budrovka' 47.2% linalool. Major differences were observed in the content of linalyl acetate, where lavandin EO 'Bila' contained 6.6%, lavandin EO 'Budrovka' SN 5.3%, and lavandin EO 'Budrovka' 26.7% linalyl acetate. Interestingly, lavandin EO 'Bila' and lavandin EO 'Budrovka' SN were comparable in composition, whereas lavandin EO 'Budrovka' showed remarkable differences, aside from its higher linalyl acetate content and its low content of lavandulol, endo-borneol, (Z)-β-ocimene, camphor, terpinene-4-ol and (E)-β-farnesene. In contrast, the content of 1,8-cineol was similar in all EOs (Table 2).

Table 2. Identification of the main components of the lavandin EOs.

Retention Time	Retention Index [a]	Compound [b]	Quantification of Total [c]		
			Lavandula × *Intermedia* 'Bila'	*Lavandula* × *Intermedia* 'Budrovka' SN	*Lavandula* × *Intermedia* 'Budrovka'
5.126	926	α-Thujene	0.086	0.139	0.012
5.301	932	α-Pinene	0.635	0.813	0.317
5.680	946	Camphene	0.248	0.33	0.031
6.349	973	Sabinene	0.173	0.196	0.178
6.442	975	β-Pinene	0.882	0.98	0.685
6.710	979	3-Octanon	tr	tr	0.601
6.851	991	Myrcen	0.27	0.311	0.343
7.449	1010	Δ3-Carene	0.235	0.222	tr
7.925	1023	p-Cymene	0.275	0.263	0.132
8.126	1030	1,8-Cineol	14.091	12.585	14.211
8.378	1037	(Z)-β-Ocimene	2.565	4.047	0.44
8.754	1047	(E)-β-Ocimene	0.128	0.27	0.046
9.115	1058	γ-Terpinene	0.104	0.165	tr
9.392	1065	cis-Sabinenhydrate	0.059	0.088	0.025
9.595	1071	cis-Linalool oxide (furanoid)	tr	0.027	0.116
10.187	1087	trans-Linalool oxide (furanoid)	tr	tr	0.097
10.198	1088	Terpinolene *	0.14	0.22	n.d.
10.662	1100	Linalool	40.412	43.058	47.206
11.141	1112	Octen-3-yl-1-acetate	0.05	0.024	0.235
12.323	1142	Camphor	2.998	1.371	0.383
12.616	1150	Hexyl-2-methylpropanoate	0.099	0.087	0.135
13.209	1163	endo-Borneol + Lavandulol	13.946	14.053	0.121
13.706	1175	Terpinen-4-ol	8.37	8.813	0.962
14.271	1190	α-Terpineol	1.159	0.827	1.106
14.418	1192	Hexylbutanoate	0.753	0.739	0.628
15.793	1227	endo-Bornylformiate *	0.23	0.171	n.d.
16.290	1237	Hexyl-2-methylbutanoate	0.206	0.194	0.276
16.497	1242	Hexylisovalerate	0.058	0.047	0.128
17.069	1256	Linalylacetate	6.645	5.264	26.709
18.577	1291	Lavandulylacetate	0.879	0.693	0.105
22.607/22.676	1387/1390	Hexylhexanoate + 7-epi-Sesquiphellandrene	0.148	0.118	0.069
23.773	1419	trans-Caryophyllene	0.663	0.625	1.704
25.423	1457	(E)-β-Farnesene	2.611	2.151	0.123
25.782	1466	Lavandulyl-butanoate *	0.102	0.051	n.d.
26.265	1480	Germacrene D	0.357	0.431	0.162
27.549	1510	Lavandulyl-isovalerate *	0.309	0.219	n.d.
30.174	1579	trans-Caryophyllenoxide	tr	0.018	0.341
34.016	1682	α-Bisabolol	tr	0.033	0.89

[a] Linear Retention Index relative to n-alkanes on HP-5-MS column; [b] Compounds identified by mass spectral libraries [23,24]; [c] Quantification by normalization (area percent method) without considering calibration factors. tr—in traces; n.d.—not determined; * not determined in *Lavandula* × *Intermedia* 'Budrovka'.

2.2. Anti-Campylobacter Activity of Lavandin Formulations

In order to evaluate the anti-Campylobacter activities of the lavandin EOs and ethanolic extracts (EFs and EWMs), their minimal inhibitory concentration (MIC) against *C. jejuni* NCTC 11,168 and *C. jejuni* 11168ΔluxS were determined (Table 3). The lavandin formulations showed antimicrobial efficacy against *C. jejuni* NCTC 11168 at a concentration ranging between 0.25–1 mg/mL. The most favorable effect was shown by samples from the group of EOs: the MICs for all EOs were 0.25 mg/mL. Slightly weaker antimicrobial activity was shown by a group of samples of ethanolic extracts, where lavandin EFs showed better

performance compared to lavandin EWMs (Table 3). The same MIC values were also determined against *C. jejuni* 11168ΔluxS, where concentration ranged between 0.25–1 mg/mL. Here, samples of EOs showed the best antimicrobial activity, while lavandin EWM proved to be less effective (Table 3).

Table 3. Minimal inhibitory and subinhibitory concentration determined against *C. jejuni* NCTC 11168 and *C. jejuni* 11168ΔluxS for the lavandin formulations (EOs, EFs and EWMs).

Sample	*C. jejuni* NCTC 11168		*C. jejuni* 11168ΔluxS	
	MIC (mg/mL)	0.25 × MIC (mg/mL)	MIC (mg/mL)	0.25 × MIC (mg/mL)
EO 'Bila'	0.25	0.062	0.25	0.062
EO 'Budrovka' SN	0.25	0.062	0.25	0.062
EO 'Budrovka'	0.25	0.062	0.25	0.062
EF 'Bila'	0.5	0.125	0.25	0.062
EF 'Budrovka' SN	1	0.25	0.5	0.125
EF 'Budrovka'	0.5	0.125	0.5	0.125
EWM 'Bila'	1	0.25	1	0.25
EWM 'Budrovka' SN	1	0.25	1	0.25
EWM 'Budrovka'	1	0.25	1	0.25

Determining the antibacterial activity of the lavandin formulations was crucial for further experiments. Based on the determined MIC values, a subinhibitory concentration (0.25 × MIC) was calculated to avoid the effect of the lavandin formulations on bacterial growth during the experiments (Table 3) [25]. Thus, the focus of this study was to monitor potential changes in *C. jejuni* properties that are important for biofilm establishment, i.e., intercellular signaling, adhesion, and biofilm formation, while exposed to lavandin formulations at subinhibitory concentration.

2.3. Modulation of Campylobacter Intercellular Signaling by Lavandin Formulations

The effect of lavandin formulations on the intercellular signaling of *C. jejuni* was verified indirectly by measuring the emitted bioluminescence of the biosensor strain *Vibrio harveyi* MM30. This biosensor was chosen because of its mutation in the luxS gene, which consequently does not synthesize AI-2 signaling molecules but can detect external AI-2 released into the growth medium by *C. jejuni* [26,27]. The intensity of the bioluminescence signal is proportional to the signal concentration in the tested spent medium (SM) [27].

C. jejuni NCTC 11168 and *C. jejuni* 11168ΔluxS were cultivated without or with the addition of the lavandin EOs and ethanolic extracts (EFs and EWMs) at a subinhibitory concentration (0.25 × MIC). Before determining the effect of lavandin formulations on the intercellular signaling of *C. jejuni*, the colony-forming units (CFUs) were determined to verify the effect on bacterial growth. Indeed, the used formulations did not significantly affect the growth of *C. jejuni* NCTC 11168 and *C. jejuni* 11168ΔluxS at a concentration of 0.25 × MIC ($p > 0.05$) (Supplementary Table S1). SMs of *C. jejuni* NCTC 11168 and *C. jejuni* 11168ΔluxS were further analyzed with the biosensor *V. harveyi* MM30, and emitted bioluminescence was measured for 15 h. The reduction of bioluminescence was calculated using Equation (1). This was the indirect measure for the reduction of *C. jejuni* intercellular signaling.

All lavandin EFs significantly reduced *C. jejuni* intercellular signaling ($p < 0.05$) (Figure 1). Lavandin EWM 'Bila' and EWM 'Budrovka' SN were also successful in reducing *C. jejuni* intercellular signaling ($p < 0.05$), while lavandin EOs did not have a significant effect on *C. jejuni* intercellular signaling ($p > 0.05$) (Figure 1). Lavandin EFs 'Bila' and 'Budrovka' and lavandin EWM 'Bila' reduced *C. jejuni* intercellular signaling by approximately 95% (Supplementary Table S2).
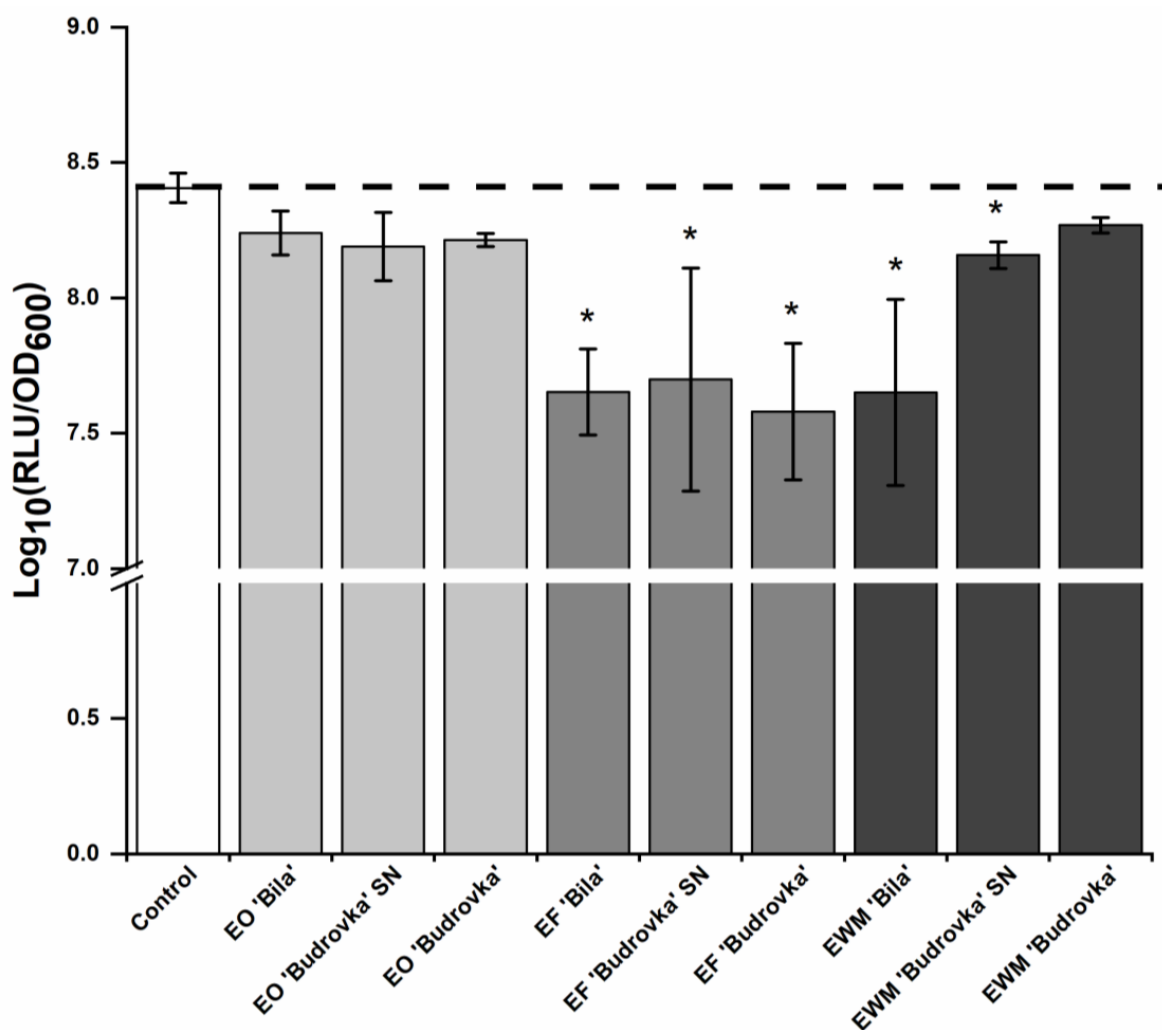
Figure 1. Effect of different lavandin formulations (EOs, EFs and EWMs) at subinhibitory concentration (0.25 × MIC) on the intercellular signaling of *C. jejuni* NCTC 11168. *C. jejuni* NCTC 11168 was cultivated for 24 h without or with the addition of lavandin formulations at subinhibitory concentration. Afterwards, SMs were prepared and added to *V. harveyi* MM30 biosensor strain. *V. harveyi* MM30 bioluminescence response was the indirect measure for *C. jejuni* intercellular signaling. Log_{10} average values $\pm$ SD are shown. * $p < 0.05$, vs. control. (EO, essential oil; EF, ethanolic extract prior to distillation; EWM, ethanolic extract of post-distillation waste material).

2.4. Modulation of Campylobacter Adhesion by Lavandin Formulations

Lavandin EOs, EFs, and EWMs were used at a subinhibitory concentration (0.25 × MIC) in order to prevent the adhesion of *C. jejuni* to a polystyrene surface. Results are shown in Figure 2. The adhesion of *C. jejuni* to a polystyrene surface was significantly reduced by all lavandin EOs and ethanolic extracts (EFs and EWMs), with the exception of lavandin EWM 'Budrovka' SN ($p < 0.05$). Within the exact group of lavandin formulations, EOs, EFs and EWMs had a similar effect on *C. jejuni* adhesion (Figure 2).
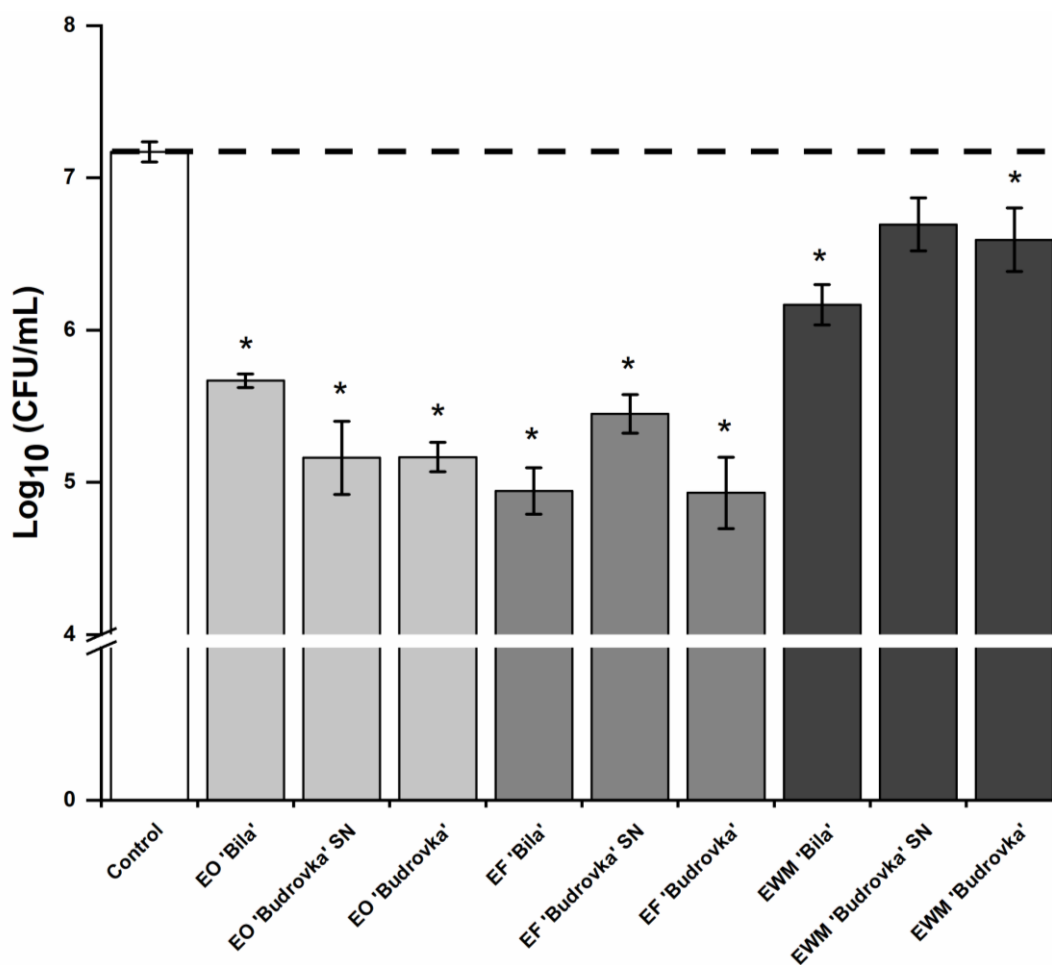
Figure 2. Effect of different lavandin formulations (EOs, EFs and EWMs) at subinhibitory concentration (0.25 × MIC) on the adhesion of *C. jejuni* NCTC 11168 to a polystyrene surface. *C. jejuni* NCTC 11168 was cultivated in a polystyrene microtiter plate without or with the addition of lavandin formulations at subinhibitory concentration in a micro-aerobic atmosphere at 42 °C for 24 h. Attached cells were suspended by sonication and their concentration was determined by plate counting. Log_{10} average values ± SD are shown. * $p < 0.05$, vs. control. (EO, essential oil; EF, ethanolic extract prior to distillation; EWM, ethanolic extract of post-distillation waste material).

Lavandin EF 'Bila' and 'Budrovka' proved slightly more effective, with an almost 99% reduction of adhesion (i.e., a reduction of 2 log_{10}). Lavandin EF 'Bila' was more effective on *C. jejuni* adhesion compared to EO and EWM 'Bila' ($p < 0.05$). There were no significant differences in the effects of EO and EWM 'Bila' ($p > 0.05$). Lavandin EO 'Budrovka' SN and 'Budrovka' were more effective than the lavandin EWMs ($p < 0.05$), but there were significant differences compared to EFs 'Budrovka' SN and 'Budrovka' ($p > 0.05$). All lavandin EFs were more effective in reducing *C. jejuni* adhesion to the polystyrene surface compared to the lavandin EWMs ($p < 0.05$).

2.5. Modulation of Campylobacter Biofilm Formation by Lavandin Formulations

The biofilm formation of *C. jejuni* was observed on a glass surface, which presented the model of an abiotic surface. Lavandin formulations at subinhibitory concentration were used in order to prevent biofilm formation. Coverage of the glass surface with *C. jejuni* NCTC 11,168 biofilm at air/liquid interface was determined after 72 h of exposure to lavandin formulations. Every 24 h, the SM was replaced with a fresh one, where lavandin formulations at subinhibitory concentration were added. This step was important

because, in this way, *C. jejuni* was constantly exposed to the same concentration and form of lavandin formulations.

All lavandin EOs and ethanolic extracts (EFs) significantly reduced the biofilm formation of *C. jejuni* on the glass surface ($p < 0.05$) (Figure 3). Among the lavandin EWMs, only lavandin EWM 'Bila' significantly reduced biofilm formation ($p < 0.05$). Once again, it is obvious that, within the exact group of lavandin formulations, EOs, EFs and EWMs had a similar effect on *C. jejuni* biofilm formation.
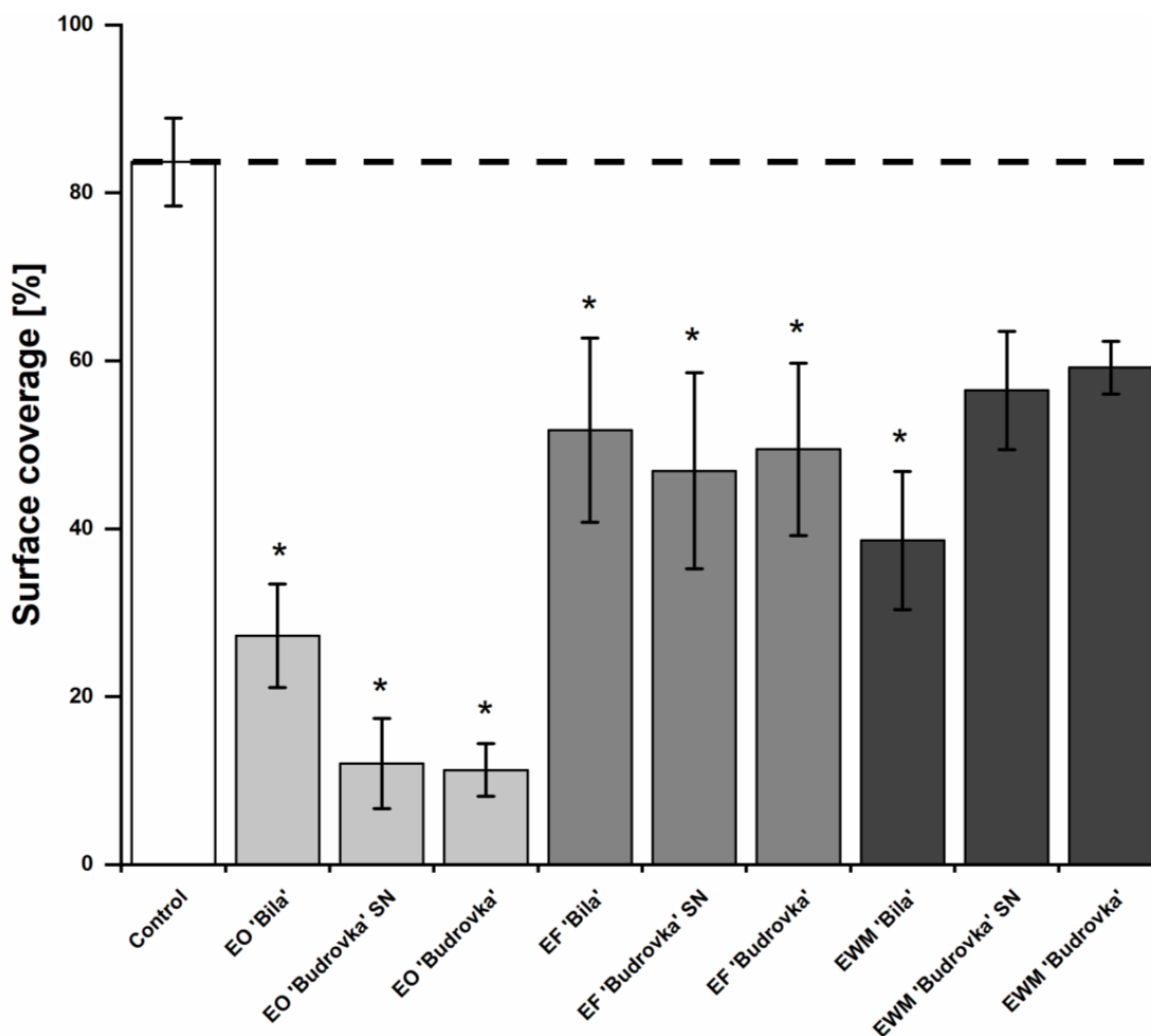

Figure 3. Effect of different lavandin formulations (EOs, EFs and EWMs) at subinhibitory concentration ($0.25 \times$ MIC) on biofilm formation of *C. jejuni* NCTC 11168. *C. jejuni* NCTC 11,168 was cultivated on a glass surface without or with the addition of lavandin formulations at subinhibitory concentration in a micro-aerobic atmosphere at 42 °C for 72 h. Every 24 h, the SM was replaced with a fresh Muller–Hinton (MH) broth, where lavandin formulations at subinhibitory concentration were added. After 72 h of incubation, microscopic slides were rinsed and stained with 1% [*v/v*] crystal violet. Biofilms were examined at air/liquid interface and surface coverage was measured. Average values ± SD are shown. * $p < 0.05$, vs. control. (EO, essential oil; EF, ethanolic extract prior to distillation; EWM, ethanolic extract of post-distillation waste material).

Lavandin EOs proved most effective against *C. jejuni* biofilm formation, where lavandin EO 'Budrovka' SN and 'Budrovka' reduced the biofilm formation by approximately 85%. Interestingly, lavandin EO 'Bila' reduced biofilm formation by approximately 67%, and its effect was not significantly different from the effect of lavandin EF 'Bila' and EWM 'Bila' ($p > 0.05$).

Lavandin ethanolic extracts (EFs and EWMs) had a weaker effect on *C. jejuni* biofilm formation. Among the ethanolic extracts, the most effective was lavandin EWM 'Bila', with a biofilm reduction of approximately 44%. The effect of lavandin EWM 'Bila' was not significantly different from the effect of lavandin EF 'Bila'.

2.6. Correlation between MIC and C. jejuni Intercellular Signaling, Adhesion and Biofilm Formation

In order to test whether the measured parameter MIC and *C. jejuni* properties—i.e., intercellular signaling, adhesion, and biofilm formation—were in correlation, Pearson's correlation test was used (Figure 4). There was a weak and negative correlation ($p < 0.01$) between MIC and *C. jejuni* intercellular signaling (Figure 4), meaning that the increment of MIC leads to the reduction of intercellular signaling. A medium and positive correlation ($p < 0.01$) was found between *C. jejuni* intercellular signaling and adhesion (Figure 4), meaning that the reduction of intercellular signaling leads to the reduction of adhesion. A medium and positive correlation ($p < 0.01$) was also observed for *C. jejuni* adhesion and biofilm formation (Figure 4), meaning that the reduction of adhesion leads to the reduction of biofilm formation.
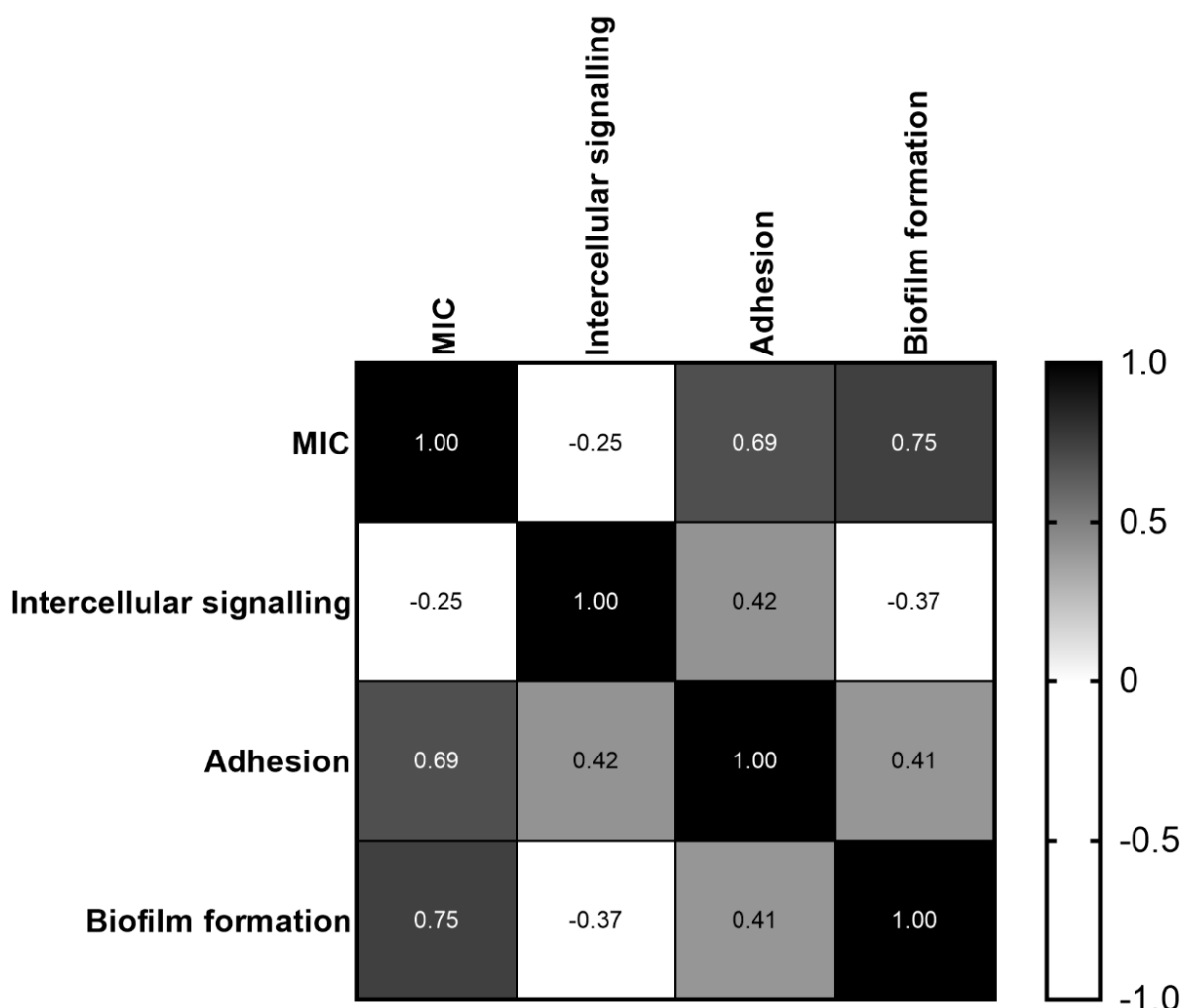
Figure 4. Correlation between MIC of lavandin formulations, *C. jejuni* intercellular signaling, adhesion and biofilm formation. Pearson's correlation test was used in order to determine the correlation among variables. For the Pearson correlation, an absolute value of 1 indicates a perfect linear relationship. A correlation close to 0 indicates no linear relationship between the variables. The sign of the coefficient indicates the direction of the relationship. Correlation was significant at the level < 0.01.

2.7. Antioxidant Activity of Lavandin Formulations

The antioxidant activity of the lavandin formulations was determined using the DPPH radical scavenging assay. Lavandin EOs were tested at a concentration of 40 mg/mL. Lavandin EO 'Bila' and 'Budrovka' showed similar results, with lavandin EO 'Bila' having a scavenging activity of 75.03 ± 11.33% and lavandin EO 'Budrovka' having a scavenging activity of 70.85 ± 2.80%. Lavandin EO 'Budrovka' SN had better antioxidant activity, with 90.17% ± 0.45% scavenging activity.

The lavandin ethanolic extracts (EFs and EWMs) were tested for antioxidant activity at a much lower concentration compared to the lavandin EOs. EFs were tested at a concentration of 2.5 mg/mL, while EWMs were tested at a concentration of 1 mg/mL. EF 'Bila' and 'Budrovka' SN had similar results, with EF 'Bila' having a scavenging activity of 86.73 ± 2.81% and EF 'Budrovka' SN of 83.54 ± 4.58%. EF 'Budrovka' had the best antioxidant activity among the lavandin EFs, with a scavenging activity of 93.87 ± 0.67%.

All three EWMs had a similar scavenging activity, with lavandin EWM 'Bila' having a scavenging activity of 92.16 ± 1.73, EWM 'Budrovka' SN of 94.38 ± 1.19, and EWM 'Budrovka' of 92.94 ± 0.38%.

3. Discussion

Current measures that are used to combat the persistence of *C. jejuni* in the food production chain are not fully effective, so there is a need for new approaches to control *C. jejuni* across the whole food production chain from farm to fork. In order to find potential antimicrobials that will be able to prevent or reduce *C. jejuni* biofilm establishment on abiotic surfaces, dried flowers of *Lavandula × intermedia* 'Bila', 'Budrovka SN, and 'Budrovka' were used to prepare EOs, ethanolic extracts of lavandin flowers prior to distillation (EFs) and ethanolic extracts of lavandin post-distillation waste material (EWMs). Prepared lavandin formulations were used to target *C. jejuni* intercellular signaling, adhesion, and biofilm formation in order to combat biofilm establishment. Subinhibitory concentration was used to avoid effects on *C. jejuni* growth.

Prior to the experiments at the biological level, the chemical composition of lavandin EOs, EFs and EWMs was investigated to gain insight into the chemical profile of prepared lavandin formulations. EFs and EWMs had a similar chemical composition, where phenols were the major compounds detected. However, it is important to note that the extraction yield was higher for waste material compared to flowers prior to the distillation (Supplementary Figure S1). This can be due to better accessibility of waste material to the solvent, as by hydrodistillation, the plant material was cooked for the time of hydrodistillation. Therefore, the plant cellular matrix was better solubilized, and extractive compounds were more easily available. Moreover, 3-(3,4-dihydroxyphenyl)lactic acid, the hydrolysis product of rosmarinic acid, as well as salvianolic acid A, could only be detected in the extract from waste materials after hydrodistillation, indicating that artifact formation during hydrodistillation has to be taken into account. In addition, the flavones apigenin-7-O-glucoside and ladanein were detected. A comparable composition was reported for *L. × intermedia* waste material, where chlorogenic acid and a number of flavone glycosides were also found [18]. A similar composition for *Lavandula* ethanolic extracts was also reported in our previous study [22]. Mass spectrometry and UV-VIS data were used for the identification of phenols, so the sugar moieties were only designated as hexosides; however, according to other reports for *Lavandula* spp., glucosidation is most likely to occur [18,28].

The complete chemical profile was determined for all three lavandin EOs. Linalool, linalyl acetate, 1,8-cineol, and camphor were the major compounds found in tested EOs. This confirms that tested EOs belonged to the genus *Lavandula*, more specifically to the hybrid *L. × intermedia* [29,30]. The EO of *L. × intermedia* 'Budrovka' contained the highest percentage of linalool (47.2%) and linlyl acetate (26.7%) compared to the percentage of linalool and linalyl acetate found in *L. × intermedia* 'Bila' and 'Budrovka' SN (40.4–43.1% and 5.3–6.6%, respectively). This is especially interesting because *L. × intermedia* 'Budrovka' and 'Budrovka' SN were cultivated at the same geographic location but in different fields,

which indicates that ontogenetic and morphogenetic factors can also influence the chemical variability, either to a quantitative or qualitative extent [31].

Among tested lavandin formulations, all three lavandin EOs were shown to possess the best antibacterial activity, with MIC values of 0.25 mg/mL. The antibacterial activity of *L. × intermedia* 'Budrovka' and *L. angustifolia* EOs were observed against different Gram-positive and Gram-negative bacteria [29]. In our previous study [22], the same MIC was determined for *L. angustifolia* EO against *C. jejuni*. Regarding the information provided, *C. jejuni* seems most sensitive to *Lavandula* formulations among all tested bacteria. This could be due to the type of microorganism, the inoculum volumes, and the culture medium used, together with the pH, temperature, and incubation time. Type and storage, as well as the method for plant formulation preparation, can also influence antimicrobial activity [32].

EFs and EWMs had a moderate but comparable effect against *C. jejuni*, although weaker than EOs. It is most likely that this can be explained by the glycosidic nature of the major constituents of the ethanolic extracts resulting in decreased cell wall permeability. Nevertheless, EFs and EWMs still contain a diverse pool of bioactive compounds and are effective antibacterial agents. This is in agreement with previous studies on post-distillation thyme waste, pinot noir grape skins and seeds, juniper fruit waste, and *Lavandula* waste material, which also showed great antimicrobial activity [22,33,34].

In further experiments, lavandin formulations were used at a subinhibitory concentration as a novel approach to control biofilm development, focusing on *C. jejuni* properties: intercellular signaling and adhesion. All lavandin EFs and lavandin EWMs 'Bila' and 'Budrovka' SN significantly reduced *C. jejuni* intercellular signaling, proving to be more effective than the lavandin EOs. It is hypothesized that the signaling molecules were bound to the solid aggregates of the precipitate in the samples of the ethanolic extracts, which became apparent during the preparation of the SMs and were removed along with the bacteria during filtration. Moreover, the process of intercellular signaling can be disrupted by different mechanisms: reducing the activity of receptor protein or synthase; inhibiting the production of signaling molecules; degrading the signaling molecules; mimicking the signaling molecules primarily by using the analogs of signal molecules (e.g., secondary metabolites of natural formulations) [35]. A comparable result was reported for *L. hybrida* EO at subinhibitory concentration, which inhibited the intercellular signaling of *C. jejuni* by approximately 66% [25]. Similarly, a strong effect on the inhibition of *C. jejuni* intercellular signaling was also found for the ethanolic fruit extract *Euodia ruticarpa*, which showed a reduction of more than 90% [36].

Adhesion is a bacterial feature affected by intercellular signaling. It is crucial for the development of *C. jejuni* biofilm, so it is necessary to inhibit it in order to prevent biofilm establishment [9]. A statistically significant effect on the reduction of *C. jejuni* adhesion to a polystyrene surface was confirmed for all tested lavandin preparations, with the exception of the lavandin EWM 'Budrovka' SN. There were no statistically significant differences between the anti-adhesion effect of lavandin EOs and EFs. Moreover, a slightly better effect could be observed for lavandin EF 'Bila' and 'Budrovka' compared to their EOs, where lavandin EF 'Budrovka' reduced adhesion by >99%. This is comparable with the results gained for thyme ethanolic extracts [33]. An excellent anti-adhesion effect was also observed for the *L. hybrida* EO, which reduced the adhesion of *C. jejuni* to the polystyrene surface by 96% [25]. This is comparable to the observed results for the lavandin EOs. Similar results for lavender formulations were shown in our previous study [22], where it was confirmed that lavender EOs were able to affect the expression of genes carrying the transcript for the outer membrane proteins involved in the initial adhesion of *C. jejuni* to contact surfaces. Moreover, a moderate and positive correlation was found between intercellular signaling and adhesion, indicating that a decrease in intercellular signaling leads to a decrease in the adhesion of bacterial cells to abiotic surfaces. These results are supported by the research by [25], who also found a correlation between the reduction of intercellular signaling and the reduction of adhesion. Altogether, these findings confirm that formulations from the genus *Lavandula* have great anti-adhesion potential against

C. jejuni and that intercellular signaling is an important target of *Lavandula* preparations to combat the adhesion of *C. jejuni*.

It is clear that the lavandin formulations successfully reduced *C. jejuni* adhesion, but the most important question was whether the lavandin formulations could reduce biofilm development even after 72 h of incubation. Indeed, all lavandin EOs and EFs, as well as lavandin EWM 'Bila', significantly reduced the biofilm development of *C. jejuni* on a glass surface even after 72 h of incubation ($p < 0.05$). A moderate and positive correlation was found between reducing adhesion and biofilm formation, confirming that reducing adhesion is a crucial step in combating bacterial biofilm, but a correlation between reducing intercellular signaling and biofilm was not found, which was expected, as biofilm formation is a multifactorial event and does not only depend on intercellular signaling. If we consider all the facts together, it is evident that intercellular signaling is the primary mechanism that needs to be reduced in order to reduce adhesion and, consequently, biofilm establishment. The lavandin EOs had the most favorable inhibitory effect against biofilm establishment. The latter can be attributed to the higher content of bioactive secondary metabolites in EO. It is interesting that there were no significant differences between the effects of lavandin EO, EF, and EWM 'Bila', indicating that waste material can match EO in its effects. Studies have also shown the anti-biofilm activity of linalool against different bacteria [9,29], but not as good as for EO. Naturally, linalool is one of the major compounds found in the tested EOs, but it is important to emphasize that the action of EO comes from the action of all the bioactive compounds found in EO [22].

Finally, the antioxidant activity of prepared lavandin formulations was tested. The antioxidant activity of natural compounds is important because it can reduce the oxidation of food products that come to consumers, thus improving food quality [37]. Among all the lavandin formulations, lavandin EWM had the best antioxidant activity and scavenging activity of more than 90% at a concentration of 1 mg/mL. In order to gain a similar effect with lavandin EFs and EOs, a concentration 2.5 times or 40 times higher had to be used. Similar results were found for the ethanolic extract *Ocimum basilicum*, which had better antioxidant activity than the EO of *O. basilicum* [38]. The better antioxidant activity of lavandin ethanolic extract formulations can be attributed to their strongly different chemical composition compared to EOs. For example, ladanein, which was found in the tested ethanolic extracts, is known to be a good antioxidant agent [39]. Moreover, lavandin EWMs had a relatively higher concentration of some identified compounds than EFs (concluded from the mass spectrometry and UV-VIS data), which can explain their better antioxidant activity. Similar results were found for lavandin 'Budrovka' EO, which had an IC_{50} value of 21.6 mg/mL [29]. By comparing our results with the research carried out on lavandin 'Sumiens', 'Super A' and 'Grosso', it was recognized that tested cultivars 'Bila', 'Budrovka' SN, and 'Budrovka' had an antioxidant activity that was twice as good [40]. Such an effect is probably the result of synergistic interactions between EOs constituents, as linalool and linlyl acetate had much higher IC_{50} values (218.6 mg/mL or 157.1 mg/mL, respectively) than lavandin EO [29].

4. Material and Methods

4.1. Chemicals

The MH agar was from BioMéroeux (Marcy-l'Étoile, France), the MH broth was from Oxoid (Hampshire, UK) and the Karmali agar was from Biolife (Milan, Italy). The glycerol solution was from Kemika (Zagreb, Croatia), the phosphate-buffered saline (PBS) was from Oxoid, and the kanamycin, dimethylsulphoxide (DMSO), resazurin, menadione, and Folin–Ciocalteu reagent were from Sigma Aldrich (Steinheim, Germany). The sodium chloride, magnesium sulfate heptahydrate, L-arginine, and 96% ethanol were from Merck (Darmstadt, Germany). The casamino acid was from Thermo Fisher Scientific (Carlsbad, CA, USA).

4.2. Lavandin Formulations

Three *Lavandula × intermedia* cultivars ('Bila', 'Budrovka' SN and 'Budrovka') were used in this study. *Lavandula × intermedia* 'Bila' was cultivated in Spodnje Pitve, Hvar, Croatia (43°09′06″ N, 16°40′35″ E), while *L. × intermedia* 'Budrovka' SN and *L. × intermedia* 'Budrovka' were cultivated in Jelsa, Hvar, Croatia (43°09′23″ N, 16°41′04″ E). The samples were collected in the afternoon hours during July 2019. Dried flowers were used to prepare the lavandin EOs and ethanolic extracts (EFs).

The EOs were prepared by hydrodistillation [41], with about 200 g of flowers distilled in two liters of water in a Clevenger-type apparatus for three to four hours and then stored at 4 °C. The waste material obtained after the hydrodistillation of the lavandin flowers was also used for the preparation of the ethanolic extracts (EWMs).

The ethanolic extracts from the lavandin dried flowers (EFs) and waste material (EWMs) gained after the hydrodistillation process were prepared by a four-to-six-hour ethanol extraction (Soxhlet extraction) of 20 g dried flowers in 150 mL 96% ethanol. These were then concentrated in a rotary evaporator (Laborota 4000; Heidolph Instruments, Germany) at 40 °C and 175 mbar pressure and stored at 4 °C.

4.3. Phytochemical Analysis of Lavandin Ethanolic Extracts

The identification of the phenolic compounds in lavandin ethanolic extracts (EFs and EWMs) was carried out using liquid chromatography—photo diode array—electrospray ionization mass spectrometry (LC-MS) following the protocol described in [22] (for details, see Supplementary Methods, LC-MS Conditions). The compounds eluted were determined by their UV-VIS and mass spectra, in comparison with the literature [18,42–46].

4.4. GC–MS Analysis of Lavandin EOs

The identification of the main compounds in lavandin EOs was carried out by GC–MS following the protocol described in [19] (for details, see Supplementary Methods, GC–MS Conditions). The compounds were identified by their retention indices according to [44] and by comparing their mass spectra with spectral data libraries [23,24,47] and with the laboratory's own database.

4.5. Bacterial Strains and Growth Conditions

C. jejuni NCTC 11168 and *C. jejuni* 11168ΔluxS [48] were used in this study. The strains were stored at −80 °C in a 20% glycerol and 80% MH broth. Prior to the experiments, *C. jejuni* NCTC 11168 was subcultivated on Karmali agar, and *C. jejuni* 11168ΔluxS on an MH agar supplemented with 30 mg/L kanamycin for 24 h at 42 °C under micro-aerobic conditions (85% N_2, 5% O_2, 10% CO_2). The strains were further subcultured in an MH broth under the same conditions, and bacterial OD was determined by spectrophotometric measurements of absorbance at 600 nm after the incubation. The inoculum was prepared in an MH broth at 10^5 CFU/mL for determination of the MICs and assays that targeted *C. jejuni* intercellular signaling and adhesion. For counting, strains were plated on an MH agar under conditions described above in this section, and the colonies were counted and expressed as CFU/mL.

For the autoinducer-2 bioassay, the biosensor strain *V. harveyi* MM30 [22] was used. The strain was stored at −80 °C in a 20% glycerol and 80% autoinducer bioassay (AB) medium composed of NaCl [0.02 g/L], MgSO4 + 7 H2O [0.01 g/L], casamino acid [0.002 g/L], PBS [1 M], L-arginine [0.1 M] and glycerol [50% (*v/v*)] [49]. Prior to the experiments, strains were subcultured for 16 h aerobically at 30 °C in an AB liquid medium.

4.6. Antimicrobial Potential of Lavandin Formulations

The MICs against *C. jejuni* NCTC 11168 and *C. jejuni* 11168Δ*luxS* were determined by the broth microdilution method, as previously described [50]. Stock solutions of lavandin EOs and ethanolic extracts (EFs and EWMs) were prepared in DMSO at 40 mg/mL. Serial dilutions of stock solutions were performed in an MH broth in a 96-well microtiter plate

(NUNC 266 120 polystyrene plates; Nunc, Denmark), after which bacterial inoculum was added, prepared as described in Section 2.5. During experiments, the DMSO in the MH broth did not exceed a concentration of 1% [*v/v*], which did not influence the growth of bacteria [25]. In further experiments, a concentration of 0.25 × MIC was used, as this concentration was the first concentration that did not influence the growth of *C. jejuni* [25].

4.7. Targeting Intercellular Signaling of C. jejuni

Overnight cultures of *C. jejuni* NCTC 11168 and *C. jejuni* 11168ΔluxS were inoculated in an MH broth until OD600 0.1 (10^7 CFU/mL). For further experiments, the cultures were diluted 100-fold in an MH broth, and an MH broth supplemented with lavandin formulations (EOs and ethanolic extracts [EFs and EWMs]) at subinhibitory concentration (0.25 × MIC). The cultures were further incubated for 24 h at 42 °C under micro-aerobic conditions. After the incubation, bacterial growth was determined using the plate counting method as described previously (Section 2.5), and cultures were further filtrated through 0.2 μm syringe filters to gain an SM where no bacteria were present. SMs were stored at −80 °C until further experiments.

V. harveyi MM30 was used for the biosensor assay in order to test the effect of lavandin formulations on *C. jejuni* intercellular signaling. An overnight culture of *V. harveyi* MM30 was diluted 5000-fold in an AB liquid medium to contain approximately 10^3 CFU/mL and was used in further experiment. *C. jejuni* NCTC 11168 SM (CJ–SM) and *C. jejuni* 11168ΔluxS SM (LUXS–SM), untreated or treated with lavandin formulations at subinhibitory concentration, were added to the suspension of the biosensor to a final concentration of 5% (*v/v*) of each (i.e., 10 μL of CJ–SM, 10 μL of LUXS–SM and 180 μL of the biosensor strain) in 96-well white microtiter plates with a transparent bottom (Greiner Bio-One, Kremsmünster, Austria). LUXS–SM, untreated or treated with lavandin formulations at subinhibitory concentration, was used as the blank [5% (*v/v*) LUXS–SM, 95% (*v/v*) AB medium], while the negative control was a 5% (*v/v*) LUXS–SM and 95% (*v/v*) *V. harveyi* suspension. The relative luminescence signals, expressed as relative luminescence units (RLU), and a growth of *V. harveyi* MM30, expressed as OD600, after the addition of CJ–SM (treated or untreated), LUXS–SM (treated or untreated), and MH broth, were measured with a microplate reader (Varioskan Lux, Thermo Scientific, Waltham, MA, USA) at 30 min intervals over 15 h at 30 °C.

The measured values (RLU and OD600) of LUXS–SM (treated or untreated), used as blank, were deducted from the values (RLU and OD600) gained for the bioluminescence response and the growth of the *V. harveyi* MM30 biosensor after the addition of CJ–SM and LUXS–SM (both treated or untreated). Results from the bioluminescence response were normalized with OD600. The reduction of bioluminescence was calculated by Equation (1):

$$\% \ bioluminescence \ reduction = 100 - \left(\frac{11168T - luxST}{11168C - luxSC} \right) \times 100\%, \tag{1}$$

where 11168T is the normalized bioluminescence response of *V. harveyi* MM30 after the addition of CJ–SM treated with lavandin formulations at subinhibitory concentration, luxST is the normalized bioluminescence response of *V. harveyi* MM30 after the addition of LUXS–SM treated with lavandin formulations at subinhibitory concentration, 11168C is the normalized bioluminescence response of *V. harveyi* MM30 after the addition of untreated CJ–SM and luxSC is the normalized bioluminescence response of *V. harveyi* MM30 after the addition of untreated LUXS–SM.

4.8. Anti-Adhesion Potential of Lavandin Formulations

The adhesion of *C. jejuni* NCTC 11168 was investigated under treatments with lavandin formulations at subinhibitory concentration. Inoculum was prepared as described in Section 2.5 and treated with lavandin EOs, and ethanolic extracts (EFs and EWMs) at 0.25 × MIC Polystyrene microtiter plates with 96 wells (Nunc 266 120 polystyrene plates; Nunc, Denmark) were prepared as described in [22] and were incubated for 24 h. The ad-

hesion of cells was determined as CFU/mL, as previously described [22,33]. The untreated culture was used as a negative control.

4.9. Anti-Biofilm Potential of Lavandin Formulations

The anti-biofilm potential of lavandin EOs and ethanolic extracts (EFs and EWMs) was evaluated according to the previously reported method [22]. Briefly, in a 50 mL centrifuge tube (Sarstedt, Nümbrecht, Germany), 20 mL of MH broth supplemented with lavandin formulations at subinhibitory concentration (0.25 × MIC) were added and were inoculated with 5% [*v/v*] inoculum of *C. jejuni* overnight culture (10^8 CFU/mL). Autoclaved microscope slides (26 × 76 mm; Deltalab, Barcelona, Spain) were used as a model for a glass surface and were vertically inserted into the centrifuge tube after inoculation of the medium. The cultures were incubated without shaking in a micro-aerobic atmosphere for 72 h at 42 °C, in a damp environment. After 24 h, microscopic slides were transferred to new centrifuge tube where 20 mL of fresh MH broth, supplemented with lavandin formulations at subinhibitory concentration (0.25 × MIC), were added. The same was repeated after an additional 24 h of incubation. Untreated cultures were used as negative controls. After 72 h of incubation, the microscopic slides were rinsed three times with PBS to remove weakly adhered cells and stained with a 1% [*v/v*] crystal violet stain. The biofilms on the air/liquid interface were investigated with a light microscope (DM750, Leica, Germany) equipped with a camera (ICC50 W, Leica, Germany) under a 400× *g* magnification. For each sample, five technical replicates of vertically connected images of biofilm at the air/liquid interface were captured (5 × 1 mosaic images; total analyzed surface per image, 1600 μm × 1200 μm). The images were processed using the Fiji program [51] as described in [22], with minor modifications. Based on the image processing, the surface coverage in percent was determined.

4.10. Free Radical Scavenging Activity Assay (DPPH Assay)

The free radical scavenging activities of the lavandin EOs and ethanolic extracts (EFs and EWMs) were evaluated using the stable DPPH radicals as previously described [29]. Briefly, the DPPH was prepared at a concentration of 0.2 mg/mL in 96% ethanol. The lavandin EOs were assayed at a concentration of 40 mg/mL in 96% ethanol, lavandin ethanolic extracts (EFs) at a concentration of 2.5 mg/mL in 96% ethanol and lavandin ethanol extracts (EWMs) at a concentration of 1 mg/mL in 96% ethanol. We added 20 μL of DPPH to 60 μL of the lavandin samples (EOs, EFs, and EWMs) in a non-sterile 96-well polystyrene microtiter plate (Brand, Wertheim, Germany). For blank, 20 μL of 96% ethanol was added to 60 μL of the lavandin samples (EOs, EFs, EWMs), and for a negative control, 20 μL of DPPH solution was added to 60 μL of the 96% ethanol. The microtiter plate was shaken for 1 min at 600 rpm in a microplate shaker (Eppendorf, Hamburg, Germany) and incubated for 30 min in the dark at room temperature. After incubation, the absorbance was measured at 517 nm on the microplate reader. The scavenging activity was calculated using the following Equation (2):

$$\% \, SA = \left(1 - \left(\frac{A \, (sample) - (A(blank)}{A(neg.control)} \right) \right) \times 100 \qquad (2)$$

4.11. Statistical Analysis

All the experiments were carried out in triplicate as three or more independent experiments. The data are expressed as means ± standard deviation, with analysis using Origin 2018 (OriginLab, Northampton, MA, USA). Statistical analysis was performed using IBM SPSS Statistics 23 (Statsoft Inc., Tulsa, OK, USA). In order to determine the distribution and homogeneity of the data, the Kolmogorov–Smirnov test of normality and the homogeneity of variances test were performed. The data were normally distributed and variances were equal across groups. Statistical significances were determined using the One-Way ANOVA test. Data were accepted as significant at $p < 0.05$. Pearson's correlation

test was used to determine the correlation between MIC and *C. jejuni* intercellular signaling, adhesion, and biofilm formation. The correlation was significant at the level $p < 0.01$.

5. Conclusions

This comparative study aimed to find antimicrobials that were potentially able to reduce *C. jejuni* biofilm establishment on abiotic surfaces. Prepared EOs, EFs, and EWMs of *Lavandula × intermedia* 'Bila', 'Budrovka' SN, and 'Budrovka' showed great antibacterial activity against one of the major food-borne pathogens, *C. jejuni*. Their effect against *C. jejuni* intercellular signaling, adhesion, and biofilm formation at subinhibitory concentration was confirmed, making lavandin formulations antimicrobial agents that can be used as an innovative approach to control *C. jejuni* biofilm development. Moreover, a correlation was confirmed between the reduction of *C. jejuni* intercellular signaling and the reduction of *C. jejuni* adhesion, two interrelated properties that can be easily controlled simultaneously. It is important to emphasize that lavandin ethanolic extracts showed better activity against *C. jejuni* intercellular signaling and adhesion, as well as better antioxidant activity, which makes them competitive with EOs. These findings mean that novel bacterial targets are of interest for biofilm control with alternative natural agents throughout the whole food production chain.

Supplementary Materials: The following supporting information can be downloaded at https://www.mdpi.com/article/10.3390/antibiotics11070854/s1: Method S1. LC-MS Conditions; Method S2. GC–MS Conditions; Table S1. Growth of *C. jejuni* NCTC 11168 and *C. jejuni* 11168ΔluxS in MH broth without or with the addition of lavandin formulations (EOs, EFs and EWMs) at subinhibitory concentration (0.25 × MIC) after 24 h of incubation in a micro-aerobic atmosphere. Average values of CFU/mL are shown ± SD; Table S2. Reduction of *C. jejuni* NCTC 11168 intercellular signaling after the addition of lavandin formulations (EOs, EFs and EWMs) at subinhibitory concentration (0.25 × MIC). Average values in % are shown ± SD; Figure S1. Yield of ethanol extraction for lavandin ethanolic extracts, i.e., lavandin EFs and lavandin EWMs. Figure S2. HPLC chromatogram (UV 310 nm) of the ethanolic extract of lavandin flowers prior to distillation [EFs]. * not identified (no significant ionization in ESI positive and negative mode); compound 1 was not detected; for identity of compounds 2–10, please refer to Table 1. Figure S3. HPLC chromatogram (UV 320 nm) of the ethanolic extract of lavandin postdistillation waste materials (EWMs). * not identified (no significant ionization in ESI positive and negative mode); compound 1 (3-(3,4-OH-phenyl)lactic acid was not detectable at 310 nm, but was detected in the ESI-MS base peak chromatogram; for identity of compounds 2–10, please refer to Table 1. Figure S4. Comparison of peak areas of compounds 2–10 in EF and EWM samples. Peak areas were calculated from UV chromatograms at 310 nm.

Author Contributions: D.R. and J.O. conceived and conducted the experiments. F.B. and D.R. analyzed the data. S.S.M. designed and coordinated the research. D.R. wrote the manuscript. S.S.M., B.J. and M.J. revised the manuscript. All authors have read and agreed to the published version of the manuscript.

Data Availability Statement: The data is available in supplementary materials.

Conflicts of Interest: The authors declare no conflict of interest.

References

1. Elgamoudi, B.A.; Korolik, V. *Campylobacter* biofilms: Potential of natural compounds to disrupt *Campylobacter jejuni* transmission. *Int. J. Mol. Sci.* **2021**, *22*, 12159. [CrossRef] [PubMed]
2. Galié, S.; García-Gutiérrez, C.; Miguélez, E.M.; Villar, C.J.; Lombó, F. Biofilms in the food industry: Health aspects and control methods. *Front. Microbiol.* **2018**, *9*, 898. [CrossRef] [PubMed]
3. Igwaran, A.; Okoh, A.I. Human campylobacteriosis: A public health concern of global importance. *Heliyon* **2019**, *5*, e02814. [CrossRef] [PubMed]
4. EFSA; ECDC. The European Union One Health 2020 Zoonoses Report. *EFSA J.* **2021**, *19*, 6971. [CrossRef]

5. Mavri, A.; Smole Možina, S. Development of antimicrobial resistance in *Campylobacter jejuni* and *Campylobacter coli* adapted to biocides. *Int. J. Food Microbiol.* **2013**, *160*, 304–312. [CrossRef]

6. Rozman, V.; Matijašić, B.B.; Smole Možina, S. Antimicrobial Resistance of Common Zoonotic Bacteria in the Food Chain: An Emerging Threat. In *Antimicrobial Resistance—A Global Threat*; Kumar, Y., Ed.; Intech Open: London, UK, 2018. [CrossRef]

7. Püning, C.; Su, Y.; Lu, X.; Gölz, G. Molecular mechanisms of *Campylobacter* biofilm formation and quorum sensing. *Curr. Top. Microbiol. Immunol.* **2021**, *431*, 293–319. [CrossRef]

8. Larsen, M.H.; Dalmasso, M.; Ingmer, H.; Langsrud, S.; Malakauskas, M.; Mader, A.; Møretrø, T.; Možina, S.S.; Rychli, K.; Wagner, M.; et al. Persistence of foodborne pathogens and their control in primary and secondary food production chains. *Food Control* **2014**, *44*, 92–109. [CrossRef]

9. Klančnik, A.; Šimunović, K.; Sterniša, M.; Ramić, D.; Smole Možina, S.; Bucar, F. Anti-adhesion activity of phytochemicals to prevent *Campylobacter jejuni* biofilm formation on abiotic surfaces. *Phytochem. Rev.* **2021**, *20*, 55–84. [CrossRef]

10. Kampf, G. Biocidal agents used for disinfection can enhance antibiotic resistance in Gram-negative species. *Antibiotics* **2018**, *7*, 110. [CrossRef]

11. Breijyeh, Z.; Jubeh, B.; Karaman, R. Resistance of Gram-negative bacteria to current antibacterial agents and approaches to resolve it. *Molecules* **2020**, *25*, 1340. [CrossRef]

12. Giacometti, F.; Shirzad-Aski, H.; Ferreira, S. Antimicrobials and food-related stresses as selective factors for antibiotic resistance along the farm to fork continuum. *Antibiotics* **2021**, *10*, 671. [CrossRef] [PubMed]

13. Salehi, B.; Mnayer, D.; Özçelik, B.; Altin, G.; Kasapoğlu, K.N.; Daskaya-Dikmen, C.; Sharifi-Rad, M.; Selamoglu, Z.; Acharya, K.; Sen, S.; et al. Plants of the genus *Lavandula*: From farm to pharmacy. *Nat. Prod. Commun.* **2018**, *13*, 1385–1402. [CrossRef]

14. Lesage-Meessen, L.; Bou, M.; Sigoillot, J.C.; Faulds, C.B.; Lomascolo, A. Essential oils and distilled straws of lavender and lavandin: A review of current use and potential application in white biotechnology. *Appl. Microbiol. Biotechnol.* **2015**, *99*, 3375–3385. [CrossRef]

15. Bajalan, I.; Pirbalouti, A.G. Variation in chemical composition of essential oil of populations of *Lavandula × intermedia* collected from Western Iran. *Ind. Crops Prod.* **2015**, *69*, 344–347. [CrossRef]

16. Kara, N.; Baydar, H. Determination of lavender and lavandin cultivars (*Lavandula* sp.) containing high quality essential oil in Isparta, Turkey. *Turk. J. F. Crops* **2013**, *18*, 58–65.

17. Prusinowska, R.; Śmigielski, K.; Stobiecka, A.; Kunicka-Styczyńska, A. Hydrolates from Lavender (*Lavandula angustifolia*)–Their chemical composition as well as aromatic, antimicrobial and antioxidant properties. *Nat. Prod. Res.* **2016**, *30*, 386–393. [CrossRef] [PubMed]

18. Torras-Claveria, L.; Jauregui, O.; Bastida, J.; Codina, C.; Viladomat, F. Antioxidant activity and phenolic composition of lavandin (*Lavandula × intermedia* Emeric Ex Loiseleur) waste. *J. Agric. Food Chem.* **2007**, *55*, 8436–8443. [CrossRef]

19. Méndez-Tovar, I.; Herrero, B.; Pérez-Magariño, S.; Pereira, J.A.; Manzanera, M.C.A.S. By-product of *Lavandula latifolia* essential oil distillation as source of antioxidants. *J. Food Drug Anal.* **2015**, *23*, 225–233. [CrossRef]

20. Śmigielski, K.B.; Prusinowska, R.; Krosowiak, K.; Sikora, M. Comparison of qualitative and quantitative chemical composition of hydrolate and essential oils of lavender (*Lavandula Angustifolia*). *J. Essent. Oil Res.* **2013**, *25*, 291–299. [CrossRef]

21. Bridier, A.; Sanchez-Vizuete, P.; Guilbaud, M.; Piard, J.C.; Naïtali, M.; Briandet, R. Biofilm-associated persistence of food-borne pathogens. *Food Microbiol.* **2015**, *45*, 167–178. [CrossRef]

22. Ramić, D.; Bucar, F.; Kunej, U.; Dogša, I.; Klančnik, A.; Smole Možina, S. Antibiofilm potential of *Lavandula* preparations against *Campylobacter jejuni*. *Appl. Environ. Microbiol.* **2021**, *87*, AEM0109921. [CrossRef] [PubMed]

23. Adams, R.P. *Identification of Essential Oil Components by Gas Chromatography/Quadrupole Mass Spectroscopy*, 4th ed.; Allured Publishing Corporation: Carol Stream, IL, USA, 2007.

24. NIST. *Mass Spectrometry Data Center*; NIST: Gaithersburg, MD, USA. Available online: https://chemdata.nist.gov/ (accessed on 4 June 2021).

25. Šimunović, K.; Ramić, D.; Xu, C.; Smole Možina, S. Modulation of *Campylobacter jejuni* motility, adhesion to polystyrene surfaces, and invasion of Int407 cells by quorum-sensing inhibition. *Microorganisms* **2020**, *8*, 104. [CrossRef] [PubMed]

26. Bassler, B.L.; Greenberg, E.P.; Stevens, A.M. Cross-species induction of luminescence in the quorum-sensing bacterium *Vibrio harveyi*. *J. Bacteriol.* **1997**, *179*, 4043–4045. [CrossRef] [PubMed]

27. Ramić, D.; Klančnik, A.; Smole Možina, S.; Dogša, I. Elucidation of the AI-2 communication system in the food-borne pathogen *Campylobacter jejuni* by whole-cell-based biosensor quantification. *Biosens. Bioelectron.* **2022**, *212*, 114439. [CrossRef]

28. Areias, F.M.; Valentão, P.; Andrade, P.B.; Moreira, M.M.; Amaral, J.; Seabra, R.M. HPLC/DAD analysis of phenolic compounds from Lavender and its application to quality control. *J. Liq. Chromatogr. Relat. Technol.* **2000**, *23*, 2563–2572. [CrossRef]

29. Blažeković, B.; Yang, W.; Wang, Y.; Li, C.; Kindl, M.; Pepeljnjak, S.; Vladimir-Knežević, S. Chemical composition, antimicrobial and antioxidant activities of essential oils of *Lavandula × intermedia* 'Budrovka' and *L. angustifolia* cultivated in Croatia. *Ind. Crops Prod.* **2018**, *123*, 173–182. [CrossRef]

30. Jug-Dujaković, M.; Ninčević, T.; Grdiša, M.; Liber, Z.; Šatović, Z. Genetic analysis of Lavandin (*Lavandula × intermedia* Emeric Ex Loisel.) landraces from the island of Hvar, Croatia. In *Book of Abstracts–8th CMAPSEEC*; Ibraliu: Alba, TX, USA, 2014.

31. Aprotosoaie, A.C.; Gille, E.; Trifan, A.; Luca, V.S.; Miron, A. Essential oils of *Lavandula* genus: A systematic review of their chemistry. *Phytochem. Rev.* **2017**, *16*, 761–799. [CrossRef]

32. Burt, S. Essential oils: Their antibacterial properties and potential applications in foods–A review. *Int. J. Food Microbiol.* **2004**, *94*, 223–253. [CrossRef]

33. Pogačar, M.Š.; Klančnik, A.; Bucar, F.; Langerholc, T.; Smole Možina, S. Anti-adhesion activity of thyme (*Thymus vulgaris* L.) extract, thyme post-distillation waste, and olive (*Olea europea* L.) leaf extract against *Campylobacter jejuni* on polystyrene and intestine epithelial cells. *J. Sci. Food Agric.* **2016**, *96*, 2723–2730. [CrossRef]

34. Klančnik, A.; Pogačar, M.Š.; Trošt, K.; Žnidarič, M.T.; Vodopivec, B.M.; Smole Možina, S. Anti-*Campylobacter* activity of resveratrol and an extract from waste pinot noir grape skins and seeds, and resistance of *Campylobacter jejuni* planktonic and biofilm cells, mediated via the CmeABC efflux pump. *J. Appl. Microbiol.* **2017**, *122*, 65–77. [CrossRef]

35. Kalia, V.C. Quorum sensing inhibitors: An overview. *Biotechnol. Adv.* **2013**, *31*, 224–245. [CrossRef] [PubMed]

36. Bezek, K.; Kurinčič, M.; Knauder, E.; Klančnik, A.; Raspor, P.; Bucar, F.; Smole Možina, S. Attenuation of adhesion, biofilm formation and quorum sensing of *Campylobacter jejuni* by *Euodia ruticarpa*. *Phyther. Res.* **2016**, *30*, 1527–1532. [CrossRef] [PubMed]

37. Karabagias, I.; Badeka, A.; Kontominas, M.G. Shelf life extension of lamb meat using thyme or oregano essential oils and modified atmosphere packaging. *Meat Sci.* **2011**, *88*, 109–116. [CrossRef] [PubMed]

38. Rezzoug, M.; Bakchiche, B.; Gherib, A.; Roberta, A.; Kilinçarslan, Ö.; Mammadov, R.; Bardaweel, S.K. Chemical composition and bioactivity of essential oils and ethanolic extracts of *Ocimum basilicum* L. and *Thymus algeriensis* Boiss. & Reut. from the Algerian Saharan Atlas. *BMC Complement. Altern. Med.* **2019**, *19*, 146. [CrossRef]

39. Etsassala, N.G.E.R.; Adeloye, A.O.; El-Halawany, A.; Hussein, A.A.; Iwuoha, E.I. Investigation of in-vitro antioxidant and electrochemical activities of isolated compounds from *Salvia chamelaeagnea* P.J. Bergius extract. *Antioxidants* **2019**, *8*, 98. [CrossRef]

40. Pistelli, L.; Najar, B.; Giovanelli, S.; Lorenzini, L.; Tavarini, S.; Angelini, L.G. Agronomic and phytochemical evaluation of Lavandin and Lavender cultivars cultivated in the Tyrrhenian area of Tuscany (Italy). *Ind. Crops Prod.* **2017**, *109*, 37–44. [CrossRef]

41. Meyer-Warnod, B. Natural essential oils: Extraction processes application to some major oil. *Perfum. Flavorist* **1984**, *9*, 93–104.

42. Çelik, S.E.; Tufan, A.N.; Bekdeşler, B.; Özyürek, M.; Güçlü, K.; Apak, R. Identification and determination of phenolics in *Lamiaceae* species by UPLC-DAD-ESI-MS/MS. *J. Chromatogr. Sci.* **2017**, *55*, 291–300. [CrossRef]

43. Héral, B.; Stierlin, É.; Fernandez, X.; Michel, T. Phytochemicals from the genus *Lavandula*: A review. *Phytochem. Rev.* **2021**, *20*, 751–771. [CrossRef]

44. Lesage-Meessen, L.; Bou, M.; Ginies, C.; Chevret, D.; Navarro, D.; Drula, E.; Bonnin, E.; Del Río, J.C.; Odinot, E.; Bisotto, A.; et al. Lavender- and lavandin-distilled straws: An untapped feedstock with great potential for the production of high-added value compounds and fungal enzymes. *Biotechnol. Biofuels* **2018**, *11*, 217. [CrossRef]

45. Lopes, C.L.; Pereira, E.; Soković, M.; Carvalho, A.M.; Barata, A.M.; Lopes, V.; Rocha, F.; Calhelha, R.C.; Barros, L.; Ferreira, I.C.F.R. Phenolic composition and bioactivity of *Lavandula pedunculata* (Mill.) Cav. Samples from different geographical origin. *Molecules* **2018**, *23*, 1037. [CrossRef] [PubMed]

46. Zhang, Y.; Xiong, H.; Xu, X.; Xue, X.; Liu, M.; Xu, S.; Liu, H.; Gao, Y.; Zhang, H.; Li, X. Compounds identification in *Semen cuscutae* by ultra-high-performance liquid chromatography (UPLCs) coupled to electrospray ionization mass spectrometry. *Molecules* **2018**, *23*, 1199. [CrossRef] [PubMed]

47. Joulain, D.; König, W. *The Atlas of Spectral Data of Sesquiterpene Hydrocarbons*; E.B.-Verlag: Hamburg, Germany, 1998.

48. Plummer, P.J. LuxS and quorum-sensing in *Campylobacter*. *Front. Cell. Infect. Microbiol.* **2012**, *2*, 22. [CrossRef] [PubMed]

49. Sivakumar, K.K.; Jesudhasan, P.R.; Pillai, S.D. Detection of autoinducer (AI-2)-like activity in food samples. *Methods Mol. Biol.* **2011**, *692*, 71–82. [CrossRef] [PubMed]

50. Klančnik, A.; Guzej, B.; Kolar, M.H.; Abramovic, H.; Smole Možina, S. In vitro antimicrobial and antioxidant activity of commercial rosemary extract formulations. *J. Food Prot.* **2009**, *72*, 1744–1752. [CrossRef]

51. Schindelin, J.; Arganda-Carreras, I.; Frise, E.; KAynig, V.; Longair, M.; Pietzsch, T.; Preibisch, S.; Rueden, C.; Saalfeld, S.; Schmid, B.; et al. Fiji: An open-source platform for biological-image analysis. *Nat. Methods* **2012**, *9*, 676–682. [CrossRef]

MDPI